NDOR Project No. SPR-P1(07) P596

PHASE I DEVELOPMENT OF AN AESTHETIC, PRECAST CONCRETE BRIDGE RAIL

Submitted by

Scott K. Rosenbaugh, M.S.C.E., E.I.T.
Research Associate Engineer

Ronald K. Faller, Ph.D., P.E.
Research Assistant Professor

Robert W. Bielenberg, M.S.M.E., E.I.T.
Research Associate Engineer

Dean L. Sicking, Ph.D., P.E.
Professor and MwRSF Director

John D. Reid, Ph.D.
Professor

MIDWEST ROADSIDE SAFETY FACILITY (MwRSF)
Nebraska Transportation Center
University of Nebraska-Lincoln
130 Whittier Building
2200 Vine Street
Lincoln, Nebraska 68583-0853
(402) 472-0965

Maher K. Tadros, Ph.D., P.E.
Professor

UNIVERSITY OF NEBRASKA-OMAHA
Department of Civil Engineering
Omaha, Nebraska 68182
(402) 554-4842

Submitted to

NEBRASKA DEPARTMENT OF ROADS
1500 Nebraska Highway 2
Lincoln, Nebraska 68502

MwRSF Research Report No. TRP-03-239-12

February 13, 2012

TECHNICAL REPORT DOCUMENTATION PAGE

1. Report No. TRP-03-239-12	2.	3. Recipient's Accession No.
4. Title and Subtitle Phase I Development of an Aesthetic, Precast Concrete Bridge Rail		5. Report Date February 13, 2012 6.
7. Author(s) Rosenbaugh, S.K., Faller, R.K., Bielenberg, R.W., Sicking, D.L., and Reid, J.D.		8. Performing Organization Report No. TRP-03-239-12
9. Performing Organization Name and Address Midwest Roadside Safety Facility (MwRSF) Nebraska Transportation Center University of Nebraska-Lincoln 130 Whittier Research Center 2200 Vine Street Lincoln, Nebraska 68583-0853		10. Project/Task/Work Unit No. 11. Contract © or Grant (G) No.
12. Sponsoring Organization Name and Address Nebraska Department of Roads 1500 Nebraska Highway 2 Lincoln, Nebraska 68502		13. Type of Report and Period Covered Final Report: 2006 – 2012 14. Sponsoring Agency Code NDOR Project No. SPR-P1(07) P596
15. Supplementary Notes Prepared in cooperation with U.S. Department of Transportation, Federal Highway Administration.		

16. Abstract (Limit: 200 words)

Precast concrete bridge rail systems offer several advantages over traditional cast-in-place rail designs, including reduced construction time and costs, installation in a wide range of environmental conditions, easier maintenance and repair, improved railing quality, and greater flexibility for aesthetic treatments. The objective of this project was to develop a precast concrete bridge rail system that met the TL-4 impact safety standards provided in MASH. The design criteria for the new bridge rail system included criteria for barrier geometry, provisions for open and closed rail options, constructability, weight limitations, segment length, design impact loads, connection of barrier segments, and connection to the bridge deck among other factors.

The research effort proceeded in several phases. First, the research focused on determining the overall concept for the new bridge rail system in terms of the rail configuration and geometry as well as the required barrier reinforcement. Next, design concepts for the joints connecting adjacent rail segments were designed and subjected to dynamic component testing in order to select a design capable of meeting design criteria for the precast bridge rail system. After selection of an appropriate rail joint, the researchers developed connection details for the attachment of the rail to the bridge deck. Once the design of the various precast bridge rail components was completed, a complete set of CAD details for the prototype precast concrete bridge rail system were completed. Following the design effort, recommendations were made regarding the full-scale testing required to implement the new, precast concrete bridge rail system

17. Document Analysis/Descriptors Precast Concrete, Bridge Rail, Barrier, MASH, Safety, TL-4, Bogie Testing, Crash testing, Aesthetic, Joints, Attachments, and Accelerated Bridge Construction		18. Availability Statement No restrictions. Document available from: National Technical Information Services, Springfield, Virginia 22161	
19. Security Class (this report)	20. Security Class (this page)	21. No. of Pages 345	22. Price

DISCLAIMER STATEMENT

This report was completed in part through funding from the Federal Highway Administration, U.S. Department of Transportation. The contents of this report reflect the views and opinions of the authors who are responsible for the facts and the accuracy of the data presented herein. The contents do not necessarily reflect the official views or policies of the Nebraska Department of Roads nor the Federal Highway Administration, U.S. Department of Transportation. This report does not constitute a standard, specification, regulation, product endorsement, or an endorsement of manufacturers.

UNCERTAINTY OF MEASUREMENT STATEMENT

The Midwest Roadside Safety Facility (MwRSF) has determined the uncertainty of measurements for several parameters involved in standard full-scale crash testing and non-standard testing of roadside safety features. Information regarding the uncertainty of measurements for critical parameters is available upon request by the sponsor and the Federal Highway Administration. Test nos. PCRB-1 through PCRB-5 consisted of non-compliant component tests that were conducted for research and development purposes only.

ACKNOWLEDGEMENTS

The authors wish to acknowledge several sources that made a contribution to this project: (1) the Nebraska Department of Roads for sponsoring the research study; (2) MwRSF personnel for constructing the barriers and conducting the crash tests; (3) Prestressed Concrete Association of Nebraska for their contribution in casting the concrete rail segments; and (4) L&M Construction Chemicals for donating the grout material.

A special thanks is also given to the following individuals who made a contribution to the completion of this research project.

Midwest Roadside Safety Facility

J.C. Holloway, M.S.C.E., E.I.T., Test Site Manager
K.A. Lechtenberg, M.S.M.E., E.I.T., Research Associate Engineer
C.L. Meyer, M.S.M.E., E.I.T., Research Associate Engineer
A.T. Russell, B.S.B.A., Shop Manager
K.L. Krenk, B.S.M.A, Maintenance Mechanic
A.T. McMaster, Former Laboratory Mechanic
Undergraduate and Graduate Research Assistants

Nebraska Department of Roads

Lymon Freeman, P.E., Former State Bridge Engineer
Sam Fallaha, P.E., Former Assistant State Bridge Engineer (TAC Member - Bridge)
Mark Traynowicz, P.E., State Bridge Engineer and Former Construction Engineer (TAC Member - Construction)
Phil TenHulzen, P.E., Design Standards Engineer (TAC Member - Roadway Design)
Amy Starr, P.E., Research Engineer
Jodi Gibson, Research Coordinator

Concrete Industries, Inc. (Lincoln)

Mark Lafferty, P.E., Vice President, General Manager

Coreslab Structures, Inc. (Omaha)

Todd Culp, P.E., Vice-President, Sales Manager

TABLE OF CONTENTS

TECHNICAL REPORT DOCUMENTATION PAGE i

ACKNOWLEDGEMENTS iii

TABLE OF CONTENTS iv

LIST OF FIGURES viii

LIST OF TABLES xiv

1 INTRODUCTION 1
- 1.1 Background 1
- 1.2 Research Objectives 2
- 1.3 Expected Benefits 2
- 1.4 Research Plan and Preliminary Design Considerations 3
  - 1.4.1 Bridge Railing Systems 3
  - 1.4.2 Bridge Deck and Anchorage Systems 3
  - 1.4.3 Test Level for Railing Systems 4
  - 1.4.4 Aesthetics 5
  - 1.4.5 Roadway Surfacing or Overlays 5
  - 1.4.6 Connection Design Considerations 6
  - 1.4.7 Analysis and Design 7
  - 1.4.8 Experimental Subsystem Testing – Phase I 8
  - 1.4.9 Full-Scale Vehicle Crash Testing – Phase II 8

2 LITERATURE REVIEW 10

3 DESIGN CRITERIA 12
- 3.1 Bridge Rail Cross Section Geometry 12
  - 3.1.1 Barrier Width 12
  - 3.1.2 Barrier Face Geometry 12
  - 3.1.3 Barrier Height 15
  - 3.1.4 Open and Closed Options 20
- 3.2 Design Load 20
- 3.3 Constructability Considerations 23
  - 3.3.1 Joint Tolerances 23
  - 3.3.2 Weight Limits 24
  - 3.3.3 Deck Type and Strength 24
  - 3.3.4 Rail Segment Length 25
- 3.4 Barrier Aesthetics 25

4 PRECAST BRIDGE RAIL - DESIGN CONCEPTS 26
- 4.1 Overview 26
- 4.2 Rail Concepts – No or Limited Continuity 26
  - 4.2.1 Concept A (L-Post) 26

4.2.2 Concept B (Post-Off-Deck) 41
4.2.3 Concept C (Rail Cap) 45
4.3 Rail Concepts - Moderate Continuity 50
4.3.1 Concept D (Staggered Rail) 50
4.4 Rail Concepts – High Continuity 53
4.4.1 Concept E (Ladder) 53
4.4.2 Concept F (Fence) 62
4.5 Rail Design Selection 63

5 RAIL TO RAIL JOINT DESIGNS 68
5.1 Overview 68
5.2 Joint Loading Criteria 68
5.2.1 Shear Loading 68
5.2.2 Moment Loading 69
5.3 Joint Classification 70
5.4 Dry Joint Designs 71
5.4.1 Joint Design A – Bolted Splice Plates 71
5.4.2 Joint Design B – X-Bolts 74
5.4.3 Joint Design C – Side Bolts and Center Shear Key 76
5.4.4 Joint Design D – Side Bolts and Shear Tubes 78
5.4.5 Joint Design E – Center Bolt and Shear Pipe 82
5.4.6 Joint Design F – Baluster Connection Piece 86
5.5 Grouted Joint Designs 90
5.5.1 Joint Design G – Center Bolt and Side Grout Pockets 90
5.5.2 Joint Design H – I-Shape Segments in Side Grout Pockets 94
5.5.3 Joint Design I – Side Bolts and Center Grout Pocket 96

6 RAIL JOINT BOGIE TESTING – ROUND 1 98
6.1 Purpose 98
6.2 Scope 98
6.3 Testing Facility 100
6.4 Equipment and Instrumentation 100
6.4.1 Bogie 100
6.4.2 Accelerometers 101
6.4.3 Pressure Tape Switches 102
6.4.4 Photography Cameras 102
6.5 Test Specimen – Selected Joint Designs 103
6.5.1 Test No. PCRB-1, Joint Design H 104
6.5.2 Test No. PCRB-2, Joint Design D 118
6.6 Bogie Test No. PCRB-1 134
6.6.1 Test Description 134
6.6.2 Rail Joint Component Damage 135
6.6.3 Data Analysis 136
6.7 Bogie Test No. PCRB-2 144
6.7.1 Test Description 144
6.7.2 Rail Joint Component Damage 145

6.7.3 Data Analysis 146
6.8 Round 1 Bogie Testing Discussion 155

7 RAIL JOINT DESIGN MODIFICATIONS AND IMPROVEMENTS 157
7.1 Refined Grout Joint 157
7.2 Alternate Grout Joint 159
7.3 Refined Dry Joint 163

8 RAIL JOINT BOGIE TESTING - ROUND 2 166
8.1 Scope 166
8.2 Equipment and Instrumentation 166
8.2.1 Bogie 166
8.2.2 Photography Cameras 167
8.3 Test Specimen – Joint Designs 169
8.3.1 Test No. PCRB-3, Refined Grout Joint Design 169
8.3.2 Test No. PCRB-4, Refined Dry Joint Design 186
8.3.3 Test No. PCRB-5, Alternate Grout Joint Design 210
8.4 Bogie Test No. PCRB-3 227
8.4.1 Test Description 227
8.4.2 Component Damage 227
8.4.3 Data Analysis 228
8.5 Bogie Test No. PCRB-4 234
8.5.1 Test Description 234
8.5.2 Component Damage 235
8.5.3 Data Analysis 236
8.6 Bogie Test No. PCRB-5 243
8.6.1 Test Description 243
8.6.2 Component Damage 244
8.6.3 Data Analysis 245
8.7 Round 2 –Bogie Testing Discussion 252

9 BARRIER POST TO DECK ATTACHMENT DESIGN 257
9.1 Overview 257
9.1.1 Deck Attachment A - Threaded Rods and Shear Tubes 257
9.1.2 Deck Attachment B - Threaded Rods 259
9.1.3 Deck Attachment C - Cleat 261
9.1.4 Deck Attachment D - Shear Curb 262
9.1.5 Deck Attachment E - Shear Channel 264
9.1.6 Deck Attachment Selection 265
9.2 Bridge Deck Reinforcement Design 266

10 FINAL PROTOTYPE DESIGN DETAILS 280

11 SUMMARY, CONCLUSIONS, AND RECOMENDATIONS 323
11.1 Summary and Conclusions 323
11.2 Recommendations and Future Work 327

12 REFERENCES 330

13 APPENDICES 333
APPENDIX A. Additional Rail to Rail Joint Concepts 334

LIST OF FIGURES

Figure 1. Head Ejection Envelope [8] 14
Figure 2. New Bridge Rail Geometry Using Width and Head Ejection Limits 15
Figure 3. Barrier Forces Acting on Single-Unit Truck During Impact 16
Figure 4. Maximum Roll Angle of 10000S Vehicle Impacting 34½-in. Tall, Rigid Barrier 18
Figure 5. Bridge Rail Geometric Bounds 19
Figure 6. LS-DYNA Impact Force vs. Time - MASH TL-4 Condition 22
Figure 7. Concept A (L-Post) - Overview 31
Figure 8. Concept A (L-Post) – Assembled Side View 32
Figure 9. Concept A (L-Post) – Connection Details 33
Figure 10. Concept A (L-Post) – Rail Segment Geometry 34
Figure 11. Concept A (L-Post) – Rail Segment Reinforcement 35
Figure 12. Concept A (L-Post) – Post Geometry 36
Figure 13. Concept A (L-Post) – Post Reinforcement 37
Figure 14. Concept A (L-Post) – Placement of Post Reinforcement 38
Figure 15. Concept A (L-Post) –Deck Panel Attachment Details 39
Figure 16. Concept A (L-Post) – Isotropic View 40
Figure 17. Concept B (Post-Off-Deck) - Assembled Overview 42
Figure 18. Concept B (Post-Off-Deck) – Rail Dimensions 43
Figure 19. Concept B (Post-Off-Deck) – Post Dimensions 44
Figure 20. Concept C (Rail Cap) - Assembled Overview 47
Figure 21. Concept C (Rail Cap) – Rail Dimensions 48
Figure 22. Concept C (Rail Cap) – Post Dimensions 49
Figure 23. Concept D (Staggered Rail) - Geometry 51
Figure 24. Concept D (Staggered Rail) – Isotropic View 52
Figure 25. Concept E (Ladder) - Overview 56
Figure 26. Concept E (Ladder) – Cross Section View 57
Figure 27. Concept E (Ladder) – Connection Hardware 58
Figure 28. Concept E (Ladder) – Rail Segment 59
Figure 29. Concept E (Ladder) – Post Segment 60
Figure 30. Concept E (Ladder) – Isotropic View 61
Figure 31. Concept F (Fence) - Overview 65
Figure 32. Concept F (Fence) - Geometry 66
Figure 33. Concept F (Fence) – Isotropic View 67
Figure 34. Factored Rail Moment Strength vs. Post Moment Strength 70
Figure 35. Joint Design A – Bolted Splice Plates 73
Figure 36. Joint Design B – X-Bolts 75
Figure 37. Joint Design C – Side Bolts and Center Shear Key 77
Figure 38. Joint Design D – Side Bolts and Shear Tubes 80
Figure 39. Joint Design D – Side Bolts and Shear Tubes - Assembly 81
Figure 40. Joint Design E – Center Bolt and Shear Pipe 84
Figure 41. Joint Design E – Center Bolt and Shear Pipe – Assembly and Parts 85
Figure 42. Joint Design F – Baluster Connection Piece 88
Figure 43. Joint Design F – Baluster Connection Piece – Individual Parts 89

Figure 44. Joint Design G – Center Bolt and Side Grout Pockets 92
Figure 45. Joint Design G – Center Bolt and Side Grout Pockets – Assembly 93
Figure 46. Joint Design H – Wide Flange Segments in Side Grout Pockets 95
Figure 47. Joint Design I – Side Bolts and Center Grout Pocket 97
Figure 48. Bogie Testing Set Up 99
Figure 49. Bogie Vehicle (a) Impact Head and (b) on Guidance Track 101
Figure 50. Camera Locations, Test Nos. PCRB-1 and PCRB-2 103
Figure 51. Wide Flange Joint Test Specimen, Test No. PCRB-1 106
Figure 52. Wide Flange Joint Assembly, Test No. PCRB-1 107
Figure 53. Long Rail Segment, Test No. PCRB-1 108
Figure 54. Cross Section Views of Long Rail Segment, Test No. PCRB-1 109
Figure 55. Rail Steel Reinforcement, Test No. PCRB-1 110
Figure 56. Short Rail Segment, Test No. PCRB-1 111
Figure 57. Cross Section Views of Short Rail Segment, Test No. PCRB-1 112
Figure 58. Grout Pocket Assembly and Reinforcement, Test No. PCRB-1 113
Figure 59. Left-Side Grout Pocket Details, Test No. PCRB-1 114
Figure 60. Right-Side Grout Pocket Details, Test No. PCRB-1 115
Figure 61. Pocket Reinforcement Details and Wide Flange Section, Test No. PCRB-1 116
Figure 62. Rail Component Photographs, Test No. PCRB-1 117
Figure 63. Side Bolts and Shear Tubes Joint Test Specimen, Test No. PCRB-2 121
Figure 64. Side Bolts and Shear Tubes Joint Assembly, Test No. PCRB-2 122
Figure 65. Long Rail Segment, Test No. PCRB-2 123
Figure 66. Cross Section Views of Long Rail Segment, Test No. PCRB-2 124
Figure 67. Rail Steel Reinforcement, Test No. PCRB-2 125
Figure 68. Short Rail Segment, Test No. PCRB-2 126
Figure 69. Cross Section Views of Short Rail Segment, Test No. PCRB-2 127
Figure 70. End Pockets Assembly and Reinforcement, Test No. PCRB-2 128
Figure 71. Left-Side Pocket Details, Test No. PCRB-2 129
Figure 72. Right-Side Pocket Details, Test No. PCRB-2 130
Figure 73. Pocket Gusset Plates, Shims, and Shear Bolts, Test No. PCRB-2 131
Figure 74. Connection Hardware, Test No. PCRB-2 132
Figure 75. Rail Component Photographs, Test No. PCRB-2 133
Figure 76. Sequential Photographs, Test No. PCRB-1 137
Figure 77. Additional Sequential Photographs, Test No. PCRB-1 138
Figure 78. Component Damage, Test No. PCRB-1 139
Figure 79. Component Damage – Long Rail Segment, Test No. PCRB-1 140
Figure 80. Component Damage – Short Rail Segment, Test No. PCRB-1 141
Figure 81. Bending Damage of Long Rail Segment, Test No. PCRB-1 142
Figure 82. Data Analysis Plots, Test No. PCRB-1 143
Figure 83. Sequential Photographs, Test No. PCRB-2 147
Figure 84. Additional Sequential Photographs, Test No. PCRB-2 148
Figure 85. Additional Sequential Photographs, Test No. PCRB-2 149
Figure 86. Component Damage, Test No. PCRB-2 150
Figure 87. Component Damage - Front Pocket Assembly, Test No. PCRB-2 151
Figure 88. Component Damage – Back Pocket Assembly, Test No. PCRB-2 152

Figure 89. Component Damage – Loose Concrete Removed, Test No. PCRB-2 153
Figure 90. Data Analysis Plots, Test No. PCRB-2 154
Figure 91. Data Comparison Plots, Round 1 Bogie Testing Results 155
Figure 92. Grout Rail Joint Improvements – Steel I-Shape Connector 158
Figure 93. Grout Rail Joint Improvements – Alternate Modifications 162
Figure 94. Dry Rail Joint Improvements – Shear/Tension Tube 165
Figure 95. Bogie Impact Head with Steel Tube Blockouts 167
Figure 96. Camera Locations, Test Nos. PCRB-3 and PCRB-4 168
Figure 97. Camera Locations, Test No. PCRB-5 169
Figure 98. Refined Grout Rail Joint Design, Test No. PCRB-3 172
Figure 99. Refined Grout Joint Assembly, Test No. PCRB-3 173
Figure 100. Long Rail Segment, Test No. PCRB-3 174
Figure 101. Cross Section Views of Long Rail Segment, Test No. PCRB-3 175
Figure 102. Short Rail Segment, Test No. PCRB-3 176
Figure 103. Cross Section Views of Short Rail Segment, Test No. PCRB-3 177
Figure 104. Rail Internal Steel Reinforcement, Test No. PCRB-3 178
Figure 105. Grout Pocket Assembly, Test No. PCRB-3 179
Figure 106. Grout Pocket Assembly Connections, Test No. PCRB-3 180
Figure 107. Left Grout Pocket, Test No. PCRB-3 181
Figure 108. Right Grout Pocket, Test No. PCRB-3 182
Figure 109. Grout Pocket Accessories and Shear Bolts, Test No. PCRB-3 183
Figure 110. Built Up I-Shape Connector, Test No. PCRB-3 184
Figure 111. Rail Component Photographs, Test No. PCRB-3 185
Figure 112. Refined Dry Rail Joint, Test No. PCRB-4 189
Figure 113. Refined Dry Joint Assembly, Test No. PCRB-4 190
Figure 114. Long Rail Segment, Test No. PCRB-4 191
Figure 115. Cross Section Views of Long Rail Segment, Test No. PCRB-4 192
Figure 116. Cross Section Views of Long Rail Segment, Test No. PCRB-4 193
Figure 117. Short Rail Segment, Test No. PCRB-4 194
Figure 118. Cross Section Views of Short Rail Segment, Test No. PCRB-4 195
Figure 119. Cross Section Views of Short Rail Segment, Test No. PCRB-4 196
Figure 120. Rail Internal Steel Reinforcement, Test No. PCRB-4 197
Figure 121. End Pocket Assembly, Test No. PCRB-4 198
Figure 122. Pocket Assembly Connections, Test No. PCRB-4 199
Figure 123. Left Pocket, Test No. PCRB-4 200
Figure 124. Left Pocket, Test No. PCRB-4 201
Figure 125. Right Pocket, Test No. PCRB-4 202
Figure 126. Right Pocket, Test No. PCRB-4 203
Figure 127. Shear Plates, Test No. PCRB-4 204
Figure 128. Reinforcing Rebar, Test No. PCRB-4 205
Figure 129. Shear Tube Connector, Test No. PCRB-4 206
Figure 130. Shear Tube, Shim Plates, and Gussets, Test No. PCRB-4 207
Figure 131. Dry Joint Installation Hardware, Test No. PCRB-4 208
Figure 132. Rail Component Photographs, Test No. PCRB-4 209
Figure 133. Alternate Grout Joint Design, Test No. PCRB-5 213

Figure 134. Alternate Grout Joint Assembly, Test No. PCRB-5 214
Figure 135. Long Rail Segment, Test No. PCRB-5 215
Figure 136. Cross Section Views of Long Rail Segment, Test No. PCRB-5 216
Figure 137. Short Rail Segment, Test No. PCRB-5 217
Figure 138. Cross Section Views of Short Rail Segment, Test No. PCRB-5 218
Figure 139. Rail Internal Steel Reinforcement, Test No. PCRB-5 219
Figure 140. Pocket Assembly and Anchorage, Test No. PCRB-5 220
Figure 141. Pocket Assembly Connections, Test No. PCRB-5 221
Figure 142. Left Grout Pocket, Test No. PCRB-5 222
Figure 143. Right Grout Pocket, Test No. PCRB-5 223
Figure 144. Grout Pocket Cap, Shear Plate, and Anchorage, Test No. PCRB-5 224
Figure 145. Threaded Rod Connector Assembly, Test No. PCRB-5 225
Figure 146. Rail Component Photographs, Test No. PCRB-5 226
Figure 147. Sequential Photographs, Test No. PCRB-3 229
Figure 148. Component Damage, Test No. PCRB-3 230
Figure 149. Component Damage – Steel Pockets, Test No. PCRB-3 231
Figure 150. Rail Tension Cracks and Damage to Bottom of Joint, Test No. PCRB-3 232
Figure 151. Data Analysis Plots, Test No. PCRB-3 233
Figure 152. Sequential Photographs, Test No. PCRB-4 237
Figure 153. Additional Sequential Photographs, Test No. PCRB-4 238
Figure 154. Component Damage, Test No. PCRB-4 239
Figure 155. Component Damage – Steel Pockets, Test No. PCRB-4 240
Figure 156. Component Damage – Concrete Damage, Test No. PCRB-4 241
Figure 157. Data Analysis Plots, Test No. PCRB-4 242
Figure 158. Sequential Photographs, Test No. PCRB-5 246
Figure 159. Additional Sequential Photographs, Test No. PCRB-5 247
Figure 160. Component Damage, Test No. PCRB-5 248
Figure 161. Component Damage – Short Rail Segment, Test No. PCRB-5 249
Figure 162. Component Damage – Long Rail Segment, Test No. PCRB-5 250
Figure 163. Data Analysis Plots, Test No. PCRB-5 251
Figure 164. Data Comparison Plots, Round 2 Bogie Testing Results 255
Figure 165. Joint Comparison Plots, Round 2 Bogie Testing Results 256
Figure 166. Deck Attachment A – Threaded Rods and Shear Tubes 258
Figure 167. Deck Attachment B – Threaded Rods 260
Figure 168. Deck Attachment C - Cleat 262
Figure 169. Deck Attachment D - Shear Rail 264
Figure 170. Deck Attachment E – Shear Channel 265
Figure 171. Schematic Details of Modified Bridge Deck Reinforcement 269
Figure 172. Schematic Details of Modified Bridge Deck Reinforcement 270
Figure 173. Schematic Details of Modified Bridge Deck Reinforcement 271
Figure 174. Schematic Details of Modified Bridge Deck Reinforcement 272
Figure 175. Schematic Details of Modified Bridge Deck Reinforcement 273
Figure 176. Schematic Details of Modified Bridge Deck Reinforcement 274
Figure 177. Schematic Details of Modified Bridge Deck Reinforcement 275
Figure 178. Schematic Details of Modified Bridge Deck Reinforcement 276

Figure 179. Schematic Details of Modified Bridge Deck Reinforcement 277
Figure 180. Schematic Details of Modified Bridge Deck Reinforcement 278
Figure 181. Schematic Details of Modified Bridge Deck Reinforcement 279
Figure 182. Precast Bridge Rail Segment CAD Details 284
Figure 183. Precast Bridge Rail Segment CAD Details 285
Figure 184. Precast Bridge Rail Segment CAD Details 286
Figure 185. Precast Bridge Rail Segment CAD Details 287
Figure 186. Precast Bridge Rail Segment CAD Details 288
Figure 187. Precast Bridge Rail Segment CAD Details 289
Figure 188. Precast Bridge Rail Segment CAD Details 290
Figure 189. Precast Bridge Rail Segment CAD Details 291
Figure 190. Precast Bridge Rail Segment CAD Details 292
Figure 191. Precast Bridge Rail Segment CAD Details 293
Figure 192. Precast Bridge Rail Segment CAD Details 294
Figure 193. Precast Bridge Rail Segment CAD Details 295
Figure 194. Precast Bridge Rail Segment CAD Details 296
Figure 195. Precast Bridge Rail Segment CAD Details 297
Figure 196. Precast Bridge Rail Segment CAD Details 298
Figure 197. Precast Bridge Rail System Layout 299
Figure 198. Precast Bridge Rail System Layout 300
Figure 199. Precast Bridge Rail System Layout 301
Figure 200. Precast Bridge Rail System Layout 302
Figure 201. Precast Bridge Rail System Layout 303
Figure 202. Precast Bridge Rail System Layout 304
Figure 203. Precast Bridge Rail System Layout 305
Figure 204. Precast Bridge Rail System Layout 306
Figure 205. Precast Bridge Rail System Layout 307
Figure 206. Precast Bridge Rail System Layout 308
Figure 207. Precast Bridge Rail System Layout 309
Figure 208. Precast Bridge Rail System Layout 310
Figure 209. Precast Bridge Rail System Layout 311
Figure 210. MwRSF Simulated Bridge Test Pit 312
Figure 211. Precast Bridge Rail Foam Model with 1100C Vehicle 313
Figure 212. Precast Bridge Rail Foam Model with 2270P Vehicle 314
Figure 213. Precast Bridge Rail Foam Model with 10000S Vehicle 315
Figure 214. Precast Bridge Rail Aesthetic Treatment Concepts 316
Figure 215. Precast Bridge Rail Aesthetic Treatment Concepts 317
Figure 216. Precast Bridge Rail Aesthetic Treatment Concepts 318
Figure 217. Precast Bridge Rail Aesthetic Treatment Concepts 319
Figure 218. Precast Bridge Rail Aesthetic Treatment Concepts 320
Figure 219. Precast Bridge Rail Aesthetic Treatment Concepts 321
Figure 220. Precast Bridge Rail Aesthetic Treatment Concepts 322
Figure A-1. Dry Rail Joint – Slider Tube 335
Figure A-2. Dry Rail Joint – Slider Tube Assembly 336
Figure A-3. Dry Rail Joint – Plates Underneath Rail 337

Figure A-4. Dry Rail Joint – Structural Steel Shape (C-Channel) Underneath Rail 338
Figure A-5. Dry Rail Joint – Bolts Through End Balusters..... 339
Figure A-6. Dry Rail Joint – Bolts and Shear Pipes Through End Balusters 340
Figure A-7. Dry Rail Joint – Unsymmetrical, One-Way Bolt Assembly 341
Figure A-8. Grouted Rail Joint – Side Bolts and Vertical, Center Grout Pocket 342
Figure A-9. Grouted Rail Joint – Large Grout Pocket with exposed Steel Reinforcement..... 343
Figure A-10. Grouted Rail Joint – Structural Steel Shape in Center Grout Pocket..... 344

LIST OF TABLES

Table 1. Estimated Peak Lateral Impact Force - MASH TL-4 Conditions 22
Table 2. LS-DYNA Peak Lateral Impact Force – MASH TL-4 Conditions 23
Table 3. Camera and Lens Information, Test Nos. PCRB-1 & 2 103
Table 4. Camera and Lens Information, Test Nos. PCRB-3 and PCRB-4 167
Table 5. Camera and Lens Information, Test No. PCRB-5 168

1 INTRODUCTION

1.1 Background

Historically, most open concrete bridge railings have been installed using cast-in-place concrete construction. As a result, significant labor costs are expended at the actual jobsite in order to set forms, tie steel reinforcing bars, place concrete, and allow for adequate curing while considering environmental and weather conditions. The increased labor and extended construction time results in higher construction costs and delays in opening a bridge system.

Alternatively, an open concrete bridge railing system could be developed using precast concrete construction. For this precast system, all of the bridge railing components would be fabricated offsite and then later delivered to the jobsite. Subsequently, the precast post and beam components would be erected onsite in a relatively short period of time as compared to the cast-in-place construction methods. Labor costs would be significantly reduced by eliminating the need for form construction and field placement of the reinforcement and concrete.

The design of a new, precast concrete bridge railing system would consider the following factors: aesthetics; ease of construction; maintenance and repair; load transfer; dynamic safety performance; as well as the overall economy of an "installed" barrier system. Design variations could be made to accommodate various levels of service. In addition, a precast concrete bridge railing system could be configured either as an open rail or as a closed vertical parapet. Finally, precast concrete bridge railing systems could be developed for use on either cast-in-place and precast concrete bridge decks. The development effort would consider the selection of cost-effective anchorage hardware for making the connection between the bridge railing and deck systems.

1.2 Research Objectives

For this research project, an open precast concrete bridge railing system was developed for use on cast-in-place and precast concrete bridge deck systems. In addition, conceptual modifications were developed for creating a closed version of the precast concrete railing system for use in special applications. The open and closed new railing systems were designed to meet the Test Level 4 impact safety standards provided in the American Association for State Highway and Transportation Officials (AASHTO) document entitled, *Manual for Assessing Safety Hardware* (MASH) [1].

1.3 Expected Benefits

The successful development of a new family of precast bridge railing systems will significantly reduce construction time and should ultimately reduce overall costs as contractors and precasters gain experience with the new system. Construction of precast bridge railing systems should be much less weather sensitive than cast-in-place bridge railing systems. With the reduced construction time, the roadway and bridge would be opened to the motoring public in a more-timely manner. Further, a precast barrier system will greatly simplify barrier repair should any damage occur during high-energy, impacts with trucks. Standardized barrier components will allow maintenance personnel to easily remove and replace any damaged barrier components in a timely and efficient manner without requiring long periods of lane closure. Finally, aesthetic features can be easily cast into the face of a precast barrier system without the high costs associated with field construction. Hence, the new barrier system should allow designers much greater flexibility to develop bridge designs that contribute to the overall beauty of Nebraska's highways.

1.4 Research Plan and Preliminary Design Considerations

1.4.1 Bridge Railing Systems

The preliminary plan was to develop two precast railing systems - an open concrete railing and a closed concrete parapet. In general, open concrete railings are preferred on rural highways for several reasons. First, an open railing design allows transverse water runoff to flow easily over the deck edge in applications where no traffic or pedestrians are found below the bridge system. Second, open railing systems reduce snow accumulation in front of the railing system both during snow removal operations as well as during snow storms. In addition, open railing designs arguably have more aesthetic appeal as compared to most closed concrete parapets. Closed concrete railings are typically utilized in urban applications where it is necessary to prevent water runoff from traveling over the deck edge.

1.4.2 Bridge Deck and Anchorage Systems

As previously noted, the preliminary plan was to develop railing systems for use on both cast-in-place reinforced concrete decks as well as precast reinforced concrete deck panels. As such, it was envisioned that the same steel anchorage system would be developed for use with either bridge deck type. However, it should be noted that the size, spacing, and/or configuration of the anchorage system may differ for the open and closed railing designs. For example, open concrete railings require attachment to the deck at the base of the each bridge post. Alternatively, continuous closed concrete parapets are typically anchored to the deck along the entire length of the parapet. If deemed feasible, the research and engineering team would consider the use of one anchorage system for both the open and closed railing designs.

The railing systems were to be developed for two bridge deck systems. As such, the most critical deck system would be selected for use in the crash testing program. The successful

completion of this research and development project should result in the allowance of either railing system to be anchored to both deck types. For this project, it was anticipated that the most critical bridge railing system would be tested and evaluated on a 7½ to 8½-in. (190 to 216-mm) thick deck system. In addition, it was envisioned that the transverse, precast concrete deck panels would measure approximately 12 ft (3.66 m) wide by 15 to 16 ft (4.57 to 4.88 m) long.

1.4.3 Test Level for Railing Systems

Based on discussions between Nebraska Department of Roads (NDOR) personnel and Midwest Roadside Safety Facility (MwRSF) researchers, it was anticipated that the new, precast bridge railing systems would be designed to meet the revised Test Level 4 (TL-4) condition provided in the new MASH impact safety standards. At the revised TL-4 impact condition, three full-scale vehicle crash tests are required - a 2,425-lb (1,100-kg) small car impacting at 62.1 mph (100 km/hr) and 25 degrees, a 5,000-lb (2,268-kg) pickup truck impacting at 62.1 mph (100 km/hr) and 25 degrees, and a 22,046-lb (10,000-kg) single-unit truck impacting at 55.9 mph (90 km/hr) and 15 degrees.

Using the revised TL-4 impact condition, the bridge railing and deck systems were to be designed to limit the overall damage imparted to the bridge deck. An acceptable level of deck damage was determined as damage which can be repaired through standard crack filling operations. However, any damage occurring to the rail and/or post elements that requires replacement would be deemed acceptable as long as the safety performance criteria were met.

Historically, TL-4 open concrete bridge railings and closed concrete parapets have been configured with a top mounting height which has ranged from 29 to 34 in. (737 to 864 mm). Initially, it was anticipated that the new precast railing systems would be configured with similar top railing heights, even when developed to meet the revised TL-4 impact conditions. The new,

precast concrete bridge railing systems would be developed using a vertical, or nearly vertical, front-face railing geometry in order to reduce the propensity for vehicle climb and subsequent vehicular instabilities during redirection.

1.4.4 Aesthetics

The bridge railing systems would be developed with the assumption that aesthetic features (i.e., decorative geometric features, longitudinal asperities, etc.) could be placed on the front face of the rail elements. The research team was also to consider the inclusion of decorative elements and/or medallions on the back side of the system, more specifically at the post locations, if deemed desirable by NDOR officials. It should also be noted that the appearance of the precast railing and post components could be enhanced with the use of various textures and dyes on the concrete surfaces.

Professor William Holmes, R.A., a University of Nebraska – Lincoln (UNL) faculty member with expertise in architectural design and aesthetics, was retained on this project in order to better address the overall appearance of the new bridge railing systems.

1.4.5 Roadway Surfacing or Overlays

The development of the new bridge railing systems would make accommodation for the future placement of roadway surfacing or overlays with a maximum thickness of 2 in.(51 mm). As such, the overall top mounting height of the bridge railing could be constructed 2 in. (51 mm) taller than that deemed necessary to meet the revised TL-4 test condition. For the experimental testing program, a 2-in. (51-mm) asphalt or low-strength, concrete wearing surface was to be considered over the concrete bridge deck in order to evaluate the worst case scenario.

In addition, the height of the opening below the rail element for the open concrete railing configuration would be sized to prevent small car wheel snag on the posts when no asphalt

overlay was used. However, it should be noted that the inclusion of the 2-in. (51-mm) wearing surface will reduce the propensity for wheel snag from that observed without any overlay.

1.4.6 Connection Design Considerations

For the new, precast open and closed concrete railing systems, the rail, post, and solid parapet elements would be designed to accommodate both horizontal and vertical roadway curves. Therefore, it would be necessary for NDOR officials to provide to the research team the maximum horizontal and vertical curves that could be used on future bridge systems.

In addition to the curve considerations, the post-to-deck and parapet-to-deck connections would be designed to accommodate cross slopes (i.e., roadway crown and super-elevation). As such, a shim detail would likely be necessary to construct the rail face either perpendicular to the earth or perpendicular to the deck at the appropriate locations.

Initially, it was anticipated that the rail and solid parapet elements would be fabricated using 12 or 24-ft (3.66 or 7.32-m) lengths in order to accommodate the various roadway curves. Using the 12-ft (3.66-m) wide precast deck panels, it was envisioned that a 12-ft (3.66-m) center-to-center post spacing would provide the necessary structural capacity as well as an acceptable appearance for the open concrete rail design. For open concrete railings installed on the precast deck panel systems, the posts would be attached to the deck panels at the center locations of the panels instead of the panel joint locations.

Based on prior discussions with NDOR bridge personnel regarding the open concrete railing system, two separate connections were to be considered to attach the rail to the posts and the posts to the deck. The use of separate connection details was believed to provide for an easier replacement of damaged components. For example, a vertical bolted connection was being considered to attach the posts to the deck surface, while a horizontal bolted connection was

considered to mount the rail elements to the posts. Initially, it was uncertain whether the rail splice connection detail would occur at the posts, at the midspan, or even at one of the quarter span locations. Grouted connections were to be used if deemed absolutely necessary.

1.4.7 Analysis and Design

The development of the two new, precast bridge railing systems would consider the following features: (1) prestressed and standard reinforced concrete design for the railing components; (2) smooth and/or deformed welded wire reinforcement for posts and/or rail elements; (3) standard and self-consolidating concrete mixes; (4) high-strength concrete mix designs ranging between 10,000 and 12,000 psi (68.95 to 82.74 MPa); (5) Grade 60 steel reinforcement and high-strength steel reinforcing rods, such as rods conforming to the 120,000 and 150,000 psi (827.4 to 1,034.2 MPa) specifications; and (6) tapered front-face post geometry to reduce and/or prevent wheel snag.

Standard reinforced and prestressed concrete design methods were to be utilized for configuring all of the connections details, sizing the posts, rails, and solid parapet segments, as well as the determining the required deck reinforcement adjacent to the barrier attachment locations. However, the redirective capacity of the rigid, open and closed concrete bridge railing systems would be determined using existing, yield-line analysis procedures outlined in the literature.

For the research project, all of the construction and fabrication details for the bridge railing systems, and even components, would be prepared using 3-D Solidworks CAD modeling. The use of 3-D computer-aided drafting would ensure that appropriate design tolerances were provided as well as to allow for an aesthetic evaluation of the systems prior to final fabrication of the system component.

1.4.8 Experimental Subsystem Testing – Phase I

Upon completion of the preliminary design, Phase I dynamic bogie testing would be utilized to evaluate the structural adequacy of selected subsystems of the precast bridge railings prior to conducting the full-scale vehicle crash testing program. Subsystem testing may include: cantilevered post testing with a rigid sleeve foundation or attachment to an existing, rigid section of bridge deck; three- or four-point bend testing for simply-supported rail sections; and lateral load testing of mid-span or quarter-span rail splice connections. In addition, it may be valuable to perform similar experimental testing on selected subsystems from NDOR's current bridge railing systems (i.e., open concrete railing). If this testing is deemed appropriate and necessary, those test results would be used for a baseline comparison to those results obtained from the subsystem testing of the new railing components. For this project, it was anticipated that a minimum of six (6) dynamic bogie tests would be performed on various subsystems of the precast bridge railings.

1.4.9 Full-Scale Vehicle Crash Testing – Phase II

The new, precast open concrete bridge railing system would be constructed on a full-size bridge deck and girder system located at MwRSF's outdoor test facility and within an existing bridge test pit. The existing bridge test pit is configured with two exterior abutments and two interior bents. The bridge support structure consists of two rows of longitudinal steel girders for a total of six (6) girders. The girders are configured with lateral bracing and are attached to a series of reinforced concrete bents and abutments. As previously mentioned, the precast open concrete bridge railing system would be anchored to either a cast-in-place concrete deck or a precast concrete deck panel system.

For the Phase II testing program, the bridge railing and deck systems would be constructed in the bridge test pit. Subsequently, a full-scale vehicle crash testing program would

be utilized to demonstrate the structural adequacy of the bridge railing system as well as to prove its overall crashworthiness according to the impact safety standards. Three crash tests are required according to the TL-4 impact conditions - a small car test, a pickup truck test, and a single-unit truck test. Since the railing geometry would be designed to mitigate any propensity for small car wheel snag on the railing or post components, the research team believed that the small car test would likely be waived from the test matrix. However, the pickup truck and single-unit truck crash tests would likely be required for certifying and garnering FHWA acceptance for the new bridge railing systems.

Occasionally, barrier systems are instrumented with sensors in order to determine the magnitude of the deformation, loading, stress, and/or strain imparted to selected components when subjected to dynamic vehicular impact events. As such, the research team intends to consider the instrumentation of selected steel reinforcing bars within the bridge deck system and near specific post locations in order to better evaluate the adequacy of the deck design under an impact loading scenario. This instrumentation could include the installation of strain gauges on steel reinforcing bars that are expected to experience maximum loading during both of the truck tests. However, this effort could require two different regions to be instrumented along the length of the bridge deck.

2 LITERATURE REVIEW

A literature review was performed to identify prior research, development, and testing studies pertaining to precast concrete bridge railing systems. If relevant systems were identified, then the research results would be evaluated to determine whether existing technologies and methods should be considered for the new railing system. Second, the research team also wanted to be knowledgeable of any prior successful and/or unsuccessful crash testing programs in order to guide the development of new precast, open and closed concrete bridge railing systems. From the literature review, it was discovered that very little research had been performed on the development and testing of solid concrete parapets, while no prior efforts were uncovered which involved precast open concrete bridge railings.

In the late 1980s, the L.B. Foster Company developed a half-section, precast concrete barrier and anchoring system for use on bridges [2]. The front face of the parapet resembled the New Jersey profile which extended to a height of 32 in. (813 mm). The concrete section utilized a 9¾ in. (248 mm) top width and a 19 in. (483 mm) base width. The 20-ft (6.10-m) long segments were anchored to a concrete deck using ten 1-in. (25-mm) diameter, ASTM A325 steel anchor rods that were bonded into the deck, spaced on 2 ft (610 mm) centers along the barrier length, and inserted into precast vertical holes at the barrier base. The precast bridge railing system was successfully crash tested and evaluated by the Texas Transportation Institute using the Test Level 4 (TL-4) safety performance criteria found in AASHTO's *Guide Specifications for Bridge Railings* [3]. One test was performed with the 18,000-lb (8,165-kg) single-unit truck at the approximate impact conditions of 50 mph (80.5 km/hr) and 15 degrees.

The Texas Department of Transportation (TxDOT) also utilizes a precast concrete parapet as a permanent traffic barrier [4-5]. The Type T503 and Type T504 barriers are

configured with a half-section, New Jersey safety shape using segment lengths ranging between 9 ft (2.74 m) and 31 ft - 6 in. (9.60 m). The overall height of the parapet was 32 in. (813 mm), including the use of a ½-in. (13-mm) thick grout pad. The segments were anchored to a concrete deck using seven 1-in. (25-mm) diameter, steel anchor rods that were epoxied or grouted into the deck. The steel anchor rods were noted to conform to ASTM A325, A321, or A193 B7. The precast bridge railing has been approved as meeting Test Level-4 of NCHRP Report No. 350 based on its equivalent strength to other railings with similar geometry [6].

3 DESIGN CRITERIA

3.1 Bridge Rail Cross Section Geometry

3.1.1 Barrier Width

The selection of a particular bridge railing can affect a bridge structure's width and overall cost. A top-mounted barrier with a wide footprint requires additional width of the bridge deck and support structure, while a top-mounted bridge rail with a narrow footprint reduces the overall structure width. Side-mounted bridge rails can also potentially reduce the required structure width if a greater portion of the barrier is positioned beyond the outer deck edge. In any event, narrow and/or side-mounted bridge rails should be considered when optimizing a bridge system.

For this project, the width of the new precast concrete bridge rail was to be limited in order to provide a cost-effective barrier and bridge deck system. One of the more common concrete bridge rails in use today is the 32-in. (813-mm) tall, New Jersey safety shape, single-sided, concrete bridge barrier with a top width of 6 in. (152 mm) and a base width of 15 in. (381 mm) [7]. Therefore, the maximum width of approximately 15 in. (381 mm) was targeted for the new, precast bridge railing.

3.1.2 Barrier Face Geometry

Previously, full-scale crash testing and computer simulation modeling have shown that vehicle stability is improved as the barrier face becomes more vertical [8-9]. Full-scale crash testing of vertical-faced parapets under NCHRP Report No. 350 guidelines has also demonstrated that vehicle decelerations fall below the threshold limits for occupant risk [10]. More recently, full-scale crash testing has been successfully performed on two nearly rigid, vertical-faced, concrete barriers according to the MASH impact safety standards which also

demonstrated acceptable safety performance [11-12]. Therefore, a vertical-faced geometry was selected for use in the development of a precast concrete bridge railing.

The barrier system was also designed to reduce the risk of head slap against the concrete parapet. Head slap is defined as an event where an occupant's head contacts the barrier during vehicle redirection. In 2007, MwRSF researchers preformed a study on head ejection from passenger vehicles [8]. For this effort, a head ejection envelope was developed to provide guidance regarding predicted positions for ejected heads outside of a vehicle's side window, as shown in Figure 1. The head ejection envelope was positioned at the barrier's front face to determine the upper cross section of the precast concrete bridge rail, as shown in Figure 2.

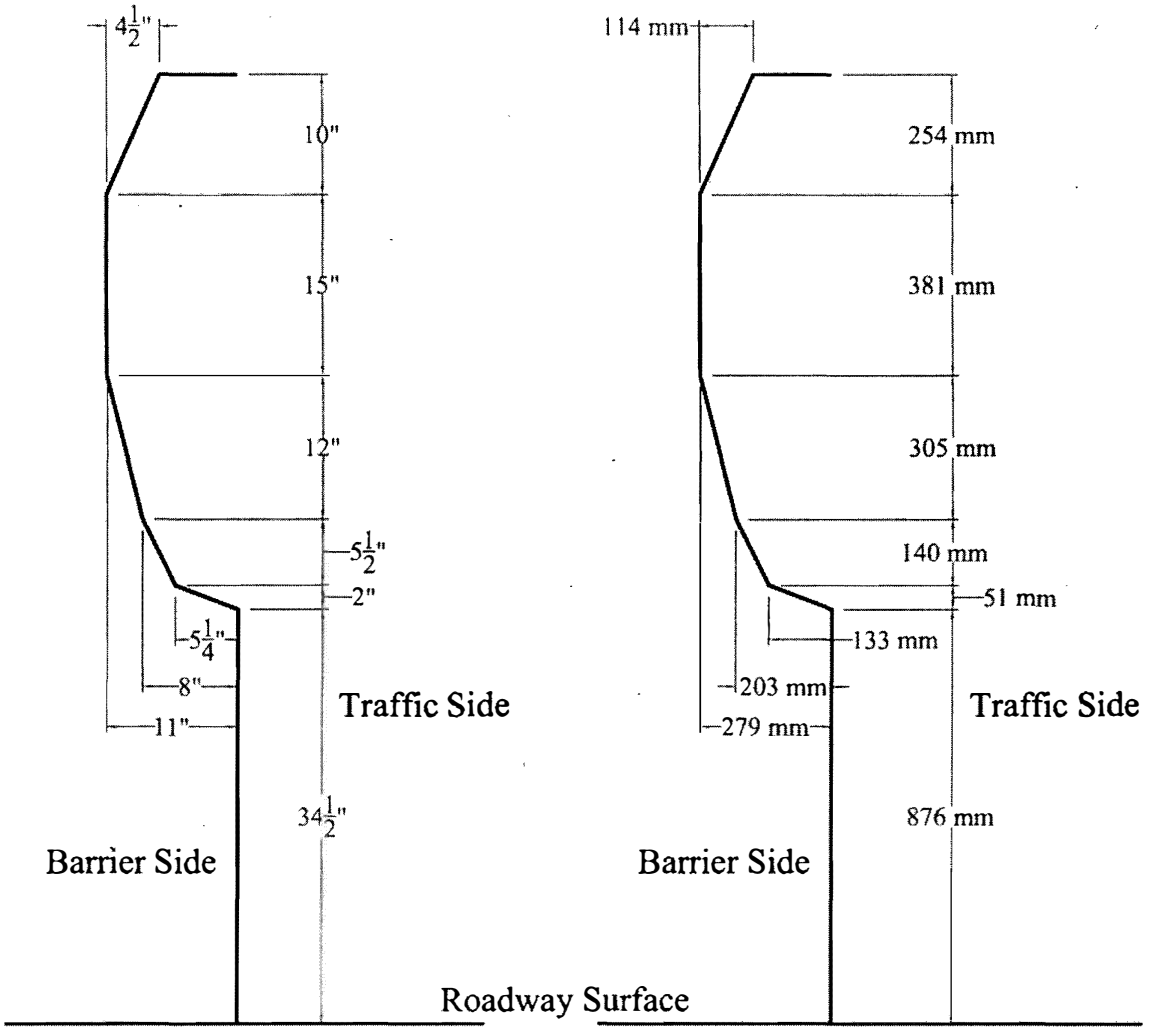

Figure 1. Head Ejection Envelope [8]

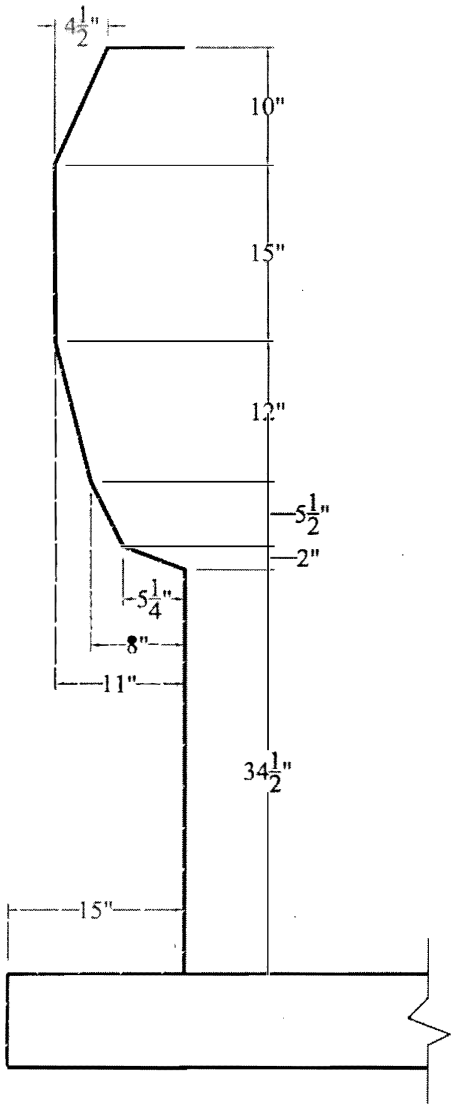

Figure 2. New Bridge Rail Geometry Using Width and Head Ejection Limits

3.1.3 Barrier Height

Concrete barrier heights typically range from 32 to 42 in. (813 to 1,067 mm). Passenger vehicles, including small cars and pickup trucks, normally have a center of gravity height below 30 in. (762 mm). As a result, passenger vehicles are normally redirected with lateral forces generated from these vehicle-to-barrier impact events. However, taller vehicles, such as single-unit trucks, have a much higher center of gravity and run the risk of rolling over the top of

shorter barriers during impact events. For example, the MASH 10000S single-unit truck (SUT) has a ballast center of gravity (c.g.) height of 63 in. (1,600 mm). Thus, these heavier and taller vehicles, such as single-unit trucks, are redirected and prevented from rolling over the top of rigid barriers due to a combination of a vertical barrier load being applied to the outer underside of the cargo box and a lateral barrier resistance imparted to the wheels and axle assemblies, as shown in Figure 3.

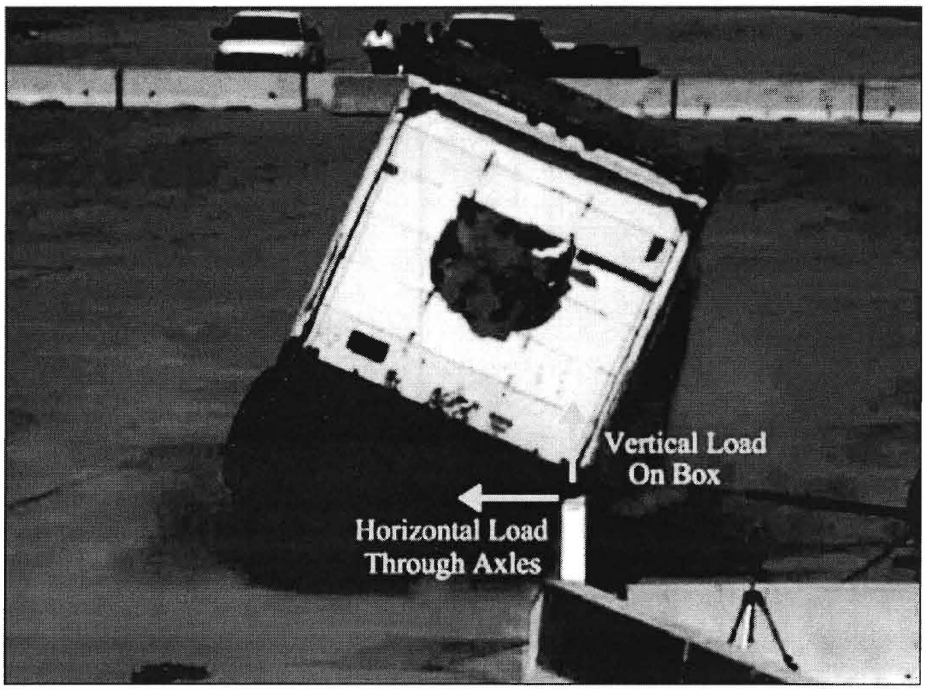

Figure 3. Barrier Forces Acting on Single-Unit Truck During Impact

Multiple 32-in. (813-mm) tall concrete barriers have been shown to redirect single-unit trucks under the TL-4 crash testing guidelines found in NCHRP Report No. 350 which have consisted of a 17,637-lb (8,000-kg) vehicle impacting at approximately 50 mph (80 km/h) and 15 degrees [13-15]. However, the new MASH guidelines modified the TL-4 test conditions for the SUT vehicle to include a weight of 22,046 lb (10,000 kg) and a speed of approximately 56 mph (90 km/h). These changes resulted in a 58 percent increase in impact severity, from 97.6 k-ft

(132 kJ) to 154.4 k-ft (209 kJ). Thus, there exists an increased risk for a SUT vehicle to roll over a 32-in. tall rigid barrier when impacted under the new TL-4 MASH criteria. In fact, previous TL-4 MASH crash tests with a 10000S vehicle on 32-in. (813-mm) tall, New Jersey safety shape bridge rails have resulted in the single-unit truck rolling over the barrier [16-17].

Subsequently, MwRSF researchers determined that barrier heights in excess of 32 in. (813 mm) would likely be required to prevent single-unit trucks from rolling over the top of common rigid barriers during TL-4 impacts under MASH. With increased barrier height, the truck box would contact the top of the barrier sooner, thus allowing the vertical force to stabilize vehicle roll before it became critical.

As such, an LS-DYNA computer simulation effort [18] was utilized to determine the barrier height necessary to prevent rollover. A 15-in. (381-mm) wide, rigid barrier was configured using a cross-sectional geometry conforming to the design limits shown in Figure 2. The barrier geometry was modeled such that the barrier height could be raised or lowered between simulation trials. A 10000S vehicle was modeled to impact the barrier under the TL-4 impact conditions of MASH. If the initial simulation provided satisfactory results (i.e., the vehicle was redirected without rolling over the barrier), then a second simulation was conducted at the same barrier height in which the suspension was disconnected from the front axle during impact. This type of vehicle damage has been commonly observed in previous TL-4 full-scale crash tests [15-16, 19-21], which can cause vehicle instabilities. LS-DYNA simulations demonstrated that a barrier height of 34½ in. (876 mm) was adequate for redirecting a single-unit truck and preventing the vehicle from rolling over the top of the barrier. Crash images depicting the vehicle's maximum roll angle when impacting a 34½-in. (876-mm) tall barrier are shown in **Error! Reference source not found.** for both the connected and deleted suspension simulations.

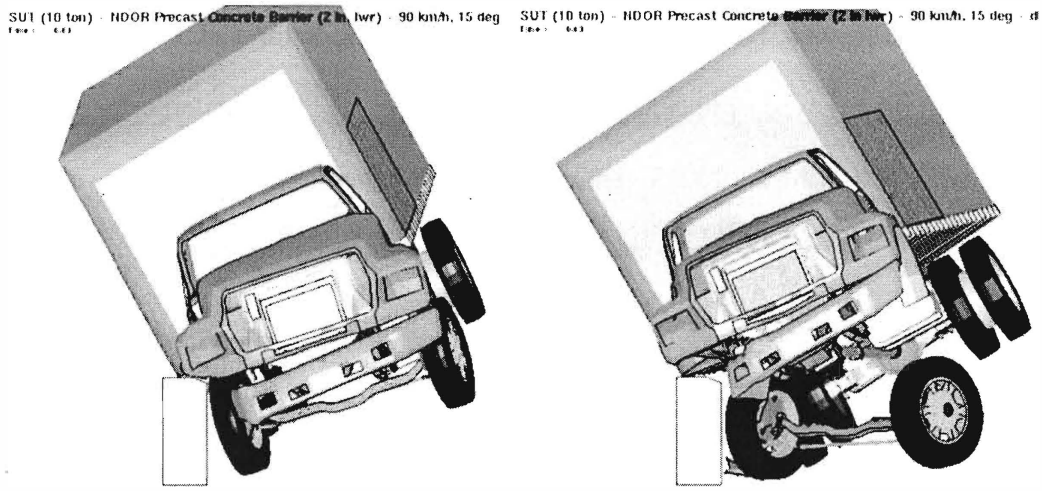

Connected Suspension Deleted Suspension @ 100 ms

Figure 4. Maximum Roll Angle of 10000S Vehicle Impacting 34½-in. Tall, Rigid Barrier

A final design criteria considered with respect to rail height was the height of the bottom of the rail for open concrete railings. The height of the bottom of the rail was critical with respect to small car vehicles in order to provide proper capture and redirection of the vehicle and to prevent the vehicle from extending too far underneath the rail and snagging on the rigid concrete posts supporting the system. In order to determine the minimum height for the bottom of the rail, the researchers reviewed previous small car testing on open concrete railings and timber railings. The results of this review found that a minimum height for the bottom of the rail was 12 in. (305 mm) above the ground in order to ensure the system functioned properly for small car vehicles.

Asphalt overlays are typically used to refurbish the wearing surfaces of a bridge deck, which would lower the bridge rail's effective height. A bridge rail should be designed to perform in an acceptable manner when the road or deck surface is expected to be treated with an asphalt overlay in the future. The presence of an asphalt overlay could increase the propensity for a heavy truck to roll over the top of the bridge rail. Therefore, the minimum rail height was raised to 36½ in. (927 mm) in order to allow for a future 2-in. (51-mm) thick overlay applied on the

bridge deck surface in front of the parapet. Using the prior width and head ejection limits in combination with the noted rail height, the geometric bounds for the new bridge rail were determined, as shown in Figure 5. However, it was noted that additional features may be incorporated into the simple geometry shown in Figure 5 as long as the head ejection envelope or lateral rail width limits are not violated.

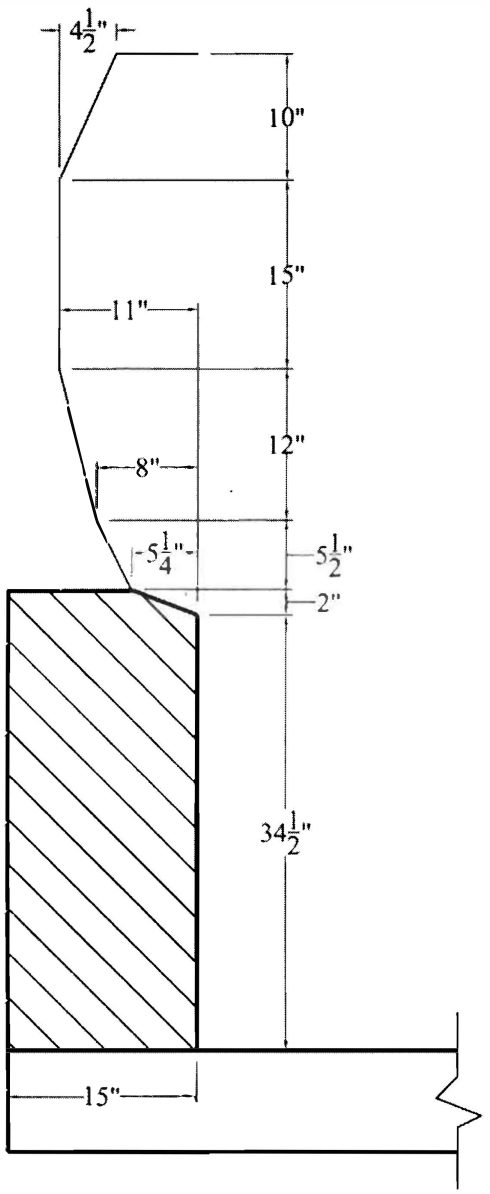

Figure 5. Bridge Rail Geometric Bounds

3.1.4 Open and Closed Options

For the new precast bridge rail, it was determined that the general configuration should be adaptable to both open and closed design variations. Open bridge rails allow water to flow off of the bridge deck and/or snow to be pushed through the barrier and off of the bridge. Closed bridge rails keep all water, snow, or debris on the bridge, thereby preventing it from falling laterally onto a lower roadway. Instead, water is often redirected into drainage systems and transported to acceptable outlet locations or to the bridge ends. The decision to use an open or a closed bridge rail is often dependent on bridge location and site constraints below the structure. Therefore, both open and closed versions were desired in order for the new precast rail to be used on the full spectrum of bridges. Open concrete bridge rails are not continuous at their base. Thus, open rails are inherently weaker than closed rails and require additional strengthening at the discrete post locations. Thus, the initial design efforts, as outlined in Chapter 4, were based on starting with an open configuration with the understanding that the system could later be easily converted to a closed configuration.

3.2 Design Load

When the design effort was initiated, the preliminary MASH guidelines had only recently been released. Thus, only a small number of full-scale crash tests with SUT vehicles had been conducted under the MASH safety standards. As such, a design impact load for the MASH TL-4 single-unit truck test had not yet been determined or estimated using crash test results. Therefore, three different methods were utilized to approximate the TL-4 design impact load for SUT vehicles, including: (1) numerical approximations; (2) scaling of previous crash test results; and (3) computer simulations.

NCHRP Report No. 86 outlines a numerical analysis used to approximate vehicle impact loads based on vehicle dimensions and impact conditions [22]. The equations used to calculate vehicle impact loads are shown below:

$$G_{LAT} = \frac{(V_I * \sin\theta)^2}{2g[AL * \sin\theta - B(1 - \cos\theta) + D]}$$

and

$$F_{LAT-AVE} = G_{LAT} * Wt$$

where V_I and θ are the initial impact speed and angle, respectively, AL is the distance from the front of the vehicle to the center of gravity, 2B is the width of the vehicle, D is the barrier lateral deflection, and g is the gravitational constant. Using the TL-4 impact conditions, AL and B distances of 16.4 and 3.5 ft (5.0 and 1.07 m), respectively, and with the assumption of a rigid barrier, the average lateral impact force was determined to be 37.5 kips (167 kN). Assuming a dynamic impact factor of 2, the lateral peak impact force was determined to be 75 kips (334 kN).

As previously stated, only a limited number of TL-4 crash tests had been performed under the MASH standards due to its recent release. Thus, the majority of single-unit truck crash tests were conducted in accordance to the TL-4 standards of NCHRP Report No. 350. Thus, results from prior NCHRP Report No. 350 TL-4 crash tests were used in combination with a scaling factor to estimate the lateral impact load. The impact force data from these previous tests were scaled to reflect the increased impact severity.

In 2007, MwRSF researchers calculated peak lateral impact forces for several full-scale crash tests using results obtained from onboard vehicle accelerometers and rate gyros [23]. For this effort, three single-unit truck crash tests into rigid parapets were considered. Subsequently, the peak lateral impact forces were multiplied by the ratio of the MASH target impact severity,

154.4 k-ft (209 kJ), divided by the actual impact severity. From this analysis, the peak loads were approximated to range between 88 and 95 kips (391 and 4,253 kN), as shown in Table 1.

Table 1. Estimated Peak Lateral Impact Force - MASH TL-4 Conditions

Test No.	Ref No.	Weight		Impact Speed		Impact Angle (deg)	Actual Impact Severity		NCHRP 350 TL-4 Peak Lateral Impact Force		MASH TL-4 Predicted Peak Lateral Impact Force	
		(lbs)	(kg)	(mph)	(km/h)		(k-ft)	(kJ)	(kips)	(kN)	(kips)	(kN)
CYRO-1	[20]	17,840	8,092	51.2	82.4	17.7	145	196	87.2	388	93.3	415
ZOI-1	[24]	17,605	7,985	50.4	81.1	15.64	108	146	66.8	297	88.7	395
ZOI-3	[24]	17,637	8,000	50.2	80.8	16.32	117	159	66.9	298	94.5	421

The third method for approximating the MASH TL-4 peak lateral impact loads consisted of LS-DYNA computer simulation. The computer simulations described in Section 3.1.3 were used to demonstrate that a 34½ in. (876 mm) tall, rigid barrier could successfully redirect a 10000S vehicle. These same simulations were also used to predict the peak lateral impact forces. Two simulations were conducted for each barrier height of 36½ and 34½ in. (927 and 876 mm). The front suspension was deleted at 100 ms for one simulation at each barrier height. Figure 6 contains force vs. time curves for all four simulations after an SAE C60 filter was applied. Table 2 contains the simulation results for the applicable TL-4 test condition.

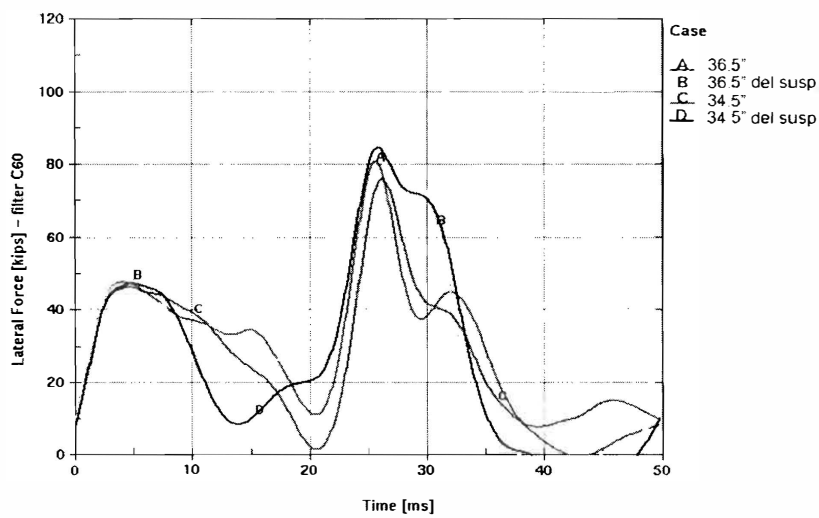

Figure 6. LS-DYNA Impact Force vs. Time - MASH TL-4 Condition

Table 2. LS-DYNA Peak Lateral Impact Force – MASH TL-4 Conditions

Case No.	Simulation Conditions	Peak Lateral Impact Load	
		(kips)	(kN)
A	36½ in. [927 mm] barrier height	81	360
B	36½ in. [927 mm] barrier height, front suspension deleted @ 100 ms	98	436
C	34½ in.[876 mm] barrier height	75	334
D	34½ in. [876 mm] barrier height, front suspension deleted @ 100 ms	86	383

In summary and as noted above, three methods were used to determine the peak lateral impact force for single-unit truck impacts into rigid parapets under the MASH TL-4 test conditions. From this analysis, the peak lateral impact force was found to range from 75 to 98 kips (334 to 436 kN). For the development of the new precast bridge railing, the research team conservatively selected a design lateral impact force of 100 kips (445 kN).

3.3 Constructability Considerations

3.3.1 Joint Tolerances

It is impractical to assume that the precast bridge rail components would fit together in a perfect manner when constructed on a real bridge deck. As such, constructions tolerances were incorporated into to each connection or interface between the adjacent precast components. Since the precast bridge railing components were to be fabricated in a controlled environment and not on site, it was determined that ½ in. (12.7 mm) of construction tolerance should be adequate. Thus, the rail-to-deck connections and the rail-to-rail connections incorporated a ½-in. (12.7-mm) construction tolerance in the longitudinal and lateral directions.

3.3.2 Weight Limits

For this R&D effort, the project team also considered the construction equipment that was deemed necessary to install the precast bridge rail segments. From discussions with Nebraska Department of Roads engineers as well as construction and maintenance personnel, a 5-ton (44.5-kN) limit was established to accommodate the most common heavy lifting machinery utilized for construction and maintenance operations on the job sites. Therefore, each precast rail component had an upper weight limit of 10,000 lbs (4,536 kg).

3.3.3 Deck Type and Strength

In recent years, much interest has been directed toward the use of accelerated bridge construction as well as precast bridge deck panels. However, many bridges are still being constructed with cast-in-place concrete bridge decks. Therefore, it was reasoned that the new precast bridge railing would be primarily designed for use on cast-in-place concrete bridge decks but with the potential for it to be later adapted to precast concrete deck panels.

Regardless of the deck type, the concrete bridge deck would need sufficient strength to resist the peak lateral impact load imparted to the deck edge without resulting in any structural damage. Damage to the precast bridge railing system was deemed tolerable; since, the damaged components could be removed and replaced with new railing hardware without closing the bridge. However, the replacement of new deck panels would be much more difficult and would likely require the bridge structure to be closed and traffic rerouted. Thus, it was determined that structural damage due to vehicular impact events should be mostly limited to the bridge railing system.

3.3.4 Rail Segment Length

In order to maximize efficiency, a rail segment length should be selected to limit the number of precast sections per bridge without exceeding the weight limit of 10,000 lbs (4,536 kg), as determined in Section 3.3.2. Also, a rail segment length should be selected to either match the width of one precast deck panel or the width of two or more panels in order to provide for a consistent installation pattern across the length of the bridge. Precast bridge deck panels are commonly fabricated in 8, 10, or 12 ft (2.4, 3.1, or 3.7 m) lengths. Assuming the cross-sectional geometry shown in Figure 5, a 16 ft (4.9 m) long rail segment would weigh about 7,500 lbs (3,400 kg) for concrete alone. Thus, the design concepts for the precast bridge rail were focused with using a 16-ft (4.9-m) long rail segment that would span two 8-ft (2.4-m) wide deck panels. Cast-in-place and precast concrete decks can be modified to contain attachment hardware at any spacing along the bridge length. Thus, the bridge rail should be applicable for use on either deck configuration.

3.4 Barrier Aesthetics

One of the primary project goals was to design a precast concrete bridge rail that was aesthetically pleasing. Historically, barrier aesthetics have often been enhanced through the use various treatments, such as: longitudinal face asperities; imprinted facial patterns; openings, such as windows; and color additives. As a result, the research team believed that the new precast concrete bridge rail would likely be innovative and attractive with the inclusion of several of these characteristics in combination with a new rail shape.

4 PRECAST BRIDGE RAIL - DESIGN CONCEPTS

4.1 Overview

Several design concepts were prepared for the new precast concrete bridge rail prior to selecting the final barrier concept, as described in Section 4.4.2. The initial design concepts were based on using separate post and rail pieces that utilized simple bolted connections to form simply-supported beams. However, the analysis and design of these barrier concepts demonstrated a need to incorporate alterations to the barrier shape as well as utilize a continuous rail in order to satisfy the criteria described in Chapter 2. Within the following sections, the major barrier concepts are presented and discussed, including CAD details which depict the evolution of the precast bridge rail.

4.2 Rail Concepts – No or Limited Continuity

4.2.1 Concept A (L-Post)

The precast concrete bridge rail was designed to incorporate separate rail and post segments. For Concept A, all posts were identical. The rail segments which spanned between posts could be configured to provide either an open or a closed bridge rail configuration. The rail-to-post and post-to-deck connections were configured to utilize either bolts or threaded rods. Thus, the precast concrete bridge railing could easily be dismantled in the event that damage occurred, and a portion of the barrier system was to be removed or replaced. Detailed drawings for this system, including internal steel reinforcement, were prepared and are shown in Figures 7 through 16.

Initially, the rail segments were designed to span across only two posts, thus resulting in unmanageable impact loads for a simply-supported configuration. Subsequently, the rails were

extended to cover two spans or three posts, thus greatly reducing the loads imparted to the posts and rail segments.

The analysis and design effort was focused on the open rail configuration; since, the closed rail configuration would likely provide greater redirective capacity. The rail segment utilized a basic rectangular shape, except for the top-front portion of the rail which was sloped to match the relevant boundaries of the head ejection envelope, as discussed in Section 3.1.2. Also, longitudinal asperities were integrated into the front face of the rail to provide more aesthetic appeal. Finally, recessed areas were placed within the rail face around the bolt holes so that the bolt heads would not extend out and become a snagging hazard. Internal steel reinforcement provided the necessary bending and shear strength to resist the impact loads. Fourteen no. 7 longitudinal bars were placed through the rail, and the no. 4 vertical stirrups were placed at 4 in. (102 mm) intervals, as shown in Figure 11. For this steel reinforcement configuration, a minimum rail width of 11 in. (279 mm) was required to provide sufficient structural strength.

The posts were L-shaped for a number of reasons. First, the taller portion of the post provides lateral restraint for the rail segments with minimal connection hardware. Next, the lower extension provided a location for bolting the post to the deck without having to extend the bolt through the entire height of the post. Finally, the lower extension also serves as a seat for the rail. With the rail supported by this seat, a gap was established below the rail, thus resulting in an open configuration. As a result, the rail-to-post bolts did not need to resist any dead weight of the beams. As shown in Figure 12, the lower extension of the post was tapered on the front corners to prevent impacting vehicles from snagging on the upstream and downstream corners of the post. Similar to the face of the rail, the areas around the bolts were recessed so that the bolt heads would not protrude from the post so that the rail could sit flush on the post seat.

Longitudinal and transverse steel reinforcement was utilized within each post, as shown in Figures 13 and 14. The longitudinal steel consisted of no. 4 stirrups and provided resistance to shear, while the transverse steel consisted of no. 6 stirrups and provided bending or overturning resistance. The minimum post length and width was 3 ft (0.9 m) and 8½ in. (216 mm), respectively. This post geometry, used in combination with the current reinforcement configuration, was deemed necessary to provide adequate strength to resist the design impact load.

Within the post-to-deck connection, the bending and shear strength were provided by separate components. Bending strength was provided by two 1⅜-in. (35-mm) diameter ASTM A193 Grade B7 threaded rods which extended through the seat of the post as well as the deck. Shear strength was provided by two 3 x 3 x ¼-in. (76 x 76 x 6-mm) steel tubes which were partially cast into the post and extended out from the bottom of the post. The exposed portion of the tube extended into sleeves which were cast into the deck. These components, along with the 1¼ in. (32 mm) diameter, SAE Grade 5 heavy hex bolt connecting the rail and post, are shown in Figure 9.

As previously mentioned, the transverse precast concrete deck panels were selected to be 8 ft (2.4 m) wide. Each panel contained two holes for the ASTM A193 Grade B7 threaded rods as well as the two 4 x 4 x ¼-in. (102 x 102 x 6-mm) steel tubes, or sleeves, for the shear tubes. These holes and sleeves were centered on each panel and spaced 18 in. (457 mm) apart, as shown in Figure 15. In the event that a cast-in-place deck is to be used, the connection hardware would need to be repeated at 8-ft (2.4-m) intervals. All of the connection holes and sleeves were designed with a construction tolerance of ¼ in. (13 mm) in both the lateral and longitudinal directions.

For this project, it was deemed important to mitigate damage to first occur to the rail and post components rather than the deck. As such, a steel angle was placed on the outside edge of the bridge deck to provide increased deck strength as well as an improved bearing surface for the posts. Also, each post had a notch integrated into the lower-back surface with the intent of weakening the concrete in the post's compression zone. This stress concentration point was expected to result in concrete crushing on the back side of the post before the deck sustains any significant damage. Finally, ⅛-in. (3-mm) thick neoprene pads were placed between every concrete-to-concrete surface to distribute bearing loads and prevent localized crushing.

Although Concept A (L-Post) had adequate strength and could easily be installed and removed, it did not satisfy all of the design criteria. For example, the system width, 20⅛ in. (511 mm), exceeded the width limit of 15 in. (381 mm). Recall, the width limit was set so that the rail would not occupy more deck space than current safety-shaped bridge rails. A wider bridge rail would require an extended bridge deck and result in an increased bridge cost for a comparable width of traveled way. Further analysis was undertaken in an attempt to decrease the width of the rail and/or posts. However, the strength requirements combined with the current quantity and layout for the steel reinforcement rendered these efforts unsuccessful.

As previously noted, there existed concerns regarding the magnitude of the impact load imparted into the rail, post, and deck components. With no or very limited rail continuity to distribute the impact load along the length of the bridge, the entire impact load could likely be transmitted into the deck through only a few posts. Under this scenario, high shear and bending moments would occur at the post locations near impact. It was feared that current precast panels, and even some cast-in-place concrete decks, would not provide adequate strength to withstand MASH TL-4 impact loads without suffering major structural damage. Recall, it was desirable for

all structural damage to only occur within the easily-replaceable precast bridge rail and post members and not within the bridge deck.

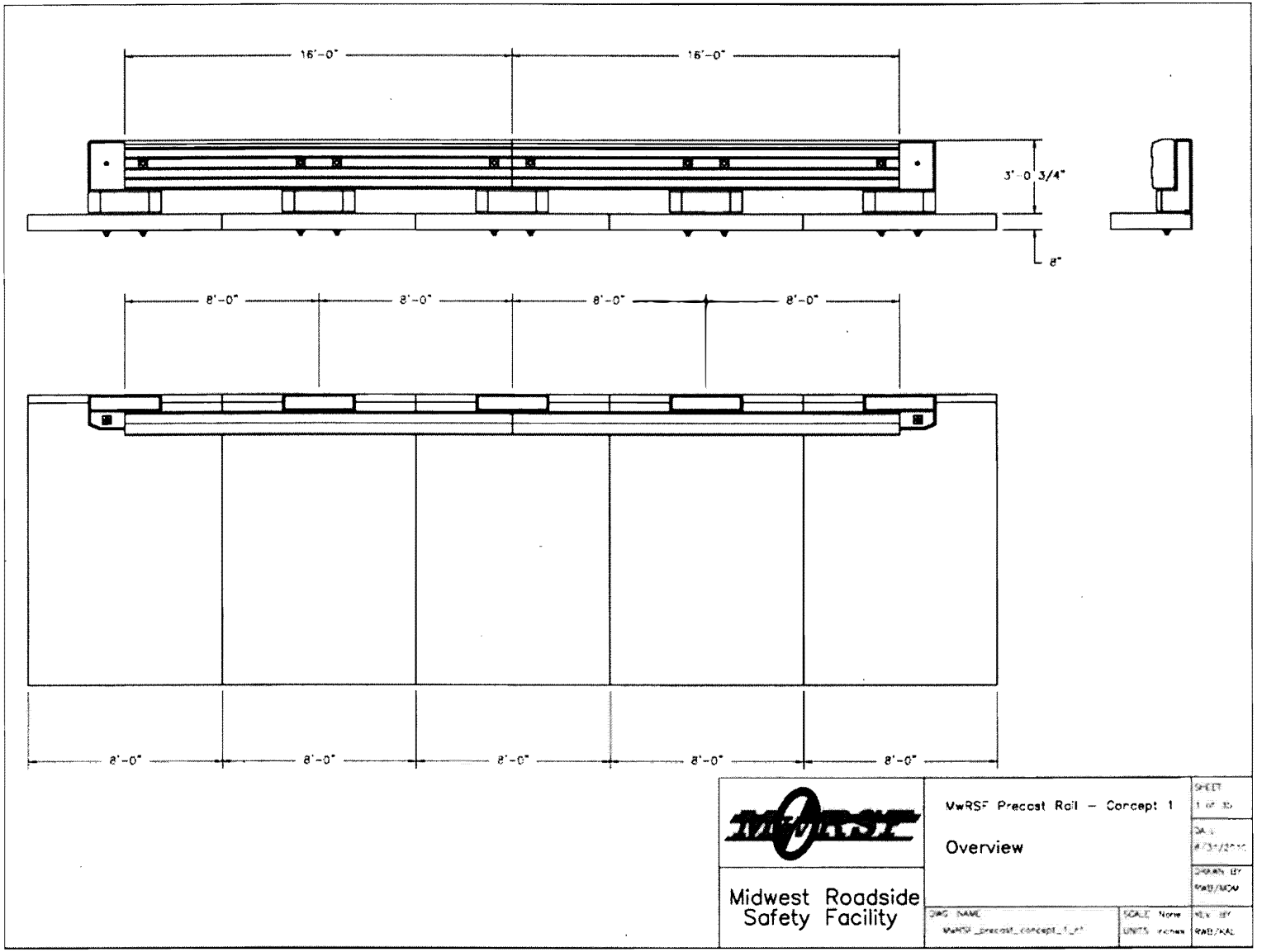

Figure 7. Concept A (L-Post) - Overview

MwRSF Precast Bridge Rail – Concept 1					
Item No.	QTY.	Description	Material Spec	Hardware Guide	File Name
a1	5	Precast Deck Panel	–	–	MwRSF_concept_1_precast deck
b1	5	Precast Post Assembly	–	–	MwRSF_concept_1_post
c1	2	Precast Bridge Rail	–	–	MwRSF_concept_1_main_rail_section
d1	20	Washer Plate 4x4x0.5x1.5	A36 – Galvanized	–	MwRSF_concept_1_washerplate_4x4x.5x.1.5_A36
d2	16	Washer Plate 4x4x0.5x1.375	A36 – Galvanized	–	MwRSF_concept_1_washerplate_4x4x.5x.1.375_A36
d3	10	Threaded Rod 1.375 – UNC 6 x 23	B7 (105 ksi) – Galvanized	–	MwRSF_concept_1_threaded_rod_1.375-6x23_b7
d4	20	Heavy Hex Nut 1.375 – UNC 6	Grade 5 – Galvanized		MwRSF_concept_1_HHNUT_1.3750-6-D-N.sldprt
d5	8	Heavy Hex Nut 1.25 – UNC 7	Grade 5 – Galvanized		MwRSF_concept_1_HHNUT_1.2500-7-D-N_Grade5.sldprt
d6	8	Heavy Hex Bolt 1.25 – UNC 7 x 18	Grade 5 – Galvanized		MwRSF_concept_1_HHBOLT_1.2500-7x18x18_N_grade5.SLDPRT

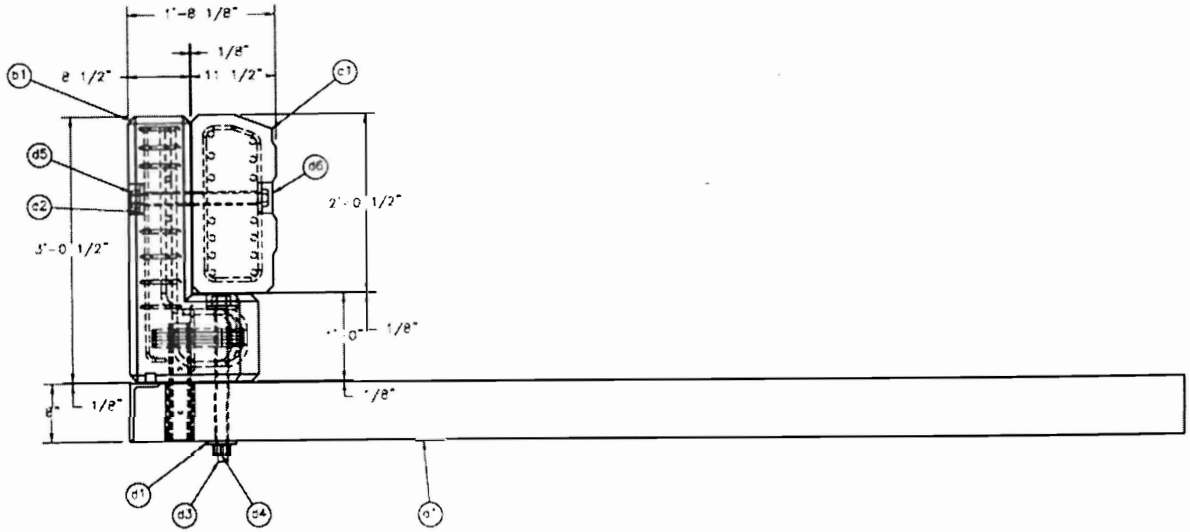

Midwest Roadside Safety Facility

MwRSF Precast Rail – Concept 1

Precast Bridge Rail Assembly Side View

Figure 8. Concept A (L-Post) – Assembled Side View

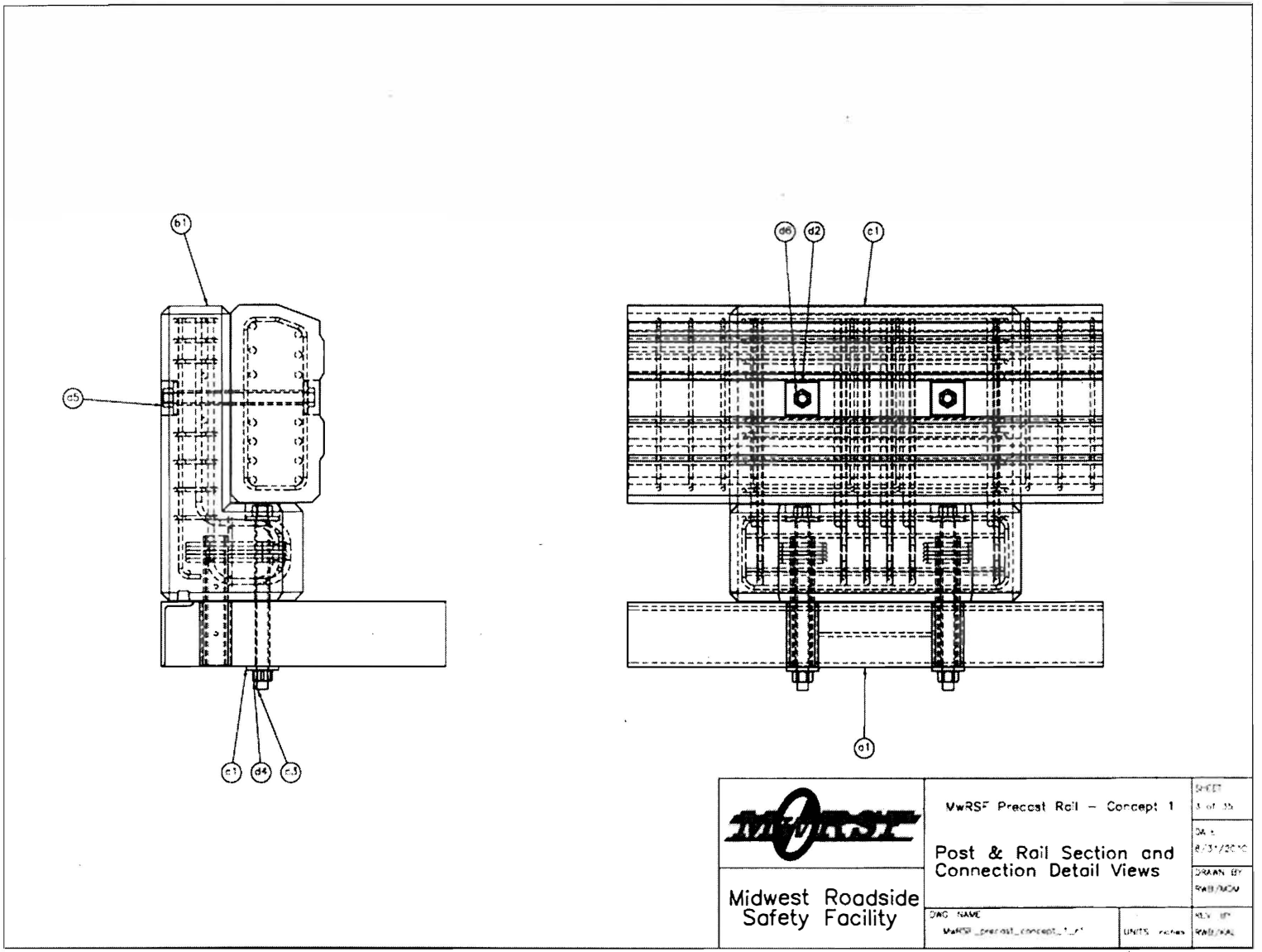

Figure 9. Concept A (L-Post) – Connection Details

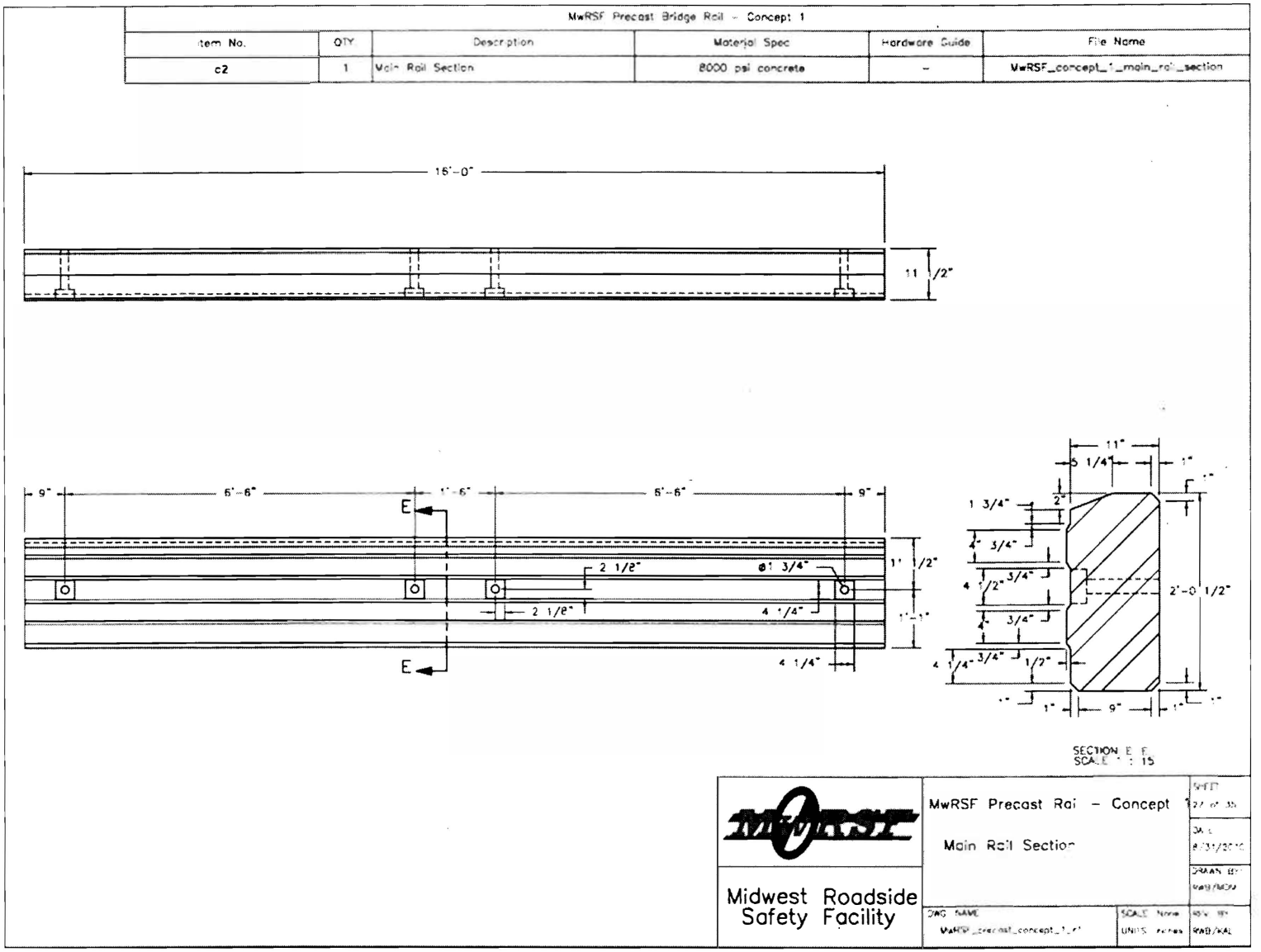

Figure 10. Concept A (L-Post) – Rail Segment Geometry

Precast Bridge Rail					
Item No.	QTY.	Description	Material Spec	Hardware Guide	File Name
c2	1	Main Rail Section	8000 psi concrete	–	MwRSF_concept_1_main_rail_section
c3	43	Rail No. 4 Stirrup	A615 Grade 60	–	MwRSF_concept_1_rail_stirrup_no4_a615gr60
c4	14	Rail No. 7 Longitudinal Rebar	A615 Grade 60	–	MwRSF_concept_1_rail_longbar_no7_a615gr60

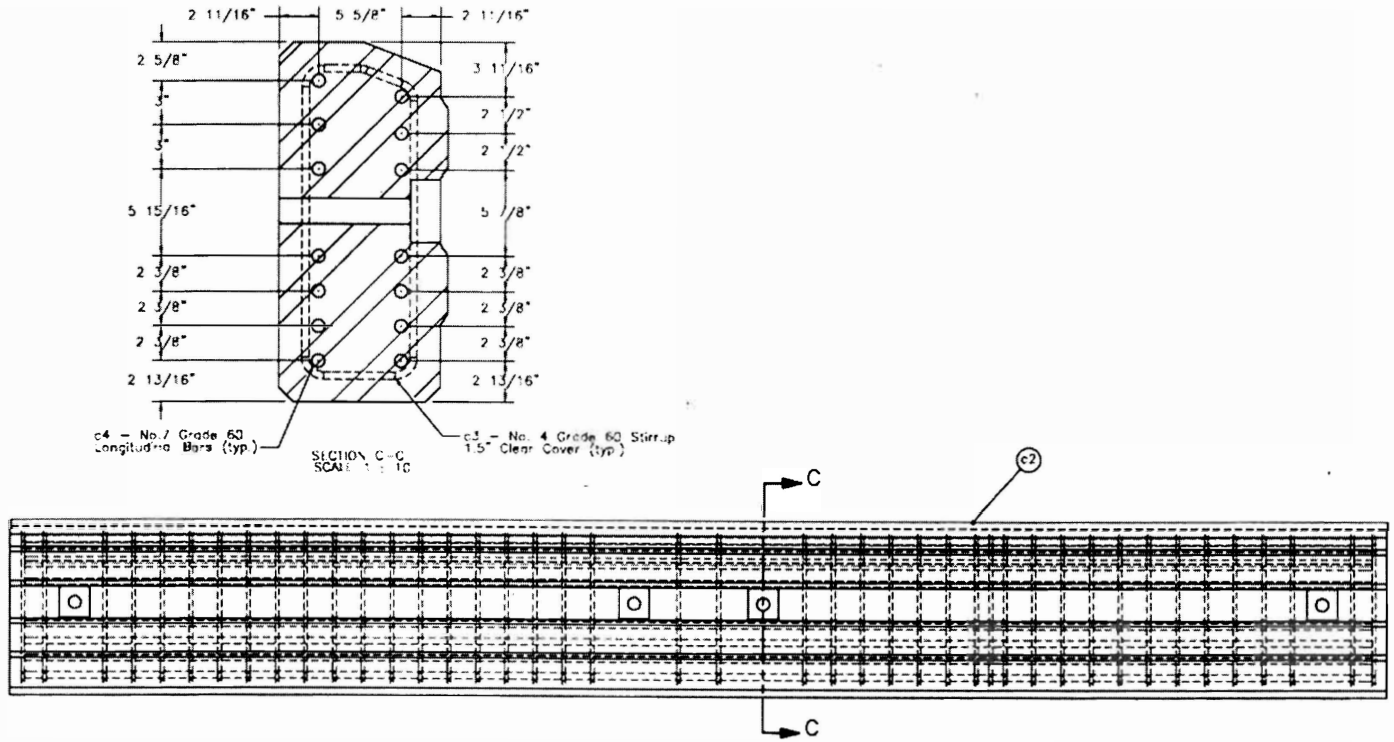

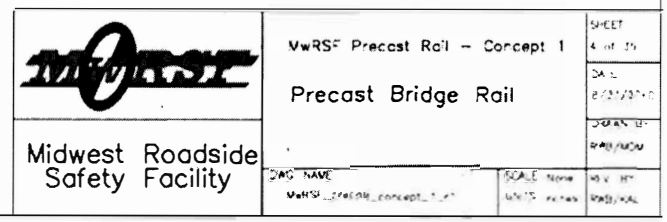

Figure 11. Concept A (L-Post) – Rail Segment Reinforcement

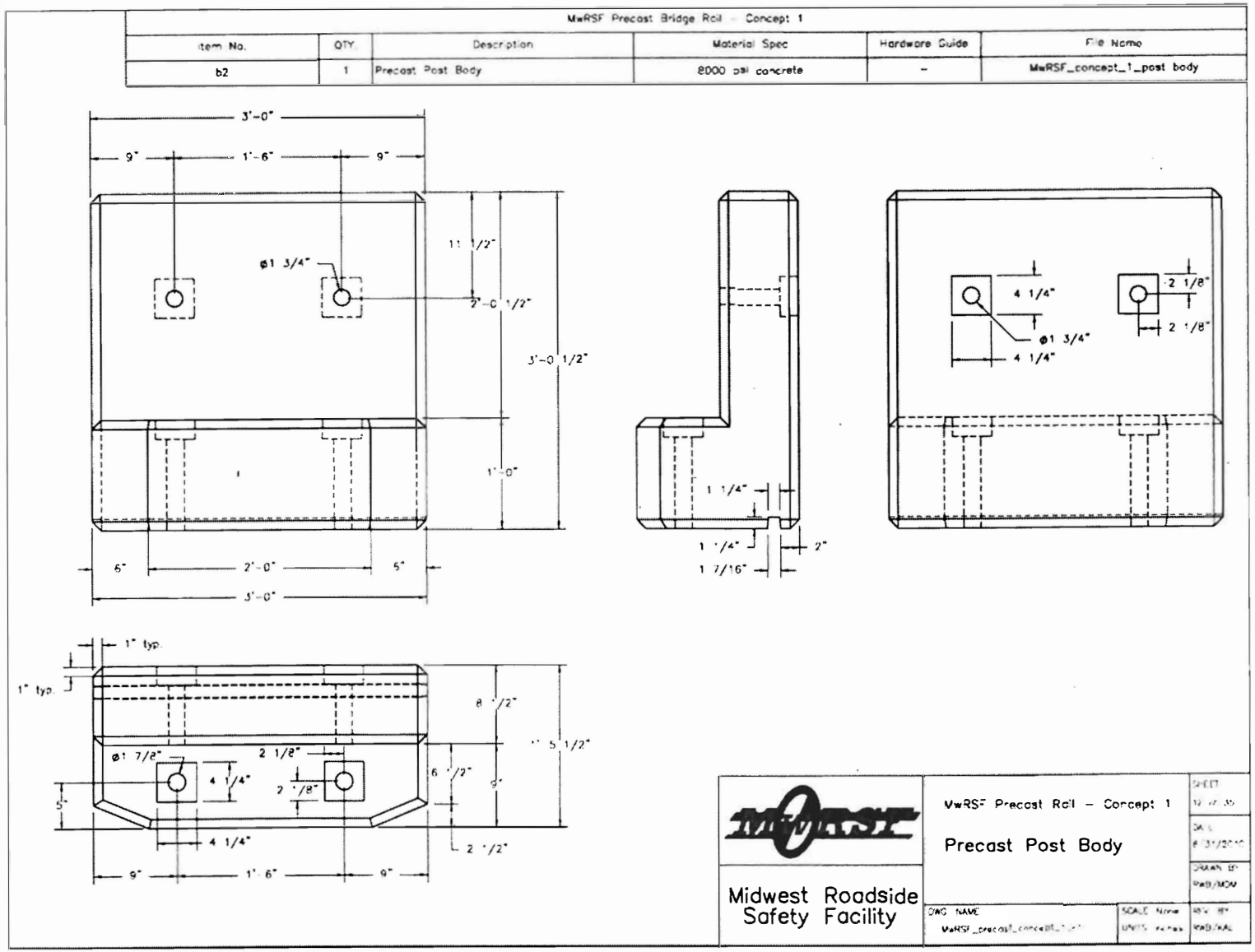

Figure 12. Concept A (L-Post) – Post Geometry

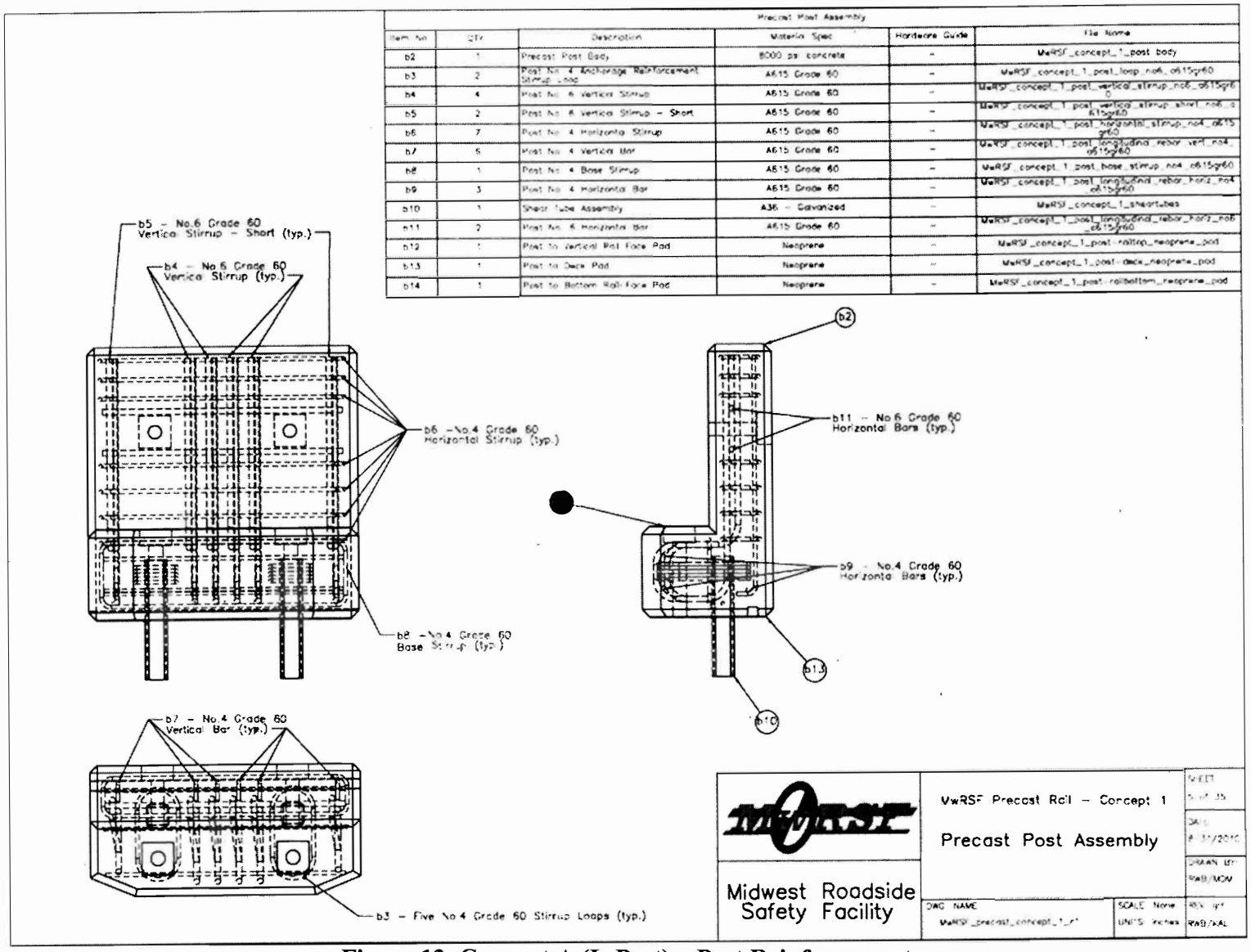

Precast Post Assembly

Item No	Qty	Description	Material Spec	Hardware Guide	File Name
b2	1	Precast Post Body	8000 psi concrete	–	MwRSF_concept_1_post body
b3	2	Post No. 4 Anchorage Reinforcement Stirrup Loop	A615 Grade 60	–	MwRSF_concept_1_post_loop_no4_a615gr60
b4	4	Post No. 6 Vertical Stirrup	A615 Grade 60	–	MwRSF_concept_1_post_vertical_stirrup_no6_a615gr60
b5	2	Post No. 6 Vertical Stirrup – Short	A615 Grade 60	–	MwRSF_concept_1_post_vertical_stirrup_short_no6_a615gr60
b6	7	Post No. 4 Horizontal Stirrup	A615 Grade 60	–	MwRSF_concept_1_post_horizontal_stirrup_no4_a615gr60
b7	6	Post No. 4 Vertical Bar	A615 Grade 60	–	MwRSF_concept_1_post_longitudinal_rebar_vert_no4_a615gr60
b8	1	Post No. 4 Base Stirrup	A615 Grade 60	–	MwRSF_concept_1_post_base_stirrup_no4_a615gr60
b9	3	Post No. 4 Horizontal Bar	A615 Grade 60	–	MwRSF_concept_1_post_longitudinal_rebar_horiz_no4_a615gr60
b10	1	Shear Tube Assembly	A36 – Galvanized	–	MwRSF_concept_1_sheartubes
b11	2	Post No. 6 Horizontal Bar	A615 Grade 60	–	MwRSF_concept_1_post_longitudinal_rebar_horiz_no6_a615gr60
b12	1	Post to Vertical Rail Face Pad	Neoprene	–	MwRSF_concept_1_post-railtop_neoprene_pad
b13	1	Post to Deck Pad	Neoprene	–	MwRSF_concept_1_post-deck_neoprene_pad
b14	1	Post to Bottom Rail Face Pad	Neoprene	–	MwRSF_concept_1_post-railbottom_neoprene_pad

Figure 13. Concept A (L-Post) – Post Reinforcement

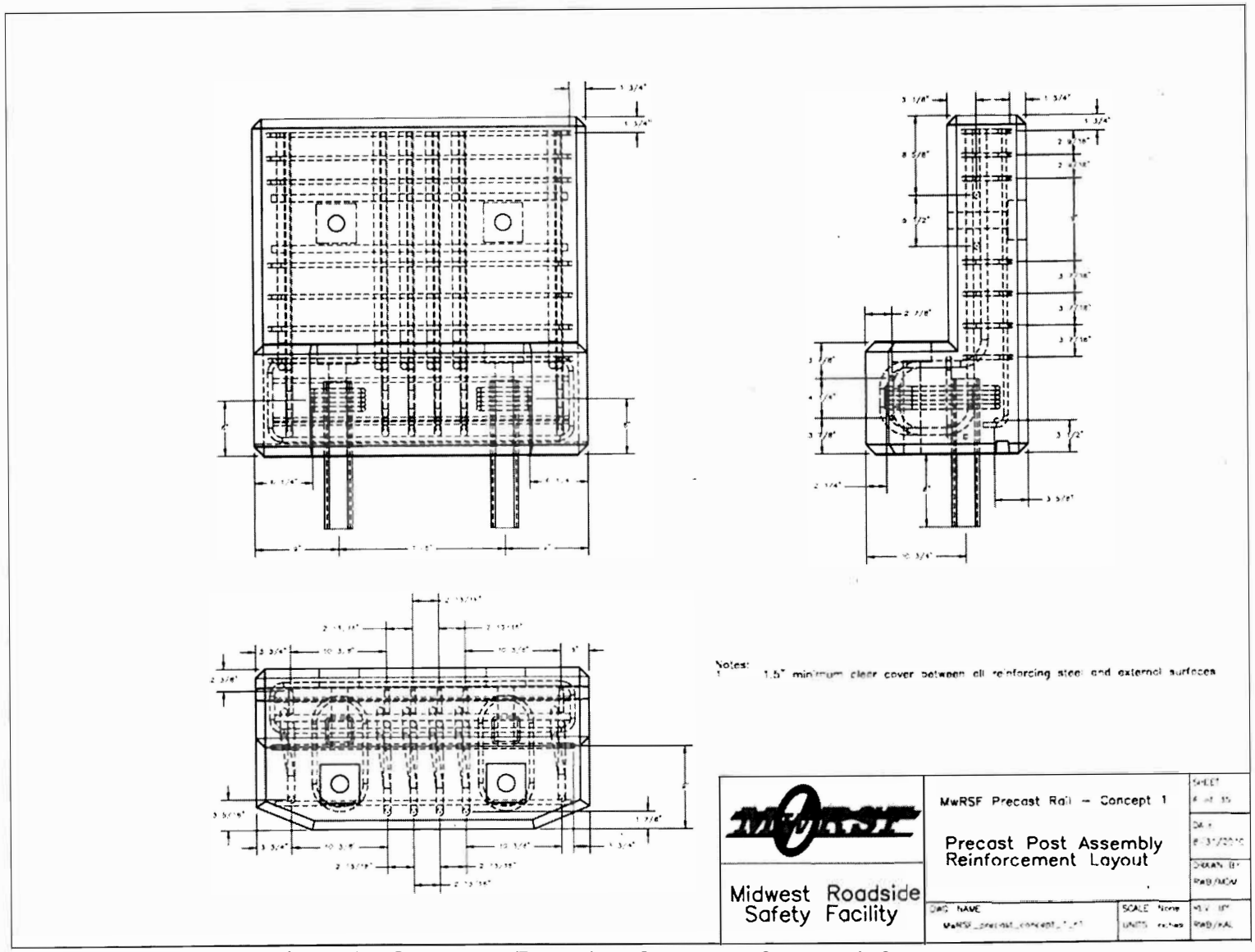

Figure 14. Concept A (L-Post) – Placement of Post Reinforcement

Precast Deck Panel					
Item No.	QTY.	Description	Material Spec	Hardware Guide	File Name
a2	1	Precast Deck Panel Body	8000 psi concrete	–	MwRSF_concept_1_precast deck
a3	1	Shear Sleeve Assembly	A36 – Galvanized	–	MwRSF_concept_1_shearsleeves
a4	1	Bearing Plate Angle L8x4x0.5x96	A36 – Galvanized	–	MwRSF_concept_1_Bearing Plate _Angle L8x4x0.5x96_A36

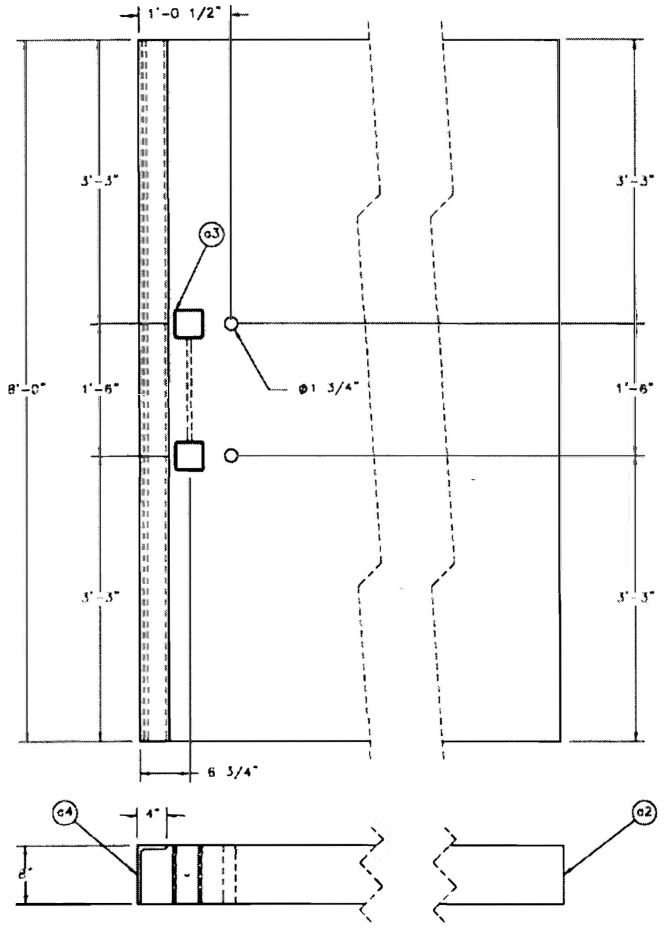

Note:
1 Deck details shown only pertain to the attachment of the precast bridge rail.
2 Complete deck dimensions and reinforcement details will be provided separately

Midwest Roadside Safety Facility

MwRSF Precast Rail – Concept 1

Precast Deck Panel Schematic

SHEET

DATE

DRAWN BY RWB/MCW

DWG NAME MwRSF_precast_concept_1.dwg

SCALE None

UNITS Inches

REV BY RWB/KAL

Figure 15. Concept A (L-Post) –Deck Panel Attachment Details

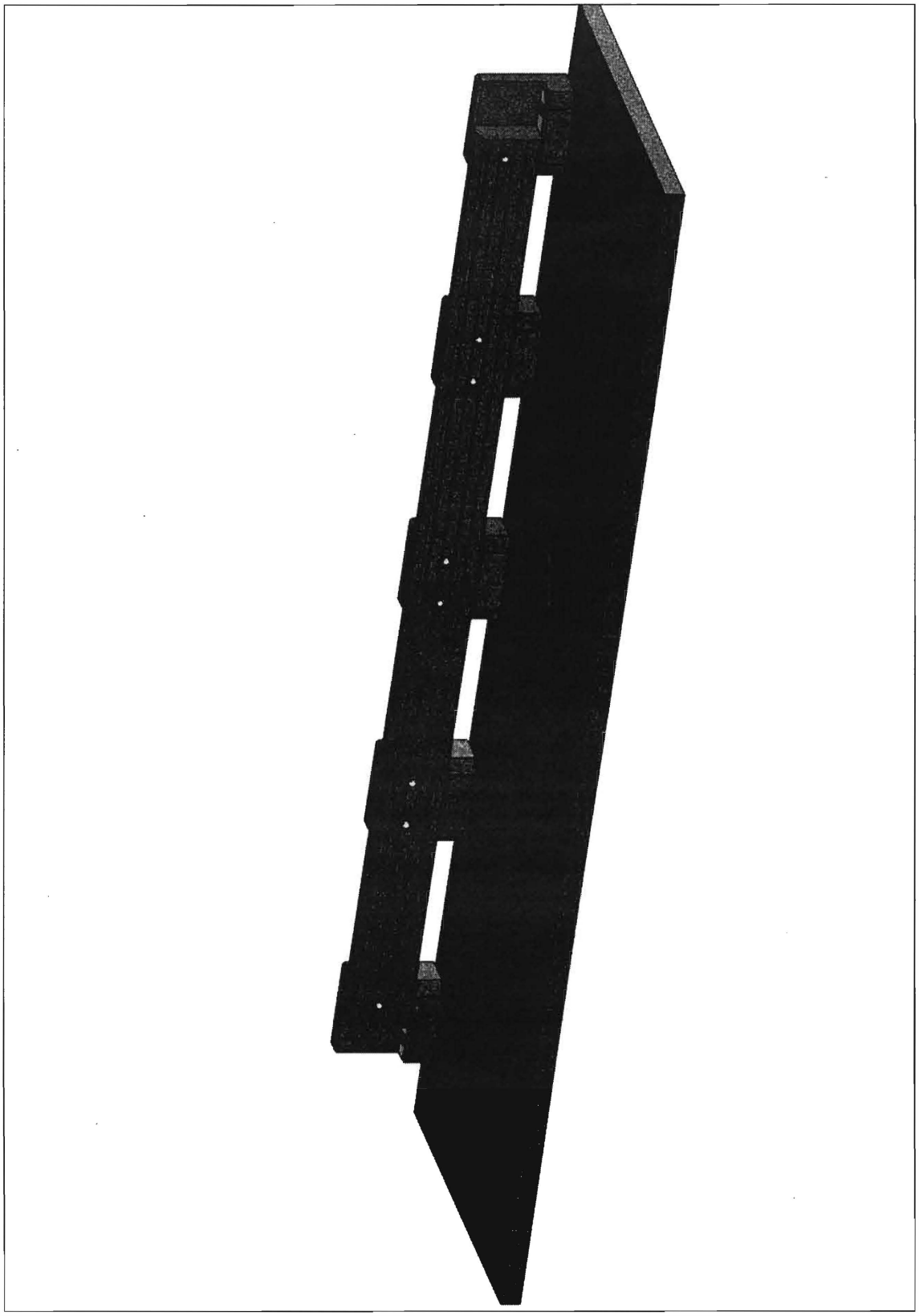

Figure 16. Concept A (L-Post) – Isotropic View

4.2.2 Concept B (Post-Off-Deck)

In an effort to improve Concept A (L-Post), the posts were altered to wrap around the edge of the bridge deck, as shown in Figures 17 through 19. As a result, the rail was shifted outward and now occupied only the outer 15 in. (381 mm) of the deck, thus satisfying the rail width requirement. The attachment hardware was similar to that used for Concept A (L-Post), which consisted of two bolts in the rail-to-post connection and three bolts in the post-to-deck connection. The bridge deck retained the steel angle on its outer edge to mitigate deck damage.

Although Concept B (Post-Off-Deck) satisfied the width criteria established in Section 3.1.1, it did not help reduce the load imparted to the bridge deck. The rail remained non-continuous and essentially simply supported, resulting in localized load transfer to the deck. The lack of load distribution again causes high shear and bending loads which can lead to structural damage to the bridge deck.

It should be noted that the design of Concept B was not completed, thus details regarding anchorage hardware as well as rebar sizes and quantities are not available.

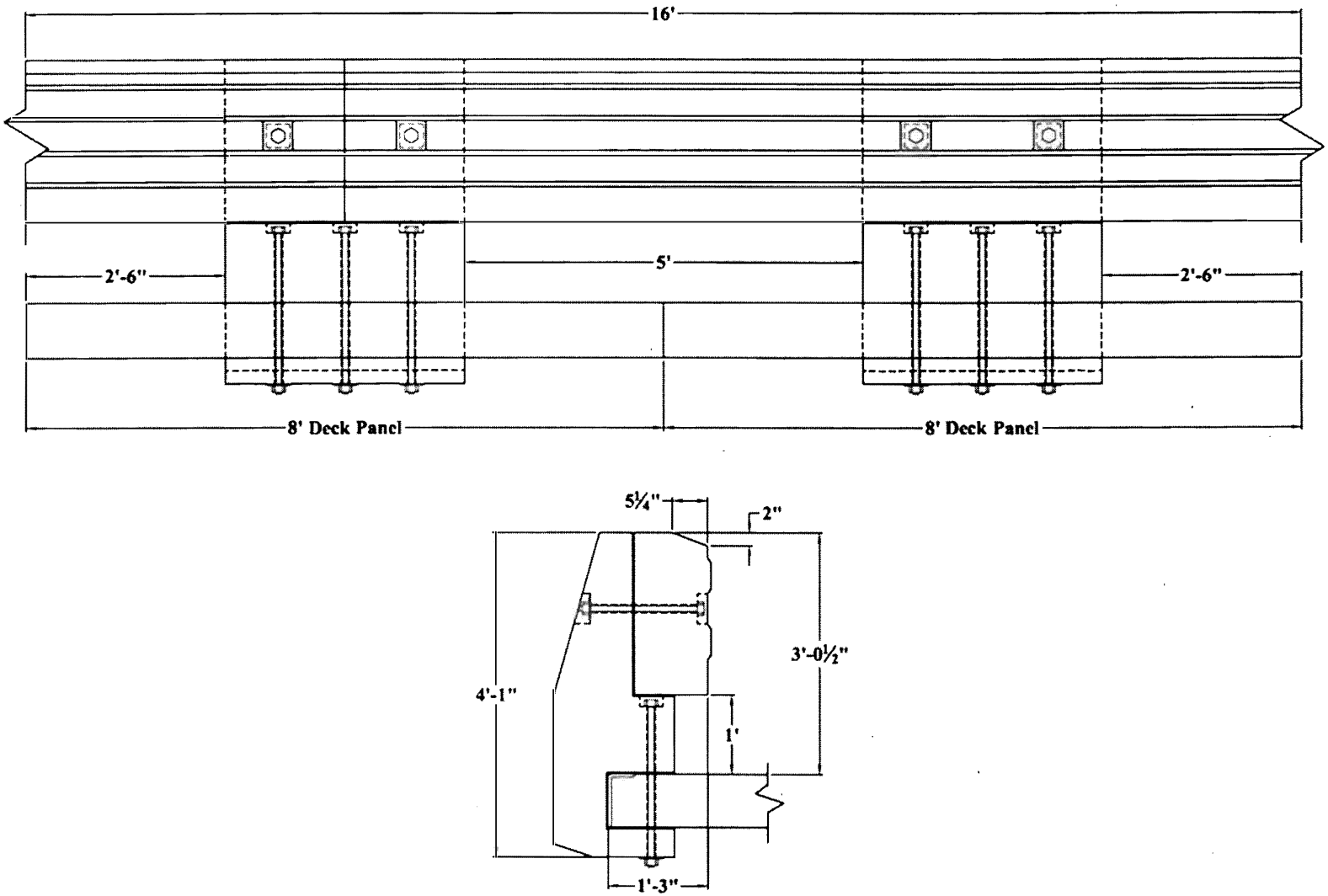

Figure 17. Concept B (Post-Off-Deck) - Assembled Overview

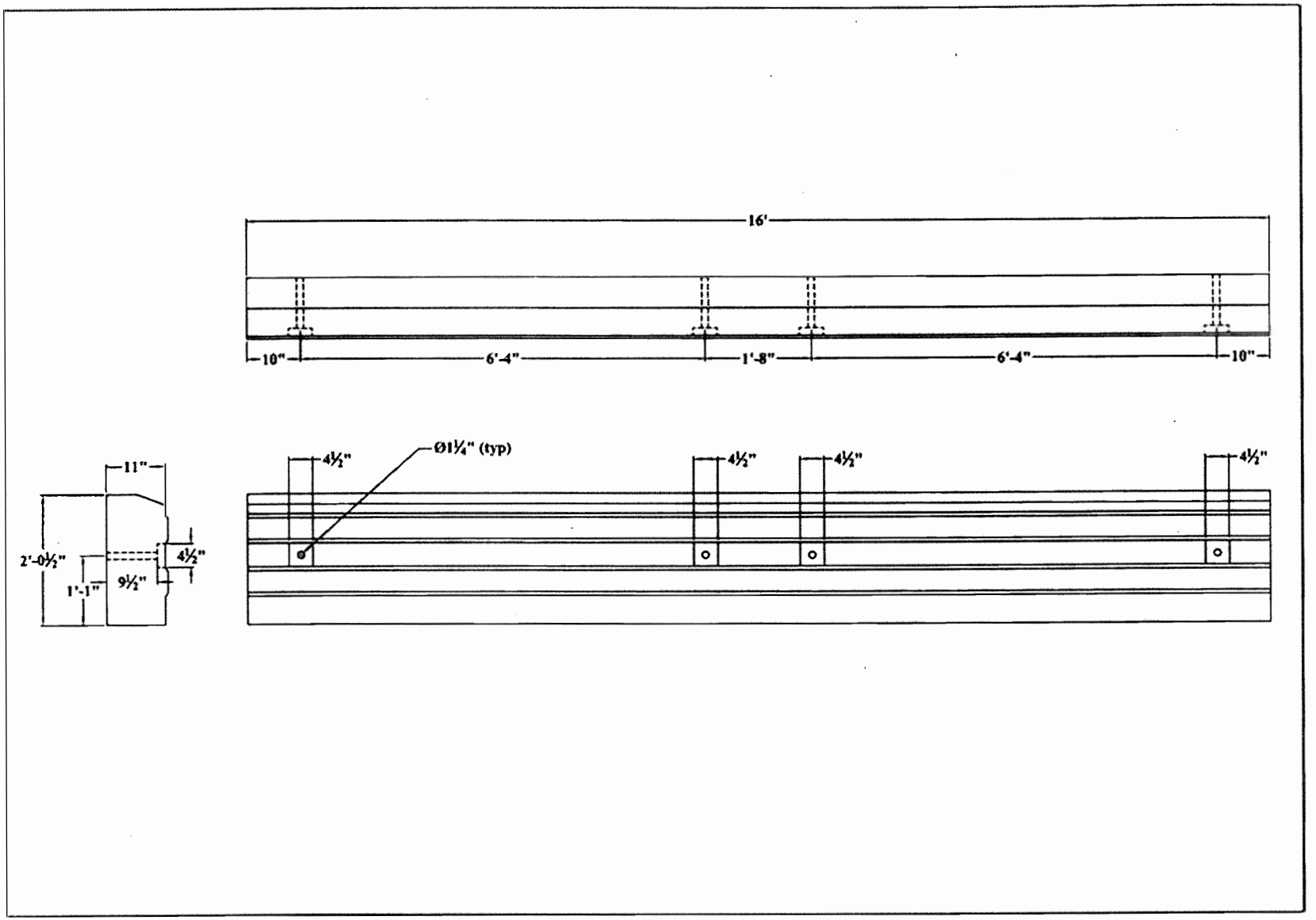

Figure 18. Concept B (Post-Off-Deck) – Rail Dimensions

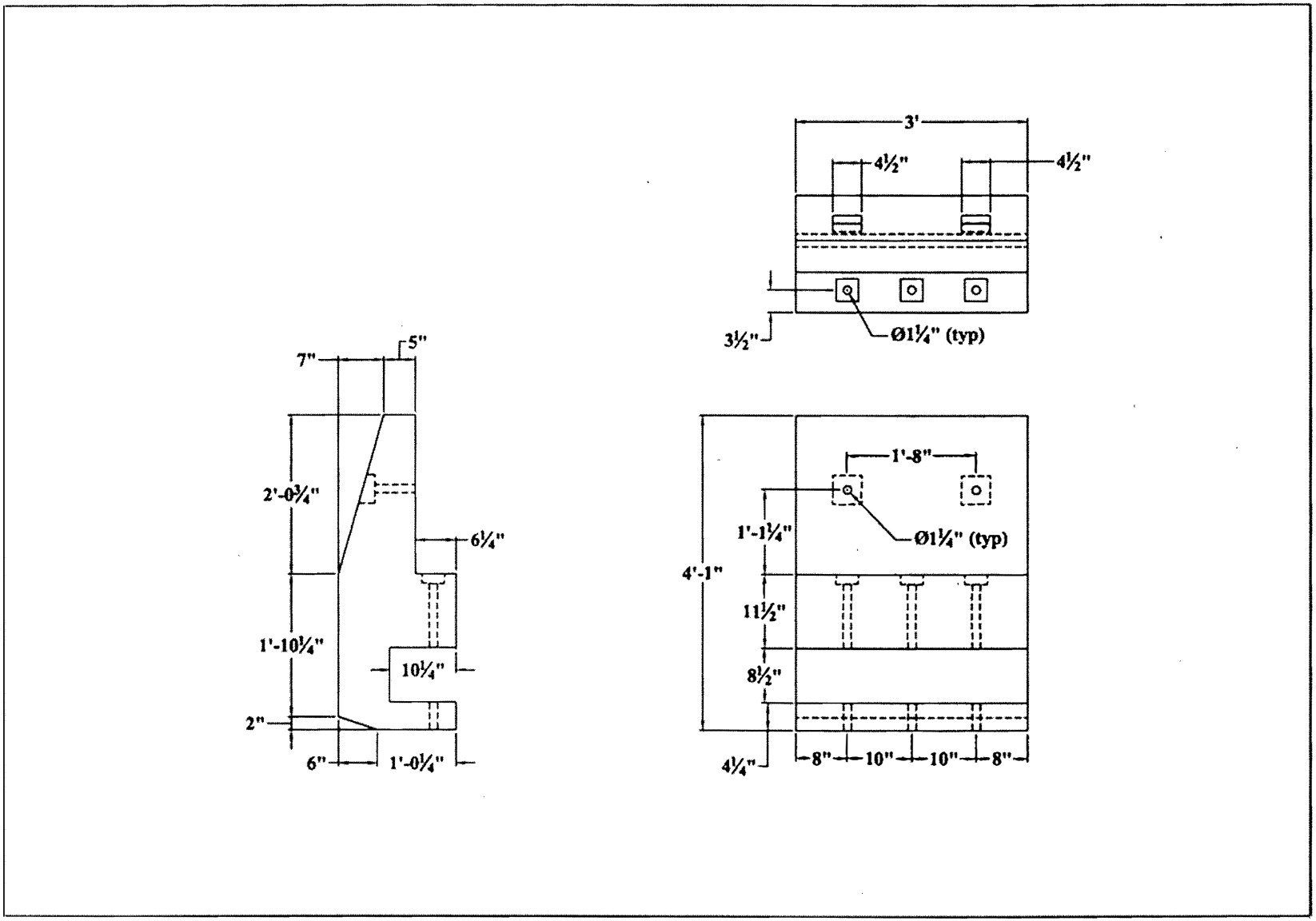

Figure 19. Concept B (Post-Off-Deck) – Post Dimensions

4.2.3 Concept C (Rail Cap)

Concept C (Rail Cap) was configured as another variation of Concept A (L-Post), which was modified to allow for the rail to be supported on top of the posts. As shown in Figures 20 through 22, the rail was designed with bottom cavities for which the posts would be inserted, similar to an extended cap. With the posts inserted 16 in. (406 mm) into the rail, no additional connection hardware was needed between the posts and rail sections. The weight of the 16-ft (4.9-m) concrete rail segments was deemed adequate to hold it in position.

The rail cross section was widened to 21 in. (533 mm) in order to ensure that adequate shear strength could be provided around the bottom cavities, as shown in Figure 21. Since the rail element was configured to cap the posts, the outer portion of the rail extended beyond the edge of the bridge deck. Although the rail section was wider than the 15-in. (381-mm) maximum width requirement, the bridge railing system occupied only 15 in. (381 mm) of deck space. Also, the increased rail width (i.e., beam depth) could likely result in reduced steel reinforcement.

As noted above, the rail was designed to cap the post instead of sit on a small extension, or post seat. Thus, the overall post width was reduced, as shown in Figure 22. Also, the post's geometry was simplified to utilize a trapezoidal shape. However, the size of the connection bolts would need to be increased due to the reduced moment arm.

As with the first two concepts, Concept C (Rail Cap) lacked continuity in the rail, thus resulting in concerns for high, localized deck loads and probable deck damage. All three of the discontinuous bridge rail concepts were deemed easy to fabricate, install, and replace. However, the simplicity of these systems caused considerable concern for high impact loading to result in structural deck damage.

It should be noted that the design of Concept C was not completed, thus details regarding anchorage hardware as well as rebar sizes and quantities are not available.

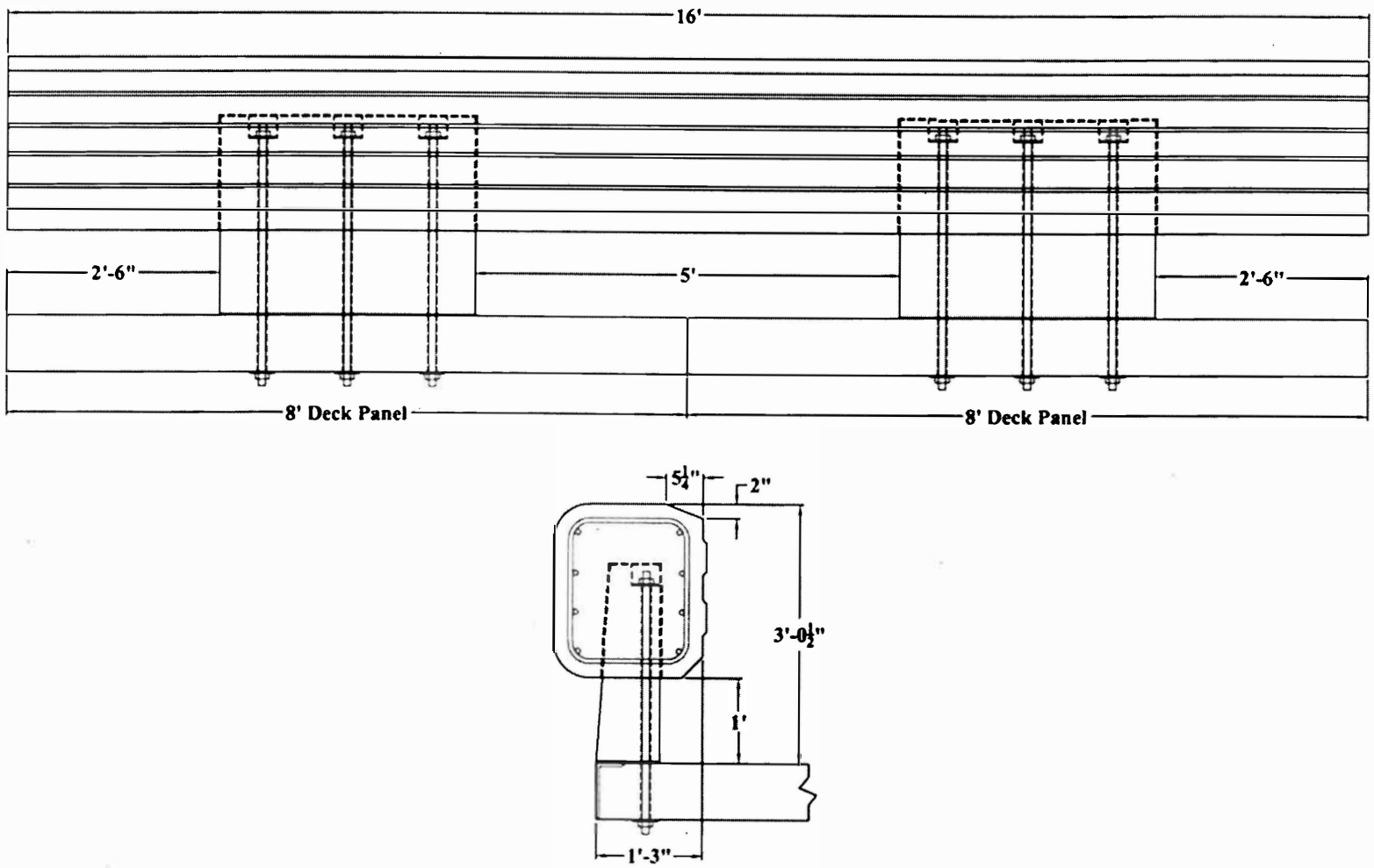

Figure 20. Concept C (Rail Cap) - Assembled Overview

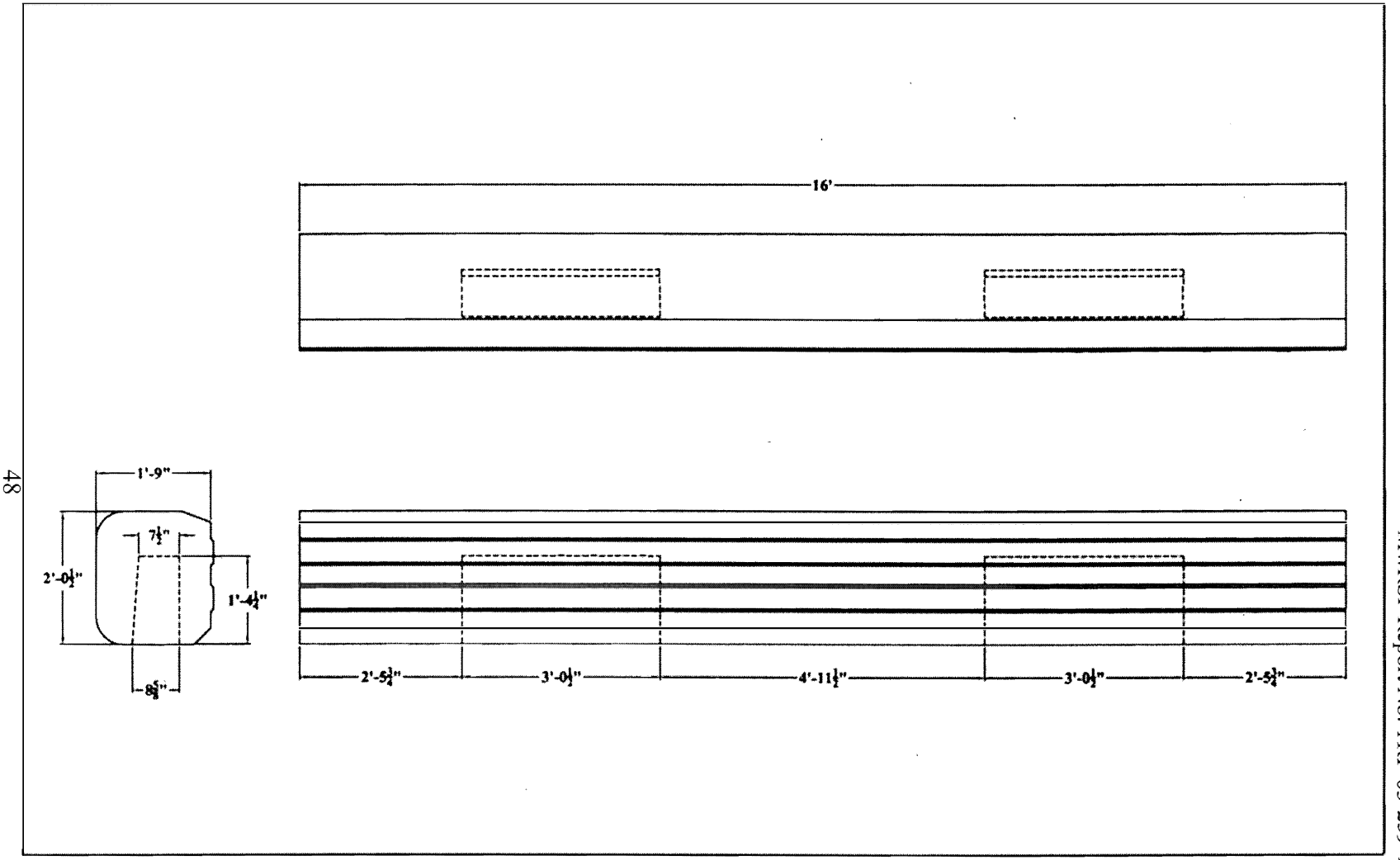

Figure 21. Concept C (Rail Cap) – Rail Dimensions

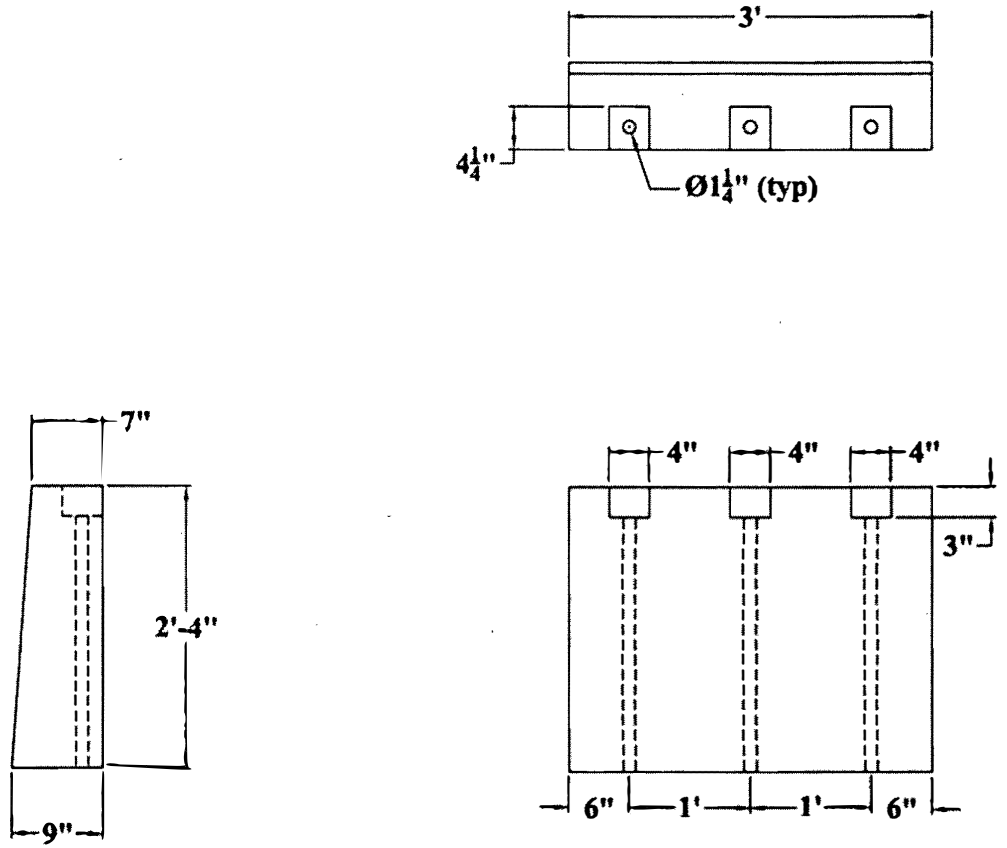

Figure 22. Concept C (Rail Cap) – Post Dimensions

4.3 Rail Concepts - Moderate Continuity

4.3.1 Concept D (Staggered Rail)

Concept D (Staggered Rail) was configured for the precast concrete bridge rail system in order to provide increased continuity and improved load distribution. This concept used two individual rails that were stacked on top one another instead of using a single rail. The two rails were staggered longitudinal such that the end of the upper rail lined up with the middle of the lower rail, as shown in Figures 23 and 24. Thus, the impact load would always be distributed to adjacent posts by at least one of the two rail segments.

The rail geometry was configured to be symmetric as well as to satisfy the head ejection envelope criteria. For this concept, the rails were stacked on top of the short posts, thus resulting in a system width below the 15-in. (381-mm) limit noted in Section 3.1.1. Although not shown in Figures 23 and 24, the connection hardware consisted of both bolts and a shear key. The vertical bolts penetrated through the top of the rails, posts, and deck and provided the post's lateral shear and moment capacities. Steel tubes were placed between the post-to-rail and rail-to-rail surfaces to act as shear keys and prevent any lateral movement between rail sections.

Although Concept D (Staggered Rail) distributed the impact forces outward another span or two beyond the prior concepts, the potential for deck damage remained. The shear and bending loads imparted to the deck still posed moderate risk of structural damage to standard bridge decks. Therefore, Concept D (Staggered Rail) was abandoned in favor of developing a more continuous bridge railing system.

It should be noted that the design of Concept D was not completed, thus details regarding anchorage hardware as well as rebar sizes and quantities are not available.

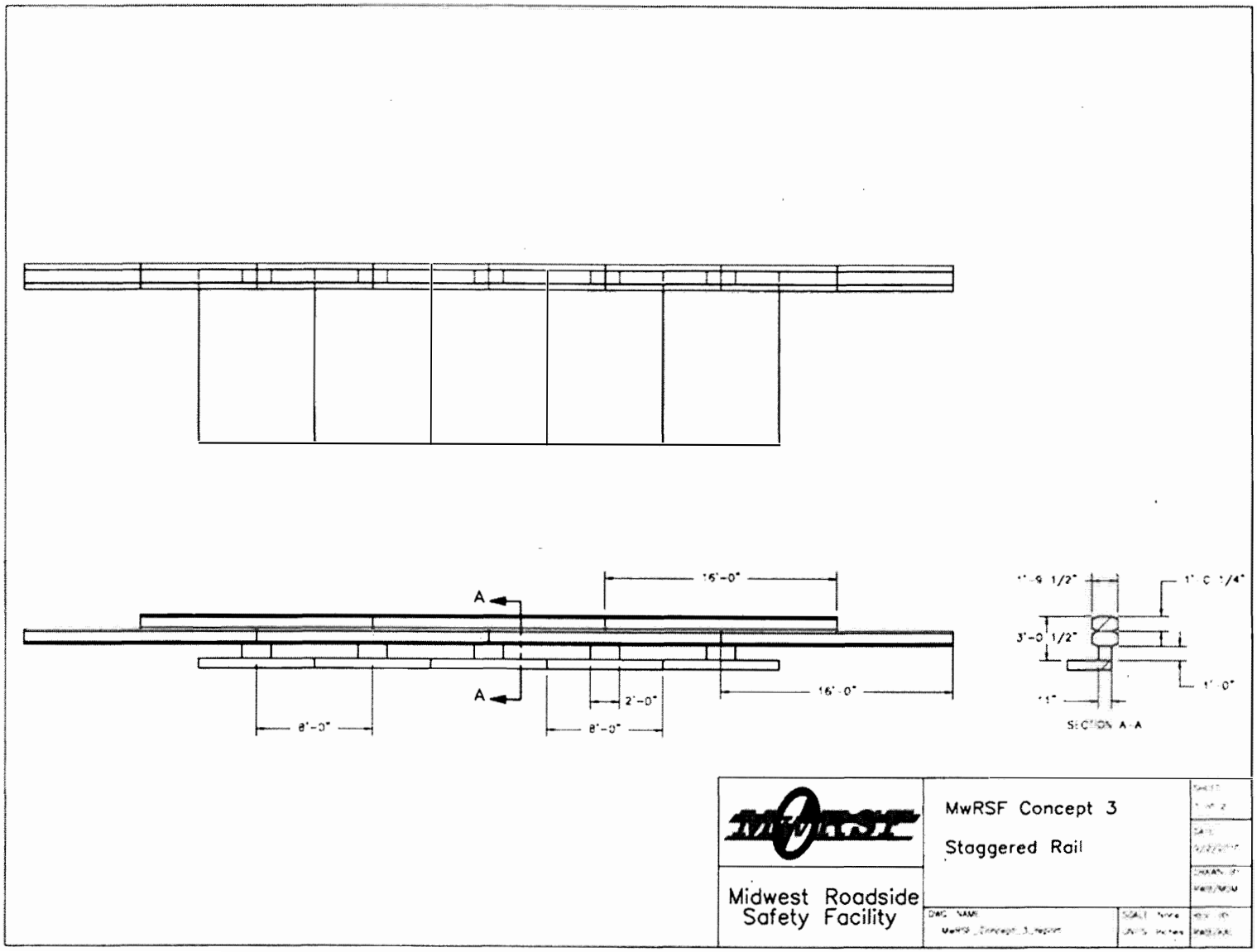

Figure 23. Concept D (Staggered Rail) - Geometry

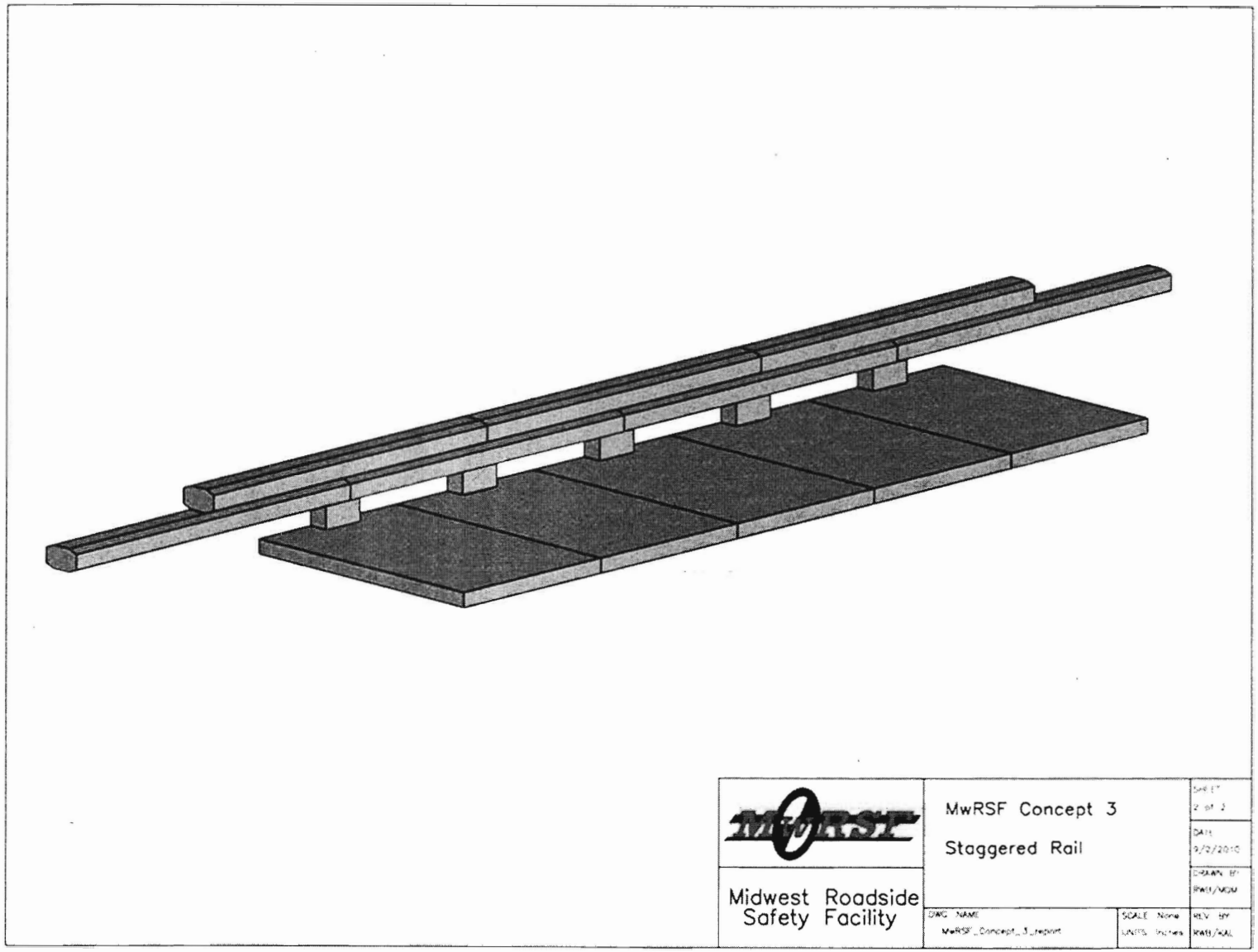

Figure 24. Concept D (Staggered Rail) – Isotropic View

4.4 Rail Concepts – High Continuity

4.4.1 Concept E (Ladder)

During the development of Concepts A through D, the research team had concerns as to whether cost-effective bridge railing systems with limited continuity could reasonably withstand TL-4 impact loading without incurring significant damage to the bridge deck. As previously noted, the prior concepts were associated with greater risk of structural deck damage due to high shear and bending loads concentrated at the post locations nearest to impact. Therefore, it was deemed necessary to utilize a continuous railing system that would provide shear and moment transfer between adjacent rail segments and better distribute the impact load along the length of the bridge.

Concept E (Ladder) was similar to prior concepts as it was comprised of separate post and rail segments. However, Concept E was also much different as each rail utilized two rails separated by diaphragms, thus creating many void spaces between rails, as shown in Figures 25 through 30. For this concept, steel connection hardware was placed between adjacent rail segments on the inside of the rails, effectively shielding the joint hardware from view on either side. Thus, a rigid rail-to-rail joint was created without sacrificing aesthetics. Since the middle region of the rail had many void regions, the railing system was lighter per unit length than a solid rail. In addition, the rail segments were extended to a length of 24 ft (7.3 m) to reduce the number of rail segments necessary to span a bridge.

As noted above, multiple diaphragms or spacers were used to connect the two rail segments throughout the length of the segment at a consistent offset, as shown in Figure 28. These spacers served multiple purposes. First, the spacers functioned similar to the web of an I-shape beam by shear transfer across the beam depth, thus allowing the built-up section to provide

increased bending strength and act as a single structural element. The diaphragms were also intermittently spaced to allow for drainage of water as well as aid in controlling weight and material costs. The spacers were strategically positioned to allow for the posts to be easily attached to the rail segments, as shown in Figure 25.

For Concept E (Ladder), the posts measured 24 in. (610 mm) wide by 11 in. (279 mm) deep. Vertical bolts were placed through the posts and deck to anchor the bridge railing to the bridge deck surface. Corbels were added to the upstream and downstream sides of the posts, as shown in Figure 29, to support the rail diaphragms or spacers on both sides of the post. Since the two rails and attached diaphragms completely surrounded each post and were supported on the corbels, a rail-to-post connection may not be warranted. However, horizontal bolts would ensure that the rail does not move vertically during impact loading, as shown in Figure 27.

After the Concept E (Ladder) was configured, some concerns remained regarding the overall system width and shear strength. The back side of the rail extended off of the deck edge and still occupied 20½ in. (546 mm) of deck space, exceeding the 15-in. (381-mm) limit established in Section 3.1.1. Unfortunately, the current rail width could not easily be reduced to satisfy this limit for two reasons. First, the 11 in. (279 mm) post depth was necessary to develop the bending strength at the post-to-deck interface. Second, the depth of both rails was already narrow and further reductions would cause concern for inadequate shear strength.

In addition, the two rail sections were attached to one another with discrete spacer blocks and not a solid, continuous midsection of the rail. With this configuration, there remained concerns that inadequate shear capacity would be provided within a single, thin rail section. An impact load located between spacers would cause the front rail to carry the entire shear load until the load path reached a spacer block and was distributed to the back face. The same would be

true for impacts near, but not yet on, a post. Only with extensive steel reinforcement could a 7-in. (178-mm) deep rail resist the significant impact loading.

Concept E (Ladder) was deemed aesthetic through the use of unique geometry and rail asperities. The rail contained steel joint hardware within the middle cavity, thus creating a continuous bridge rail system without taking away from the aesthetic appeal. Unfortunately, competing demands remained due to the need to widen the individual rails to resist high shear loading in conjunction with the need to narrow overall system width to meet the 15-in. (381-mm) limit. Therefore, this concept was abandoned.

It should be noted that the design of Concept E was not completed, thus only partial details are available for the anchorage hardware as well as rebar sizes and quantities.

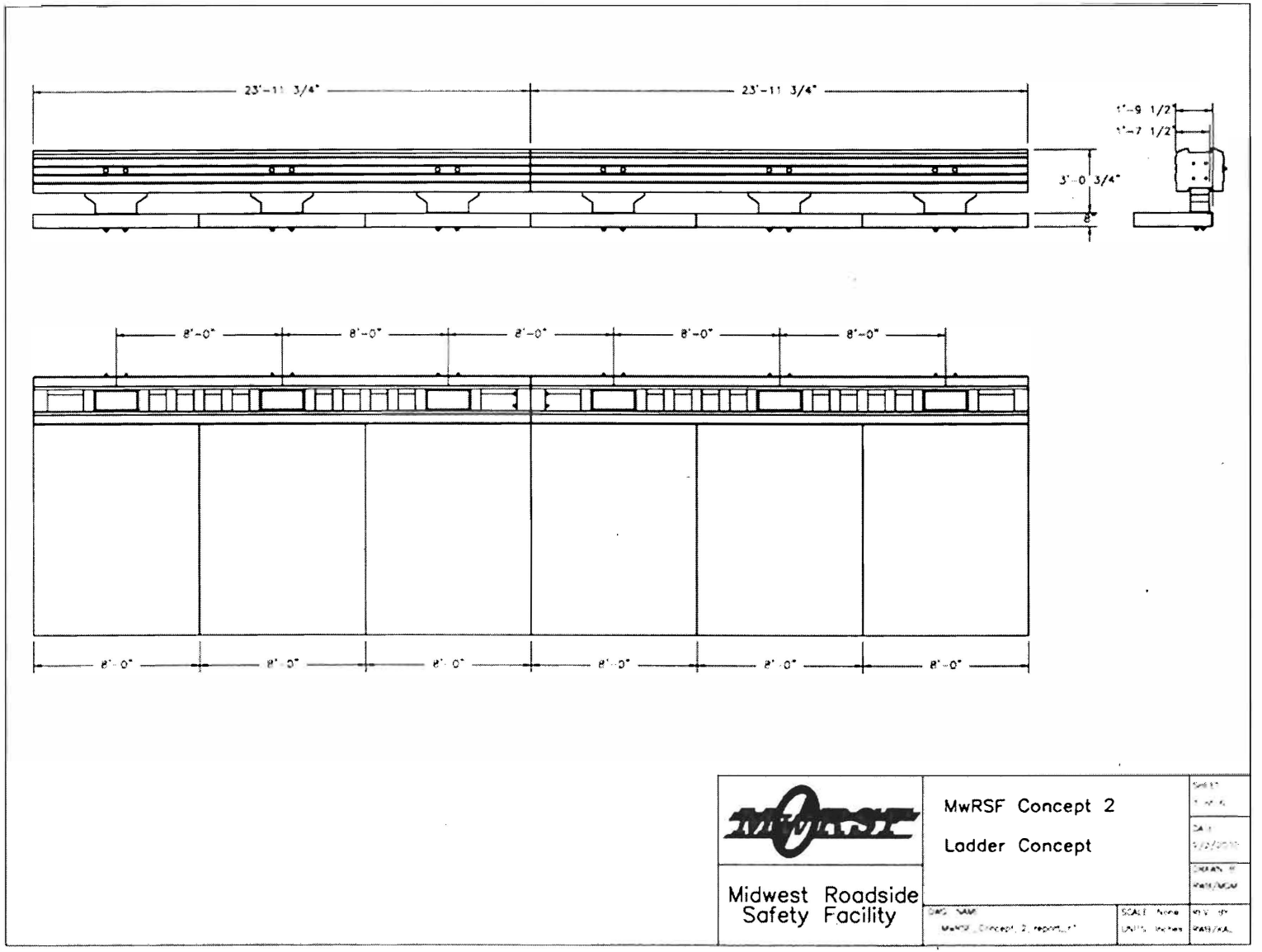

Figure 25. Concept E (Ladder) - Overview

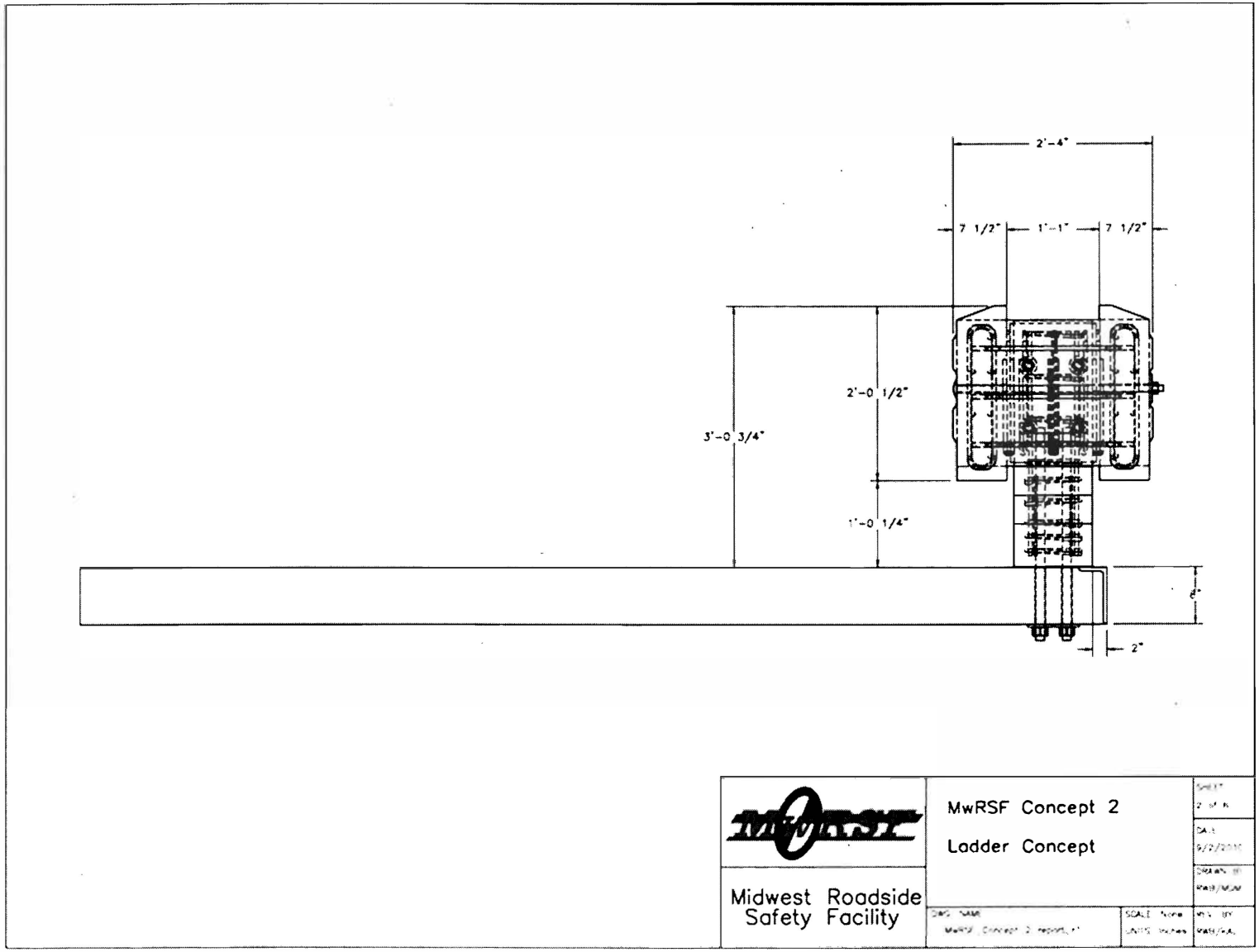

Figure 26. Concept E (Ladder) – Cross Section View

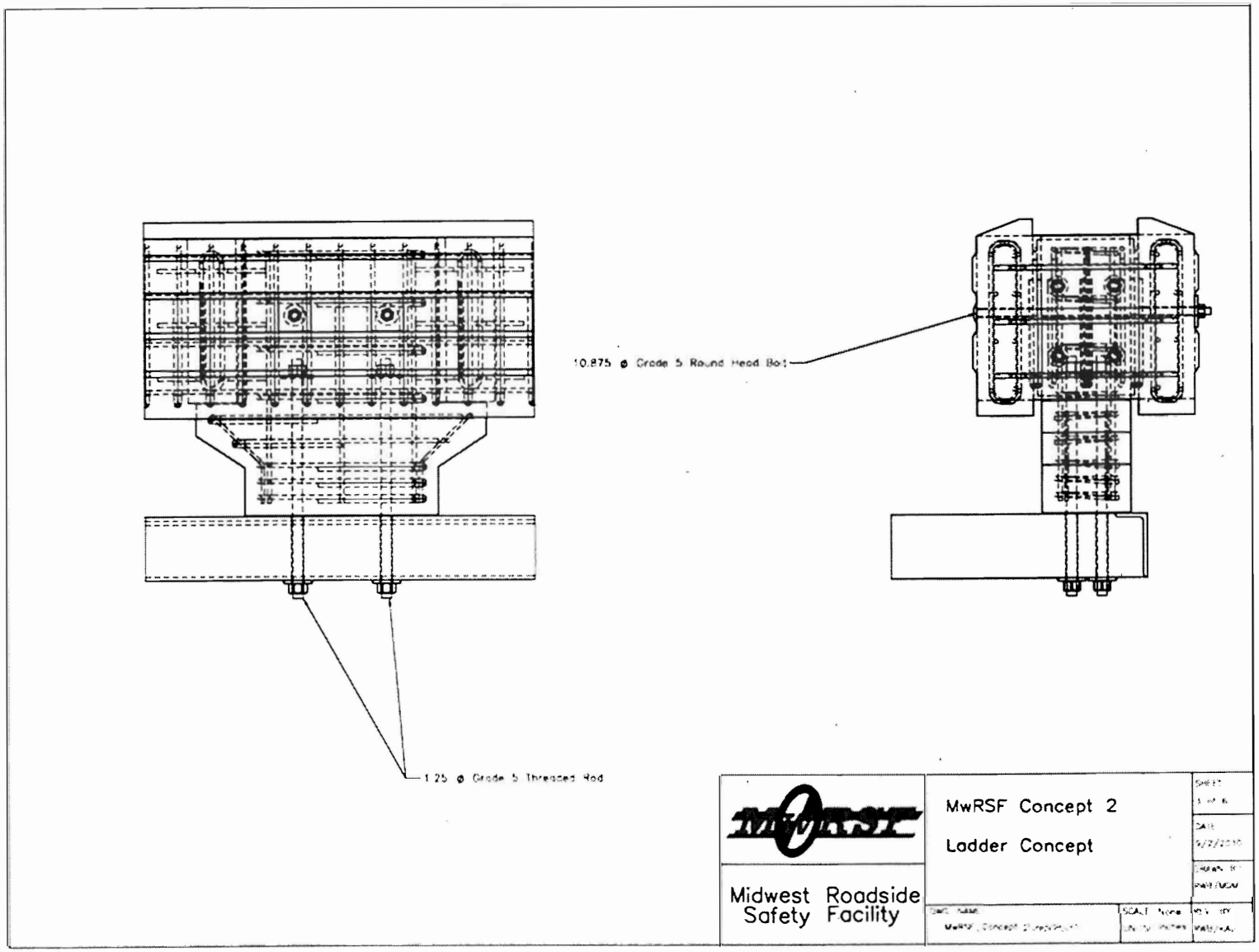

Figure 27. Concept E (Ladder) – Connection Hardware

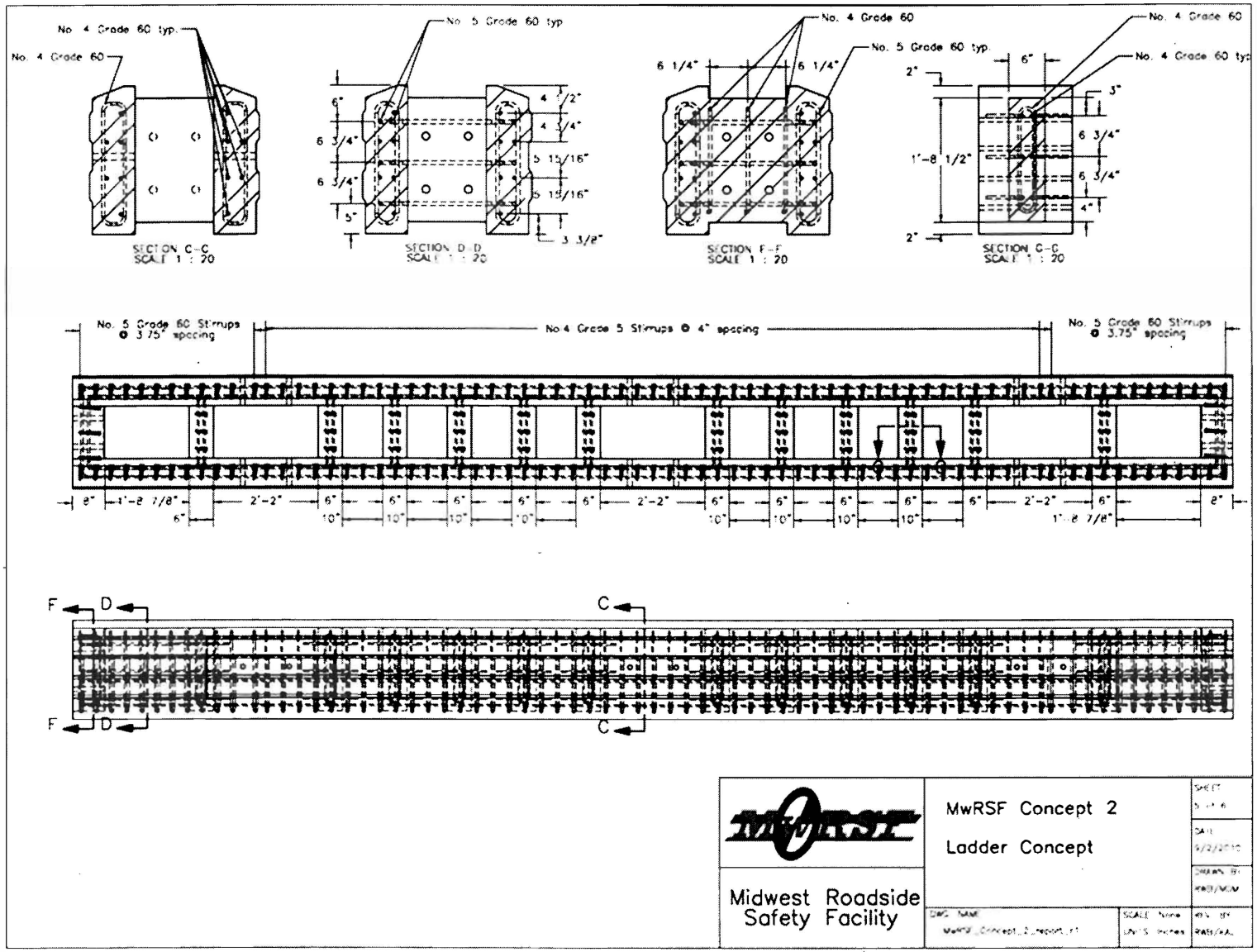

Figure 28. Concept E (Ladder) – Rail Segment

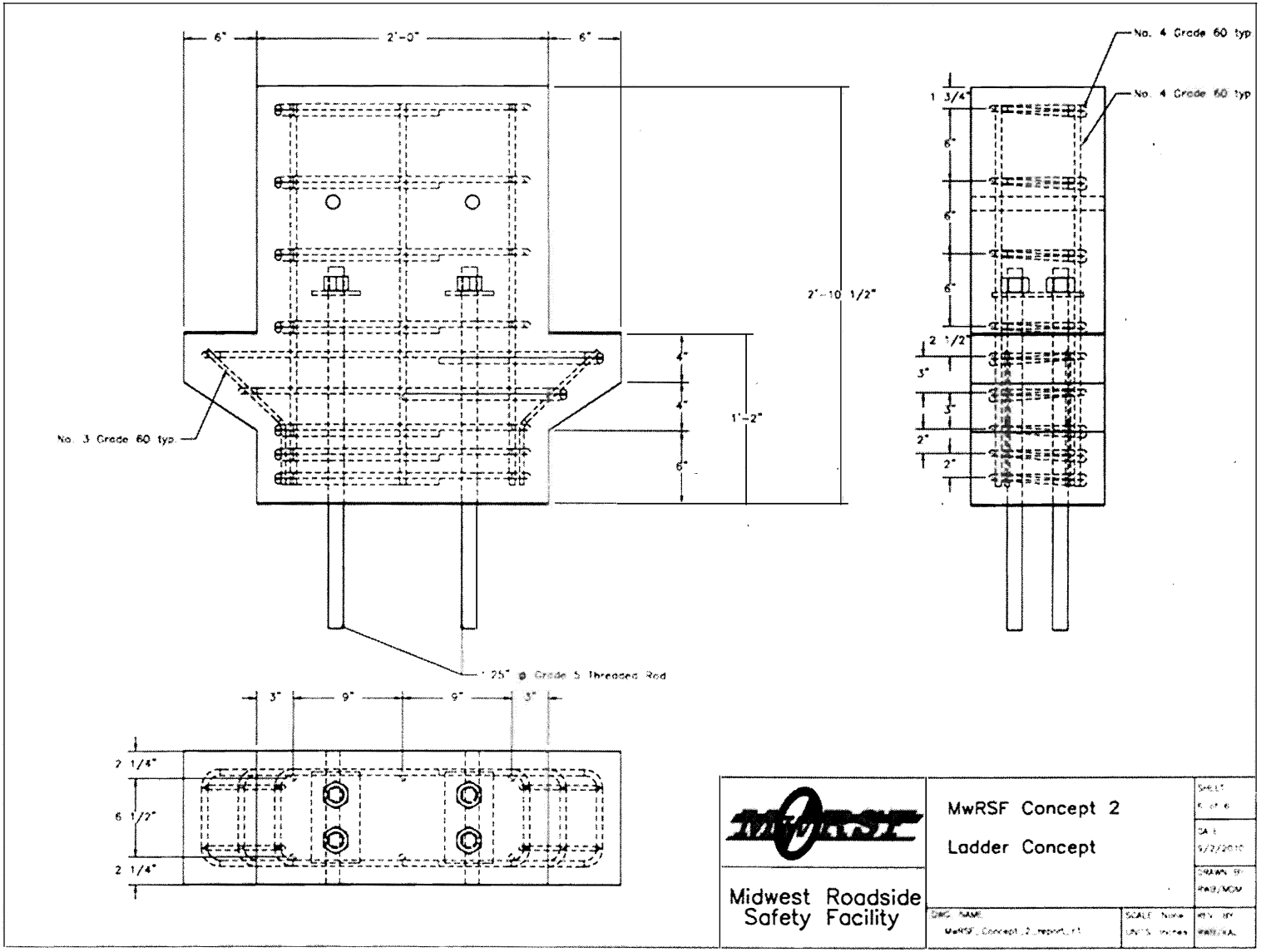

Figure 29. Concept E (Ladder) – Post Segment

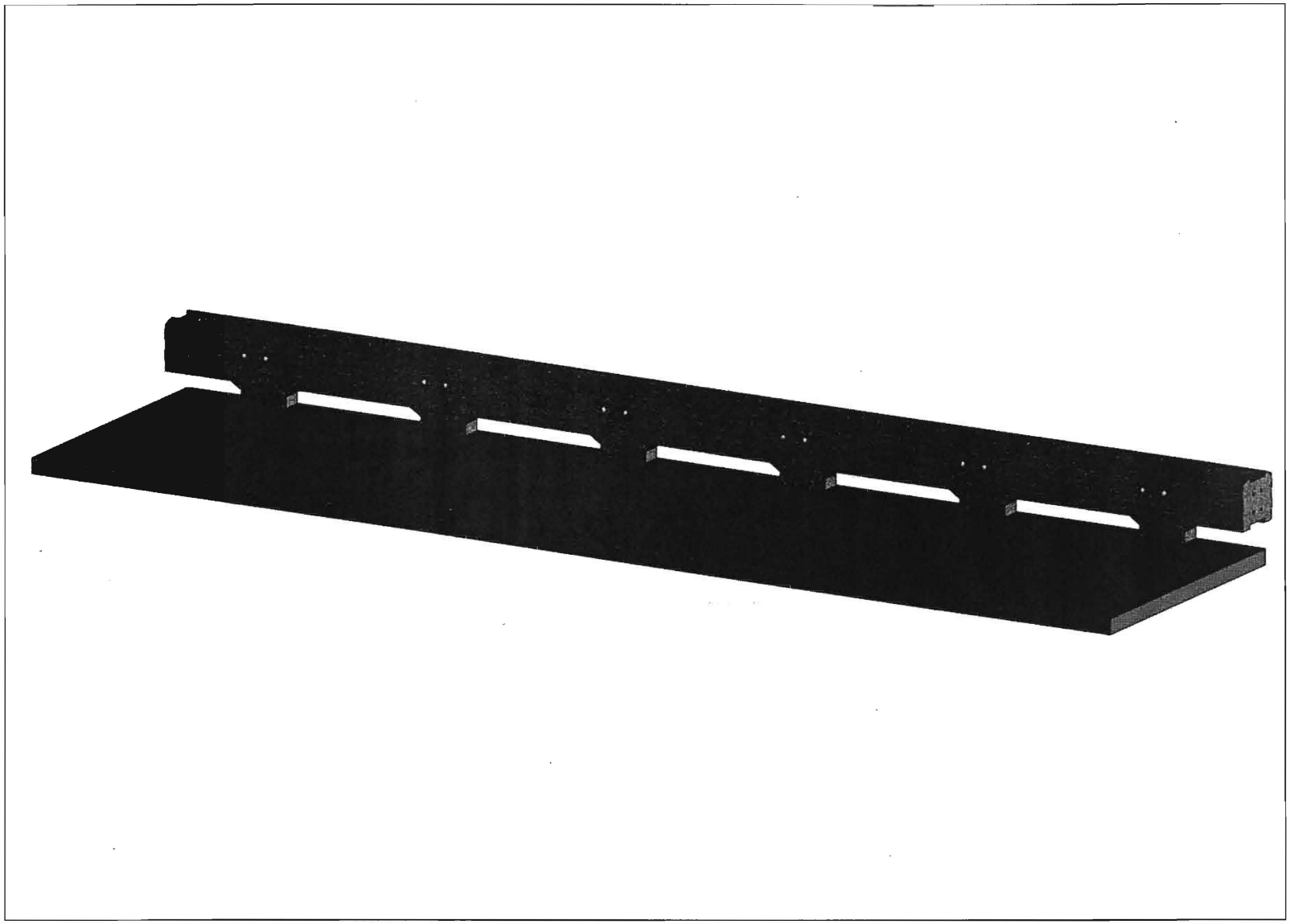

Figure 30. Concept E (Ladder) – Isotropic View

4.4.2 Concept F (Fence)

Concept F (Fence) was similar to the previous continuous rail design in that it also incorporated two longitudinal rails. However, the rails in Concept F (Fence) were placed on top of each other vertically instead of side by side horizontally, as shown in Figures 31 through 33. This orientation allowed for the width of each rail to extend across the full width of the barrier cross section rather than just a portion. Consequently, an increase in the width of each rail directly correlates to an increase in the shear capacity of each rail. Thus, concerns associated with insufficient shear capacity encountered with the previous continuous rail design were eliminated. As such, a width of 19 in. (483 mm) was selected for the rails. The width requirement established in Section 3.1.1 was satisfied by centering the rails over the 11-in. (279-mm) deep posts. This geometry left 4 in. (102 mm) of rail hanging off the deck edge and occupied only 15 in. (381 mm) of deck space, as shown in Figure 32.

The two rails were set apart to create an aesthetic opening in the bridge rail system. Balusters, similar to the spacer blocks described for Concept E (Ladder), were utilized to span the opening and connect the rails. The height (i.e., vertical distance between rails) and the offset distance from the face of the rail to each baluster were set at 8 ½ in. (216 mm) and 4 in. (102 mm), respectively. These cross sectional dimensions and individual rail heights satisfied all of the geometry requirements specified in Section A13.1.1 of the AASHTO LRFD Bridge Design Specifications [25]. In addition, the top rail geometry conformed to the geometric bounds set forth in Section 3.1.3 regarding the head ejection envelope.

The post dimensions remained the same from earlier design configurations, 24 in. wide by 11 in. deep (610 by 279 mm) at 8-ft (2.4-m) spacing. Further, the post and rail components were integrated to form a single bridge rail segment, as shown in Figure 31. Thus, there was no

need for connection hardware between the post and the rail. However, integrating both components significantly increased the weight of each bridge rail segment. As such, the heavy combination rail made it necessary to utilize a 16 ft (4.9 m) segment length rather than a 24 ft (7.3 m) segment length to satisfy the 10,000-lb (4,500-kg) weight requirement established in Section 3.3.2.

Although the unique geometry of Concept F (Fence) contained many aesthetically appealing features, it did not conceal the connection hardware between the rails as well as other previous concepts had. Still, it was felt that numerous simple rail-to-rail joints could be developed without sacrificing a significant portion of aesthetic appeal. Rail-to-rail joints are explored in detail in the following chapter.

4.5 Rail Design Selection

After significant consideration, it was concluded that Concept F (Fence) was the most appealing of all the bridge rail concepts discussed herein for numerous reasons. First, the openings between the upper and lower rails presented an extra aesthetic appeal that would remain whether the bridge rail was specified to be open or closed. Another unique geometrical feature that added aesthetic appeal to the concept was a draft along to the top and bottom of the rails and also along the upstream and downstream faces of each post. Moreover, this draft alignment was also a functional part of the design which allows for the easy removal of form work after casting of the bridge rail segment is completed. Finally, Concept F (Fence) called for the fewest assembly components for each segment. In fact, the posts and rails in an individual segment were cast together and did not require a connection or joint between them during installation.

In addition, Concept F (Fence) met all of the design criteria discussed in Chapter 2: each bridge rail only occupied 15 in. (381 mm) of transverse deck space; each segment of rail weighed less than 10,000 lb (4,536 kg); and the design satisfied the geometric bounds established to prevent vehicle rollover and occupant head slap. Also, the relatively large size of individual rail and post elements allowed for numerous possible solutions for rigid rail-to-rail joints and post-to deck attachments. These connections, explored in detail in the following chapters, should provide the rail segments with the ability to form a rigid, continuous bridge rail system and thereby decrease impact loading and subsequent damage to the deck. Considering all these factors, Concept F (Fence) was selected by engineers, fabricators, and researchers at NDOR, PCAN, and MwRSF for further development and testing.

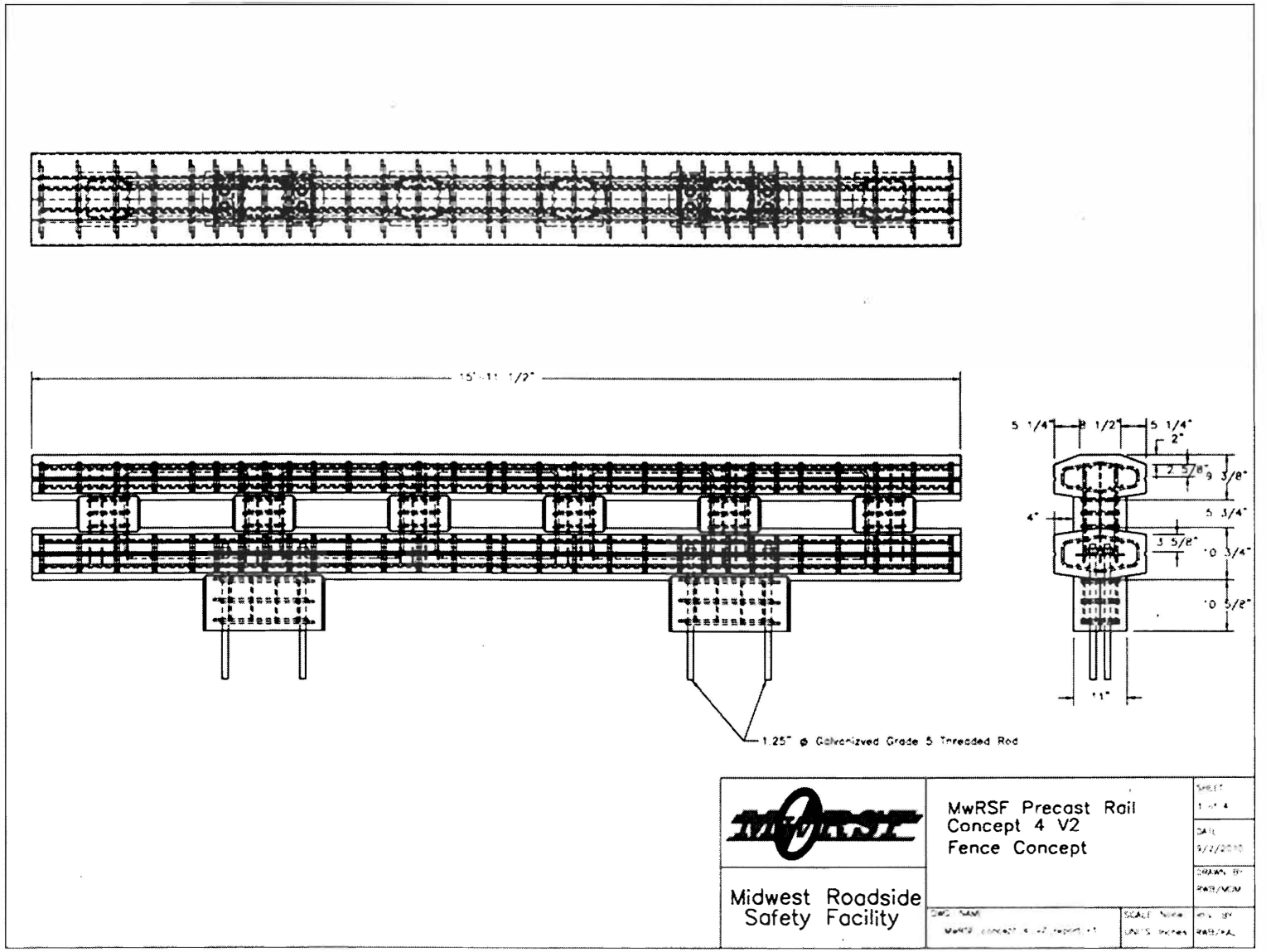

Figure 31. Concept F (Fence) - Overview

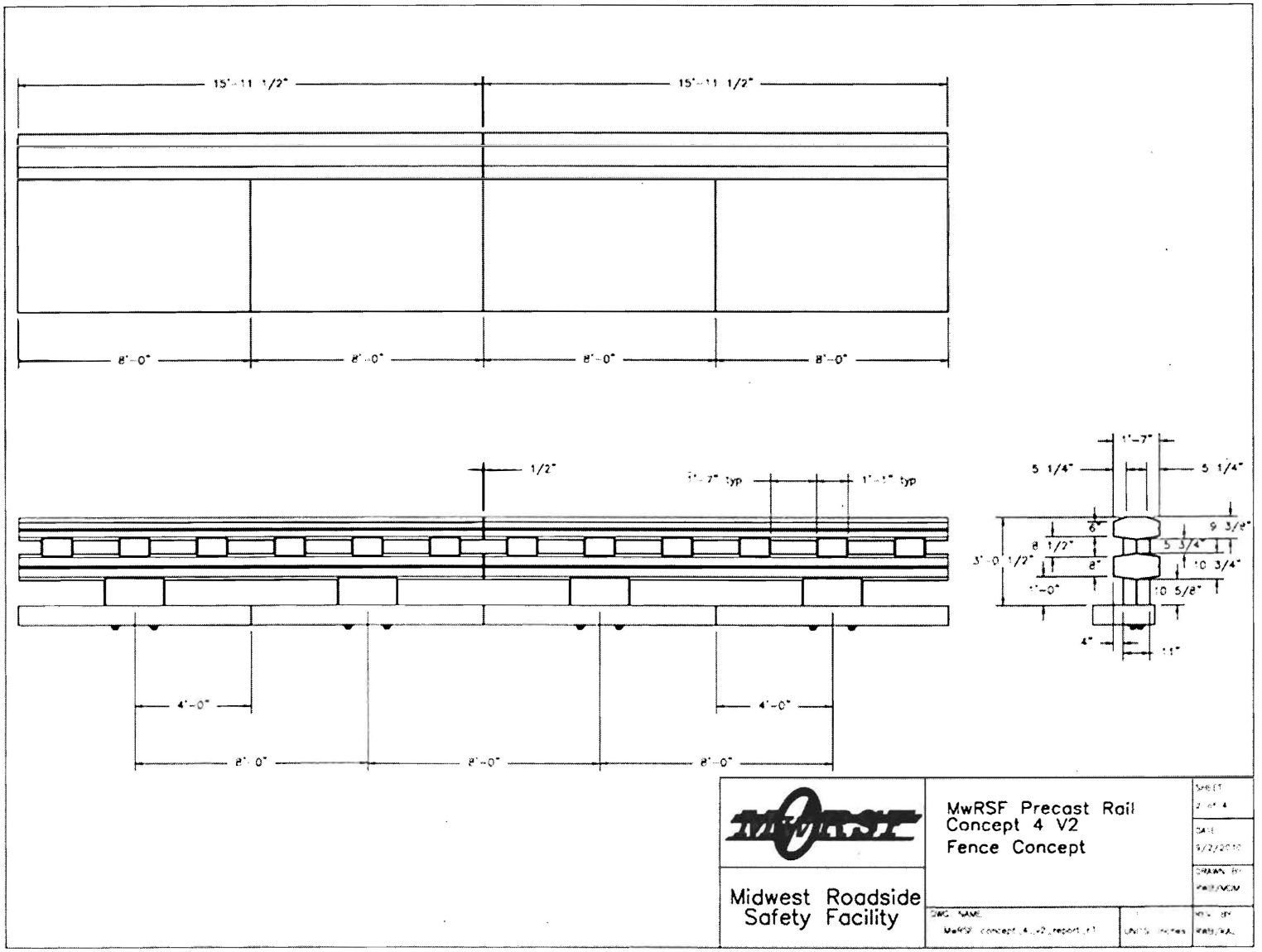

Figure 32. Concept F (Fence) - Geometry

Figure 33. Concept F (Fence) – Isotropic View

5 RAIL TO RAIL JOINT DESIGNS

5.1 Overview

As described in Chapter 4, it was necessary to design the precast bridge rail system as a continuous structure in order to withstand TL-4 impacts and prevent structural damage to the bridge deck. Thus, adjacent precast segments of the bridge rail system required the utilization of a rigid joint which was capable of transferring both shear and moment loadings. Although the upper and lower rails contained different cross sectional geometries, it was desired to design a single joint that would utilize identical installation hardware for either rail. As such, the design effort focused on creating a compatible joint for the smaller and thus more critical upper rail. Joint hardware designed for the upper rail would be assumed to have an adequate capacity if utilized for the lower rail.

It should be noted that the selected precast bridge rail design, as described in Section 4.4.2, was symmetric both through its cross section and also along its length. This eliminated the need to classify one end as either upstream or downstream. Preserving this symmetry was a priority in rail joint design. Also, it was essential for the joint to accommodate both straight and curved sections of a bridge for the same precast segments. Finally, it was important to incorporate the construction tolerances established in Section 3.3.1 into the joint design.

5.2 Joint Loading Criteria

5.2.1 Shear Loading

Recall from Section 3.2, the design impact load to the bridge rail system was determined to be 100 kips (445 kN). As such, shear and moment design loads were determined for both the upper and lower rails for impacts of this magnitude. To ensure the rail joints would not

prematurely fail, the rail joints were designed to have minimum shear and moment capacities equal to or greater than the rail itself.

A conservative estimate for the maximum shear force through the rail sections was determined by placing the impact load near midspan of two consecutive post locations. This resulted in a maximum rail shear load of 50 kips (223 kN) between consecutive posts in the impact region of the bridge rail. However, the maximum load imparted to each rail joint would not be of this magnitude since the upper and lower rails need only resist some fraction of this load individually. It is important to clarify that loads would not necessarily be divided equally between the upper and lower rails for every impact scenario. For example, passenger vehicles would be more likely to impart a greater load upon the lower rail, while single unit trucks with a higher center of gravity would be more likely to impart a greater load upon the upper rail. Therefore, it was conservatively determined that each individual rail would be designed to carry two-thirds of the maximum rail design shear, or 35 kips (156 kN).

5.2.2 Moment Loading

The required moment strength for the joint was estimated using Yield Line Theory [26]. In particular, parameters corresponding to a design capacity equal to 100 kips (445 kN), a barrier height of 36 ½ in. (927 mm), and a 24-in. (610-mm) wide post at 8 ft-(2.44-m) spacing were utilized to calculate the required total moment resistance of the rails, M_b, as a function of the post bending moment, M_c. A safety reduction factor of Φ=0.75 was applied to both M_b and M_c during yield line calculations to account for any material defects, installation problems, or tolerance issues. A plot showing the relationship between rail strength and post strength is shown in Figure 34.

The plot shown in Figure 34 was used to analyze the effects rail strength had on post strength, and vice versa. A value of 1,000 k-in. (113 kN-m) was selected as the design moment for the rail beams, which corresponded to a post bending value equal to 800 k-in (90 kN-m). Note that this post bending value will be used to design the post to deck attachment hardware in Chapter 9. Again, the rail design moment was allocated accordingly between the upper and lower rails. Estimating that up to two-thirds of the impact load could be applied to a single rail, a design moment of 700 k-in (79 kN-m) was prescribed for each rail.

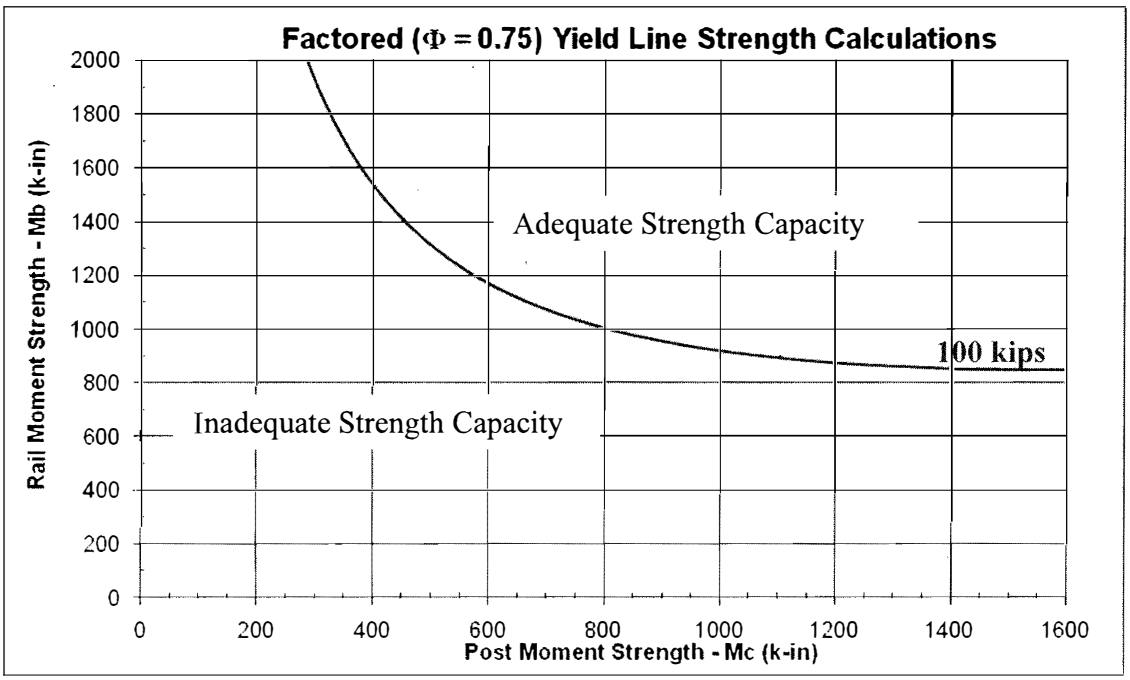

Figure 34. Factored Rail Moment Strength vs. Post Moment Strength

5.3 Joint Classification

During the initial design stages, two different methods emerged as ways to provide stiffness and strength to the rail joint. The first method employed standard steel hardware (i.e., bolts, threaded rods, etc.) in combination with shim plates. The general purpose of the shim plates was to fill gaps left in the joint for tolerance purposes and/or bridge curvature. By eliminating this gap the shims were able to provide immediate stiffness to the joint, thus

significantly reducing the possibility of undesirable deck damage. Joint designs which utilized only steel hardware and/or shims were termed "dry" joints. Dry joints had an advantage that allowed them to be quickly assembled in the field. Further, dry joints could also easily be disassembled for the repair or replacement of damaged segments. However, dry joints generally consisted of multiple installation parts and often included specific steel hardware that would need to be fabricated.

The second method for connecting the rails involved the use of grout to fill voids in the joint. Although grout represents an easy solution to initial rigidity, tolerance, and curvature issues, it also posed a few problems of its own. Grouted joints generally consisted of fewer parts than dry joints, but did require an additional skill for field assembly. Also, using grout would prolong the opening of the bridge since it would require time to cure and harden. Finally, if a segment of rail was damaged and needed to be replaced, disassembling a grouted joint would be more difficult and time consuming than disassembling a dry joint.

Ultimately, both dry and grouted joints were developed. Bogie component testing would later be utilized to determine the optimum joint design.

5.4 Dry Joint Designs

5.4.1 Joint Design A – Bolted Splice Plates

One of the simplest solutions to forming a rigid joint between rail ends was to utilize bolted splice plates. The relatively large moment arm created by mounting splice plates on opposite faces of the joint allowed for an extremely efficient use of steel to resist bending. Further, this configuration also created a mechanism for lining up the precast bridge rail segments longitudinally. Tightening the bolts on the plates would force adjacent rail ends flush, thus preventing any lateral misalignment of the precast segments. Subsequently, the bolts and

splice plates could be easily removed in the event that one of the precast segments were damaged and needed to be replaced.

A preliminary drawing of Joint Design A is shown in Figure 35. Recessed grooves were placed on the front and back of the rail so that the plates remained flush with the rail face. The resulting flat surface of the rail and the selected dome head bolts should prevent vehicle snag on the joint hardware.

The simplicity of this joint makes it quick and easy to assemble. However, several disadvantages were recognized with this design. First, the flat plates do not easily allow curvature in the bridge rail. Curved sections of a bridge would require the fabrication of specially angled plates for the plates to sit perfectly in the grooves. Further, the holes in the plate and the rail would need to be oversized to account for tolerance issues. As such, the play created from this tolerance would allow the rails to significantly deflect before any tension and/or compression is applied to the plates. Thus, the rails would lose continuity at the onset of impact. It was feared that this loss of continuity may result in high, localized loading and premature damage to the posts and bridge deck. Finally, the amount of exposed steel, especially the nuts and bolts on the outer face of the barrier, may detract from the unique aesthetics of the precast concrete bridge rail.

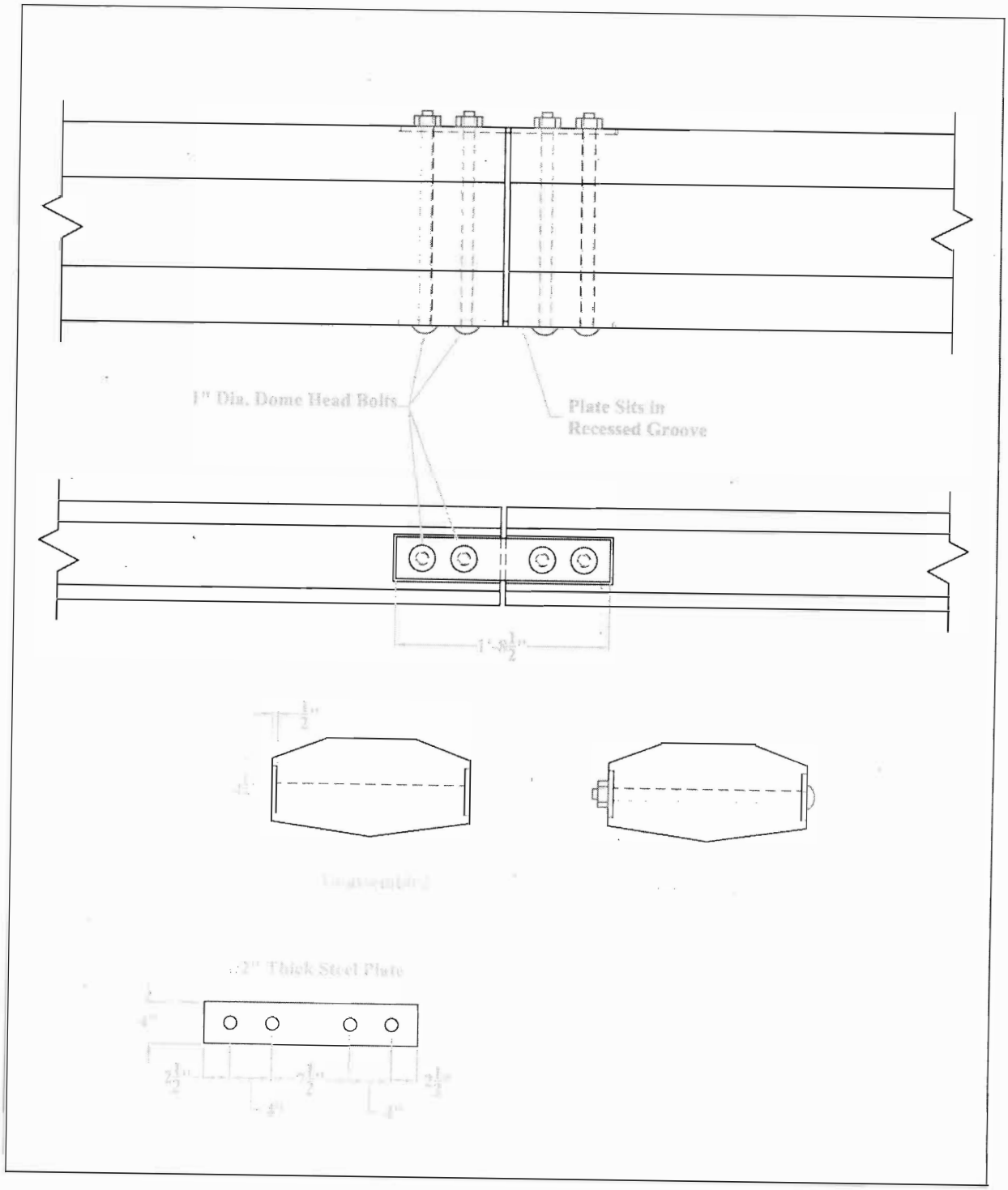

Figure 35. Joint Design A – Bolted Splice Plates

5.4.2 Joint Design B – X-Bolts

In 2005, the Texas Transportation Institute (TTI) developed a barrier-to-barrier joint in order to limit deflections in portable concrete median barrier systems [27]. This joint consisted of two bolts which crossed from the front face of one barrier to the back face of the other and vice versa. Hence, an 'X' was formed when looking down upon the joint.

Several aspects of this bolt configuration made it favorable for adaptation to Joint Design B. First, this joint prevents relative movement between barrier segments, thus providing both shear and moment resistance between rail segments. Further, the limited amount of steel hardware necessary to create the joint and the ease in which this joint can be assembled and disassembled made it appealing for accelerated construction applications. Finally, the out of plane placement of the two bolts did not detract from the overall symmetry of the precast rail segments. When facing the end of the rail, the top bolt hole always goes to the right, as shown in Figure 36. As such, the upstream and downstream ends remain identical and the precast segments could be installed with either end pointed upstream.

Unfortunately, a major issue developed upon further examination of the cross bolt joint: the size of the bolts needed to significantly increase. The original cross bolt joint design by TTI utilized ⅞-in. (22-mm) diameter bolts. However, the design criteria used in that study corresponded to a NCHRP Report No. 350 TL-3 barrier, whereas the design criteria for the proposed precast bridge rail in this project corresponds to a MASH TL-4 barrier. Consequently, impact loading conditions vary between the two designations. In fact, the proposed precast barrier is required to resist much higher force levels than the original TTI design. Thus, larger bolts and more anchorage in the rail segment ends were necessary. The task of increasing the size of the bolts while still providing adequate concrete cover proved to be too difficult.

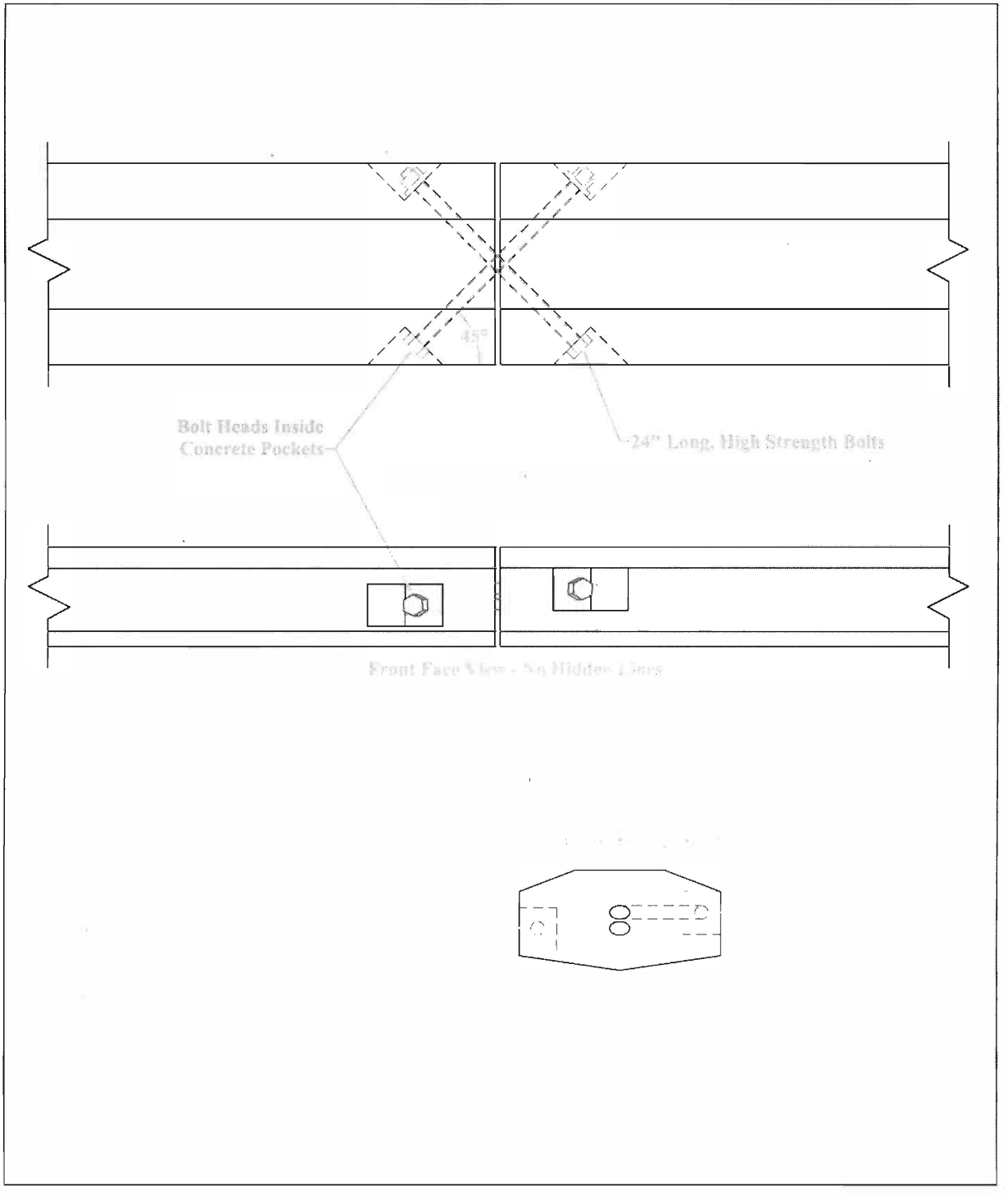

Figure 36. Joint Design B – X-Bolts

5.4.3 Joint Design C – Side Bolts and Center Shear Key

Joint Design C attempted to reduce the size of the steel joint hardware by designating specific components for isolated loading conditions. Components which provided shear resistance were analyzed separately from those components which provided moment resistance (tension and compression). Bending resistance between rail ends was provided by bolts placed inside steel pockets cast into the rails while shear resistance between rail ends was provided by a steel shear plate, as shown in Figure 37.

The steel pockets utilized for bending resistance would be cast into both the front and back faces of the rails. This maximized the distance between the tension and compression load paths during bending. The steel pockets were open to the bottom of the rail, which enabled installation of the bolts from underneath the rail. This method removed the bolts from the visibility of motorists. Large circular washers were placed around the bolts and used as shims to fill the gap between rail ends. This provided an immediate compression load path through the steel pockets. The amount, or thickness, of the shims could be varied to adjust for curvature in the bridge. The plates utilized for shear resistance would simply drop into notches cast into the top of the rail. The shear plates would be short enough as to not prohibit any curvature in the bridge rail system.

With only two bolts and a simple drop in shear plate, Joint Design C permitted quick and easy joint assembly on site. However, the steel pockets required more material and labor during the fabrication process than the previous joint designs. Thus, this design had a higher initial cost than previous designs. Further, the steel pockets themselves were visible from the sides of the rail while the shear plates were visible from the top of the rail. These exposed features had the potential to detract from the aesthetics of the precast concrete bridge rail system.

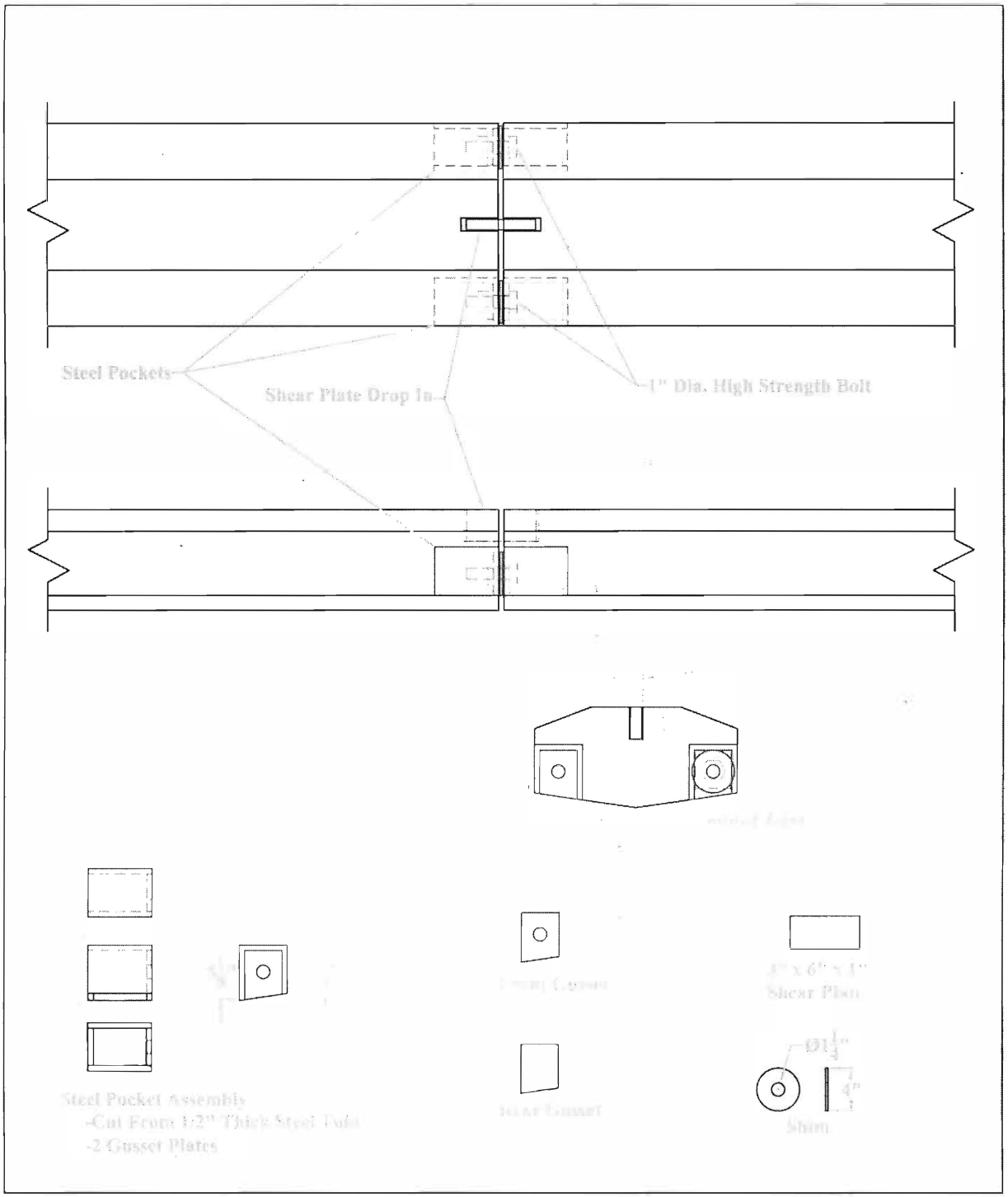

Figure 37. Joint Design C – Side Bolts and Center Shear Key

5.4.4 Joint Design D – Side Bolts and Shear Tubes

Similar to the previous joint design, Joint Design D used separate hardware to provide shear and bending resistance. Again, bolts placed inside of steel pockets and shims placed between rail ends were used to provide the bending resistance. The unique aspect of this design was that it utilized steel tubes for shear resistance. The shear tubes were small enough to fit inside the steel pockets, but large enough to fit around the bolts. This allowed both the separate shear and moment resistive mechanisms to be hidden from view inside the steel pockets, as shown in Figure 38.

Circular and square shapes were both considered for the shear tubes, but square shear tubes were ultimately selected for two reasons: (1) the flat faces of the square shear tube created a larger bearing surface between the tubes and the pocket wall than a circular tube, and (2) the square cross section allowed the shim plates to rest directly on top of the shear tubes which prevented the shims from rotating. To create the largest possible compression area, the shims were designed to match the geometry of the barrier cross section. Thinner shims were selected to be used in combination on each side of adjacent rails rather than a thicker individual shim so that each rail could be shimmed independently to create a tight joint for curved bridges.

Joint assembly was a process that required several steps. First, the shear tubes must be placed into the steel pockets. Next, the bolts must be inserted into the backside of the steel pockets and pushed through the gusset plates and into the shear tubes. Then, the shims must be lowered into the gap between the rails and over the shear tubes. Finally, the washers and nuts can be applied and tightened to secure the joint and compress the shim plates. The assembly process is shown in Figure 39.

Although Joint Design D eliminated the visibility of the shear plate from the top of the rail, the sides of the steel pockets were still exposed to view and may reduce the precast rails aesthetic appeal. In addition, the steel pockets required more fabrication during casting than other joint designs.

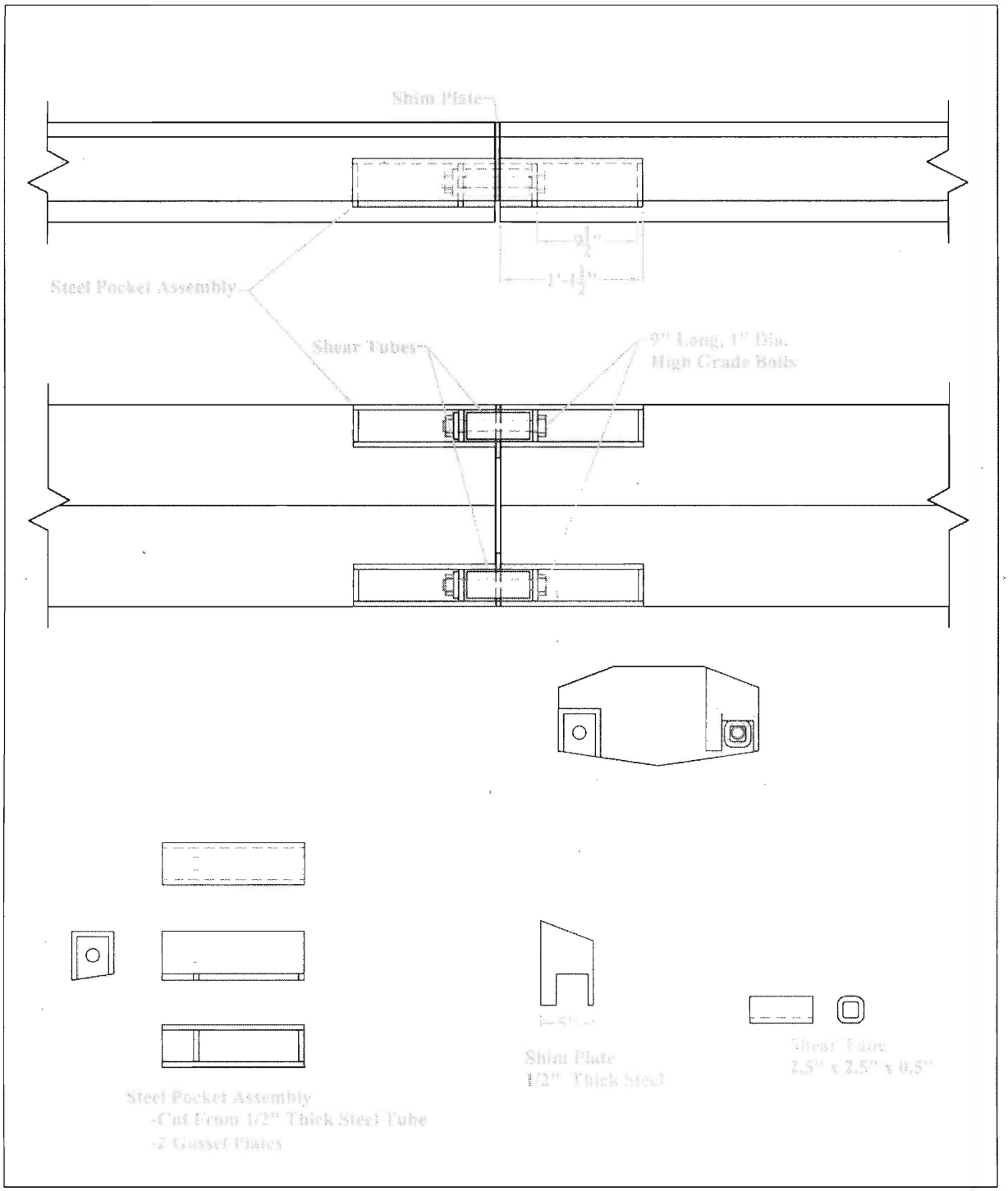

Figure 38. Joint Design D – Side Bolts and Shear Tubes

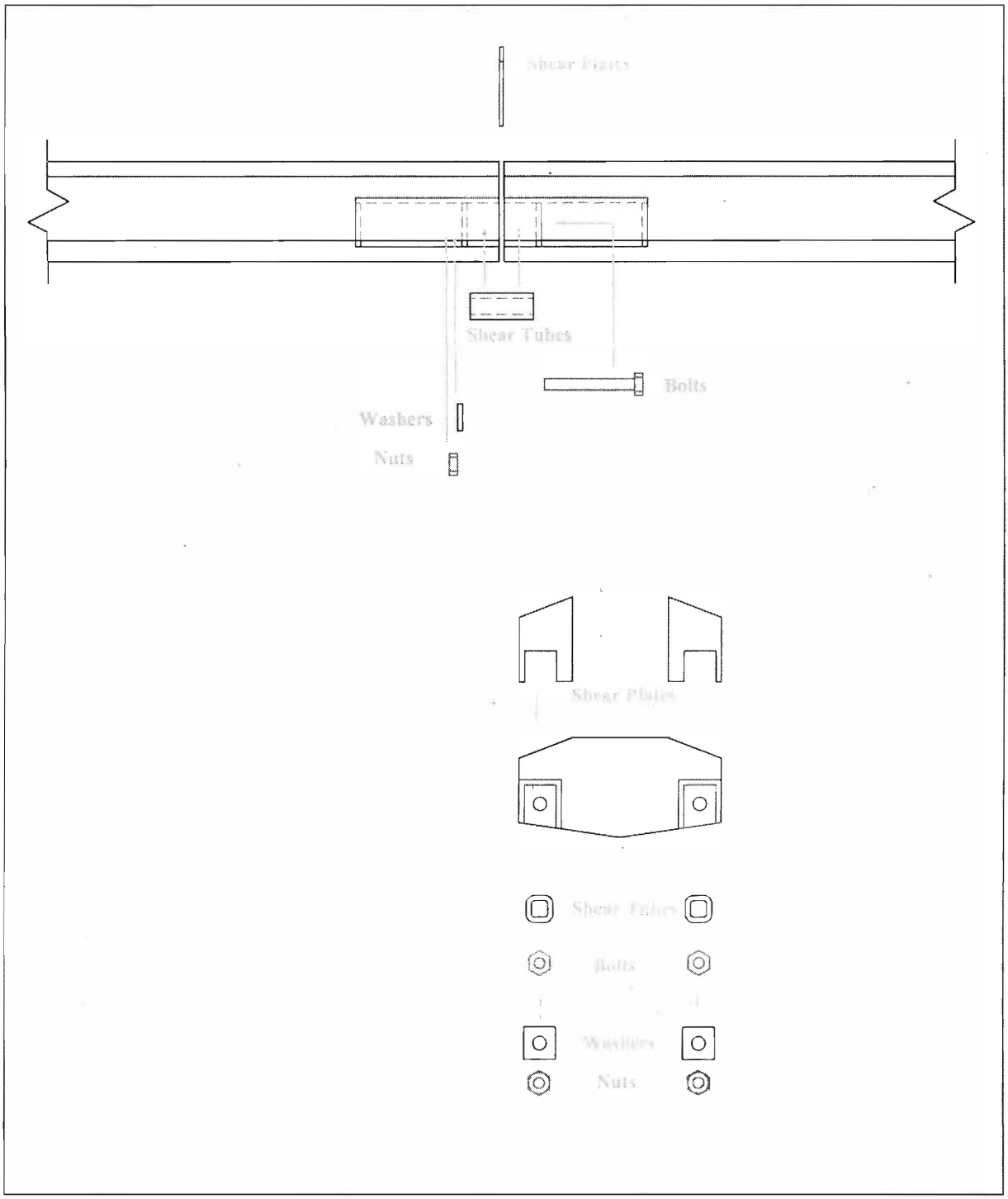

Figure 39. Joint Design D – Side Bolts and Shear Tubes - Assembly

5.4.5 Joint Design E – Center Bolt and Shear Pipe

Joint Design E was designed to contain all of the steel joint hardware in the center of the rails. As such, no exposed steel elements would be located on the face of the precast concrete rail system. A steel pipe was utilized to transfer shear between rails, while a high strength rod in combination with shims were designed to transfer moment between rails, as shown in Figure 40.

Placing the hardware in the center of the rail essentially cut the moment arm in half and doubled the necessary tension load for moment transfer. Thus, a large B7 threaded rod was specified instead of the lower grade bolts used in previous designs. Further, placing all of the joint hardware in a single location resulted in concentrated stresses during loading. As such, the probability of localized failure and/or steel hardware components pulling through the concrete rail was increased. To prevent the rail ends from premature failure, a steel end cap was created to distribute the load throughout the rail cross section. The end cap consisted of a plate in the shape of the rail cross section with a short length of pipe welded near the center. Shims had to be designed to create compression zones near both the front face and the back face of the rail. However, only the shear pipe in the center of the rail provided a location for the shims to attach to. Thus, the shims were made to span the entire rail cross section. Small pins inserted through tabs on both sides of the shim were required to prevent the shim from rotating and dropping out of the joint. Both the shim plates and the pins are shown in Figure 41.

Joint assembly was a process that required several steps. First, both the shear pipe and the threaded rod must be inserted into hollow pockets in the rail and fed across the joint through the end caps. The threaded rod fits inside the shear pipe, similar to previous joint designs. Next, shims matching the cross section of the rail are lowered into place, resting on the shear pipes. Then, the small pins are inserted through the tabs on both sides of the shim. Finally, the joint is

completed with the addition of washers and nuts to secure the threaded rod. Note the shear pipe is encased inside the rail cap by the washers. The assembly process is shown in Figure 41.

Although locating the joint hardware in the center of rail eliminated steel from the rail face and reduced the amount of parts necessary for installation, it did create other problems. Without a moment arm for bending transfer, the threaded rod had to be larger and of higher strength material than in other joint designs. Also, due to the hollow pocket for hardware in the center of the rail, a steel end cap assembly was necessary to distribute the loads and prevent concrete failure to the reduced rail section. Finally, since the shims covered the entire rail width and not individual sides, creating a tight joint in a curved bridge rail system would be difficult.

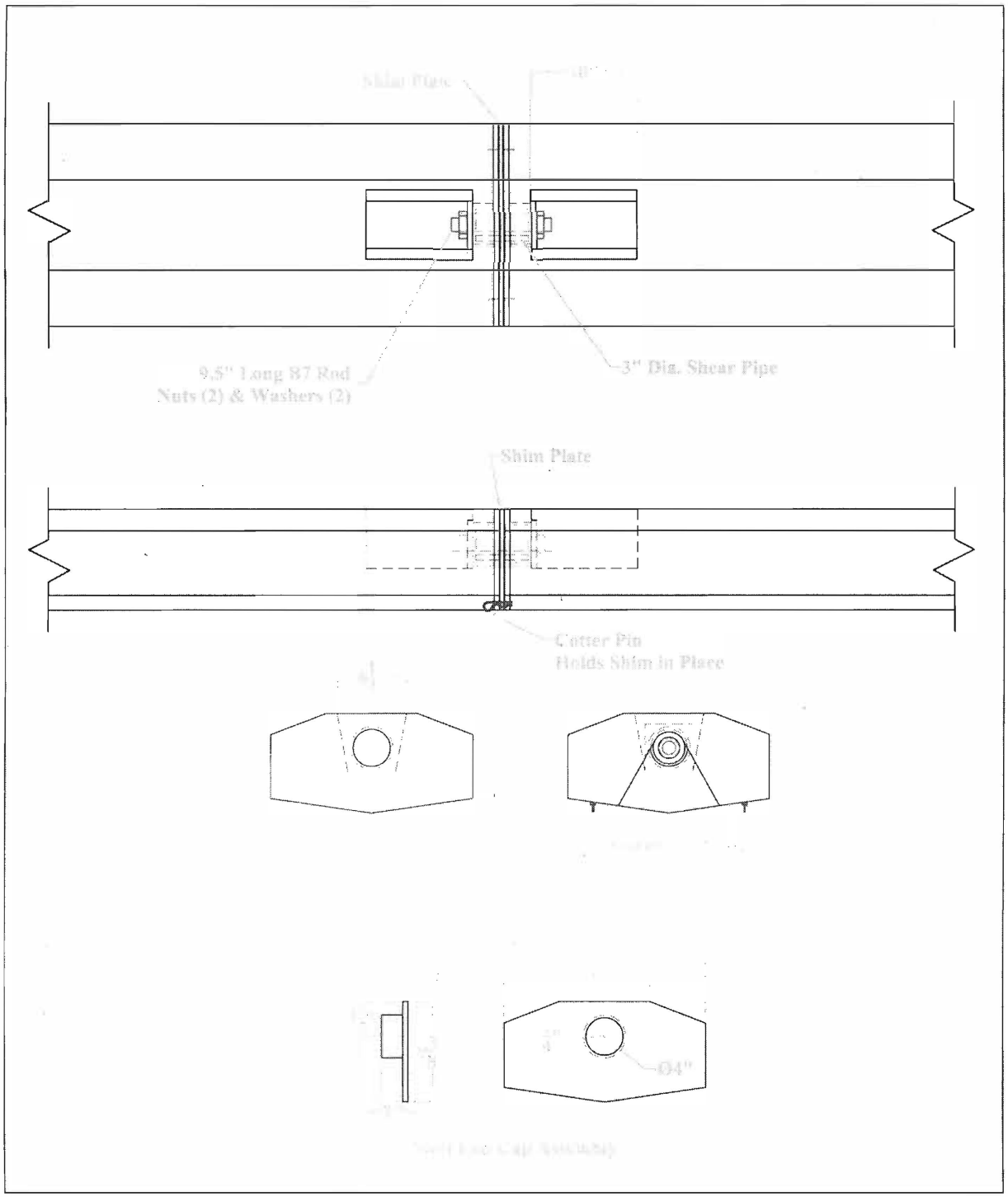

Figure 40. Joint Design E – Center Bolt and Shear Pipe

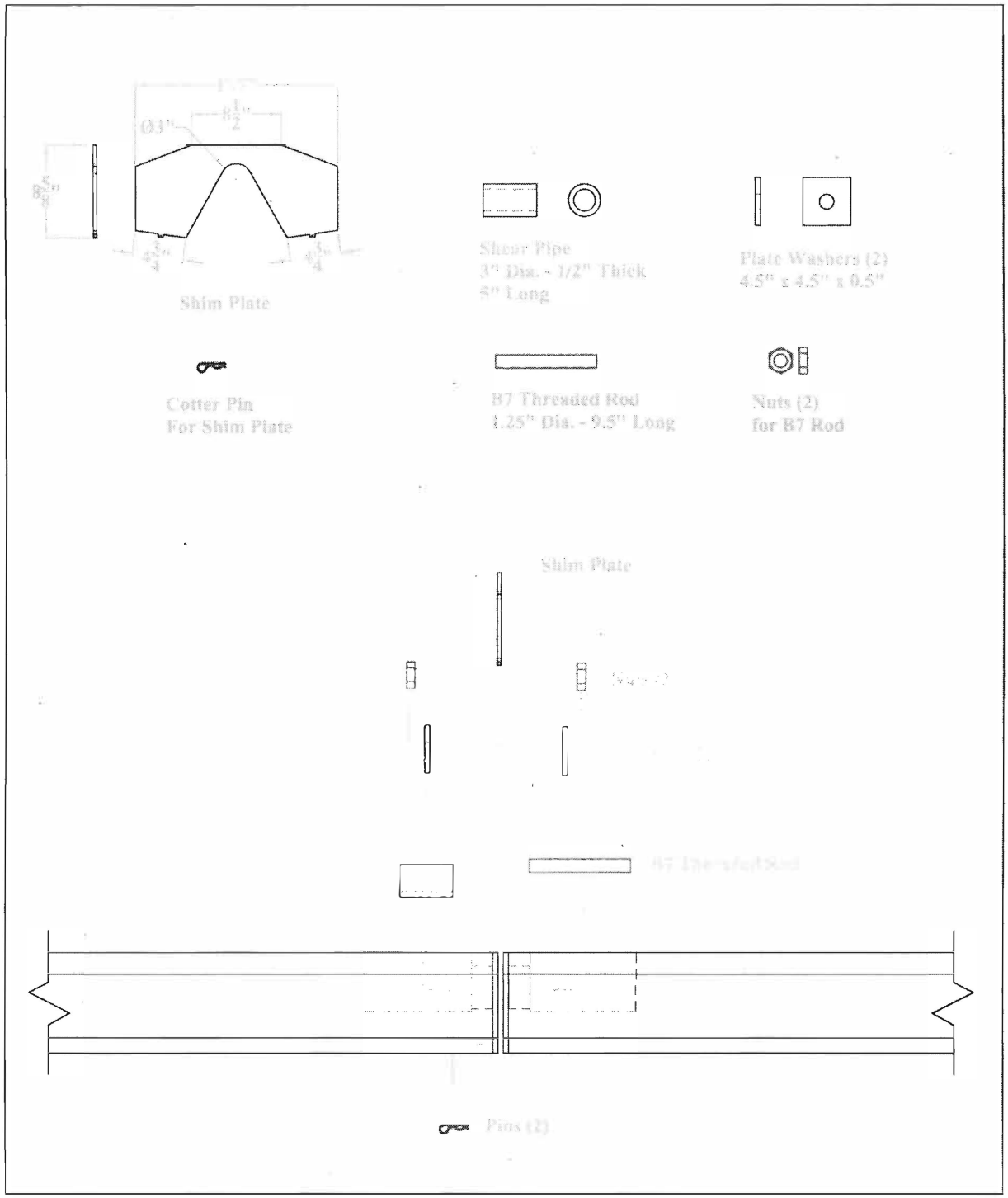

Figure 41. Joint Design E – Center Bolt and Shear Pipe – Assembly and Parts

5.4.6 Joint Design F – Baluster Connection Piece

Joint Design F utilized a baluster as the load transfer mechanism. This load transfer baluster was separate from those connecting the vertically mounted rails in each segment, as shown in Figures 42 and 43. The position of the balusters through the length of the precast rail segment was shifted such that one of the load transfer balusters would be centered across each joint. The baluster at this location would not be cast in with the rest of the precast rail segment. Instead, it would be a separate precast piece bolted to the rail segments during installation to create the necessary rigid joint.

By using a separate baluster piece to transfer the load between rail segments, much of the extra fabrication and installation efforts associated with other designs were eliminated. For this joint design, only a few vertical bolt holes need to be cast into the rail segment ends. The joint design contained no extra pockets or steel pieces that needed to be specially fabricated. Even during installation, only the baluster pieces and few bolts would be necessary to assemble the joint. This joint should be quick to assemble and easy to take apart if a segment needed replacement. Also, this joint design nearly eliminated all exposed steel and preserved the aesthetic appeal of the precast bridge rail. The only exposed steel parts were the nuts and bolt heads. However, the nuts were underneath the bottom rail and the dome head bolts, used to prevent vehicle snag, would not attract as much attention as standard hex head bolts.

A negative aspect of this design was that the concrete baluster, at an estimated 75 lb (34 kg), may not be easy to transport and position during installation. Also, the balusters require heavy reinforcement in order to transfer the entire load between both the upper and lower rails. Steel plates embedded inside the baluster may be necessary. Finally, the oversized bolt holes,

needed to account for tolerances, may allow significant movement in the rail before transferring load.

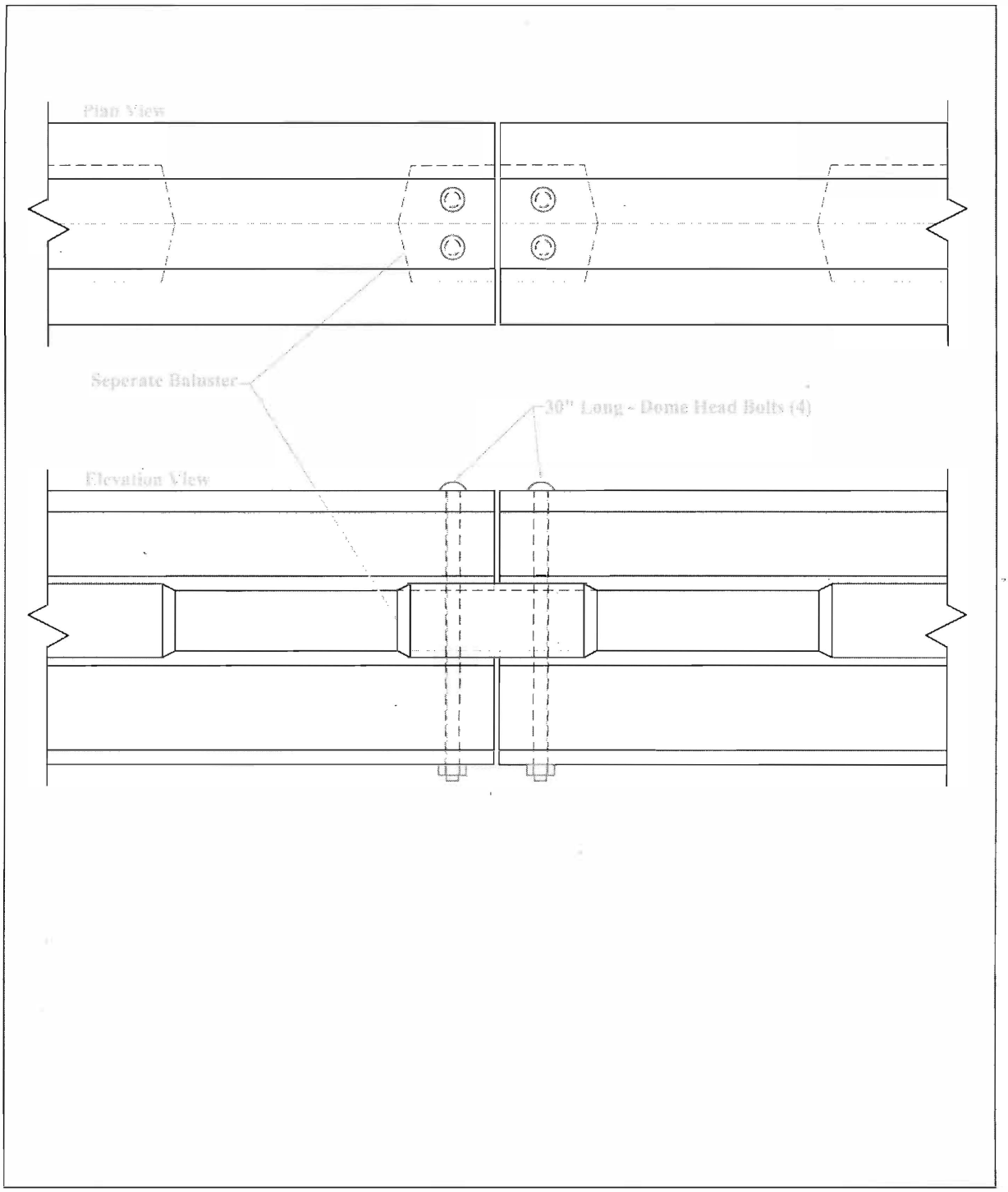

Figure 42. Joint Design F – Baluster Connection Piece

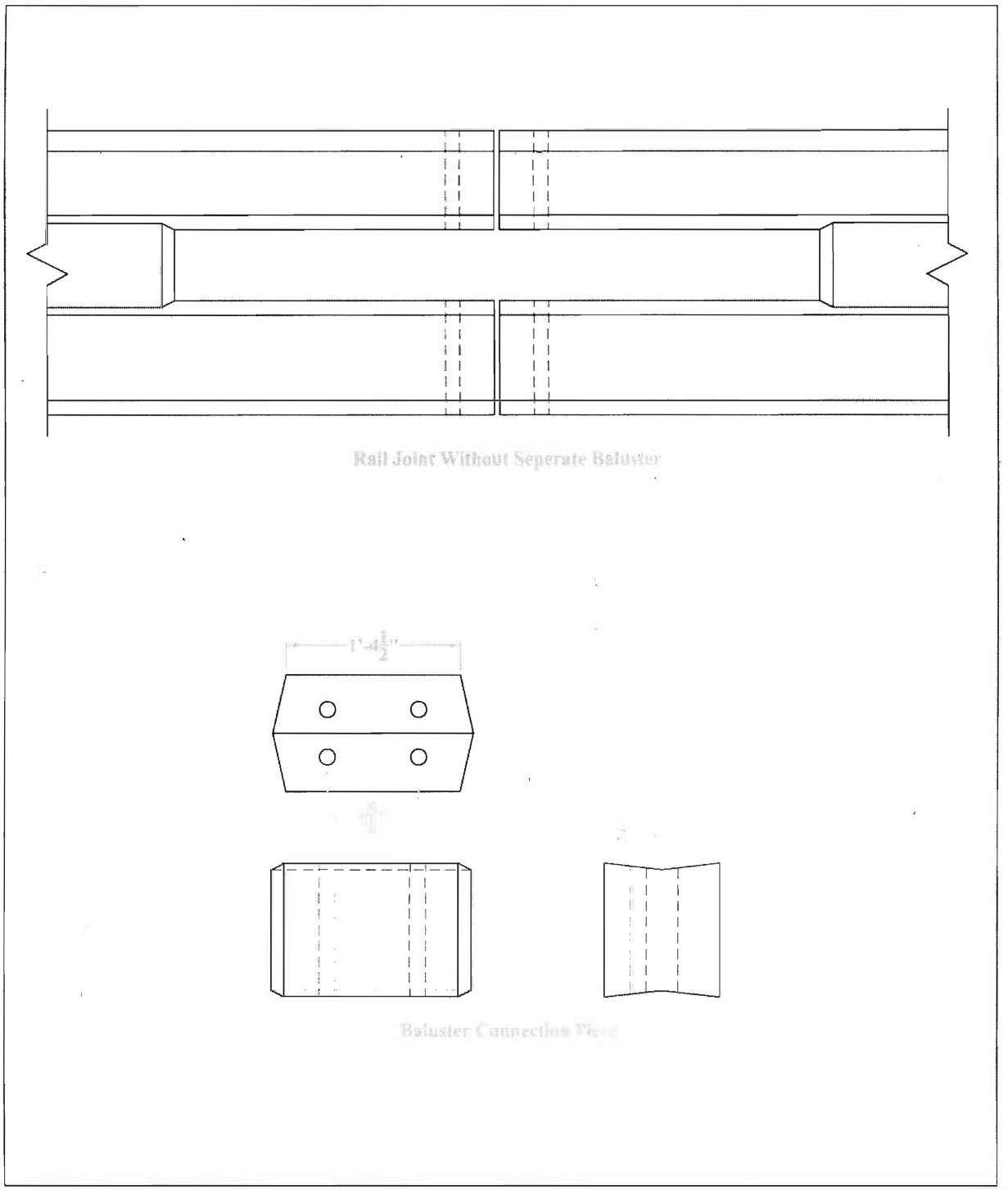

Figure 43. Joint Design F – Baluster Connection Piece – Individual Parts

5.5 Grouted Joint Designs

5.5.1 Joint Design G – Center Bolt and Side Grout Pockets

Joint Design G consisted of a center tension rod with front and back grout pockets, as shown in Figure 44. Described in Section 5.4.5, when the tension member is located in the center of the rail, the moment arm is effectively cut in half and the tension required to transfer the design moment doubles. As such, a threaded B7 rod was used instead of a standard grade bolt. Hollow pockets underneath the rails allow the B7 rod to connect the rail end caps without being visible from the roadway, as shown in Figure 45. Thick plate washers were used to distribute the tensile load from the B7 rod and prevent excessive deformation in the rail end cap.

Similar to the Joint Design E, a steel end cap was necessary to anchor the B7 rod. However, a cavity plate was welded to the rail end cap to help anchor the cap in tension and form the pocket underneath the rail used to install the B7 rod. Also, an 8 x 4 x ½-in. (203 x 102 x 13-mm) steel tube was cut in half and welded to each side of the rail end cap to form the grout pockets. Finally, a thin steel plate was welded to the bottom of the tubes to contain the grout during installation. The entire rail end cap assembly is shown in Figure 44.

Grout pockets spanned between adjacent rail ends on both the front and back faces of the rail. Steel U-shape sections welded to both sides of the end caps formed the pockets while grout and a steel sleeve were used to fill the pocket. These grout pockets served multiple functions. First, the grout provided a mechanism for compression between the rail ends to complete the moment transfer. Second, the steel sleeve lining the pocket provided shear transfer between the rails and effectively confined the grout to prevent fracture across the gap. Finally, filling in the pockets with grout created a strong and rigid joint that can adapt to both tolerance and curvature requirements in the bridge rail.

Joint Design G was one of the most robust of all joint designs described in this chapter. However, this strength and durability came at the expense of an elaborate rail end cap which required six different steel pieces to be fabricated and welded together. Also, installation on the joint required multiple steel hardware pieces and grout. Thus, this joint was considered one of the more expensive joint to fabricate and to install. Further, a reduction in the aesthetic appeal of the precast concrete bridge rail was another concern with the design. This joint contained both exposed steel to the rail faces and grout on the top surfaces of each rail. The entire bridge rail system may have to be painted to preserve the appeal of the precast bridge rail system.

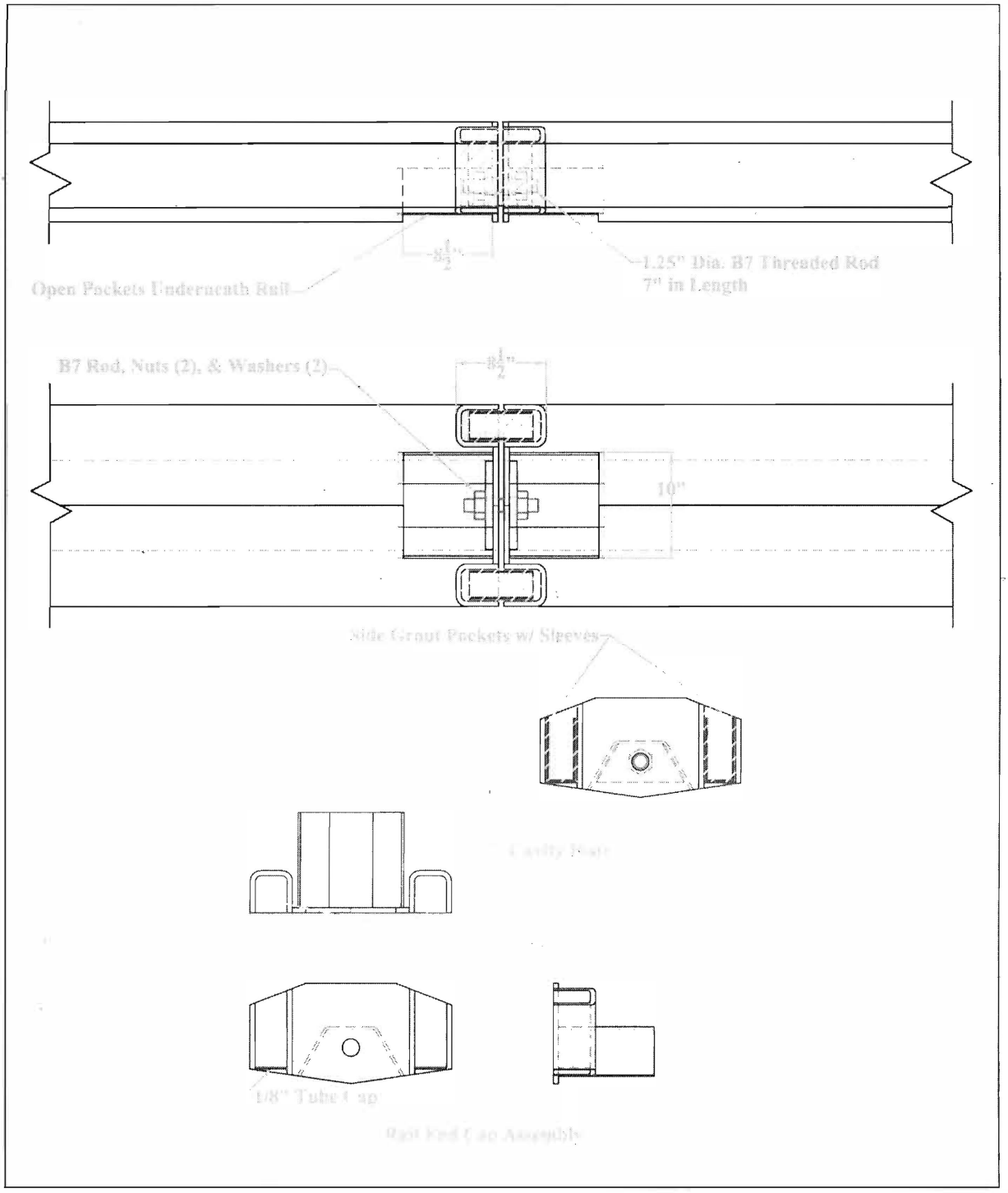

Figure 44. Joint Design G – Center Bolt and Side Grout Pockets

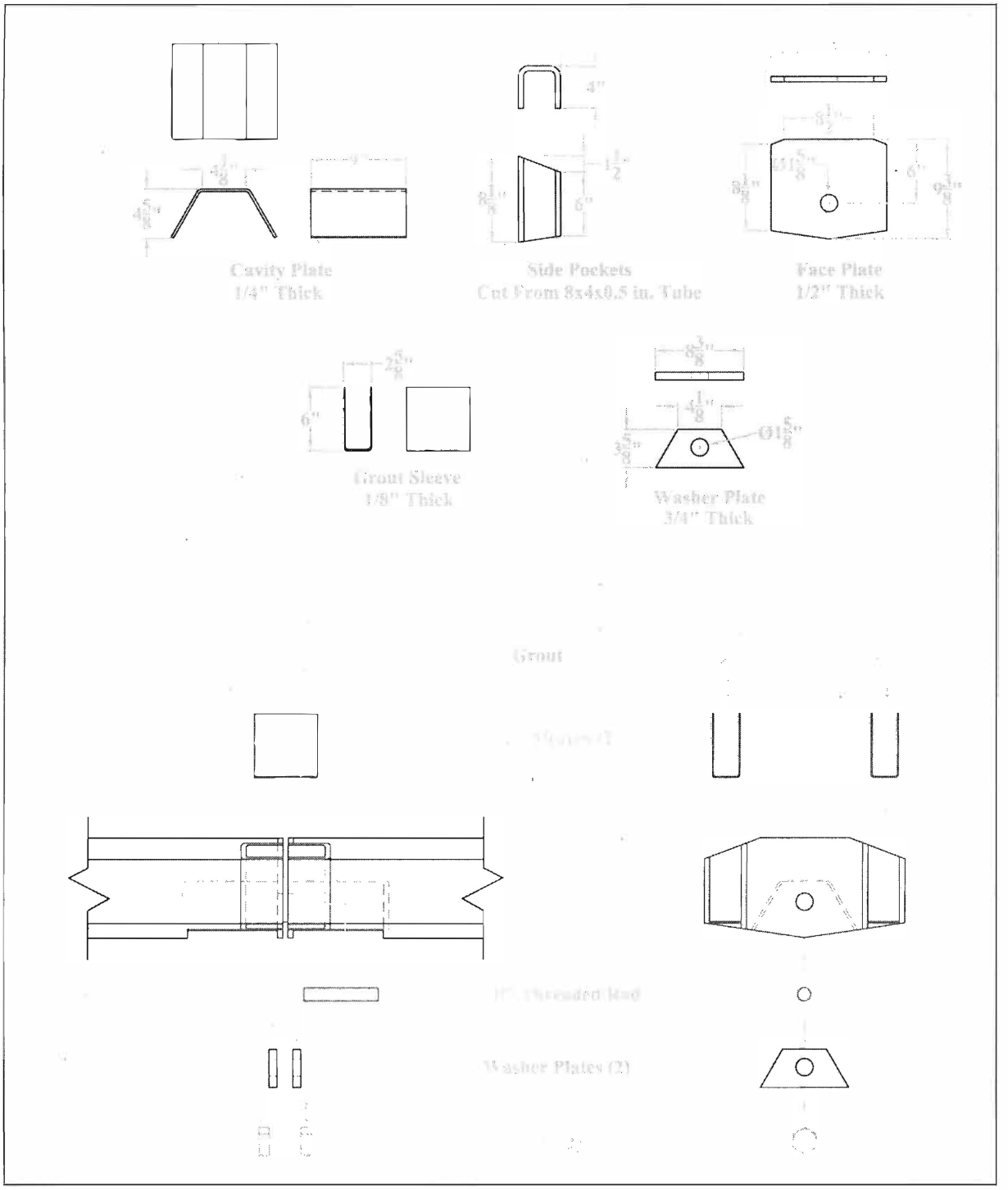

Figure 45. Joint Design G – Center Bolt and Side Grout Pockets – Assembly

5.5.2 Joint Design H – I-Shape Segments in Side Grout Pockets

Joint Design H utilized short segments of steel I-shapes to transfer load between rail segments. The I-shape segments were placed inside steel pockets on both the front and back sides of the rail, and the pockets were filled with grout, as shown in Figure 46. The I-shape connectors were designed to transfer both shear and moment loads across the joint while the grout held them rigidly in place.

This unique joint design had many advantages over other joint designs. First, it required only two steel parts for field assembly, both of which simply dropped into place. The slots in the steel pockets were cut wider than the web of the I-shape to allow the joint to handle all tolerance issues as well as curvature in the bridge. Further, filling the inside of the pockets with grout created a rigid joint that was capable of transferring load instantly upon impact. Finally, all of the steel pieces needed for the joint can be cut from standard sections, thus fabrication was limited to cutting and tack welding a plate to the inside of the pocket to hold in the grout.

Although the grout pocket solved many of the joint issues, it still contained the same issues mentioned in previous sections regarding the installation of the grout itself. These issues include additional installation labor, additional time for the grout to cure, and difficult joint disassembly. Also, the exposed grout on the top surface and the exposed steel of the pocket may take away from the aesthetic appeal of the precast concrete bridge rail system unless the system is painted after installation.

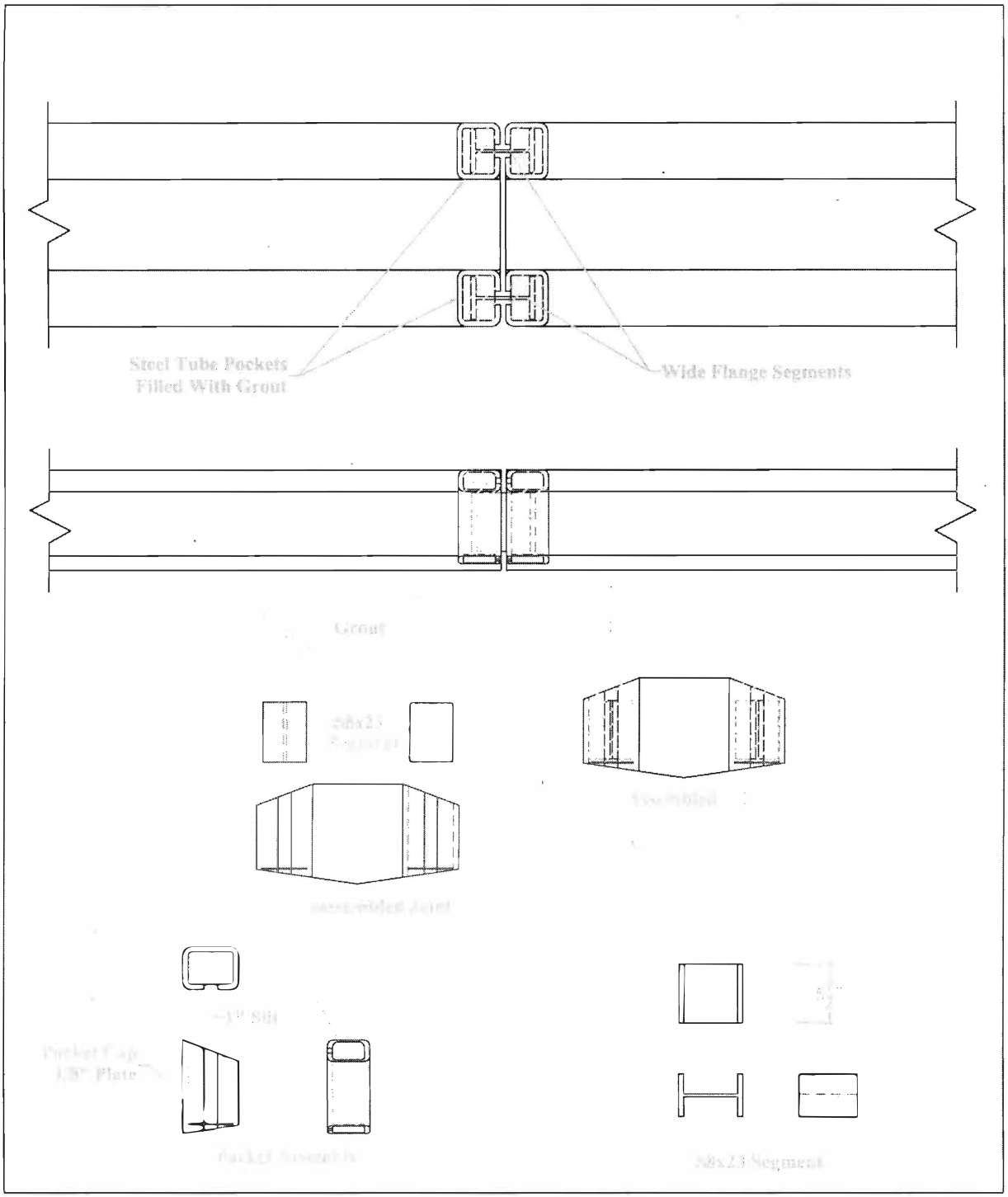

Figure 46. Joint Design H – Wide Flange Segments in Side Grout Pockets

5.5.3 Joint Design I – Side Bolts and Center Grout Pocket

Joint Design I was designed to create a grouted joint that could be easily disassembled. As such, the grout was limited to a single pocket running along the top of the rails, as shown in Figure 47. A steel pocket liner was designed to sit inside the pocket and create a barrier between the grout and the precast concrete rail. Thus, the grout was used as the mechanism to provide instantaneous shear transfer across the joint. The pocket liner itself allowed the grout to be removed from the pocket without damage to the rail. Additional pockets were created on the front and back faces of the rail by steel angles and gussets. Bolts were inserted into the pockets and across the joint to carry tension and provide moment resistance. Shims were not necessary for this design because the grout pocket carried both the compression load for moment resistance as well as the shear load.

Separating the grout from the rest of the precast rail and connection hardware created a joint that could be assembled and disassembled quickly and easily. However, this ease in field labor was the result of pre-construction fabrication which required multiple steel pieces to complete the joint. Although the steel pocket assemblies were small, they required both cutting and welding to attach the gussets. Also, the grout pocket liner was not created from a standard steel shape, thus it required specific fabrication as well. Further, the side pockets may also be the source of future problems. Since the pockets were designed open to the sides, they increase the risk of vehicle snag on the joint during impacts. The pockets may also result in a reduction in aesthetic appeal to the precast concrete rail that painting could not cover up.

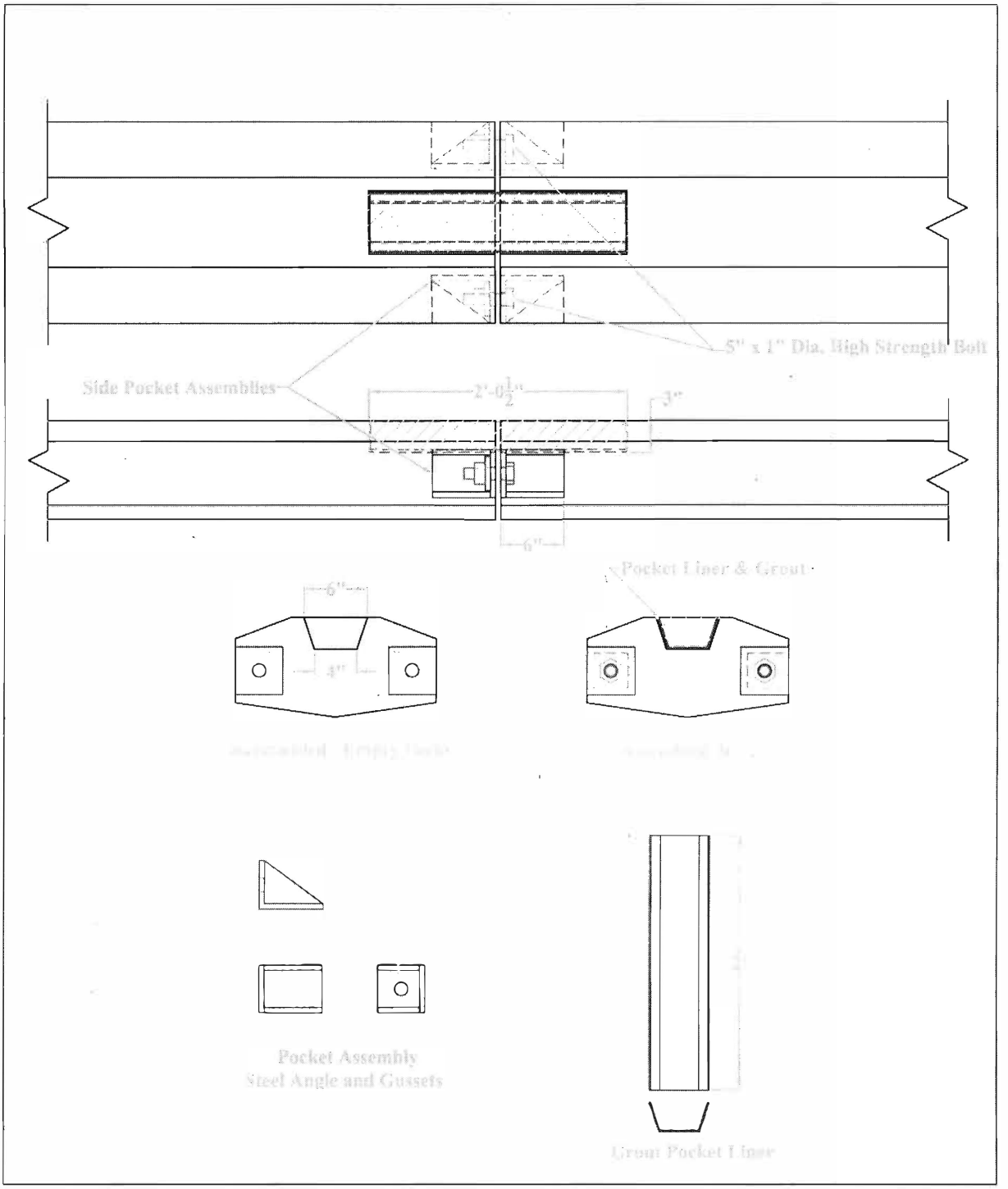

Figure 47. Joint Design I – Side Bolts and Center Grout Pocket

6 RAIL JOINT BOGIE TESTING – ROUND 1

6.1 Purpose

To determine the optimum joint design from the options presented in Chapter 5, a bogie testing program was initiated. These bogie tests were used to evaluate selected rail joint designs in multiple areas including strength, stiffness, toughness, constructability, and ability to disassemble the joint after loading.

6.2 Scope

Two of the most promising rail joint designs from Chapter 5 were selected for component testing using a dynamic impact bogie vehicle. The joints were used to connect two segments of concrete beams with the same cross section as the upper rail of the Concept F (Fence) bridge rail design. The upper rail geometry was selected because it has a smaller cross-sectional area than the lower rail. Thus, it would represent the weaker of the two rails. The segments measured 9 ft – 6 in. (2.90 m) and 5 ft (1.52 m) long. The adjacent ends of the rails were spaced ½ in. (13 mm) apart to represent the maximum tolerance of the joint gap in the actual bridge rail. Wood blocks were used to vertically support the concrete segments and position the center of the segments in plane with the center of the bogie impact head. The interface between the blocks and the rails was coated with grease to allow the rails to move and rotate during testing. Three anchor posts spaced 72 in. (1,829 mm) apart were used to laterally brace the rails and generate the desired shear and moment loads at the joint. The first anchor post was centered 41 in. (1,041 mm) and 35 in. (889 mm) away from the rail joint and bogie impact location, respectively, as shown in Figure 48. These specified dimensions for anchor post spacing, joint location, and impact location were selected such that an impact force of 62 kips (276 kN) would result in the design shear and moment loads through the joint of 35 kips (156 kN) and 700 k-in (79 kN-m), respectively.

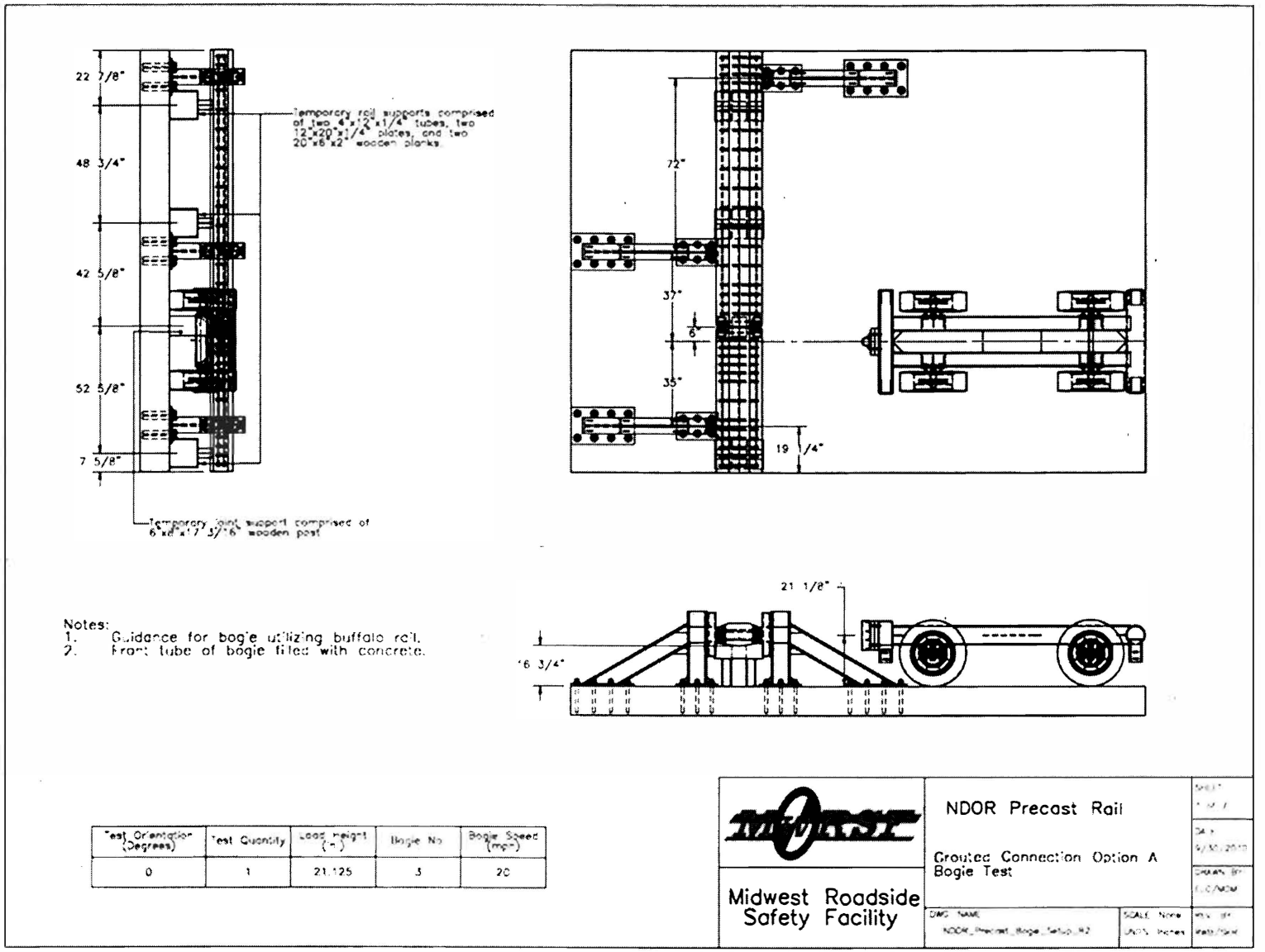

Figure 48. Bogie Testing Set Up

6.3 Testing Facility

Physical bogie testing of the two rigid rail-to-rail joint designs was conducted at the MwRSF testing facility which is located at the Lincoln Air Park on the Northwest side of the Lincoln Municipal Airport. The facility is approximately 5 miles (8 km) northwest from the University of Nebraska-Lincoln's city campus.

6.4 Equipment and Instrumentation

Equipment and instrumentation utilized to collect and record data during the dynamic bogie tests included a bogie, accelerometers, pressure tape switches, high-speed and standard-speed digital video, and still cameras

6.4.1 Bogie

A rigid frame bogie was used to impact the posts. A variable height, detachable impact head was constructed and used in the testing. The bogie head was constructed of 3-in. (76-mm) diameter steel pipe welded to a ½-in. (13-mm) thick steel plate using multiple gussets. Also, the steel tube was filled with concrete to prevent damage to the impact head. The impact head assembly was bolted to the bogie vehicle at a centered height of 21⅛ in. (537 mm) above the ground. The bogie with attached impact head is shown on the guidance track in Figure 49. The weight of the bogie with the addition of the mountable impact head was 1,616 lbs (733 kg).

A pickup truck with a reverse cable tow system was used to propel the bogie down the guidance track to a target impact speed of 22 mph (35 km/h). When the bogie reached the end of the guidance system, it was released from the tow cable, allowing it to be free rolling when it impacted the rail joint specimen. A remote braking system was installed on the bogie allowing it to be safely brought to rest after the test.

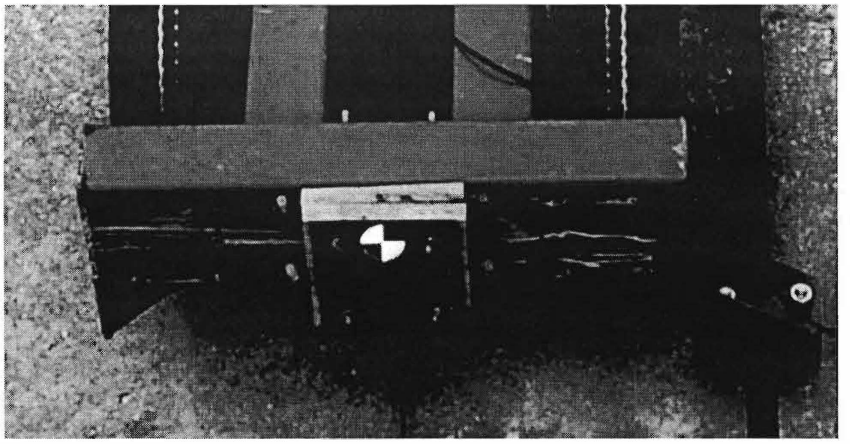

(a)

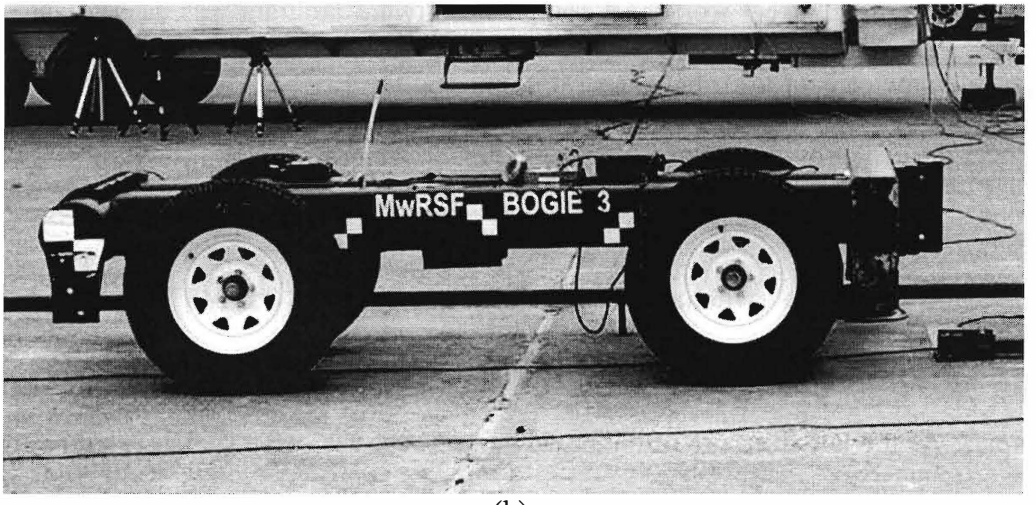

(b)

Figure 49. Bogie Vehicle (a) Impact Head and (b) on Guidance Track

6.4.2 Accelerometers

Two environmental shock and vibration sensor/recorder systems were used to measure the accelerations in the longitudinal, lateral, and vertical directions. One triaxial piezoresistive accelerometer system, Model EDR-3, was developed by Instrumented Sensor Technology (IST) of Okemos, Michigan. The EDR-3 was configured with 256 kB of RAM memory, a range of ±200 g's, a sample rate of 3,200 Hz, and a 1,120 Hz lowpass filter.

The second accelerometer was a two-Arm piezoresistive accelerometer system developed by Endevco of San Juan Capistrano, California. Three accelerometers were used to measure each

of the longitudinal, lateral, and vertical accelerations independently at a sample rate of 10,000 Hz. Data was collected using a Sensor Input Module (SIM), Model TDAS3-SIM-16M, which was developed by Diversified Technical Systems, Inc. (DTS) of Seal Beach, California. The SIM was configured with 16 MB SRAM memory and 8 sensor input channels with 250 kB SRAM/channel. The SIM was mounted on a TDAS3-R4 module rack. The module rack is configured with isolated power/event/communications, 10BaseT Ethernet and RS232 communication, and an internal back-up battery. Both the SIM and module rack are crashworthy. A customized Microsoft Excel worksheet computer software program was used to analyze and plot the accelerometer data from both the DTS unit and the EDR-3. Both accelerometers were mounted near the center of gravity of the test vehicles.

6.4.3 Pressure Tape Switches

Three pressure tape switches spaced at approximately 18 in. (457 mm) intervals and placed near the end of the bogie guidance track were used to determine the speed of the bogie before impact. As the left-front tire of the bogie passed over each tape switch, a strobe light was fired sending an electronic timing signal to the data acquisition system. The system recorded the signals and the time each occurred. The speed was then calculated using the spacing between the sensors and the time between the signals.

6.4.4 Photography Cameras

For test nos. PCRB-1 and PCRB-2, three high-speed AOS VITcam video cameras, three JVC digital video cameras, and one Canon digital video camera were utilized to record the crash test. Camera details, lens information, and camera operating speeds are shown in Table 3. A schematic of the camera locations is shown in Figure 50. A Nikon D50 digital camera was used to document pre- and post-test conditions for each rail joint specimen.

Table 3. Camera and Lens Information, Test Nos. PCRB-1 & 2

	No.	Type	Operating Speed (frames/sec)	Lens	Lens Setting
High-Speed Video	1	Vitcam CTM	500	Cosmicar12.5 Fixed	
	2	Vitcam CTM	500	Sigma 70-200	200
	WEIN	Vitcam CTM	500	Sigma 24-70	70
Digital Video	3	JVC – GZ-MC40U (Everio)	29.97		
	4	JVC – GZ-MC40U (Everio)	29.97		
	5	JVC – GZ-MC40U (Everio)	29.97		
	8	JVC – GZ-MC40U (Everio)	29.97		

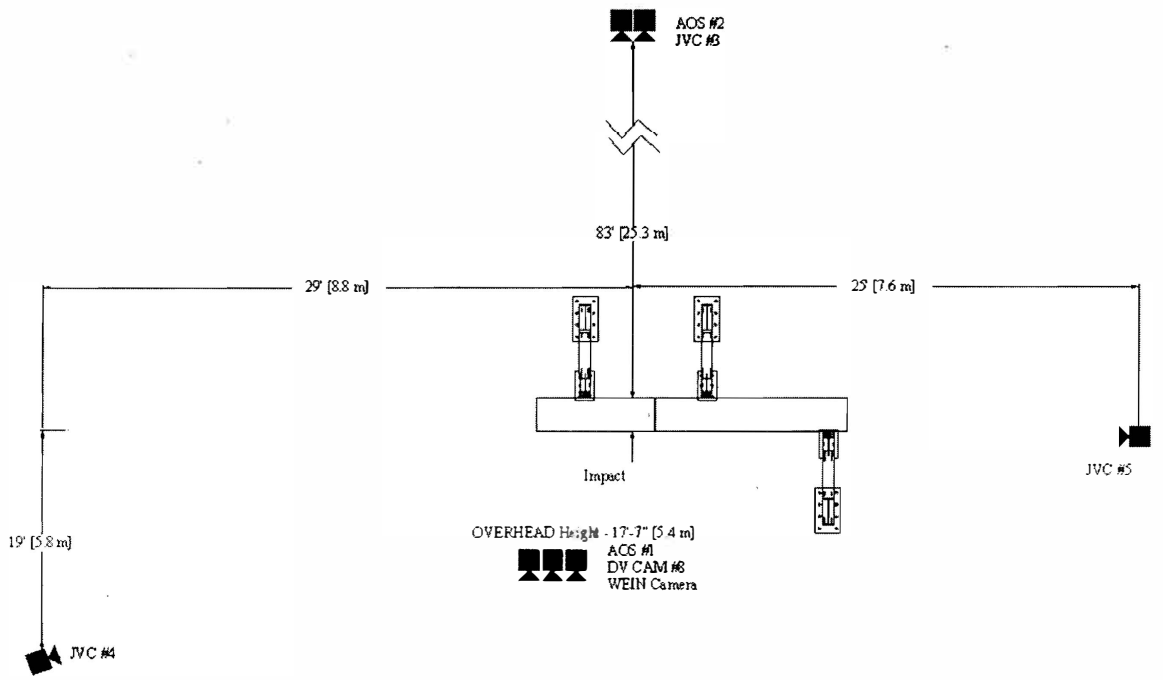

Figure 50. Camera Locations, Test Nos. PCRB-1 and PCRB-2

6.5 Test Specimen – Selected Joint Designs

The most promising rail joint design from each of the two rail connection categories, grouted and dry, was selected. Recall, grouted joint designs were seen as initially stiffer and better equipped to handle tolerances and curvature, while dry joint designs were seen as easier and quicker to construct and disassemble. Both of the joints were expected to provide adequate

shear and moment capacity. Thus, testing one of each joint type helped evaluate the benefits of one design method over the other in terms of maximum strength, toughness, and constructability. The two selected joints, Joint Design H and Joint Design D, are described in detail in Sections 6.5.1 and 6.5.2, respectively.

6.5.1 Test No. PCRB-1, Joint Design H

The test specimen used for bogie test no. PCRB-1 consisted of two reinforced concrete rail segments connected by two I-shaped steel sections and grout, as shown in Figures 51 through 62. The cross-sectional geometry of the concrete rail segments resembled that of the upper rail of the selected bridge rail design, Concept F (Fence). One rail segment had a length of 9 ft – 6 in. (2.90 m) while the other had a length of 5 ft (1.52 m). The concrete used to construct each rail had a design strength of 5,000 psi (34 MPa).

Both stirrups and longitudinal bars were used as steel reinforcement for the rail segments, as shown in Figures 53 through 57. The closed loop stirrups were bent from no. 4 rebar and were spaced at 8 in. (203 mm). Near the ends of the segments this spacing was reduced to 4 in. (102 mm) to protect against localized damage from the anchor post supports and the impact head. All stirrups were given a minimum clear cover of 1½ in. (38 mm). Two no. 5 longitudinal bars were placed on each side of the rail and two no. 4 bars were placed in the middle for a total of six (6) longitudinal bars. All of the internal reinforcement for the rail segments was epoxy coated Grade 60 rebar.

One end of each rail was configured with steel pockets on the front and back faces of the rail segment. These pockets were 6 x 6 x ½-in. (152 x 152 x 13-mm) A500 Grade C steel tubes cut to match the cross section geometry, as shown in Figures 59 and 60. Also, a ¾-in. (19-mm) wide vertical slot was cut through the side of the tube on the end plane to allow the web of the I-

shaped steel section to span between the pockets. To hold the I-shape segment and the grout in the pocket, a ⅛-in. (3-mm) thick steel plate was welded to the bottom of the pocket as an end cap. Gusset plates measuring ¼ in. (6 mm) thick were welded to the inside corners of the tubes to prevent the pockets from prying open during loading. They were positioned such that the steel segment could still drop in from the top. The gusset plates and end caps were all made from A572 Grade 50 steel and are shown in Figures 58 and 61.

Steel rebar was welded to the outside of the pockets to anchor the pockets to the concrete rails, as shown in Figure 58. A no. 4 bar was welded between the pockets to provide shear reinforcement and resist lateral movement. Also, two no. 6 bars were welded to the back of each pocket and lay adjacent to the no. 5 longitudinal bars in the concrete rail. These no. 6 bars provided anchorage for the pockets and transferred tension loads to the longitudinal bars of the concrete rail. All of the components comprising the end pocket assembly were galvanized.

The rail segments were placed on wooden support blocks and positioned as prescribed by Section 6.2 and Figure 48. To assemble the rail joint, two wide flange segments were dropped into the pockets with the web spanning across the ½-in. (13-mm) wide gap between rail ends. The steel segments were 5⅜-in. (137-mm) long S8x23 (S200x34) members. Once the segments were in place, L&M Crystex grout with a design strength of 10,000 psi (68.9 MPa) was used to fill the pockets and secure the steel sections. Photographs of the assembled joint specimen are shown in Figure 62.

Wide Flange Connection – Option B					
Item No.	QTY.	Description	Material Spec	Comment	File Name
p1	1	Wide Flange Connection Option B – 9.5 ft Beam	–	–	Beam_1–Grouted_Wide_Flange_Option-B_9.5ft
p2	1	Wide Flange Connection Option B – 5 ft Beam	–	–	Beam_1–Grouted_Wide_Flange_Option-B_5ft
e5	2	Option B L&M Crystex Grout	L&M Crystex Grout – f'c = 10000 psi	–	Beam_1–Grouted_Wide_Flange_Option_B_grout
e6	2	Option B S8x23	A36 Steel – Galvanized	–	Beam_1–Grouted_Wide_Flange_Option_B_S8x23

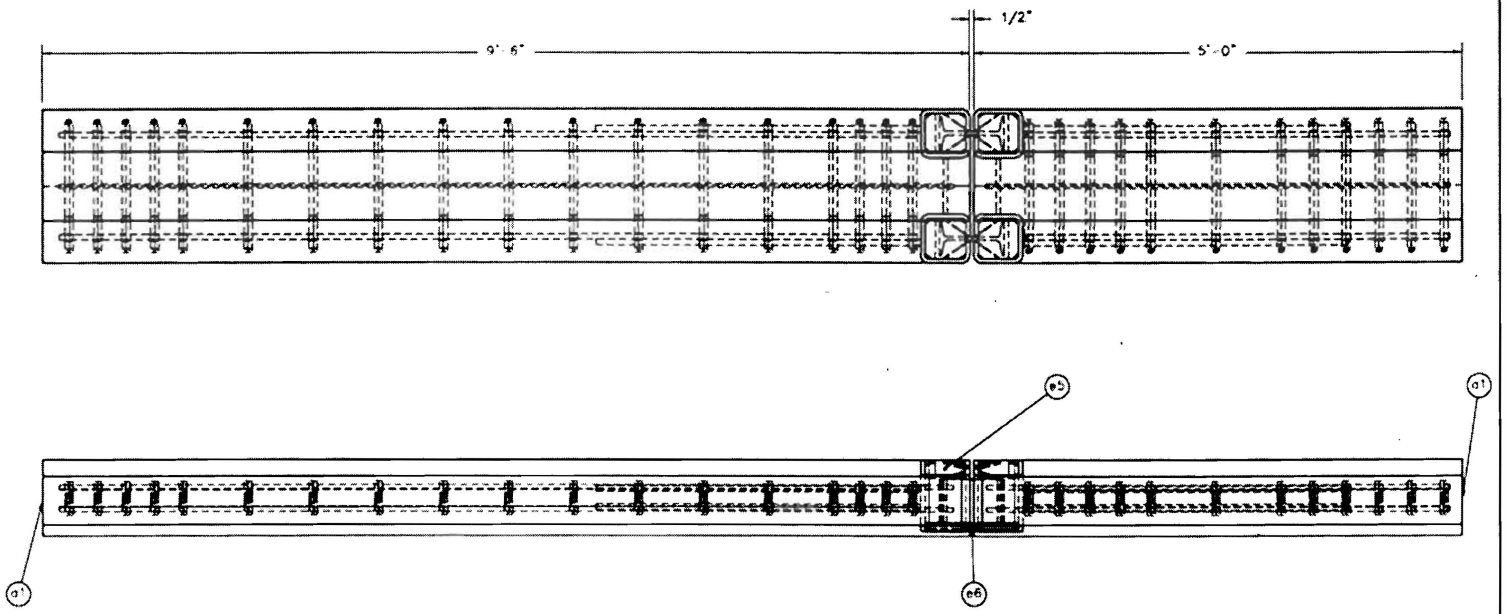

Midwest Roadside Safety Facility

Wide Flange Connection Option B

Assembled Beams

Figure 51. Wide Flange Joint Test Specimen, Test No. PCRB-1

Wide Flange Connection – Option B

Item No.	QTY.	Description	Material Spec	Comment	File Name
p1	1	Wide Flange Connection Option B – 9.5 ft Beam	–	–	Beam_1–Grouted_Wide_Flange_Option-B_9.5ft
p2	1	Wide Flange Connection Option B – 5 ft Beam	–	–	Beam_1–Grouted_Wide_Flange_Option-B_5ft
e5	2	Option B L&M Crystex Grout	L&M Crystex Grout – f'c = 10000 psi	–	Beam_1–Grouted_Wide_Flange_Option_B_grout
e6	2	Option B S8x23	A36 Steel – Galvanized	–	Beam_1–Grouted_Wide_Flange_Option_B_S8x23

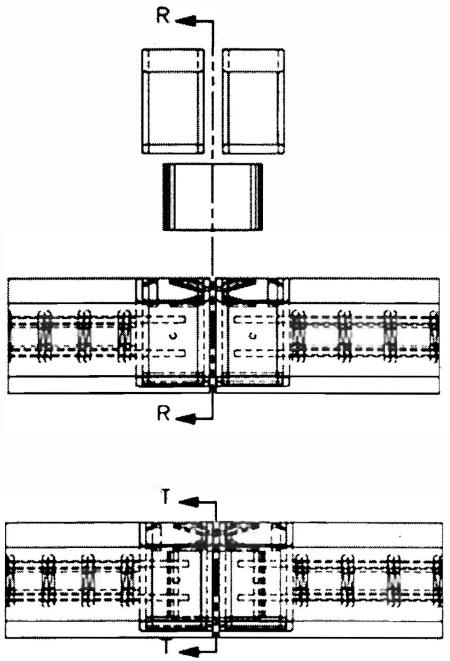

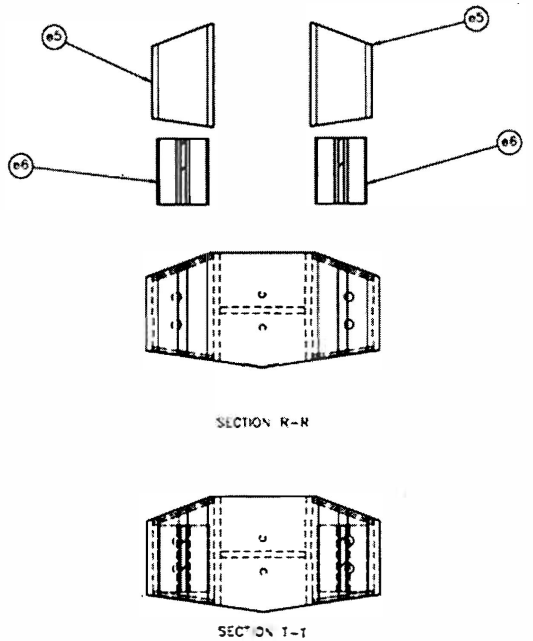

Midwest Roadside Safety Facility

Wide Flange Connection Option B

Connection Detail

Figure 52. Wide Flange Joint Assembly, Test No. PCRB-1

Wide Flange Connection – Option B

Item No.	QTY	Description	Material Spec	Comment	File Name
a1	1	Precast Concrete Bridge Rail Section	SSC f'c = 5000 psi	–	Beam_1–Grouted_Wide_Flange_Option_B_body_9.5ft
b1	18	No. 4 Top Rail Stirrup	A615 Grade 60 – Epoxy Coated	–	Beam_1–Grouted_Wide_Flange_toprail_stirrup_No.4_Grade60
b2	2	No. 4 Longitudinal Rebar	A615 Grade 60 – Epoxy Coated	–	Beam_1–Grouted_Wide_Flange_Option_B_9.5ft_longbar_No.4_Grade60
b3	4	No. 5 Longitudinal Rebar	A615 Grade 60 – Epoxy Coated	–	Beam_1–Grouted_Wide_Flange_Option_B_9.5ft_longbar_No.5_Grade60
d1	1	Wide Flange Connection Option B	–	–	Beam_1–Grouted_Wide_Flange_Option_B

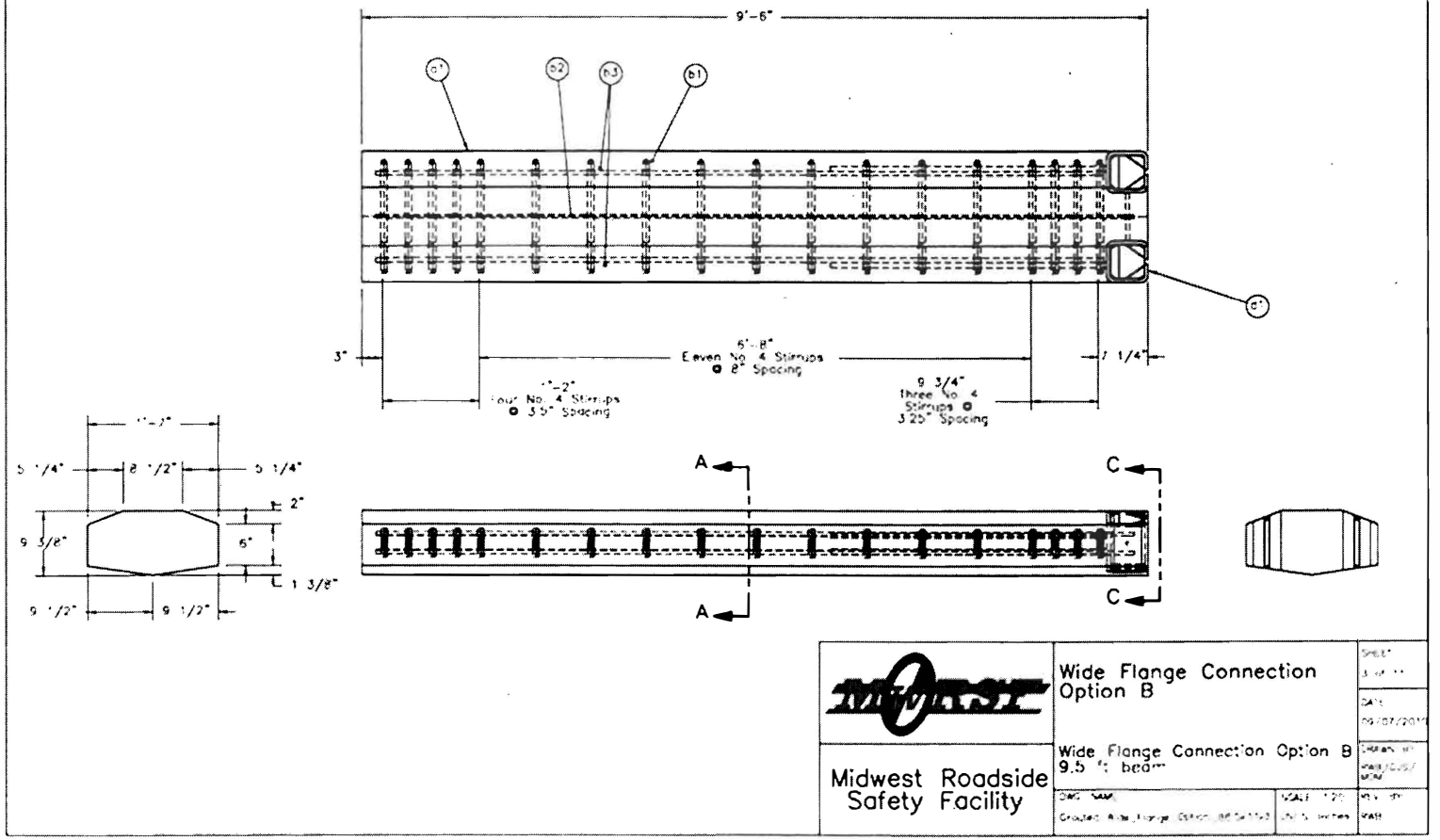

Figure 53. Long Rail Segment, Test No. PCRB-1

Wide Flange Connection – Option B					
Item No.	QTY	Description	Material Spec	Comment	File Name
a1	1	Precast Concrete Bridge Rail Section	SSC f'c = 5000 psi	–	Beam_1 – Grouted_Wide_Flange_Option_B_body_9.5ft
b1	18	No. 4 Top Rail Stirrup	A615 Grade 60 – Epoxy Coated	–	Beam_1 – Grouted_Wide_Flange_toprail_stirrup_No.4_Grade60
b2	2	No. 4 Longitudinal Rebar	A615 Grade 60 – Epoxy Coated	–	Beam_1 – Grouted_Wide_Flange_Option_B_9.5ft_longbar_No.4_Grade60
b3	4	No. 5 Longitudinal Rebar	A615 Grade 60 – Epoxy Coated	–	Beam_1 – Grouted_Wide_Flange_Option_B_9.5ft_longbar_No.5_Grade60

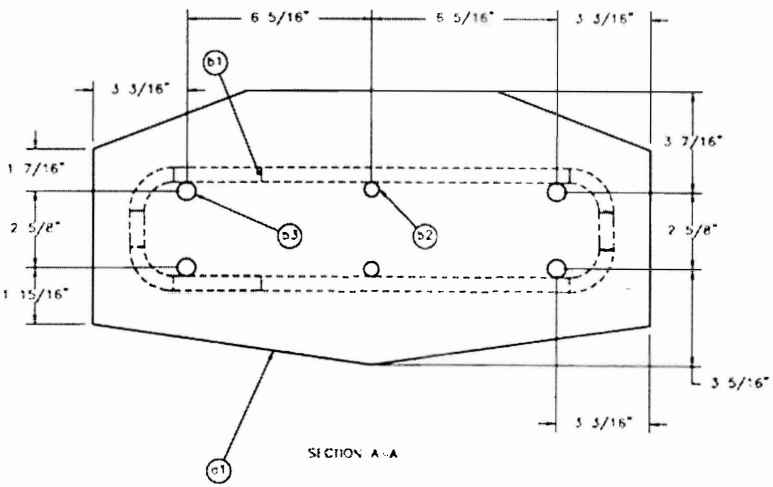

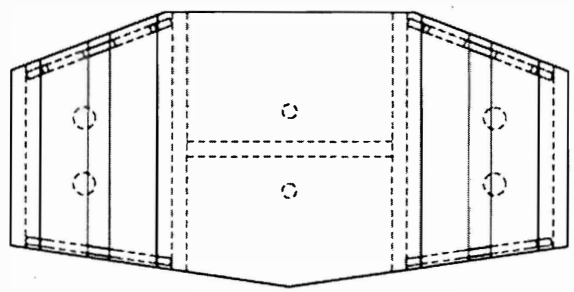

Note:
1. Stirrup clear cover is 1.5" on the side and 2.625" from the top face of the rail section

Midwest Roadside Safety Facility	Wide Flange Connection Option B Main Beam Reinforcement 9.5 ft Beam and Connection End View	SHEET DATE DRAWN BY REV. BY
	DWG. NAME SCALE UNITS	

Figure 54. Cross Section Views of Long Rail Segment, Test No. PCRB-1

Wide Flange Connection – Option B					
Item No.	QTY.	Description	Material Spec	Comment	File Name
b1	1	No. 4 Top Rail Stirrup	A615 Grade 60 – Epoxy Coated	–	Grouted_Wide_Flange_Beam_1–top rail_stirrup_No.4_Grade60
b2	1	No. 4 Longitudinal Rebar	A615 Grade 60 – Epoxy Coated	–	Grouted_Wide_Flange_Beam_1–Option_B_9.5ft_longbar_No.4_Grade60
b3	1	No. 5 Longitudinal Rebar	A615 Grade 60 – Epoxy Coated	–	Grouted_Wide_Flange_Beam_1–Option_B_9.5ft_longbar_No.5_Grade60
b4	1	No. 5 Longitudinal Rebar	A615 Grade 60 – Epoxy Coated	–	Grouted_Wide_Flange_Beam_1–Option_B_5ft_longbar_No.5_Grade60
b5	1	No. 4 Longitudinal Rebar	A615 Grade 60 – Epoxy Coated	–	Grouted_Wide_Flange_Beam_1–Option_B_5ft_longbar_No.4_Grade60

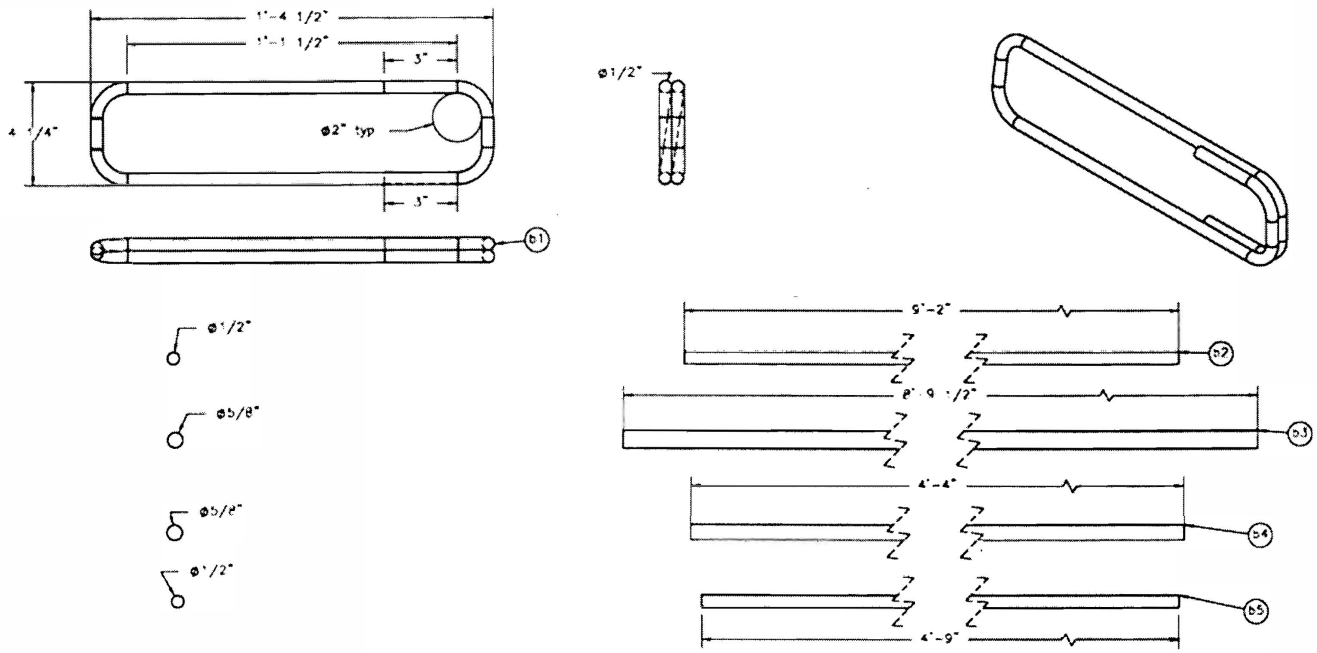

Midwest Roadside Safety Facility

Wide Flange Connection
Option B

Reinforcing Steel
9.5 ft Beam
5 ft Beam

Figure 55. Rail Steel Reinforcement, Test No. PCRB-1

Wide Flange Connection – Option B

Item No.	QTY	Description	Material Spec	Comment	File Name
a1	1	Precast Concrete Bridge Rail Section	SSC f'c = 5000 psi	–	Beam_1–Grouted_Wide_Flange_Option_B_body_5ft
b1	12	No. 4 Top Rail Stirrup	A615 Grade 60 – Epoxy Coated	–	Beam_1–Grouted_Wide_Flange_toprail_stirrup_No.4_Grade60
b4	4	No. 5 Longitudinal Rebar	A615 Grade 60 – Epoxy Coated	–	Beam_1–Grouted_Wide_Flange_Option_B_5ft_longbar_No.5_Grade60
b5	2	No. 4 Longitudinal Rebar	A615 Grade 60 – Epoxy Coated	–	Beam_1–Grouted_Wide_Flange_Option_B_5ft_longbar_No.4_Grade60
d1	1	Wide Flange Connection Option B	–	–	Beam_1–Grouted_Wide_Flange_Option_B

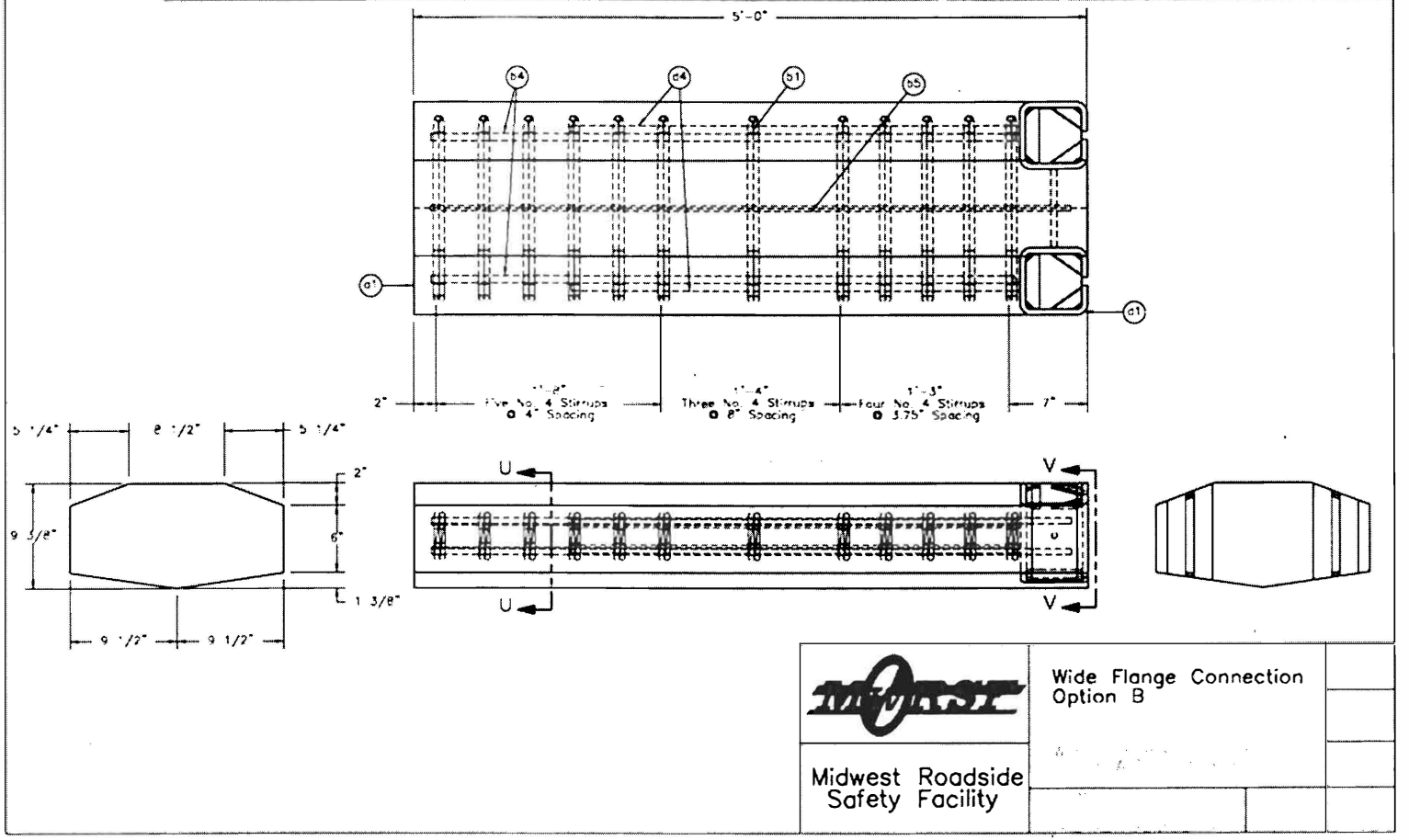

Figure 56. Short Rail Segment, Test No. PCRB-1

Wide Flange Connection – Option B					
Item No.	QTY	Description	Material Spec	Comment	File Name
a1	1	Precast Concrete Bridge Rail Section	SSC f'c = 5000 psi	–	Beam_1 – Grouted_Wide_Flange_Option_B_body_5ft
b1	12	No. 4 Top Rail Stirrup	A615 Grade 60 – Epoxy Coated	–	Beam_1 – Grouted_Wide_Flange_toprail_stirrup_No.4_Grade60
b4	4	No. 5 Longitudinal Rebar	A615 Grade 60 – Epoxy Coated	–	Beam_1 – Grouted_Wide_Flange_Option_B_5ft_longbar_No.5_Grade60
b5	2	No. 4 Longitudinal Rebar	A615 Grade 60 – Epoxy Coated	–	Beam_1 – Grouted_Wide_Flange_Option_B_5ft_longbar_No.4_Grade60

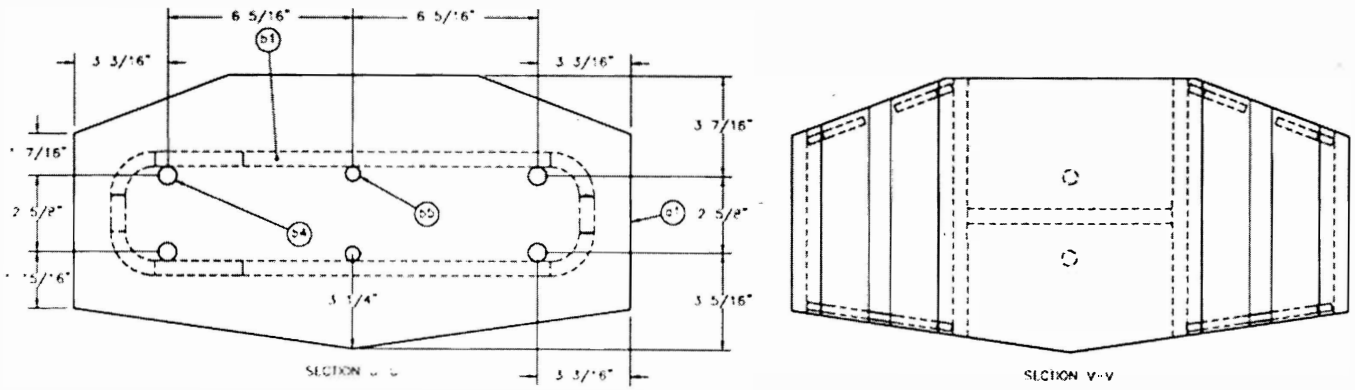

Midwest Roadside Safety Facility

Wide Flange Connection
Option B

Main Beam Reinforcement
5 ft Beam and
Connection End View

DWG. NAME: Grouted_Wide_Flange_Option_B8.5x11x3
SCALE: 1:5
UNITS: Inches
REV. BY: RWB

Figure 57. Cross Section Views of Short Rail Segment, Test No. PCRB-1

Wide Flange Connection - Option B

Item No.	QTY.	Description	Material Spec	Comment	File Name
d2	1	Option B Grout Tube Left 6x6x0.5	A500 Grade C - Galvanized	-	Grouted_Wide_Flange_Option_B_grout_pocket_left_6x6x0.5
d3	1	Option B Grout Tube Right 6x6x0.5	A500 Grade C - Galvanized	-	Grouted_Wide_Flange_Option_B_grout_pocket_right_6x6x0.5
d4	4	Option B No. 6 dbo	A706 Grade 60 - Galvanized	-	Grouted_Wide_Flange_Option_B_No.6_Grade60_dbo
d5	2	Option B Grout Tube Cap	A572 Grade 50 - Galvanized	-	Grouted_Wide_Flange_Option_B_grout_pocket_cap
d6	4	Option B Grout Tube Gusset	A572 Grade 50 - Galvanized	-	Grouted_Wide_Flange_Option_B_grout_pocket_gusset
d7	1	Option B No. 4 dbo	A706 Grade 60 - Galvanized	-	Grouted_Wide_Flange_Option_B_No.4_Grade60_dbo
d8	2	Option B Grout Pocket Back Gusset	A572 Grade 50 - Galvanized	-	Grouted_Wide_Flange_Option_B_grout_pocket_back_gusset

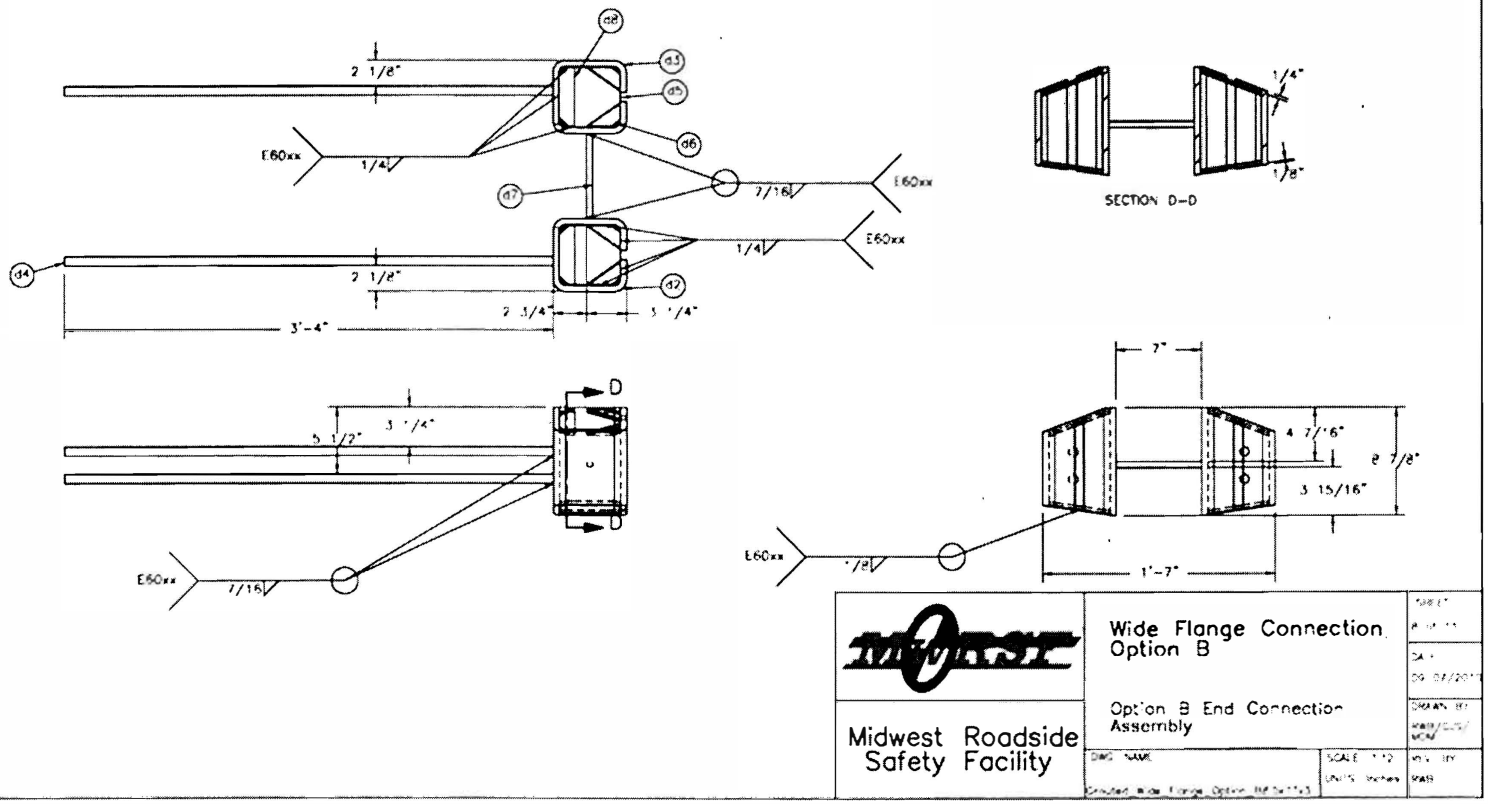

Figure 58. Grout Pocket Assembly and Reinforcement, Test No. PCRB-1

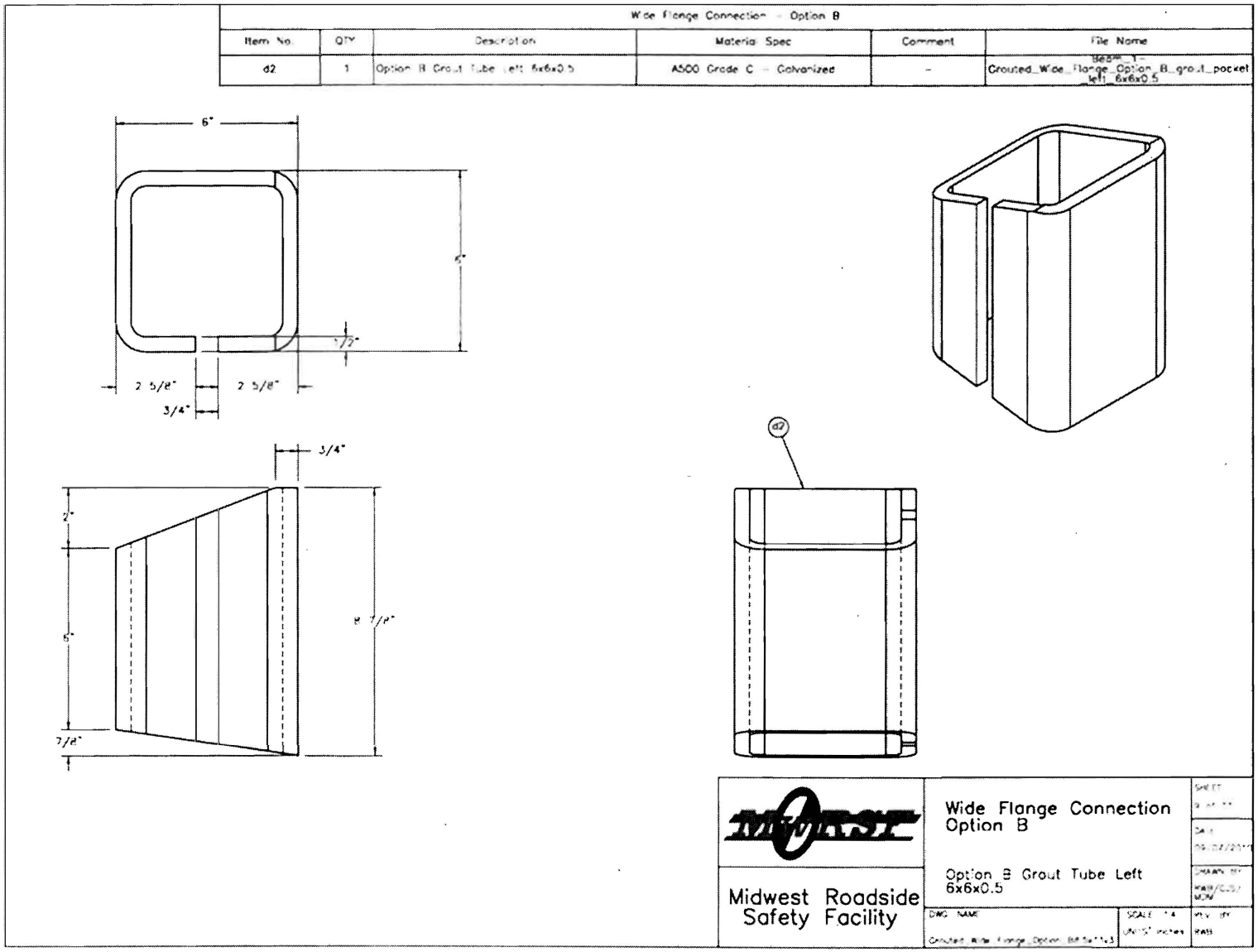

Figure 59. Left-Side Grout Pocket Details, Test No. PCRB-1

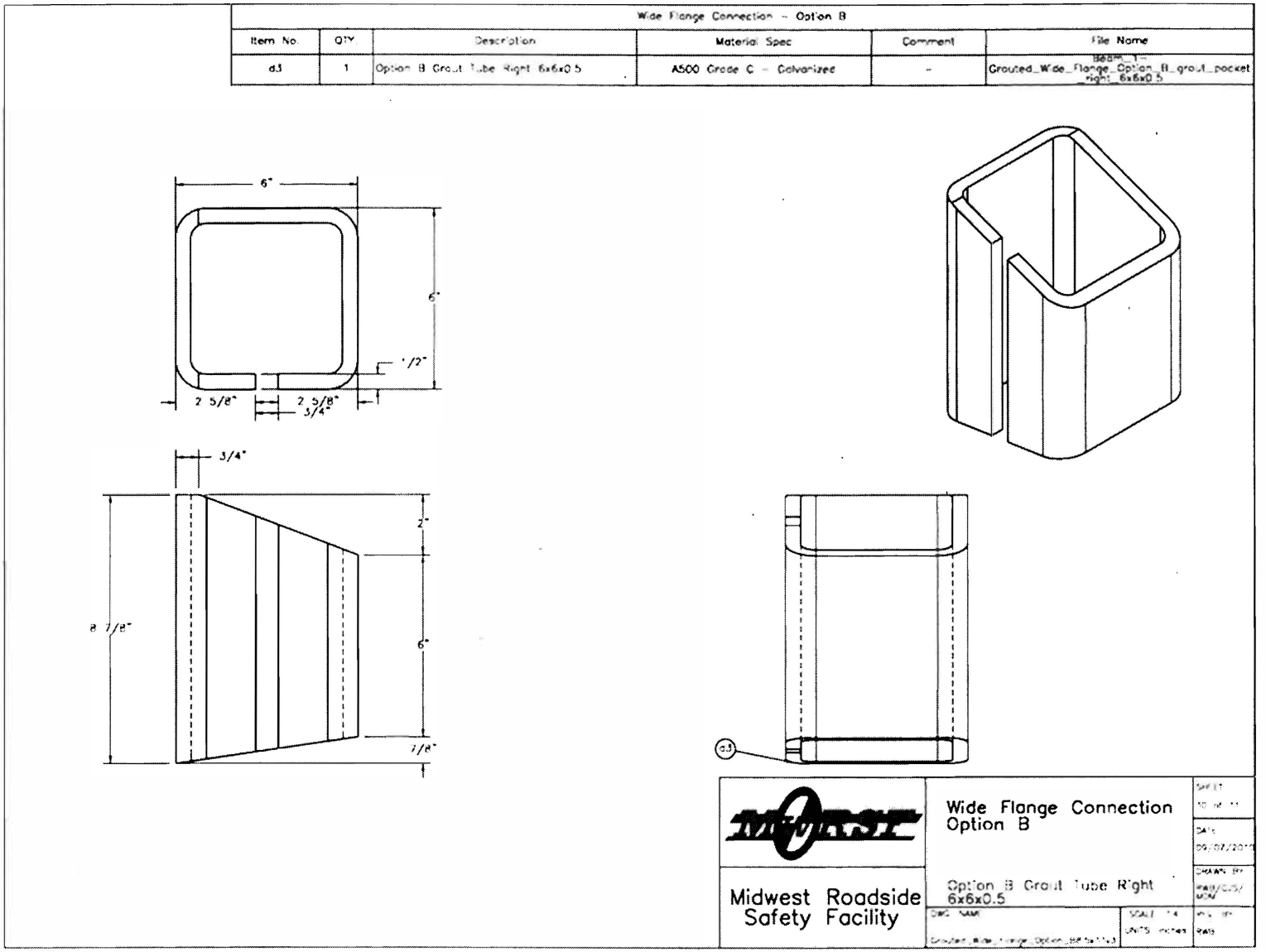

Figure 60. Right-Side Grout Pocket Details, Test No. PCRB-1

Wide Flange Connection – Option B					
Item No	QTY	Description	Material Spec	Comment	File Name
c6	1	Option B S8x23	A36 Steel – Galvanized	–	Beam_1–Grouted_Wide_Flange_Option_B_S8x23
d4	*	Option B No. 6 dbs	A706 Grade 60 – Galvanized	–	Beam_1–Grouted_Wide_Flange_Option_B_No.6_Grade60_dbs
d5	*	Option B Grout Tube Cap	A572 Grade 50 – Galvanized	–	Beam_1–Grouted_Wide_Flange_Option_B_grout_pocket_cap
d6	1	Option B Grout Tube Gusset	A572 Grade 50 – Galvanized	–	Beam_1–Grouted_Wide_Flange_Option_B_grout_pocket_gusset
d7	*	Option B No. 4 dbs	A706 Grade 60 – Galvanized	–	Beam_1–Grouted_Wide_Flange_Option_B_No.4_Grade60_dbs
d8	1	Option B Grout Pocket Block Gusset	A572 Grade 50 – Galvanized	–	Beam_1–Grouted_Wide_Flange_Option_B_grout_pocket_block_gusset

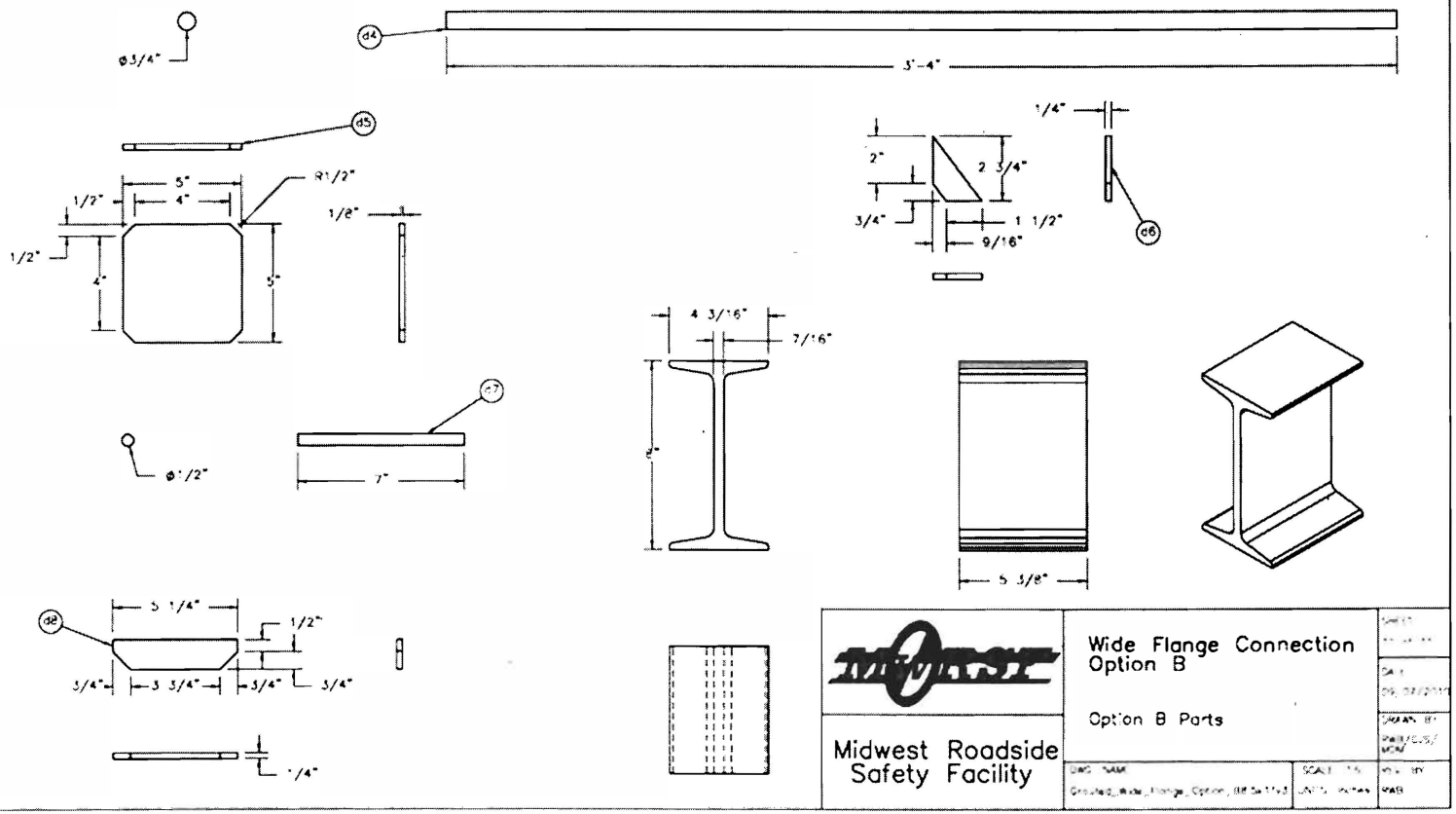

Figure 61. Pocket Reinforcement Details and Wide Flange Section, Test No. PCRB-1

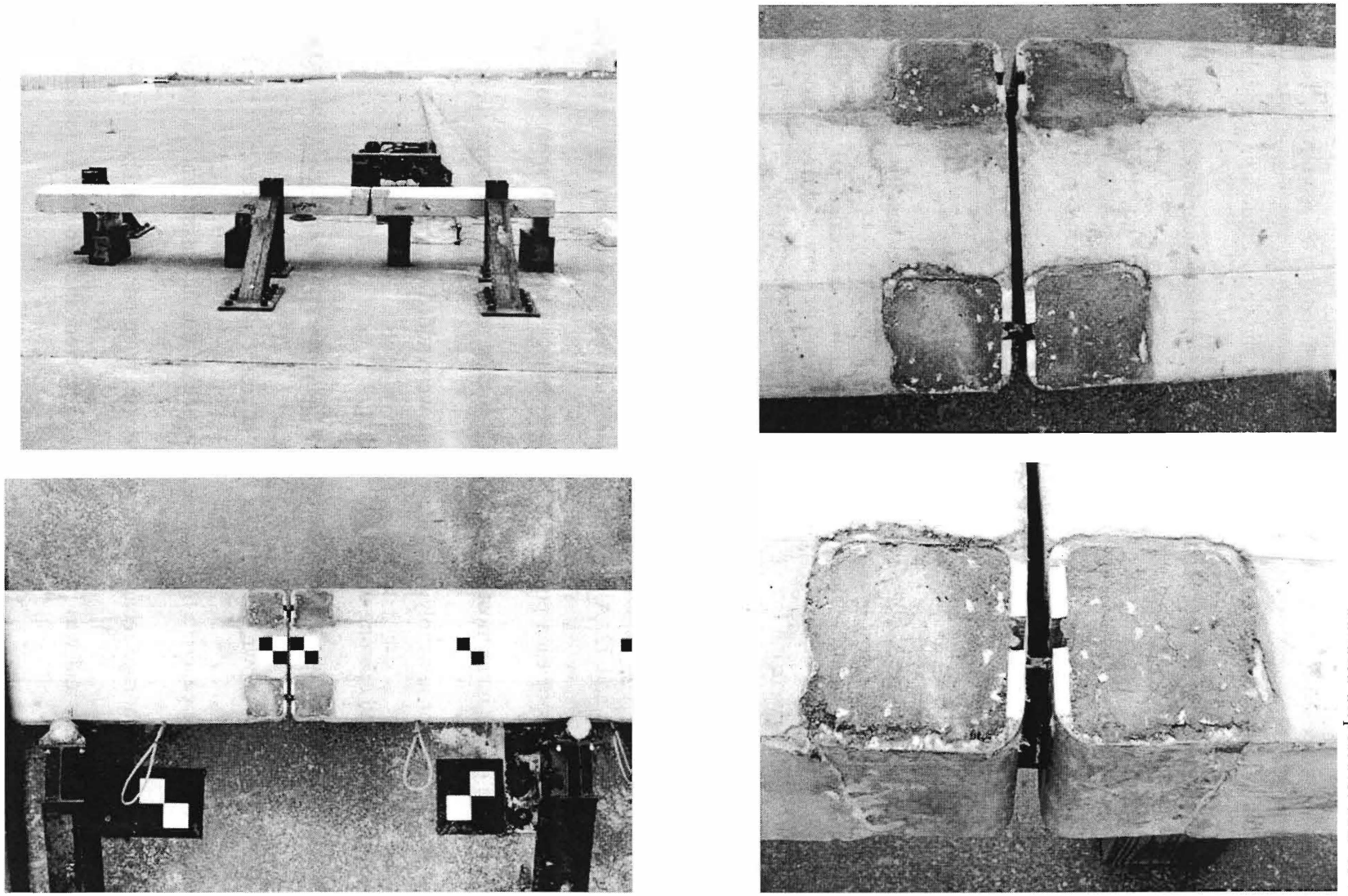

Figure 62. Rail Component Photographs, Test No. PCRB-1

6.5.2 Test No. PCRB-2, Joint Design D

The test specimen used for bogie test no. PCRB-2 consisted of two reinforced concrete rail segments connected by two bolts and two shear tubes, as shown in Figures 63 through 75. The concrete rail segments had the same lengths, cross sectional geometries, and steel reinforcement configurations as the rail segments used during test no. PCRB-1. These dimensions and reinforcement configurations are shown in Figures 65 through 69. The concrete design strength remained at 5,000 psi (34 MPa) and the use of epoxy coated Grade 60 rebar was again used for all internal reinforcing bars.

As opposed to the previous joint design test, this joint design test specified the rail end pockets as open on the underside of the rail. This configuration concealed all of the joint hardware. The steel pockets were cut from a 14½-in. (368 mm) long piece of 10 x 4 x ½-in. (254 x 102 x 13-mm) A500 Grade C steel tubing such that two pockets were created from each section of tube. The tubes were cut to follow the bottom geometry of the rail for both sides of the rail, as shown in Figures 71 and 72. Also, ½-in. (13-mm) diameter holes were placed near the bottom corner on both sides of each pocket for the shear bolts. A nut for the shear bolts was welded over the hole on the inner most surface of each pocket, as shown in Figure 70, so that only the bolt was needed for assembly. The shear bolts were added to prevent the side of the steel tube from deforming and opening under shear loading.

Two ½-in. (13-mm) thick gusset plates made from A572 Grade 50 steel were welded inside each of the pockets, as shown in Figure 70. A solid gusset plate was welded near the back end of the pocket to prevent concrete from entering the pocket during casting and to provide a welding surface for the anchorage rebar. The second gusset plate contained a 1⅛-in. (29-mm) diameter hole near its center and was placed 3 in. (76 mm) from the end of the pocket. This

gusset enabled pockets from adjacent rail segments to be bolted together. Both gusset plates are shown in Figure 73.

Steel bars and plates were used to anchor the pockets in both the lateral and longitudinal directions. A $^{5}/_{16}$-in. (8-mm) thick A572 Grade 50 steel plate was welded between the pockets near the end of the rail, while two no. 5 bars were welded between the pockets near the middle and at the opposite end of the pockets. To anchor the pockets longitudinally, two no. 6 bars were welded to each pocket and extended into the rail. One rebar was welded directly to the back gusset plate while the other was welded to the face of the inner most surface of each pocket. Both the lateral and longitudinal anchorage bars and plates are shown in Figures 70 and 73. All of the steel components of the end pocket assembly, including gusset plates and anchorage bars, were galvanized.

The following hardware was necessary to assemble the joint between rail segments: two 1-in. (25-mm) diameter, 9-in. (229-mm) long Grade 5 bolts, four ½-in. (13-mm) diameter by 5-in. (127-mm) long Grade 5 bolts, two shear tubes made from 2 ½ x 2 ½ x ¼-in. (64 x 64 x 6-mm) A500 Grade C steel tubing, and two ½-in. (13-mm) thick shim plates. All of this hardware is shown in Figure 74. During assembly, first a shear tube was positioned inside adjacent pockets spanning the ½-in. (13-mm) gap between rail segments, as shown in Figure 64. Next, a 1-in. (25-mm) diameter bolt was inserted into a pocket between the gusset plates and slid through the gusset plate, shear tube, and gusset plate of the adjacent pocket. This process was repeated for the other side of the rail joint. Shims were then positioned in the gap between the rail segments and surrounding the shear tubes, as shown in Figure 64. The shim plates were intended to close the gap between rail ends left as a result of tolerance issues and provide a compression zone for bending resistance. The nuts and bolts were then tightened bringing the rail segments together

and clamping down on the shim plates. Finally, the ½-in. (13-mm) diameter shear bolts were inserted through the holes of each pocket and tightened into place to prevent the pockets from bending out during loading and to hold the shear tubes in place vertically.

The segments were set in the same positions as the segments in test no. PCRB-1, only the rail system was flipped upside down so that the joint hardware could be viewed from the overhead video during the test. Photographs of the assembled joint specimen for test no. PCRB-2 are shown in Figure 75.

Dry Connection					
Item No.	QTY	Description	Material Spec	Comment	File Name
p1	1	Dry Connection – 9.5 ft Beam	–	–	Beam2_Dry_9.5ft
p2	1	Dry Connection – 5 ft Beam	–	–	Beam2_Dry_5ft
f1	2	1.0 UNC-8 x9x 9 Grade 5 Heavy Hex Bolt	Grade 5 – Galvanized	–	HHBOLT 1.0000-8x8.5x2.5-C
f2	2	1.0 Heavy Hex Nut	Grade 5 – Galvanized	–	HHNUT 1.0000-8-D-C
f3	2	Shear Tube 2.5x2.5x0.25 with 0.125 shims	A500 Grade C – Galvanized	–	Beam2_Dry_sheartube_2.5x2.5x0.25_w_0.12 5shim
f4	2	Dry Connection Shim Plate	A36 Steel – Galvanized	Material will likely change following component testing	Beam2_Dry_shimplate

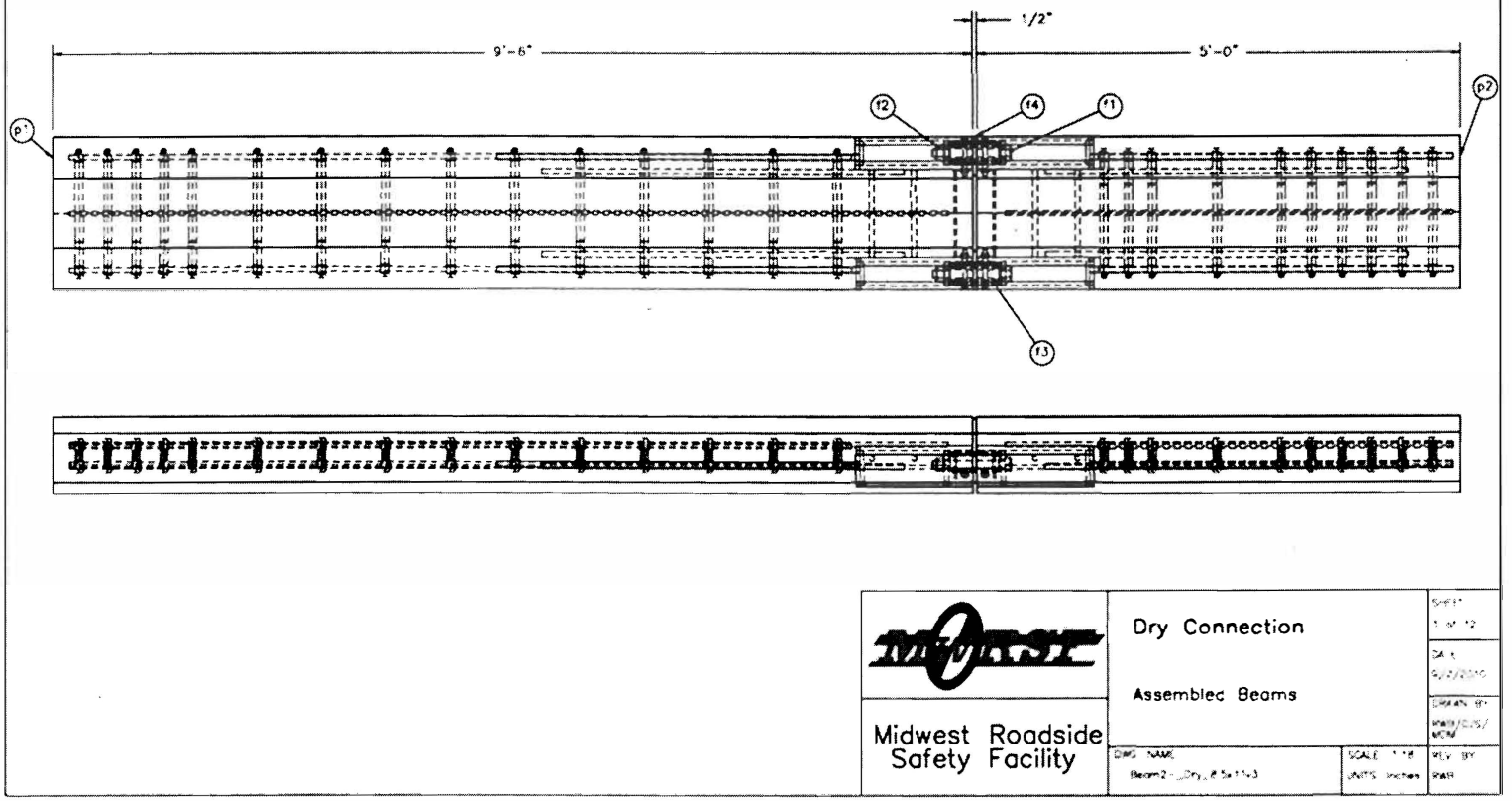

Figure 63. Side Bolts and Shear Tubes Joint Test Specimen, Test No. PCRB-2

Dry Connection					
Item No.	QTY	Description	Material Spec	Comment	File Name
p1	1	Dry Connection – 9.5 ft Beam	–	–	Beam2_Dry_9.5ft
p2	1	Dry Connection – 5 ft Beam	–	–	Beam2_Dry_5ft
f1	2	1.0 UNC-8 x9x 9 Grade 5 Heavy Hex Bolt	Grade 5 – Galvanized	–	HHBOLT 1.0000-8x8.5x2.5-C
f2	2	1.0 Heavy Hex Nut	Grade 5 – Galvanized	–	HHNUT 1.0000-8-D-C
f3	2	Shear Tube 2.5x2.5x0.25 with 0.125 shims	A500 Grade C – Galvanized	–	Beam2_Dry_shear tube_2.5x2.5x0.25_w_0.125shim
f4	2	Dry Connection Shim Plate	A36 Steel – Galvanized	Material will likely change following component testing	Beam2_Dry_shimplate

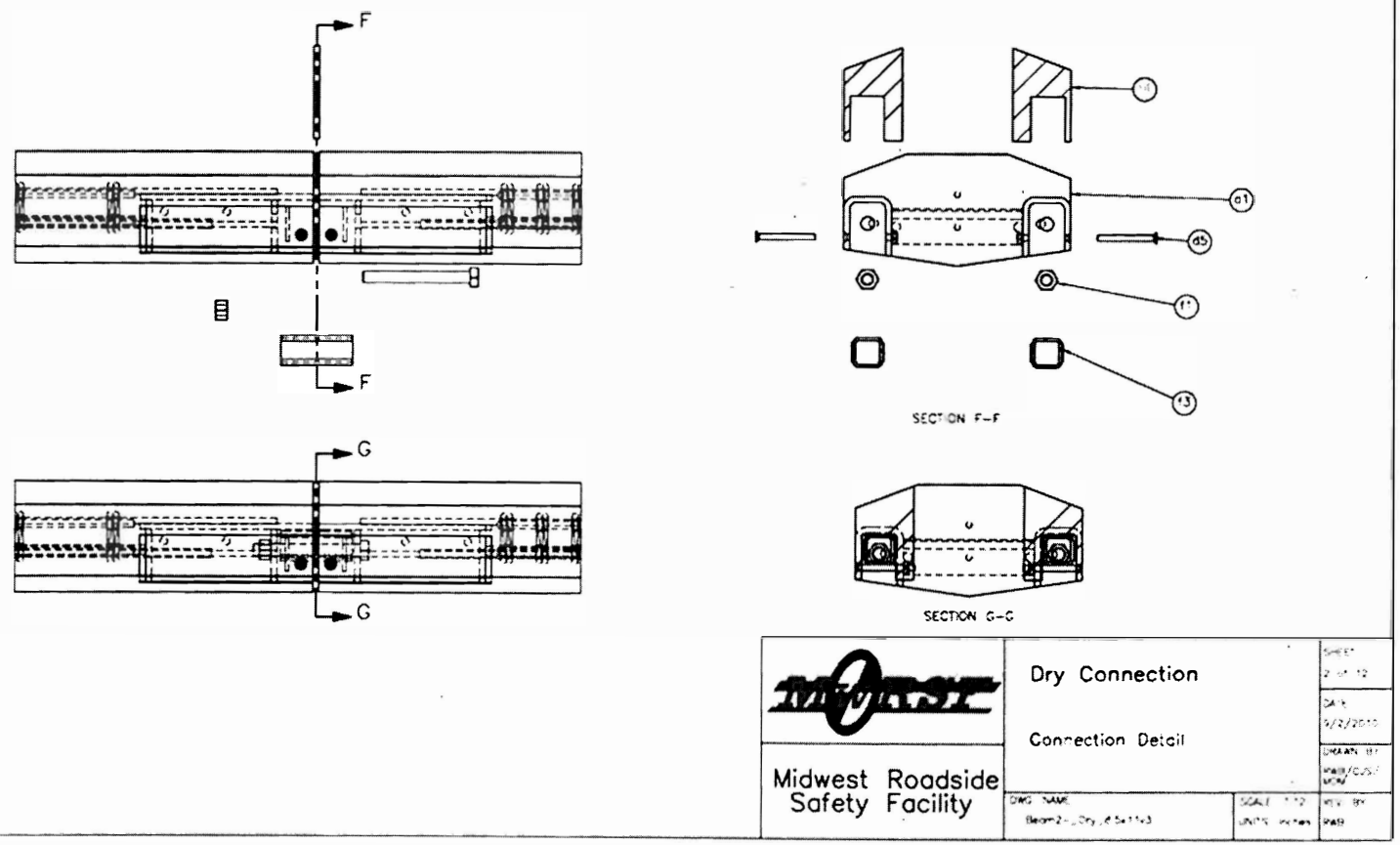

Figure 64. Side Bolts and Shear Tubes Joint Assembly, Test No. PCRB-2

Dry Connection					
Item No.	QTY	Description	Material Spec	Comment	File Name
a1	1	Precast Concrete Bridge Rail Section	SSC f'c = 5000 psi	–	Beam2_Dry_body_9.5ft
b1	15	No. 4 Top Rail Stirrup	A615 Grade 60 – Epoxy Coated	–	Beam2_Center_Bolt_and_Dry_toprail_stirrup_No.4_Grade60
b2	2	No. 4 Longitudinal Rebar	A615 Grade 60 – Epoxy Coated	–	Beam2_Dry_9.5ft_longbar_No.4_Grade60
b3	4	No. 5 Longitudinal Rebar	A615 Grade 60 – Epoxy Coated	–	Beam2_Dry_9.5ft_longbar_No.5_Grade60
c1	1	Dry Connection End Assembly	–	–	Beam2_Dry_end_connection_assembly

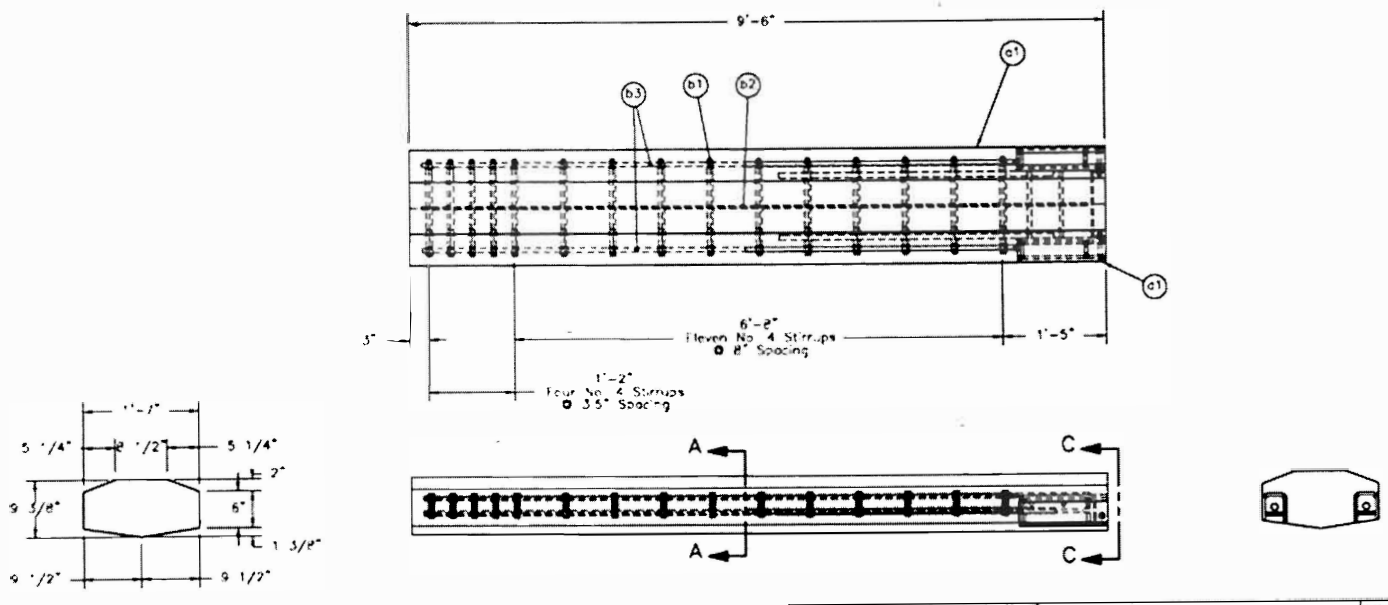

Midwest Roadside Safety Facility

Dry Connection

Dry Connection
9.5 ft Beam

Figure 65. Long Rail Segment, Test No. PCRB-2

Dry Connection					
Item No.	QTY	Description	Material Spec	Comment	File Name
a1	1	Precast Concrete Bridge Rail Section	SSC f'c = 5000 psi	–	Beam2_Dry_body_9.5ft
b1	15	No. 4 Top Rail Stirrup	A615 Grade 60 – Epoxy Coated	–	Beam2_Center_Bolt_and_Dry_toprail_stirrup_No.4_Grade60
b2	2	No. 4 Longitudinal Rebar	A615 Grade 60 – Epoxy Coated	–	Beam2_Dry_9.5ft_longbar_No.4_Grade60
b3	4	No. 5 Longitudinal Rebar	A615 Grade 60 – Epoxy Coated	–	Beam2_Dry_9.5ft_longbar_No.5_Grade60

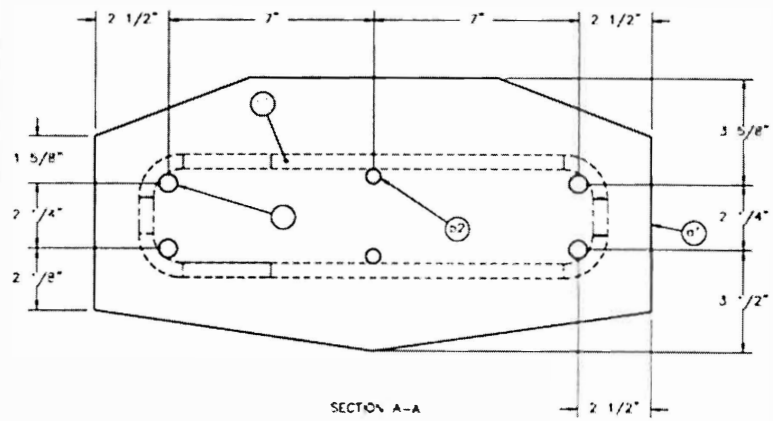

SECTION A–A

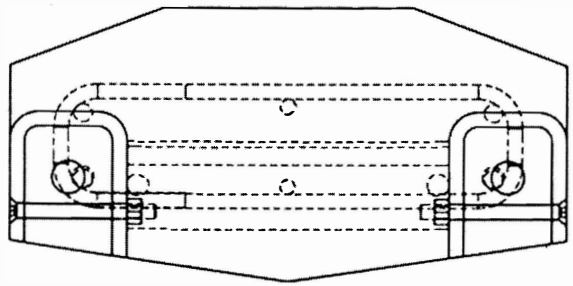

SECTION C–C

Note:
1 Stirrup clear cover is 1.5" on each side and 2.626" from the top face of the rail section

Midwest Roadside Safety Facility

Dry Connection

Main Beam Reinforcement
9.5 ft Beam and
Connection End View

Figure 66. Cross Section Views of Long Rail Segment, Test No. PCRB-2

Dry Connection					
Item No.	QTY.	Description	Material Spec	Comment	File Name
b1	1	No. 4 Top Rail Stirrup	A615 Grade 60 – Epoxy Coated	–	Beam2_Center_Rail_and_Dry_topra_stirrup_No.4_Grade60
b2	1	No. 4 Longitudinal Rebar	A615 Grade 60 – Epoxy Coated	–	Beam2_Dry_9.5ft_longbar_No.4_Grade60
b3	1	No. 5 Longitudinal Rebar	A615 Grade 60 – Epoxy Coated	–	Beam2_Dry_9.5ft_longbar_No.5_Grade60
b4	1	No. 4 Longitudinal Rebar	A615 Grade 60 – Epoxy Coated	–	Beam2_Dry_5ft_longbar_No.4_Grade60
b5	1	No. 5 Longitudinal Rebar	A615 Grade 60 – Epoxy Coated	–	Beam2_Dry_5ft_longbar_No.5_Grade60

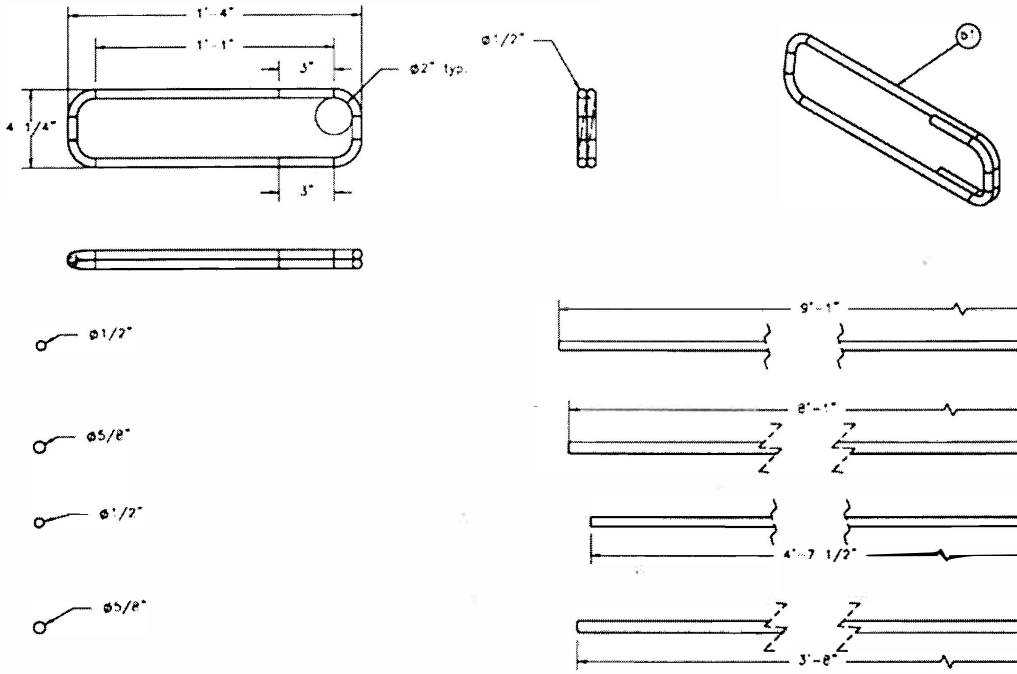

Midwest Roadside Safety Facility

Dry Connection

Reinforcing steel
9.5 ft Beam and
5 ft Beam

Figure 67. Rail Steel Reinforcement, Test No. PCRB-2

Dry Connection					
Item No.	QTY	Description	Material Spec	Comment	File Name
a1	1	Precast Concrete Bridge Rail Section	SSC f'c = 5000 psi	–	Beam2_Dry_body_5ft
b1	10	No. 4 Top Rail Stirrup	A615 Grade 60 – Epoxy Coated	–	Beam2_Center_Bolt_and_Dry_toprail_stirrup_No.4_Grade60
b4	2	No. 4 Longitudinal Rebar	A615 Grade 60 – Epoxy Coated	–	Beam2_Dry_5ft_longbar_No.4_Grade60
b5	4	No. 5 Longitudinal Rebar	A615 Grade 60 – Epoxy Coated	–	Beam2_Dry_5ft_longbar_No.5_Grade60
d1	1	Dry Connection End Assembly	–	–	Beam2_Dry_end_connection_assembly

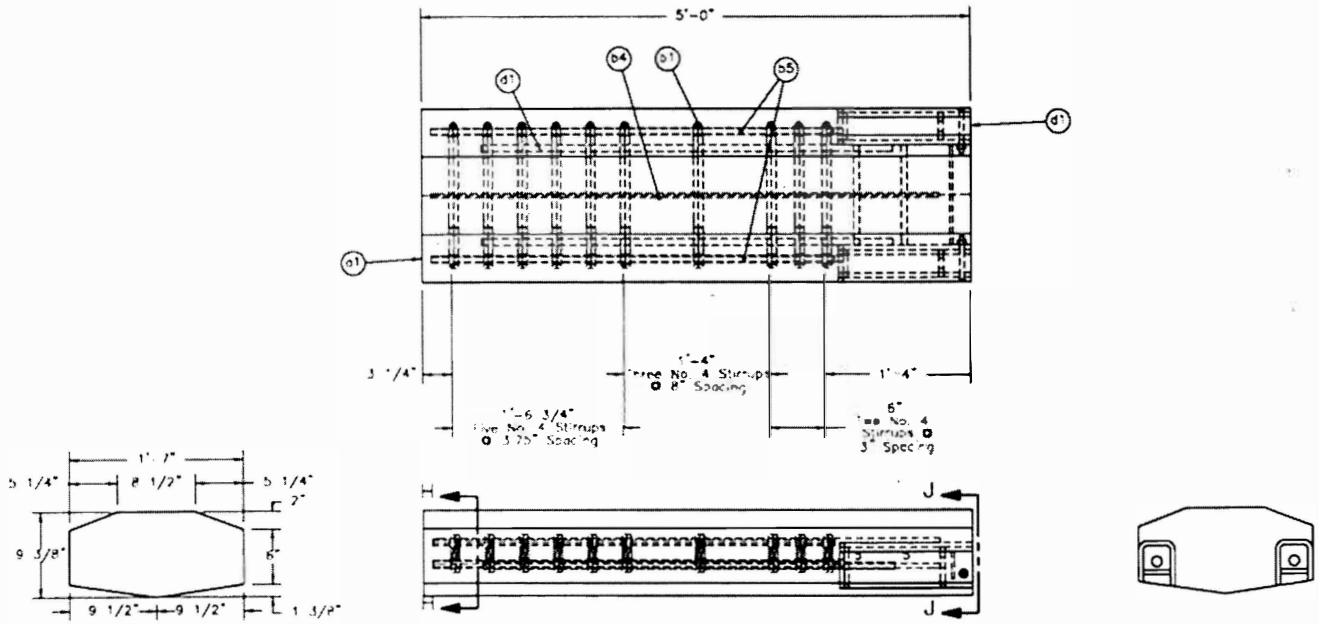

Midwest Roadside Safety Facility

Dry Connection

Dry Connection
5 ft Beam

Figure 68. Short Rail Segment, Test No. PCRB-2

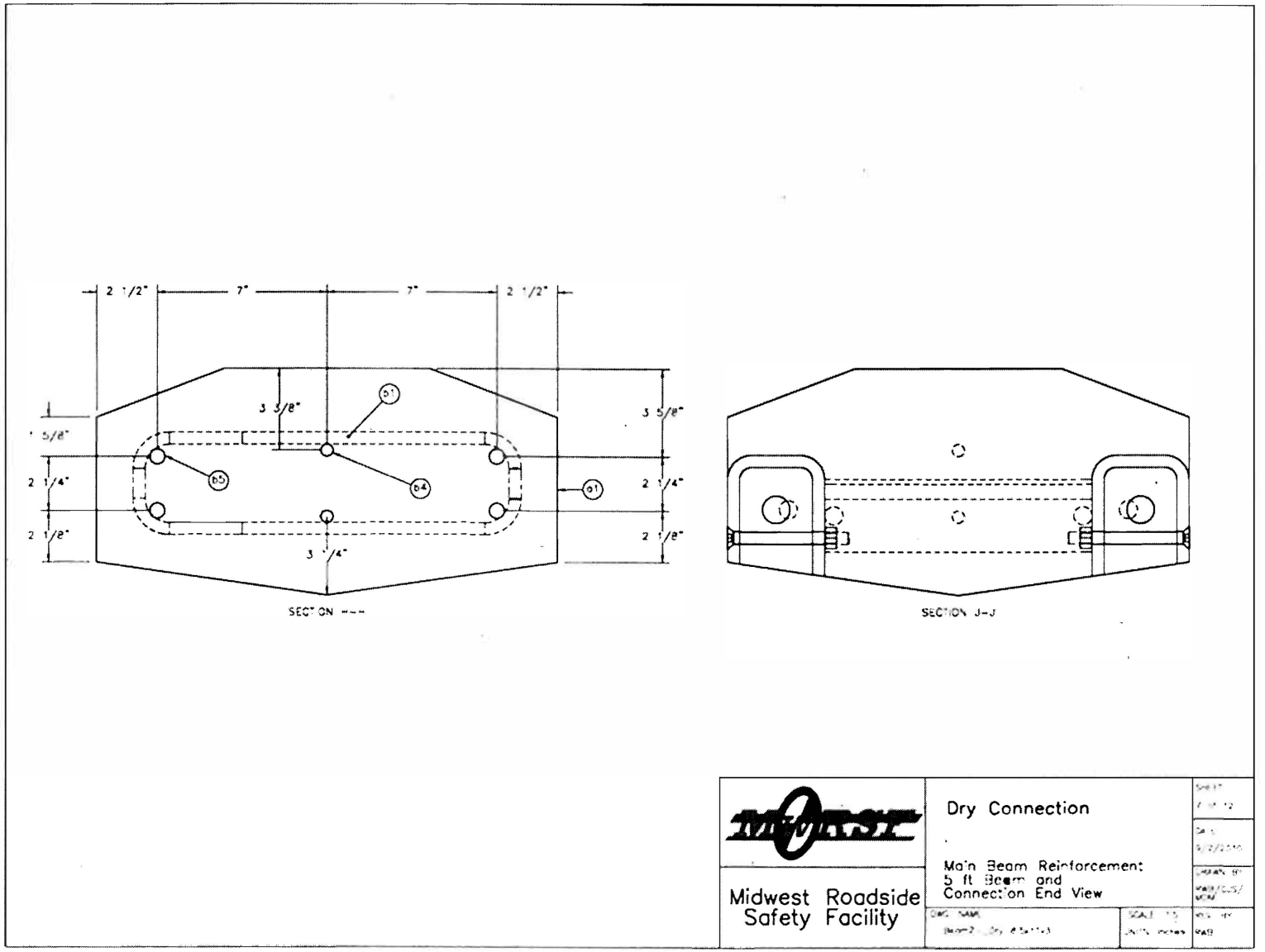

Figure 69. Cross Section Views of Short Rail Segment, Test No. PCRB-2

Dry Connection					
Item No.	QTY	Description	Material Spec	Comment	File Name
d2	1	Dry Connection Bolt Pocket Left	A500 Grade C Galvanized	Cut section of 10x4x0.5 tube	Beam2_Dry_bolt_pocket_4x4.5x0.5_left
d3	1	Dry Connection Bolt Pocket Right	A500 Grade C – Galvanized	Cut section of 10x4x0.5 tube	Beam2_Dry_bolt_pocket_4x4.5x0.5_right
d4	2	Dry Connection Bolt Pocket Cap	A572 Grade 50 – Galvanized	–	Beam2_Dry_bolt_pocket_cap
d5	2	0.5 UNC 13 x 5 Counter Sunk Allen Head Bolt	Grade 5 – Galvanized	–	SCHCSCREW 0.5–13x5x1.75–HX–C
d6	2	0.5 UNC 13 Heavy Hex Nut	Grade 5 – Galvanized	–	HHNUT 0.5000–13–D–N
d7	1	Dry Connection Shear Plate	A572 Grade 50 – Galvanized	–	Beam2_Dry_shear_plate_A572Gr50
d8	2	No. 5 Shear dbo	A706 Grade 60 – Galvanized	–	Beam2_Dry_dbo_No.5_Grade60
d9	4	Dry Connection No. 6 dbo	A706 Grade 60 – Galvanized	–	Beam2_Dry_No.6_Grade60_dbo
d10	2	Dry Connection Bolt Pocket End Cap	A572 Grade 50 – Galvanized	–	Beam2_Dry_bolt_pocket_end_cap

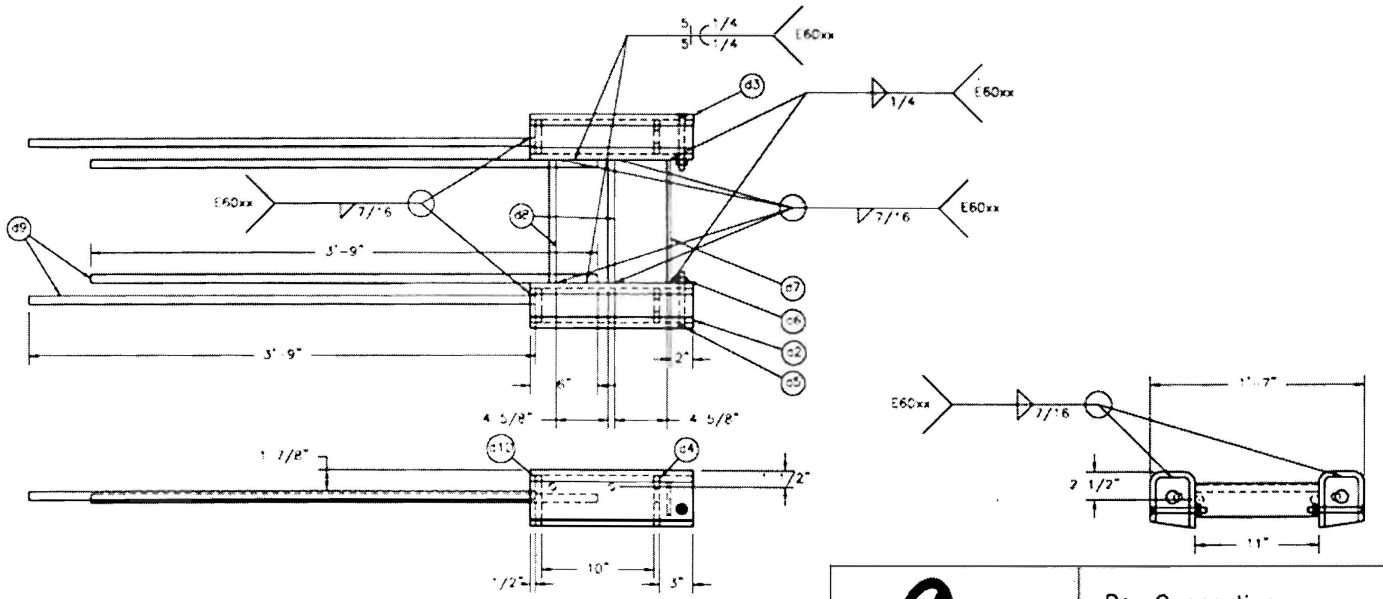

Midwest Roadside Safety Facility

Dry Connection

Connection Assembly

Figure 70. End Pockets Assembly and Reinforcement, Test No. PCRB-2

Dry Connection					
Item No.	QTY.	Description	Material Spec	Comment	File Name
d2	1	Dry Connection Bolt Pocket Left	A500 Grade C Galvanized	Cut section of 10x4x0.5 tube	Beam2_Dry_bolt_pocket_4x4.5x0.5_left

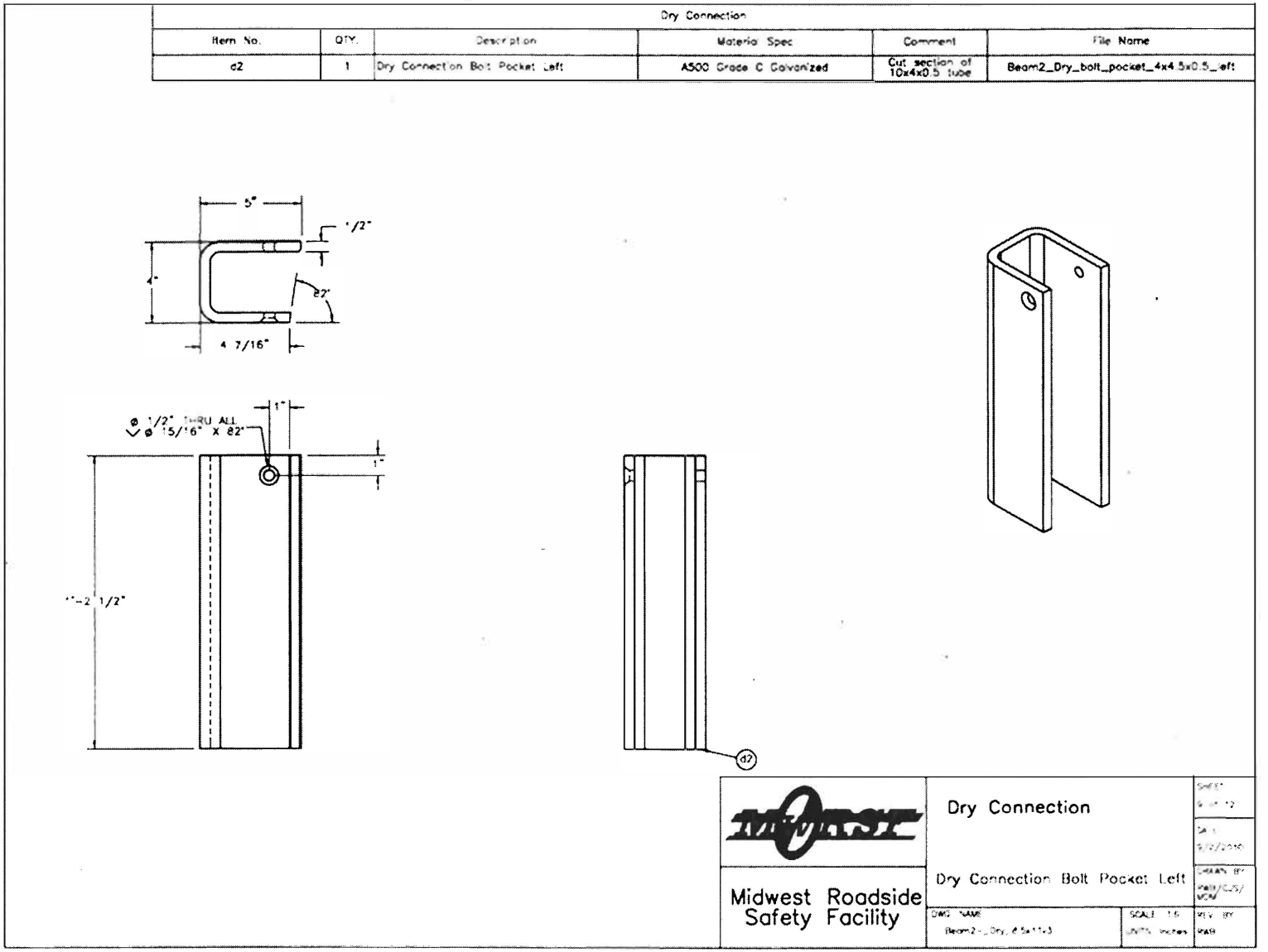

Figure 71. Left-Side Pocket Details, Test No. PCRB-2

Dry Connection					
Item No.	QTY	Description	Material Spec	Comment	File Name
d3	1	Dry Connection Bolt Pocket Right	A500 Grade C – Galvanized	Cut section of 10x4x0.5 tube	Beam2_Dry_bolt_pocket_4x4.5x0.5_right

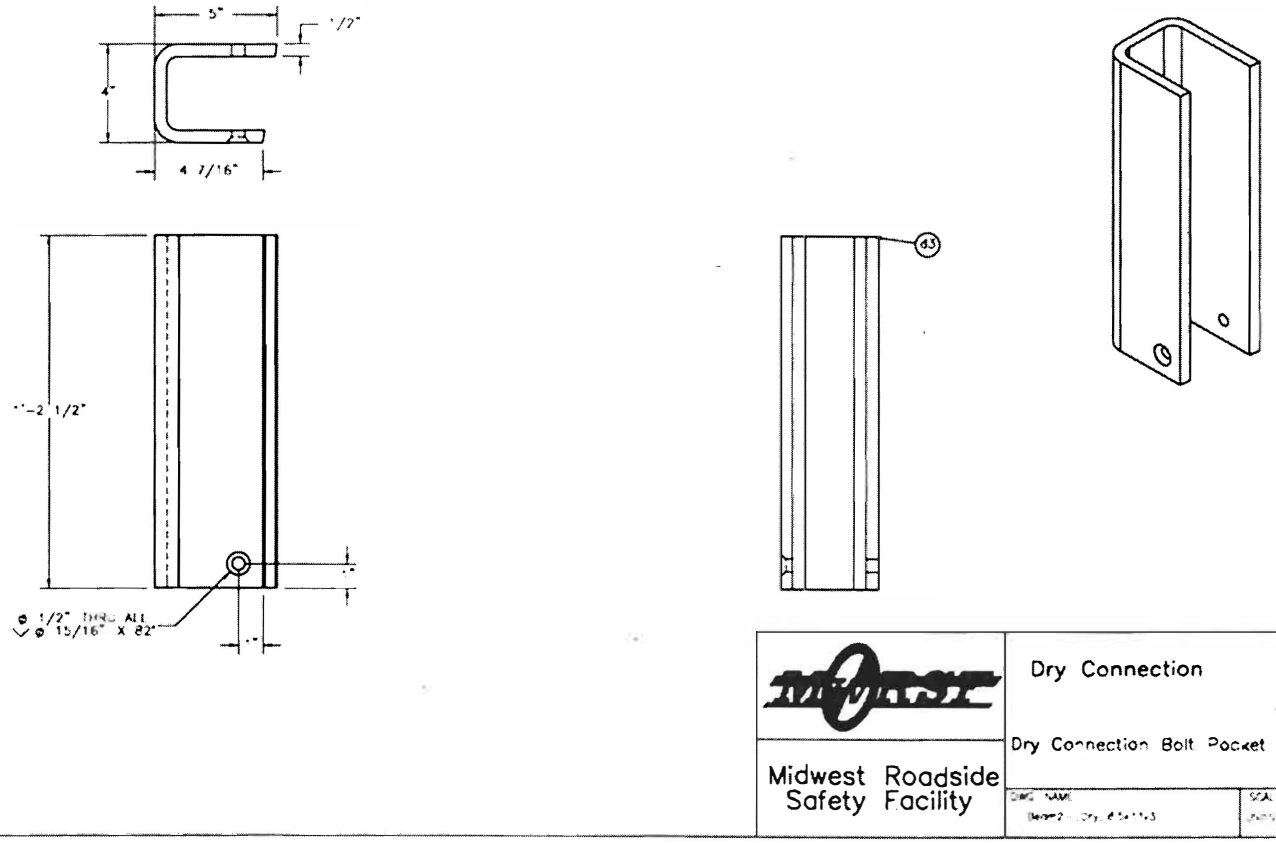

Figure 72. Right-Side Pocket Details, Test No. PCRB-2

Dry Connection					
Item No.	QTY.	Description	Material Spec	Comment	File Name
d4	1	Dry Connection Bolt Pocket Cap	A572 Grade 50 – Galvanized	–	Beam2_Dry_bolt_pocket_cap
d5	1	0.5 UNC-13 x 5 Counter Sunk Allen Head Bolt	Grade 5 – Galvanized	–	SCHCSCREW 0.5-13x5x1.75-HX-C
d6	1	0.5 UNC-13 Heavy Hex Nut	Grade 5 – Galvanized	–	HHNUT 0.5000-13-D-N
d7	1	Dry Connection Shear Plate	A572 Grade 50 – Galvanized	–	Beam2_Dry_shear_plate_A572G-50
d8	1	No. 5 Shear dba	A706 Grade 60 – Galvanized	–	Beam2_Dry_dba_No.5_Grade60
d9	1	Dry Connection No. 6 dba	A706 Grade 60 – Galvanized	–	Beam2_Dry_No.6_Grade60_dba
d10	1	Dry Connection Bolt Pocket End Cap	A572 Grade 50 – Galvanized	–	Beam2_Dry_bolt_pocket_end_cap

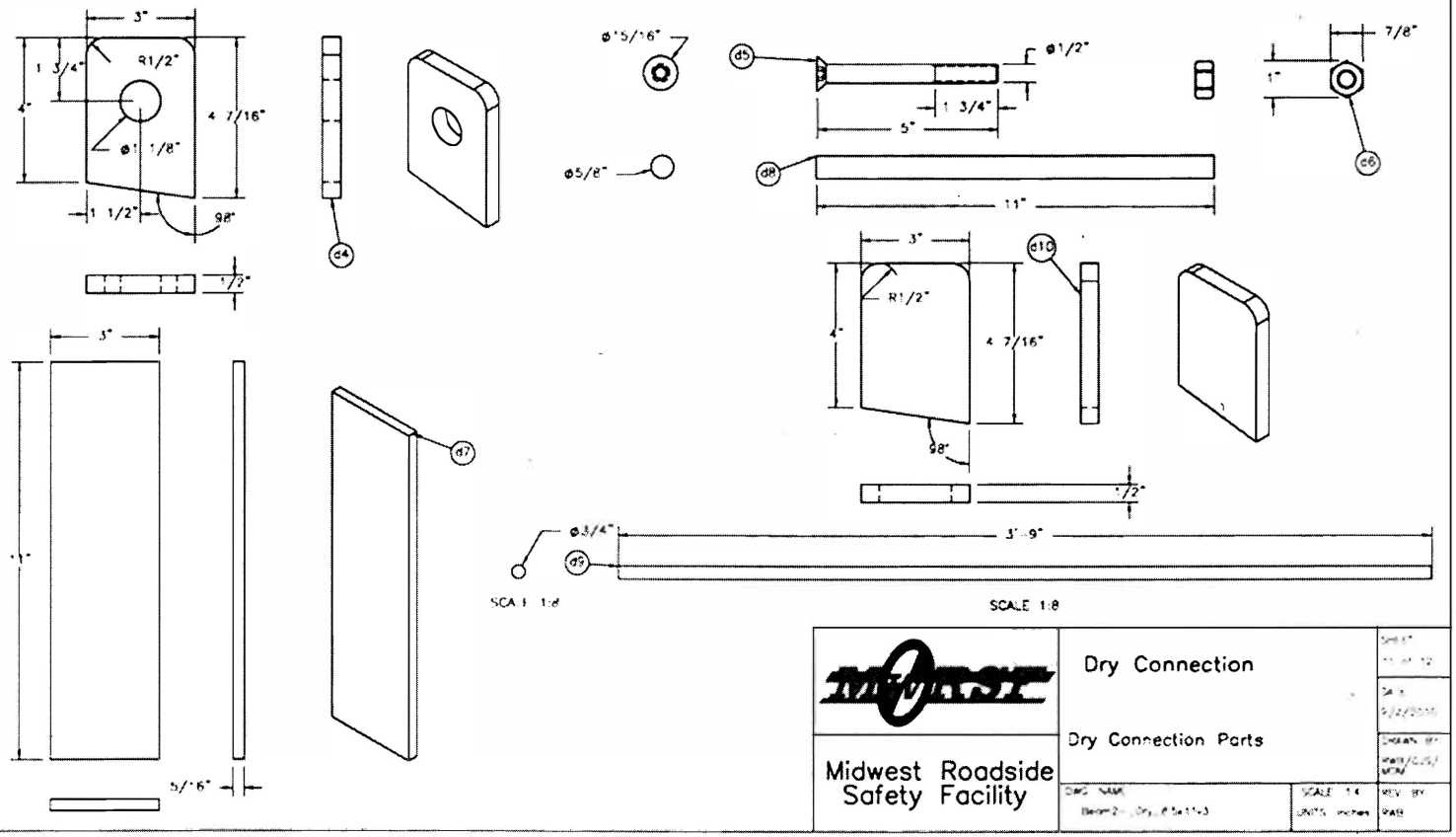

Figure 73. Pocket Gusset Plates, Shims, and Shear Bolts, Test No. PCRB-2

Dry Connection					
Item No.	QTY	Description	Material Spec	Comment	File Name
f1	1	1.0 UNC-8 x9x 9 Grade 5 Heavy Hex Bolt	Grade 5 – Galvanized	–	Beam2_Dry_--B0_" 1.0000-8x9x9-C
f2	1	1.0 Heavy Hex Nut	Grade 5 – Galvanized	–	HHNUT 1.0000-8-D-C
f3	1	Shear Tube 2.5x2.5x0.25 with 0.125 shims	A500 Grade C – Galvanized	–	Beam2_Dry_shearTube_2.5x2.5x0.25_w_0.125shim
f4	1	Dry Connection Shim Plate	A36 Steel – Galvanized	Material will likely change following component testing	Beam2_Dry_shimplate

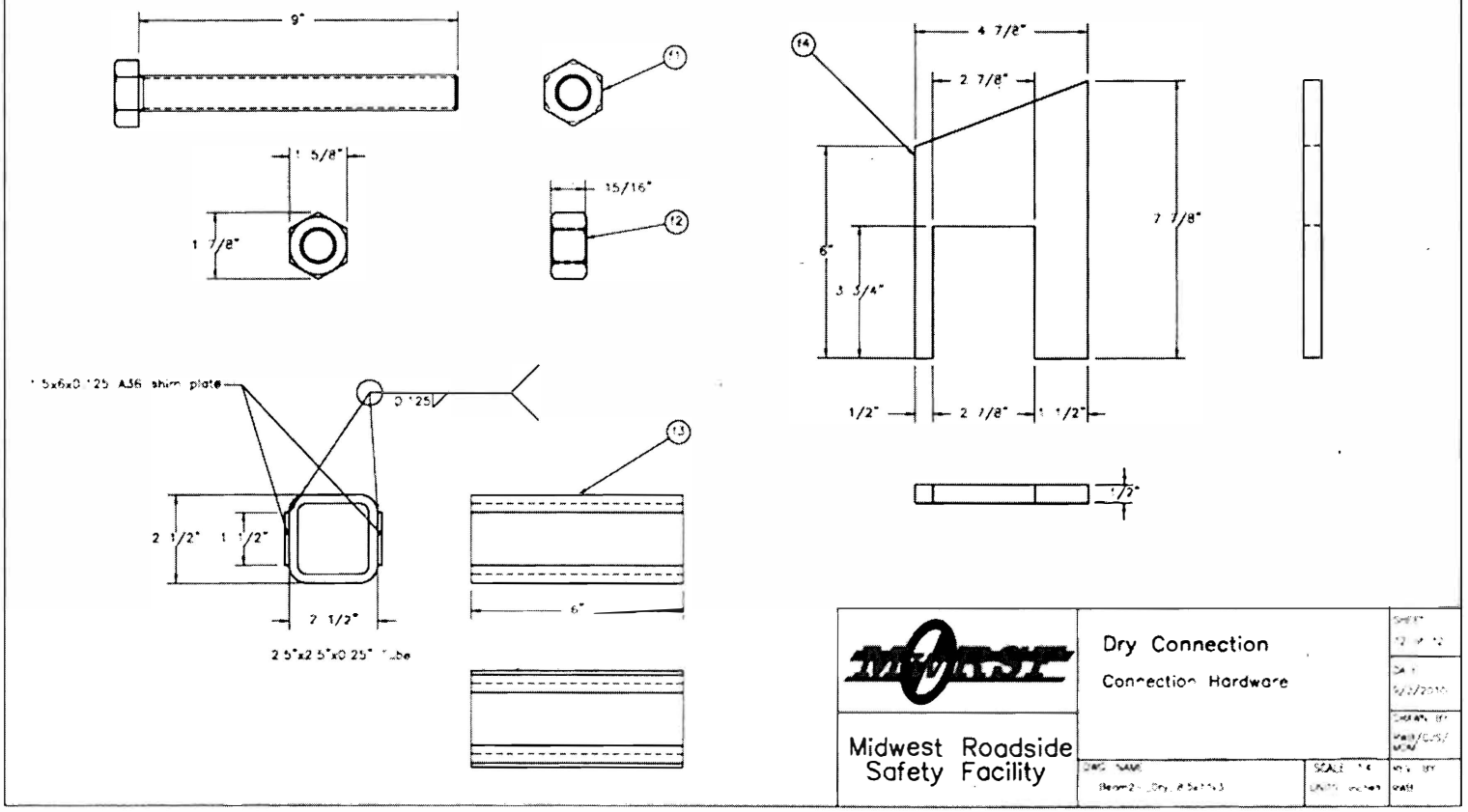

Figure 74. Connection Hardware, Test No. PCRB-2

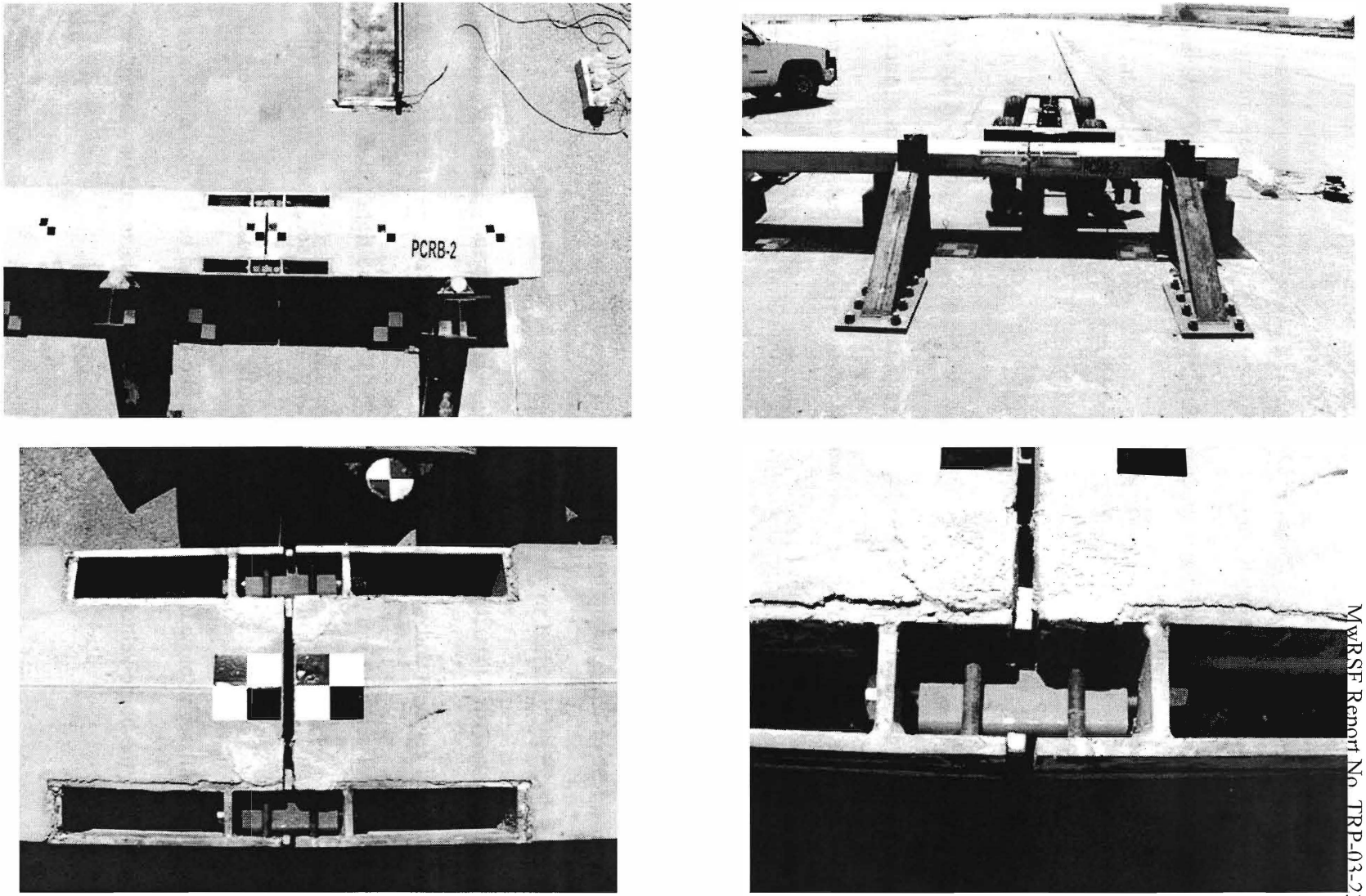

Figure 75. Rail Component Photographs, Test No. PCRB-2

6.6 Bogie Test No. PCRB-1

6.6.1 Test Description

The 1,616-lb (733-kg) bogie vehicle impacted the reinforced concrete rail specimen 6 in. (152 mm) from the centerline of the joint at a speed of 23.4 mph (37.7 km/h). At 0.002 seconds after impact, cracks had formed through both the front grout pocket of the short rail segment and the back grout pocket of the long rail segment. At 0.004 sec, the short rail segment had begun to deflect backward. Shear cracks had also formed on the short rail segment, extending from the front grout pocket to the backside of the rail. At the same time, the back grout pocket of the long rail segment had begun to rotate clockwise and break away from the rest of the rail. Concrete spalling was visible around this grout pocket as it broke away. At 0.006 sec, the front grout pocket of the short rail segment had experienced noticeable deformation which allowed the crack through its center to expand. At the same time, localized crushing and spalling near the impact point was observed. By 0.008 sec, the back grout pocket of the long rail had completely separated from the rest of the concrete rail. However, the grout pocket and the steel I-shape connector remained rigidly attached to the back grout pocket of the short rail segment as it continued to rotate backward. At 0.020 sec, the I-shape connector had pried open the front grout pocket of the short rail segment and was pulling pieces of fractured grout out of the pocket. At this point, the short rail segment was rotating freely. At 0.032 sec, the right side of the bogie vehicle's frame contacted the front of the long rail segment. At 0.034 sec, shear and bending cracks appeared in the long rail segment around the middle anchor post. By 0.038 sec, the cracking in the long rail segment had propagated on both the front and back faces and caused spalling. At 0.044 sec, the bogie vehicle had reached its maximum displacement into the system

and began to redirect in the opposite direction. Sequential photographs of the impact event are shown in Figures 76 and 77.

6.6.2 Rail Joint Component Damage

During bogie test no. PCRB-1, the joint failed and the rail segments completely separated, as shown in Figure 78. After the joint failed, the short rail segment (e.g., impact side) spun off of the wood block supports and fell to the ground. The long rail segment (e.g., non-impact side) remained on top of its supports, but had rotated away from the anchor posts following the redirection of the bogie vehicle.

As shown in Figure 79, the I-shape connector used to connect the front grout pockets remained attached to the long rail segment. However, it was bent nearly 90 degrees toward the center of the rail. The back grout pocket of the long rail segment had completely broken away from the rest of the rail. Both of the butt welds attaching the pocket to the longitudinal reinforcement of the rail segment had failed. Also, the rebar running between the grout pockets was bent out toward the joint and the butt weld connecting the rebar to the back pocket had failed. Concrete spalling was located around the area in which the back grout pocket was originally positioned.

The front grout pocket on the short rail segment was pried open, as shown in Figure 80. Subsequently, the I-shape connector and fragments of grout had been pulled out of the pocket. Concrete shear cracks were found running from the front grout pocket to the back grout pocket. The back grout pocket remained intact. Only minor cracks had formed between the steel pocket and the surrounding concrete rail. The back grout pocket that had been removed from the long rail segment remained attached to the back grout pocket of the small rail segment via the steel I-

shape segment. Both pockets appeared to be in good condition with only minor cracking of the grout.

Bending cracks were found in the long rail segment, as shown in Figure 81. Also, a large amount of spalling was observed on the back face of the rail segment. Both the spalling and the bending cracks were located near the middle anchor post and were caused by the bogie frame impacting the long rail segment after the joint had failed. Although this damage was not directly related to the strength of the joint, it was documented to demonstrate that the strength of the rail cross section was adequate to carry the design load with only minor damage.

6.6.3 Data Analysis

Data from the accelerometers was used to calculate and analyze the loads imparted to the rail component during test no. PCRB-1. The data collected by the DTS was unusable. EDR-3 plots depicting force vs. time and force vs. displacement are shown in Figure 82. The data illustrates an initial force spike that reached 143 kips (636 kN). However, this spike had quickly subsided by 0.01 seconds into impact, or 2 in. (51 mm) of deflection. This corresponded well with the video analysis in that the back grout pocket was almost immediately detached from the rail. Although a portion of this initial force spike represents the strength of the joint before failure, the majority of the spike is a result of inertia. As such, the strength of the joint is considerably less than this maximum recorded force. A second force spike reaching 75 kips (334 kN) was recorded between 6 and 7 inches (152 and 178 mm) of deflection. This spike corresponds to the impact between the bogie vehicle frame and the long rail segment after the joint had failed.

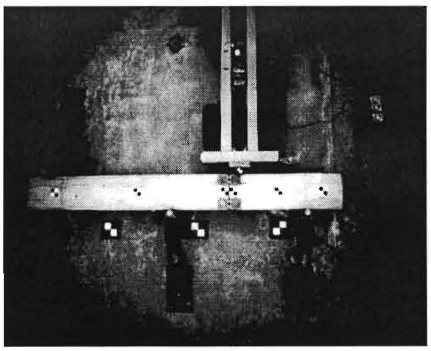
0.000 sec

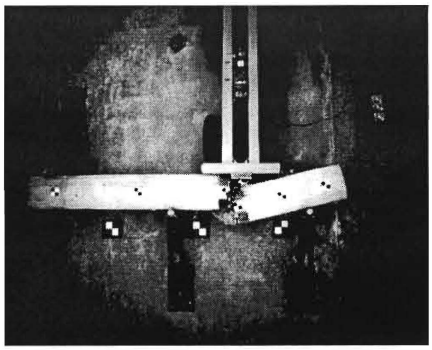
0.032 sec

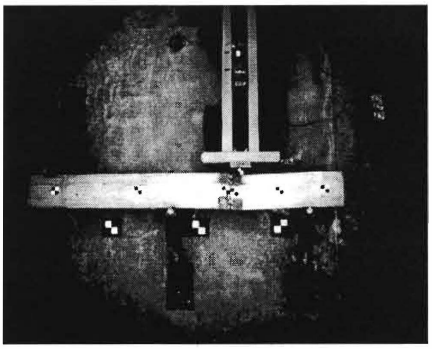
0.004 sec

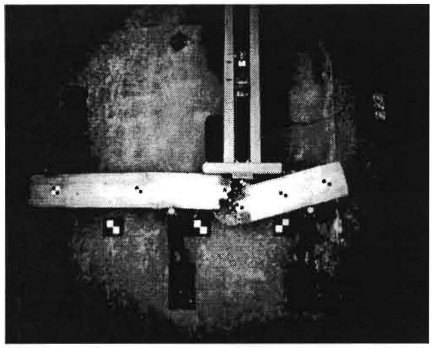
0.044 sec

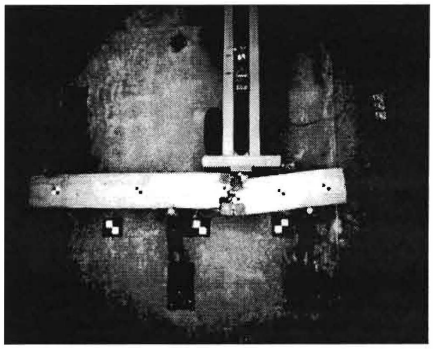
0.014 sec

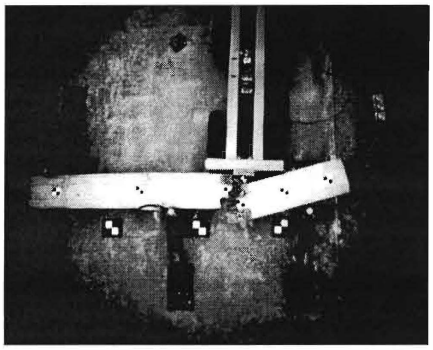
0.098 sec

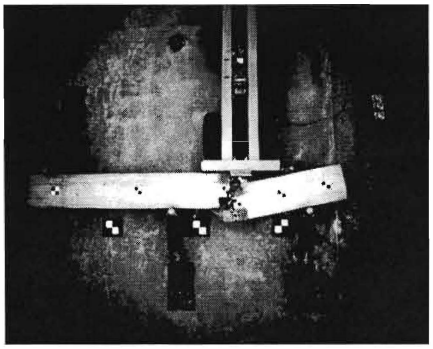
0.026 sec

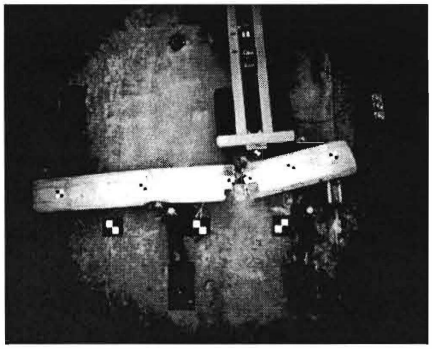
0.566 sec

Figure 76. Sequential Photographs, Test No. PCRB-1

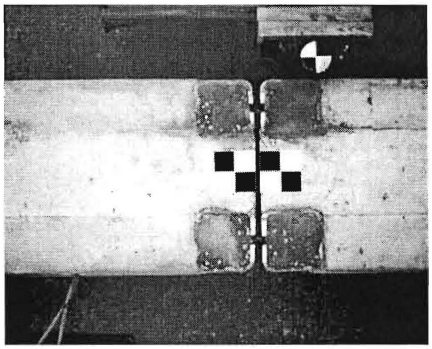
0.000 sec

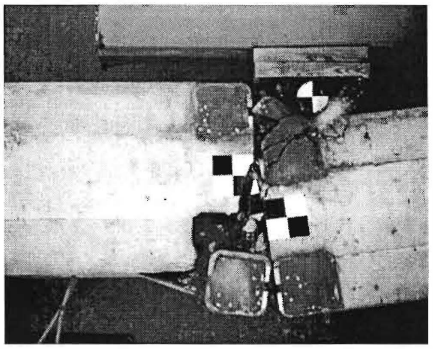
0.014 sec

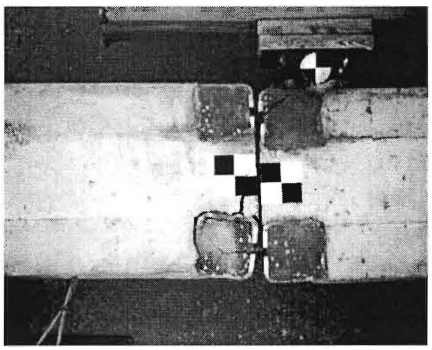
0.002 sec

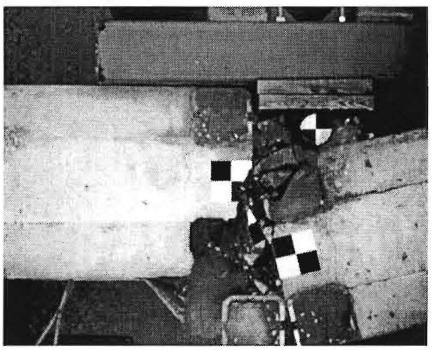
0.032 sec

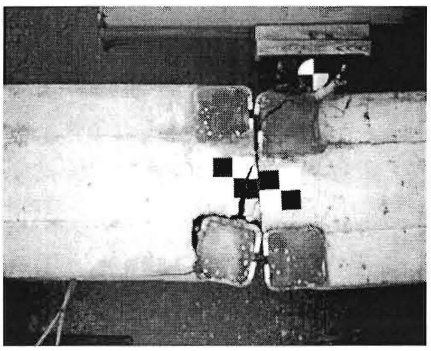
0.004 sec

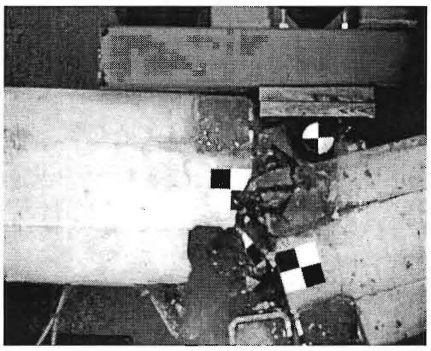
0.042 sec

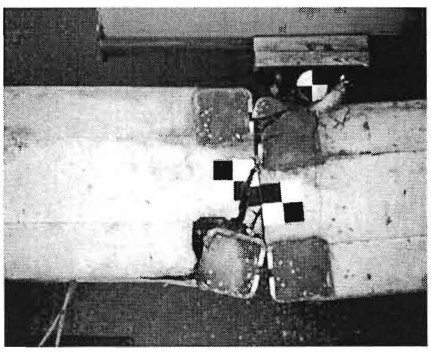
0.008 sec

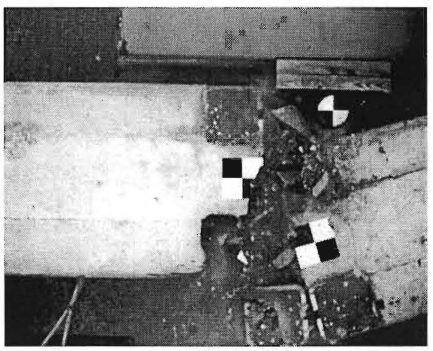
0.110 sec

Figure 77. Additional Sequential Photographs, Test No. PCRB-1

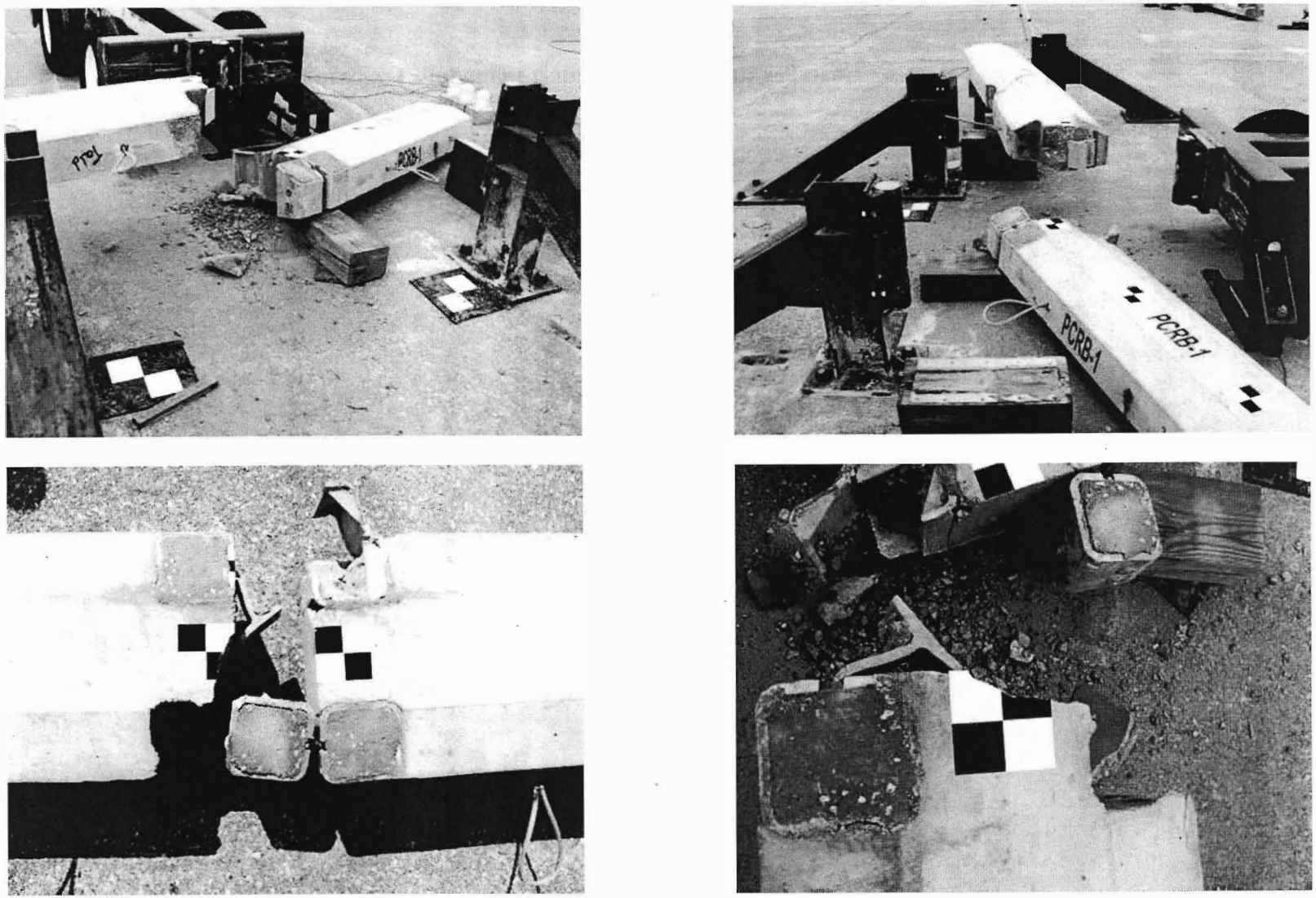

Figure 78. Component Damage, Test No. PCRB-1

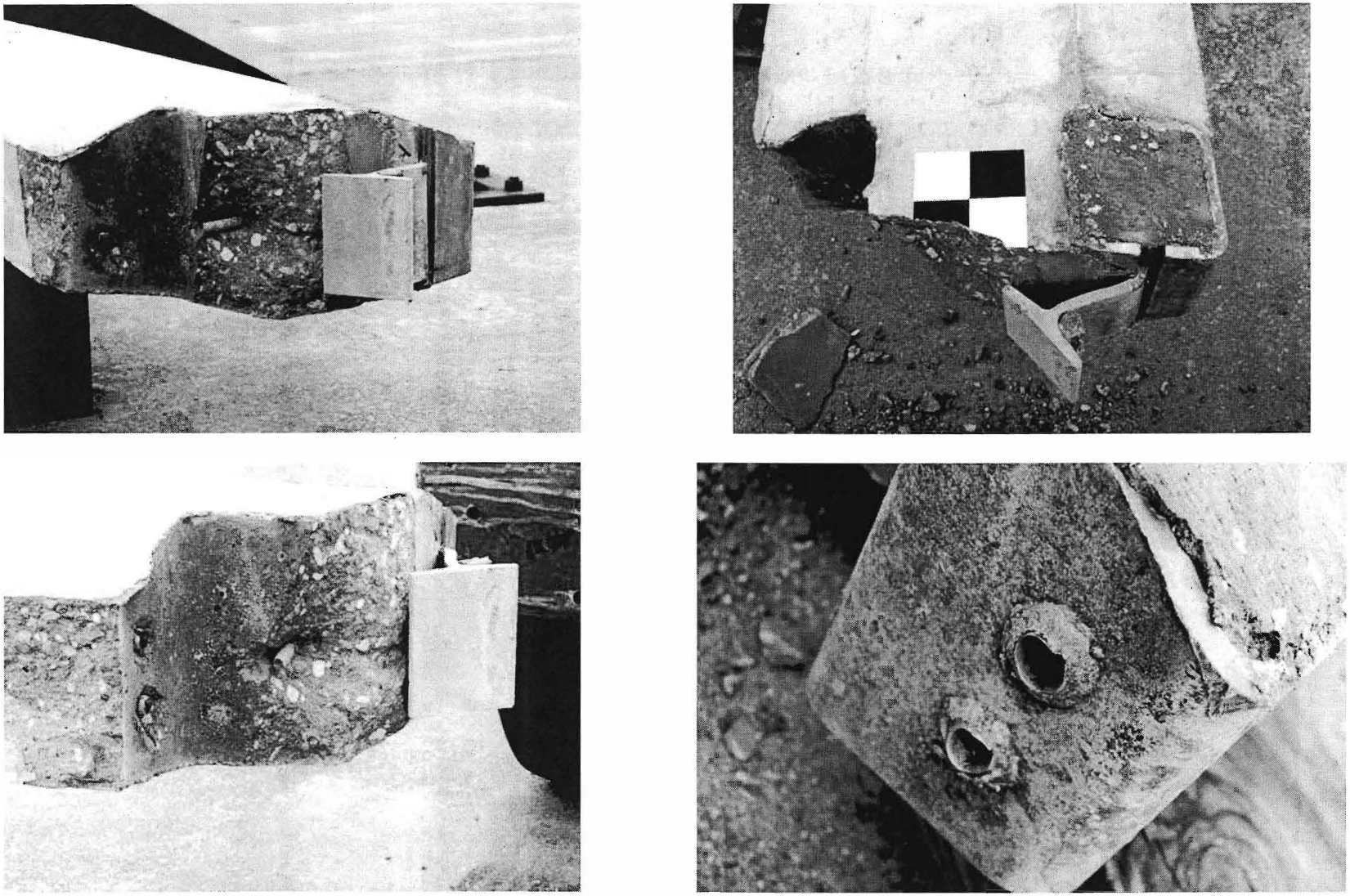

Figure 79. Component Damage – Long Rail Segment, Test No. PCRB-1

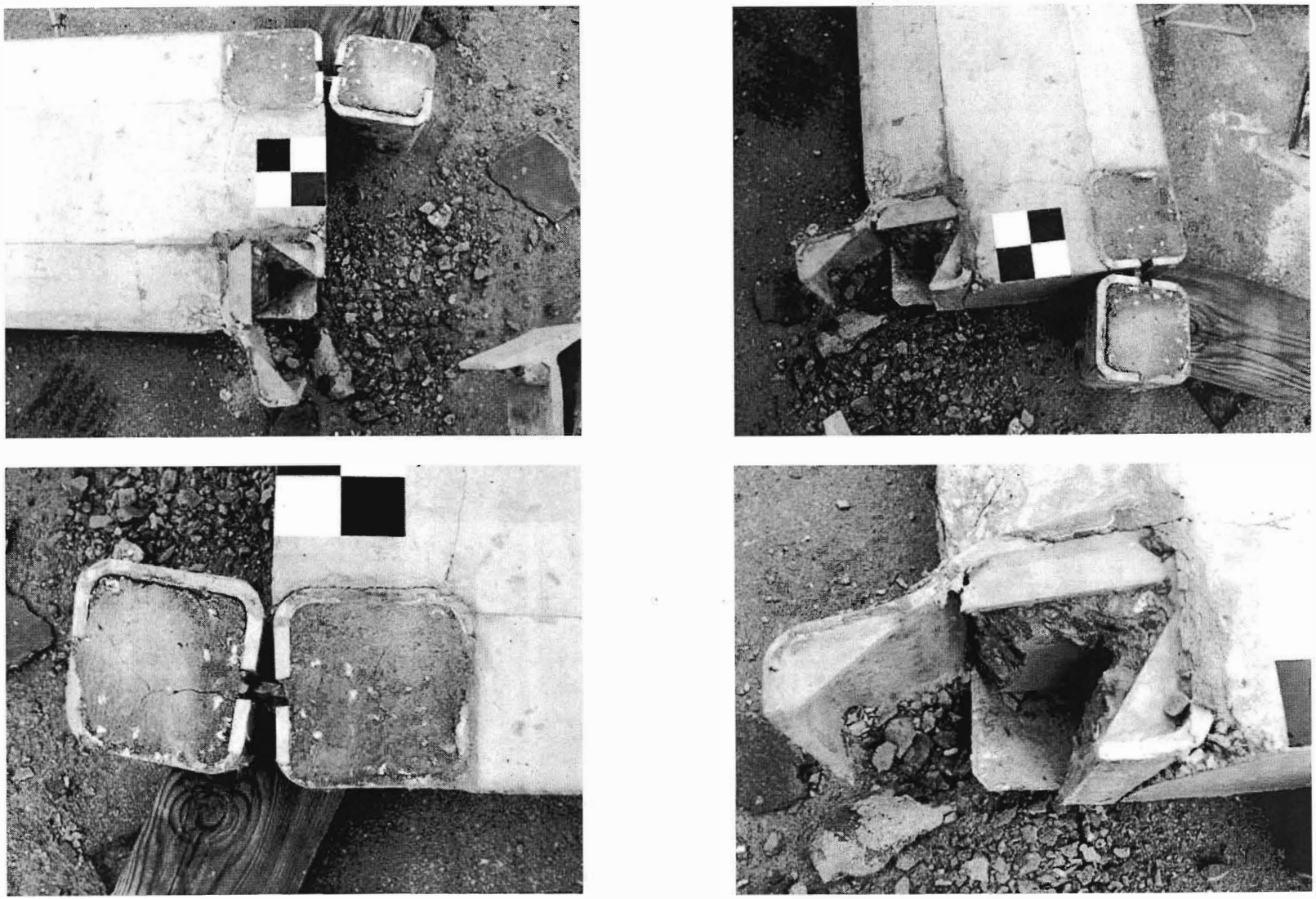

Figure 80. Component Damage – Short Rail Segment, Test No. PCRB-1

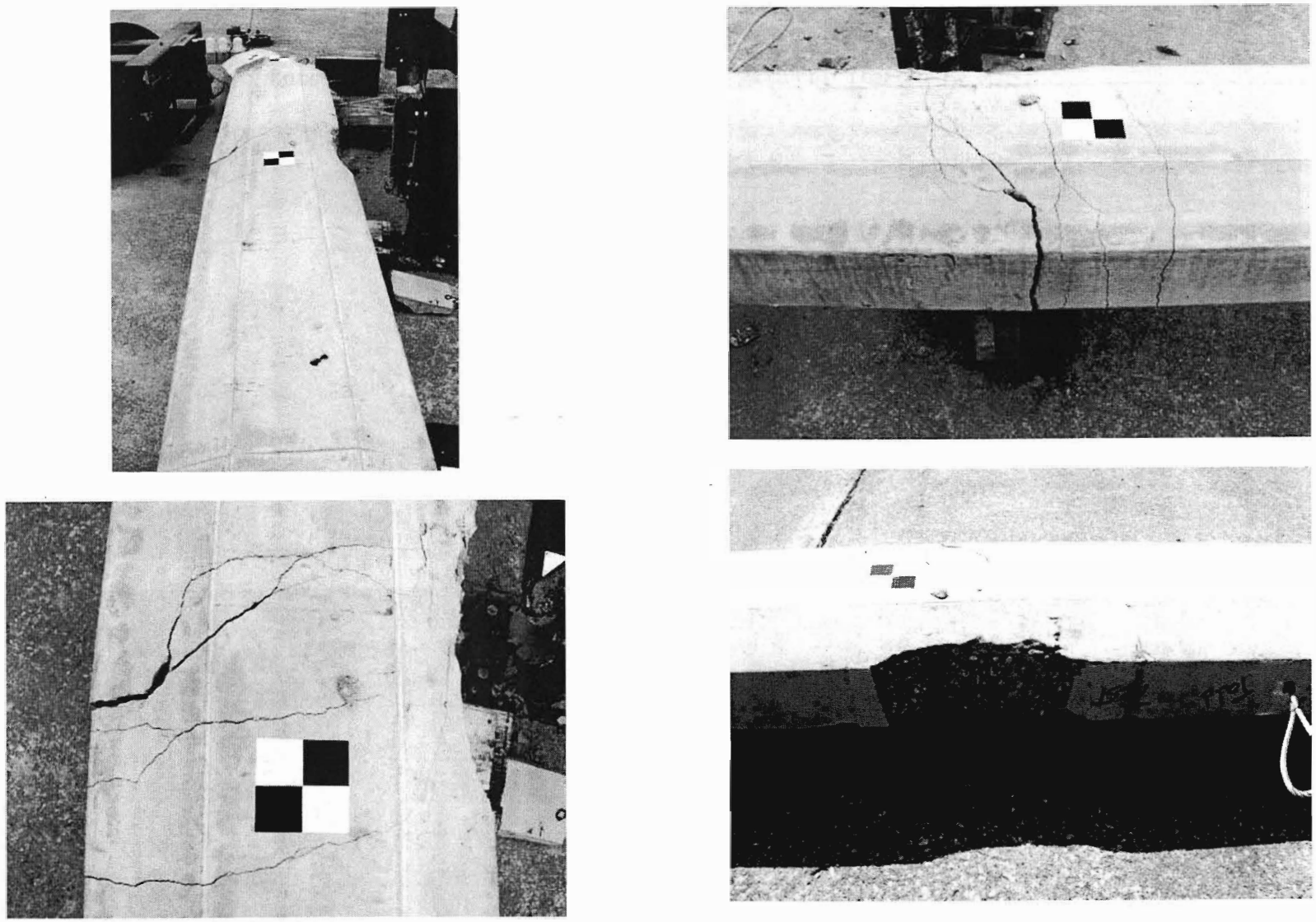

Figure 81. Bending Damage of Long Rail Segment, Test No. PCRB-1

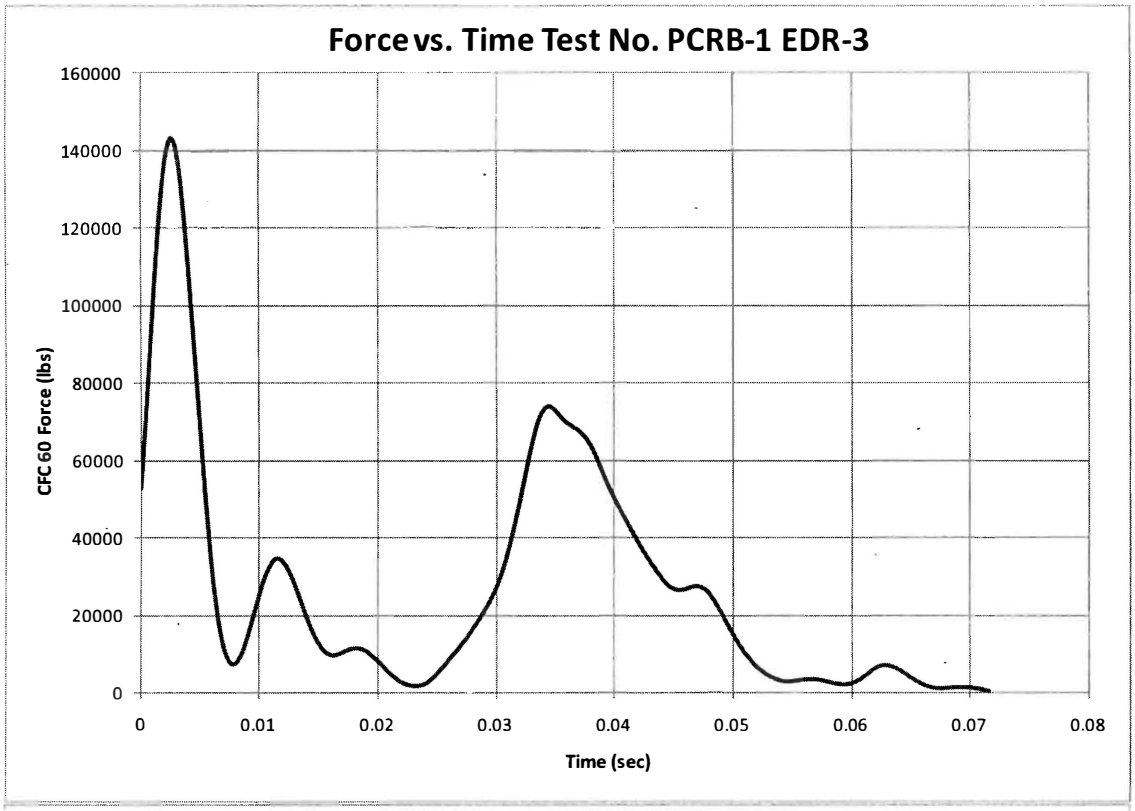

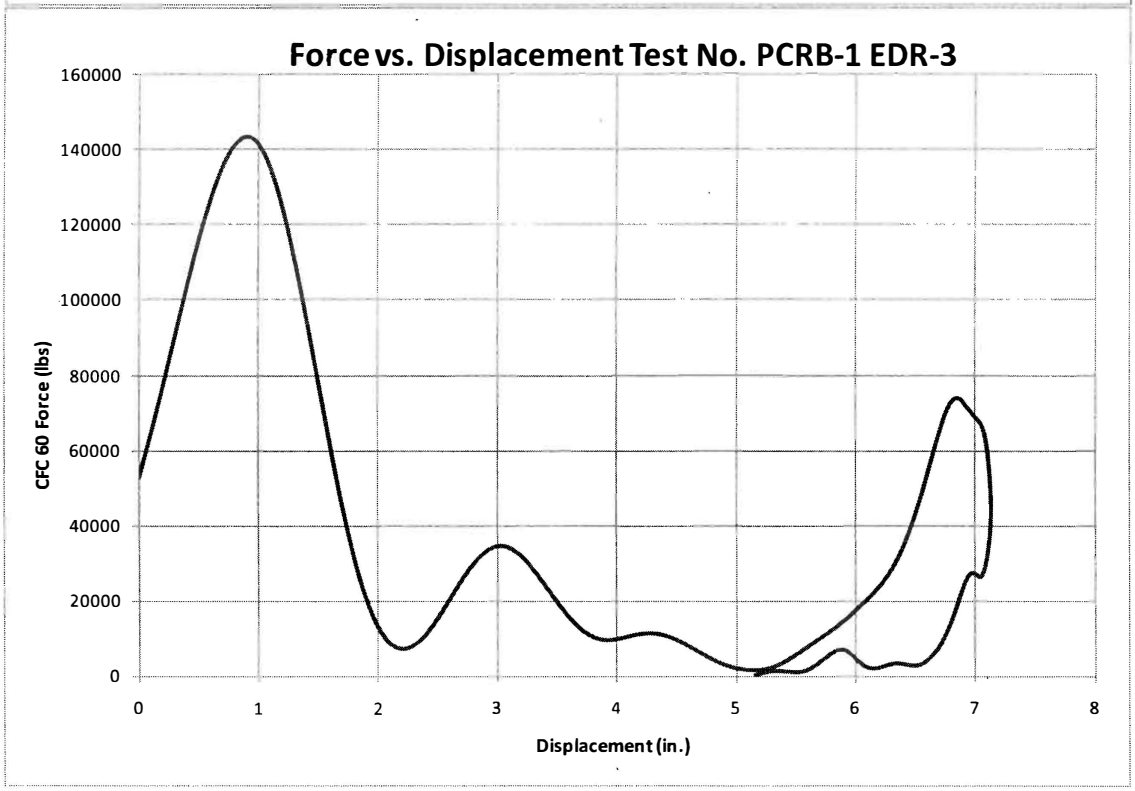

Figure 82. Data Analysis Plots, Test No. PCRB-1

6.7 Bogie Test No. PCRB-2

6.7.1 Test Description

The 1,616-lb (733-kg) bogie vehicle impacted the reinforced concrete rail specimen 6 in. (152 mm) from the centerline of the joint at a speed of 23.4 mph (37.7 km/h). At 0.002 seconds after impact, the short rail segment (e.g., impact side) had begun to deflect. At this same time, the top portion of the wood blockout attached to the impact head of the bogie vehicle splintered. At 0.004 sec, the pockets had engaged the shear tubes and both rail segments began to deflect together. At this same time, cracks developed between the pockets of both rail segments. At 0.008 sec, the rails continued to deflect together as more cracks formed between the steel pockets of both rail segments. At this same time, the back side of the joint had begun to widen. This meant that the front shear tube would be responsible for transferring the majority of the load for the remainder of the test. At 0.010 sec, the bolt connecting the back pockets had fractured in tension as the cracks further propagated and expanded in the rails. This allowed fragments of concrete between the rail pockets to break free. At this same time, the head broke off of the shear bolt holding together the front pocket of the short rail segment, while the pocket itself began to deform around the impact head. By 0.016 sec, large fragments of concrete had broken away from the bottom of the rail segments (as oriented in the test) and had fallen to the ground. At 0.020 sec, the cracking between rail pockets was severe enough that the long rail segment pockets began to rotate independently from the rest of the rail. At 0.026 sec, the back of the joint had widened enough for the shear tube to pop out of the back pocket of the long rail. At 0.030 sec, the back side shim plate became loose and began to fall toward the ground. At 0.048 sec, the rails continued to deform while many concrete fragments broke away from between the pockets of the long rail segment. At 0.068 sec, the bogie vehicle reached its maximum displacement into

the system and began to redirect in the opposite direction. At 0.132 sec, the impact head was no longer in contact with the rail joint component. Also by this time, all of the concrete between the steel pockets of the long rail joint had broken apart. By 0.228 sec, the internal steel of the long rail segment was exposed. At 0.588 sec, the rail joint component had stopped rebounding from the impact and was no longer in motion. Sequential photographs of the impact event are shown in Figures 83 through 85.

6.7.2 Rail Joint Component Damage

During bogie test no. PCRB-2, the rail-to-rail joint was severely damaged, but it held together, as shown in Figure 86. The concrete between the steel pockets of the long rail segment had completely broken apart. Only the internal steel rebar was preventing the loose concrete from falling to the ground. Due to the loss of concrete, the rebar anchoring the steel pockets to the rest of the long rail segment had bent. This allowed the pockets to rotate backward slightly. Concrete fragments had also broken off of the short rail segment near the joint and on the bottom face (as oriented in the test). Additional concrete cracks were found stemming from the steel pockets of both rail segments.

Damage to the front pocket assembly consisted mostly of deformations to the steel pocket walls. The exposed pocket wall of the short rail segment was bent outward, while the inner pocket wall of the long rail segment was bent toward the center of the rail, as shown in Figure 87. The bogie impact head had caused the pocket to pinch together slightly at the point of impact, and the shear bolt on the front pocket of the short rail segment had fractured at the base of the head. Also, the deformation in the joint caused the longitudinal bolt connecting the front pockets to bend.

The tension bolt connecting the back pockets had completely fractured, as shown in Figure 88. The bolt had fractured through the threaded portion near the nut. The back side of the joint had widened apart, and the shear tube had popped out of the back pocket of the long rail segment.

The loose concrete remaining on the rails was removed revealing damage to the interior steel reinforcement of the long rail segment. Similar to test no. PCRB-1, the butt welds used to attach rebar between the steel pockets had failed, as shown in Figure 89. The welds holding the shear plate to the steel pockets remained intact, but the shear plate itself was bent.

6.7.3 Data Analysis

Data from the accelerometers was used to calculate and analyze the loads imparted to the rail component during test no. PCRB-2. The data from EDR-3 was unusable. DTS plots depicting force vs. time and force vs. displacement are shown in Figure 90. Similar to bogie test no. PCRB-1, inertia resulted in an initial force spike that reached 102 kips (454 kN). Immediately following the inertia spike, a second force spike was recorded reaching 92 kips (409 kN) at 0.008 seconds into impact, or 2.4 in. (61 mm) of deflection. This second force spike represented the strength capacity of the rail section before the tension bolt fractured. Recall, the overhead video illustrated the tension bolt had fractured before 0.010 seconds.

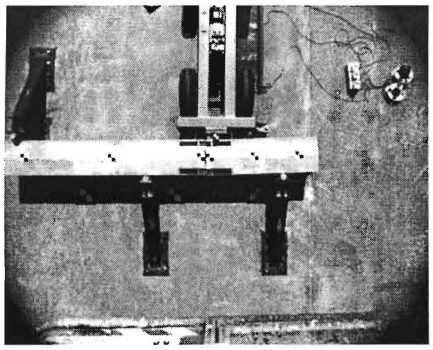
0.000 sec

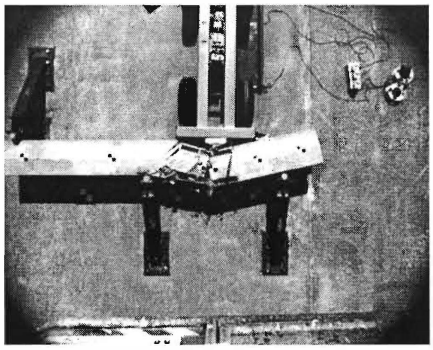
0.050 sec

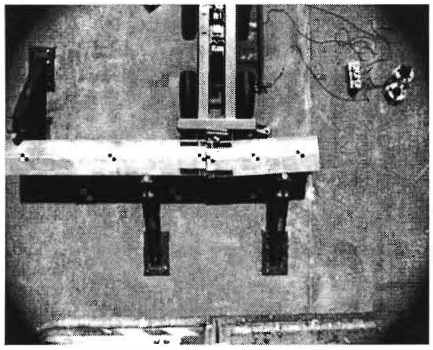
0.004 sec

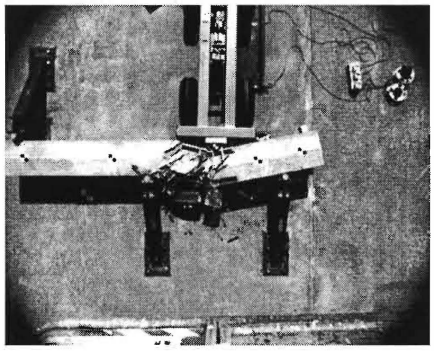
0.100 sec

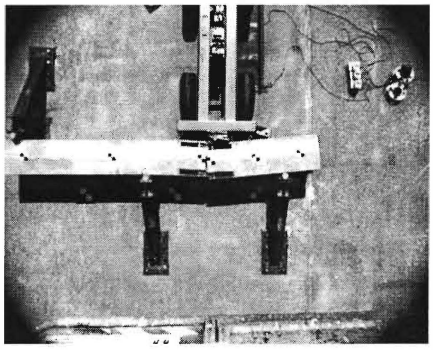
0.010 sec

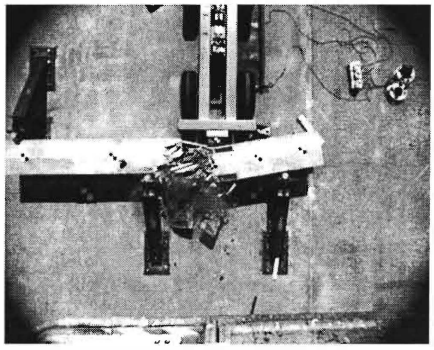
0.210 sec

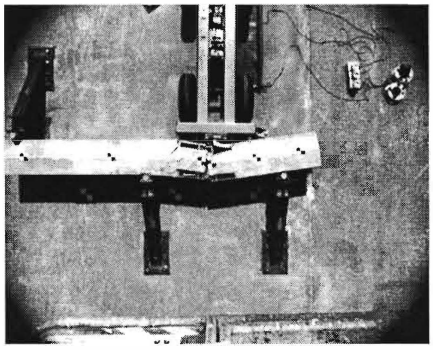
0.020 sec

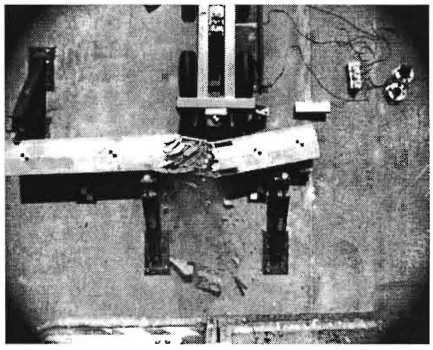
0.560 sec

Figure 83. Sequential Photographs, Test No. PCRB-2

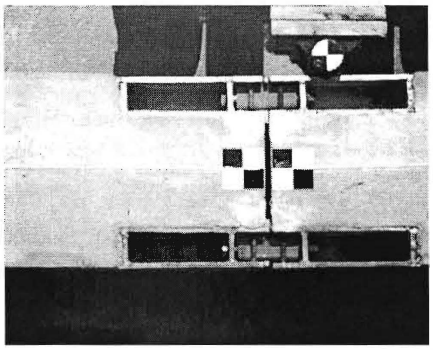
0.000 sec

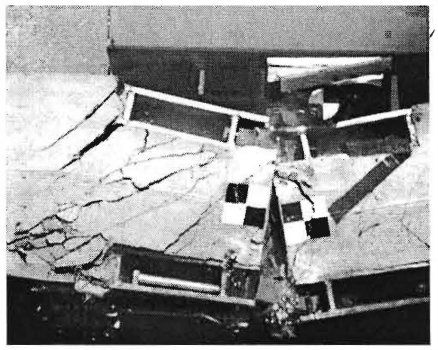
0.032 sec

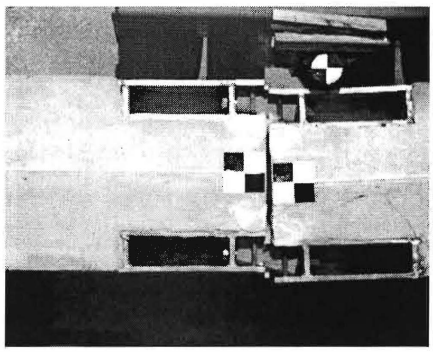
0.004 sec

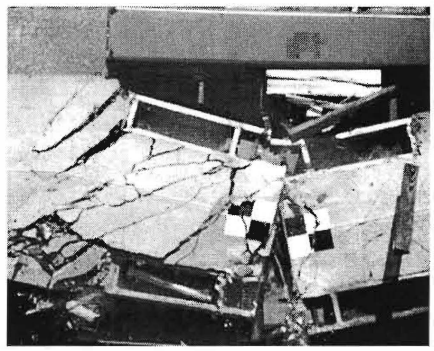
0.052 sec

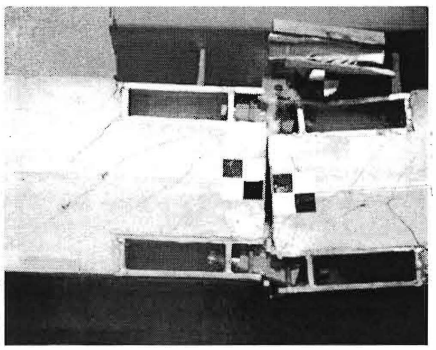
0.010 sec

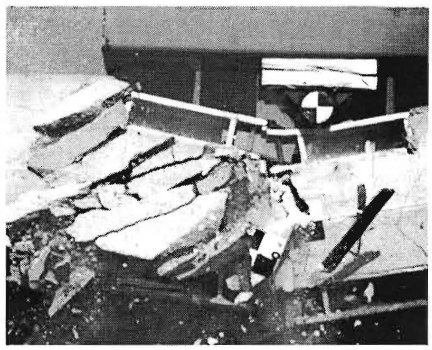
0.120 sec

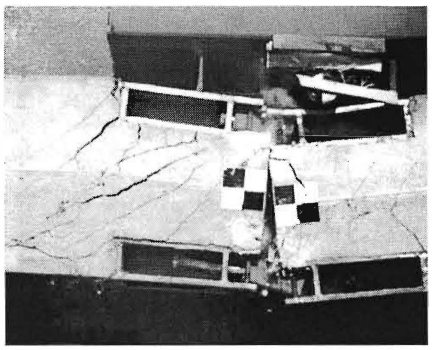
0.016 sec

0.296 sec

Figure 84. Additional Sequential Photographs, Test No. PCRB-2

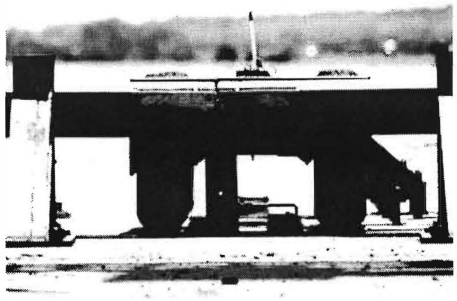

0.000 sec

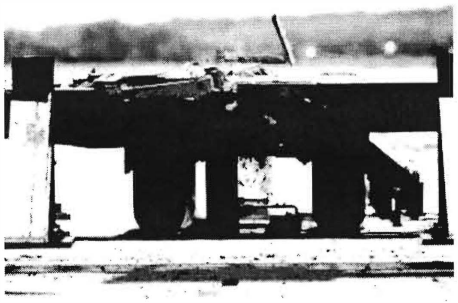

0.050 sec

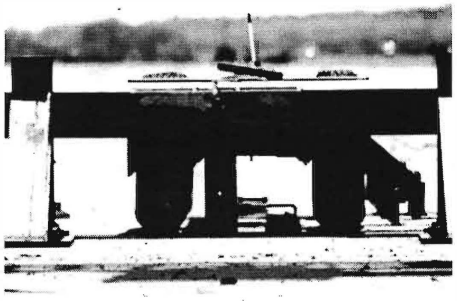

0.010 sec

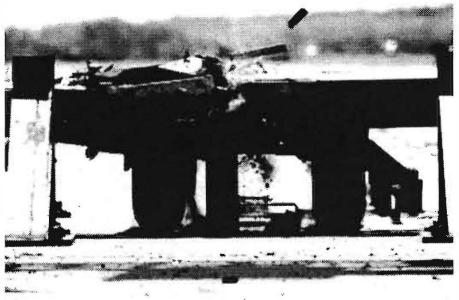

0.068 sec

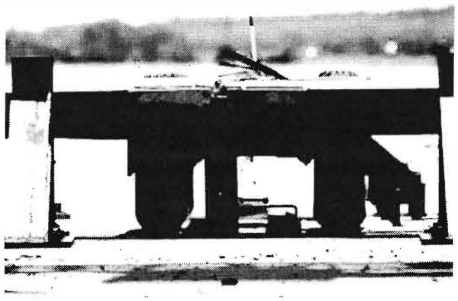

0.018 sec

0.124 sec

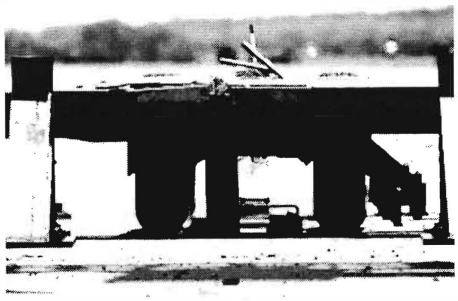

0.026 sec

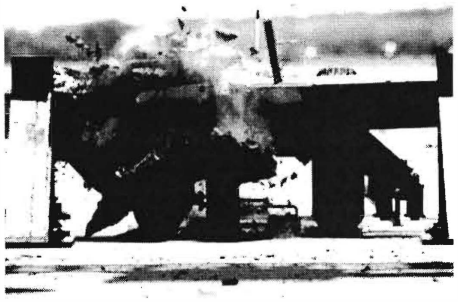

0.196 sec

Figure 85. Additional Sequential Photographs, Test No. PCRB-2

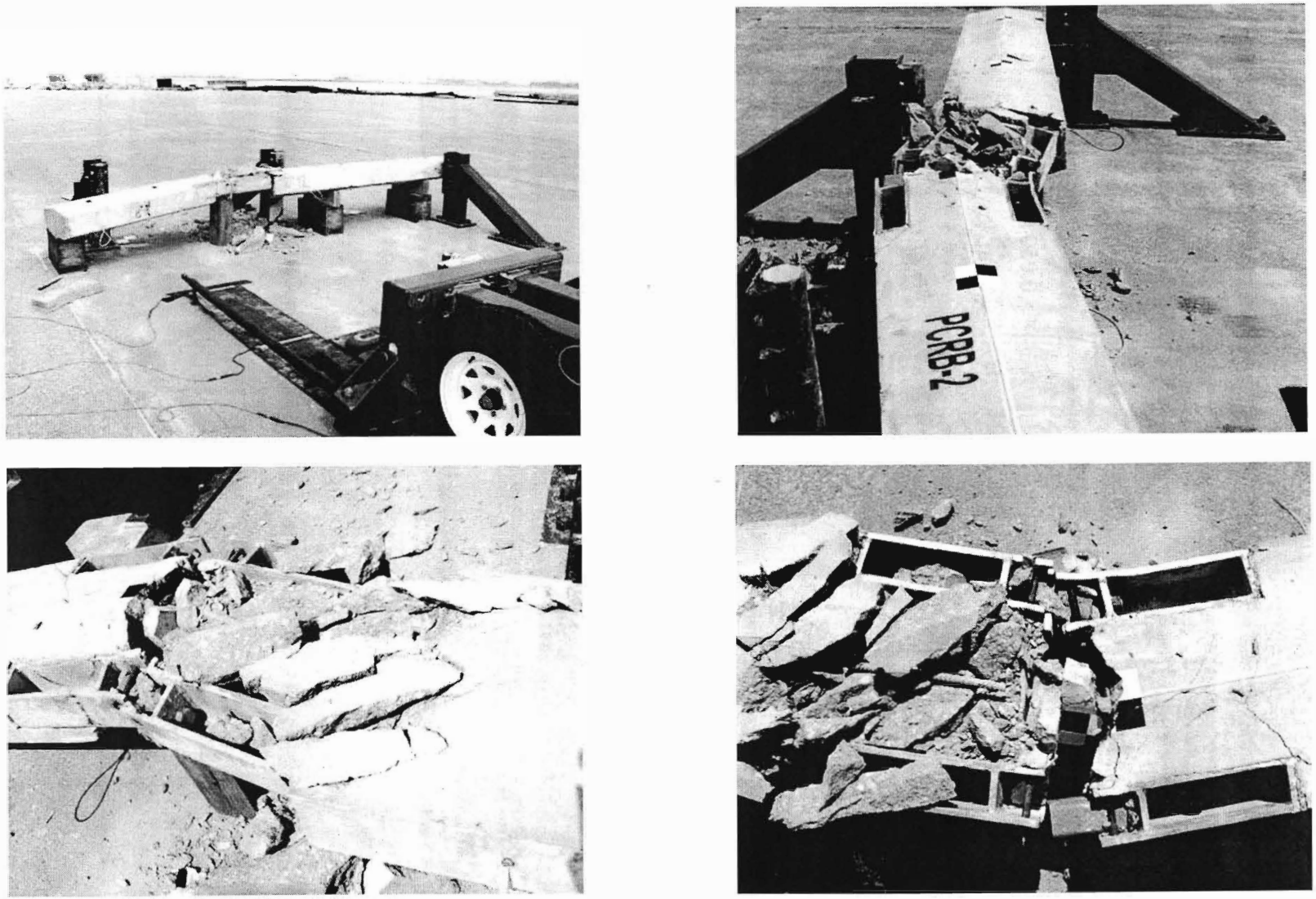

Figure 86. Component Damage, Test No. PCRB-2

Figure 87. Component Damage - Front Pocket Assembly, Test No. PCRB-2

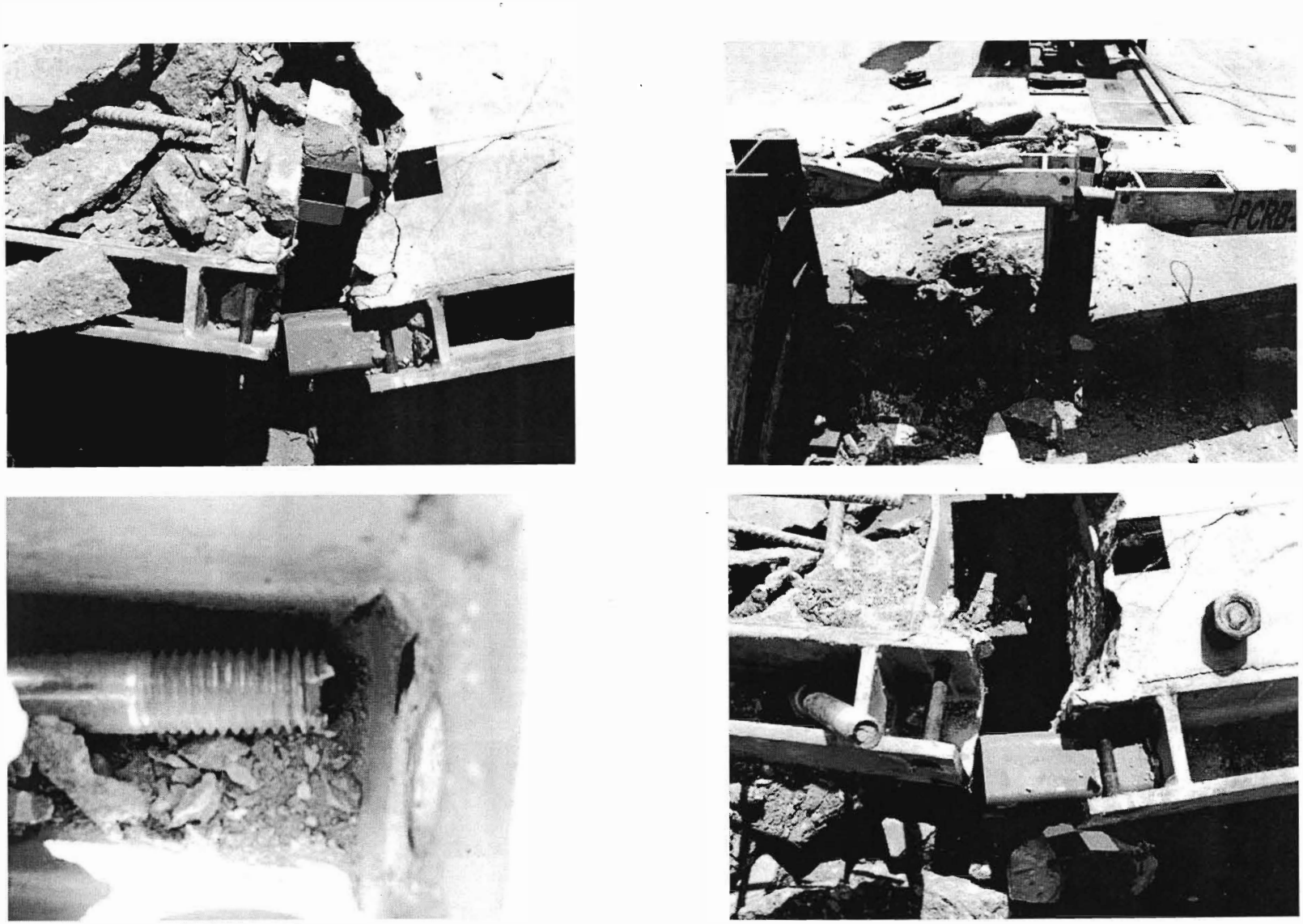

Figure 88. Component Damage – Back Pocket Assembly, Test No. PCRB-2

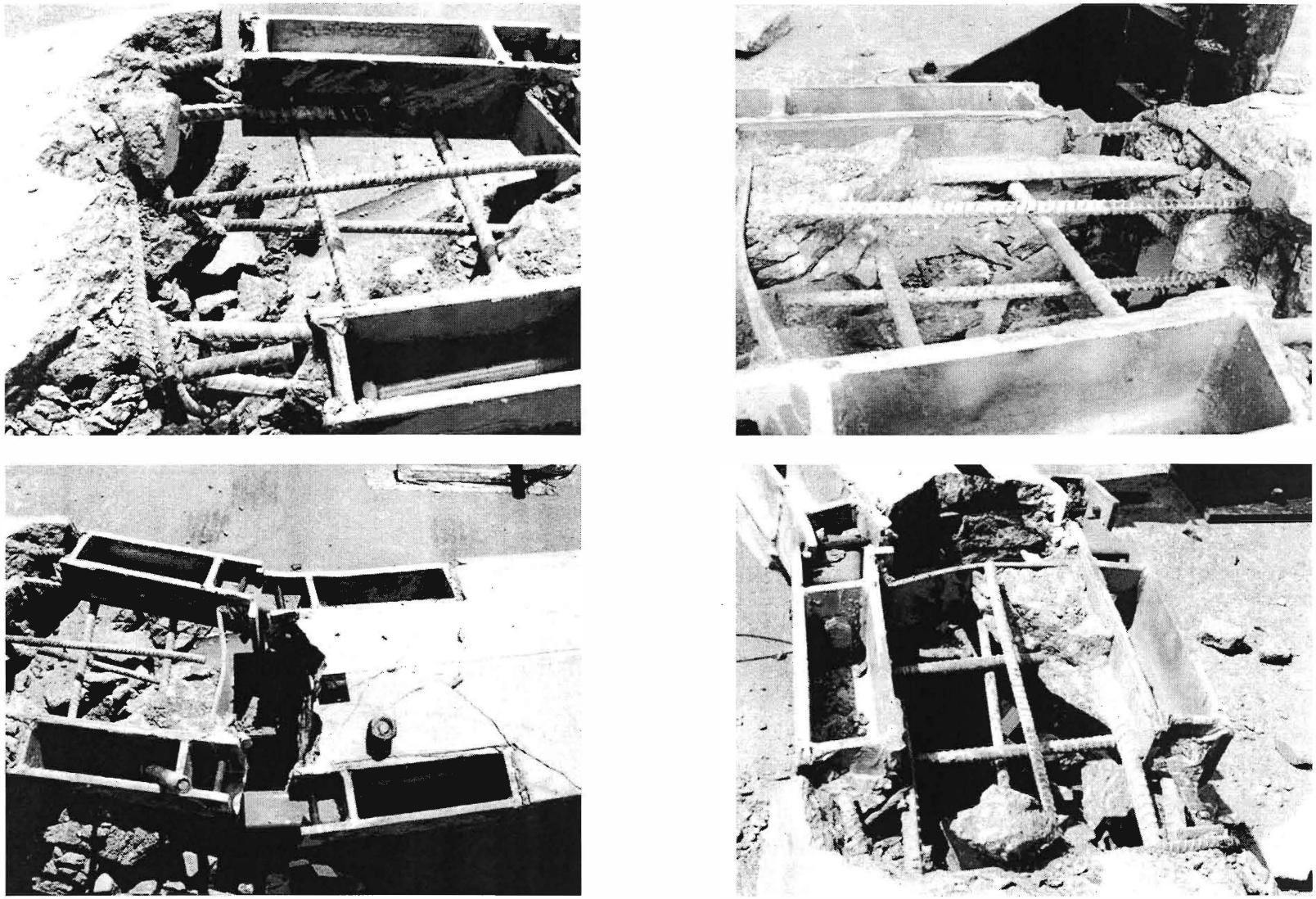

Figure 89. Component Damage – Loose Concrete Removed, Test No. PCRB-2

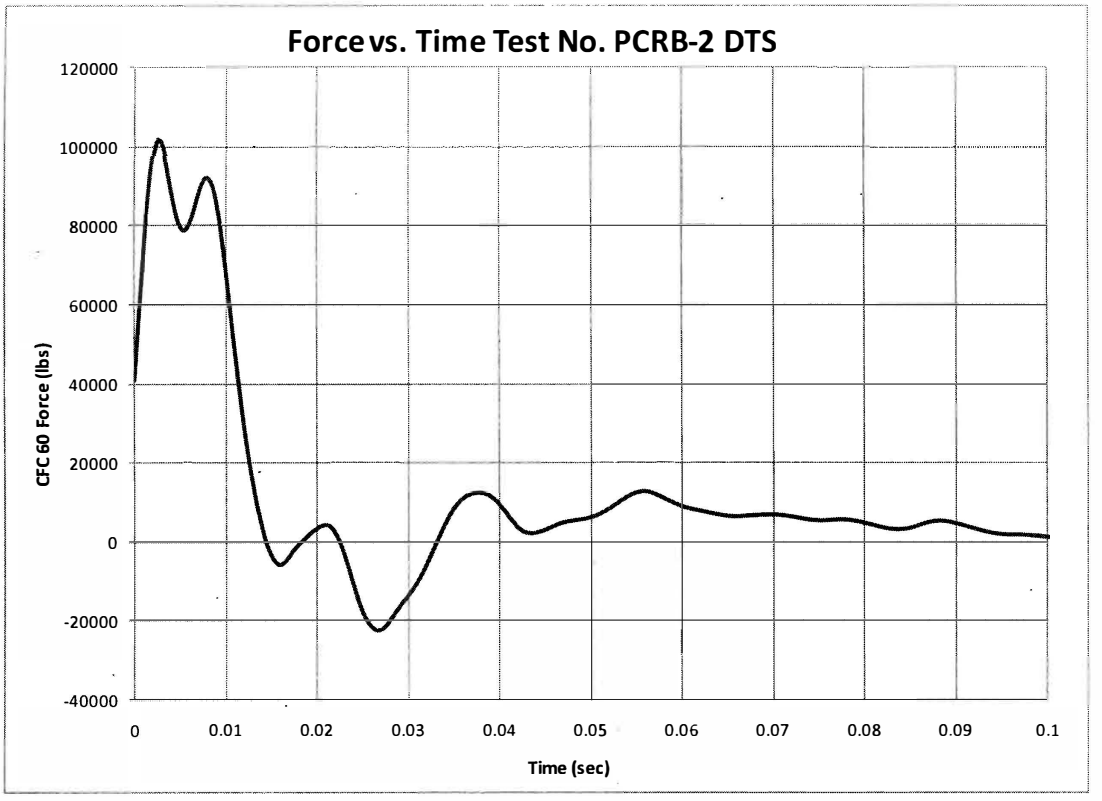

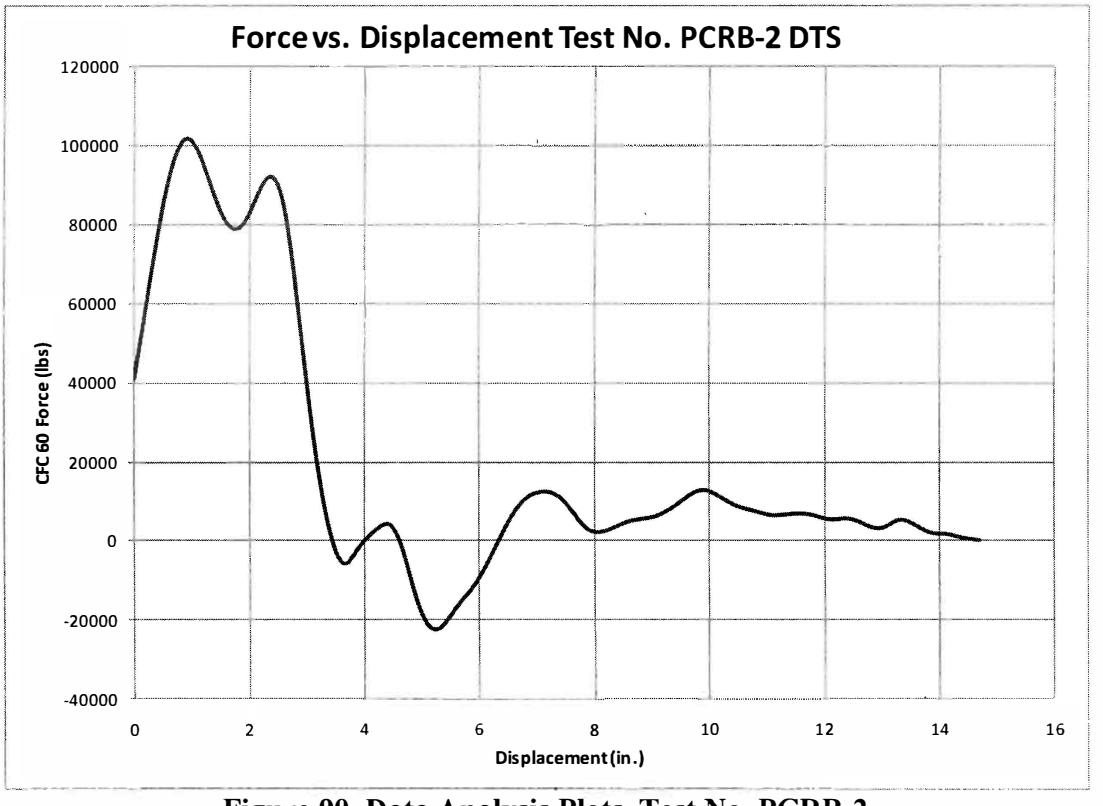

Figure 90. Data Analysis Plots, Test No. PCRB-2

6.8 Round 1 Bogie Testing Discussion

Recall from Section 6.2, an impact force of 62 kips (276 kN) would result in predicted shear and moment loads through the joint of 35 kips (156 kN) and 700 k-in (79 kN-m), respectively. As shown in Figure 91, both test nos. PCRB-1 and PCRB-2 initially exceeded this target impact force. However, the majority of the initial force spike observed in both tests was attributed to inertia. Thus, the actual strengths of the joints were much less than these inertial force spikes at 1 in. (25 mm) of displacement. Only the second force peak of test no. PCRB-2, which reached 92 kips (409 kN), demonstrated adequate strength. Also, neither of the joints demonstrated much ductility as both joints began to fail before 3 in. (76 mm) of deflection. Providing some measure of ductility to the joint increases the joints ability to absorb energy, decreases the forces in the joint and the railing and improves the overall toughness of the joint.

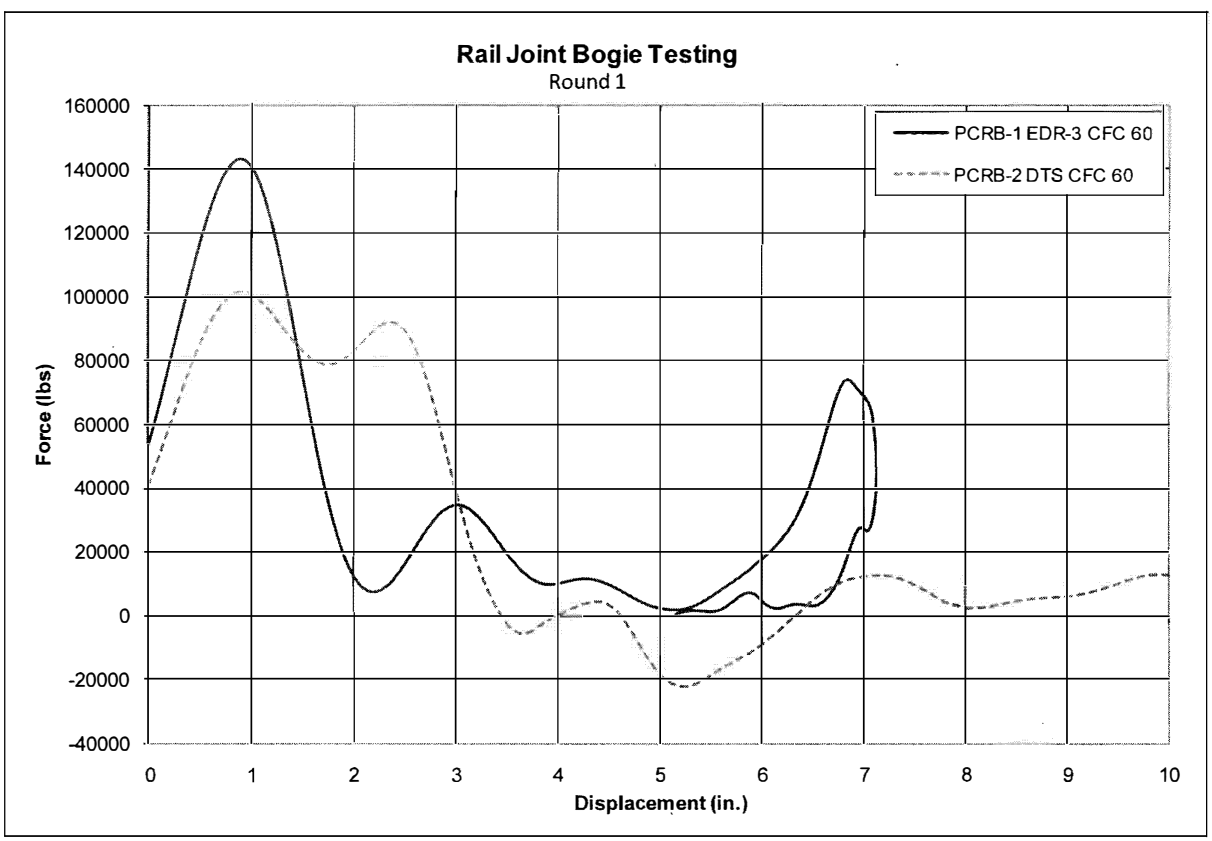

Figure 91. Data Comparison Plots, Round 1 Bogie Testing Results

Additional undesirable results were observed for both joint designs. The grouted joint of test no. PCRB-1 was determined to be very brittle due to the short amount of time and distance that significant forces were recorded. As such, the system did not absorb much energy before the joint failed. Also, the butt welds utilized to attach steel rebar to the pockets proved too weak to anchor the joint pockets. All three of the butt welds on the back pocket of the long rail segment failed during the test. Finally, the steel pockets proved to be susceptible to prying action, as observed during the opening of the front pocket of the short rail segment during test no. PCRB-1.

Although the dry joint of test no. PCRB-2 demonstrated an adequate ultimate strength and an improved ductility over the grouted joint, it took much longer to transfer the load across the joint. The impacted side of the joint moved approximately ½ in. (13 mm) before engaging the shear tubes. Ideally, load transfer should occur earlier in the impact event to maintain a continuous rail joint through the entirety of the event. In addition, the butt welds used on the rebar connecting the pockets failed, similar to the result observed in the grouted joint. However, the fillet welds and the flare bevel welds used elsewhere on the pocket sides held together. Thus, it was determined that premature weld failure may be limited to only butt welds. Finally, the concrete required more confinement to prevent large concrete fragments from falling off of the bridge rail system and onto the roadway. These fragments could become a hazard to ensuing motorists, or worse, they could fall onto traffic below the bridge.

7 RAIL JOINT DESIGN MODIFICATIONS AND IMPROVEMENTS

7.1 Refined Grout Joint

After evaluating the results of the grouted rail joint in bogie test no. PCRB-1, multiple design weaknesses were identified. These weaknesses included lateral and longitudinal anchorage of the pockets, weld strength, pocket resistance to prying action, and the bending capacity of the I-shape steel section. Each of these design aspects was refined to make the grouted joint stronger and more ductile, as shown in Figure 92.

The biggest change to the grouted rail design was that the longitudinal steel of the rail was directly used to anchor the grout pockets. During test no. PCRB-1, rebar was attached to the back of each pocket using butt welds. A lap splice was used to transfer load from the anchorage rebar to the longitudinal rebar of the rail segment. These anchorage bars and the weak butt welds that connected them to the grout pockets were removed. Also, the no. 5 longitudinal rebar was changed to no. 7 threaded rebar. These threaded rebar were inserted through holes cut in the back of the grout pocket, and nuts were used to fasten the pocket to the longitudinal threaded bars. The increase in bar size from no. 5 bars to no. 7 bars increased both the pocket anchorage strength and the bending strength of the rail. With the increase in rail bending strength, the two no. 4 longitudinal bars in the center of the rail cross section were no longer necessary and were therefore removed. To fit the threaded rebar and nuts inside the pockets and still leave room for the steel I-section, 6 x 8 x ½-in. (152 x 203 x 13-mm) steel tubes were utilized for the pockets instead of the previous 6 x 6 x ½-in. (152 x 152 x 13-mm) tubes. Overall, these simple changes significantly increased both the strength of the grout pocket longitudinal anchorage and the rail bending strength. Further, these changes also eliminated all butt welds and reduced the number of longitudinal reinforcing bars in the rail.

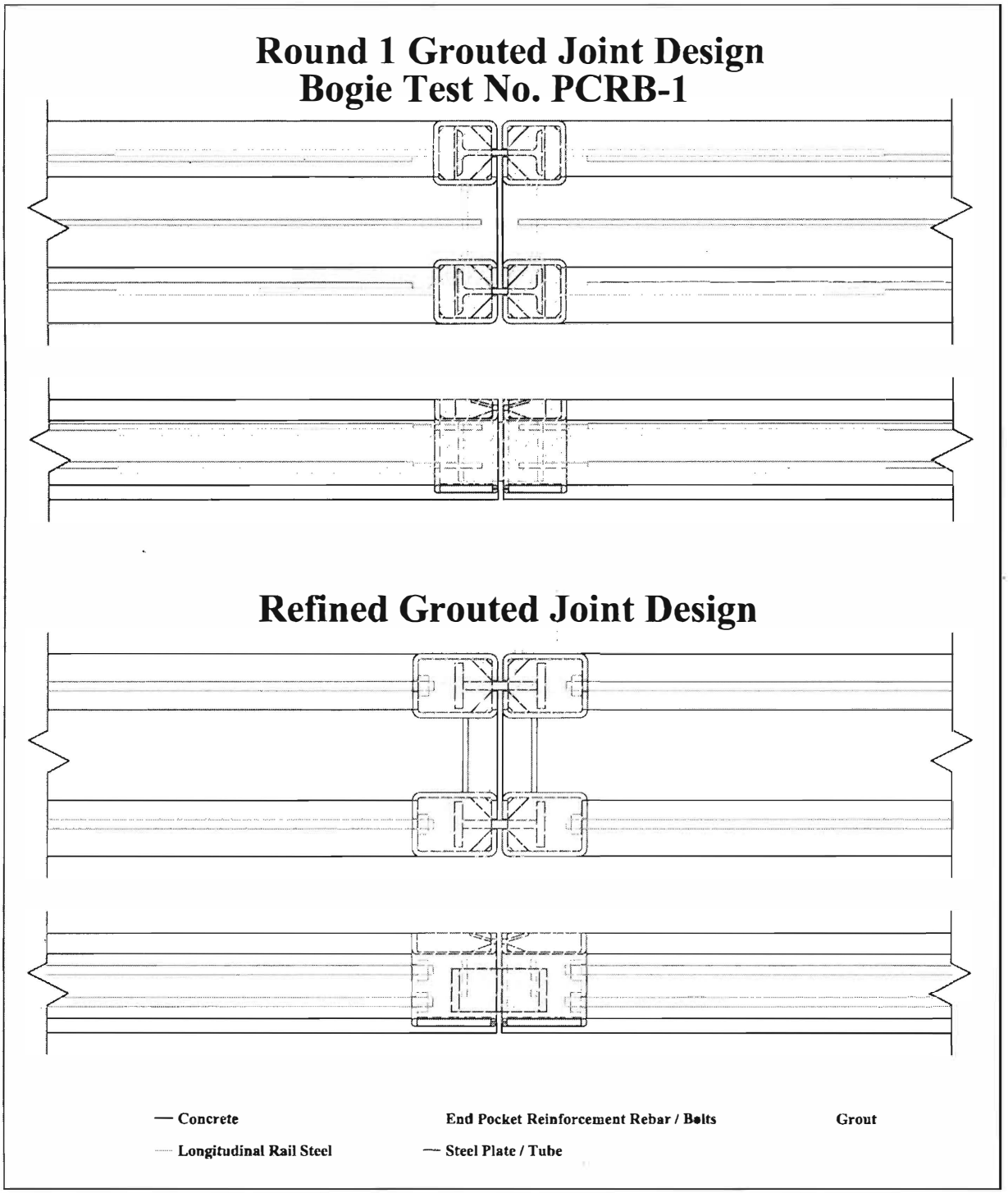

Figure 92. Grout Rail Joint Improvements – Steel I-Shape Connector

The shear reinforcement was also modified to allow for a greater resistive strength. The no. 4 rebar which tied the pockets together was replaced by a $^{5}/_{16}$-in. (8-mm) thick plate, as shown in Figure 92. Fillet welds on both sides of the plate were utilized to replace the unreliable butt welds. Thus, the strength of both the connecting element and the welds were greatly increased.

Two changes were made to the reinforcement of the pocket to prevent it from prying open. First, a 5/8-in. (16-mm) diameter, Grade 5 shear bolt was placed near the top front corner of the pocket to prevent the outside wall of the tube from prying open. Similar to the shear bolt used in the dry design in test no. PCRB-2, a nut was welded to the inside of the pocket before casting so that only the bolt was needed during construction. Second, the thickness of the grout tube cap at the bottom of the pocket was increased from ⅛ in. (3 mm) to ¼ in. (6 mm). This increase in thickness allowed the cap to act as a gusset plate and help prevent the pocket from prying open.

The final change to the grouted joint design was to use a built-up, steel I section instead of the previous S8x23 (S200x34) section. An increase in web thickness was desired for increased bending strength. However, all standard sections were too deep to fit into the available space. Therefore, the I-shaped section was fabricated from three ¾-in. (19-mm) thick plates that were welded to together to form the desired section.

7.2 Alternate Grout Joint

During the refinement of the grouted joint described in Section 7.1, design alternatives arose which concerned both pocket anchorage and the prevention of pocket prying action. These alternate ideas were combined to create a second grouted joint design. Instead of a steel I-shaped connector, the alternate joint utilized a threaded rod assembly to connect adjacent rail pockets.

This assembled connector consisted of a threaded rod, four nuts, and two washer plates, as shown in Figure 93. The threaded rod spanned between grout pockets of adjacent rail segments and two nuts were used to secure a washer plate at each end of the threaded rod. The washer plates acted similar to the flanges of the previous I-section by preventing longitudinal movement inside the grout pocket. Thus, the rod provided both tensile and compressive resistance. The threaded rod was designed to transfer all loads across the joint, similar to the web of the I-section.

The advantage of using the threaded rod connector instead of an I-section was that the rod could slide through holes in adjacent grout pockets and then be assembled inside the pockets. Thus, the slots cut into the grout pockets in previous designs were replaced by a hole. Since the pocket was a complete steel tube without the slot cut down one side, it was much stronger. Further, the removal of the slot eliminated the potential for the pocket to pry open. Therefore, the gusset plates at the top of the pocket were unnecessary and removed.

Similar to the refined grouted joint discussed in Section 7.1, the longitudinal anchorage of the grout pocket was altered to eliminate weak butt welds and reduce the number of reinforcing bars. The two no. 5 longitudinal bars on each side of the rail were replaced by a single no. 8 bar with threaded ends. The threaded ends were inserted into the backside of the grout pocket and nuts fastened the pocket to the longitudinal bar. The no. 8 bars were positioned in line with the threaded rod joint connectors to create concentric loading during load transfer. Also similar to the grout joint modifications of Section 7.1, the pocket had to be extended longitudinally in order for both the joint connector and the longitudinal bar to fit inside the pocket.

Lateral pocket anchorage consisted of a ½-in. (13-mm) thick shear plate running between the pockets. Fillet welds were used to fasten the shear plate to the grout pockets, thus removing the butt welds that failed during test no. PCRB-1. Also, three U-shaped no. 4 bars were wrapped around the plate and extended into the rail. These U-bars provided additional longitudinal pocket anchorage as well as reinforcement to prevent concrete failures on the plane directly behind the pockets.

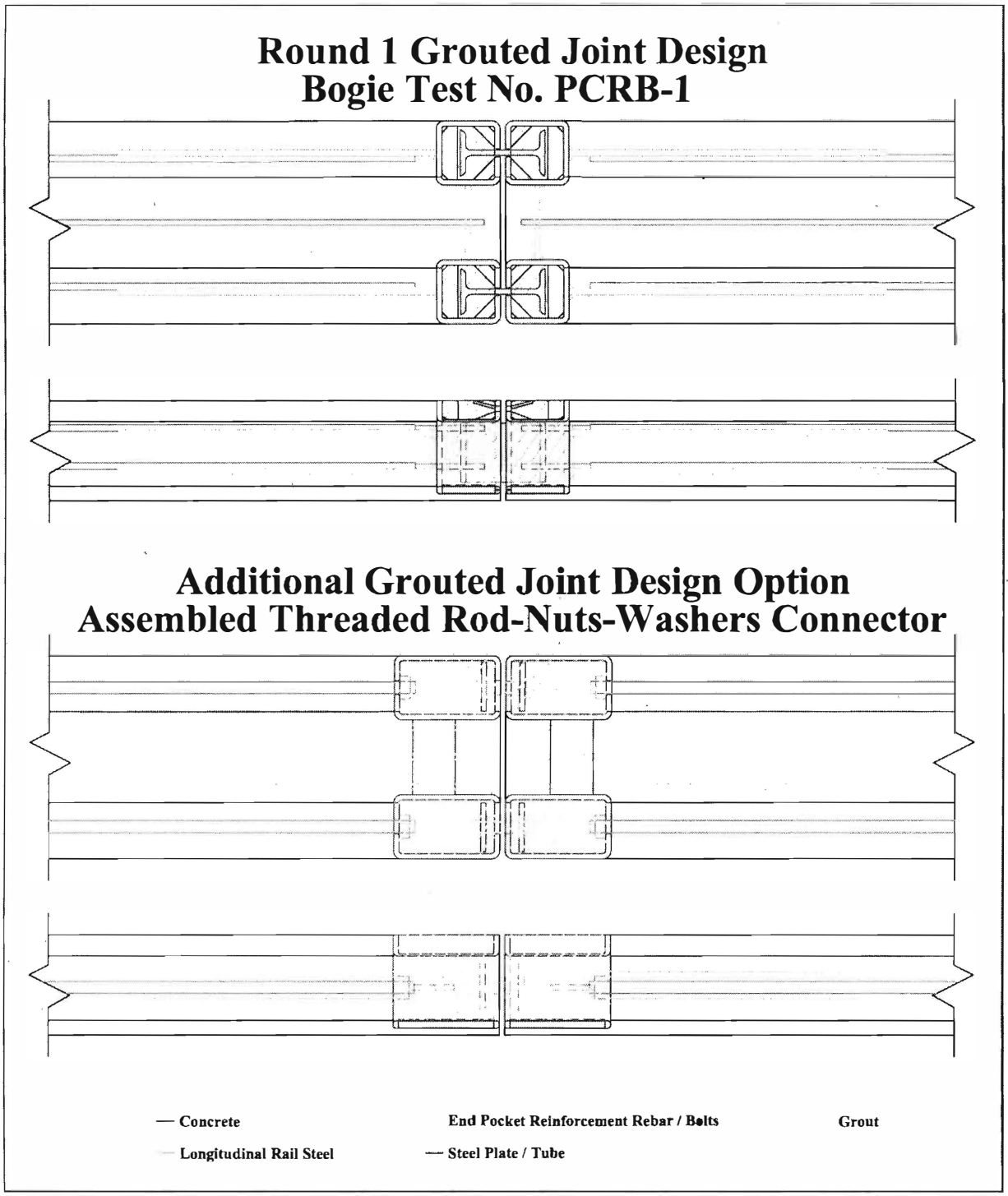

Figure 93. Grout Rail Joint Improvements – Alternate Modifications

7.3 Refined Dry Joint

After evaluating the results of the dry rail joint in bogie test no. PCRB-2, multiple design weaknesses were identified. First, the shear tubes length was insufficient to prevent significant lateral movement of one side of the joint relative to the other before load transfer occurred. Second, the butt welds used to attach anchorage rebar to the steel pockets proved too weak and subsequently failed. Third, the anchorage bars needed to be optimized with a focuse on reducing the number of bars required to adequately anchor the pockets while simultaneously confining the concrete around the pockets. All of these design aspects were incorporated in the refined design to increase the capacity and improve the load transfer of the dry joint. The refined dry joint is shown in Figure 94.

As described previously in the modifications to the grouted joints, the longitudinal steel used in the refined dry joint was altered to eliminate butt welds and increase efficiency. One of the two no. 5 longitudinal bars on each side of the original rail segment was replaced with a threaded no. 8 bar. Due to this additional strength, the two no. 4 bars running down the center of the rail were removed. The remaining no. 5 bars, one on each side of the rail, stopped at the pocket edge, while the ends of the no. 8 bars extended into the steel pockets at the ends of the rail. However, the no. 8 bars were not fastened to the pocket itself like the other refined joint designs. Instead the no. 8 bars were fastened to a redesigned shear tube connector inside the rail end pockets. This new connector directly tied the longitudinal bars of adjacent rail together and was designed to transfer both shear and tension loads across the joint. As such, the tension bolt from the previous dry joint design was removed.

The new shear tube connectors were cut from a 25½ in. (648 mm) long, 8 x 4 x ½-in. (203 x 102 x 13-mm) steel tube to form two 4 x 4 x ½-in. (102 x 102 x 13-mm) U-shape pieces.

End caps measuring ⅝ in. (16 mm) thick were welded at each end of these U-shape connectors. Slots measuring 1⅜ in. (35 mm) wide were cut into the top of the shear tube connectors on the outer 5 in. (127 mm) of each end. These slots were extended down into the gusset plates 1⅝ in. (41 mm). During construction of the joint, the shear tube would be inserted into the adjacent rail pockets and the no. 8 bars would pass through the slots and into the center of the shear tube connector. Washer plates and nuts would then be applied to each of the threaded no. 8 bars to secure the shear tube connector in place and link the longitudinal steel of adjacent rails together. The new shear tube connector improved the joint design by increasing the size and length of the tube to improve load capacity and to ensure that the load transfer would occur more rapidly.

The size of the joint connection pockets increased in the refined dry joint design. The new joint pockets were formed by cutting a 12 x 6 x ½-in. (305 x 152 x 13-mm) tube to match the rail geometry. The length of the pocket was increased to 14 in. (356 mm). A 5/8-in. (16-mm) diameter, Grade 5 shear bolt was placed near the open end of the pocket to prevent the outside wall of the tube from prying open. Changes were also made to the shear reinforcement anchoring the steel pockets together. The two rebar segments that connected to the pockets with butt welds were each replaced by a $^{5}/_{16}$-in. (8-mm) thick steel plate and fillet welds. Therefore, two steel plates were used as lateral reinforcement, one near the joint and the second near the far end of the pockets. Also, three galvanized no. 3 bars were welded across the tops of the pockets to better confine the concrete near the end of the rail.

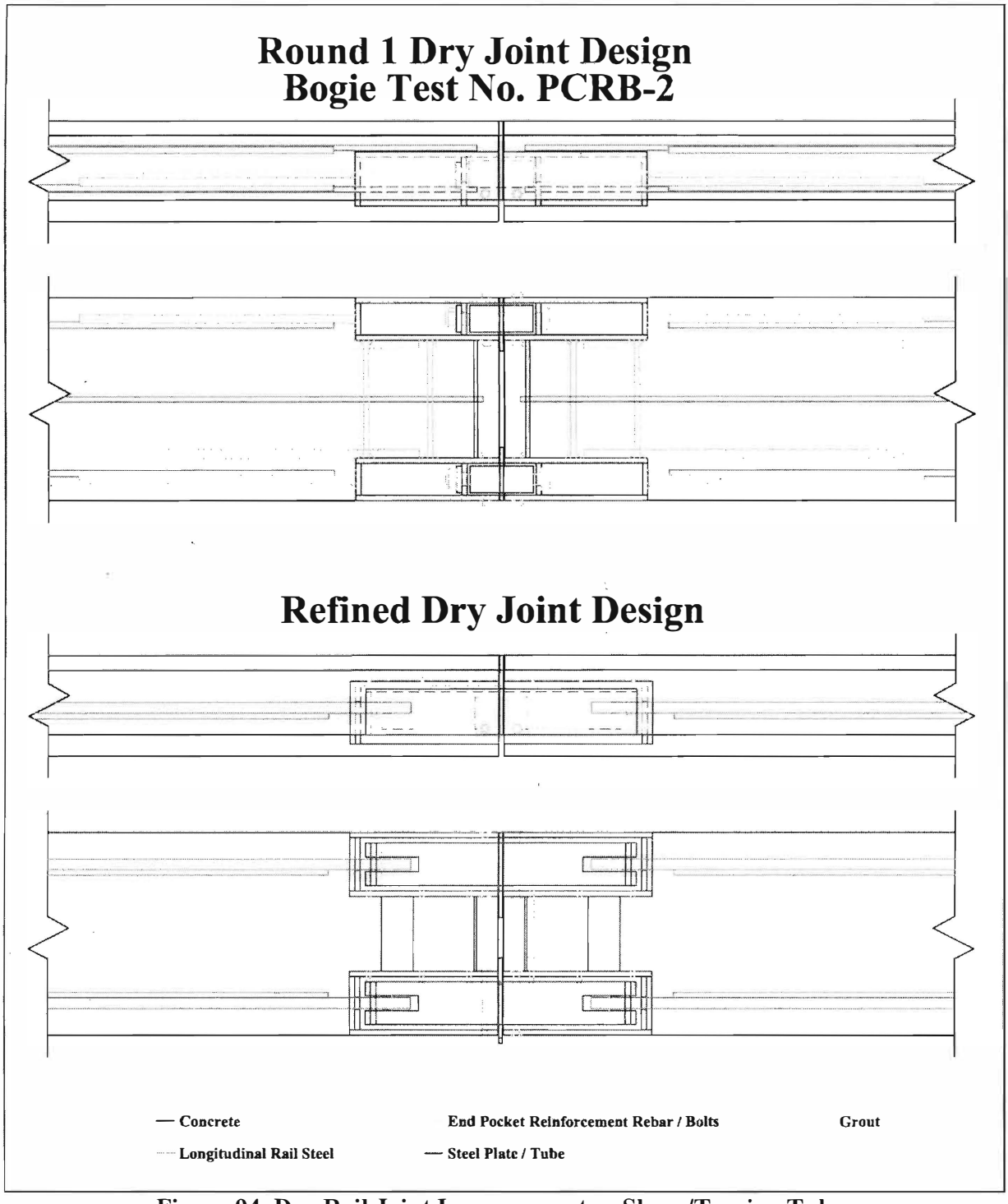

Figure 94. Dry Rail Joint Improvements – Shear/Tension Tube

8 RAIL JOINT BOGIE TESTING - ROUND 2

8.1 Scope

The first round of bogie tests, as described in Chapter 6, helped identify weaknesses in each of the selected grouted and dry rail-to-rail joint designs. Refinements to these rail joint concepts resulted in the three improved joint concepts (i.e., two grouted and one dry) as discussed in Chapter 7. Each of these three rail joints were used to connect short segments of concrete beams with the same cross section shape as the upper rail of the selected bridge rail design. The joint components were dynamically tested with the same set-up and under the same conditions as the first round of bogie tests. General details describing the bogie tests and testing facility can be found in Section 6.2 and 6.3, respectively.

8.2 Equipment and Instrumentation

The same accelerometers and pressure tape switches from the first round of bogie testing were used during the second round of testing. Accelerometer and pressure tape switch details can be found in Section 6.4.

8.2.1 Bogie

The same bogie vehicle from the first round of bogie testing was used during the second round of testing. However, the wooden blockouts used to offset the bogie head from the vehicle frame were damaged during test no. PCRB-2. As such, steel tubes were used instead of wooden blockouts to provide a more robust bogie head. These steel tubes were filled with concrete and capped with a steel plate, as shown in Figure 95. The weight of the bogie with the addition of concrete filled steel tubes to the impact head was 1,707 lbs (774 kg).

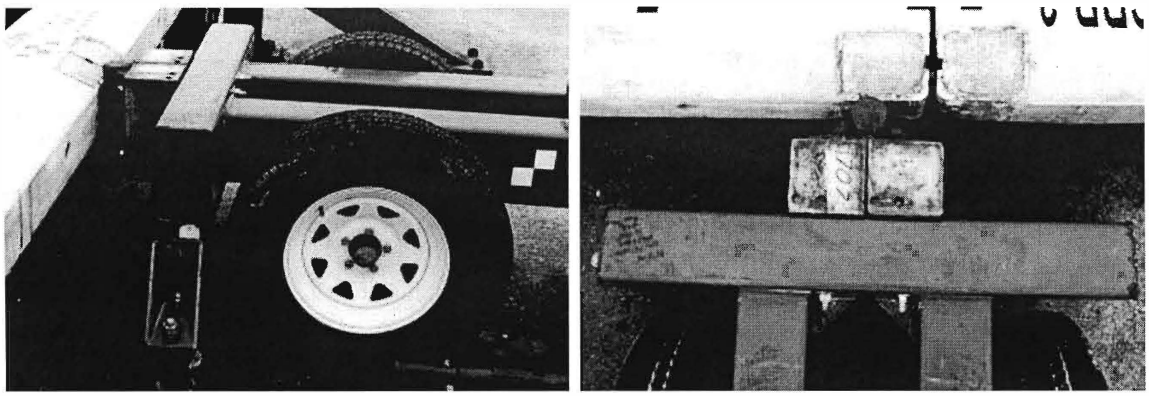

Figure 95. Bogie Impact Head with Steel Tube Blockouts

8.2.2 Photography Cameras

For test nos. PCRB-3 and PCRB-4, three high-speed AOS VITcam video cameras and four JVC digital video cameras were utilized to record the crash test. Camera details, lens information, and camera operating speeds are shown in Table 4. A schematic of the camera locations is shown in Figure 96. A Nikon D50 digital camera was used to photograph pre- and post-test conditions for each joint component.

Table 4. Camera and Lens Information, Test Nos. PCRB-3 and PCRB-4

	No.	Type	Operating Speed (frames/sec)	Lens	Lens Setting
High-Speed Video	1	Vitcam CTM	500	Signma 24-70	70
	2	Vitcam CTM	500	Cosmicar 12.5 Fixed	--
	5	Vitcam CTM	500	Sigma 50 Fixed	--
Full-Speed Video	2	JVC-GZ-MC40u (Everio)	29.97		
	3	JVC-GZ-MC40u (Everio)	29.97		
	4	JVC-GZ-MC40u (Everio)	29.97		
	5	JVC-GZ-MC27u (Everio)	29.97		

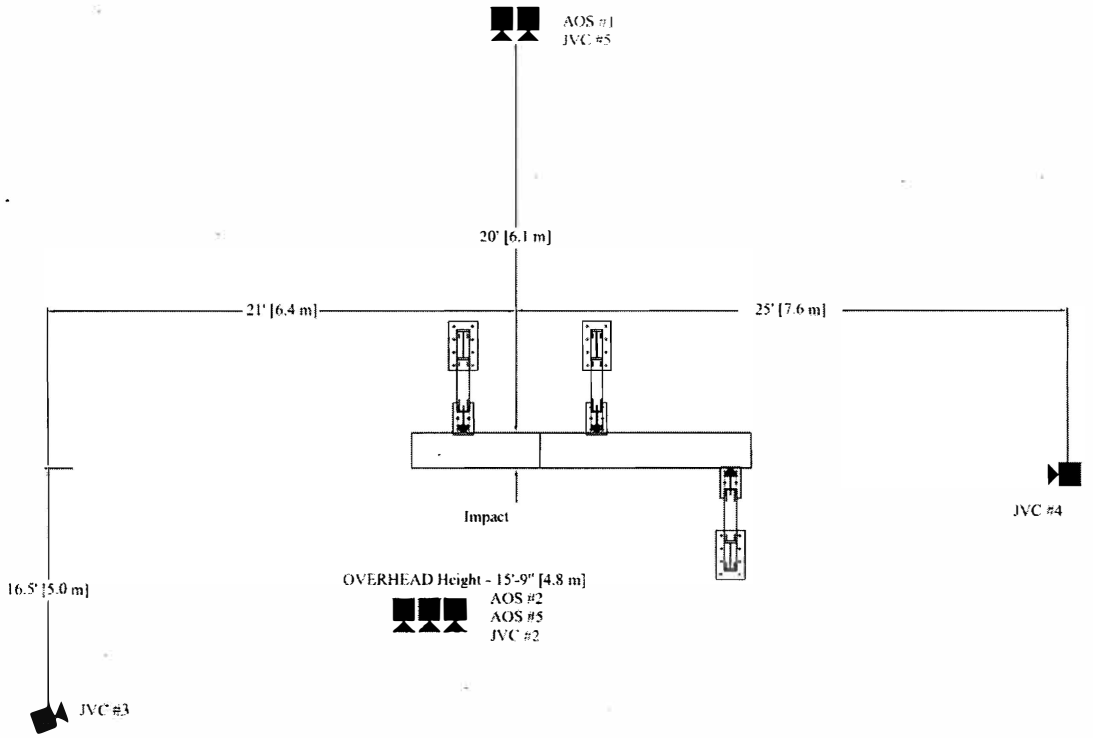

Figure 96. Camera Locations, Test Nos. PCRB-3 and PCRB-4

For test no. PCRB-5, three high-speed AOS VITcam video cameras and four JVC digital video cameras were utilized to record the crash test. Camera details, lens information, and camera operating speeds are shown in Table 5. A schematic of the camera locations is shown in Figure 97. A Nikon D50 digital camera was used to document pre- and post-test conditions for each joint component.

Table 5. Camera and Lens Information, Test No. PCRB-5

	No.	Type	Operating Speed (frames/sec)	Lens	Lens Setting
High-Speed Video	1	Vitcam CTM	500	Sigma 50 Fixed	--
	2	Vitcam CTM	500	Cosmicar 12.5 Fixed	--
	5	Vitcam CTM	500	Sigma 24-70	24
Full-Speed Video	2	JVC-GZ-MC40u (Everio)	29.97		
	3	JVC-GZ-MC40u (Everio)	29.97		
	4	JVC-GZ-MC40u (Everio)	29.97		
	5	JVC-GZ-MC27u (Everio)	29.97		

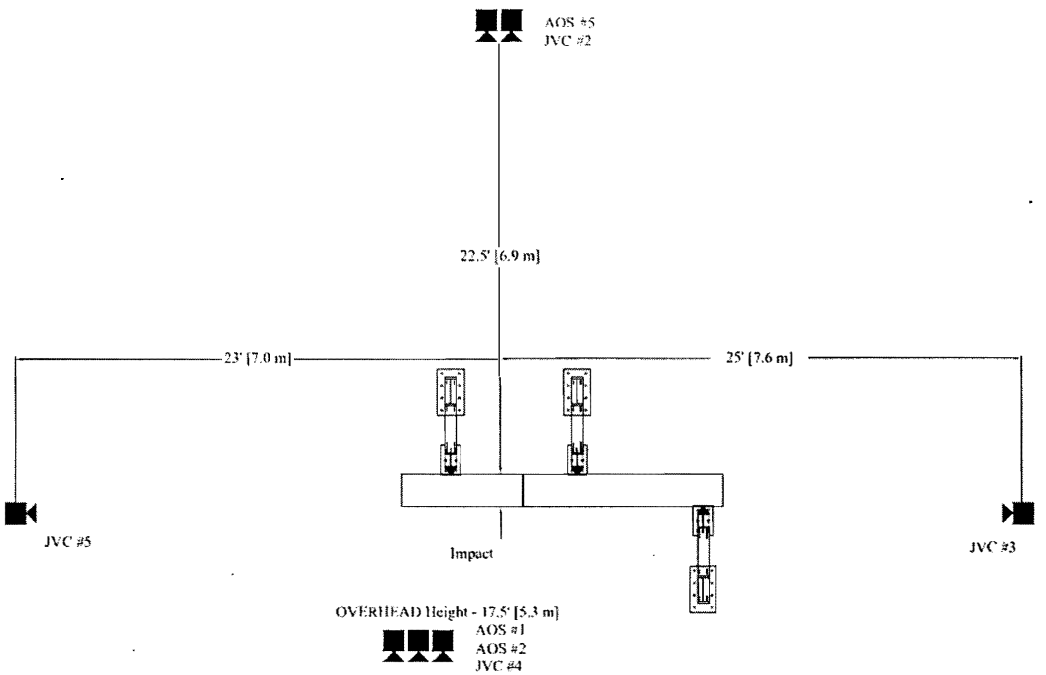

Figure 97. Camera Locations, Test No. PCRB-5

8.3 Test Specimen – Joint Designs

8.3.1 Test No. PCRB-3, Refined Grout Joint Design

The test specimen used for test no. PCRB-3 consisted of two reinforced concrete rail segments connected by two I-shaped steel sections and grout, as shown in Figures 98 through 111. The cross sectional geometry of the concrete rail segments was the same as the upper rail of the selected bridge rail design, Concept F (Fence). One rail segment had a length of 9 ft – 6 in. (2.90 m), while the other segment had a length of 5 ft – 9 in. (1.75 m). The concrete used in the construction of the rails had a design strength of 5,000 psi (34 MPa).

Both stirrups and longitudinal bars were used as steel reinforcement for the rail segments, as shown in Figures 100 through 104. The closed loop stirrups were epoxy coated no. 4 rebar with a 8 in. (203 mm) spacing. Near the ends of the segments this spacing was reduced to 4 in. (102 mm) to protect against localized damage from the anchor post supports and the impact

head. All stirrups were given a minimum clear cover of 1½ in. (38 mm). The longitudinal reinforcement consisted of two no. 7 threaded rebar placed on each side of the rail cross section. All four threaded bars were galvanized grade 60 bars

One end of each rail segment was configured with steel pockets on both the front and back faces of the rail. These pockets were composed of 6 x 8 x ½-in. (152 x 203 x 13-mm) ASTM A500 Grade C steel tubes cut to match the cross section geometry of the rail, as shown in Figures 107 and 108. The back side of these pockets had two 1⅛-in. (29-mm) diameter holes in which the rail longitudinal steel was extended through. A hex nut was used to fasten each bar inside the pockets. Also, the front face of the pockets had a 1-in. (25-mm) wide slot cut into it which allowed the web of the steel I-shape segment to pass between adjacent pockets. Shear bolt holes measuring $^{11}/_{16}$ in. (17 mm) in diameter were placed on both the left and right sides of each pocket. A hex nut was welded over the shear bolt hole on the inside face of the pocket so that only the ⅝-in. (16-mm) diameter shear bolt was needed during assembly.

To hold the steel I-segment and grout inside the pocket during assembly, a ¼-in. (6-mm) thick plate was welded to the bottom of the pocket as a cap. Also, two ¼-in. (6-mm) thick gusset plates were welded to the inside corners near the top of each pocket to prevent the pocket from prying open. Finally, a $^{5}/_{16}$-in. (8-mm) thick, 3½-in. (89-mm) wide shear plate was welded between the pockets for lateral support. All steel plates and gussets were made from A572 Grade 50 steel and are shown in Figures 105, 106, and 109. The entire end pocket assembly was galvanized.

Three pieces of ¾-in. (19-mm) thick galvanized, ASTM A572 Grade 50 steel plate were used to create each 4-in. (102-mm) tall I-shape connector, as shown in Figure 110. The web was

7 in. (178 mm) long, and the flanges were 4¼ in. (108 mm) wide. Pairs of ½-in. (13-mm) fillet welds were used to secure the flanges to the web.

The rail segments were placed on wooden support blocks and positioned as prescribed by Section 6.2 and Figure 48. To assemble the rail joint, two I-shape connectors were dropped into the pockets with the web spanning across the ½-in. (13-mm) wide gap between rail ends. Next, a ⅝-in. (16-mm) diameter shear bolt was inserted through the $^{11}/_{16}$-in. (17-mm) diameter holes of each pocket and turned through the fixed nut on the inside surface of each pocket. Once the connectors and shear bolts were in place, L&M Crystex grout with a strength of 10,000 psi (69 MPa) was used to fill the pockets and secure the steel I-shape connectors. Photographs of the assembled joint specimen are shown in Figure 111.

Wide Flange Connection – Option A					
Item No.	QTY	Description	Material Spec	Comment	File Name
p1	1	Wide Flange Connection Option A – 5.75 ft Beam	–	–	Beam_1–Grouted_Wide_Flange_OptionA_5.75ft
p2	1	Wide Flange Connection Option A – 9.5 ft Beam	–	–	Beam_1–Grouted_Wide_Flange_OptionA_9.5ft
e1	2	Option A L&M Crystex Grout	L&M Crystex Grout – f'c = 10000 psi	–	Beam_1–Grouted_Wide_Flange_Option_A_grout
e2	2	Option A Built Up Wide Flange Section	A572 Grade 50 – Galvanized	–	Beam_1–Grouted_Wide_Flange_Option_A_W-section
c8	4	Heavy Hex Bolt 0.625–11x7x1.25	Grade 5 – Galvanized	–	Beam_1–Grouted_Wide_Flange_Option_A_HHBOLT 0.6250–11x7x1.25–C

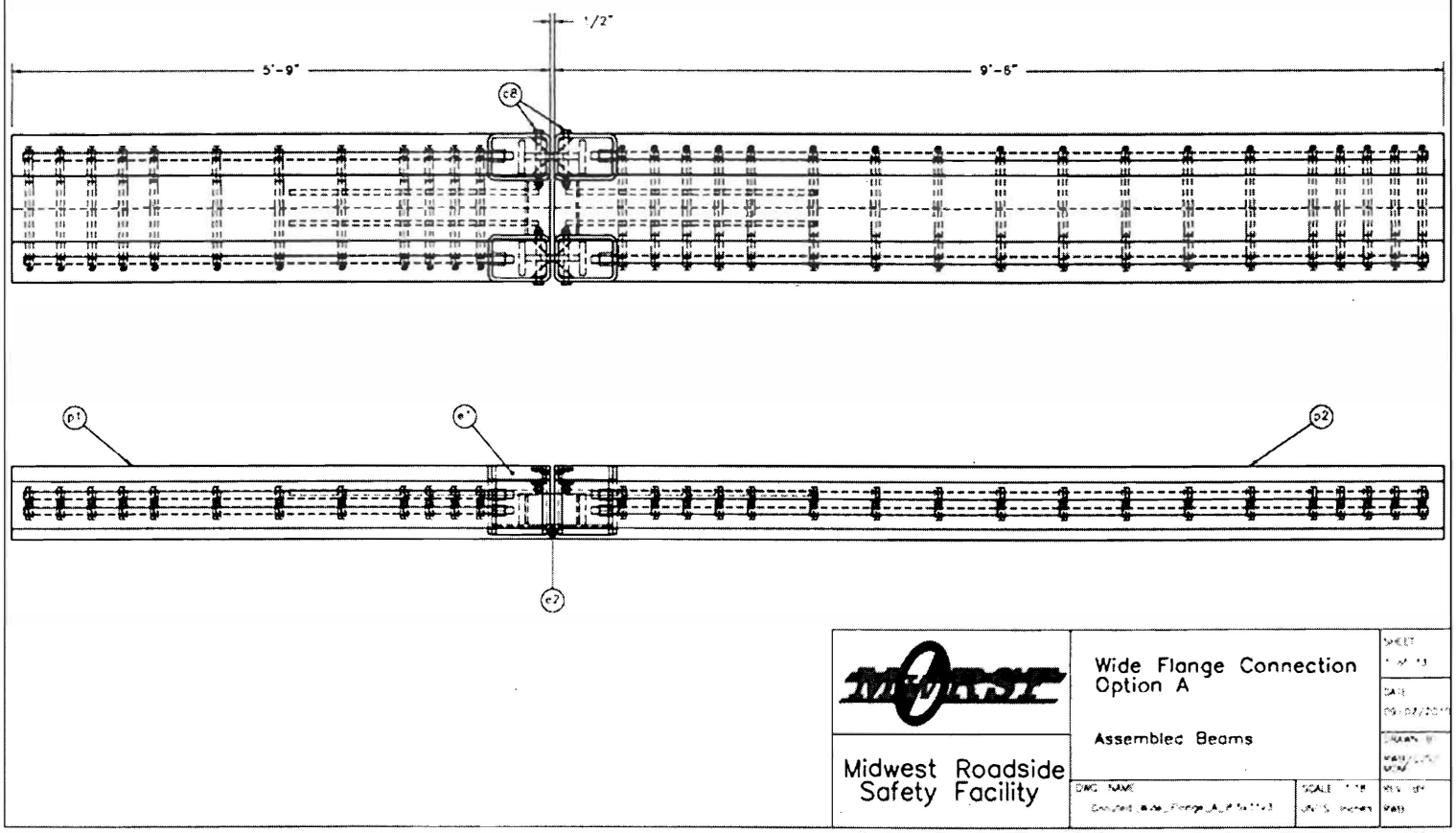

Figure 98. Refined Grout Rail Joint Design, Test No. PCRB-3

Wide Flange Connection – Option A

Item No.	QTY	Description	Material Spec	Comment	File Name
p1	1	Wide Flange Connection Option A – 5.75 ft Beam	–	–	Beam_1-Grouted_Wide_Flange_OptionA_5.75ft
p2	1	Wide Flange Connection Option A – 9.5 ft Beam	–	–	Beam_1-Grouted_Wide_Flange_OptionA_9.5ft
e1	2	Option A L&M Crystex Grout	L&M Crystex Grout – f'c = 10000 psi	–	Beam_1-Grouted_Wide_Flange_Option_A_grout
e2	2	Option A Built up Wide Flange Section	A572 Grade 50 – Galvanized	–	Beam_1-Grouted_Wide_Flange_Option_A_W-section
c8	4	Heavy Hex Bolt 0.625-11x7x1.25	Grade 5 – Galvanized	–	HHBOLT 0.6250-11x7x1.25-C

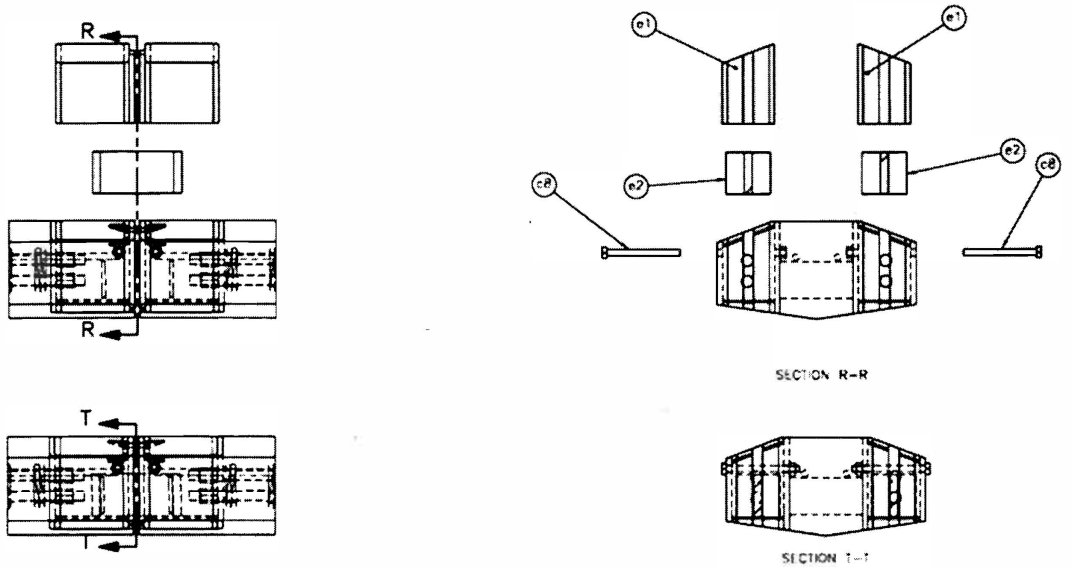

Midwest Roadside Safety Facility

Wide Flange Connection Option A

Connection Detail

Figure 99. Refined Grout Joint Assembly, Test No. PCRB-3

Wide Flange Connection – Option A					
Item No.	QTY	Description	Material Spec	Comment	File Name
a1	1	Precast Concrete Bridge Rail Section	SSC f'c = 5000 psi	–	Beam_1–Grouted_Wide_Flange_Option_A_body_9.5ft
b1	18	No. 4 Top Rail Stirrup	A615 Grade 60 – Epoxy Coated	–	Beam_1–Grouted_Wide_Flange_toprail_stirrup_No.4_Grade60
c1	1	Wide Flange Connection Option A	–	–	Beam_1–Grouted_Wide_Flange_Option_A
c10	4	Williams R53-07 Hex Nut	Galvanized	–	HNUT 0.8750-9-D-N
c12	4	No. 7 Williams Grade 60 All-Thread Rebar – R50-07	Grade 60 – Galvanized	–	Beam_1–Grouted_Wide_Flange_Option_A_9.5ft_No.7_Grade60_threadbarR50-07

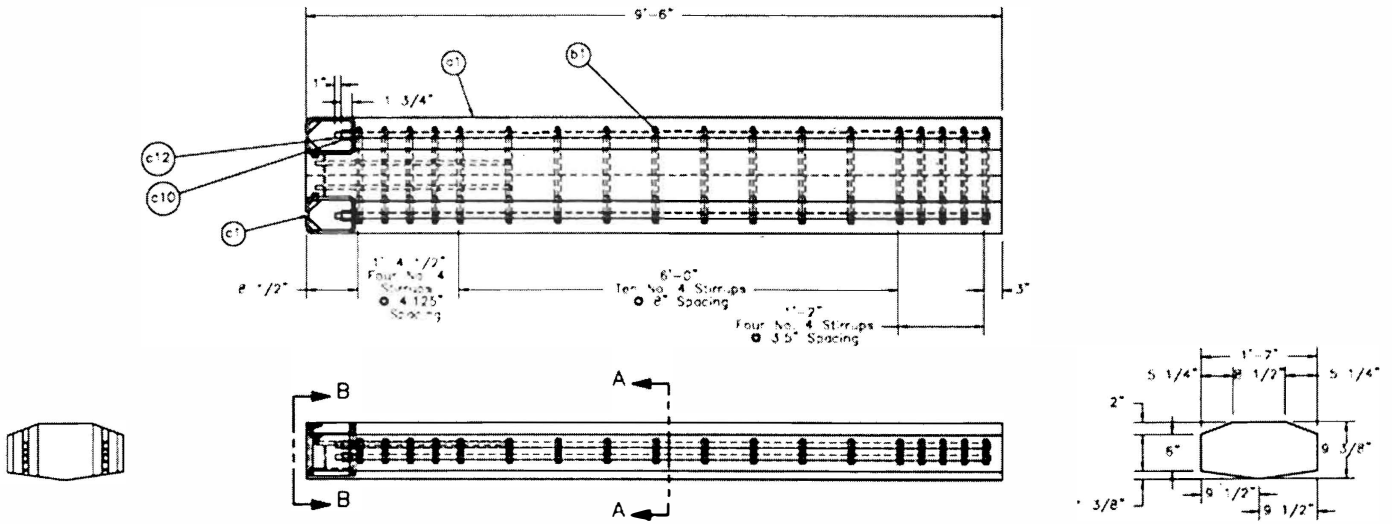

Notes:

1. Design shown with Williams Form Engineering Grade 60 All-Thread Rebar and hex nut hardware. Dywidag Threadbar products and hext nut hardware with similar capacity can be substituted if desired.

Midwest Roadside Safety Facility

Wide Flange Connection Option A

Wide Flange Connection Option A 9.5 ft Beam

SCALE 1:24
UNITS inches

Figure 100. Long Rail Segment, Test No. PCRB-3

Wide Flange Connection – Option A					
Item No	QTY	Description	Material Spec	Comment	File Name
a1	1	Precast Concrete Bridge Rail Section	SSC f'c = 5000 psi	–	Beam_1–Grouted_Wide_Flange_Option_A_body_9.5ft
b1	18	No. 4 Top Rail Stirrup	A615 Grade 60 – Epoxy Coated	–	Beam_1–Grouted_Wide_Flange_toprail_stirrup_No.4_Grade60
c10	4	Williams R53-07 Hex Nut	Galvanized	–	HNUT 0.8750-9-D-N
c12	4	No. 7 Williams Grade 60 All-Thread Rebar – R50-07	Grade 60 – Galvanized	–	Beam_1–Grouted_Wide_Flange_Option_A_9.5ft_No.7_Grade60_threadbarR50-07

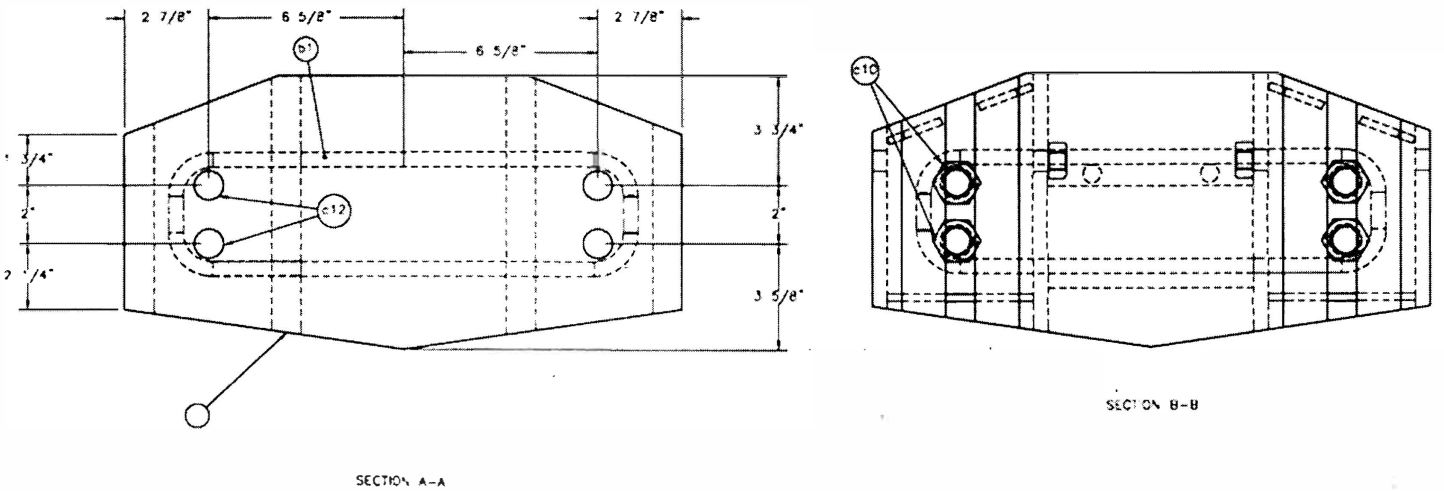

Note:
1. Stirrup clear cover is 1.5" on the side and 2.625" from the top face of the rail section

Midwest Roadside Safety Facility

Wide Flange Connection Option A

Figure 101. Cross Section Views of Long Rail Segment, Test No. PCRB-3

Wide Flange Connection – Option A					
Item No.	QTY.	Description	Material Spec	Comment	File Name
a2	1	Precast Concrete Bridge Rail Section	SSC f'c = 5000 psi	–	Beam_1–Grouted_Wide_Flange_Option_A_body_5.75ft
b1	12	No. 4 Top Rail Stirrup	A615 Grade 60 – Epoxy Coated	–	Beam_1–Grouted_Wide_Flange_toprail_stirrup_No.4_Grade60
c1	1	Wide Flange Connection Option A	–	–	Beam_1–Grouted_Wide_Flange_Option_A
c10	4	Williams R53-07 Hex Nut	Galvanized	–	HNUT 0.8750-9-D-N
c13	4	No. 7 Williams Grade 60 All Thread Rebar R50-07	Grade 60 – Galvanized	–	Beam_1–Grouted_Wide_Flange_Option_A_5.75ft_No.7_Grade60_threadbarR50-07

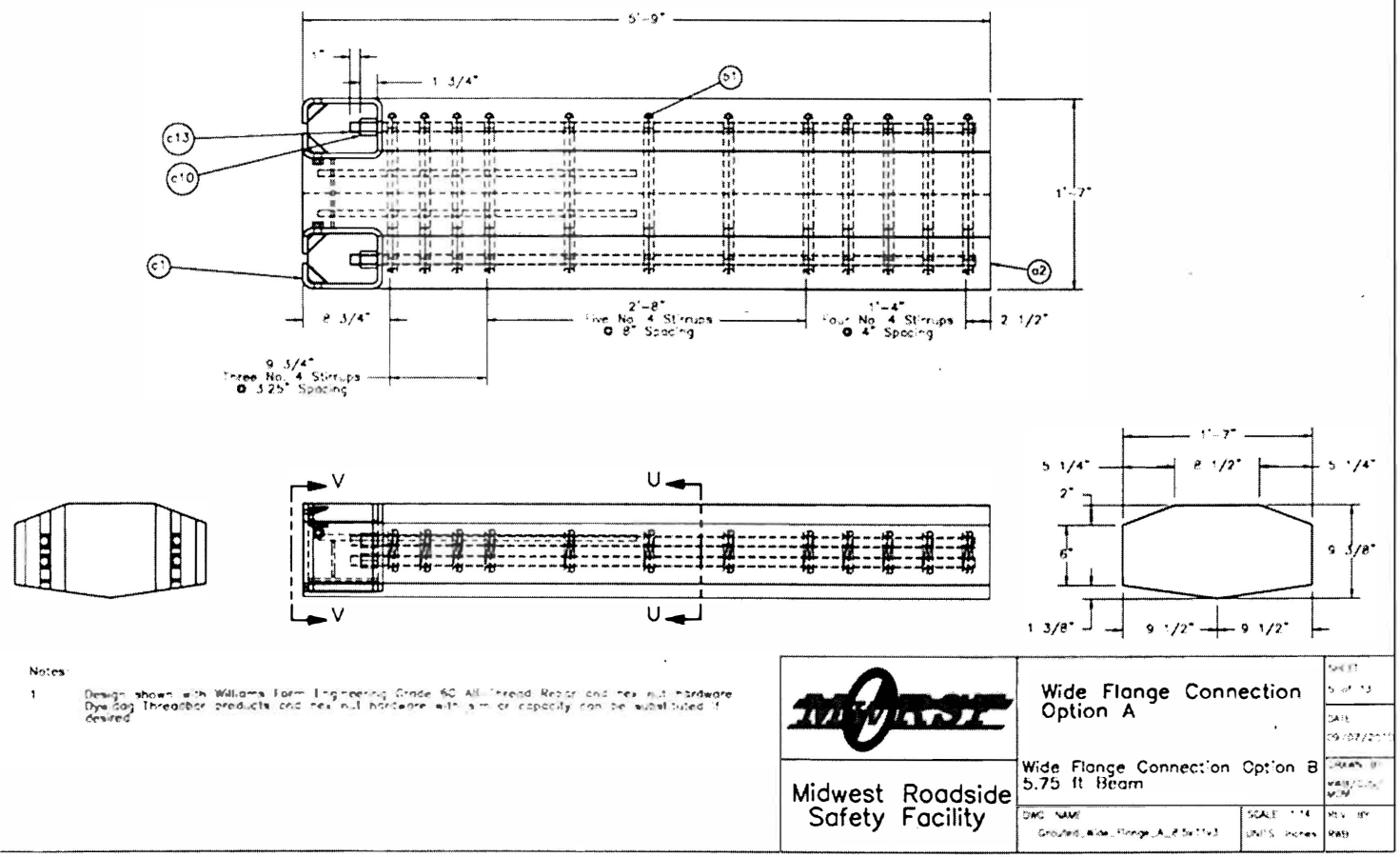

Figure 102. Short Rail Segment, Test No. PCRB-3

Wide Flange Connection – Option A					
Item No.	QTY	Description	Material Spec	Comment	File Name
a2	1	Precast Concrete Bridge Rail Section	SSC f'c = 5000 psi	–	Beam_1–Grouted_Wide_Flange_Option_A_body_5.75ft
b1	12	No. 4 Top Rail Stirrup	A615 Grade 60 – Epoxy Coated	–	Beam_1–Grouted_Wide_Flange_toprail_stirrup_No.4_Grade60
c10	4	Williams R53-07 Hex Nut	Galvanized	–	HNUT 0.8750-9-D-N
c13	4	No. 7 Williams Grade 60 All-Thread Rebar – R50-07	Grade 60 – Galvanized	–	Beam_1–Grouted_Wide_Flange_Option_A_5.75ft_No.7_Grade60_threadbarR50-07

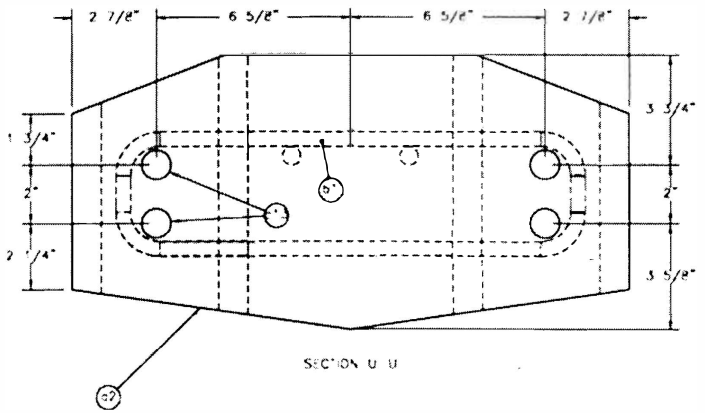

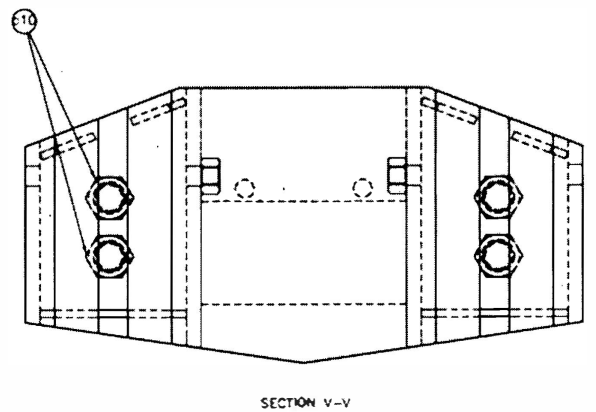

Note
1. Stirrup clear cover is 1.5" on the side and 2.625" from the top face of the rail section

Midwest Roadside Safety Facility

Wide Flange Connection Option A

Main Beam Reinforcement 5.75 ft beam and Connection End View

DWG NAME: Grouted_Wide_Flange_A_8.5x11x3
SCALE: 1:5
UNITS: Inches
REV BY: RWB

Figure 103. Cross Section Views of Short Rail Segment, Test No. PCRB-3

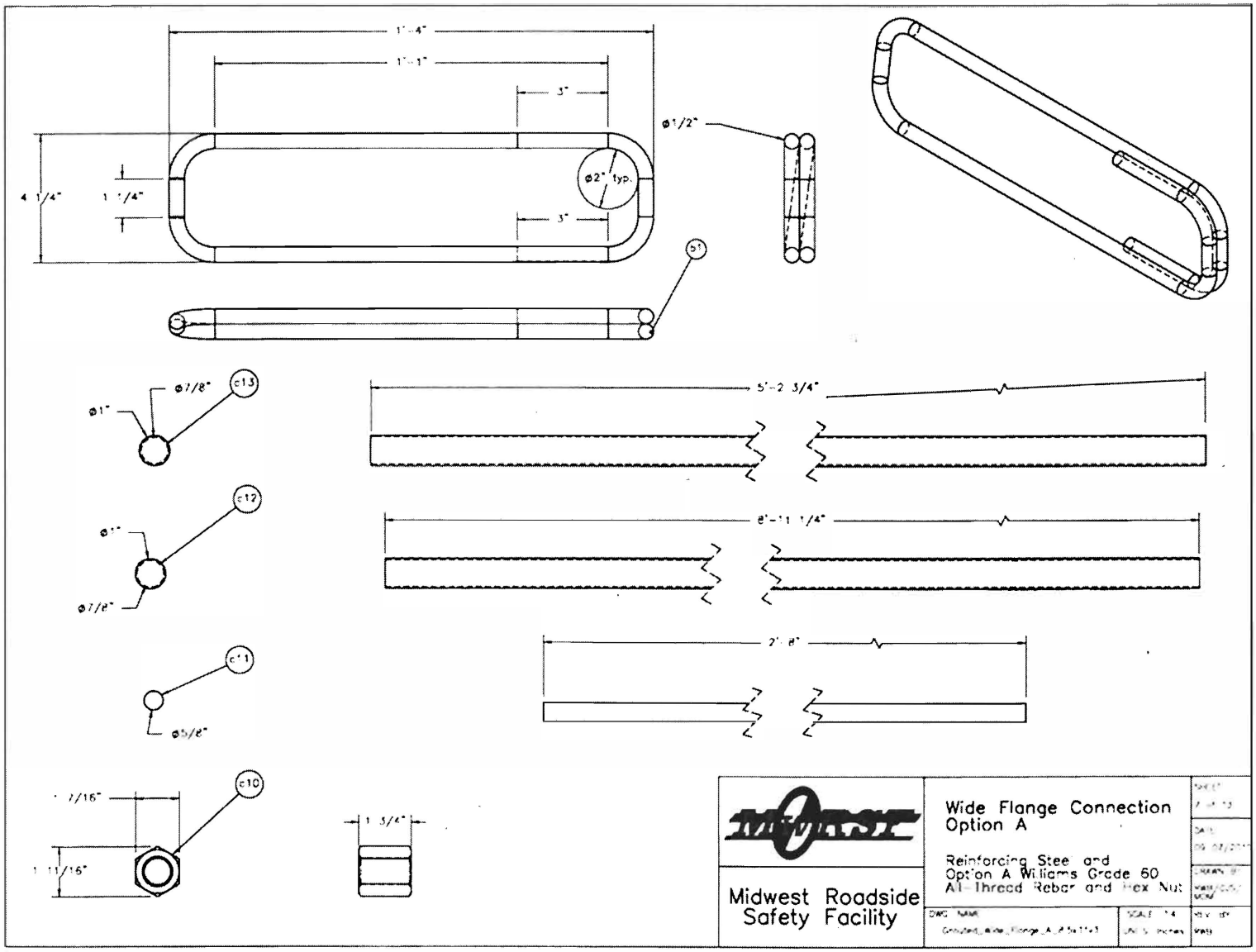

Figure 104. Rail Internal Steel Reinforcement, Test No. PCRB-3

Wide Flange Connection – Option A					
Item No.	QTY	Description	Material Spec	Comment	File Name
c2	1	Option A Left Grout Pocket Tube 6x8x0.5	A500 Grade C – Galvanized	–	Grouted_Wide_Flange_Option_A_grout_pocket left 6x8x0.5
c3	1	Option A Right Grout Pocket Tube 6x8x0.5	A500 Grade C – Galvanized	–	Grouted_Wide_Flange_Option_A_grout_pocket right 6x8x0.5
c5	2	Option A Grout Tube Cap	A572 Grade 50 – Galvanized	–	Grouted_Wide_Flange_Option_A_grout_pocket cap
c6	1	Option A Shear Plate	A572 Grade 50 – Galvanized	–	Grouted_Wide_Flange_Option_A_shear_plate A572Gr50
c7	2	0.625 UNC-11 Heavy Hex Nut	Grade 5 – Galvanized	–	HHNUT 0.6250-11-D-C
c9	4	Option A Grout Tube Gusset	A572 Grade 50 – Galvanized	–	Grouted_Wide_Flange_Option_A_grout_tube_gusset
c11	2	Option A No. 5 Baluster Reinforcement	A615 Grade 60 – Epoxy Coated	–	Grouted_Wide_Flange_Option_A_No.5_Grade60_baluster

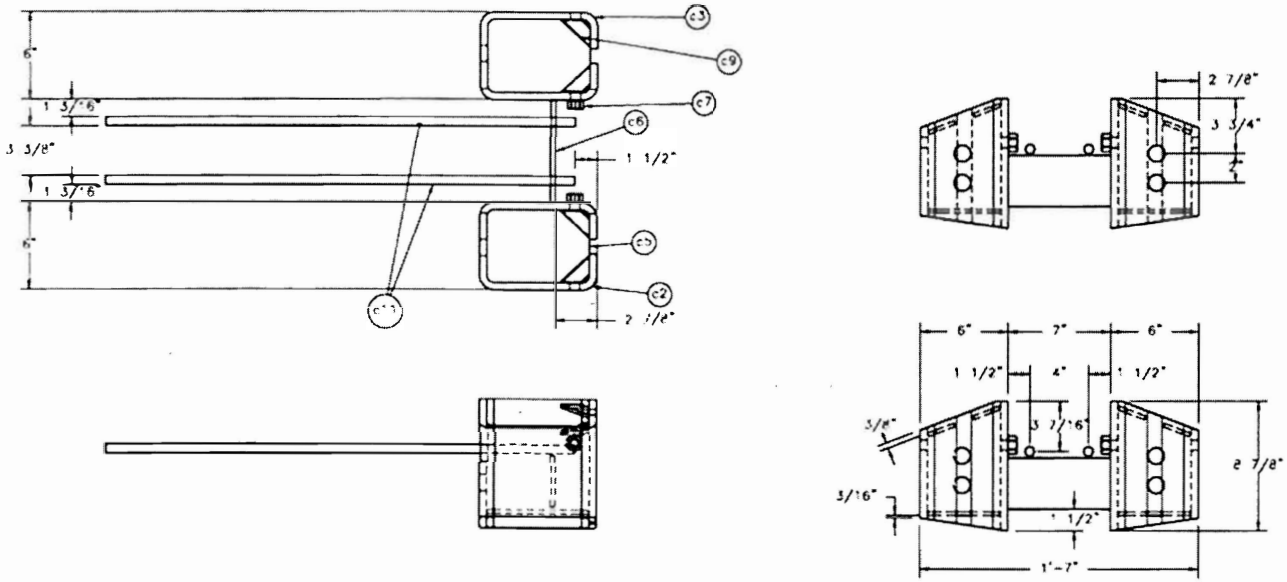

Midwest Roadside Safety Facility

Wide Flange Connection Option A

Option A End Connection Assembly

Figure 105. Grout Pocket Assembly, Test No. PCRB-3

Wide Flange Connection – Option A					
Item No.	QTY	Description	Material Spec	Comment	File Name
c2	1	Option A Left Grout Pocket Tube 6x8x0.5	A500 Grade C – Galvanized	–	Grouted_Wide_Flange_Option_A_grout_pocket left_6x8x0.5
c3	1	Option A Right Grout Pocket Tube 6x8x0.5	A500 Grade C – Galvanized	–	Grouted_Wide_Flange_Option_A_grout_pocket right_6x8x0.5
c5	2	Option A Grout Tube Cap	A572 Grade 50 – Galvanized	–	Grouted_Wide_Flange_Option_A_grout_pocket cap
c6	1	Option A Shear Plate	A572 Grade 50 – Galvanized	–	Grouted_Wide_Flange_Option_A_shear_plate_A572Gr50
c7	2	0.625 UNC-11 Heavy Hex Nut	Grade 5 – Galvanized	–	HHNUT 0.6250-11-0-C
c9	4	Option A Grout Tube Gusset	A572 Grade 50 – Galvanized	–	Grouted_Wide_Flange_Option_A_grout_tube_gusset
c11	2	Option A No. 5 Baluster Reinforcement	A615 Grade 60 – Epoxy Coated	–	Grouted_Wide_Flange_Option_A_No.5_Grade60_baluster

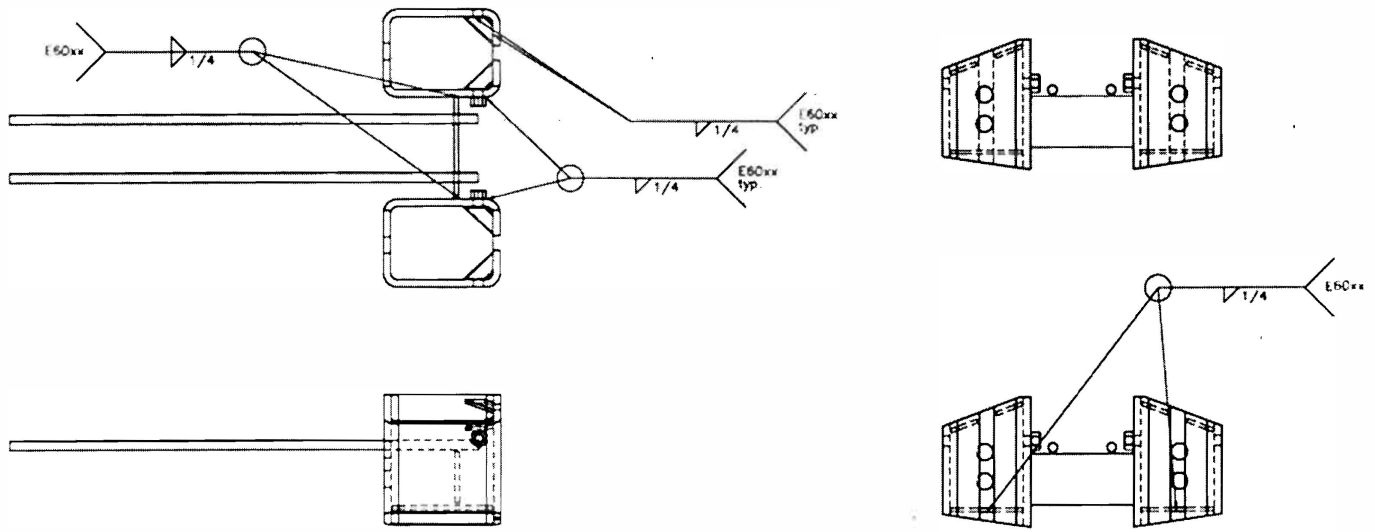

Midwest Roadside Safety Facility

Wide Flange Connection Option A

Connection Weld Details

Figure 106. Grout Pocket Assembly Connections, Test No. PCRB-3

Wide Flange Connection – Option A

Item No	QTY	Description	Material Spec	Comment	File Name
c2	1	Option A Left Grout Pocket Tube 6x8x0.5	A500 Grade C – Galvanized	–	Grouted_Wide_Flange_Option_A_grout_pocket_left_6x8x0.5

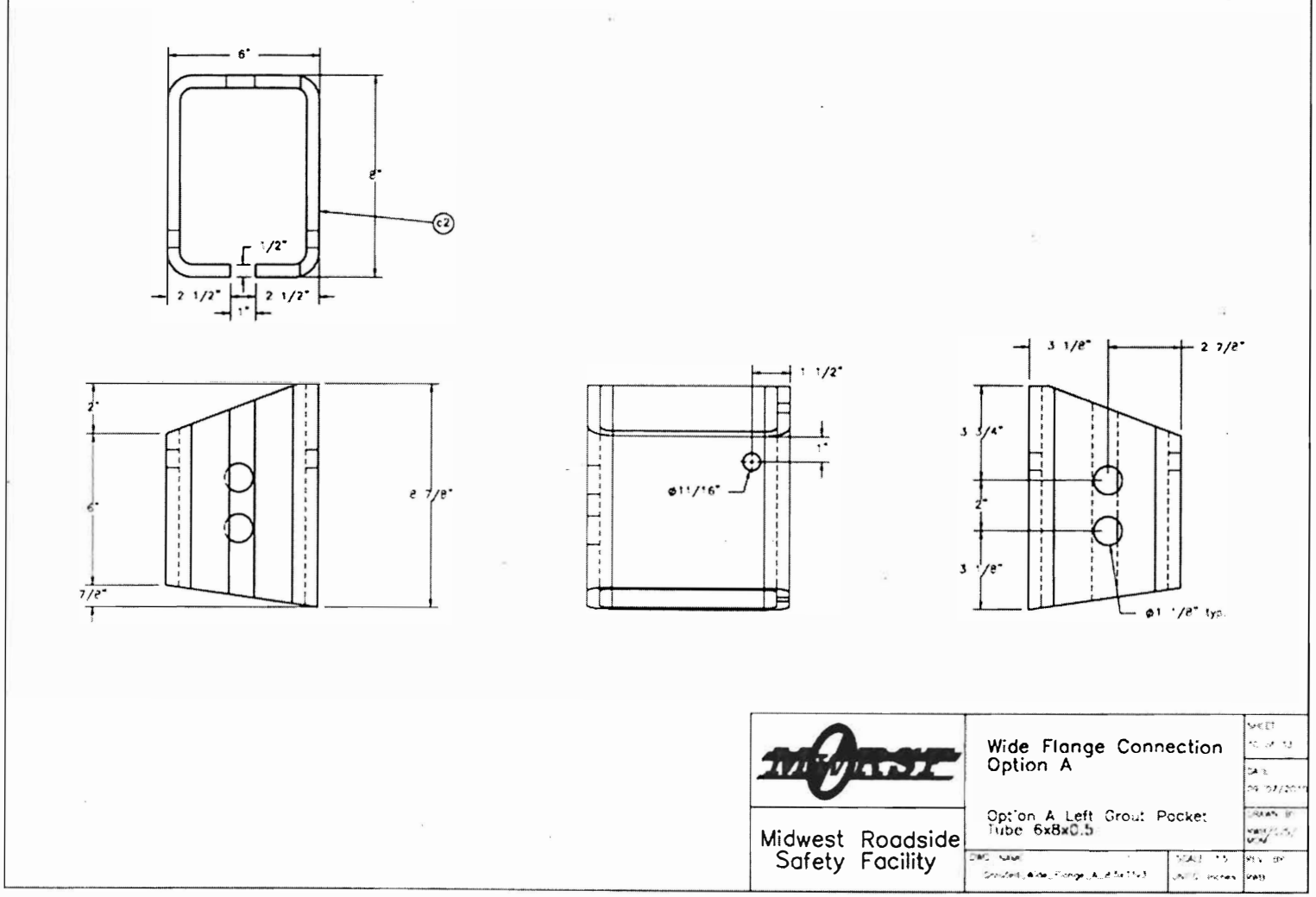

Figure 107. Left Grout Pocket, Test No. PCRB-3

Wide Flange Connection – Option A

Item No	QTY	Description	Material Spec	Comment	File Name
c3	1	Option A Right Grout Pocket Tube 6x8x0.5	A500 Grade C – Galvanized	–	Grouted_Wide_Flange_Option_A_grout_pocket_right_6x8x0.5

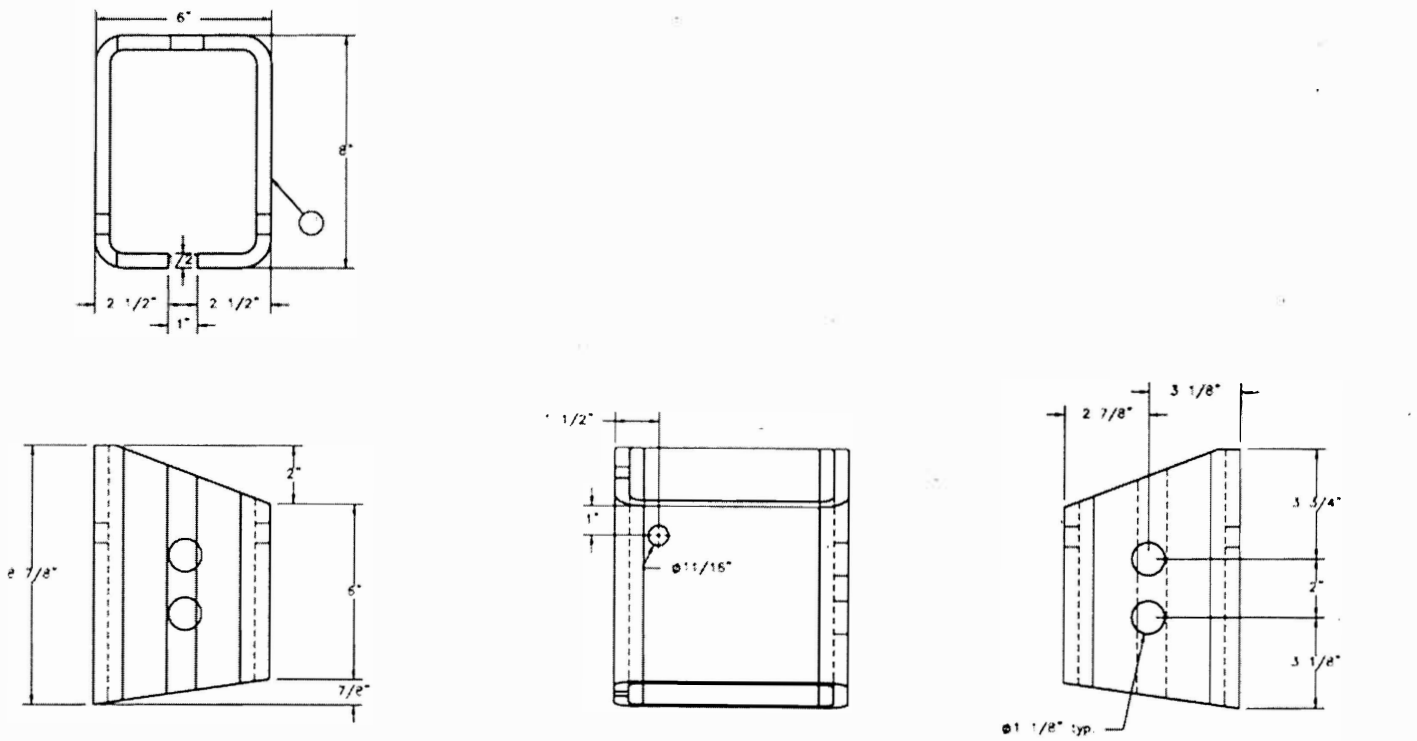

Midwest Roadside Safety Facility

Wide Flange Connection Option A

Option A Right Grout Pocket Tube 6x8x0.5

Figure 108. Right Grout Pocket, Test No. PCRB-3

Wide Flange Connection – Option A

Item No.	QTY.	Description	Material Spec	Comment	File Name
c5	1	Option A Grout Tube Cap	A572 Grade 50 – Galvanized	–	Grouted_Wide_Flange_Option_A_grout_pocket cap
c6	1	Option A Shear Plate	A572 Grade 50 – Galvanized	–	Grouted_Wide_Flange_Option_A_shear_plate_A572Gr50
c7	1	0.625 UNC 11 Heavy Hex Nut	Grade 5 – Galvanized	–	HHNUT 0.6250-11-D-C
c8	1	Heavy Hex Bolt 0.625-11x7x1.25	Grade 5 – Galvanized	–	HHBOLT 0.6250-11x6x1.25-C
c9	1	Option A Grout Tube Gusset	A572 Grade 50 – Galvanized	–	Grouted_Wide_Flange_Option_A_grout_tube_gusset

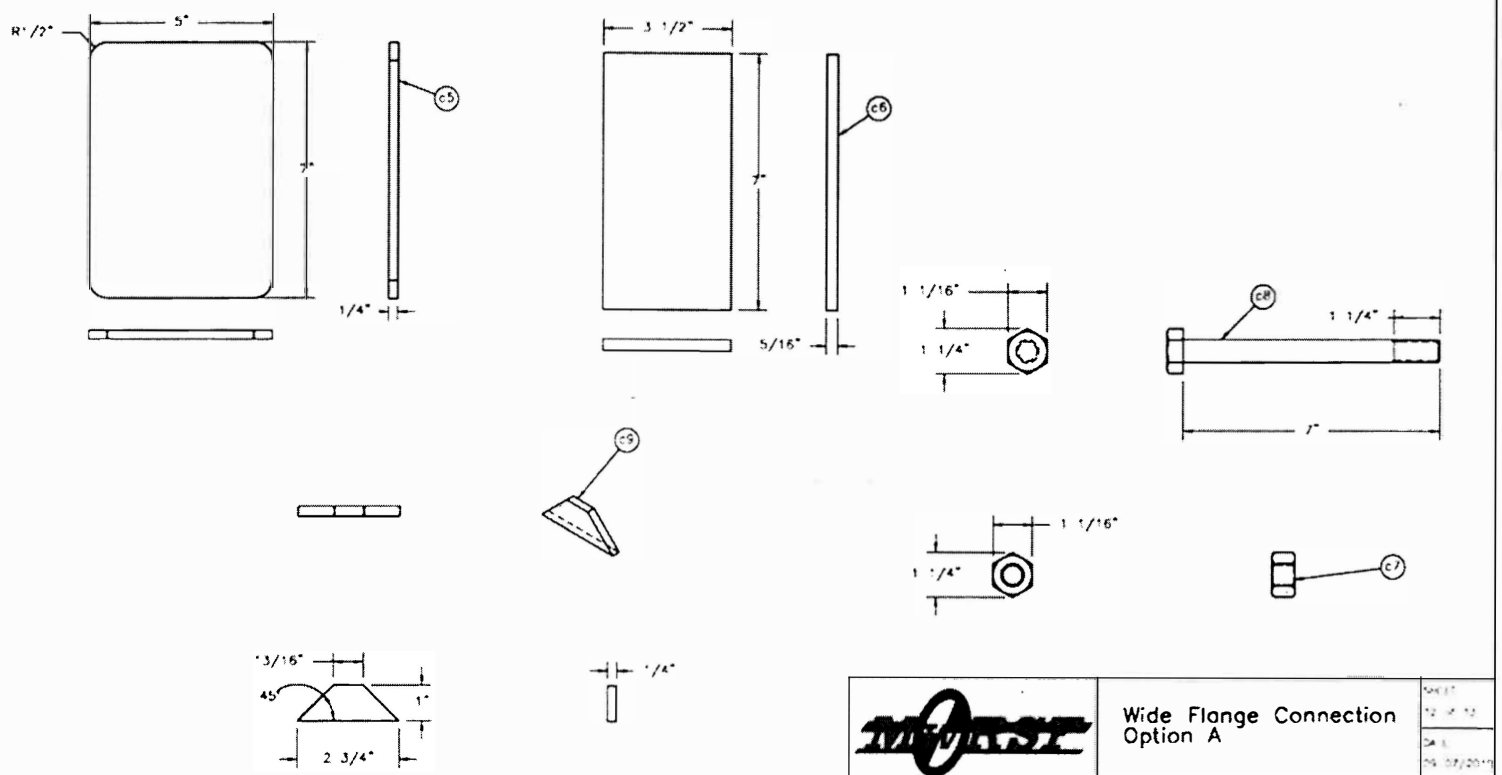

Midwest Roadside Safety Facility

Wide Flange Connection Option A

Option A Parts

Figure 109. Grout Pocket Accessories and Shear Bolts, Test No. PCRB-3

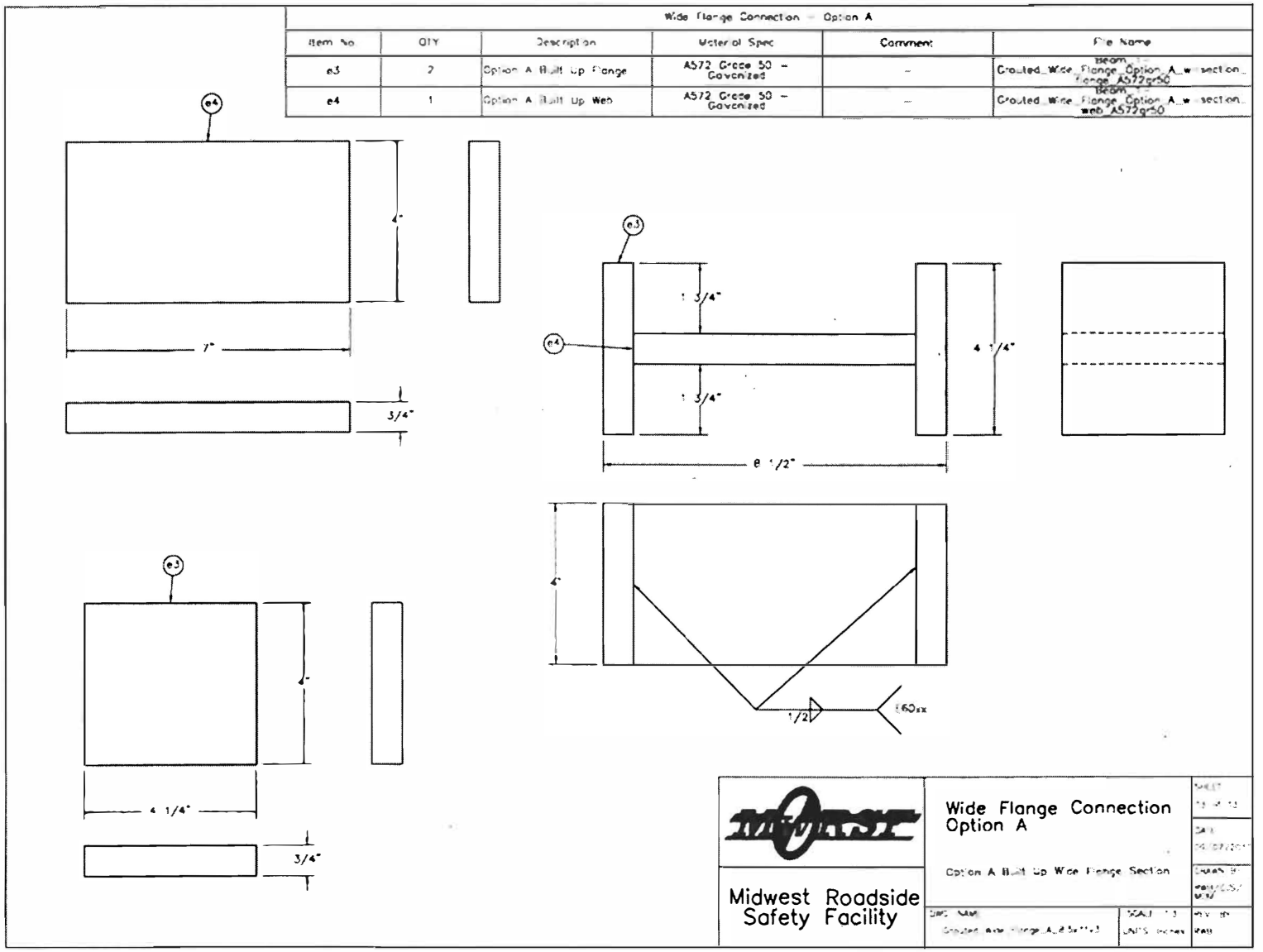

Figure 110. Built Up I-Shape Connector, Test No. PCRB-3

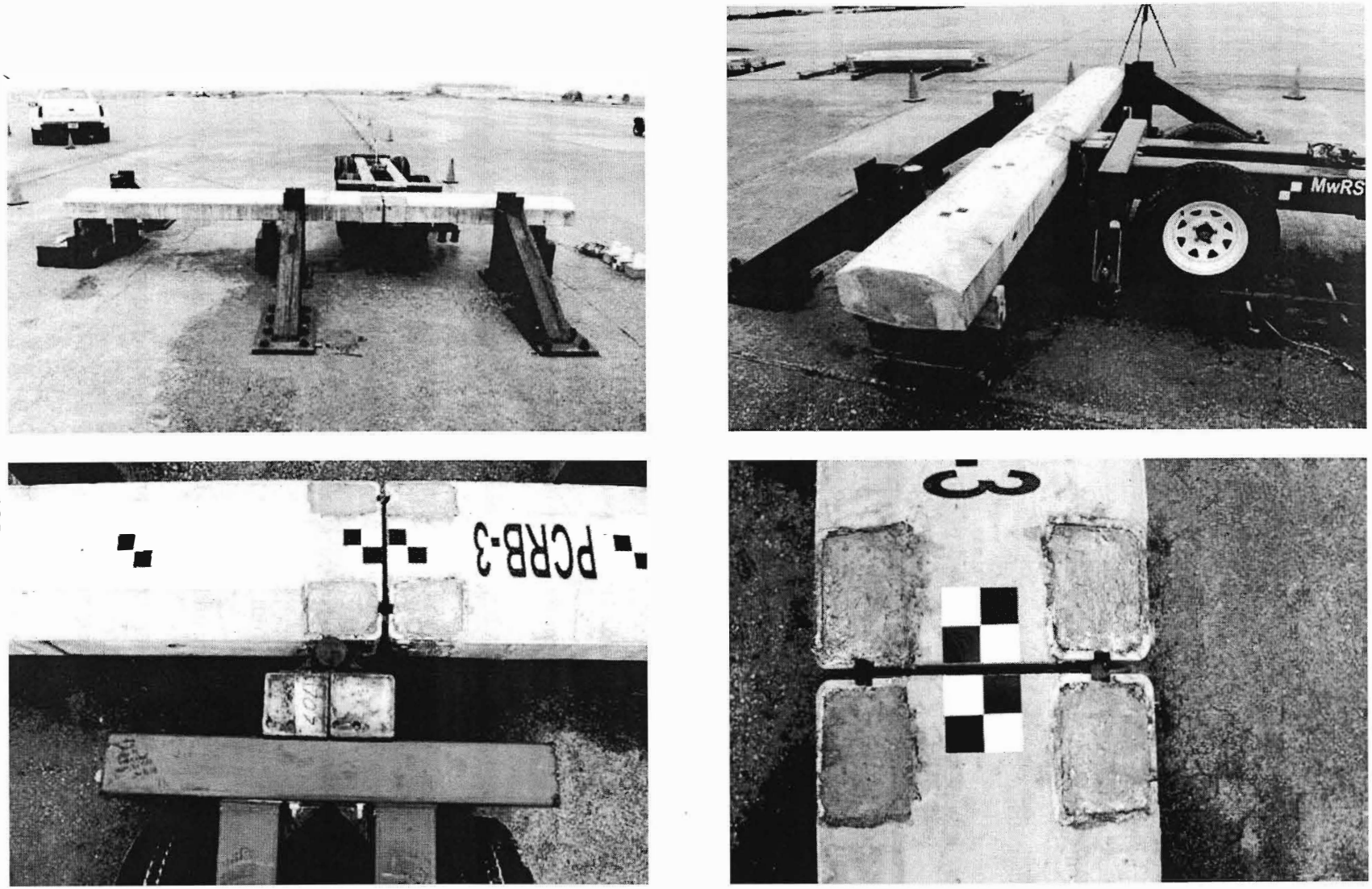

Figure 111. Rail Component Photographs, Test No. PCRB-3

8.3.2 Test No. PCRB-4, Refined Dry Joint Design

The test specimen used for test no. PCRB-4 consisted of two reinforced concrete rail segments connected by two shear tube connectors, as shown in Figures 112 through 132. Both the cross sectional geometry and lengths of each rail segment were the same as the previously described specimen for test no. PCRB-3. Also carried over from the previous design were the concrete strength of 5,000 psi (34 MPa) and the epoxy coated no. 4 rebar stirrups spaced at 8 in. (203 mm) intervals.

The rail longitudinal steel consisted of a no. 5 rebar and no. 8 threaded rebar running down each side of the rail for a total of four bars, as shown in Figures 114 through 120. The no. 5 bars were epoxy coated, while the threaded no. 8 bars were galvanized. For the short rail segment, adequate development length was not available for the no. 8 bars. Thus, for the short segment only, the no. 8 bars were extended out the far end of the concrete rail and were fastened to a steel end plate with heavy hex nuts. The end plate was ¼-in. (6-mm) thick, as shown in Figure 120, and made of ASTM A752 Grade 50 steel.

One end of each rail segment was configured with steel U-shape pockets that opened to the underside of the rail. These 5⅞ x 6 x ½-in. (149 x 152 x 13-mm) U-shape pockets were 14 in. (356 mm) long and fabricated from ASTM A500 Grade C steel, as shown in Figures 123 through 126. One side of the pocket was cut to a height of 5 in. (127 mm) to match the cross section geometry of the rail. An end cap measuring ½-in. (13-mm) thick was welded near the back of each pocket. The end cap was cut from galvanized ASTM A572 Grade 50 steel and contained a 1¼-in (32-mm) diameter hole in the middle. This hole allowed the threaded no. 8 bars to extend into the pockets. During assembly, the no. 8 bars are directly attached to the shear tube connector using Williams R63-08, Grade 75 hex nuts.

Similar to the dry joint design from the first round of bogie testing, a shear bolt was used to prevent the pocket from prying open. As such, an $^{11}/_{16}$-in. (17-mm) diameter hole was placed on both the outside and inside arms of the U-shape pocket near the end of the segment. Also repeated from previous designs, a nut was welded around the hole on the inside face of the pocket so that only the bolt was needed for assembly. These holes are shown in Figures 123 through 126, while the nuts are shown in Figures 121, 122, and 128.

Two shear plates were welded between the pockets for lateral anchorage. These shear plates were cut from galvanized A572 Grade 50 steel and measured $^{5}/_{16}$ in. (8 mm) thick by 3 in. (76 mm) wide. Also, three galvanized no. 3 bars were welded across the tops of the pockets to better confine the concrete near the end of the rail. The locations of both the shear plates and the no. 3 bars are shown in Figures 121 and 122, while the pieces are shown independently in Figures 127 and 128.

The rail segments were placed on wooden support blocks and positioned as prescribed by Section 6.2 and Figure 48. Just as the previous dry joint bogie test, the rail was positioned upside down so that the joint hardware was visible to the overhead, high-speed camera used to document the test.

Assembling the joint required the shear tube connector and the additional hardware shown in Figure 131 which included shims, washers, nuts, and bolts. The joint shims were cut from ½-in. (13-mm) thick ASTM A36 steel plate to match the cross section geometry of the rail and to fit over the shear tube connector. A 7-in. (178-mm) long, ⅝-in. (16-mm) diameter Grade 5 bolt was used as the shear bolt. Plate washers were cut from ½-in. (13-mm) thick ASTM A572 Grade 50 steel plate. Each measured 2¾ x 2¼ in. (70 x 57 mm) with a 1¼-in. (32-mm) diameter

hole in its center. Finally, 1-in (25-mm) diameter Schedule 80 pipe was used as the collars around the shear bolt to prevent the shear tube connector from pinching.

The shear tube was a 25½-in. (648-mm) long, 4 x 4 x ½-in. (102 x 102 x 13-mm) U-shape that was cut from an 8 x 4 x ½-in. (203 x 102 x 13-mm), ASTM A500 Grade C steel tube, as shown in Figures 129 and 130. A 1⅜-in. (35-mm) wide slot was cut into the top of the shear tube on the outer 5 in. (127 mm) of each end. Gusset plates cut from ⅝-in. (16-mm) thick, ASTM A572 Grade 50 steel were welded inside the shear tube at each end. A 1⅜-in. (35-mm) wide slot was also cut into the gusset plates beginning at the top of the gusset plate and continuing to the middle. Two 1 x ¾-in. (25 x 19-mm) slots were cut near the middle of the shear tube, which allowed the shear bolts to pass through the connector during assembly of the joint. Shim plates were welded to the sides of the shear tube to reduce the gaps between the shear tube and the inside pocket walls. The shim plates were 25½ in. (648 mm) long by 2½ in. (64 mm) wide by 3/8 in. (10 mm) thick and had the same shear bolt slots cut into them.

Assembly of the joint began with the shear tube connector being inserted into adjacent pockets such that the longitudinal rail steel (i.e., threaded no. 8 bars) passed through the slots cut into the top of the connector and gusset plates. Next, washers and nuts were placed on the threaded no. 8 bars inside the shear tube connector to hold the connector in place. Shims were dropped into the ½-in. (13-mm) gap between rail ends and over the connectors. Then, the nuts were tightened which pulled the rail ends together on the shim plates and tied the longitudinal steel from adjacent rails together through the shear tube connector. Finally, shear bolts were slid into place through the pocket, shear tube connector, and collars and were fastened to the pocket by the nut welded to the inside of the pocket. Photographs of the assembled joint specimen are shown in Figure 132.

Dry Connection					
Item No.	QTY	Description	Material Spec	Comment	File Name
p1	1	Dry Connection – 9.5 ft Beam	–	–	Dry_Connection_v4_9.5ft
p2	1	Dry Connection – 5.75 ft Beam	–	–	Dry_Connection_v4_5.75ft
c10	4	Williams R63-08 Hex Nut	Galvanized	–	Dry_Connection_v4_No.8_Grade75_threadbar_R63-08_hexnut SLOPRT
f1	2	Dry Connection V4 Shear Tube Assembly	–	–	Dry_Connection_v4_sheartube
f2	4	Dry Connection V4 Shear Tube Washer	A572 Grade 50 – Galvanized	–	Dry_Connection_v4_sheartube_washer_A572_gr50
f4	4	Dry Connection V4 Shear Tube Pipe	1" Schedule 80 Pipe – Galvanized	–	Dry_Connection_v4_sheartube_Pipe_0.75_XS pipe
f6	4	0.625-UNC 11x7x1.25 Heavy Hex Bolt	Grade 5 – Galvanized	–	HHBOLT 0.6250-11x6x1.25-C
f8	2	Dry Connection Shim Plate	A36 Steel – Galvanized	Material will likely change following component testing	Dry_Connection_v4_shimplate

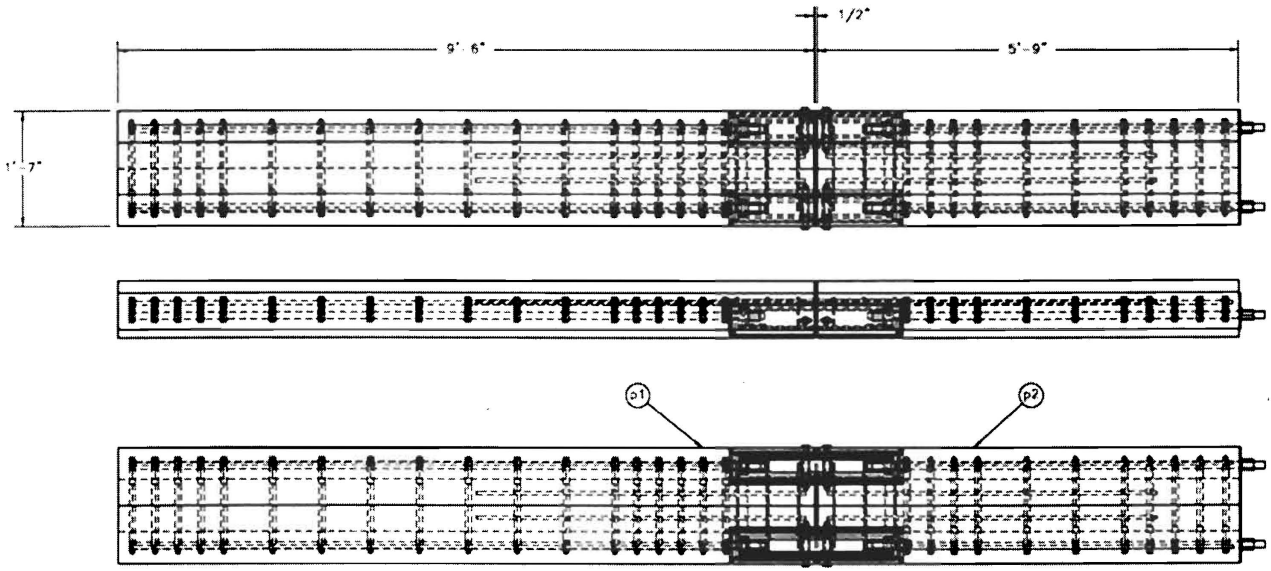

Midwest Roadside Safety Facility

Dry Connection
Version 4

Assembled Beams

SCALE 1:24

Figure 112. Refined Dry Rail Joint, Test No. PCRB-4

Dry Connection					
Item No.	QTY	Description	Material Spec	Comment	File Name
p1	1	Dry Connection – 9.5 ft Beam	–	–	Dry_Connection_v4_9.5ft
p2	1	Dry Connection – 5.75 ft Beam	–	–	Dry_Connection_v4_5.75ft
c10	4	Williams R63-08 Hex Nut	Galvanized	–	Dry_Connection_v4_No.8_Grade75_threadbar_R63-08_hexnut SLDPRT
f1	2	Dry Connection V4 Shear Tube Assembly	–	–	Dry_Connection_v4_sheartube
f2	4	Dry Connection V4 Shear Tube Washer	A572 Grade 50 – Galvanized	–	Dry_Connection_v4_sheartube_washer_A572_gr50
f4	4	Dry Connection V4 Shear Tube Pipe	1" Schedule 80 Pipe – Galvanized	–	Dry_Connection_v4_sheartube_Pipe_0.75_XS pipe
f6	4	0.625-UNC 11x7x1.25 Heavy Hex Bolt	Grade 5 – Galvanized	–	HHBOLT 0.6250-11x6x1.25-C
f8	2	Dry Connection Shim Plate	A36 Steel – Galvanized	Material will likely change following component testing	Dry_Connection_v4_shimplate

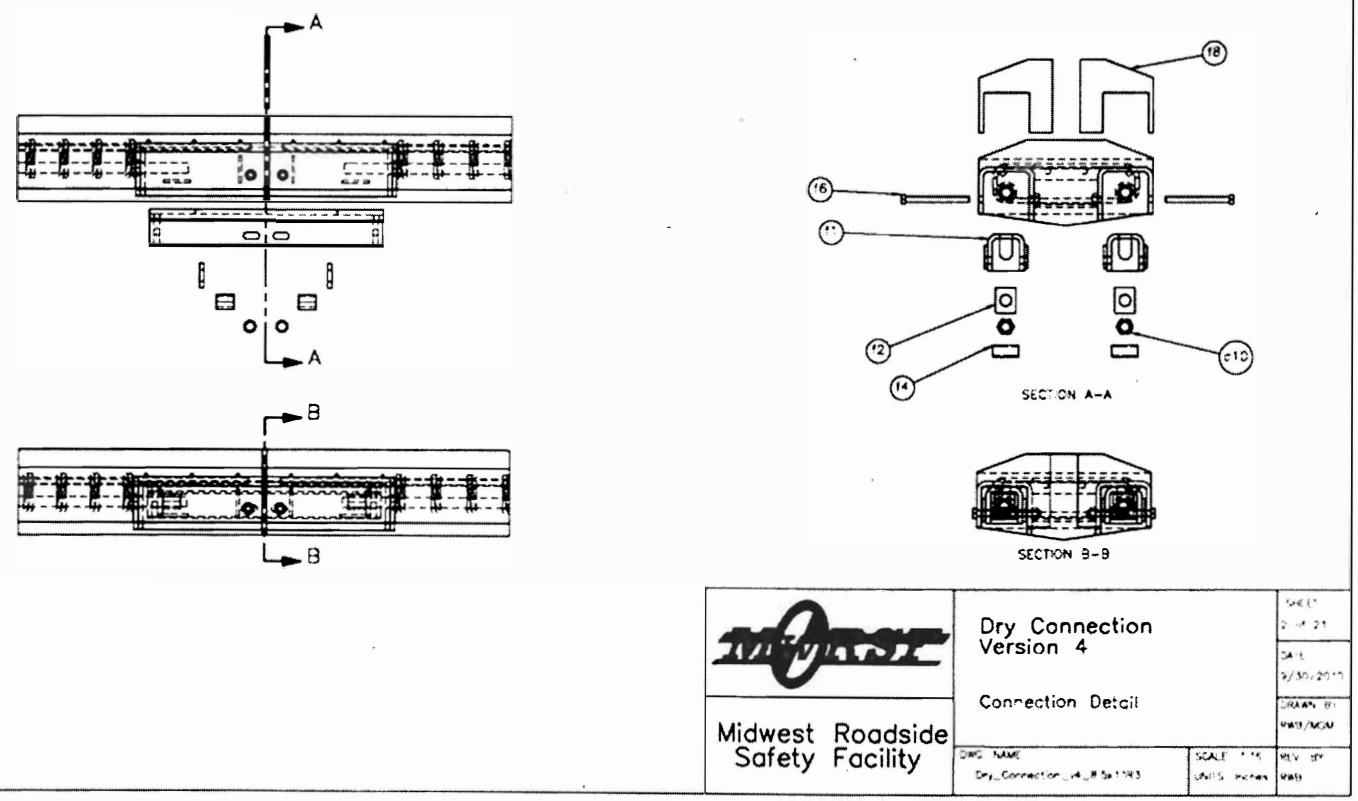

Figure 113. Refined Dry Joint Assembly, Test No. PCRB-4

Dry Connection					
Item No.	QTY	Description	Material Spec	Comment	File Name
a1	1	Precast Concrete Bridge Rail Section	SSC f'c = 5000 psi	–	Dry_Connection_v4_body_9.5ft
b1	18	No. 4 Top Rail Stirrup	A615 Grade 60 – Epoxy Coated	–	Dry_Connection_v4_toprail_stirrup_No.4_Grade60
b2	2	No. 5 Longitudinal Rebar	A615 Grade 60 – Epoxy Coated	–	Dry_Connection_v4_9.5ft_longbar_No.5_Grade60
d1	1	Dry Connection End Assembly	–	–	Dry_Connection_v4_end_connection_assembly
c8	2	No. 8 Williams Grade 75 All-Thread Rebar – R61-08	Grade 75 – Galvanized	–	Dry_Connection_v4_No.8_Grade75_9.5ft_threadbarR61-08
c11	2	Williams R63-08JN Jam Nut	ASTM 108 – Galvanized	–	Dry_Connection_v4_No.8_Grade75_threadbar_R63-08JN_jamnut.SLDPRT

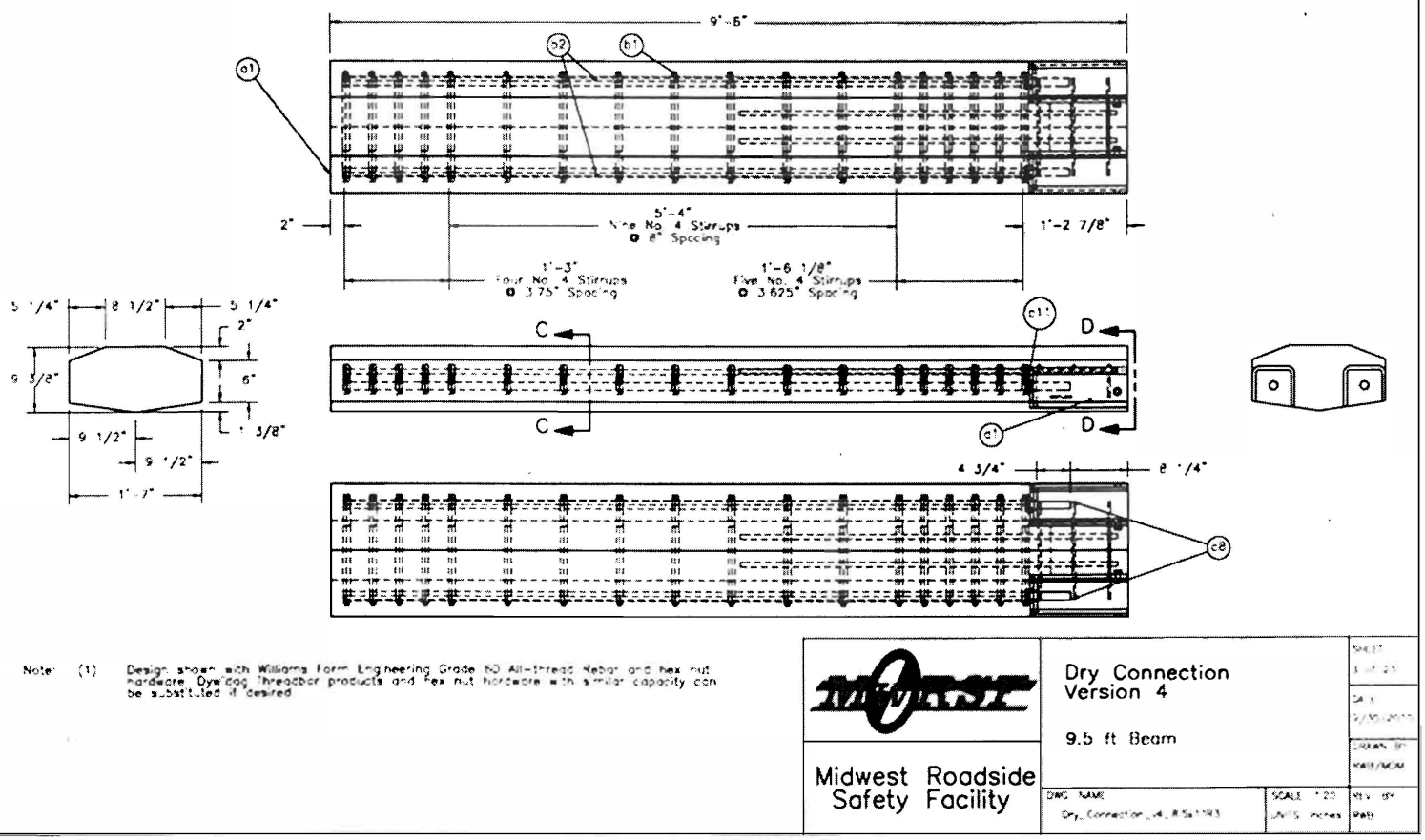

Figure 114. Long Rail Segment, Test No. PCRB-4

Precast Bridge Rail – Single Rail Section					
Item No.	QTY	Description	Material Spec	Comment	File Name
a1	1	Precast Concrete Bridge Rail Section	SSC f'c = 5000 psi	–	Dry_Connection_v4_body_9.5ft
b1	18	No. 4 Top Rail Stirrup	A615 Grade 60 – Epoxy Coated	–	Dry_Connection_v4_toprail_stirrup_No.4_Grade60
b2	2	No. 5 Longitudinal Rebar	A615 Grade 60 – Epoxy Coated	–	Dry_Connection_v4_9.5ft_longbar_No.5_Grade60
c8	2	No. 8 Williams Grade 75 All-Thread Rebar R61-C8	Grade 75 – Galvanized	–	Dry_Connection_v4_No.8_Grade75_9.5ft_threadbarR61-D8

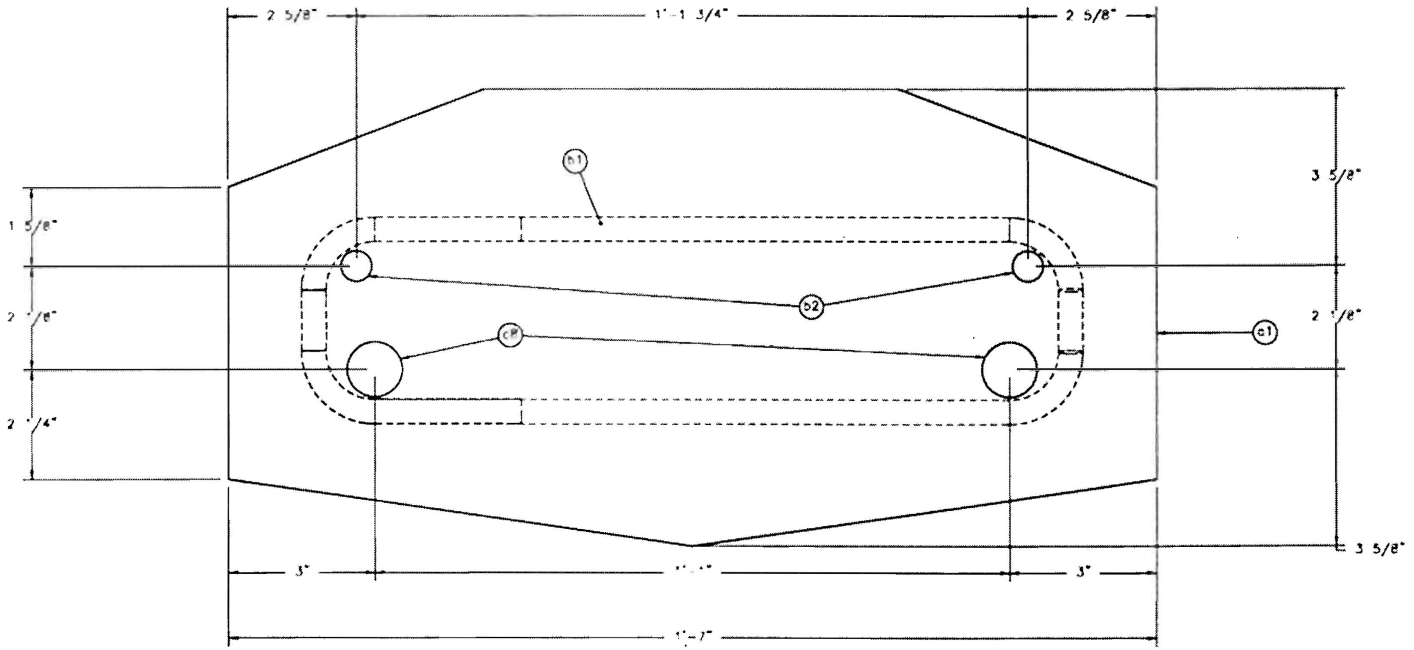

SECTION C-C

Note: Stirrup cover is 1.5" on each side and 2.625" from the top face of the rail section

Midwest Roadside Safety Facility

Dry Connection Version 4

Main Beam Reinforcement 9.5 ft Beam

SHEET 4 of 21

DATE 9/30/2010

DRAWN BY RWB/MDM

DWG. NAME Dry_Connection_v4_8.5x1193

SCALE 1:1

UNITS: Inches

REV. BY RWB

Figure 115. Cross Section Views of Long Rail Segment, Test No. PCRB-4

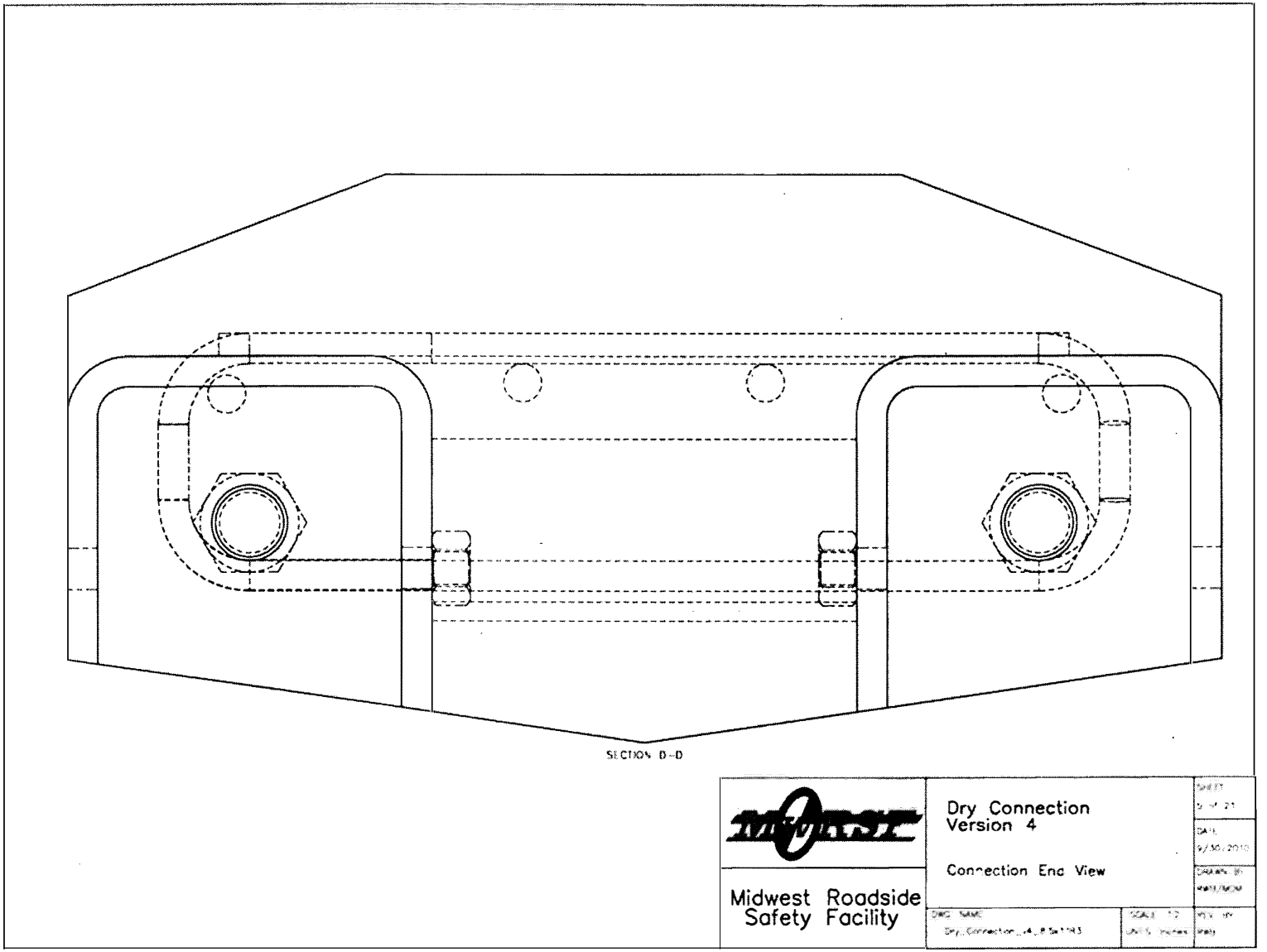

Figure 116. Cross Section Views of Long Rail Segment, Test No. PCRB-4

Dry Connection					
Item No.	QTY.	Description	Material Spec	Comment	File Name
a1	1	Precast Concrete Bridge Rail Section	SSC f'c = 5000 psi	–	Dry_Connection_v4_body_5.75ft
b1	11	No. 4 Top Rail Stirrup	A615 Grade 60 – Epoxy Coated	–	Dry_Connection_v4_toprail_stirrup_No.4_Grade60
b4	2	No. 5 Longitudinal Rebar	A615 Grade 60 – Epoxy Coated	–	Dry_Connection_v4_5.75ft_longbar_No.5_Grade60
c7	2	No. 8 Williams Grade 75 All Thread Rebar – R61 08	Grade 75 – Galvanized	–	Dry_Connection_v4_No.8_Grade75_5.75ft_threadbarR61-08
c11	2	Williams R63-08JN Jam Nut	ASTM 108 – Galvanized	–	Dry_Connection_v4_No.8_Grade75_threadbar_R63-08JN_jamnut.SLDPRT
c12	2	Dry Connection V4 Threaded Rebar Washer R9F-08-436	ASTM F 436	–	Dry_Connection_v4_No.8_Grade75_threadbar_R9F-08-436_washer
d1	1	Dry Connection End Assembly	–	–	Dry_Connection_v4_end_connection_assembly
d6	1	Dry Connection Base Plate	A572 Grade 50 – Galvanized	–	Dry_Connection_v4_5.75ft_endplate_6x19x0.5_A572_gr50

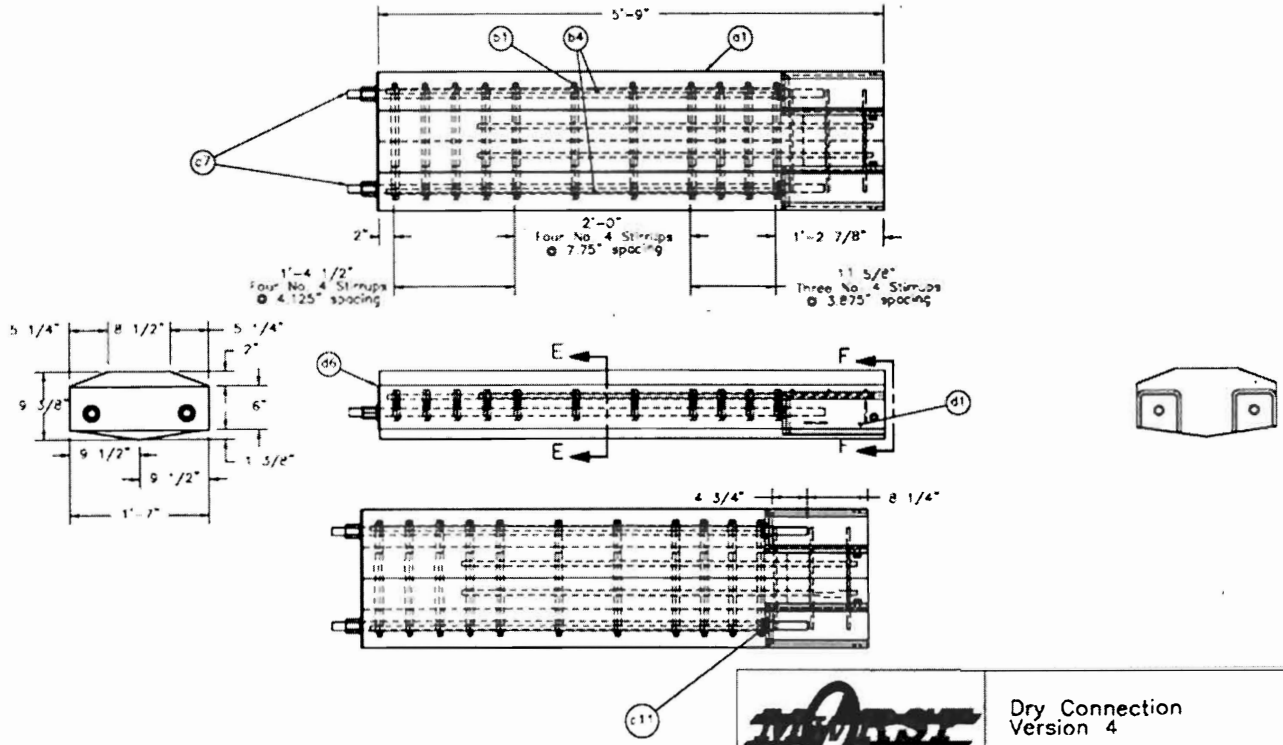

Midwest Roadside Safety Facility

Dry Connection
Version 4

Dry Connection
5.75 ft Beam

Figure 117. Short Rail Segment, Test No. PCRB-4

Dry Connection

Item No.	QTY	Description	Material Spec	Comment	File Name
a1	1	Precast Concrete Bridge Rail Section	SSC f'c = 5000 psi	–	Dry_Connection_v4_body_5.75ft
b1	11	No. 4 Top Rail Stirrup	A615 Grade 60 – Epoxy Coated	–	Dry_Connection_v4_toprail_stirrup_No.4_Grade60
b4	2	No. 5 Longitudinal Rebar	A615 Grade 60 – Epoxy Coated	–	Dry_Connection_v4_5.75ft_longbar_No.5_Grade60
c7	2	No. 8 Williams Grade 75 All-Thread Rebar R61-08	Grade 75 – Galvanized	–	Dry_Connection_v4_No.8_Grade75_5.75ft_threadbarR61-08

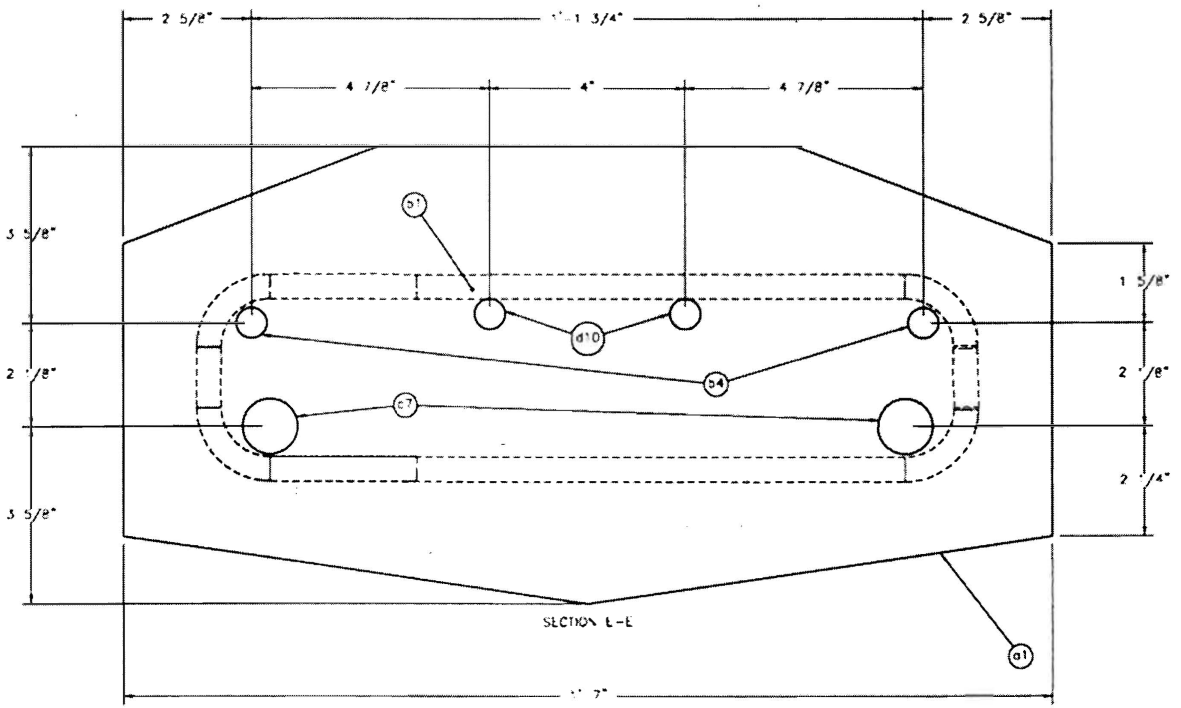

Midwest Roadside Safety Facility

Dry Connection
Version 4

Main Beam Reinforcement
5.75 ft Beam

Figure 118. Cross Section Views of Short Rail Segment, Test No. PCRB-4

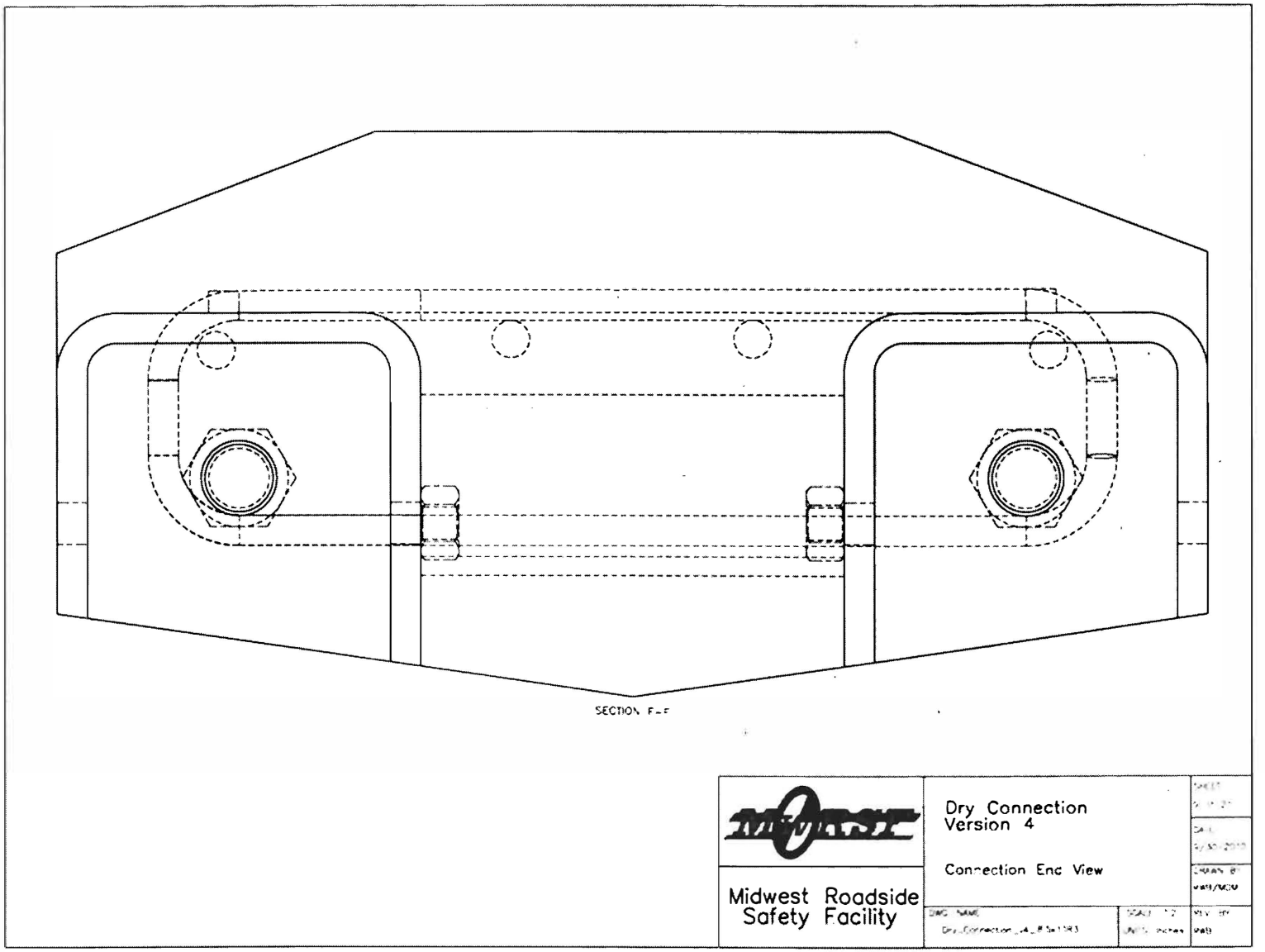

Figure 119. Cross Section Views of Short Rail Segment, Test No. PCRB-4

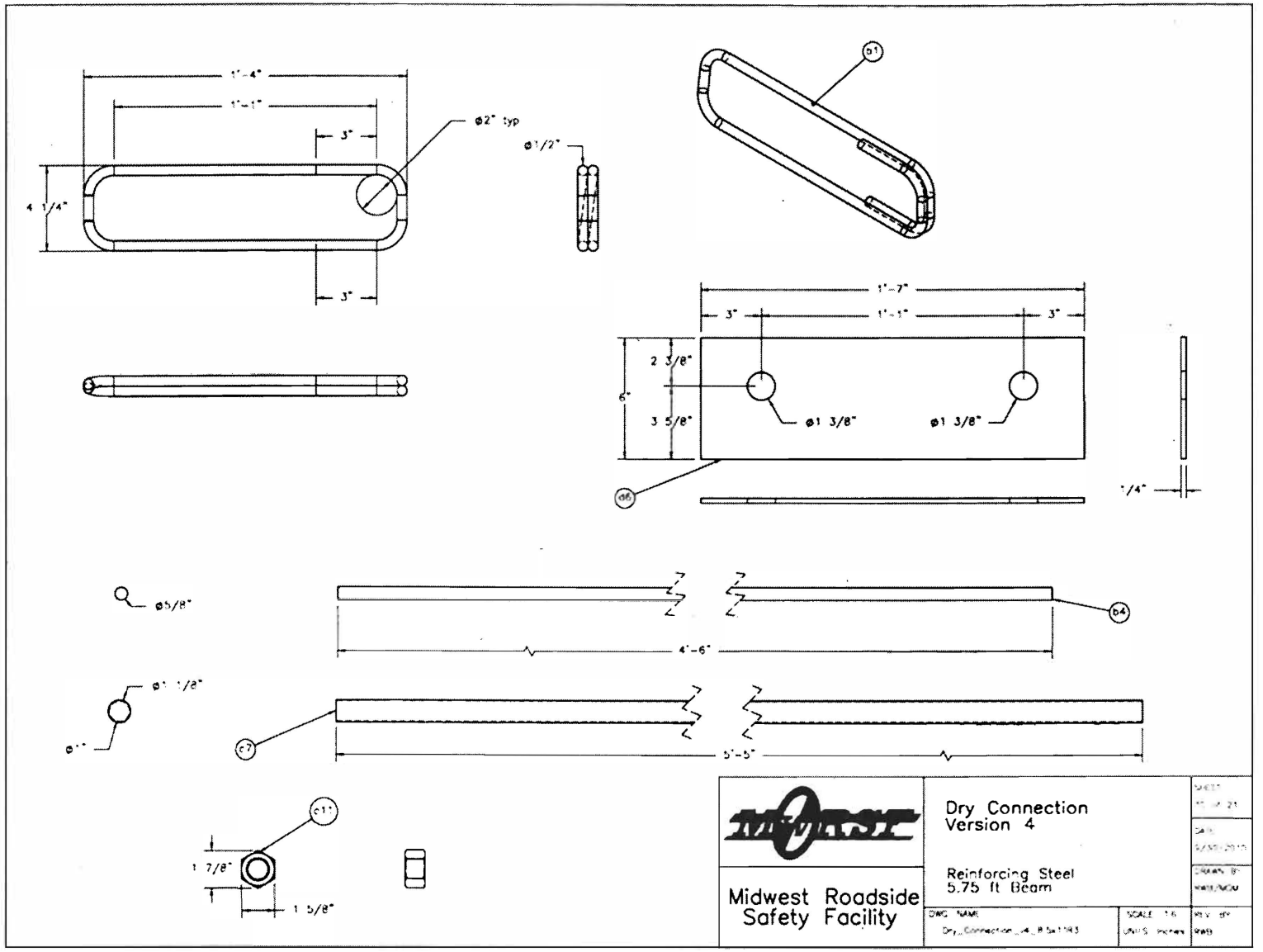

Figure 120. Rail Internal Steel Reinforcement, Test No. PCRB-4

Dry Connection					
Item No.	QTY.	Description	Material Spec	Comment	File Name
d2	1	Dry Connection Bolt Pocket Left	–	–	Dry_Connection_v4_bolt_pocket_left_assembly
d3	1	Dry Connection Bolt Pocket Right	–	–	Dry_Connection_v4_bolt_pocket_right_assembly
d4	2	Dry Connection Shear Plate	A572 Grade 50 – Galvanized	–	Dry_Connection_v4_shear_plate_A572Gr50
d7	3	Dry Connection No. 3 Shear Stirrup	A706 Grade 60 – Galvanized	–	Dry_Connection_v4_No.3_Grade60_top_confinement
d9	2	0.625 UNC-11 Heavy Hex Nut	Grade 5 – Galvanized	–	HHNUT 0.6250-11-D-C
d10	2	Dry Connection No. 5 Baluster Reinforcement	A615 Grade 60 – Epoxy Coated	–	Dry_Connection_v4_No.5_Grade60_baluster

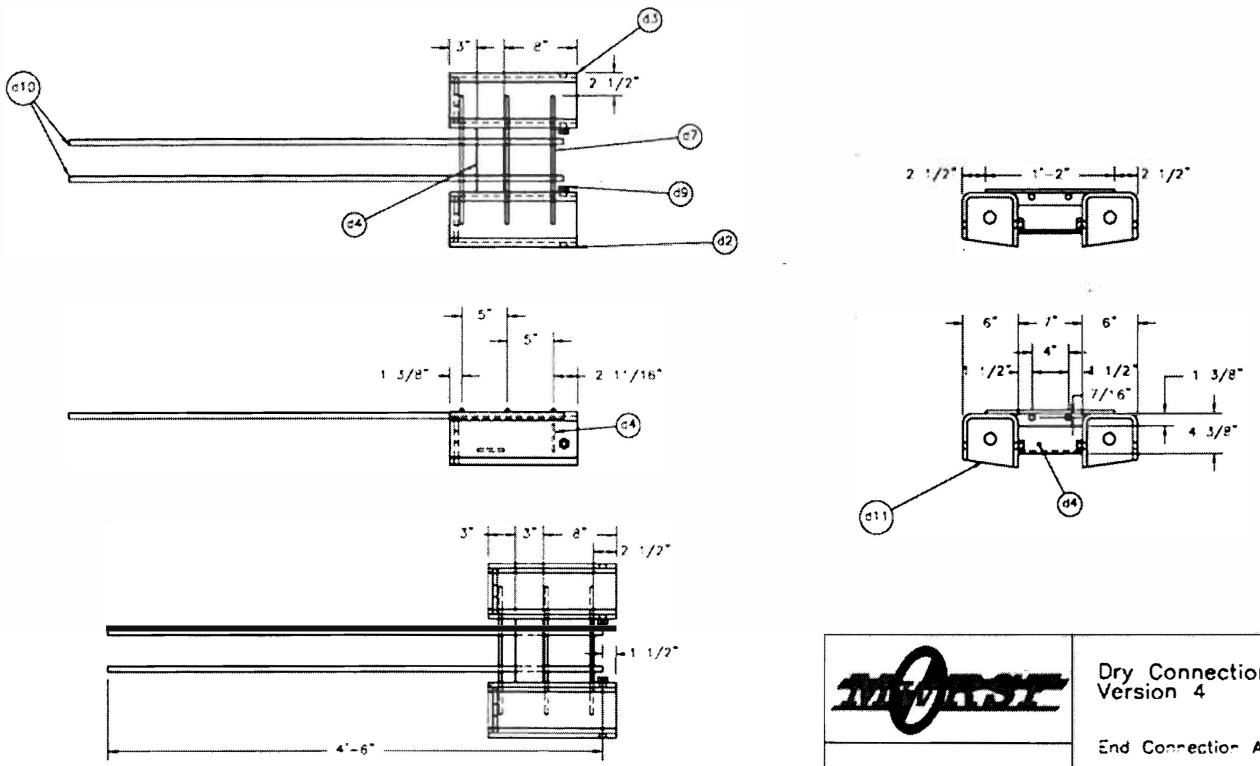

Midwest Roadside Safety Facility

Dry Connection
Version 4

End Connection Assembly

Figure 121. End Pocket Assembly, Test No. PCRB-4

Dry Connection					
Item No.	QTY	Description	Material Spec	Comment	File Name
d2	1	Dry Connection Bolt Pocket Left	–	–	Dry_Connection_v4_bolt_pocket_left_assembly
d3	1	Dry Connection Bolt Pocket Right	–	–	Dry_Connection_v4_bolt_pocket_right_assembly
d4	2	Dry Connection Shear Plate	A572 Grade 50 – Galvanized	–	Dry_Connection_v4_shear_plate_A572Gr50
d7	3	Dry Connection No. 3 Shear Stirrup	A706 Grade 60 – Galvanized	–	Dry_Connection_v4_No.3_Grade60_top_confinement
d10	2	Dry Connection No. 5 Baluster Re-forcement	A615 Grade 60 – Epoxy Coated	–	Dry_Connection_v4_No.5_Grade60_baluster
d9	2	0.625 UNC-11 Heavy Hex Nut	Grade 5 – Galvanized	–	HHNUT 0.6250-11-D-C

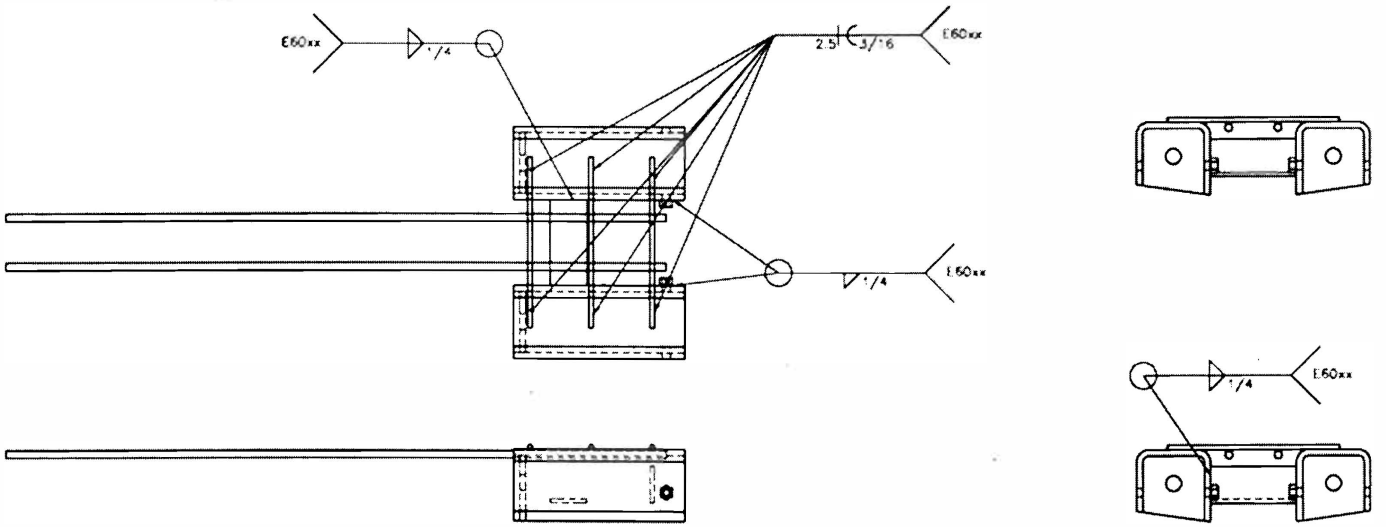

Midwest Roadside Safety Facility

Dry Connection
Version 4

End Connection Assembly Welds

SCALE 1:12
UNITS Inches

Figure 122. Pocket Assembly Connections, Test No. PCRB-4

Dry Connection

Item No.	QTY	Description	Material Spec	Comment	File Name
d10	1	Dry Connection Bolt Pocket Tube Left	A500 Grade C – Galvanized	Cut from section of 12x8x0.5 tube	Dry_Connection_v4_bolt_pocket_6x5x0.5_left
d11	1	Dry Connection Bolt Pocket End Cap Left	A572 Grade 50 – Galvanized	–	Dry_Connection_v4_bolt_pocket_end_cap_left

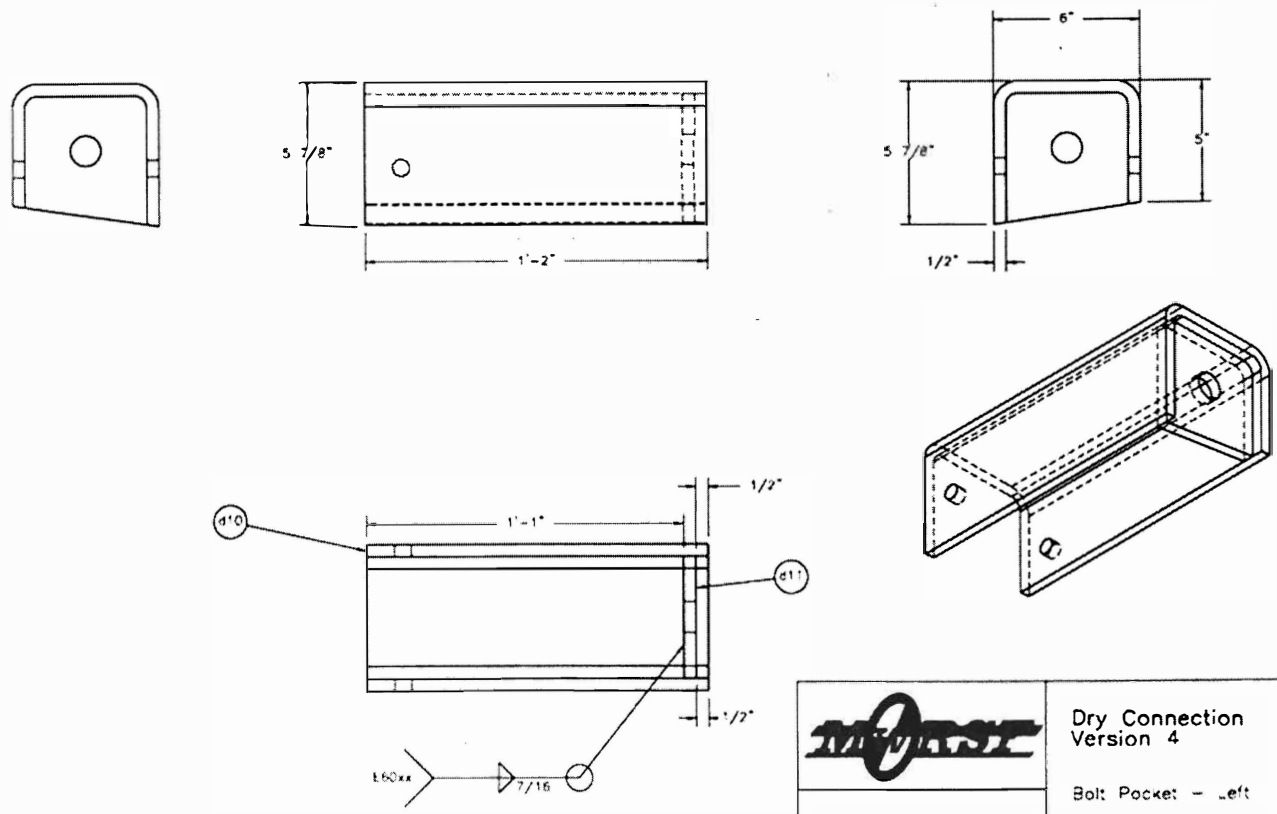

Midwest Roadside Safety Facility

Dry Connection
Version 4

Bolt Pocket – Left

Figure 123. Left Pocket, Test No. PCRB-4

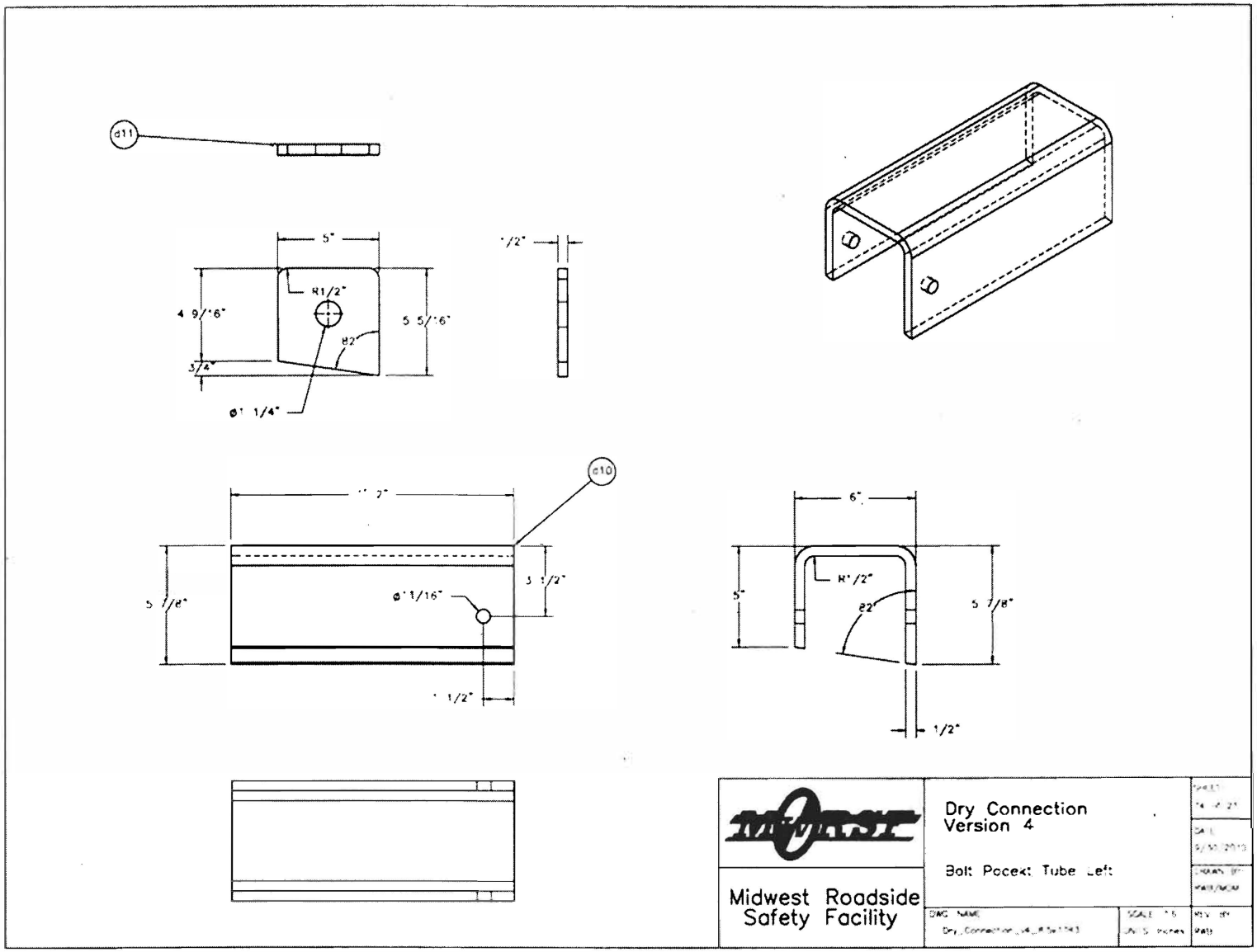

Figure 124. Left Pocket, Test No. PCRB-4

Dry Connection					
Item No.	QTY	Description	Material Spec	Comment	File Name
d13	1	Dry Connection Bolt Pocket Tube Right	A500 Grade C – Galvanized	–	Dry_Connection_v4_bolt_pocket_6x5x0.5_right
d14	1	Dry Connection Bolt Pocket End Cap Right	A572 Grade 50 – Galvanized	–	Dry_Connection_v4_bolt_pocket_end_cap_right

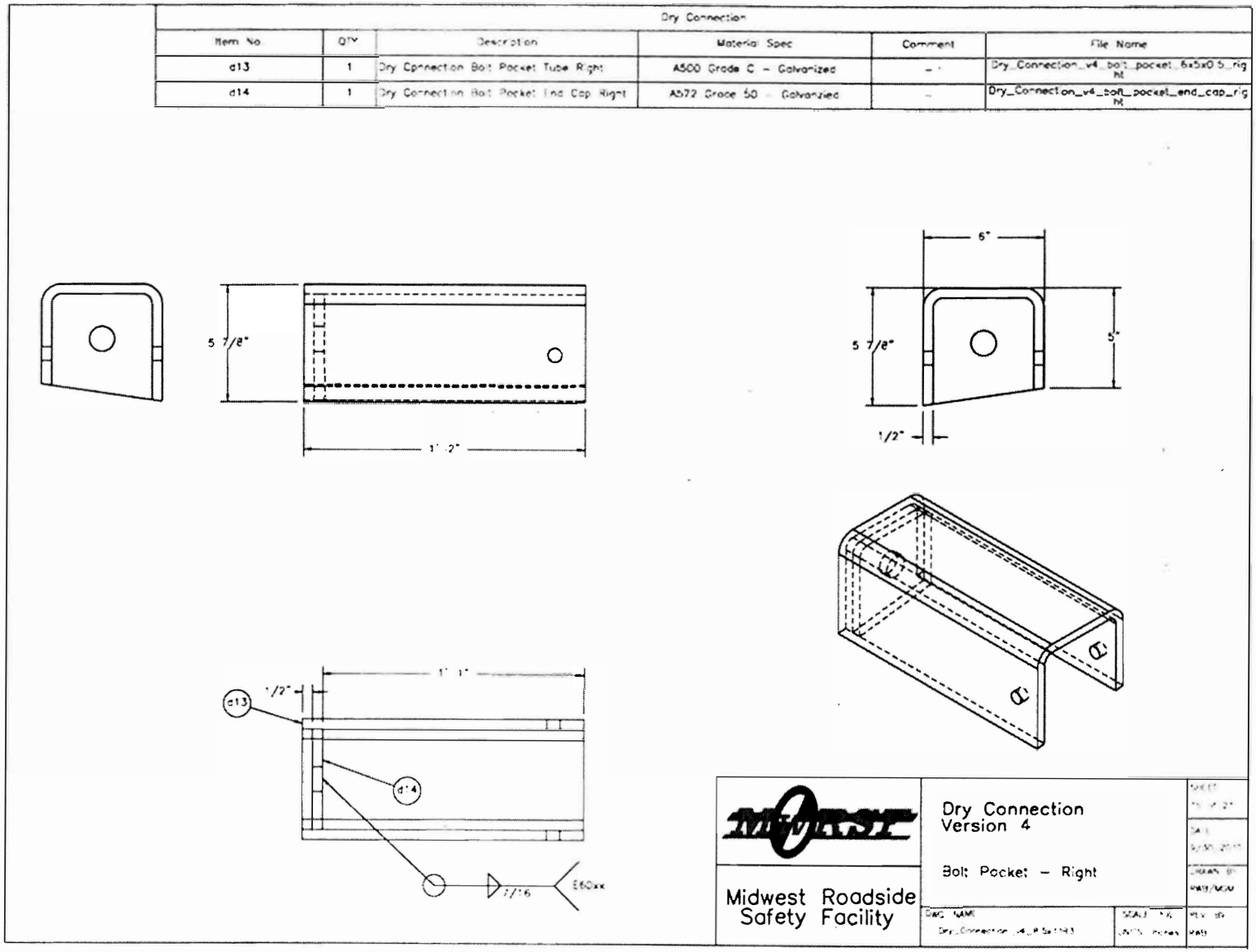

Figure 125. Right Pocket, Test No. PCRB-4

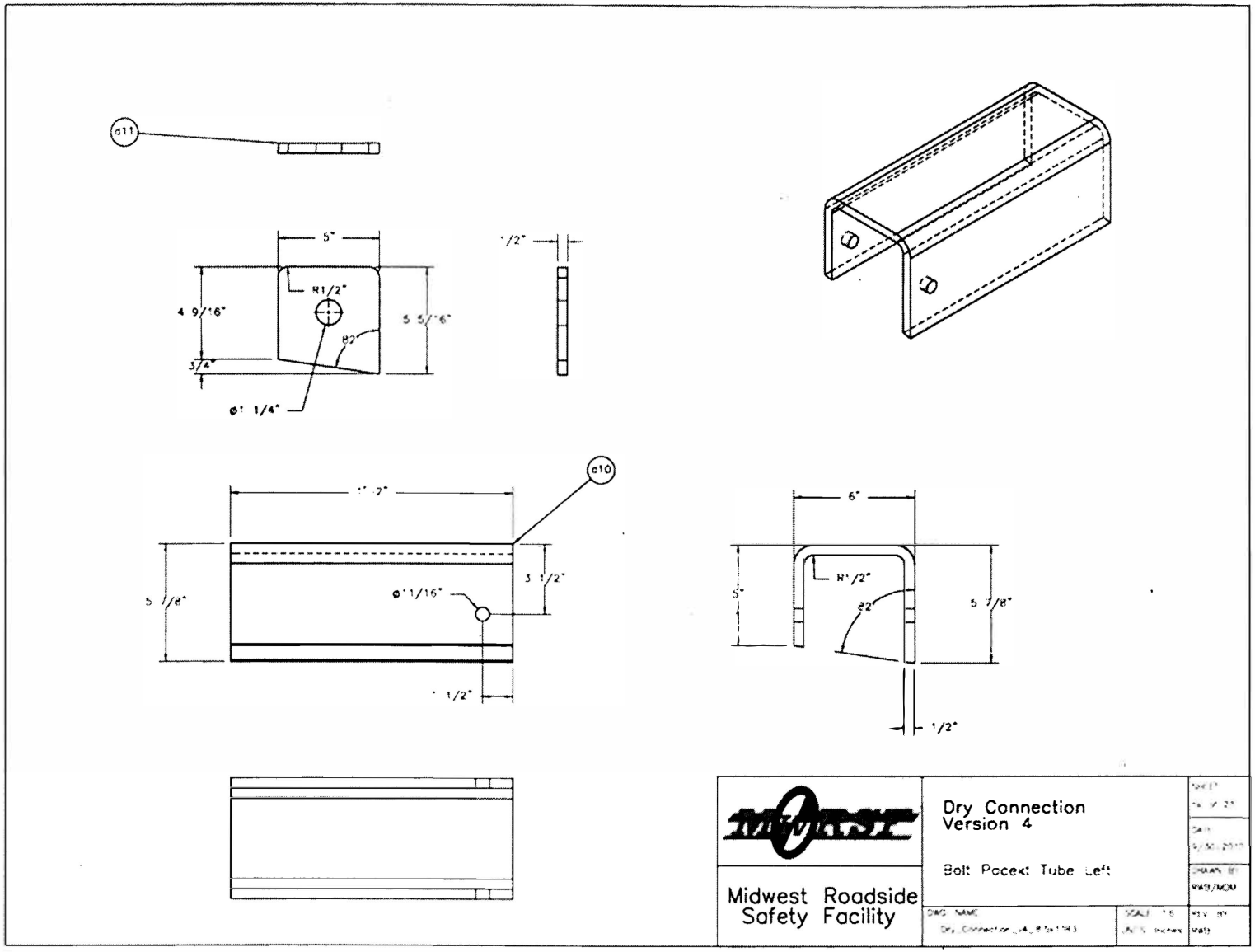

Figure 126. Right Pocket, Test No. PCRB-4

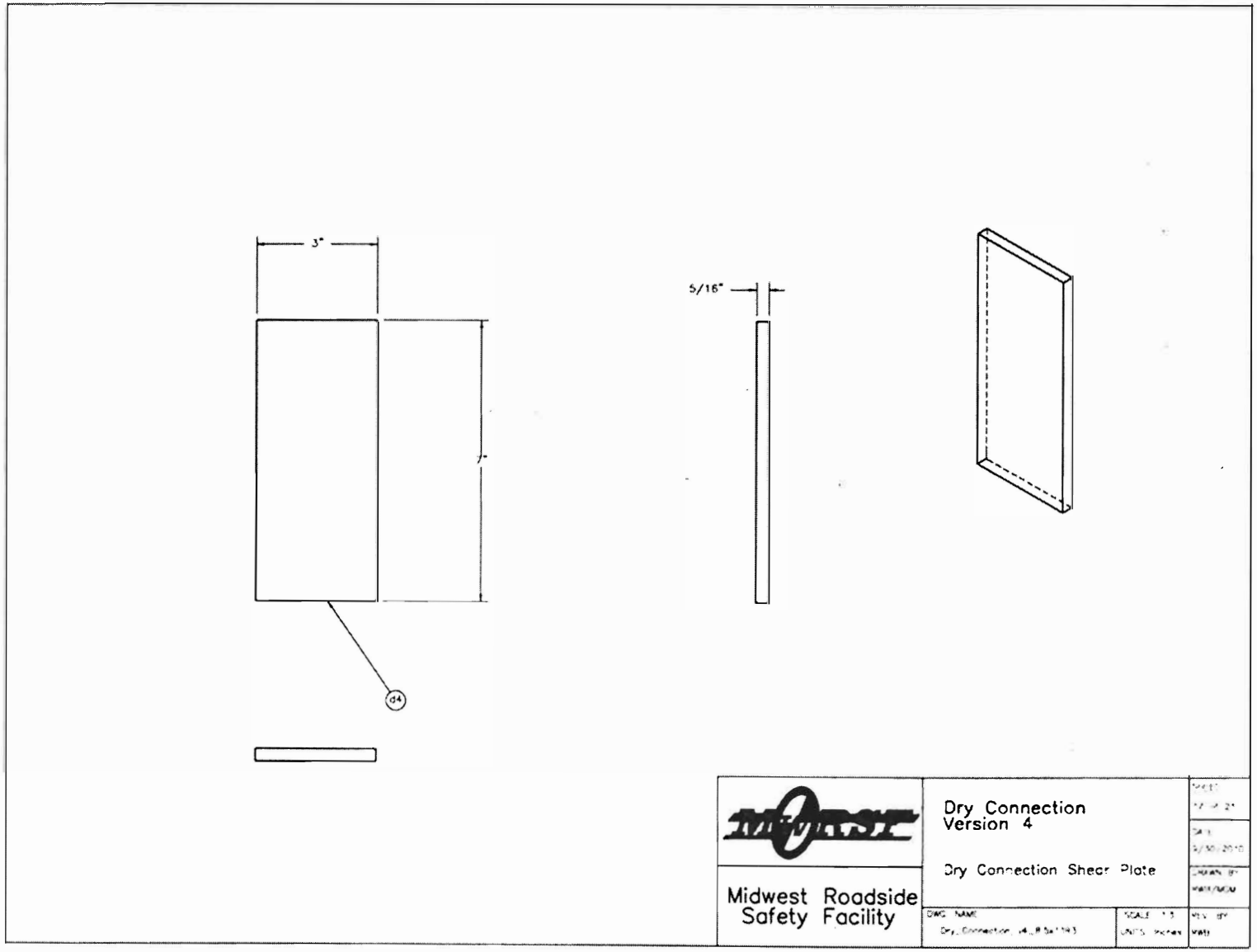

Figure 127. Shear Plates, Test No. PCRB-4

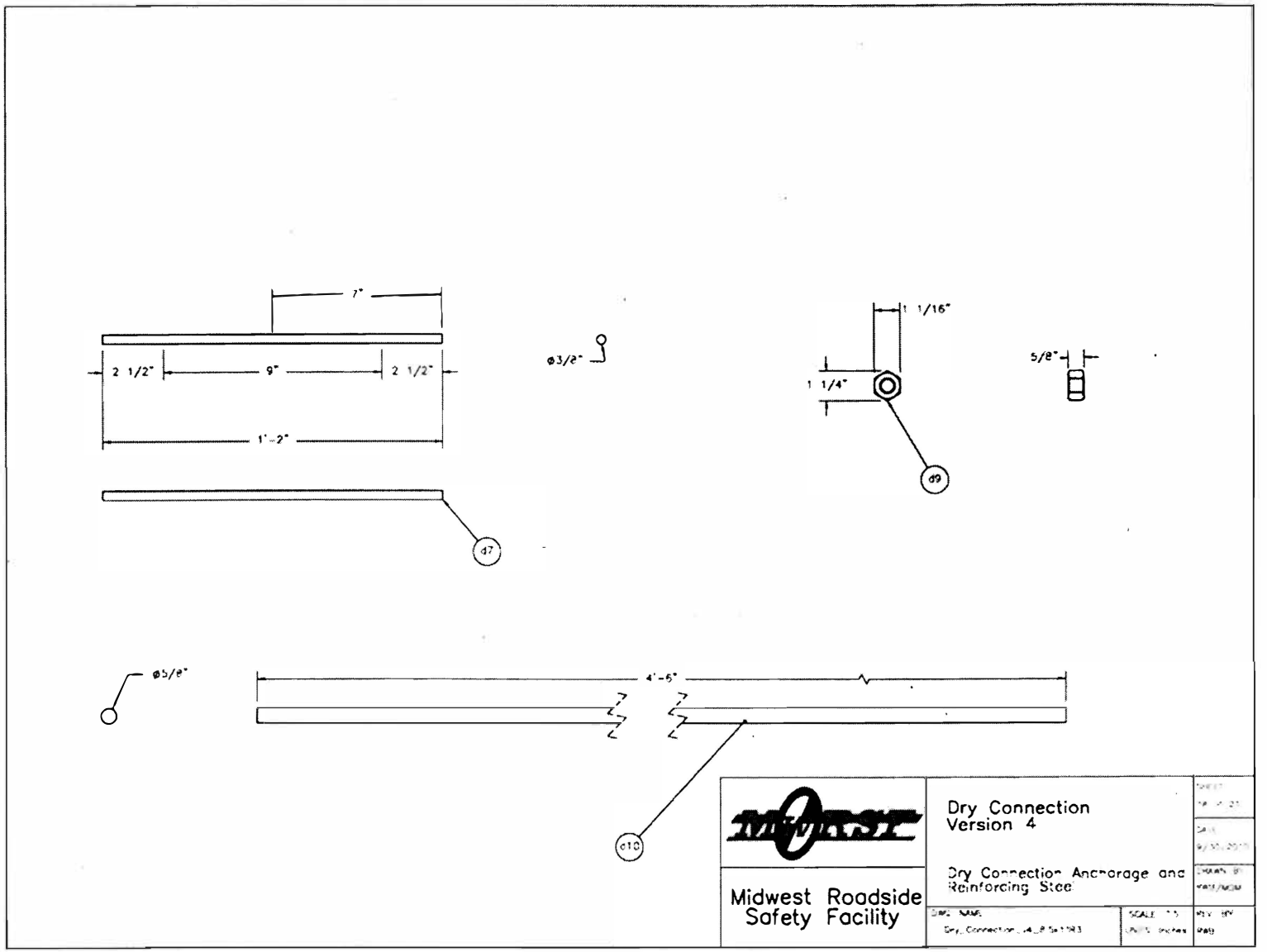

Figure 128. Reinforcing Rebar, Test No. PCRB-4

Dry Connection					
Item No.	QTY	Description	Material Spec	Comment	File Name
f3	1	Dry Connection Shear Tube Body	A500 Grade C – Galvanized	Half Section of 8x4x0.5 Tube	Dry_Connection_v4_sheartube_4.0x4.0x0.5_A500GrC
f5	2	Dry Connection Shear Tube End Cap	A572 Grade 50 – Galvanized	–	Dry_Connection_v4_sheartube_endcap_A572_gr50
f7	2	Dry Connection Shear Tube Shim	A36 – Galvanized	–	Dry_Connection_v4_sheartube_shim_A572_gr50

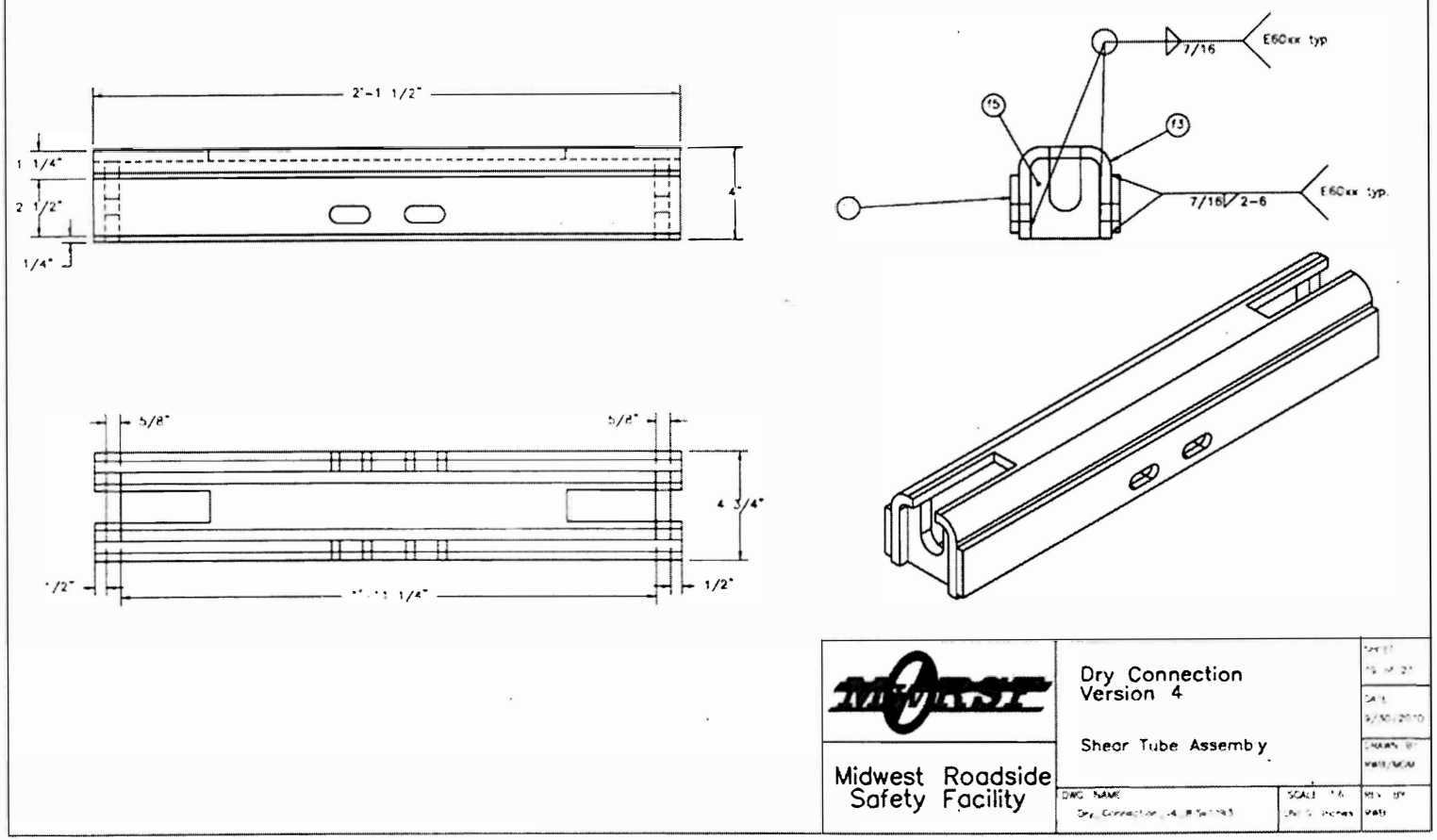

Figure 129. Shear Tube Connector, Test No. PCRB-4

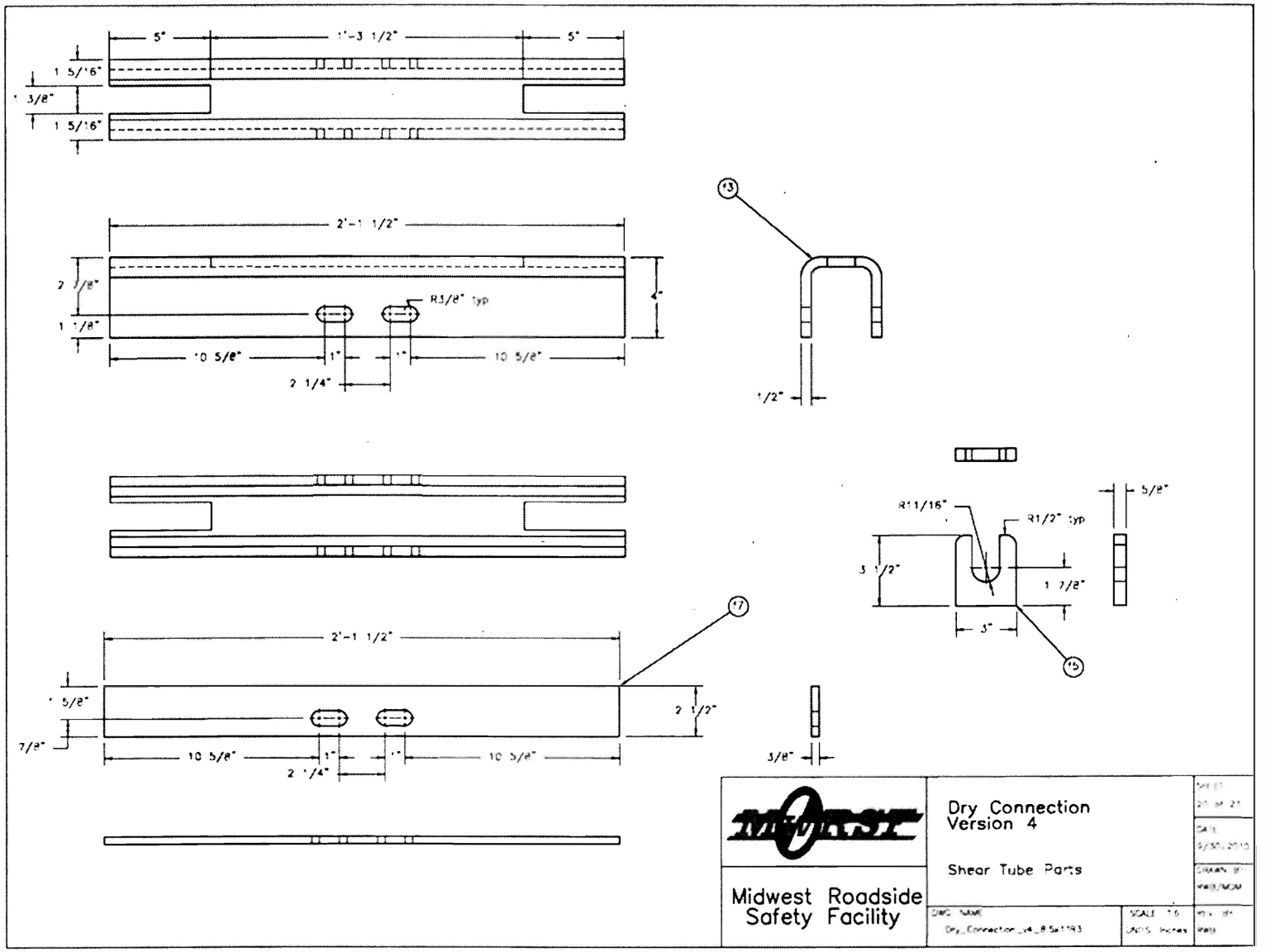

Figure 130. Shear Tube, Shim Plates, and Gussets, Test No. PCRB-4

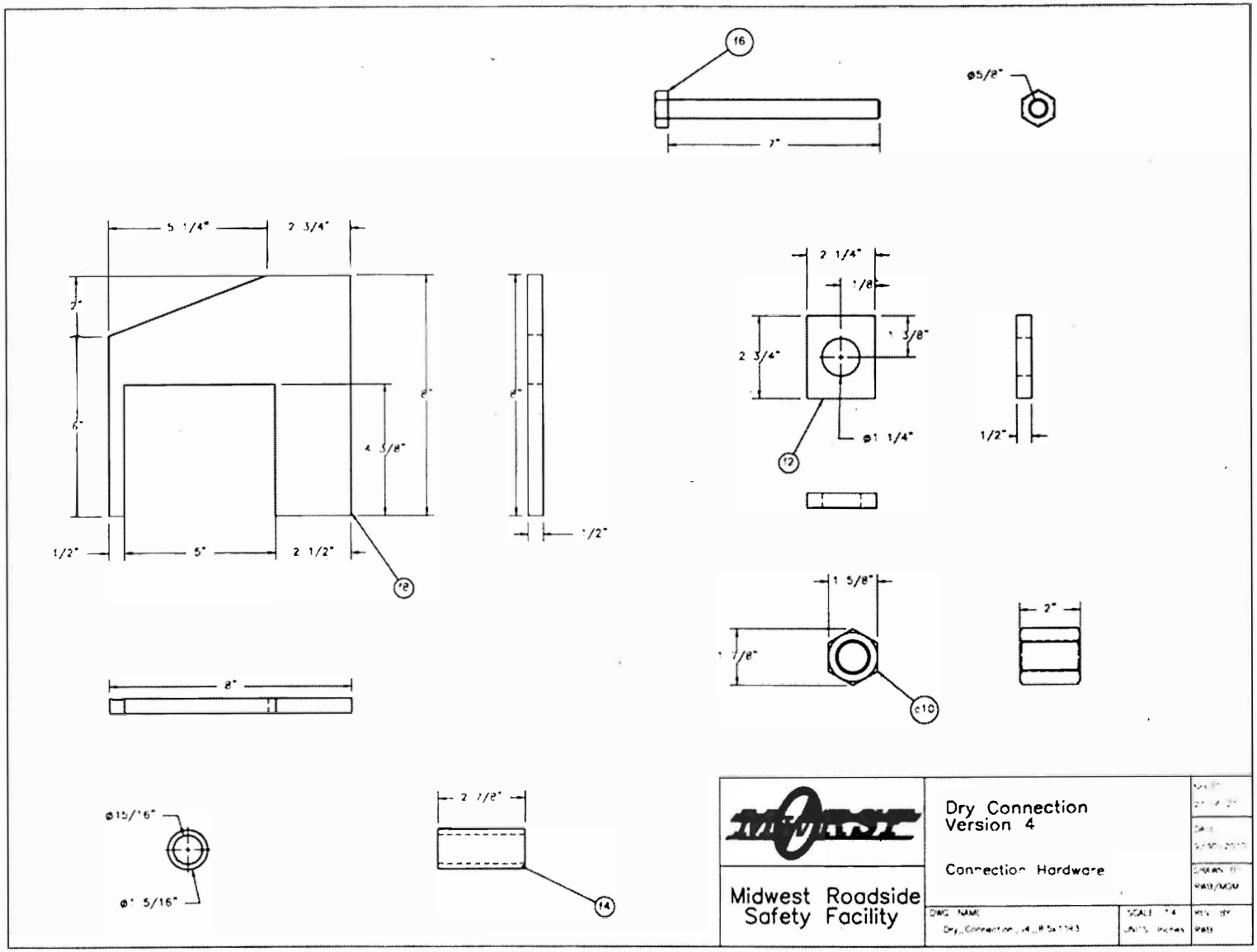

Figure 131. Dry Joint Installation Hardware, Test No. PCRB-4

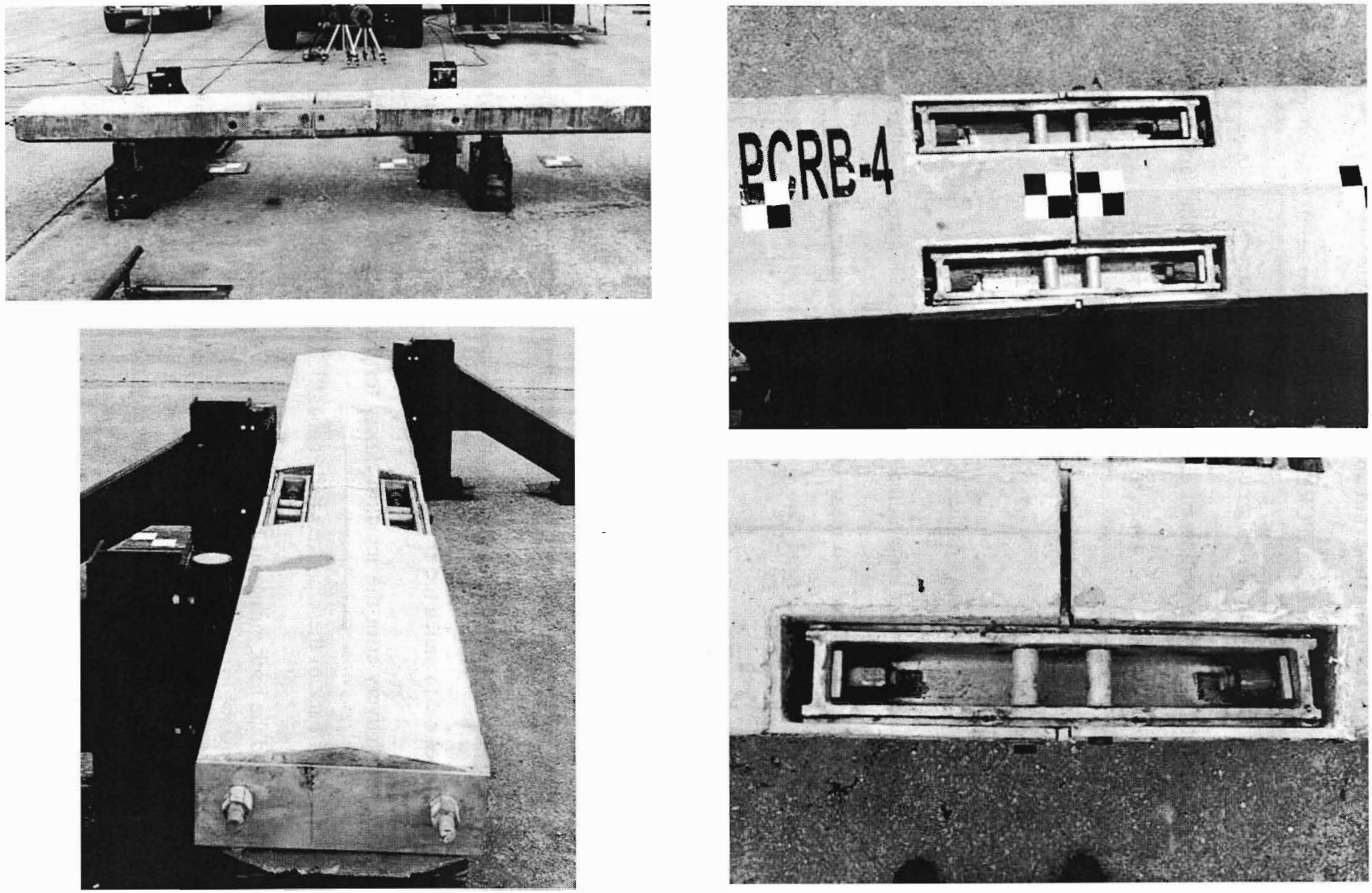

Figure 132. Rail Component Photographs, Test No. PCRB-4

8.3.3 Test No. PCRB-5, Alternate Grout Joint Design

The test specimen used for test no. PCRB-5 consisted of two reinforced concrete rail segments connected by two threaded rods and grout, as shown in Figures 133 through 146. Both the cross sectional geometry and the lengths of each rail segment were the same as the two previously described specimens for test nos. PCRB-3 and PCRB-4. Similar to previous testing, the concrete strength of 5,000 psi (34 MPa) and the epoxy coated no. 4 rebar stirrups spaced at 8-in. (203-mm) intervals were used.

The longitudinal steel in the rail consisted of two no. 4 rebar and two 1-in. (25-mm) diameter smooth bars for a total of four longitudinal bars, as shown in Figures 135 through 139. The no. 4 bars were epoxy coated Grade 60 rebar and ran down the center of the rail segments. The 1-in. (25-mm) diameter smooth bars were galvanized A449 rods with threaded ends and were positioned along each side of the rail cross section. The threaded ends allowed the rod to be fastened to the inside of the steel pockets at the ends of every bridge rail segment and provide the anchorage needed to develop tension.

One end of each rail segment was configured with steel pockets on both the front and back faces of the rail. These pockets were galvanized 6 x 10 x ½-in. (152 x 254 x 13-mm) ASTM A500 Grade C steel tubes cut to match the cross section geometry of the rail, as shown in Figures 142 and 143. Due to a delivery error the actual thickness for the pockets tested were ⅝ in. (16 mm) thick. The front and back of these pockets had concentric holes. The front measured 1⅜ in. (35 mm) in diameter, and the back measured 1⅛ in. (29 mm) in diameter. The front hole allowed the threaded rod connector to extend between grout pockets of adjacent rails for assembly. The threaded ends of the longitudinal rods were inserted through the back hole of each pocket and a heavy hex nut fastened the two components together.

Since the pockets were only located on one end of each rail segment test specimen, an alternate method of anchoring the smooth steel rods had to be utilized on the opposite end of the segment. At these locations the threaded portions actually extended out of the end of the concrete rail. A ¼-in. (6-mm) thick, ASTM A572 Grade 50 steel plate with two 1⅛-in. (29-mm) diameter holes was placed on the rods and pressed against the rail end. Heavy hex nuts were fastened to the rods and anchored the longitudinal steel in the rail. The anchorage plate and nuts are shown in Figures 135, 137, and 144.

To hold the grout in the pocket during assembly, a ¼-in. (6-mm) thick steel plate was welded to the bottom of each grout pocket. Also, a ½-in. (13-mm) thick, 6-in. (152-mm) wide steel shear plate was welded between the pockets to provide both lateral and additional longitudinal anchorage for the pockets. The additional longitudinal anchorage was developed by three U-bars which wrapped around the shear plate and extended into the rail. The U-bars were bent from epoxy coated no. 4 rebar, while the plates were galvanized, ASTM A572 Grade 50 steel. The completed pocket assembly and the individual parts are shown in Figures 140 and 141.

The connector assembly consisted of a threaded rod, two washer plates, and four heavy hex nuts, as shown in Figure 145. The threaded rod was made from B7 steel and measured 7½ in. (191 mm) in length and 1 in. (25 mm) in diameter. The washers were 4½ in. (114 mm) square, ½-in. (13-mm) thick plates cut from ASTM A572 Grade 50 steel.

To assemble the rail joint, the rail segments were first placed on wooden support blocks and positioned as prescribed by Section 6.2 and Figure 48. Next, the ASTM A193 B7 rod was inserted into one of the pockets and slid through the front holes of the adjacent pocket so that half of the rod was in each pocket. Then, two nuts were used to secure a washer plate to each end of the B7 rod. Once the connector was assembled and in place, L&M Crytex grout with a

strength of 10,000 psi (69 MPa) was used to fill the pockets and secure the steel connector. Photographs of the assembled joint specimen are shown in Figure 146.

Wide Flange Connection – Option C					
Item No.	QTY	Description	Material Spec	Comment	File Name
p1	1	Grouted Connection Option C – 5.75 ft Beam	–	–	Grouted_Wide_Flange_OptionC_5.75ft
p2	1	Grouted Connection Option C – 9.5 ft Beam	–	–	Grouted_Wide_Flange_OptionC_9.5ft
e1	2	Option C L&M Crystex Grout	L&M Crystex Grout – f'c = 10000 psi	–	Grouted_Wide_Flange_Option_C_grout
e2	2	Option C Connection Assembly	–	–	Grouted_Wide_Flange_Option_C_connection_piece

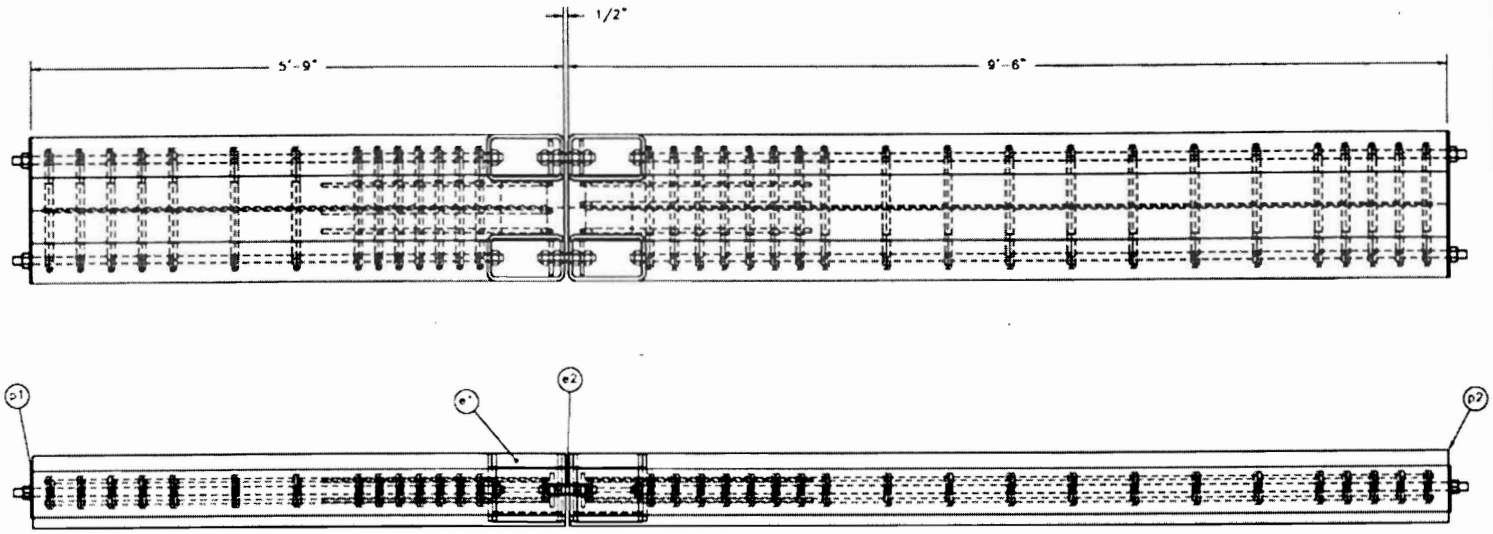

Midwest Roadside Safety Facility

Wide Flange Connection Option C

Assembled Beams

Grouted_Wide_Flange_C_6.5x11R3

SCALE 1:19

UNITS: inches

SHEET 1 of 13

DATE 9/30/2010

DRAWN BY RWB/CJS/MCM

REV. BY RWB

Figure 133. Alternate Grout Joint Design, Test No. PCRB-5

Wide Flange Connection – Option C

Item No.	QTY	Description	Material Spec	Comment	File Name
p1	1	Grouted Connection Option C – 5.75 ft Beam	–	–	Grouted_Wide_Flange_OptionC_5.75ft
p2	1	Grouted Connection Option C – 9.5 ft Beam	–	–	Grouted_Wide_Flange_OptionC_9.5ft
e1	2	Option C L&M Crystex Grout	L&M Crystex Grout – f'c = 10000 psi	–	Grouted_Wide_Flange_Option_C_grout
e2	2	Option C Connection Assembly	–	–	Grouted_Wide_Flange_Option_C_connection_piece
e3	2	Option C 1.0 UNC 8 x 7.0 Threaded Rod	B7 – Galvanized		Grouted_Wide_Flange_Option_C_threaded_connection_rod_B7
e4	4	Option C Connection Plate	A572 – Grade 50 – Galvanized		Grouted_Wide_Flange_Option_C_threaded_connection_plate_A572_Gr50
e5	8	Option C Connection 1 UNC-2 Heavy Hex Nut	ASTM 194 Grade 2H – Galvanized	–	Grouted_Wide_Flange_Option_C_HHNUT 1.0000-8-D-C

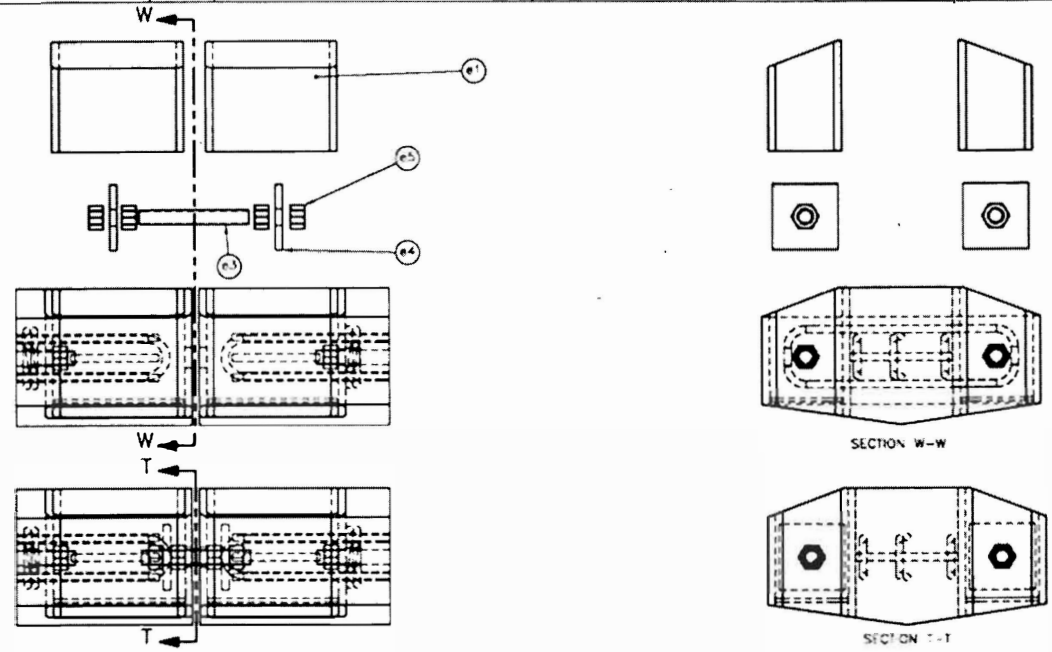

Midwest Roadside Safety Facility

Wide Flange Connection Option C

Connection Detail

Figure 134. Alternate Grout Joint Assembly, Test No. PCRB-5

Wide Flange Connection – Option C					
Item No.	QTY.	Description	Material Spec	Comment	File Name
a1	1	Precast Concrete Bridge Rail Section	SSC f'c = 5000 psi	–	Grouted_Wide_Flange_Option_C_body_9.5ft
b1	20	No. 4 Top Rail Stirrup	A615 Grade 60 – Epoxy Coated	–	Grouted_Wide_Flange_Option_C_toprail_stirrup_No 4_Grade60
b2	2	No. 4 Longitudinal Rebar	A615 Grade 60 – Epoxy Coated	–	Grouted_Wide_Flange_Option_C_9.5ft_longbar_No 4_Grade60
c1	1	Grouted Connection Option C	–	–	Grouted_Wide_Flange_Option_C
c8	2	1 UNC-8 Smooth Bar with Threaded Ends	A449 – Galvanized	–	Grouted_Wide_Flange_Option_C_No.8_9.5ft_A449_threaded_rod
d1	1	Grouted Connection Option C End Plate	A572 Grade 50 – Galvanized	–	Grouted_Wide_Flange_Option_C_5.75ft_endplate_6x19x0.5_A572_gr50
e5	4	Option C Connection 1 UNC-8 Heavy Hex Nut	ASTM 194 Grade 2H – Galvanized	–	Grouted_Wide_Flange_Option_C_HHNUT 1.0000-8-D-C

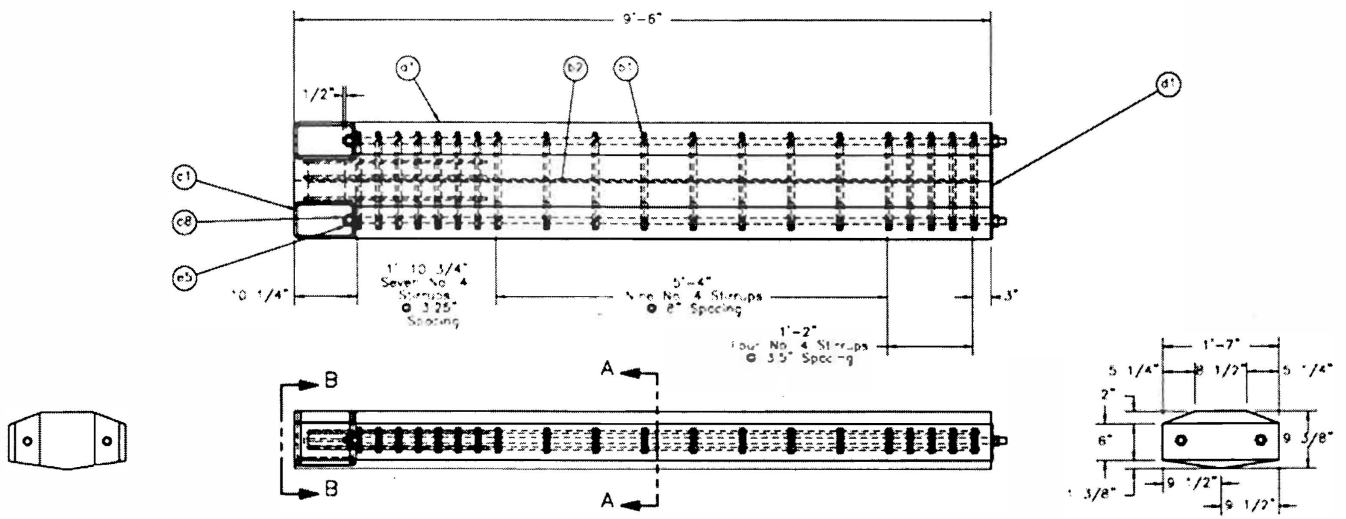

Midwest Roadside Safety Facility

Wide Flange Connection Option C

Wide Flange Connection Option C 9.5 ft Beam

DWG. NAME: Grouted_Wide_Flange_C_8.5x11R3

SCALE: 1:24

UNITS: Inches

Figure 135. Long Rail Segment, Test No. PCRB-5

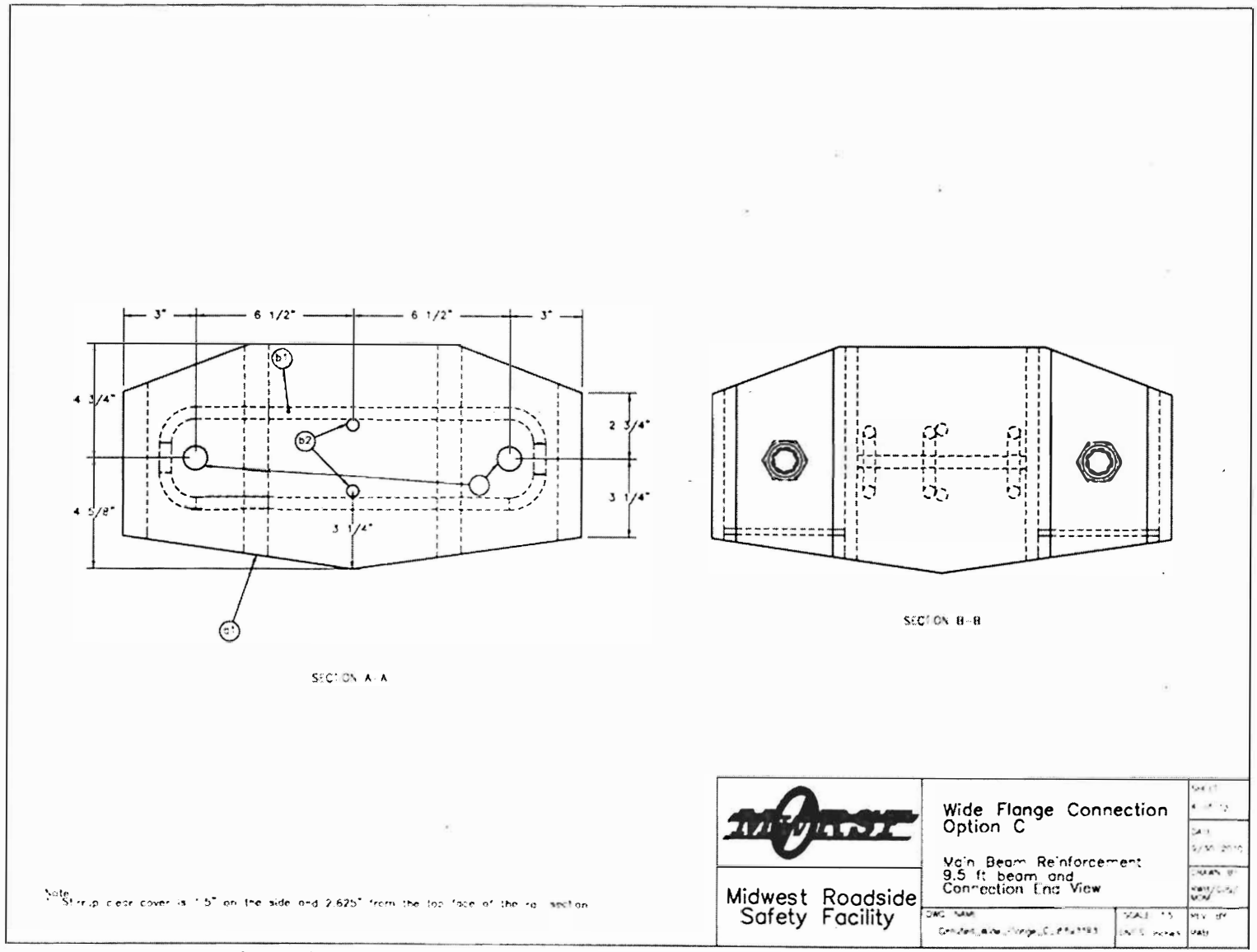

Note: Strap clear cover is 1.5" on the side and 2.625" from the top face of the rail section

Figure 136. Cross Section Views of Long Rail Segment, Test No. PCRB-5

Wide Flange Connection – Option C					
Item No.	QTY	Description	Material Spec	Comment	File Name
a2	1	Precast Concrete Bridge Rail Section	SSC f'c = 5000 psi	–	Grouted_Wide_Flange_Option_C_body_5.75ft
b1	14	No. 4 Top Rail Stirrup	A615 Grade 60 – Epoxy Coated	–	Grouted_Wide_Flange_Option_C_toprail_stirrup_No.4_Grade60
b5	2	No. 4 Longitudinal Rebar	A615 Grade 60 – Epoxy Coated	–	Grouted_Wide_Flange_Option_C_5.75ft_longbar_No.4_Grade60
c1	1	Grouted Connection Option C	–	–	Grouted_Wide_Flange_Option_C
c7	2	1"-UNC-8 Smooth Bar with Threaded Ends	A449 – Galvanized	–	Grouted_Wide_Flange_Option_C_No.8_5.75ft_A449_threaded_rod
d1	1	Grouted Connection Option C End Plate	A572 Grade 50 – Galvanized	–	Grouted_Wide_Flange_Option_C_5.75ft_endplate_6x19x0.5_A572_gr50
e5	4	Option C Connection 1"-UNC-8 Heavy Hex Nut	ASTM 194 Grade 2H – Galvanized	–	HHNUT 1.0000-8-D-C

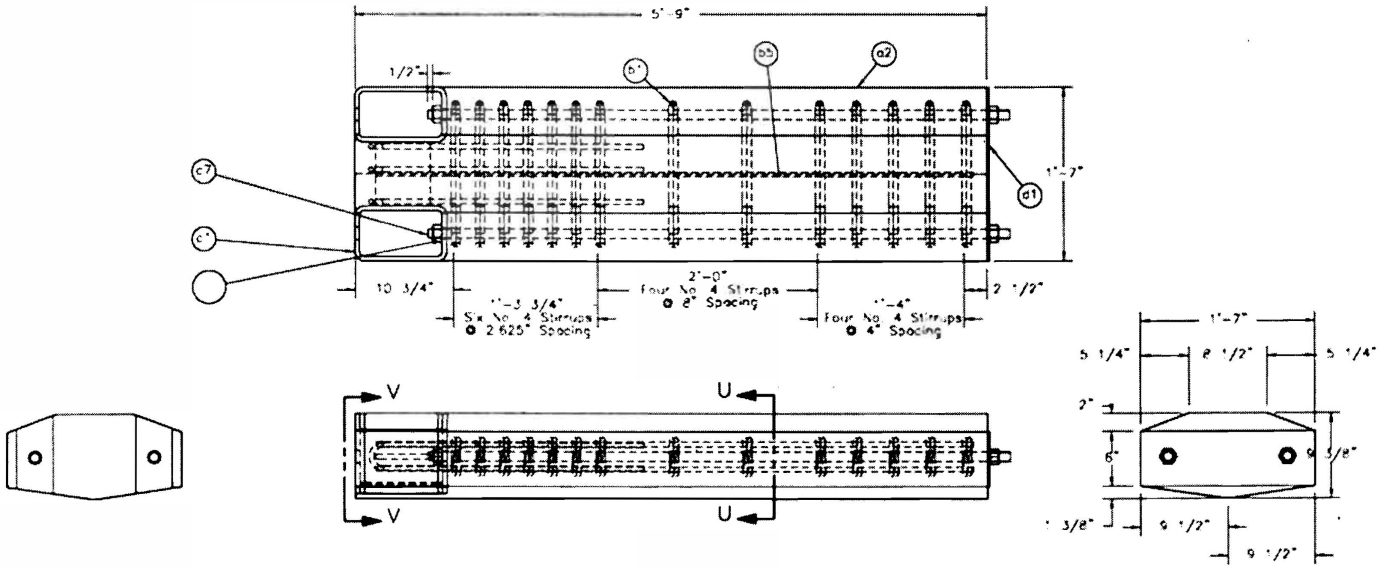

Midwest Roadside Safety Facility

Wide Flange Connection Option C

Wide Flange Connection Option C 5.75 ft Beam

Figure 137. Short Rail Segment, Test No. PCRB-5

Wide Flange Connection – Option C					
Item No.	QTY	Description	Material Spec	Comment	File Name
a2	1	Precast Concrete Bridge Rail Section	SSC f'c = 5000 psi	–	Grouted_Wide_Flange_Option_C_body_5.75ft
b1	14	No. 4 Top Rail Stirrup	A615 Grade 60 – Epoxy Coated	–	Grouted_Wide_Flange_Option_C_toprail_stirrup_No.4_Grade60
b5	2	No. 4 Longitudinal Rebar	A615 Grade 60 – Epoxy Coated	–	Grouted_Wide_Flange_Option_C_5.75ft_longbar_No.4_Grade60
c7	2	1-UNC-8 Smooth Bar with Threaded Ends	A449 – Galvanized	–	Grouted_Wide_Flange_Option_C_No.8_5.75ft_A449_threaded_rod
e5	4	Option C Connection 1 UNC-8 Heavy Hex Nut	ASTM 194 Grade 2H – Galvanized	–	HHNUT 1.0000-8-D-C

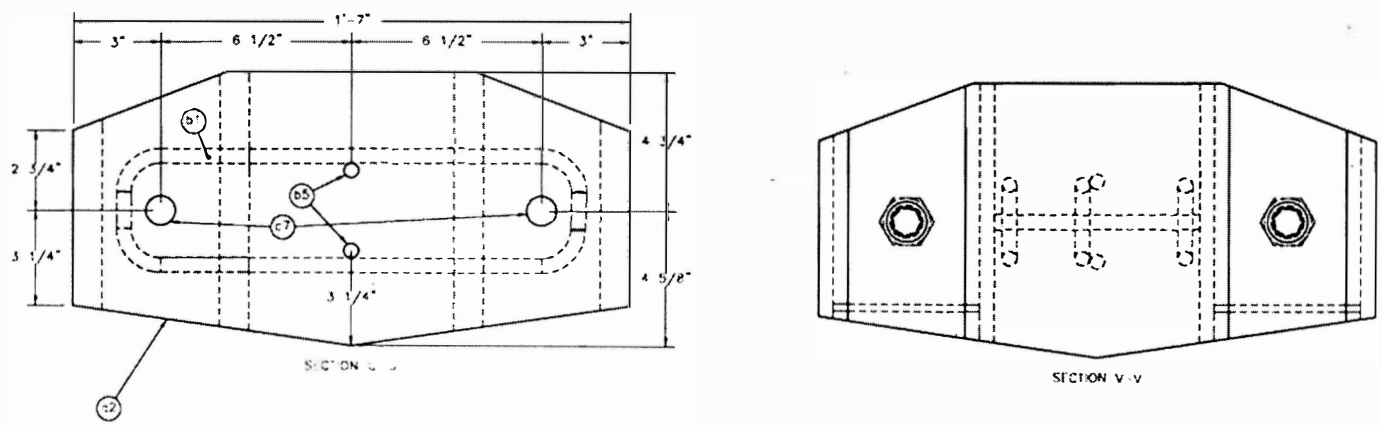

Note
* Stirrup clear cover is 1.5" on the side and 2.625" from the top face of the rail section

Midwest Roadside Safety Facility

Wide Flange Connection
Option C

Main Beam Reinforcement
5.75 ft beam and
Connection End View

DWG NAME: Grouted_Wide_Flange_C_8.5x11R3
SCALE: 1:5
UNITS: inches
REV BY: RAB

Figure 138. Cross Section Views of Short Rail Segment, Test No. PCRB-5

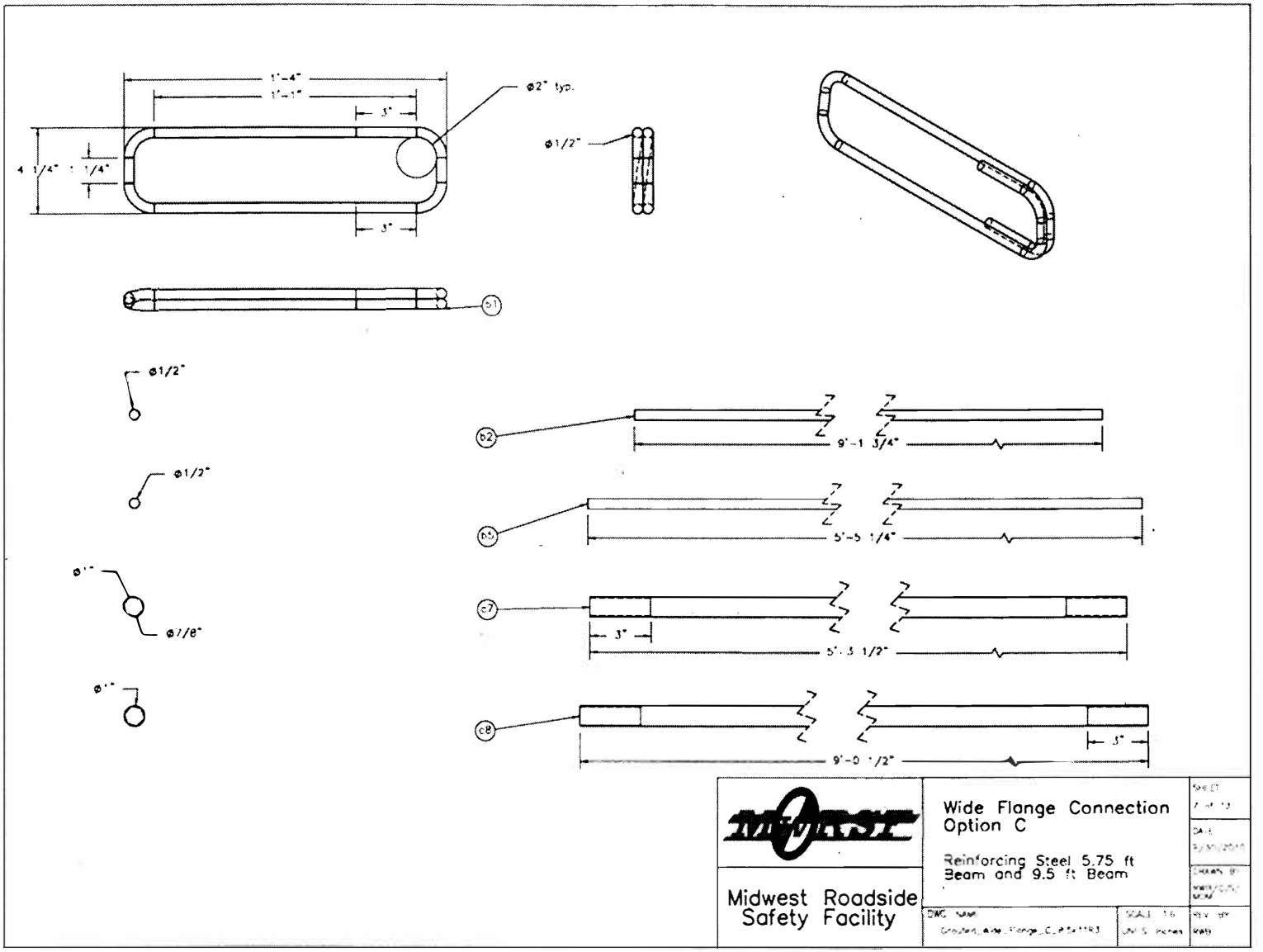

Figure 139. Rail Internal Steel Reinforcement, Test No. PCRB-5

Wide Flange Connection – Option C					
Item No.	QTY	Description	Material Spec	Comment	File Name
c2	1	Option C Left Grout Pocket Tube 6x10x0.5	A500 Grade C – Galvanized	–	Grouted_Wide_Flange_Option_C_grout_pocket_left_6x8x0.5
c3	1	Option C Right Grout Pocket Tube 6x10x0.5	A500 Grade C – Galvanized	–	Grouted_Wide_Flange_Option_C_grout_pocket_right_6x8x0.5
c5	2	Option C Grout Tube Cap	A572 Grade 50 – Galvanized	–	Grouted_Wide_Flange_Option_C_grout_pocket_cap
c6	1	Option C Shear Plate	A572 Grade 50 – Galvanized	–	Grouted_Wide_Flange_Option_C_shearplate_A572_Gr50
c9	3	Option C No. 4 U-Bars	A615 Grade 60 – Epoxy Coated	–	Grouted_Wide_Flange_Option_C_No.4_Grade60_Ubars

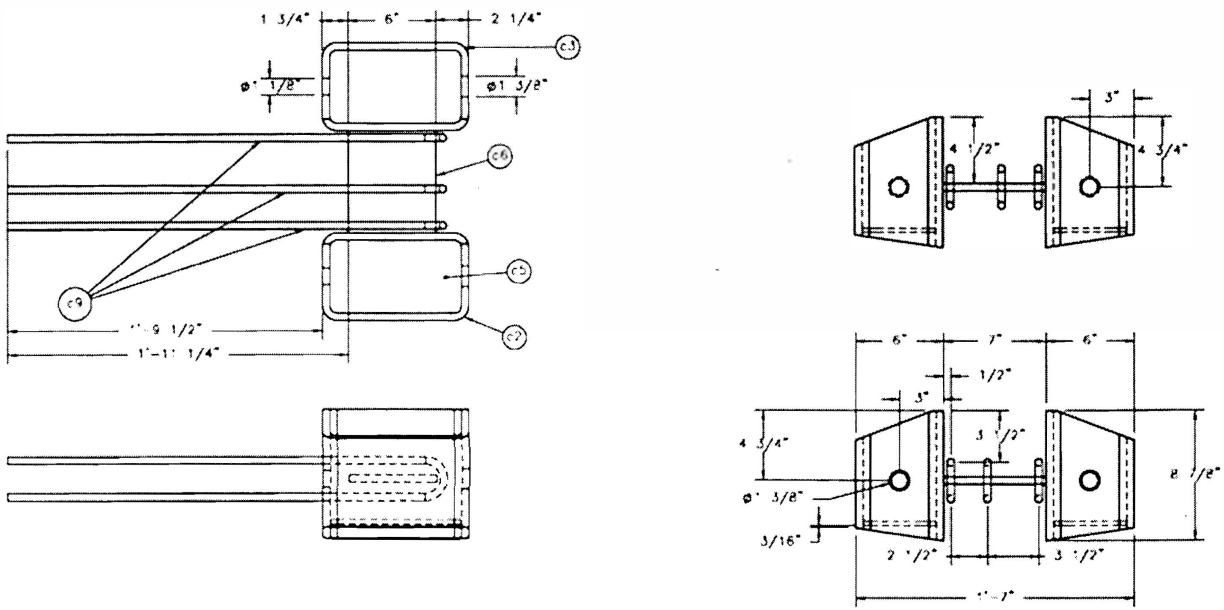

Note: The actual 6x10x0.5 tubing used in the prototype received from the precasters was 1/8" thicker than specified. This made the actual tube thickness 5/8".

Midwest Roadside Safety Facility

Wide Flange Connection Option C

Option C End Connection Assembly

DWG NAME: Grouted_Wide_Flange_C_8.5x11R3

SCALE: 1:10

UNITS: Inches

SHEET: 8 of 13

DATE: 9/30/2010

DRAWN BY: RWB/DG/MCW

REV BY: RWB

Figure 140. Pocket Assembly and Anchorage, Test No. PCRB-5

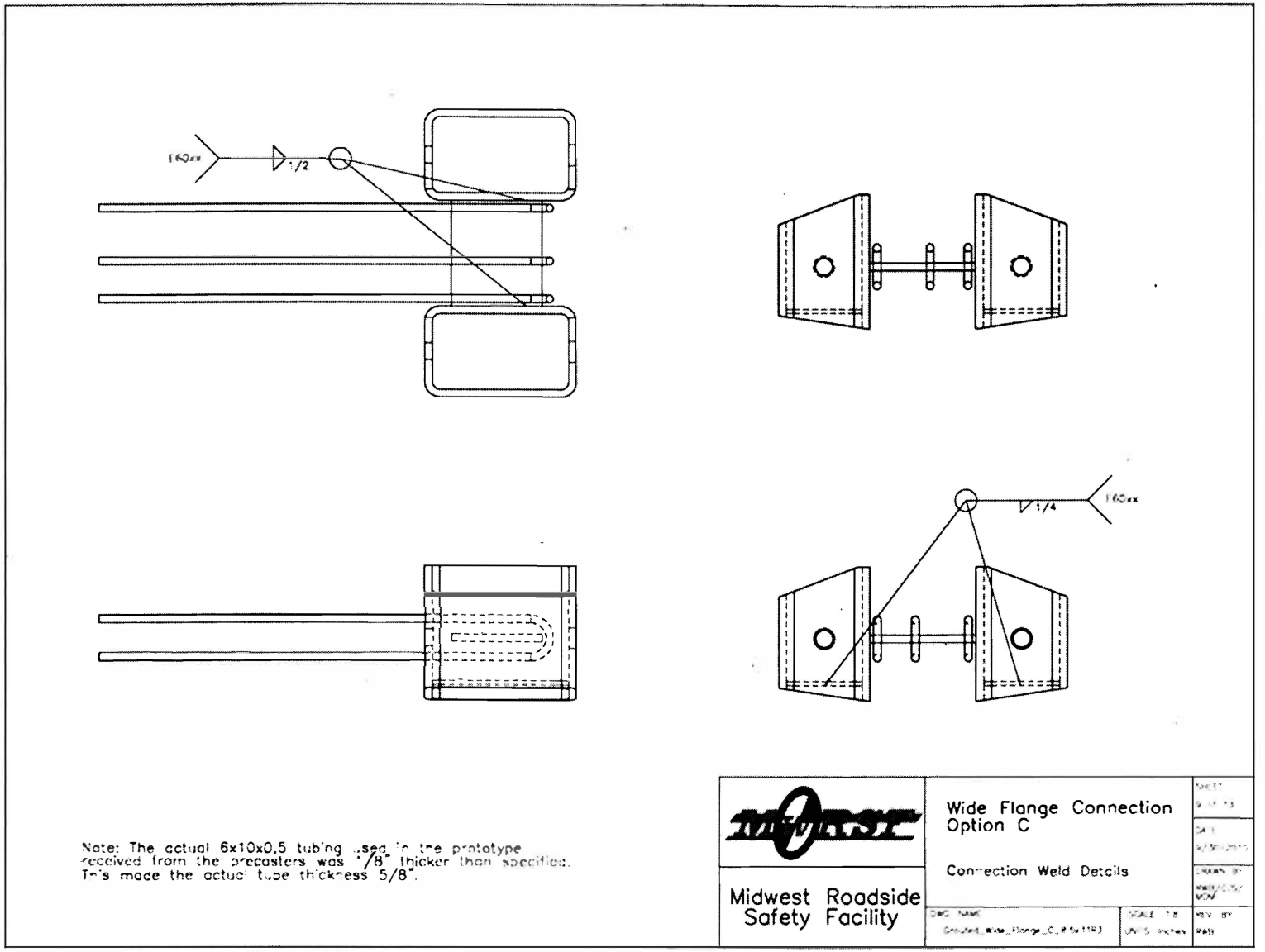

Figure 141. Pocket Assembly Connections, Test No. PCRB-5

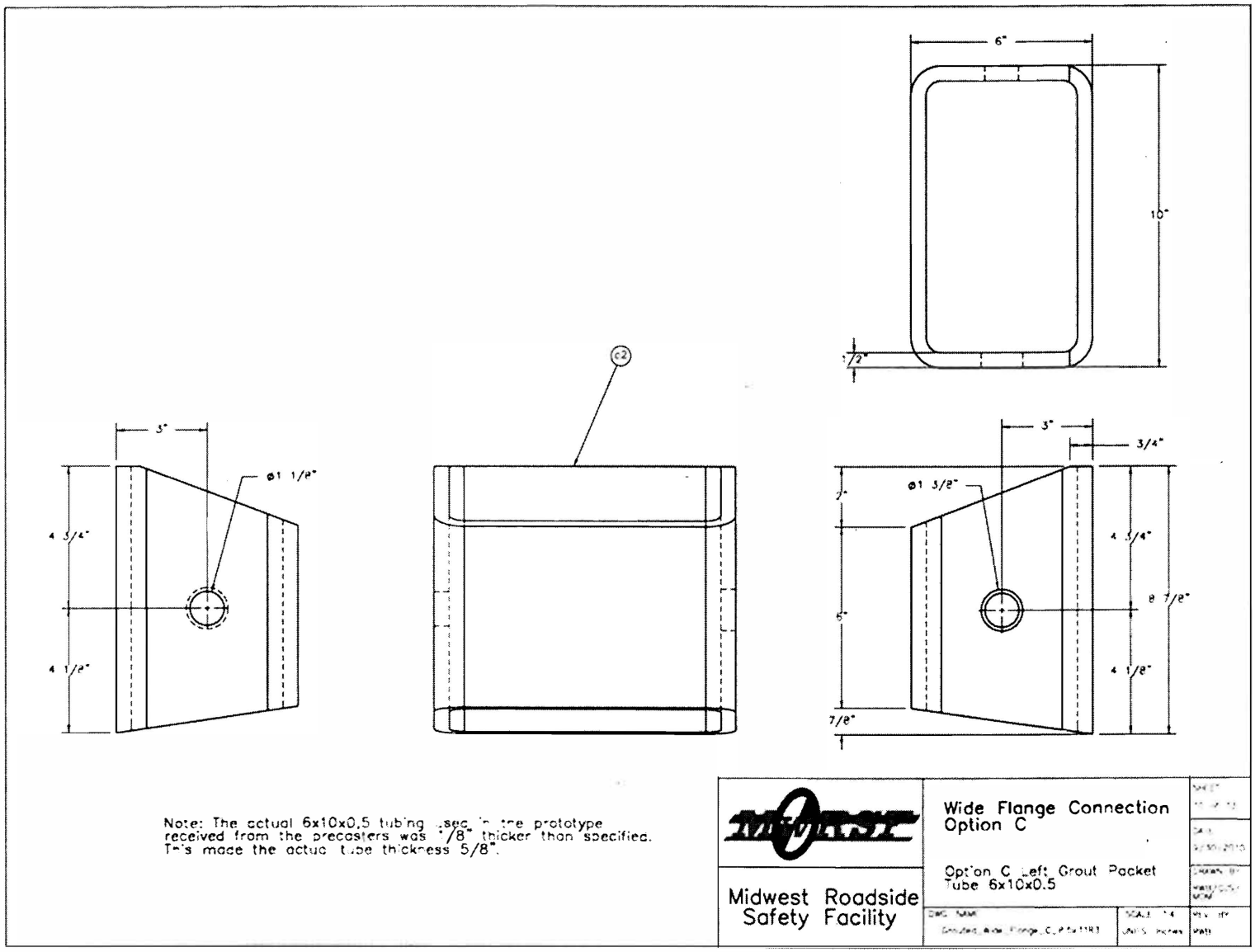

Figure 142. Left Grout Pocket, Test No. PCRB-5

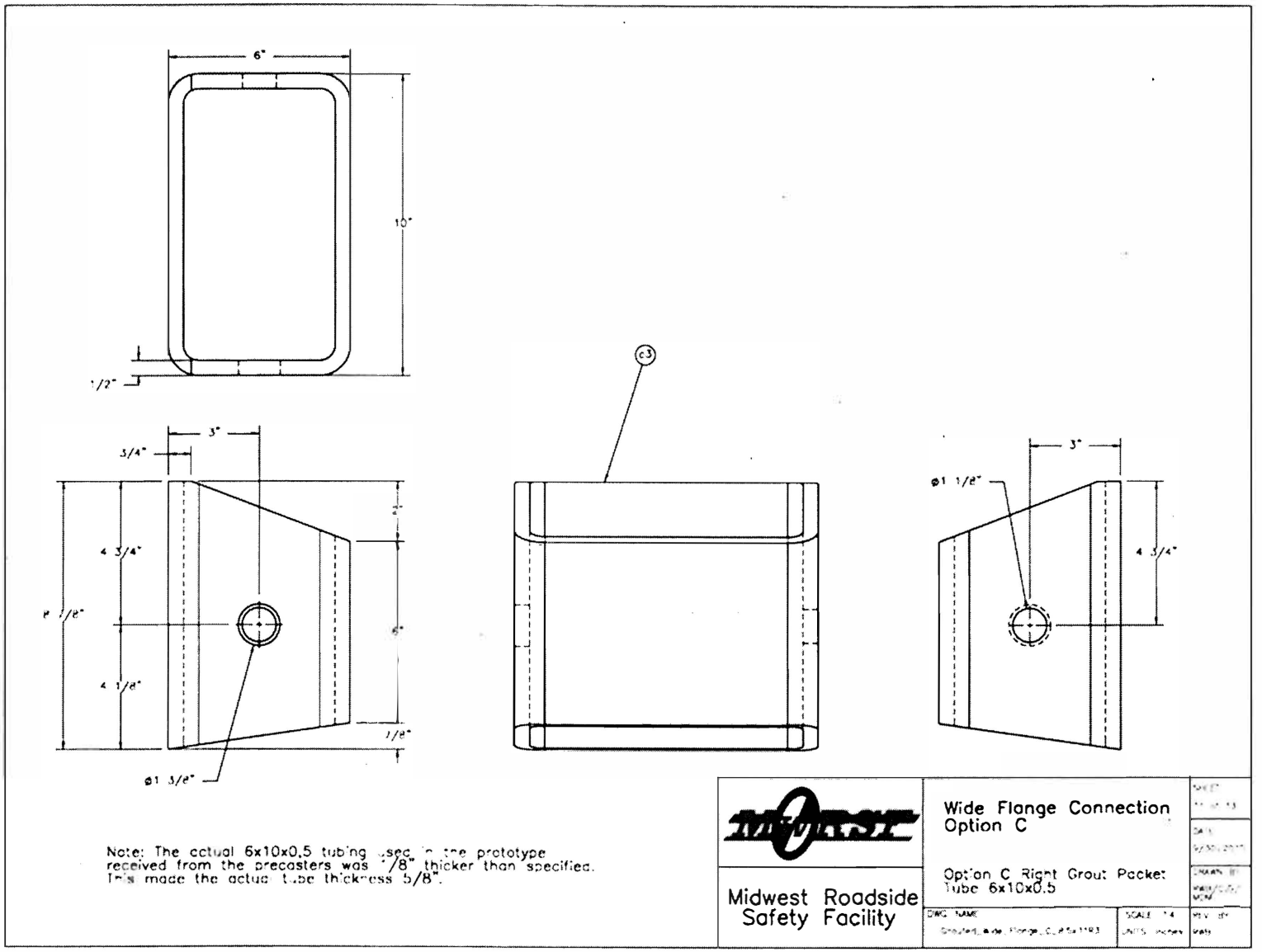

Figure 143. Right Grout Pocket, Test No. PCRB-5

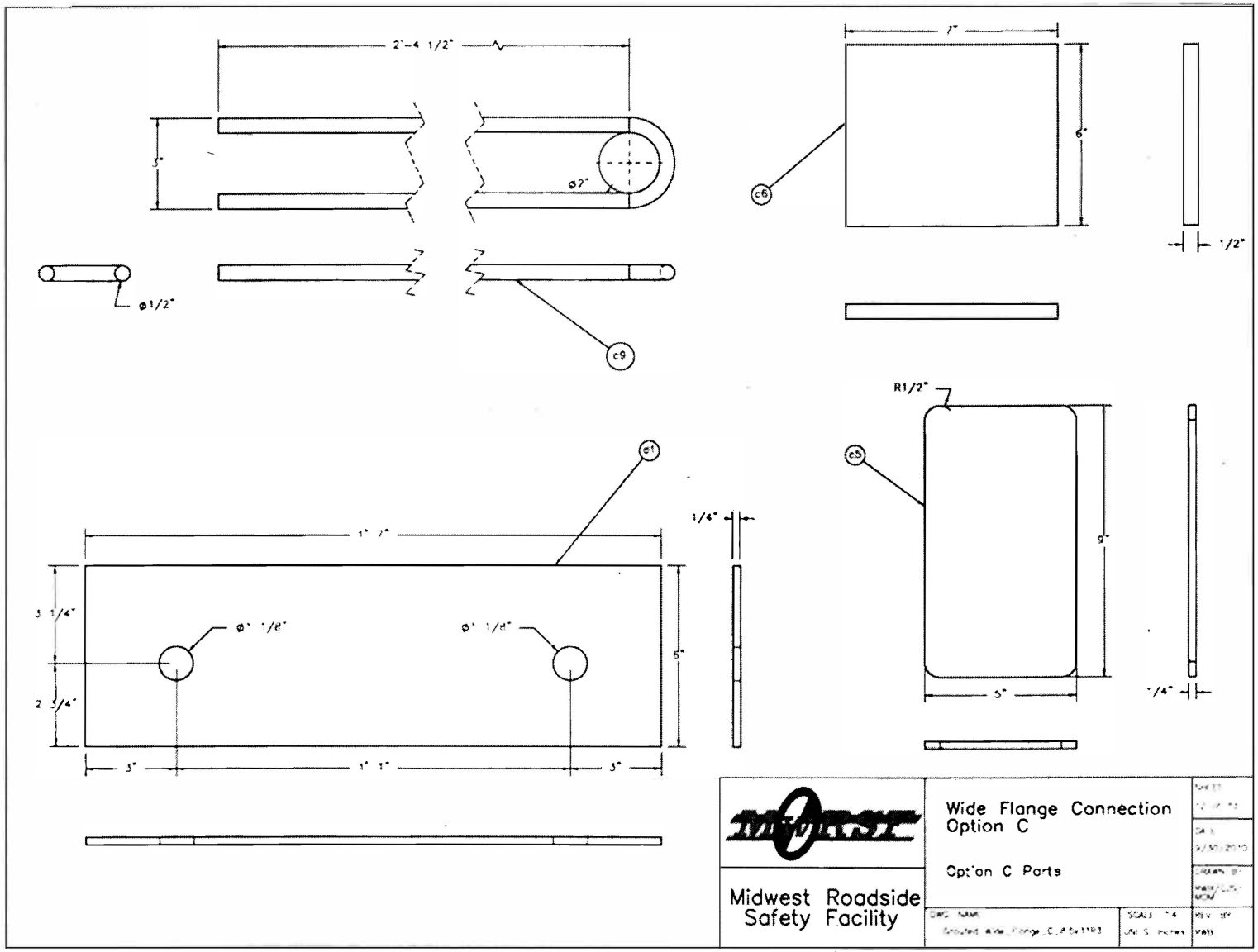

Figure 144. Grout Pocket Cap, Shear Plate, and Anchorage, Test No. PCRB-5

Wide Flange Connection – Option C

Item No.	QTY	Description	Material Spec	Comment	File Name
e3	1	Option C 1.0 UNC-8 x 7.0 Threaded Rod	B7 – Galvanized	–	Grouted_Wide_Flange_Option_C_threaded_connection_rod_B7
e4	2	Option C Connection Plate	A572 – Grade 50 – Galvanized	–	Grouted_Wide_Flange_Option_C_threaded_connection_plate_A572_Gr50
e5	4	Option C Connection 1 UNC-8 Heavy Hex Nut	ASTM 194 Grade 2H – Galvanized	–	HHNUT 1.0000-8-D-C

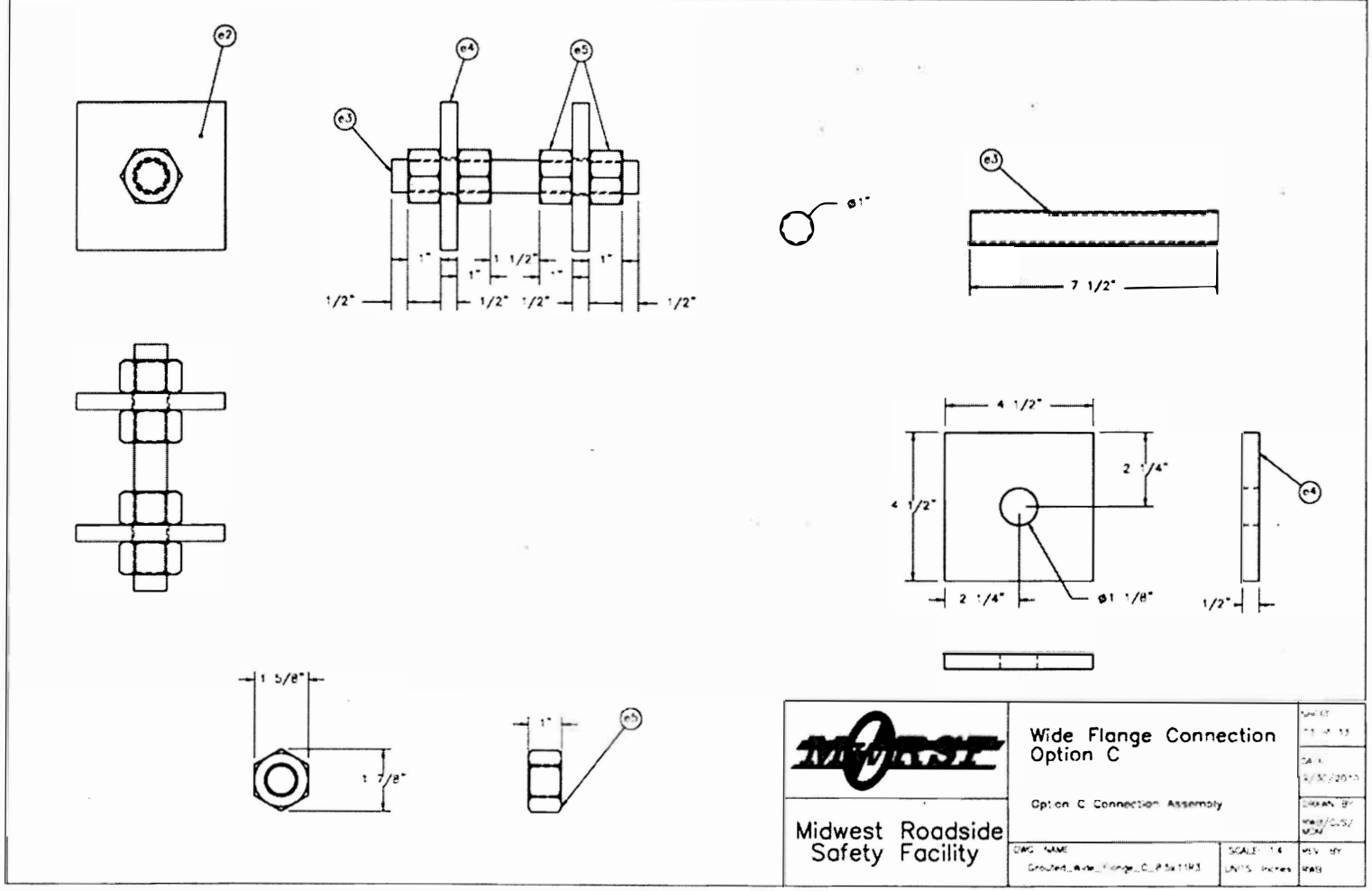

Figure 145. Threaded Rod Connector Assembly, Test No. PCRB-5

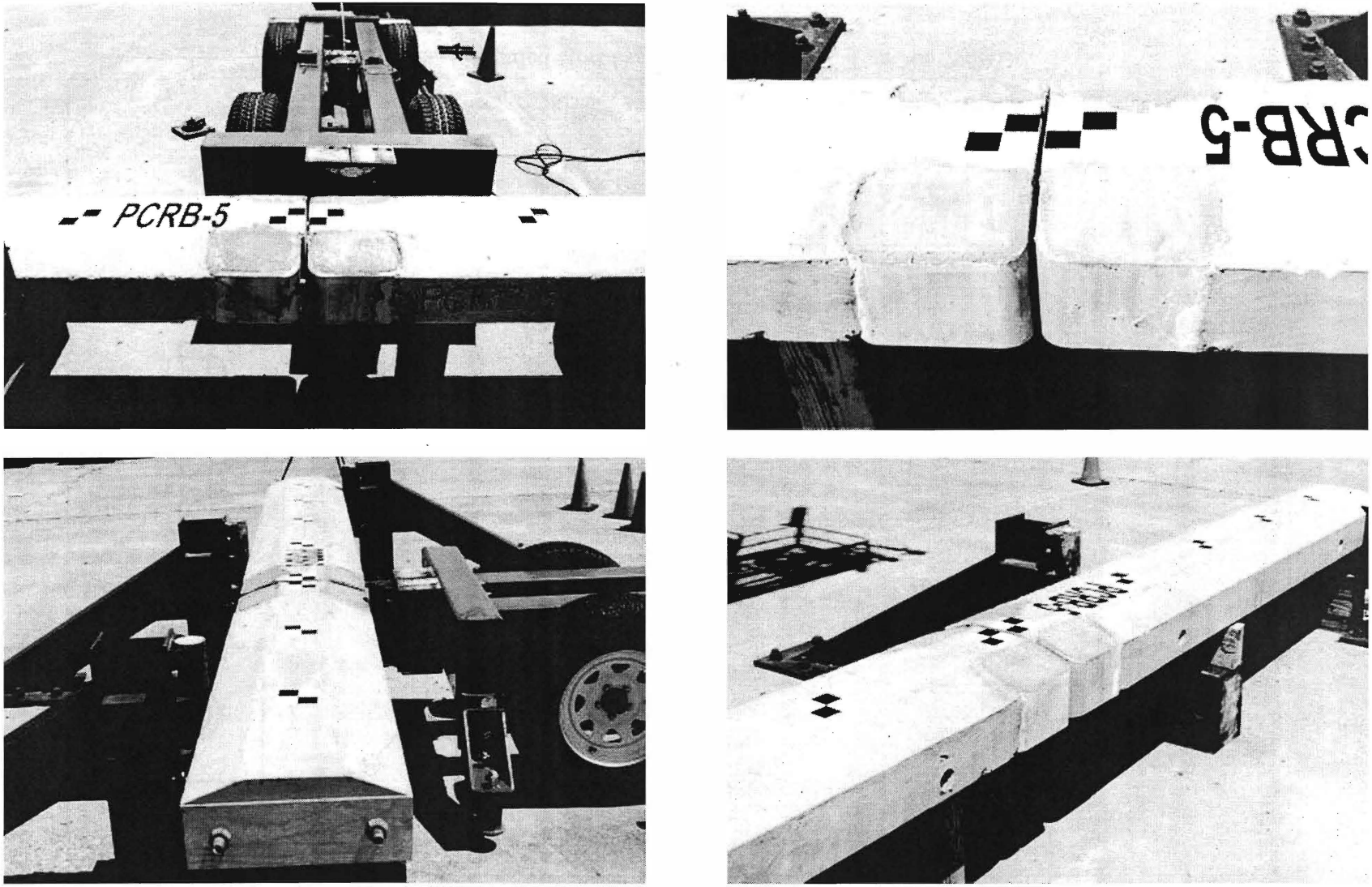

Figure 146. Rail Component Photographs, Test No. PCRB-5

8.4 Bogie Test No. PCRB-3

8.4.1 Test Description

The 1,707-lb (774-kg) bogie vehicle impacted the concrete rail specimen 6 in. (152 mm) from the centerline of the joint at a speed of 22.2 mph (35.8 km/h). At 0.002 seconds after impact, separation cracks formed between the back pockets and the concrete of both rails. Further, chipping of the grout near impact was observed. At this same time, the short rail segment developed a crack stemming from the front pocket and extending diagonally away from the joint. The long rail segment had a crack running between the steel pockets. At 0.004 sec, the rails began to deflect backward as a crack developed between the pockets of the short rail segment. At this same time, tension and shear cracks had formed in both rail segments near the anchor post supports. At 0.006 sec, the separation cracks between the back pockets and the concrete continued to expand. At 0.008 sec, the back pocket of the long rail segment rotated back slightly as a large crack opened between the pockets of the long rail segment. At 0.014 sec, the bogie and rail specimen had reached a maximum displacement of 2.1 in. (533 mm) and began to redirect in the opposite direction. At this same time, the front face of the short rail segment near the steel pocket began to spall. At 0.018 sec, minor concrete spalling was observed on both the top and bottom surfaces of either rail segment. At 0.028 sec, the bogie lost contact with the rail specimen as it continued to travel away from the test specimen. Sequential photographs of the impact event are shown in Figure 147.

8.4.2 Component Damage

Damage to the rail component consisted mainly of cracks and concrete spalling, as shown in Figures 148 through 150. Both rail segments suffered large shear cracks running between the front and back steel pockets. Also, the back pockets of both rails had separation cracks along the

interface between the steel and concrete. However, the threaded rebar remained intact with the joint and was still able to anchor the back pockets. Small separation cracks were also found on the inside of the pocket along the interface between the steel and grout. Both separation cracks and the shear cracks running between the pockets were found on the bottom surface of the rail component as well, as shown in Figure 150.

The front pocket of the short rail segment was slightly indented from direct contact with the bogie impact head. Also, a small piece of grout had chipped off from the top surface of this grout pocket, as shown in Figure 149. A 6 x 6 in. (152 x 152 mm) area of concrete spalling was located on the front face of the short rail segment adjacent to the steel pocket. Finally, tension cracks were found in the long rail segment near the location of the middle anchor post support, as shown in Figure 150.

8.4.3 Data Analysis

Data from the accelerometers was used to calculate and analyze the loads imparted to the rail component during test no. PCRB-3. The data collected by the DTS was unusable. EDR-3 plots depicting force vs. time, force vs. displacement, and energy vs. displacement are shown in Figure 151. Two force spikes were observed, the first of which was largely due to inertial effects. Beyond the inertial force spike, the joint component resisted an impact load greater than 100 kips (445 kN) until 0.015 seconds after impact. At this time both the bogie and the rail component reached maximum deflection and began to rebound. Recall form Section 6.2, the impact load for this test was 62 kips (276 kN) of which the joint was only required to resist 35 kips (156 kN). Thus, the joint used in test no. PCRB-3 provided adequate strength throughout the impact event. Also, the rail component demonstrated an ability to absorb over 330 k-in. (37 kN-m) of energy through a relatively small deflection without failing.

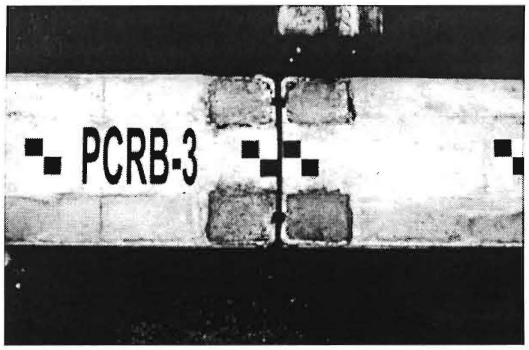

0.000 sec

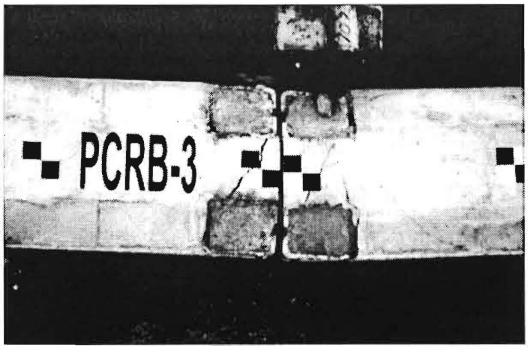

0.008 sec

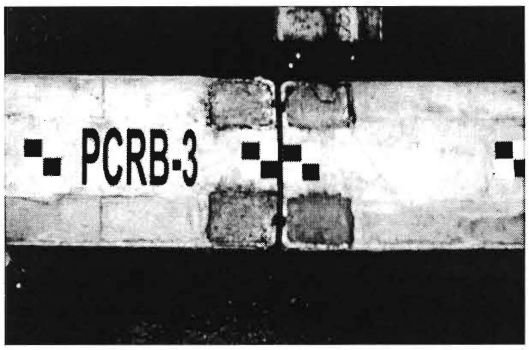

0.002 sec

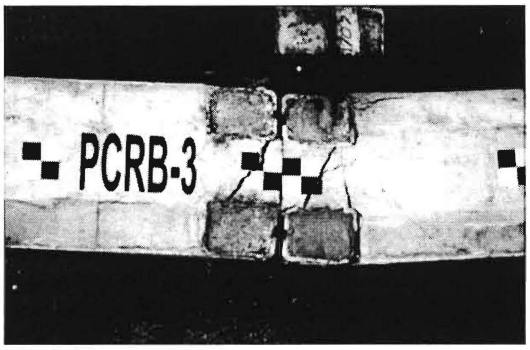

0.014 sec

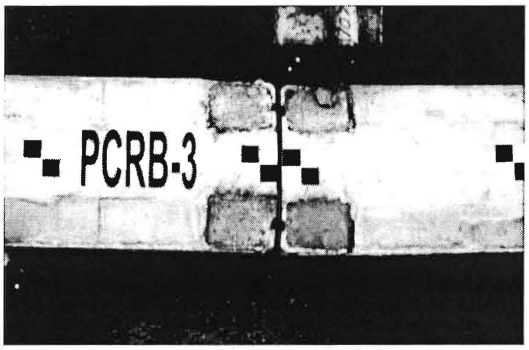

0.004 sec

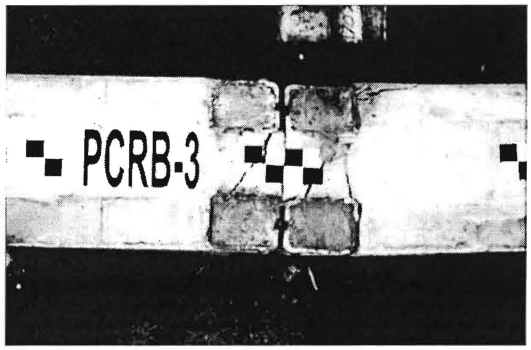

0.028 sec

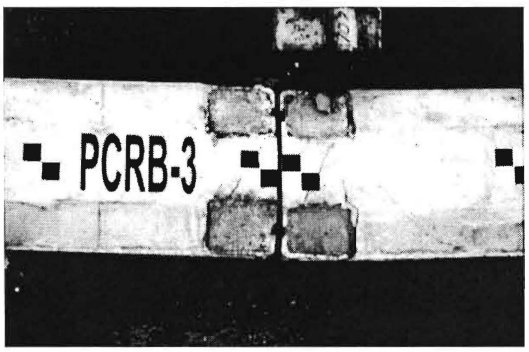

0.006 sec

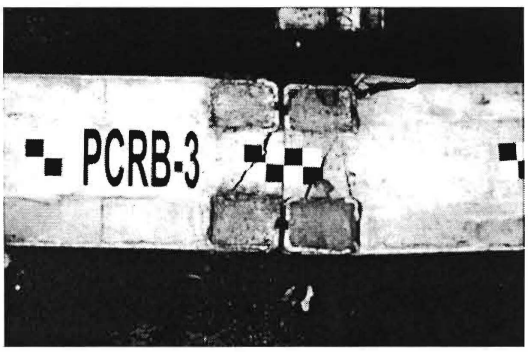

0.042 sec

Figure 147. Sequential Photographs, Test No. PCRB-3

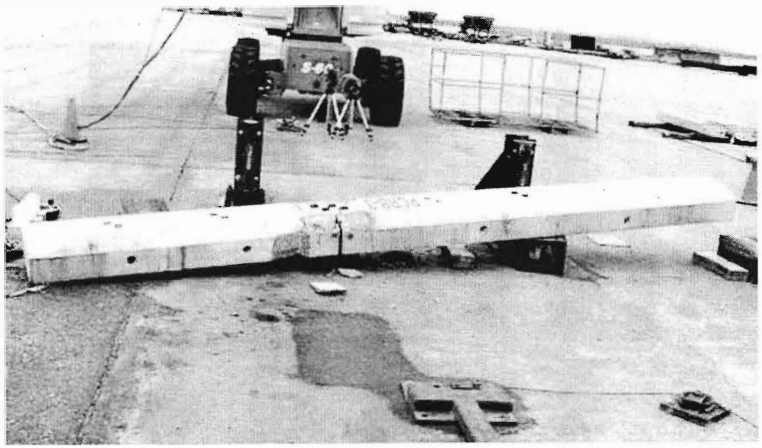

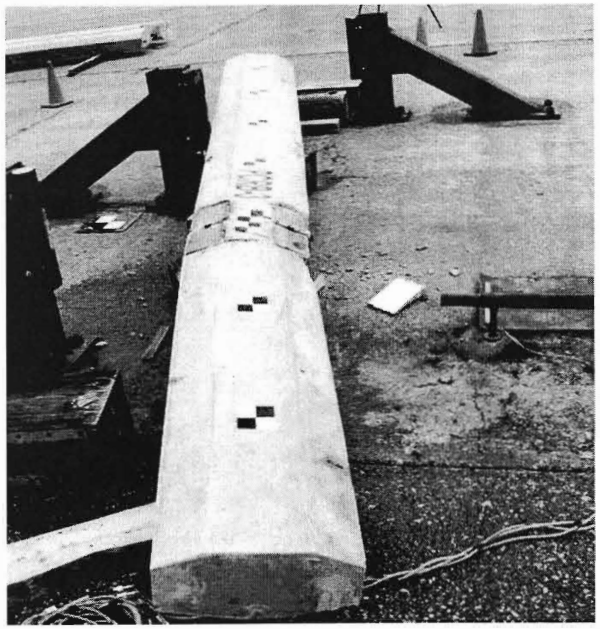

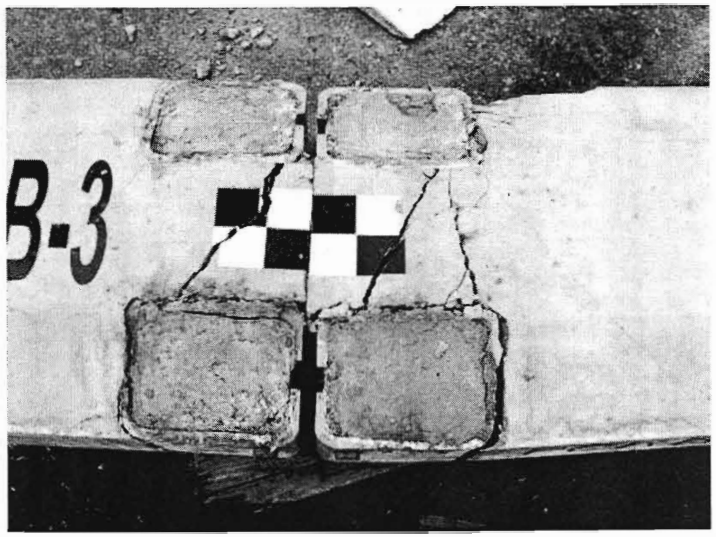

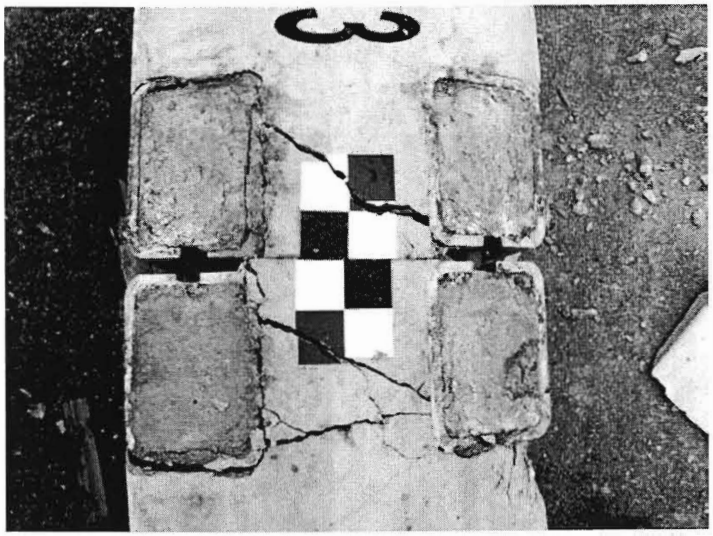

Figure 148. Component Damage, Test No. PCRB-3

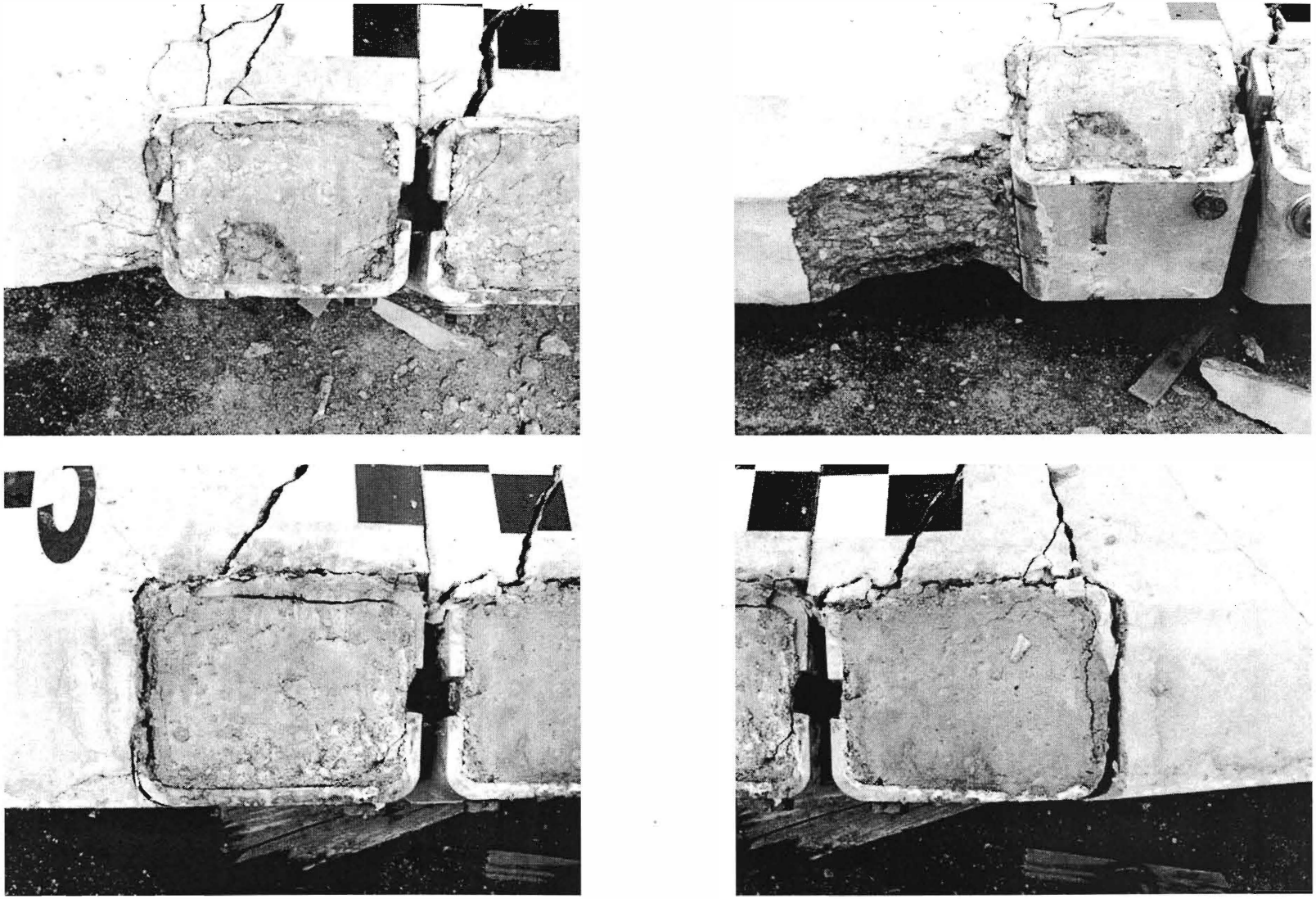

Figure 149. Component Damage – Steel Pockets, Test No. PCRB-3

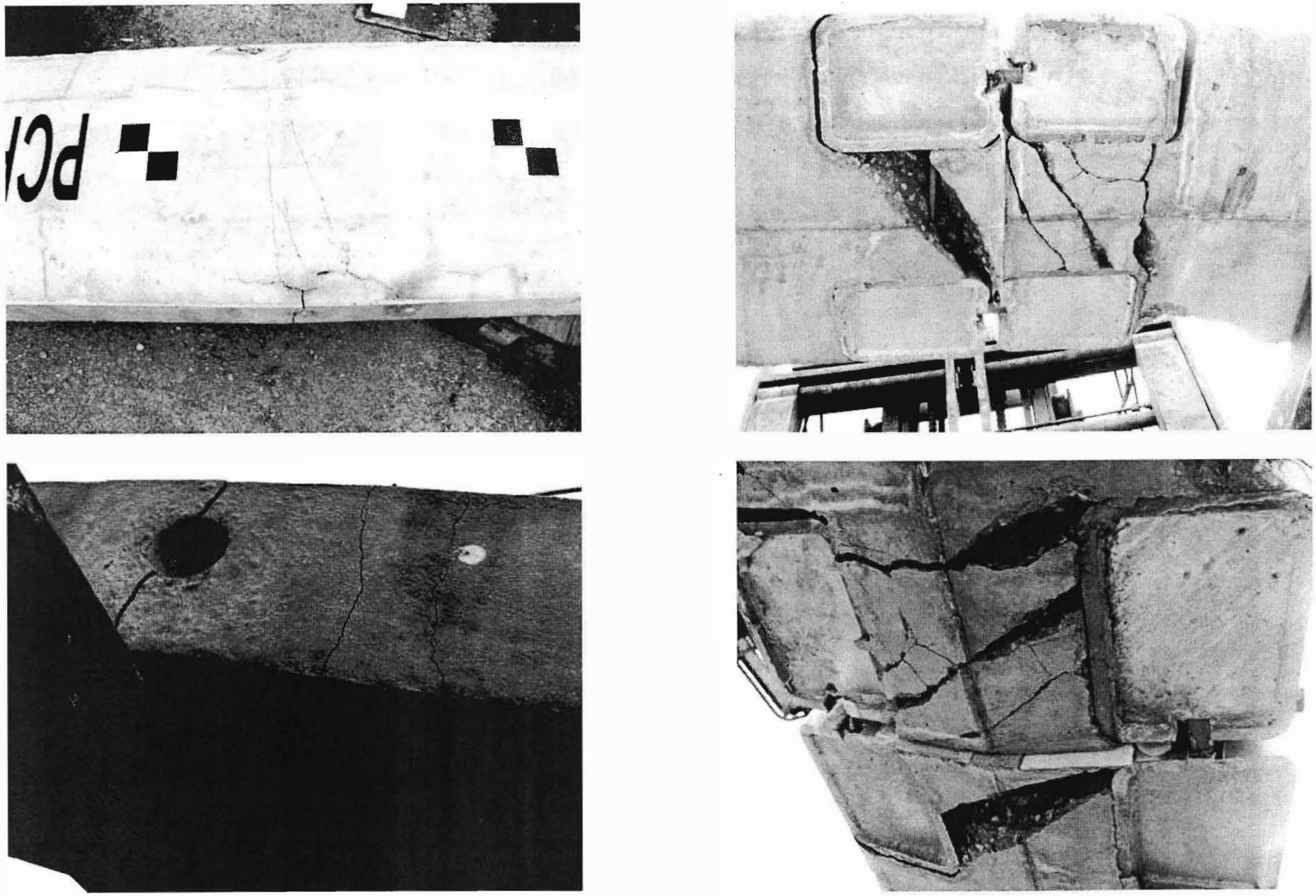

Figure 150. Rail Tension Cracks and Damage to Bottom of Joint, Test No. PCRB-3

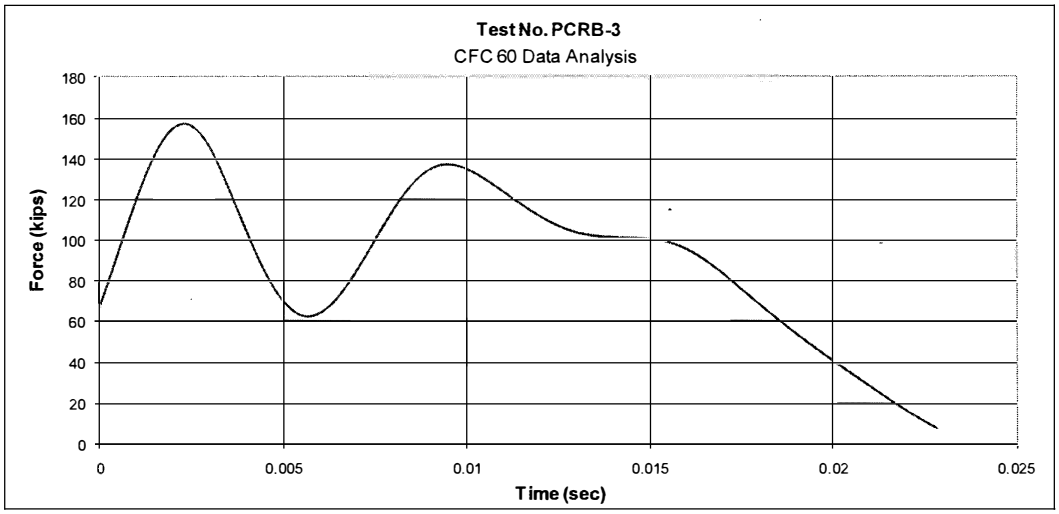

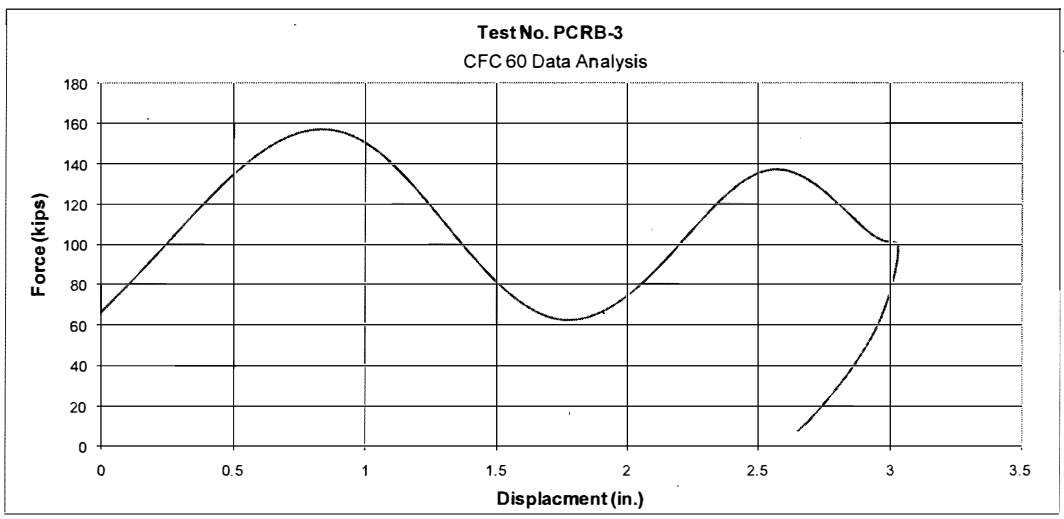

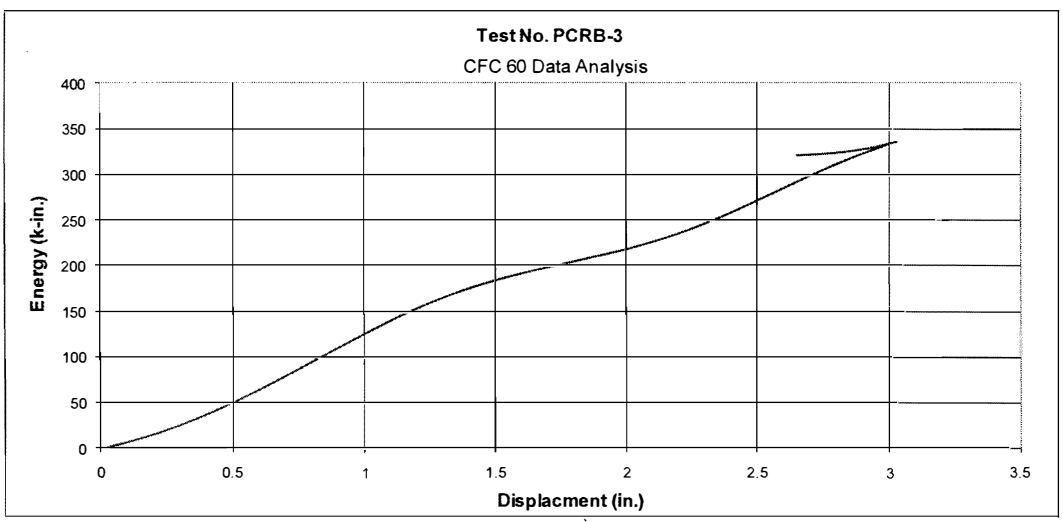

Figure 151. Data Analysis Plots, Test No. PCRB-3

8.5 Bogie Test No. PCRB-4

8.5.1 Test Description

The 1,707-lb (774-kg) bogie vehicle impacted the concrete rail specimen 6 in. (152 mm) from the centerline of the joint at a speed of 23.4 mph (37.7 km/h). At 0.002 seconds after impact, the front steel pocket of the short rail segment had bent inward. A crack developed from the corner of this pocket toward the center of the rail. At 0.004 sec, a crack developed from the corner of the front pocket of the long rail segment to the center of the rail. At this same time, both rail segments were deflecting backward. At 0.006 sec, concrete cracks development stemming from the inside faces of the back steel pockets on both rail segments. At 0.008 sec, a separation crack had developed at the interface between the steel and concrete along the edge of the back pocket in the short rail segment. At this same time, the cracks stemming from the pocket edges in both rail segments continued to grow and widen. At 0.010 sec, cracks developed in the long rail segment near the middle anchor post. Also at this time, a concrete fragment broke free from the bottom surface (as oriented in the test) of the short rail segment adjacent to the back pocket. By 0.014 sec, the cracks in the long rail segment had combined and propagated to form a large crack spanning from the front steel pocket to the middle anchor post. At 0.022 sec, the rail component reached its maximum deflection of 2.4 in. (61 mm). At this same time loose fragments of concrete began to break away from the top surface (as oriented in the test) of the rail around the large crack in the long rail segment. At 0.024 sec, large concrete fragments broke away from the bottom (as oriented in the test) of both rail components underneath the pockets. At 0.046 sec, the bogie vehicle lost contact with the rail component as many concrete fragments broke free from the long rail segment adjacent to the pocket edges. At 0.120 sec, the back shim

plate slipped out of the joint and fell to the ground. Sequential photographs of the impact event are shown in Figures 152 and 153.

8.5.2 Component Damage

Damage to the rail component consisted of bent steel hardware and concrete fracture, as shown in Figure 154. The steel joint hardware remained intact with only minor deformations. Both the front pocket of the short rail segment and the front shear tube connector were bent inward at the impact location, as shown in Figure 155. The shear bolt collar nearest to impact was pinched by the collapsing shear tube and prevented further deformation. In addition, the threaded rebar inside the back pocket of both rail segments were bent slightly inward, matching the curvature of the rail deformation during impact. The curvature also resulted in the back side of the joint opening approximately 1 in. (25 mm) and the back shim plate slipping out. However, if the rail were right side up, the shim would have been resting on the shear tube and would not have fallen to the ground.

Similar to previous test component damage, concrete cracks stemmed from the inside corner of all four steel pockets. On the short rail segment, cracks were found between the steel pockets and a loose concrete fragment was located adjacent to the back pocket, as shown in Figure 154. Also, spalling was located on the front face of the short rail segment adjacent to the front pocket. On the long rail segment, concrete fragments had broken free of the rail from the back edge of the pockets to the middle anchor post. This left the interior steel reinforcement exposed. Finally, large concrete fragments broke off of the bottom (as oriented in the test) of both rail segments exposing the internal steel rebar near the joint, as shown in Figure 156.

8.5.3 Data Analysis

Data from the accelerometers was used to calculate and analyze the loads imparted to the rail component during test no. PCRB-4. Due to unacceptable data from previous tests, the DTS unit was not used for this run. EDR-3 plots depicting force vs. time, force vs. displacement, and energy vs. displacement are shown in Figure 157. Two force spikes were clearly visible from the data. First an inertial spike followed by a resistive spike. Both were well above the design impact load of 62 kips (276 kN). In fact the impact load did not drop below 62 kips (276 kN) until after 0.015 seconds, or the time of maximum deflection and redirection. Maintaining such a high impact load resulted in the rail component absorbing over 370 k-in. (42 kN-m) of energy during the impact event.

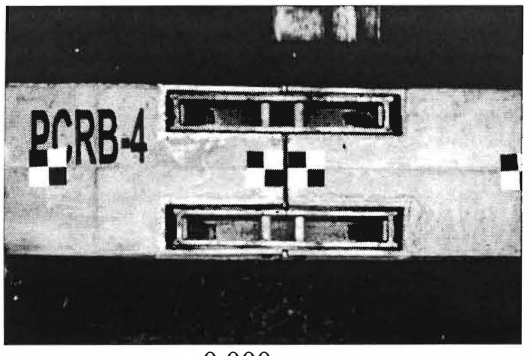

0.000 sec

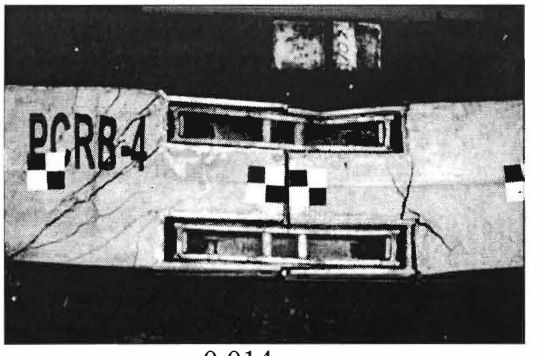

0.014 sec

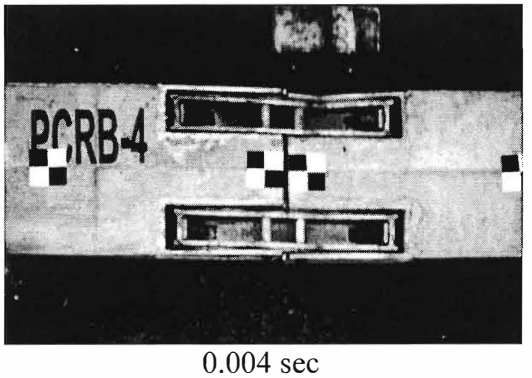

0.004 sec

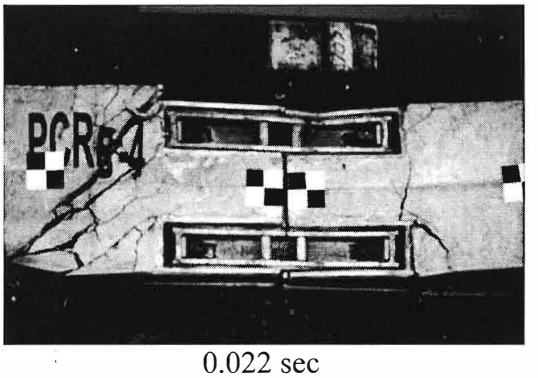

0.022 sec

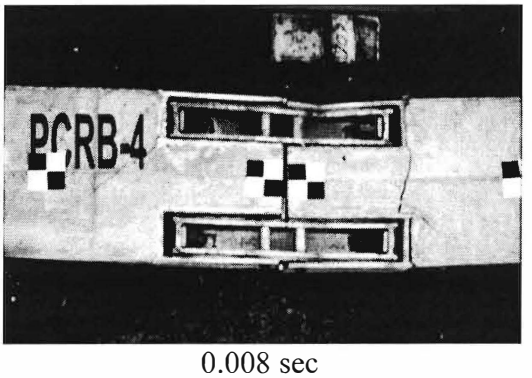

0.008 sec

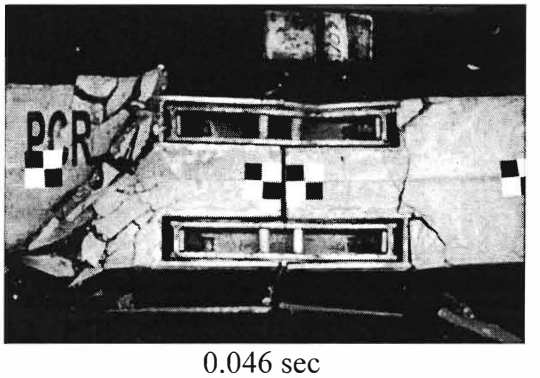

0.046 sec

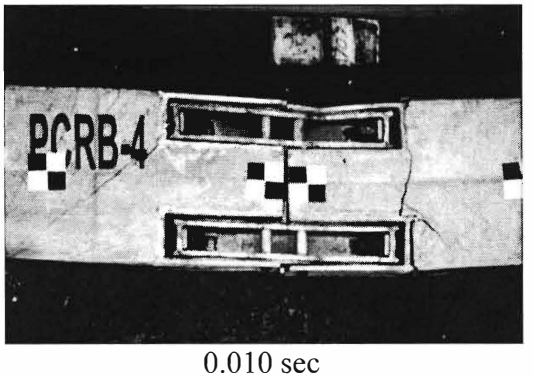

0.010 sec

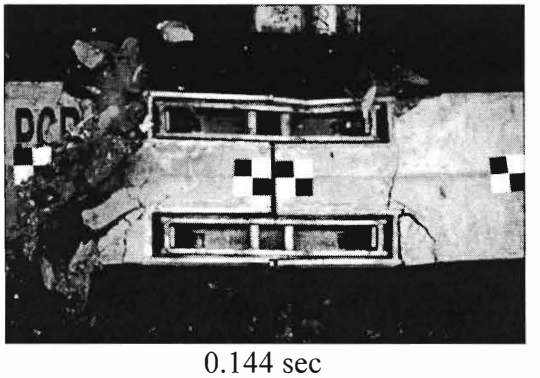

0.144 sec

Figure 152. Sequential Photographs, Test No. PCRB-4

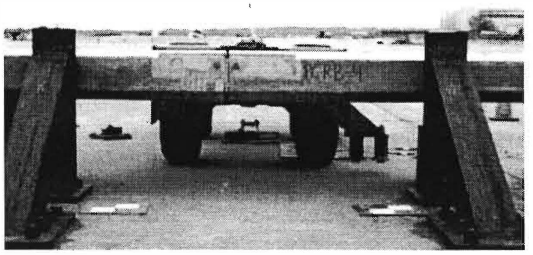
0.000 sec

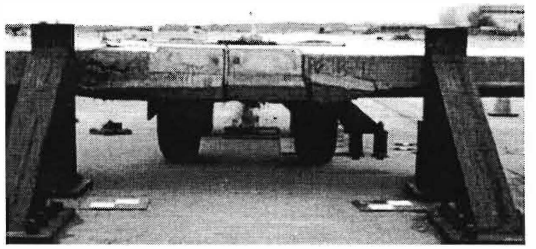
0.024 sec

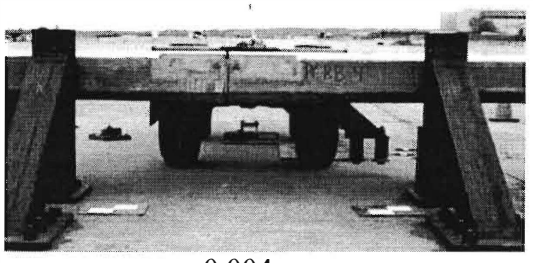
0.004 sec

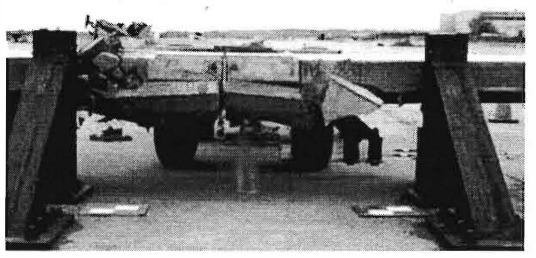
0.064 sec

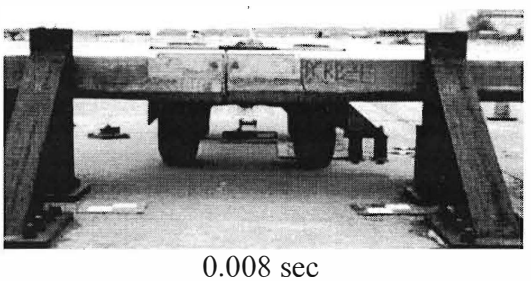
0.008 sec

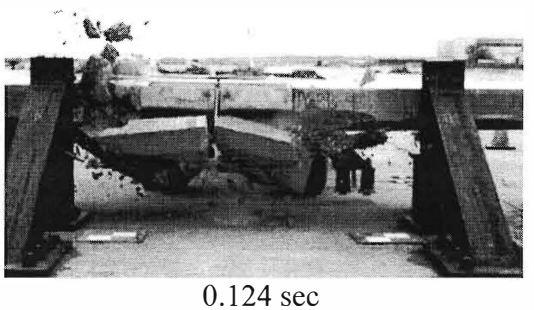
0.124 sec

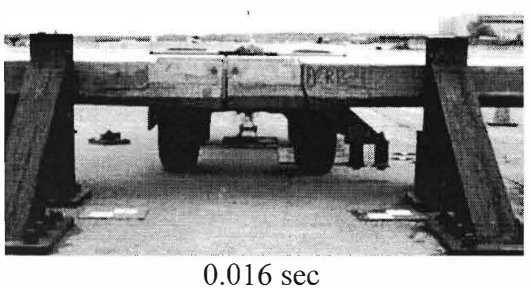
0.016 sec

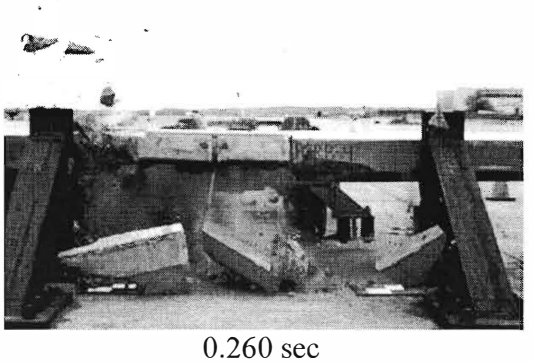
0.260 sec

Figure 153. Additional Sequential Photographs, Test No. PCRB-4

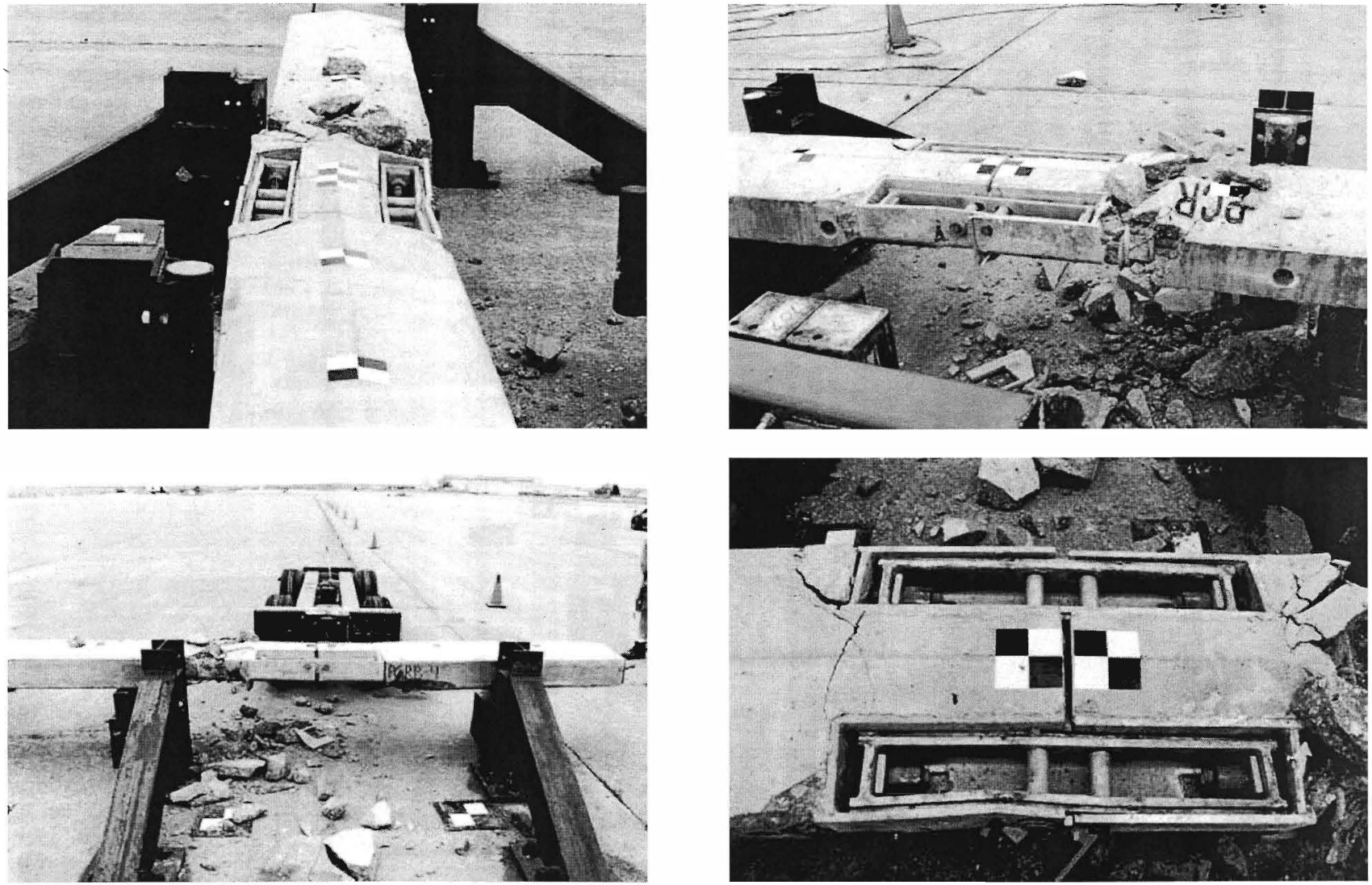

Figure 154. Component Damage, Test No. PCRB-4

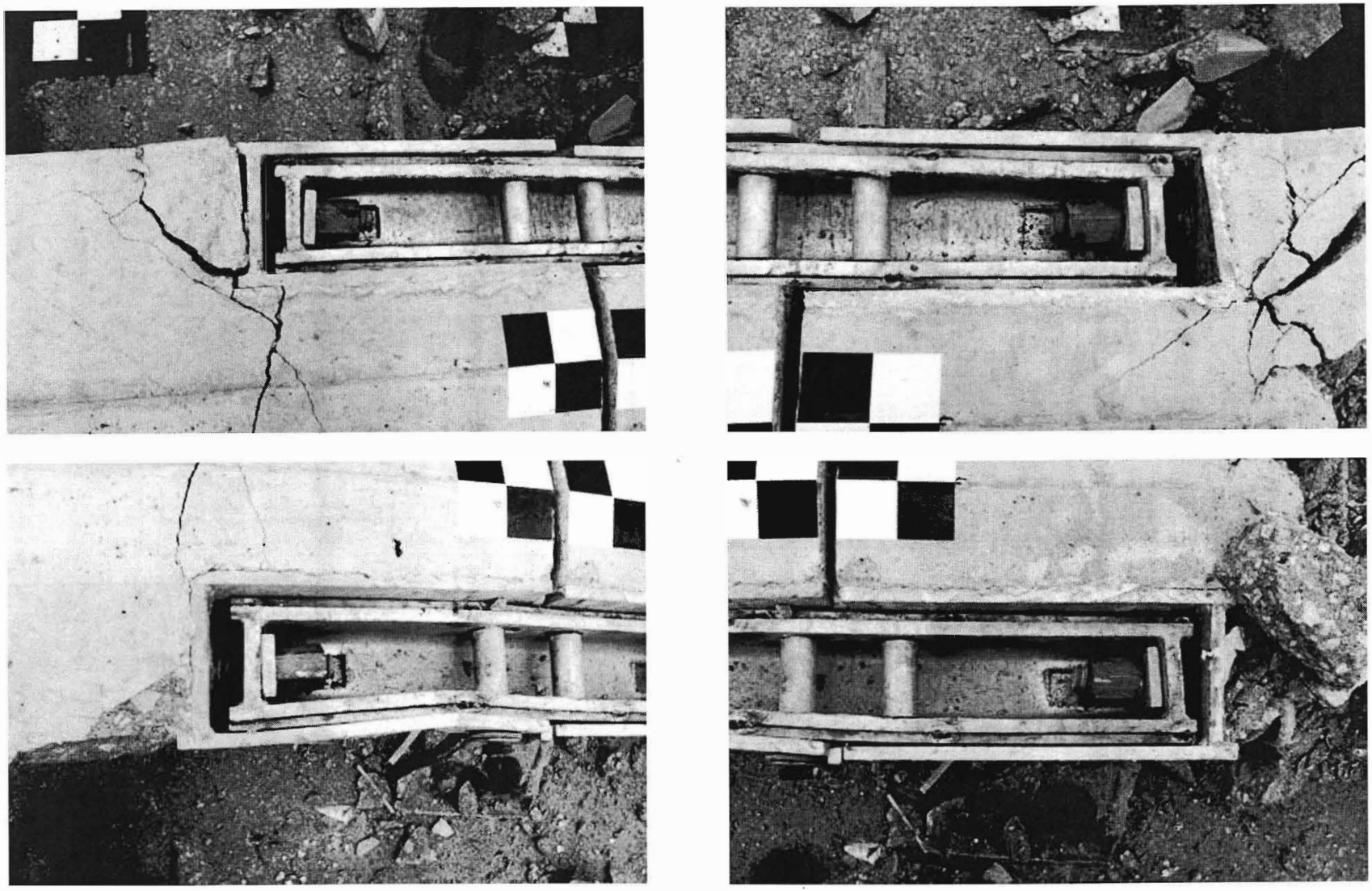

Figure 155. Component Damage – Steel Pockets, Test No. PCRB-4

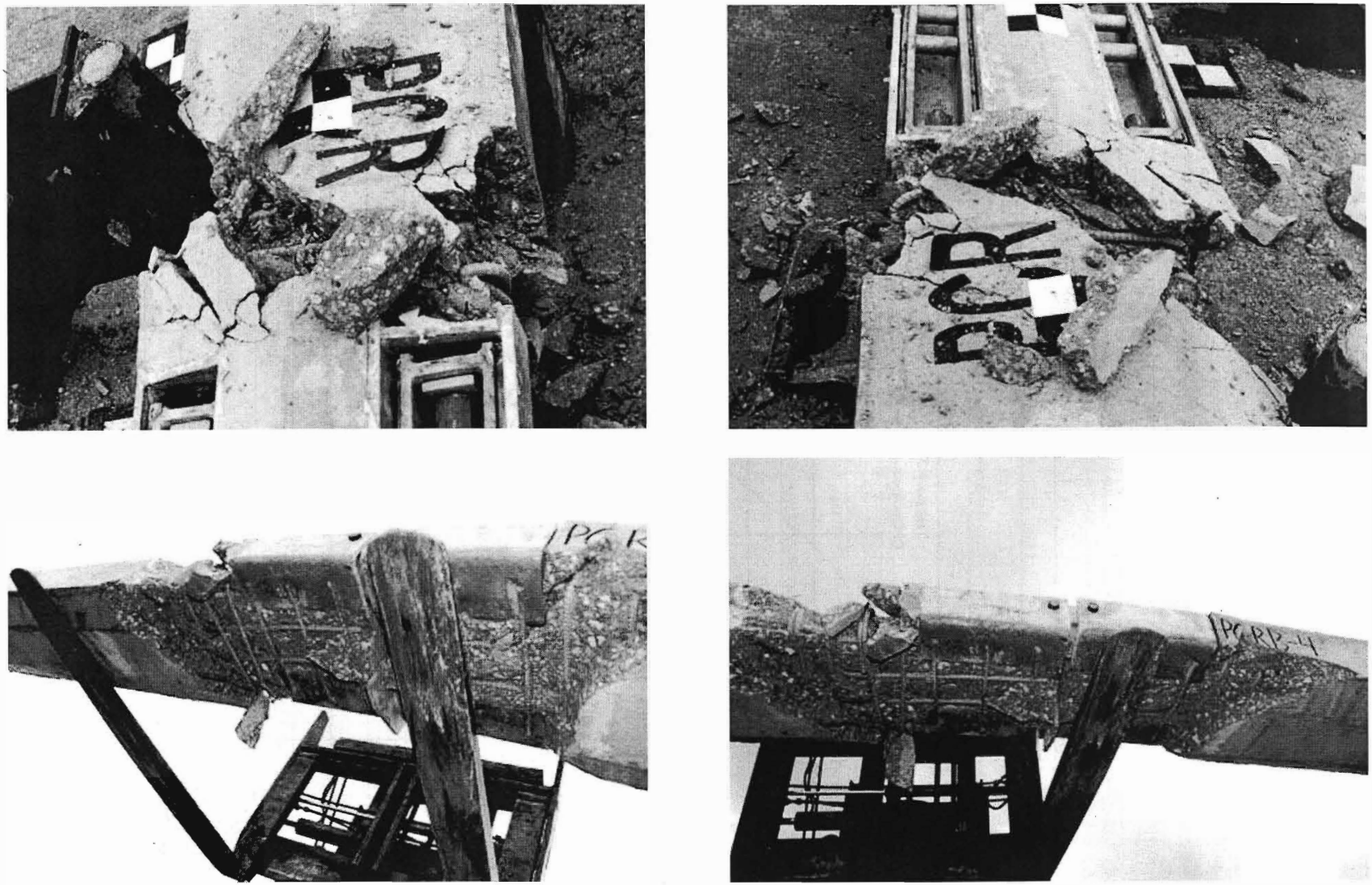

Figure 156. Component Damage – Concrete Damage, Test No. PCRB-4

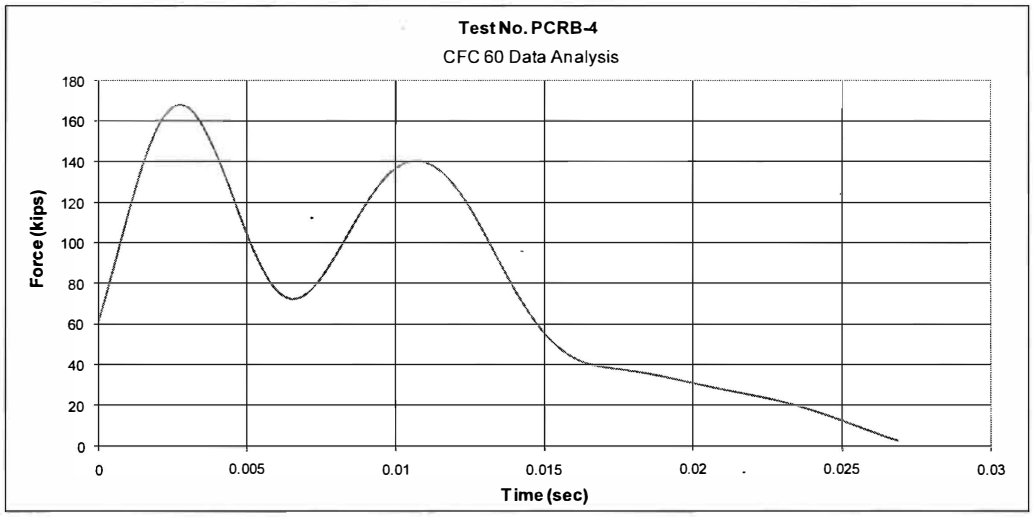

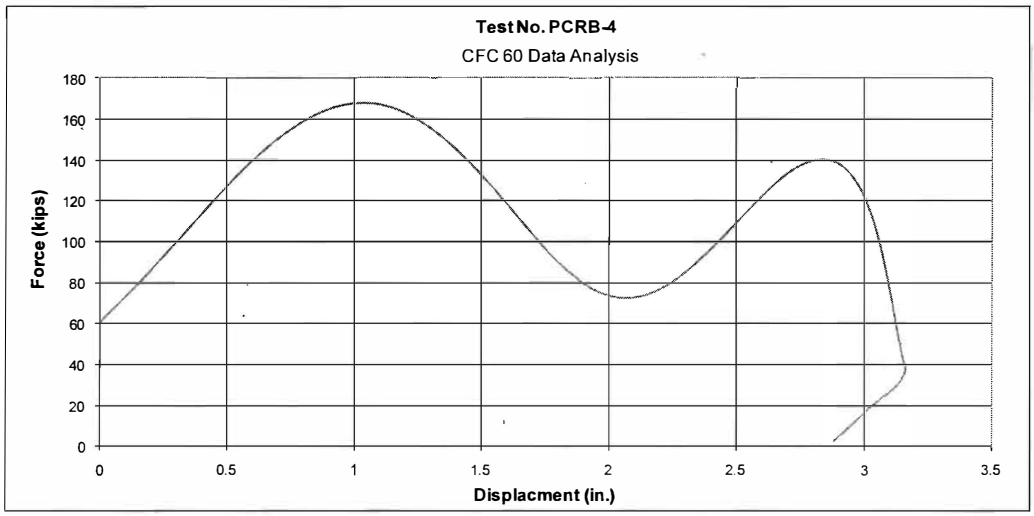

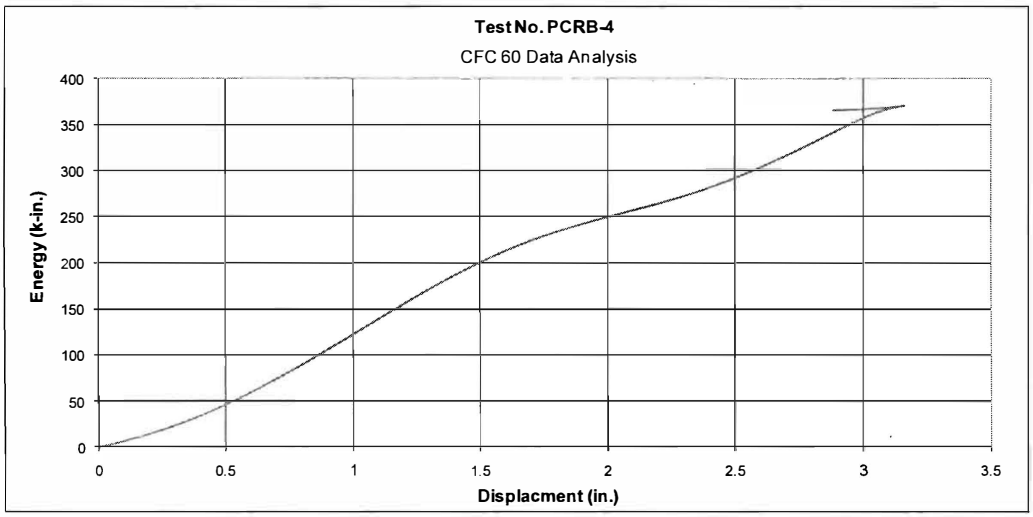

Figure 157. Data Analysis Plots, Test No. PCRB-4

8.6 Bogie Test No. PCRB-5

8.6.1 Test Description

The 1,707-lb (774-kg) bogie vehicle impacted the rail joint specimen 6 in. (152 mm) from the centerline of the joint at a speed of 22.9 mph (36.8 km/h). At 0.002 seconds after impact, two cracks developed in the short rail segment as it deflected back. The first stemmed from the inside corner of the front pocket, while the second originated on the front face near the anchor post. At 0.004 sec, the long rail segment began to deflect. At this same time, a crack formed between the pockets of the short rail segment. At 0.006 sec, tension cracks developed in the long rail segment near the middle anchor post. At this same time, small pieces of grout began to chip away from the front pocket of the short rail segment. At 0.008 sec, the threaded rod connecting the back pockets had fractured. By 0.010 sec, or a deflection of 2.5 in. (64 mm), both threaded rod connectors had fractured. Thus, the joint had failed and the small rail segment was free to rotate about the end anchor post. At 0.018 sec, the right side of the impact head contacted the end of the long rail segment. At 0.020 sec, the impact head lost contact with the short rail segment which continued to rotate about the end anchor post. At 0.028 sec, the cracks near the middle of the long rail segment were expanding as the rail continued to deflect backward. Also at this time, the back face of the long rail segment began to spall near the middle anchor post. At 0.040 sec, the long rail segment reached a maximum deflection of 2.1 in. (56 mm). The bogie vehicle had traveled 6.5 in. (165 mm) into the system. Both the long rail segment and the bogie then began to redirect into the opposite direction. At 0.066 sec, the long rail segment lost contact with the bogie vehicle. Meanwhile, the short rail segment continued to rotate freely about the end anchor post. At 0.224 sec, the free end of the short rail segment contacted the bogie vehicle stopping the rotational movement. The segment came to rest laying perpendicular to its original

position approximately 2 ft (0.6 m) in front of the end anchor post. Sequential photographs of the impact event are shown in Figures 158 and 159.

8.6.2 Component Damage

The joint for bogie test no PCRB-5 failed during the impact event. This caused the two rail segments to separate. As a result, the short rail segment ended up laying on the ground, perpendicular to its original position, as shown in Figure 160. The long rail segment remained atop the wooden support blocks, but had rotated slightly away from the anchor posts. Analysis of the threaded rods fracture patterns, as shown in Figure 162, revealed that the front threaded rod failed in shear, while the back threaded rod failed from a combination of tension and shear. Then combination tension and shear failure of the back threaded from was evidenced by the 45-degree fracture plane and the bending in the rod.

Damage to the short rail segment was minimal, as shown in Figure 161. A few concrete cracks were found in the middle of the segment near the original position of the anchor post, and another concrete crack was found spanning between the steel pockets. Also, contact marks on the short rail segment were located at the impact point and along the back face where the segment contacted the anchor post assembly while rotating.

Damage to the long rail segment consisted mainly of bending cracks and concrete spalling, as shown in Figures 160 and 162. This damage was the result of the long rail segment absorbing all of the impact energy from the bogie after the joint failed. The concrete cracks spanned from the middle anchor post to the front face of the rail. Small fragments of concrete had broken off of the rail where the cracks met the front face of the segment. Concrete spalling was found on the back face of the segment around the middle anchor post bearing location. This

spalling region measured approximately 18 in. (457 mm) wide and was as deep as 2 in. (51 mm) in the most severe areas.

8.6.3 Data Analysis

Data from the accelerometers was used to calculate and analyze the loads imparted to the rail component during test no. PCRB-5. The data collected by the DTS was unusable. EDR-3 plots depicting force vs. time, force vs. displacement, and energy vs. displacement are shown in Figure 163. The initial force spike was above the design impact load of 62 kips (276 kN). However, the majority of this spike was attributed to inertial forces. Subsequently, the force curve quickly fell below 50 kips (222 kN). As the time the impact force returned to near design levels at approximately 0.070 seconds, the joint fractured. The rail segments examined in test no. PCRB-5 were only able to absorb 208 k-in. (23.5 kN-m) of energy as a result of the premature fracture of the joint.

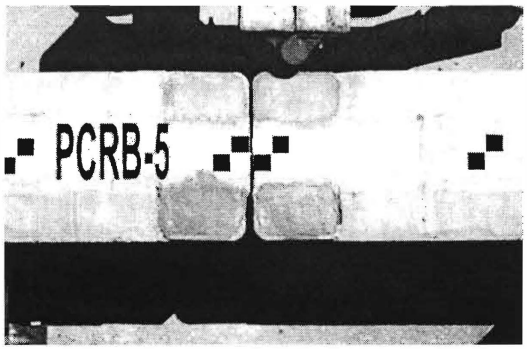

0.000 sec

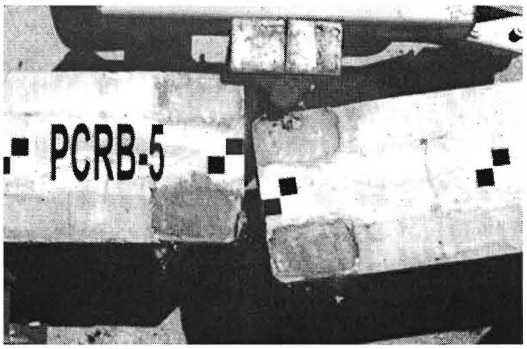

0.020 sec

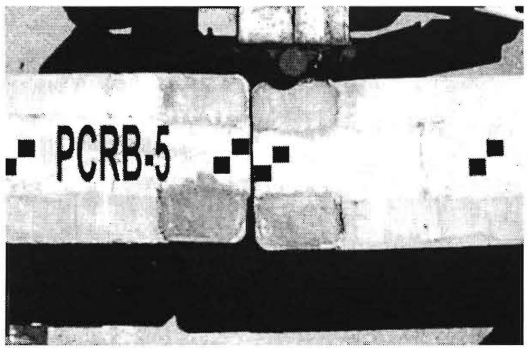

0.004 sec

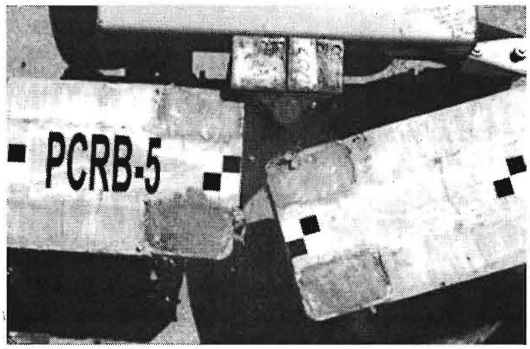

0.040 sec

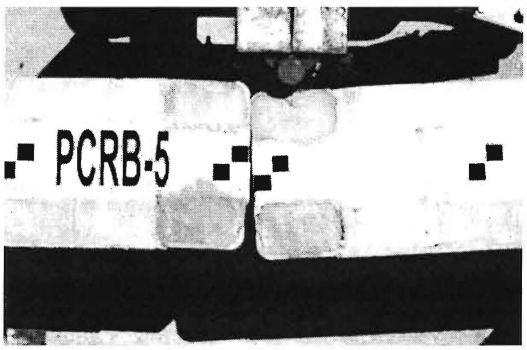

0.008 sec

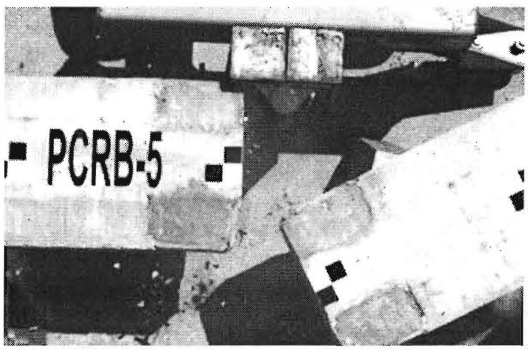

0.064 sec

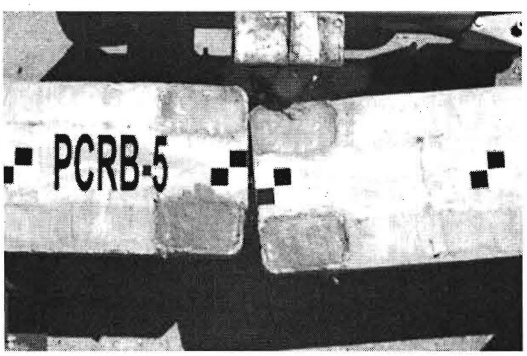

0.012 sec

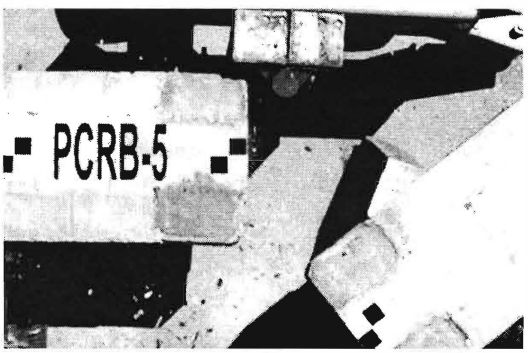

0.094 sec

Figure 158. Sequential Photographs, Test No. PCRB-5

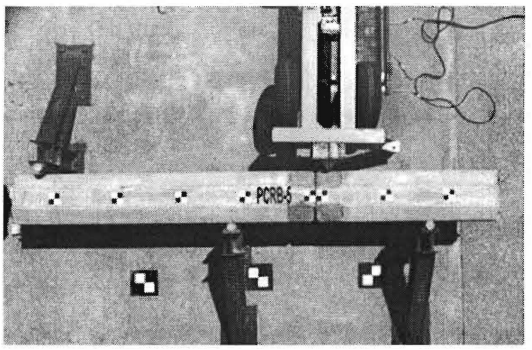

0.000 sec

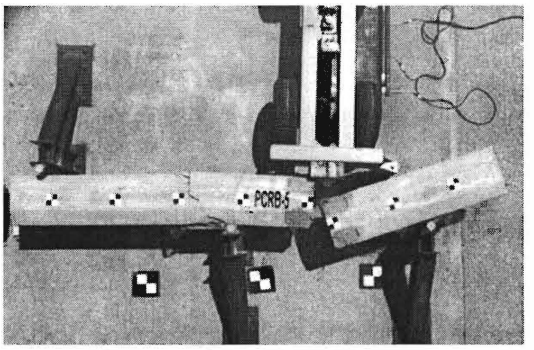

0.044 sec

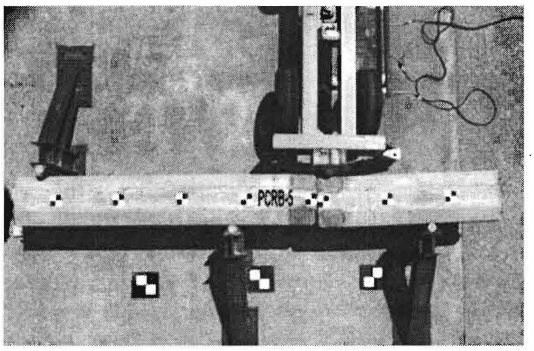

0.006 sec

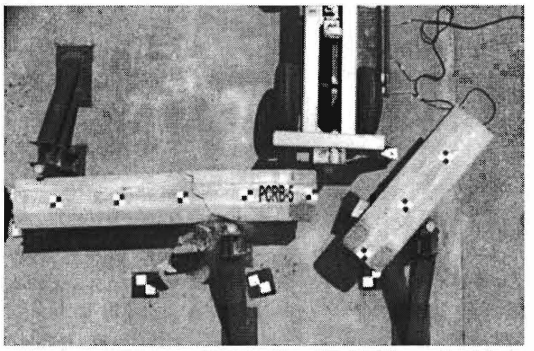

0.124 sec

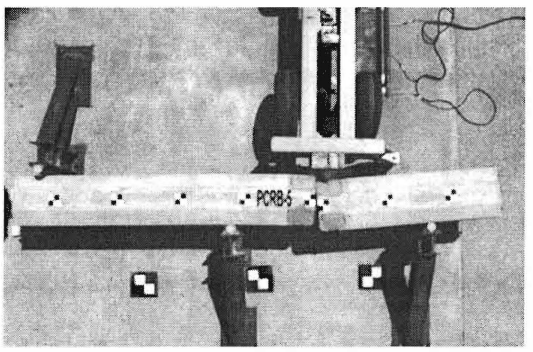

0.012 sec

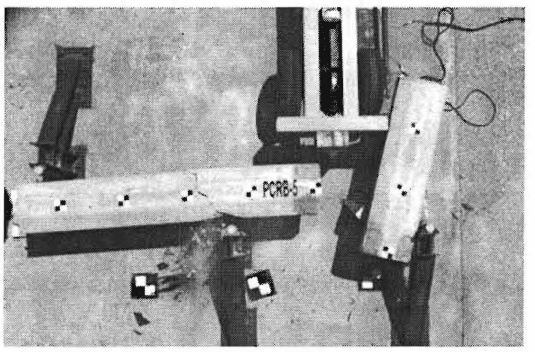

0.224 sec

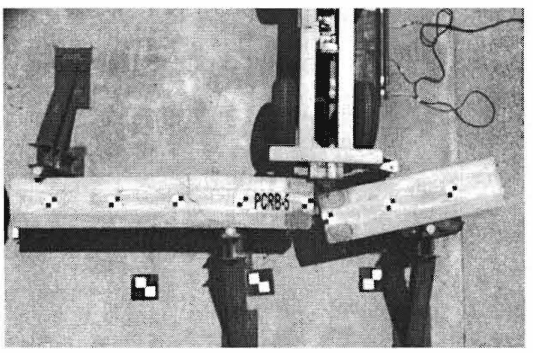

0.030 sec

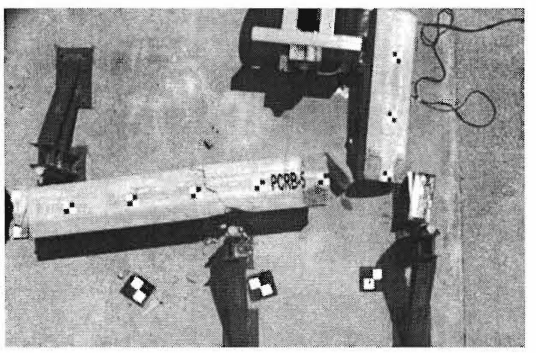

0.728 sec

Figure 159. Additional Sequential Photographs, Test No. PCRB-5

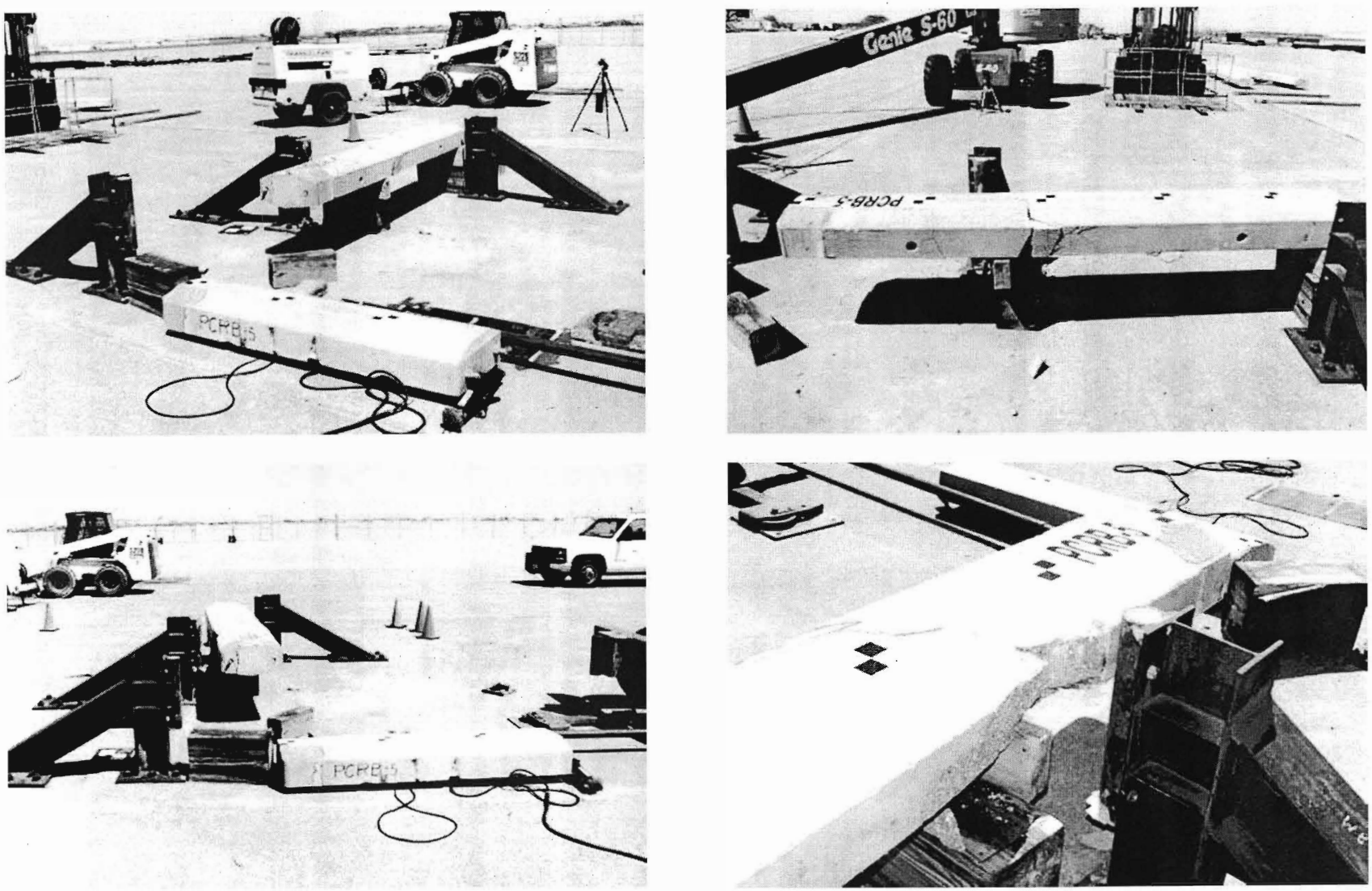

Figure 160. Component Damage, Test No. PCRB-5

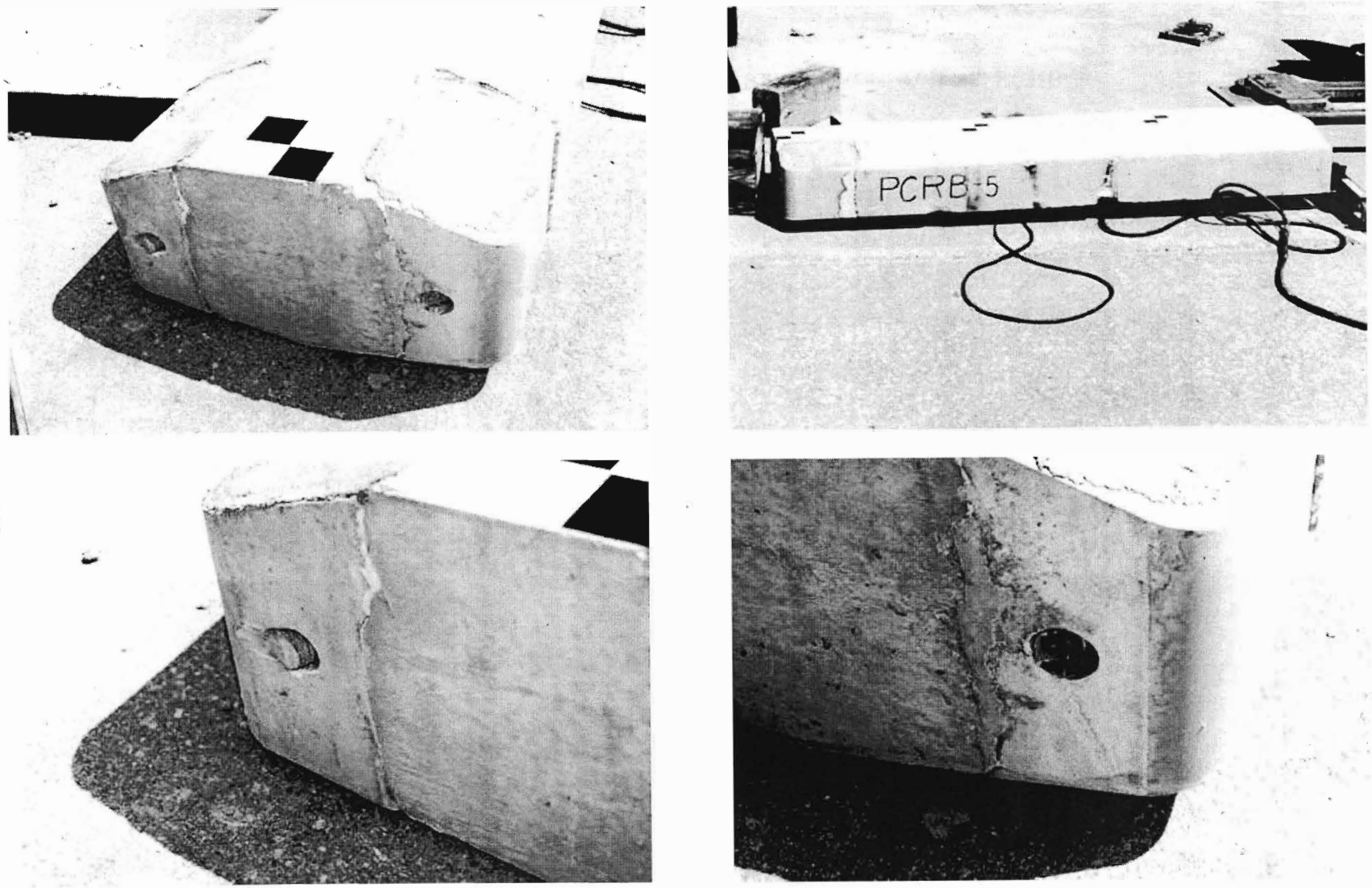

Figure 161. Component Damage – Short Rail Segment, Test No. PCRB-5

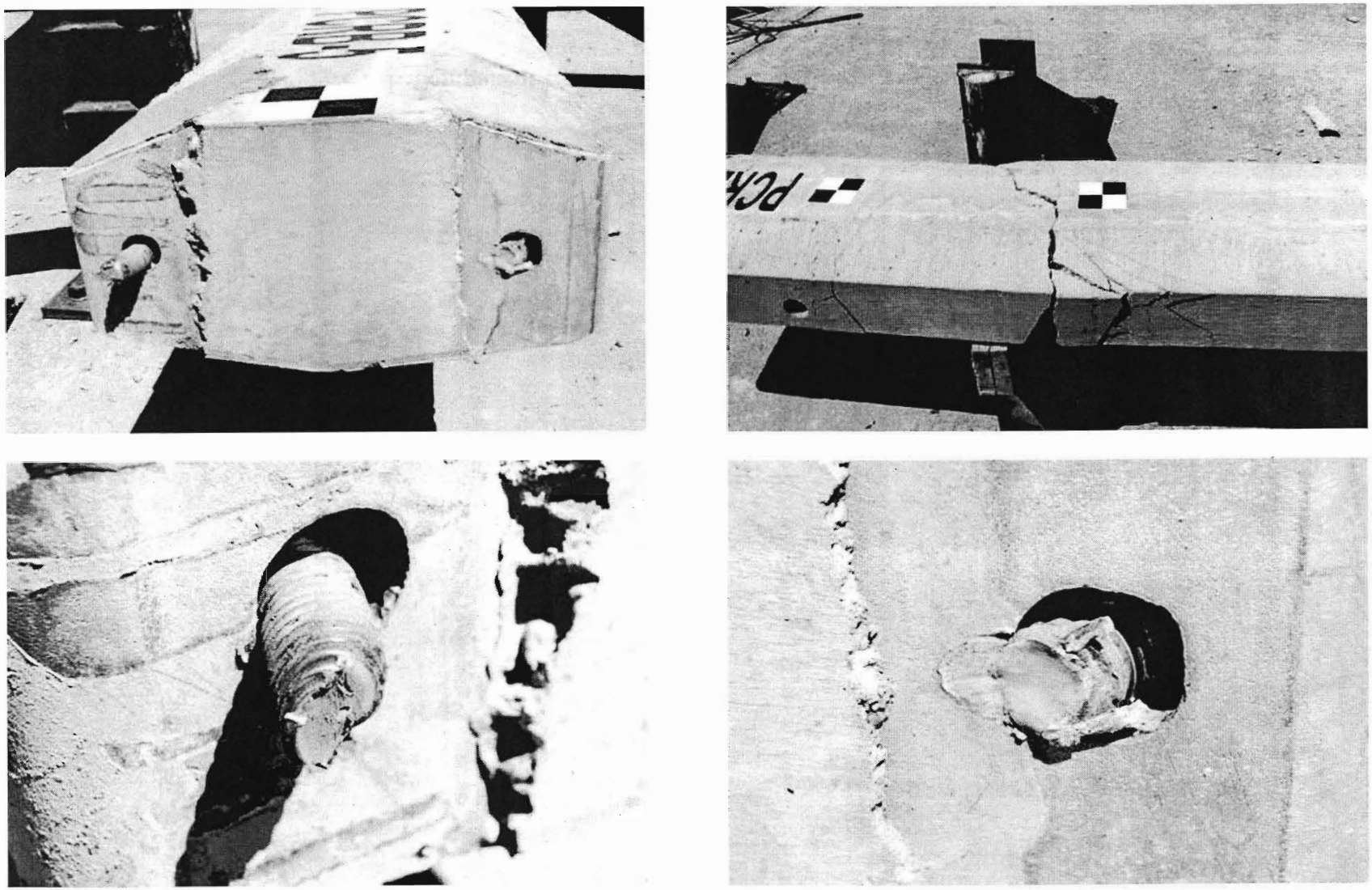

Figure 162. Component Damage – Long Rail Segment, Test No. PCRB-5

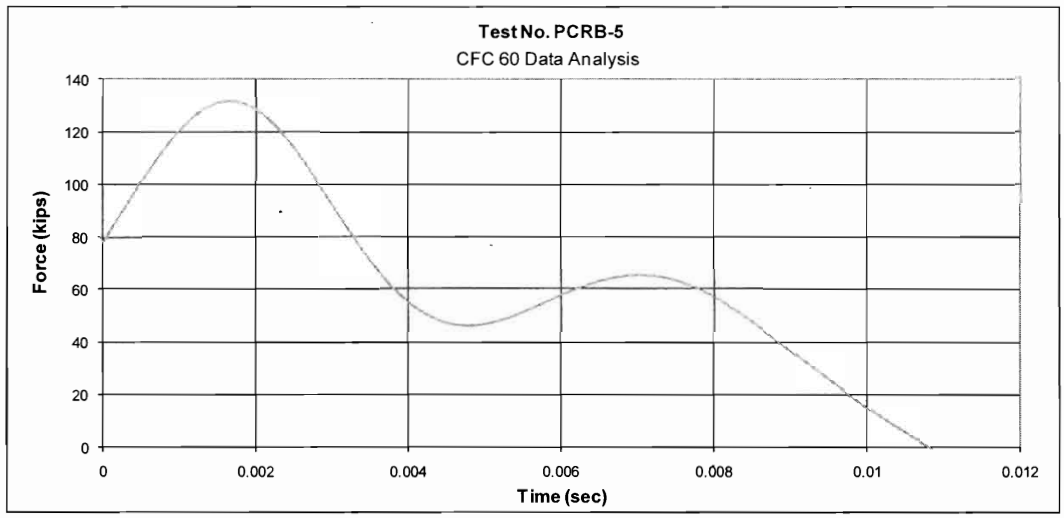

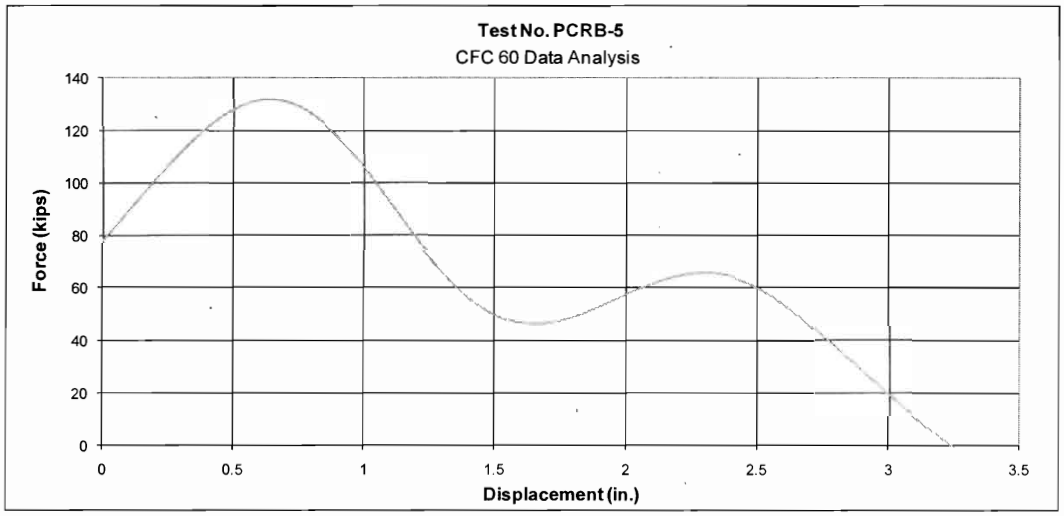

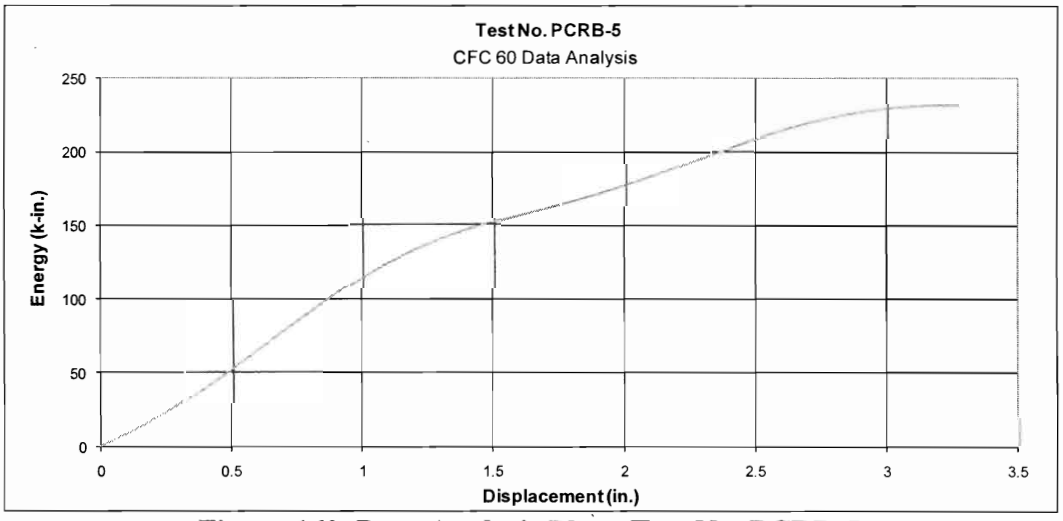

Figure 163. Data Analysis Plots, Test No. PCRB-5

8.7 Round 2 –Bogie Testing Discussion

Of the three rail-to-rail joint designs examined during the second round of bogie testing, the grouted joint which utilized I-shaped connectors (test no. PCRB-3) performed the best. Recall from Section 6.2, an impact force of 62 kips (276 kN) would result in design shear and moment loads through the joint of 35 kips (156 kN) and 700 k-in (79 kN-m), respectively. As shown in Figures 164 and 165, the grouted joint from test no. PCRB-3 met and exceeded these design loads. In fact, the joint upheld an average load of approximately 100 kips (445 kN) through the duration of the impact event. Also, this joint sustained only minimal damage from the impact, while the other joints were more severely damaged. The refinements made to the grouted joint after the first round of bogie testing proved to effectively strengthen the joint. All of the pockets remained intact without any prying or disengagement from the rail segments. Concrete cracking and spalling was minimal and was mostly limited to the area between the grout pockets. Only small pieces of concrete broke free from the bottom of the rail.

A negative aspect of the grouted joint examined in test no. PCRB-3 was that it was not easily disassembled. After the bogie test was complete, the segments were taken apart as though one segment was damaged and needed to be replaced. The shear bolts were removed easily with the use of a socket wrench, but the grout had to be chiseled out of the pockets before the I-shape connectors could be removed. Even with the use of a pneumatic chisel, it took some effort to chisel out the grout around the gusset plates on the front corners, the connecter, and threaded rebar anchored to the back of each pocket. It should be noted that the pneumatic chisel did not appear to cause damage to the beam or connection components during disassembly. Fortunately, only the grout pockets on the "undamaged" segment need to be chiseled. The damaged segment was lifted and removed with the I-shape connectors still attached. New I-shape connectors and

grout would be necessary to recreate the joint after a new segment had replaced the damaged one.

The load sustained by the dry joint in test no. PCRB-4 was very comparable to that of the grouted joint in test no. PCRB-3, as shown in Figures 164 and 165. The dry joint sustained a load that averaged over 100 kips (445 kN) and never dropped below 70 kips (312 kN) throughout the duration of the impact event. For this reason, the dry joint absorbed slightly more energy than the grouted joint. The refinements made to the joint after the first round of bogie testing improved both the initial stiffness and strength of the joint. The shear tubes transferred load almost immediately across the joint and prevented the rails from moving independent of each other at the onset of impact. Also, none of the joint hardware or the rail reinforcing steel failed during the test. However, the specimen in test no. PCRB-4 suffered much more damage than did the specimen in test no. PCRB-3. There was more concrete cracking and spalling. The largest concern, though, was the amount of concrete that broke free from the top of the rail (bottom as oriented in the test). This concrete could potentially that could fall onto another roadway below the bridge. The majority of the concrete above the top of the pockets had broken away during the test. The additional no. 3 bars spanning across the top of the pockets was only able to contain the concrete directly between the pockets.

Similar to the previous test specimen, the segments connected by the dry joint were taken apart after the bogie test was complete. Socket wrenches were used to remove the shear bolts as well as the nuts fastened to the longitudinal threaded bars. The loose washers and shim plates were removed by hand and a hammer was used to knock the shear tube connectors loose of the constricted pockets. As expected, disassembling the dry joint proved to be much easier and quicker than taking apart the grouted joint from test no. PCRB-3.

The alternative grouted joint evaluated in test no. PCRB-5 proved to be too weak to transfer the design load between rail segments. The threaded rods connecting the grout pockets failed at a load just over 60 kips (267 kN). This magnitude of load was only half as strong and had roughly 70 percent of the energy absorbing potential of the other two joints tested during the second round of bogie testing, as shown in Figure 164. Before fracturing, the rail specimen took an initial load spike of 131 kips (583 kN). However, as explained in the first round of bogie tests, the majority of the initial force spike was the result of inertia. After this inertial spike, the joint sustained an average load of only 55 kips (245 kN). Also, since the threaded rod connectors fractured so quickly, the joint in test no. PCRB-5 lacked a desired amount of ductility. In fact, the lack of damage, or even cracking, to the concrete rail segments themselves showed that the joint failed while transferring much lower loads than the previous joints.

After the second round of bogie testing, only the grouted joint design from test no. PCRB-3 satisfied all design criteria and could be implemented into the precast bridge rail design. The dry joint from test no. PCRB-4 illustrated the ability to transfer the design loads between adjacent rail segments. However, the significant amount of concrete that broke free from the rails had the potential to cause problems on the bridge or roadway below. This joint would become a feasible option for precast bridge rails if the concrete above the pockets was better confined. The alternate grout joint from test no. PCRB-5 would require major changes to strengthen and improve ductility before it was a viable option. Thus, it was decided to proceed with the grouted joint design from test no. PCRB-3 while keeping in mind that the dry joint from test no. PCRB-4 could potentially be used if additional confinement steel were added to the joint design.

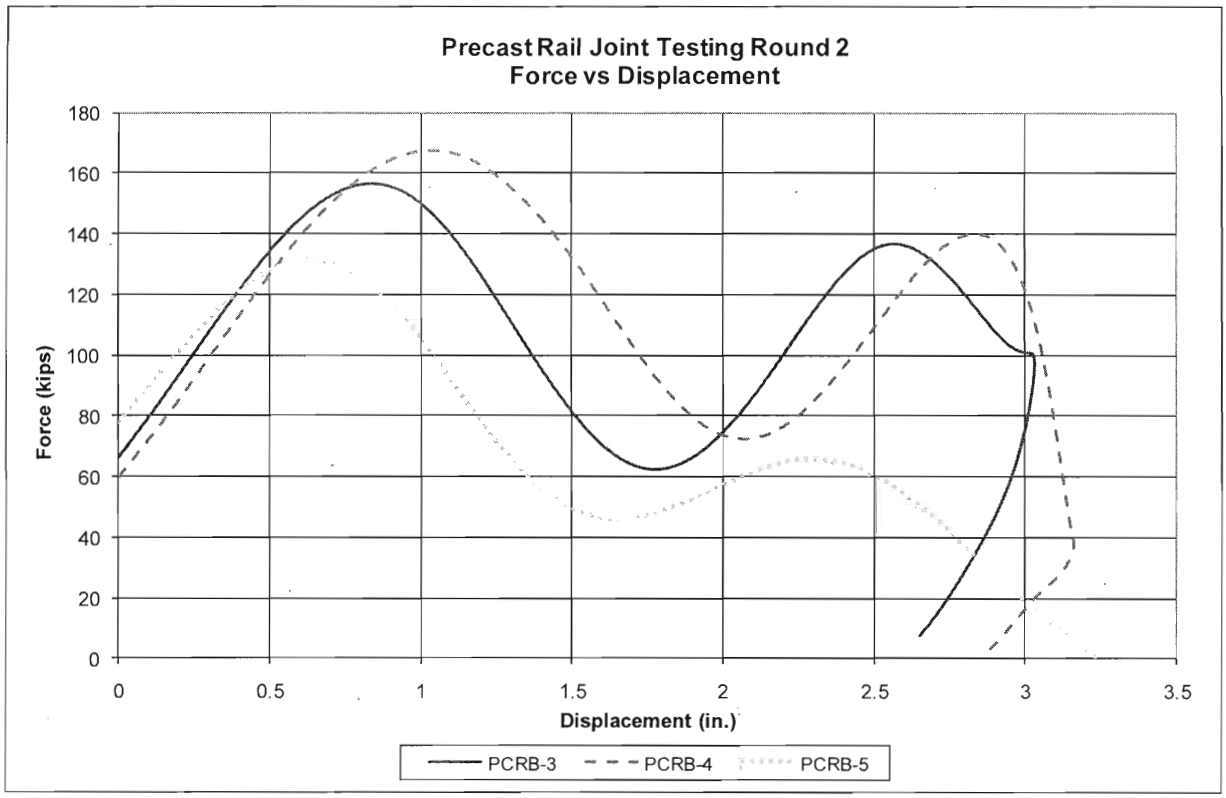

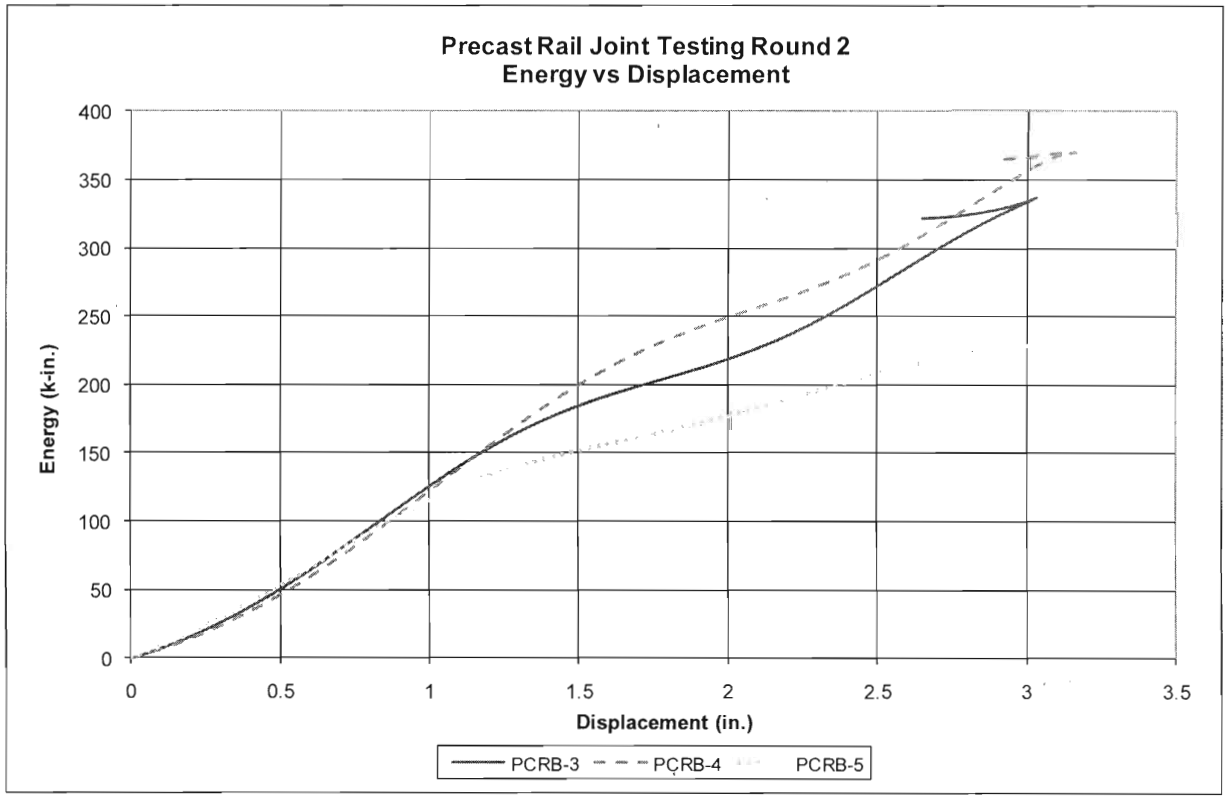

Figure 164. Data Comparison Plots, Round 2 Bogie Testing Results

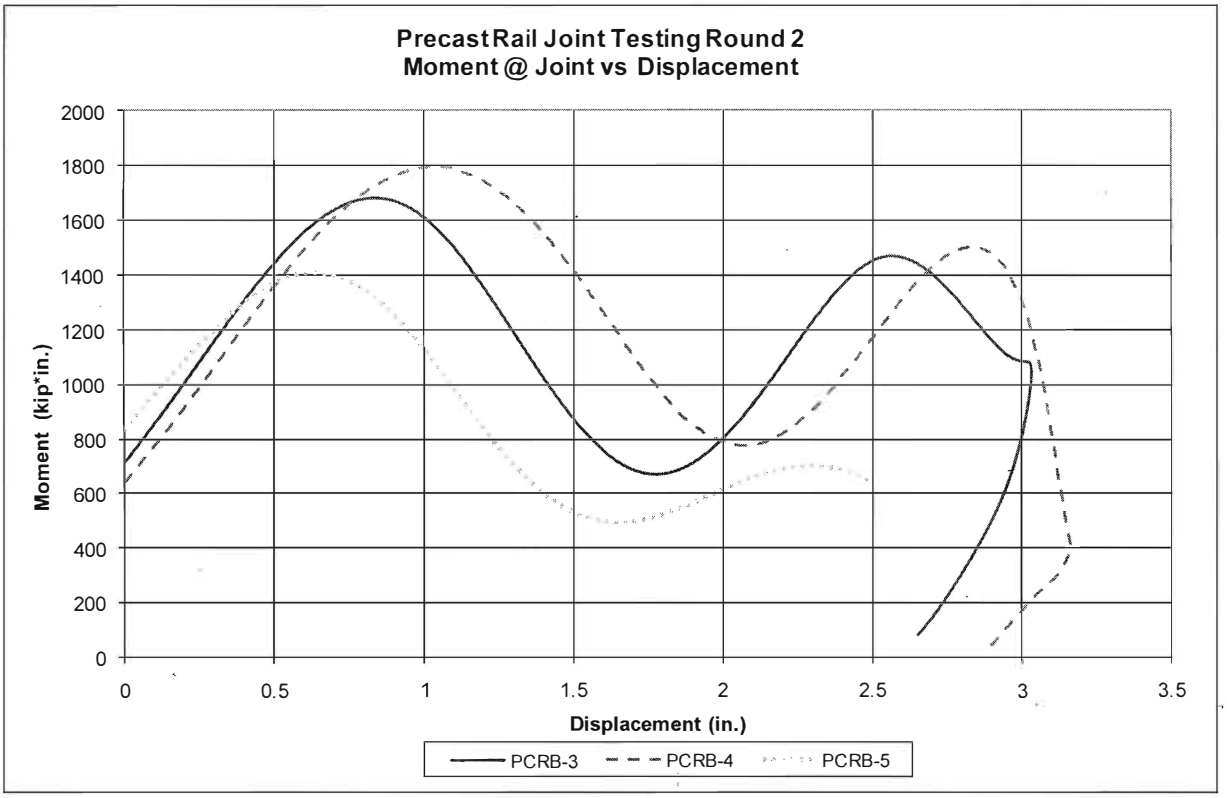

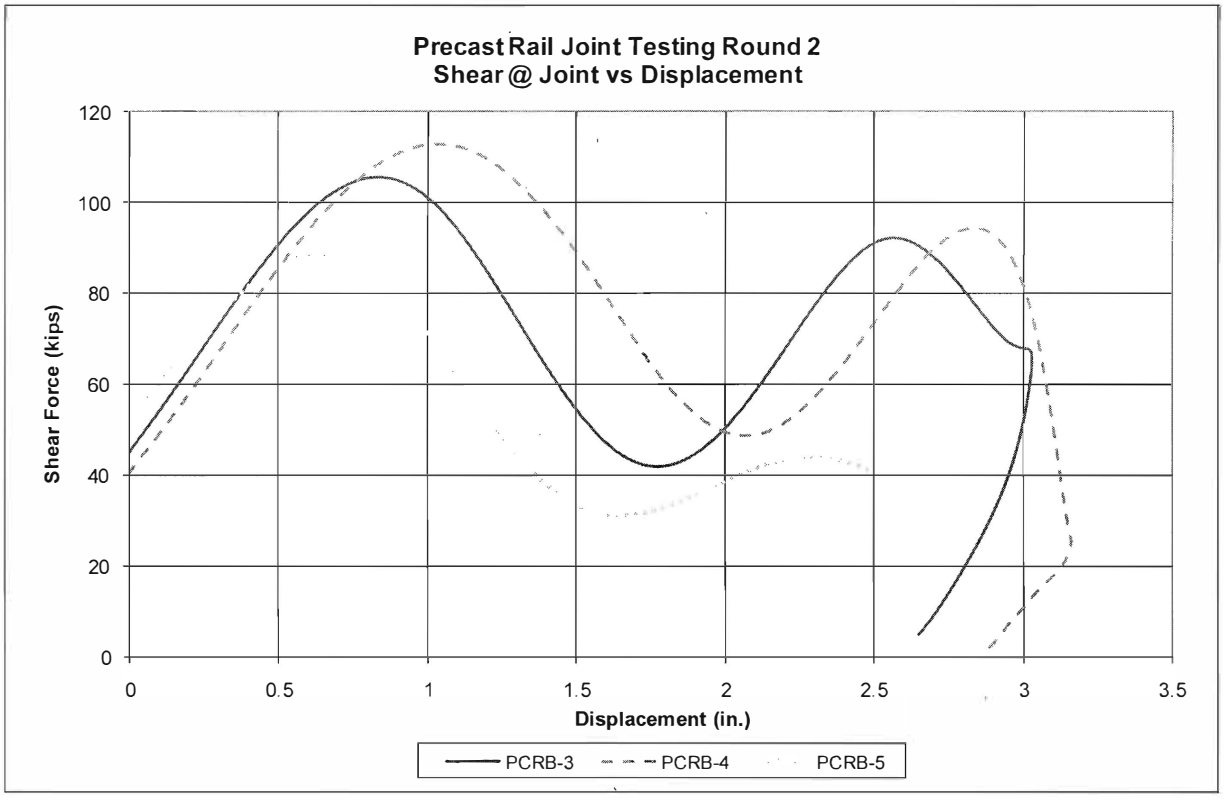

Figure 165. Joint Comparison Plots, Round 2 Bogie Testing Results

9 BARRIER POST TO DECK ATTACHMENT DESIGN

9.1 Overview

The attachment of the precast bridge rail segments to the bridge deck itself was another connection critical to the success of the barrier. It was essential that the anchorage comprising this attachment was capable of transferring both shear and moment loads to the bridge deck without causing structural damage to the deck. Further, the attachment needed to allow tolerances of ½ in. (13 mm) in both longitudinal and lateral directions during assembly. Similar to the rail-to-rail joint design, preserving the symmetry of the bridge rail segments was considered a priority, albeit not a requirement.

Recall from Section 5.2.2, Yield-Line Theory calculations were used to estimate the resistance necessary for the bridge rail to sustain a 100-kip (445-kN) impact load. These calculations led to a design moment load of 800 k-in. (90 kN-m), which each post within the bridge rail system was required to resist. The design shear load for the posts was conservatively selected as 40 kips (178 kN). Thus, it was a prerequisite that the joint utilized to attach each post to the bridge deck had resistances greater than or equal to 800 k-in. (90 kN-m) in bending and 40 kips (178 kN) in shear.

Multiple attachment designs were explored and evaluated for the post-to-deck joint. A number of these designs are presented in the following sections.

9.1.1 Deck Attachment A - Threaded Rods and Shear Tubes

Deck Attachment A consisted of two threaded rods and two shear tubes connecting each barrier post to the bridge deck, as shown in Figure 166. The threaded rods provided resistance to bending and moment loads, while the shear tubes provided resistance to lateral movement and

shear. Deck Attachment A was efficient in that each subcomponent was only required to resist forces in one direction.

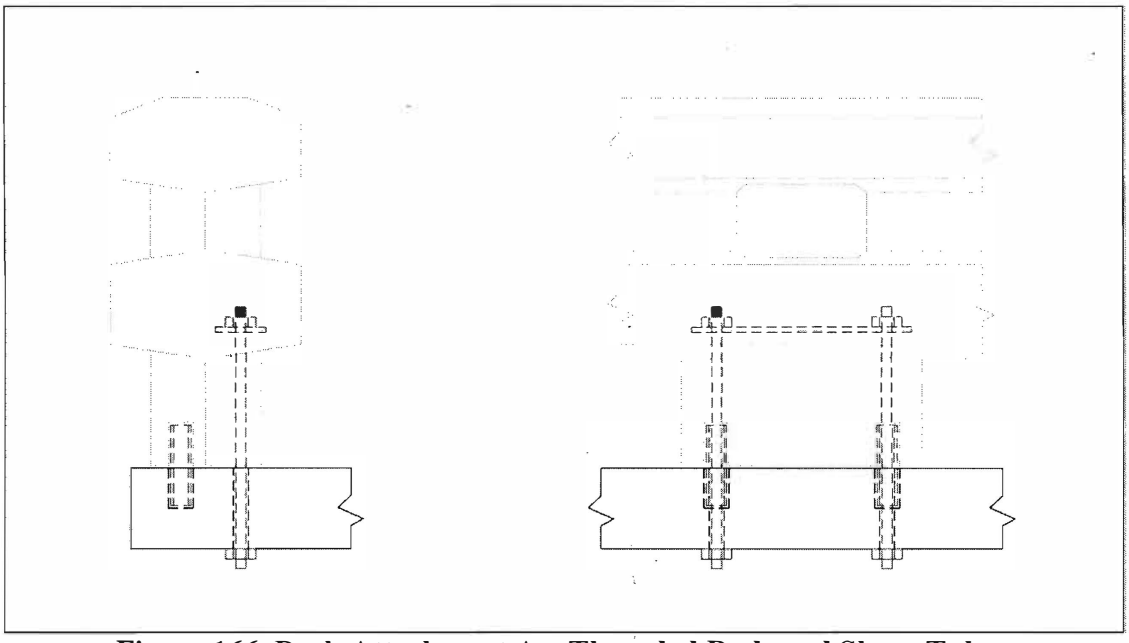

Figure 166. Deck Attachment A – Threaded Rods and Shear Tubes

The threaded rods were located near the front corners of each post and were partially embedded in the rail and post of the barrier segment during casting. The rods extended up through the post and into the lower rail of the barrier where a single washer plate and nuts were used to secure the rods inside the barrier segment. The washer plate and nuts were necessary to anchor the rods because the proper development length of the threaded rods could not be obtained within the geometry of the post. The opposite ends of the rods which protruded from the bottom of the bridge rail posts would extend through holes in the bridge deck and fasten to nuts on the bottom of the deck. Casting the rods inside the rail segment reduced the amount of hardware needed for installation as only nuts and washers were necessary to fasten the rail segments to the bridge deck.

The shear tubes were not embedded into the rail segment. Instead, cavities were cast into the bottom of the rail and the top of the deck. During installation, the shear tubes would first be placed into the cavities of the deck. Then the rail segment would be lowered into place such that the extruding rods passed through the holes in the deck and the exposed upper portion of the shear tube slid into the cavities in the post. Finally, washers and nuts would fasten the rail segment to the deck. Both the holes and the cavities in the bridge deck were oversized to satisfy tolerance issues in both the lateral and longitudinal directions. To ensure the tension rods were not loaded in shear, the holes were further oversized so that the shear tubes would engage first.

A downside to this design was that the rail segments were no longer symmetric. In fact, the threaded rods were specified in the front of rail (traffic side) while the shear tubes were specified in the back. Only one distinct orientation would allow for proper installation. Further, installation of the protruding rods into their respective cavities required a significant amount of precision, which may not be possible with cast-in-place decks. If this precision is not attained, the rods may be loaded in shear before the shear tubes. Recall, the threaded rods were not designed to sustain shear loading. Such loading could cause failure of the system. Moreover, without substantial precision, the rail segments might not fit properly on the bridge deck.

9.1.2 Deck Attachment B - Threaded Rods

Deck Attachment B consisted of four threaded rods which connected each barrier post to the bridge deck, as shown in Figure 167. Similar to the previous Deck Attachment A, the threaded rods were partially embedded into the segment post during casting. The upper end of each rod extended into the lower rail of the segment where it was anchored with a nut and washer plate. The opposite ends of each rod would extend out from the bottom of the post.

Contrary to Deck Attachment A, the post and the entire rail segment were both symmetric. A threaded rod was positioned near each one of the four corners. Also, this configuration did not require any additional vertical reinforcing steel inside the post.

During installation, the rail segments would be lowered into position by guiding the exposed rods through holes in the bridge deck. Washers and nuts would then be applied to the rods on the bottom of the deck to fasten the segment in place. As such, the only additional hardware necessary to install the rail segments are washers and nuts. This created a quick and easy installation process.

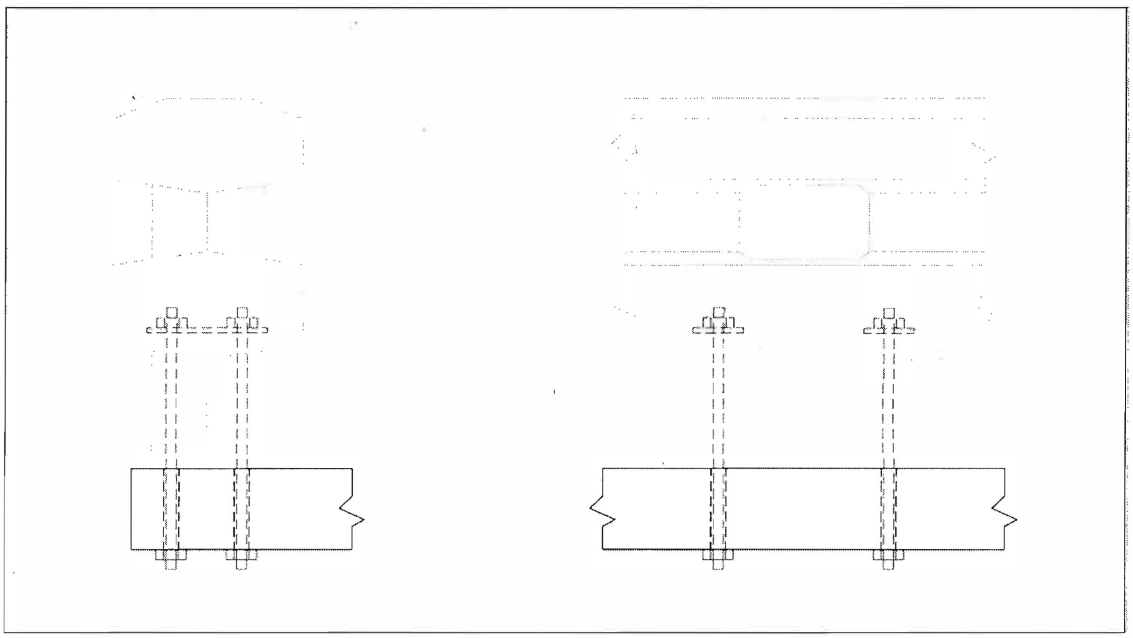

Figure 167. Deck Attachment B – Threaded Rods

During an impact, the threaded rods on the traffic side of the post would provide tension for bending and moment resistance, while the rods on the opposite side would provide shear resistance. To achieve rail symmetry it was necessary to specify all the threaded rods to be the same size. As such, the holes in the deck had to be designed so that the front rods were not

loaded in shear. Thus, the holes for on the traffic side were oversized to allow some movement before shear loading would occur.

9.1.3 Deck Attachment C - Cleat

Deck Attachment C consisted of interlocking cleats that connected rail posts to the bridge deck, as shown in Figure 168. Both the deck and the rail posts had coupled cleats that hooked onto each other when installed. It was necessary for the attachment to transfer both shear and moment, so the cleat would mutually resist both. The actual shape of the cleats could consist of a variety of shapes and was not overly important.

Cleats in the bridge deck would be partially embedded into the deck with the top extending out from the deck. The cleat in the bottom of the rail post would also be partially embedded. In order for the rail segment to rest flush on the deck, the cleat could not extend past the bottom surface of the post. As such, a cavity at the bottom of the post would contain the exposed arm of the cleat. The cavity would be centered both laterally and longitudinally along the bottom face post. The cleat would be positioned toward the traffic side of this cavity. This allowed the deck cleat to fit into the cavity during assembly. Further, this positioning created a larger moment arm and, thus, a stronger attachment.

To install the rail segment, the segment would be lowered into position such that the post cavity fit over the exposed deck cleat. Then the segment would be pushed toward the edge of the deck so that the cleats would hook onto each other and lock the segment into place. No additional hardware would be necessary for this attachment method making it the simplest and quickest to assemble.

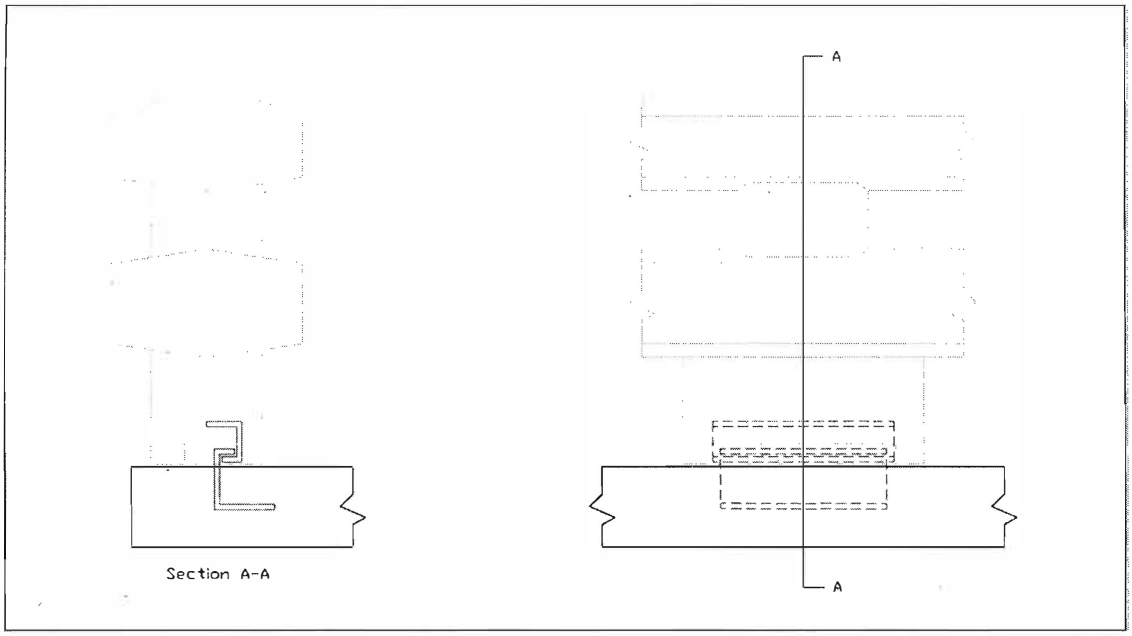

Figure 168. Deck Attachment C - Cleat

Two negative attributes could be identified with Deck Attachment C: (1) loss of rail symmetry and the possibility of a reversible rail segment and (2) damage to the cleat, or the deck, during an impact would require deck repairs or replacement. To prevent this damage, the cleat must be fabricated from strong, thick steel components, and extra deck reinforcement would be required to prevent the cleat from pulling out of the deck.

9.1.4 Deck Attachment D - Shear Curb

Deck Attachment D consisted of four threaded rods and a concrete shear curb connecting the rail posts to the bridge deck, as shown in Figure 169. The four threaded rods were the same as in Deck Attachment B, thus the rail was symmetric. Similarly, installation of the rail segments involved lowering the segment into position such that the exposed rods passed through the holes in the deck and were fastened with washers and nuts. The key difference between Deck Attachment B and Deck Attachment D was the concrete shear curb located on the edge of the deck and behind the rail post. This shear curb prevented lateral movement of the rail system and

resisted the shear component of impact. Therefore, the threaded rods were only required to carry tension loads in bending. Further, the holes in the deck did not have to be oversized to prevent shear loading.

The shear curb could be placed on the deck in two different ways. First, the entire deck could be widened to fit the shear curb behind the post. Previously, there had only been 1 in. (25 mm) of deck outside of the base of the rail system. Second, the deck could be extended only in the areas directly behind the post to account for the shear curb. However, this option created an uneven or non-uniform deck edge.

A major problem with Deck Attachment D was that a deck with a shear curb could not be easily cast in place. The addition of the shear curb to the deck resulted in the loss of a flat upper surface for the casting and curing process. This problem could be prevented in precast deck panels by casting them upside down to utilize the flat surface on the bottom of the deck. The installation of the shear curb would also use valuable deck width and would require reducing the amount of bridge deck available for travel lanes or widening the bride deck, which would incur significant cost.

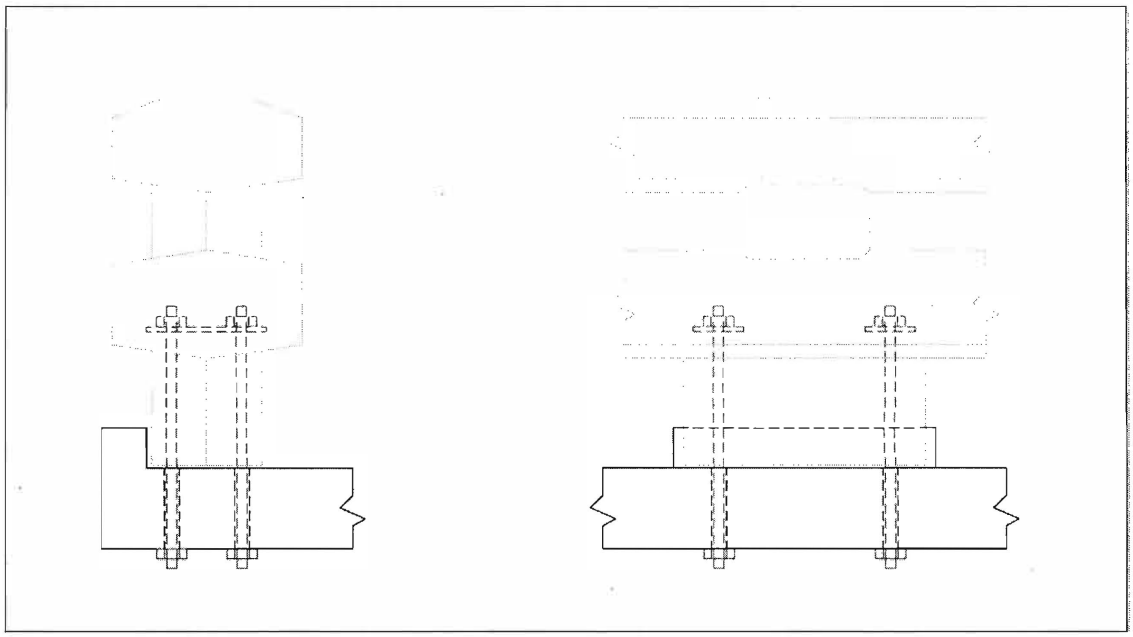

Figure 169. Deck Attachment D - Shear Rail

9.1.5 Deck Attachment E - Shear Channel

Deck Attachment E consisted of three threaded rods and a shear channel connecting the rail posts to the bridge deck, as shown in Figure 170. Similar to previous designs, the threaded rods were partially embedded into the rail post. However, instead of positioning the rods near the corners of the post, the rods were placed longitudinally in plane along the center of the post. The trapezoidal, concrete shear channel extruding from the bottom of the post would also span along the center of the post. A matching cavity would have to be cast into the deck for the shear channel to rest in. Ensuring both the threaded rods and the shear channel ran down the center of the post retained symmetry in the segments. Installation involved lowering a segment in place by guiding the shear channel into the matching cavity in the bridge deck and extending the exposed threaded rods through the holes in the deck. Washers and nuts would be used to fasten the rail segment to the deck.

As with the Deck Attachment D, the threaded rods were designed only for tension in bending and moment resistance. Additionally, the rods held the shear channel snug inside the cavity of the bridge deck to prevent lateral movement during impact. This ensured immediate shear transfer through the shear channel.

Although the channel created a strong, compact joint, the cavity in the deck resulted in a loss of deck thickness in a critically loaded area. The reduction in deck thickness ultimately would produce a corresponding reduction in both the bending and shear capacities of the deck. Consequently, the deck had an increased risk for structural damage during any significant impacts.

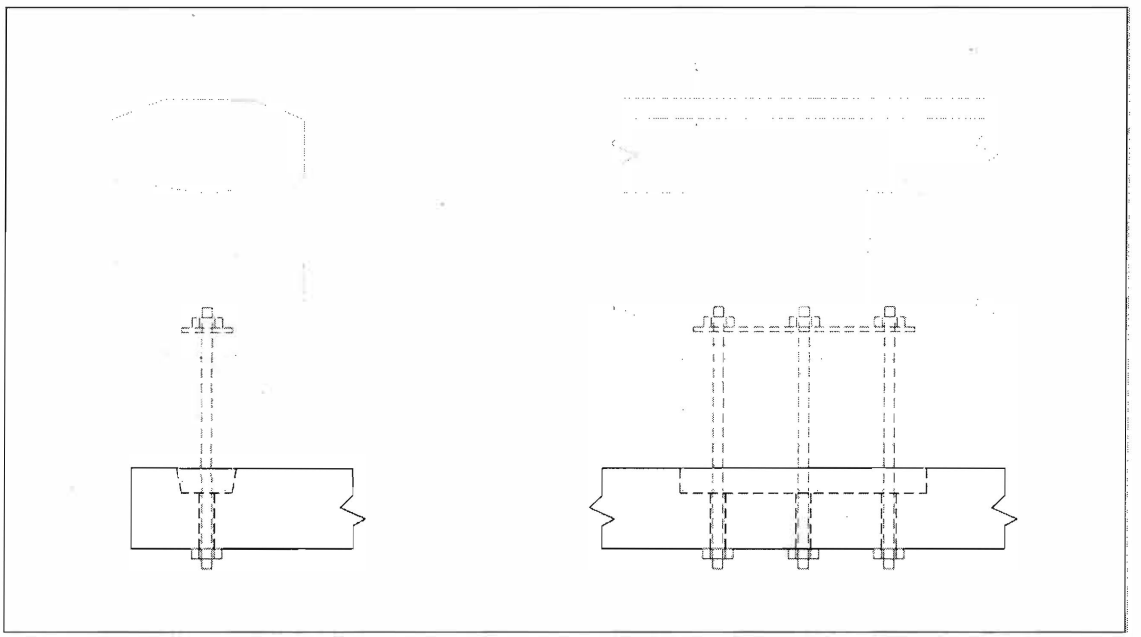

Figure 170. Deck Attachment E – Shear Channel

9.1.6 Deck Attachment Selection

Following a thorough review of all the deck attachments presented in this chapter, the designers chose Deck Attachment B as the most ideal design. This attachment employed four threaded rods of equivalent size to connect the rail posts to the bridge deck. This configuration

allowed the rail segments to remain symmetric while utilizing a quick and simple method of fastening the segments to the bridge deck. Also, the attachment did not require additional deck width nor created an increased risk for deck damage. Therefore, Deck Attachment B was selected for use in the precast bridge rail system. Analysis of the shear and tension design loads for the connection led to the selection of four 1¼-in. (32-mm) diameter, Grade 5 threaded rods for anchoring the post. The rods would be affixed to the underside of the bridge deck with ½-in. (13-mm) thick plate washers and 1¼-in. (32-mm) diameter Grade 5 heavy hex nuts.

9.2 Bridge Deck Reinforcement Design

Following the selection of the post-to-deck attachment method, it was necessary for the researchers to modify the standard bridge deck reinforcement to accept the chosen post attachment. The post-to-deck attachment method selected consisted of four threaded rods that passed from the post, through the bridge deck, and were bolted to the underside of the deck. Thus, the attachment required the creation of four holes in the deck and additional reinforcement to prevent the anchor bolts from causing damage to the deck.

The basic deck reinforcement chosen for the project was Nebraska's standard, cast-in-place bridge deck reinforcement, as supplied by NDOR bridge engineers. It was decided to design the modifications to the bridge deck reinforcement using the standard, cast-in-place deck details first, with the understanding that the reinforcing details could be adapted to other bridge deck designs and precast bridge deck panels at a later date. Nebraska's standard, cast-in-place bridge deck consisted of an 8-in. (203-mm) thick deck reinforced by a pattern of longitudinal and transverse reinforcing bars. All of the reinforcing steel consisted of Grade 60 epoxy coated rebar. The transverse steel consisted of a top and bottom mat of reinforcing bars. The top mat of transverse steel had 2½ in. (64 mm) of clear cover and used a repeated pattern of one no. 4 bar,

two no. 6 bars. All three bars were spaced at 4 in. (102 mm) on center. The bottom mat of transverse steel had 1 in. of clear cover and used repeated pattern of no. 5 bars at 12 in. (305 mm) spacing on center. The longitudinal steel was also comprised of a top and bottom mat of reinforcing bars. The top mat of longitudinal steel had 2½ in. (64 mm) of clear cover and used no. 4 bars spaced at 12 in. (305 mm) on center. The bottom mat of longitudinal steel had 1 in. of clear cover and used no. 5 bars spaced at 12 in. (305 mm) on center except for the final bar adjacent to the deck edge which was spaced at 6 in. (152 mm) on center.

Modification of the reinforcing steel for the attachment of the precast bridge rail required consideration of design loads, ease of installation, and minimizing the changes to the current reinforcement layout. The proposed modifications to the reinforcing steel are shown in Figure 171 through Figure 181. Note that the details shown show a limited length section of the bridge deck sized for mounting on girders in the existing bridge rail pit at the MwRSF test facility. The major addition to the deck reinforcement consisted of four 3-in. wide by 2-in. deep by 8-in. long by ¼-in. thick (76-mm wide by 51-mm deep by 203-mm long by 6-mm thick) steel tubes. The steel tubes served to create the holes in the deck required for the anchor rods in the post. To ease concerns with installation tolerances, the four tubes were connected by lateral and longitudinal spacer places that were welded to each tube. The spacer plates ensured that the spacing between the anchor rods on the base of post would be maintained in the bridge deck. The anchor rod tubes then needed to be tied into the existing deck. Recall that the design impact load for the bridge rail was estimated to be 100 kips (445 kN). It was conservatively assumed that the entire design load could be imparted to the deck through a single post under a worst case scenario in which the bridge rail lost it continuity. Based on this assumption, a no. 5 bar was bent around each pair of anchor and extended back laterally into the deck to resist the impact loads. In addition to these tie

back bars, a pair of longitudinal bars were mounted across the front and rear anchor tubes and spliced with the existing longitudinal reinforcement to further anchor the tubes and prevent shear cracking. The additional steel tubes and reinforcing bars required only minor modification to Nebraska's standard, cast-in-place bridge deck reinforcement. The only change to the reinforcement was the removal of one of the no. 6 bars in the top mat of the transverse steel at each of the anchor tube locations. The additional of the no. 5 tie back bar at these locations more than compensated for the removed bar.

The proposed bridge deck reinforcing steel modification for attachment of the precast bridge rail design described herein was preliminary. Further revision of the design was anticipated following additional component level or full-scale testing of the precast bridge rail when mounted on a simulated bridge deck.

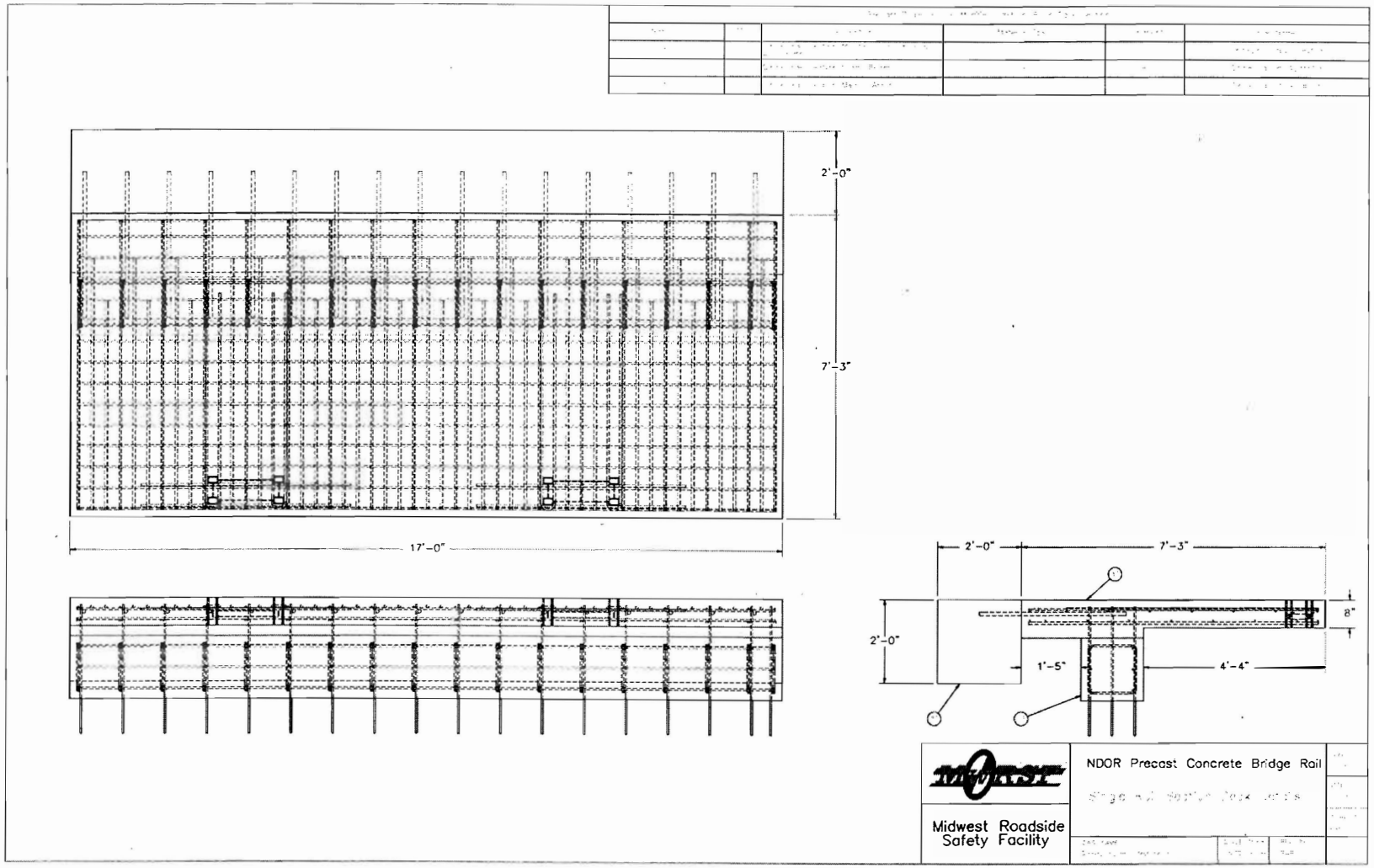

Figure 171. Schematic Details of Modified Bridge Deck Reinforcement

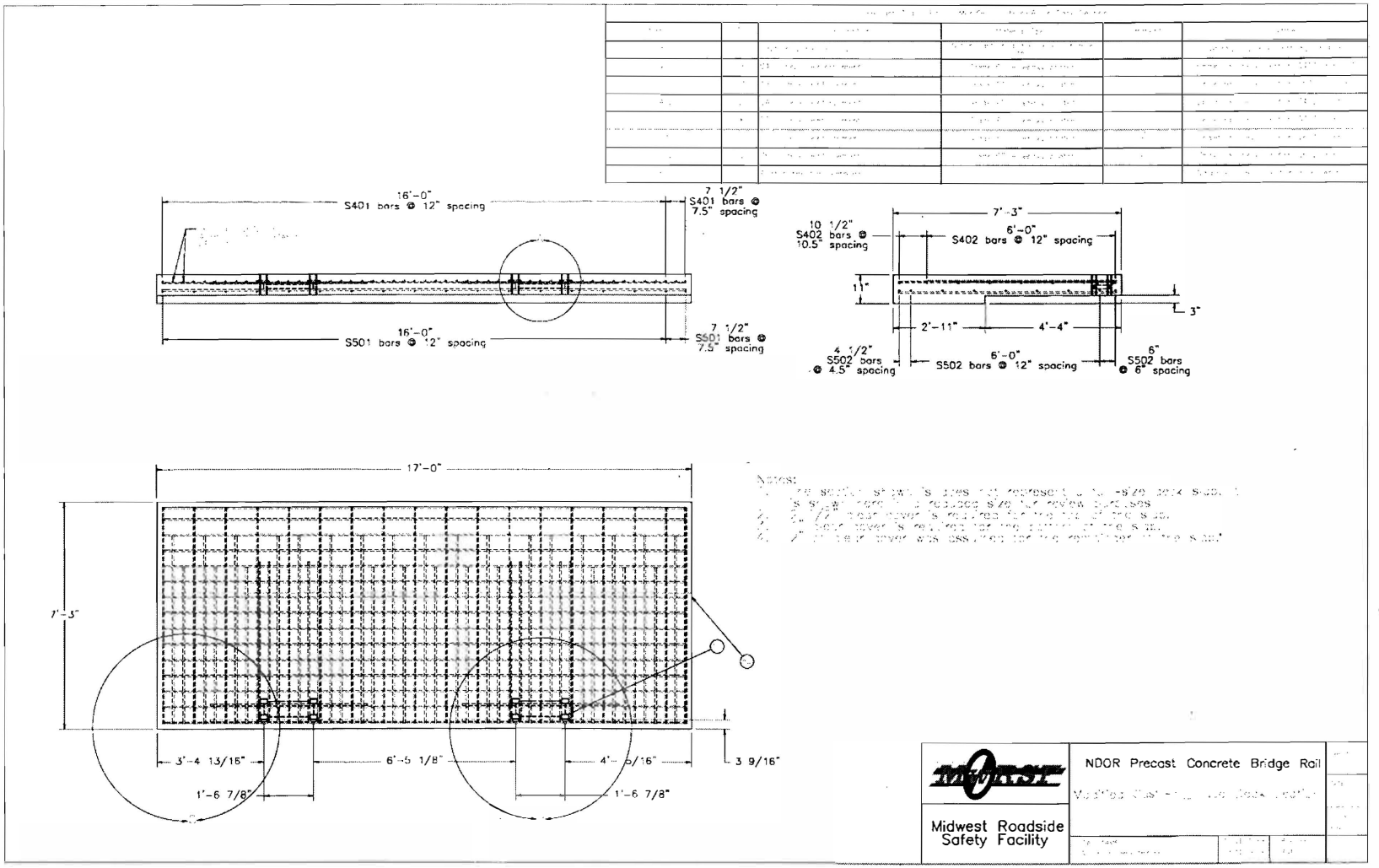

Figure 172. Schematic Details of Modified Bridge Deck Reinforcement

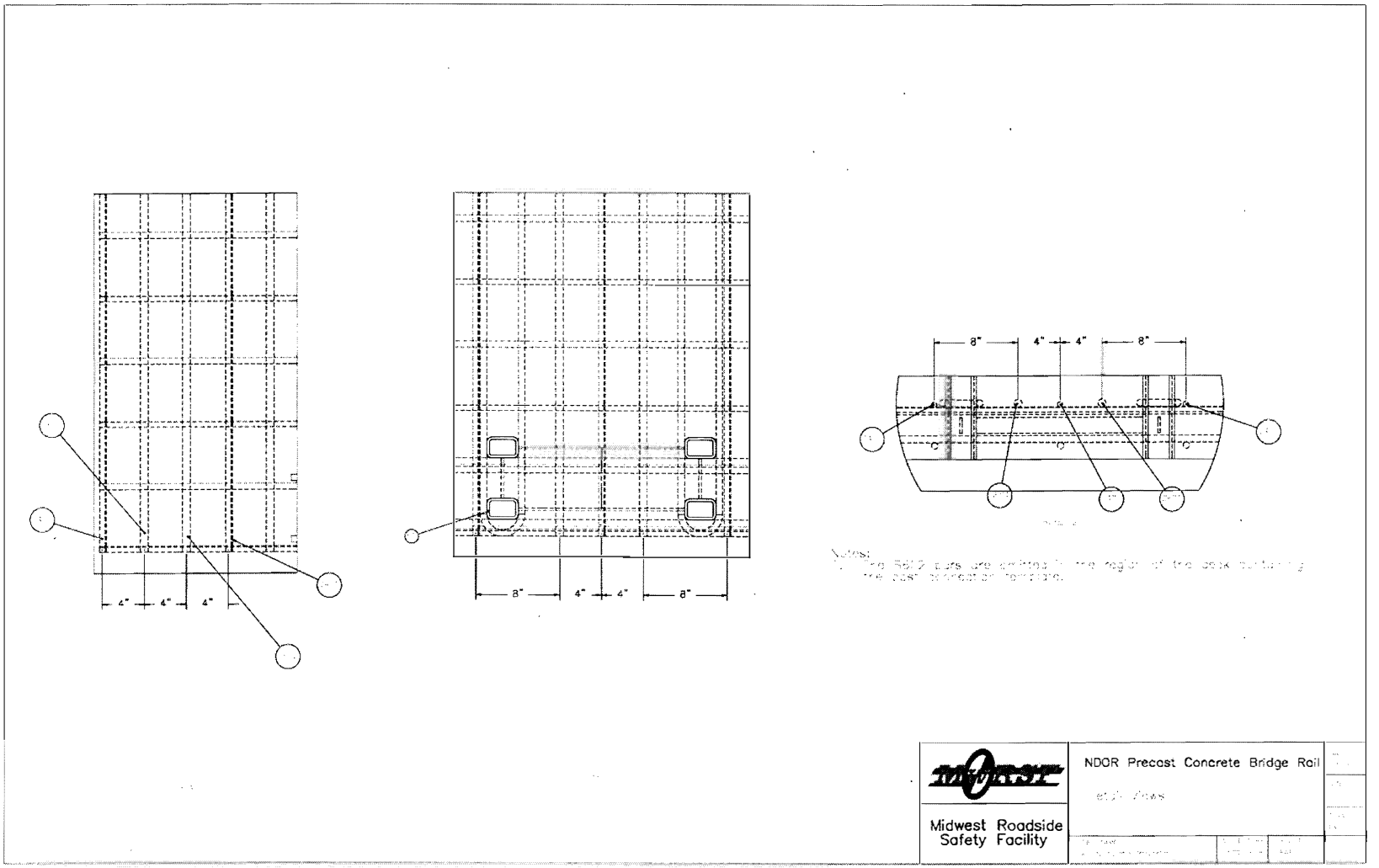

Figure 173. Schematic Details of Modified Bridge Deck Reinforcement

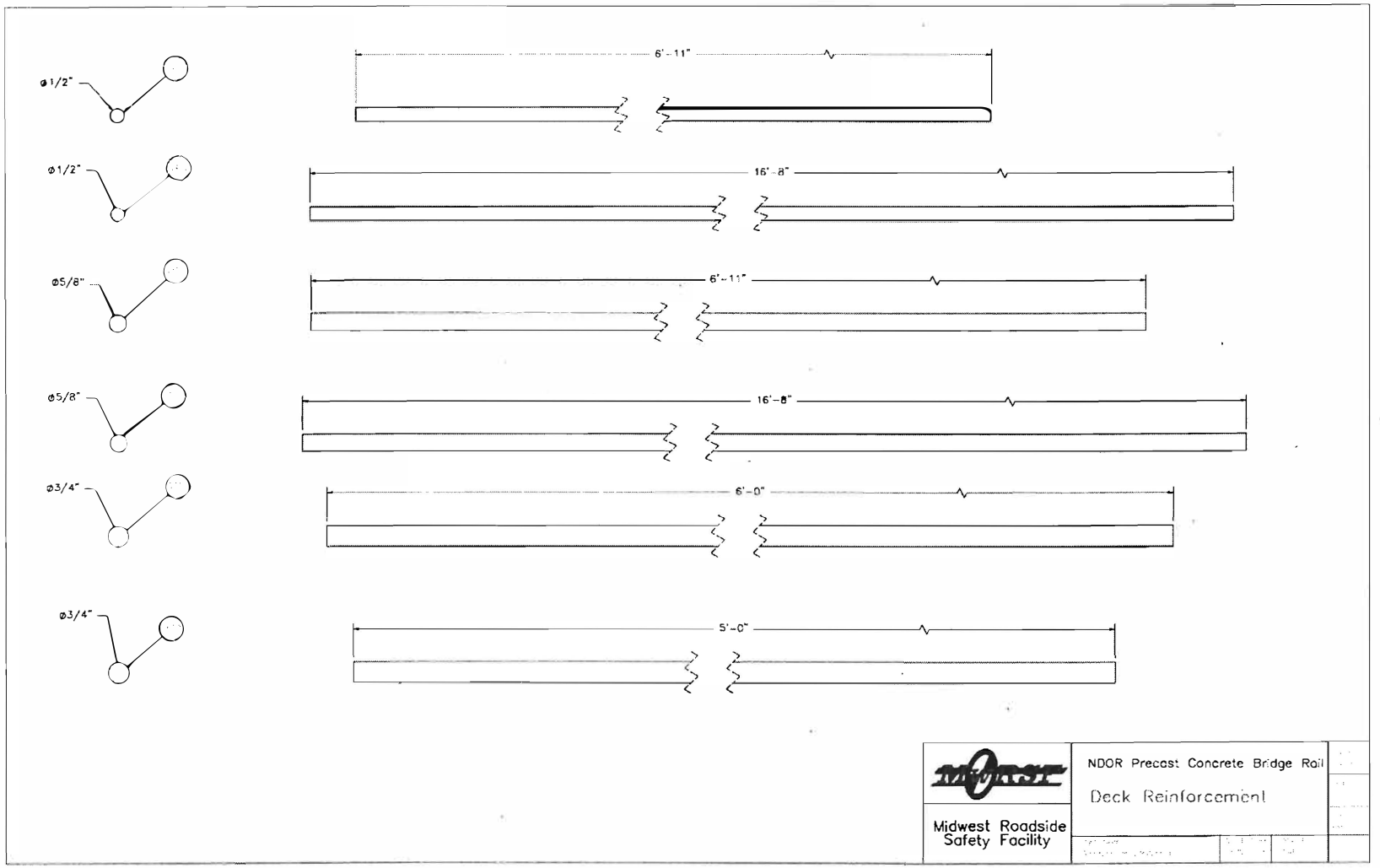

Figure 174. Schematic Details of Modified Bridge Deck Reinforcement

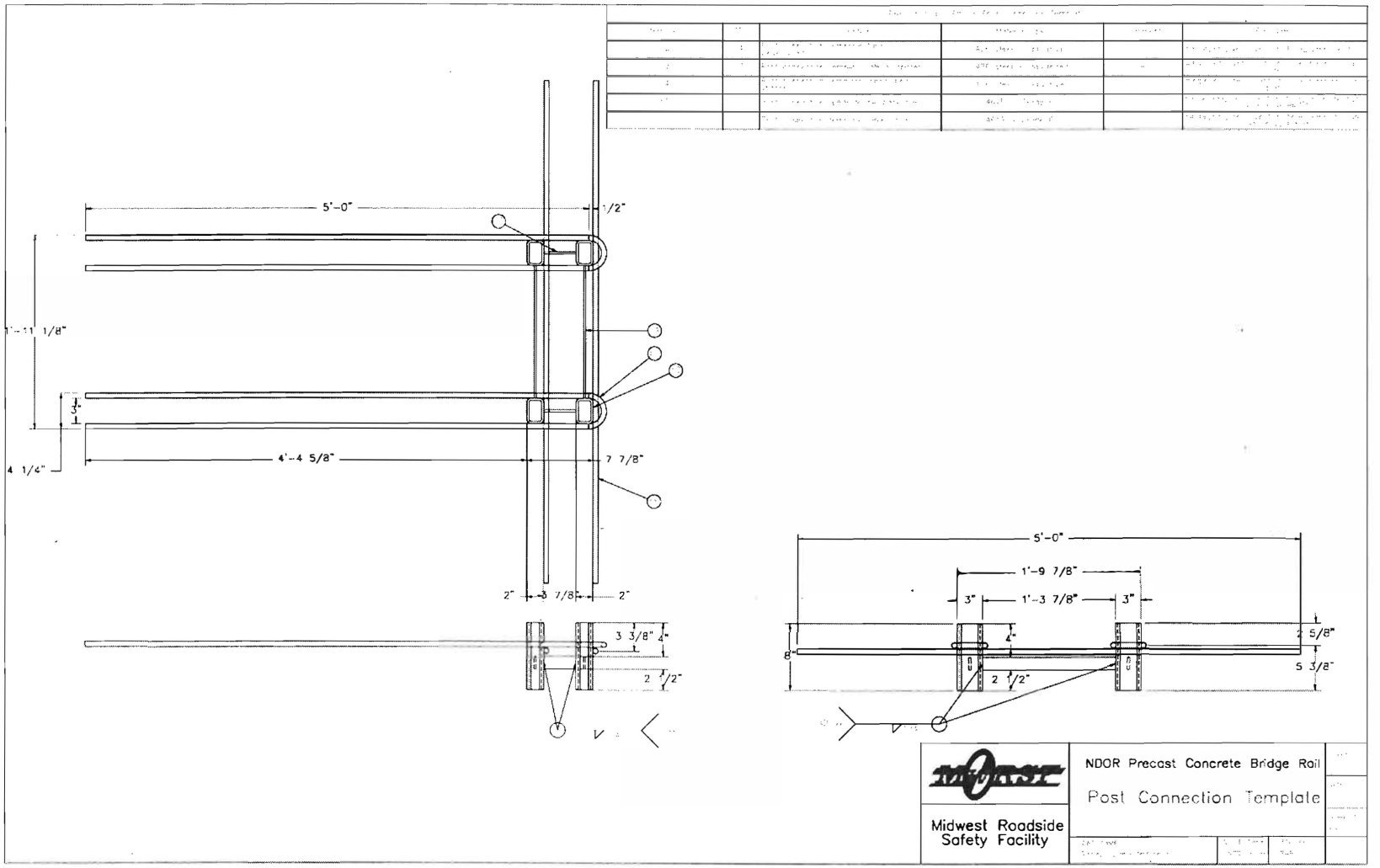

Figure 175. Schematic Details of Modified Bridge Deck Reinforcement

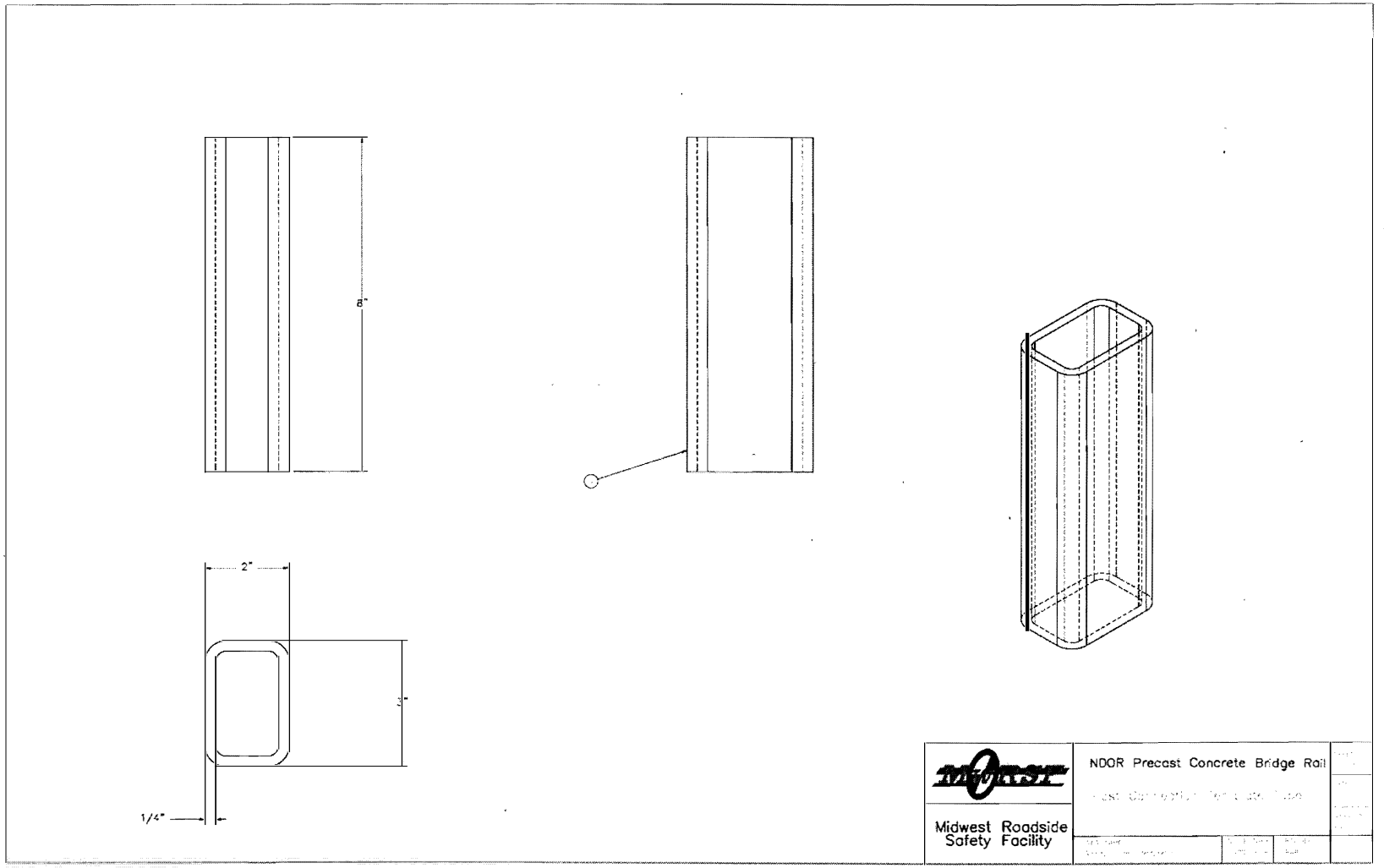

Figure 176. Schematic Details of Modified Bridge Deck Reinforcement

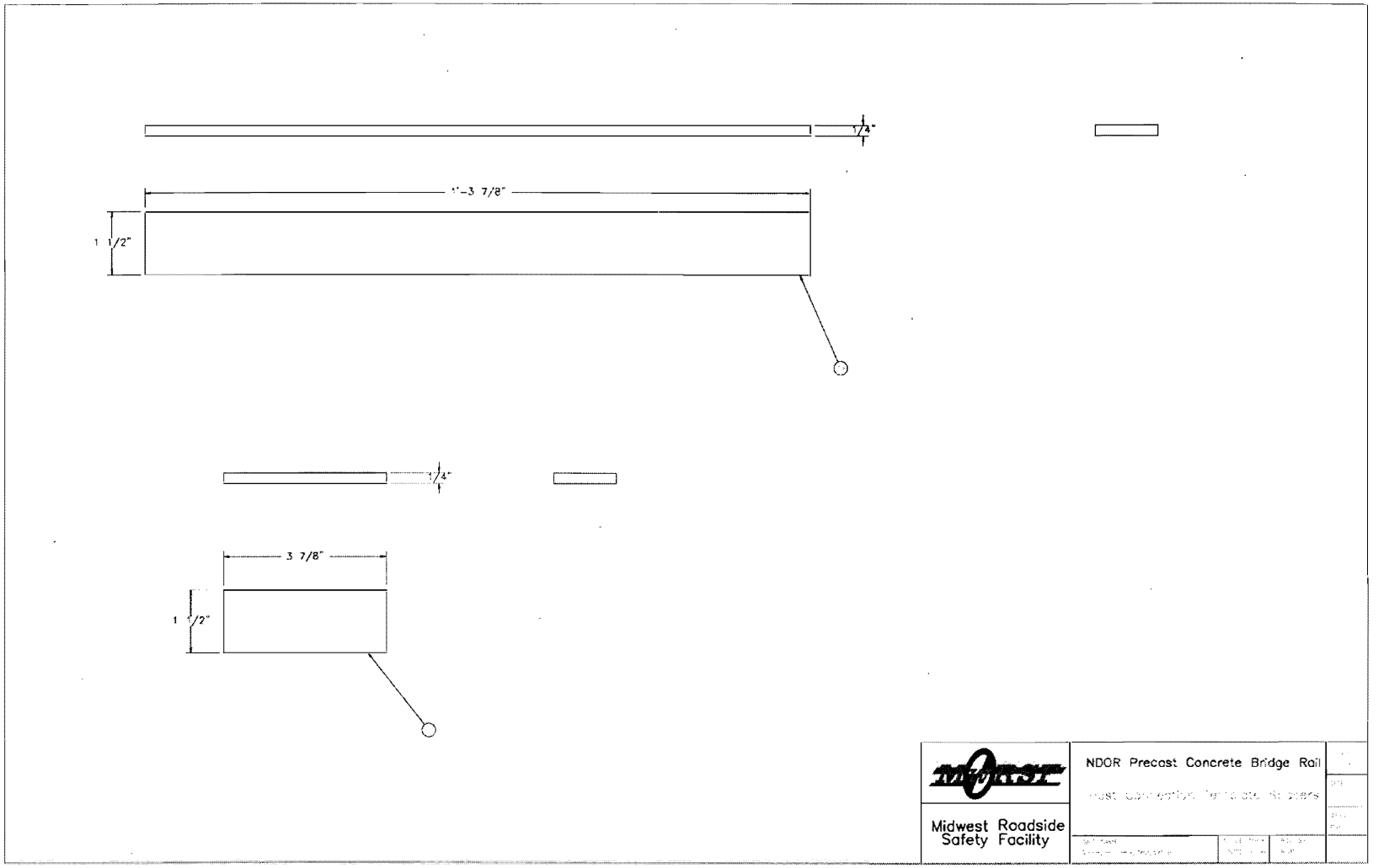

Figure 177. Schematic Details of Modified Bridge Deck Reinforcement

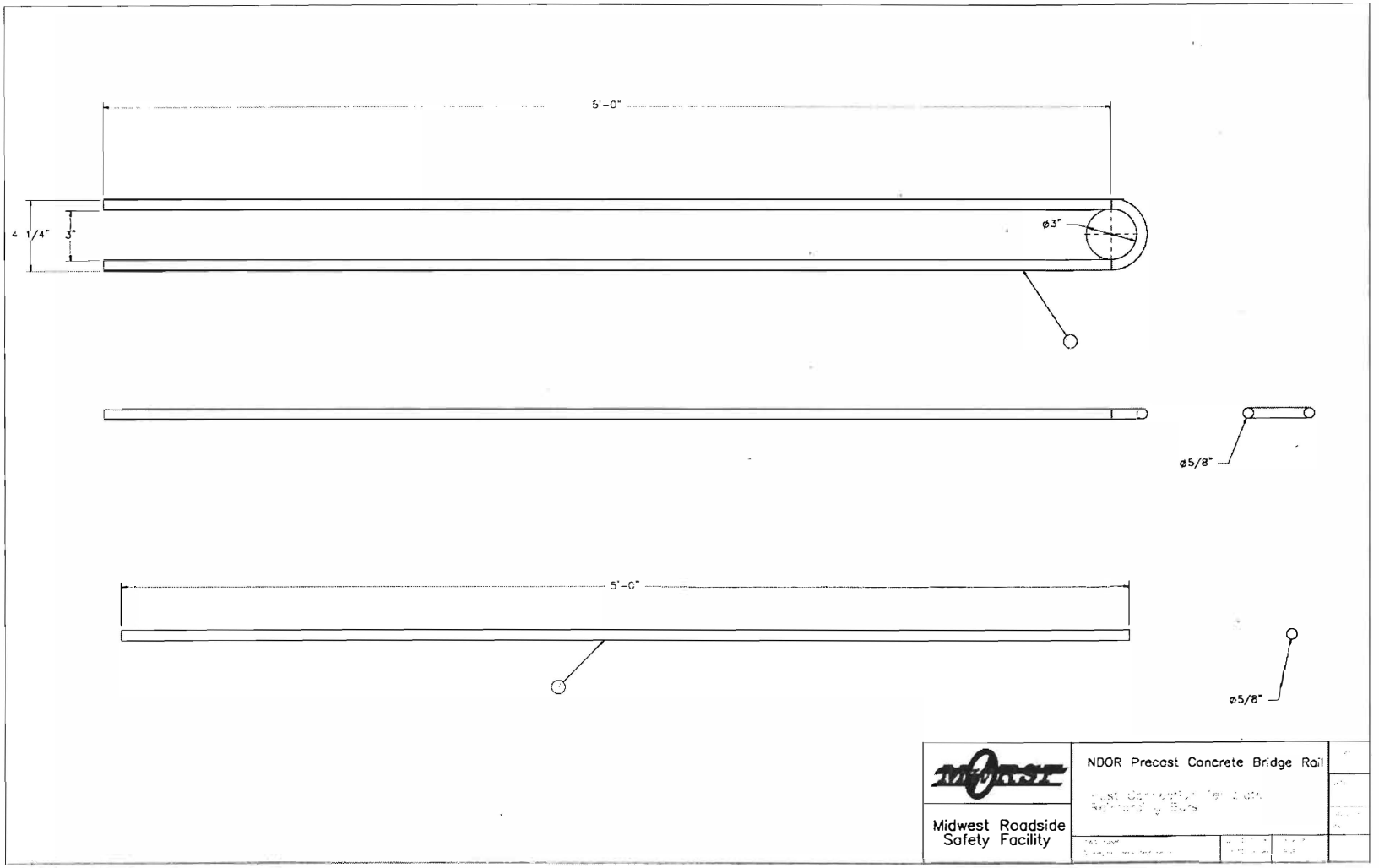

Figure 178. Schematic Details of Modified Bridge Deck Reinforcement

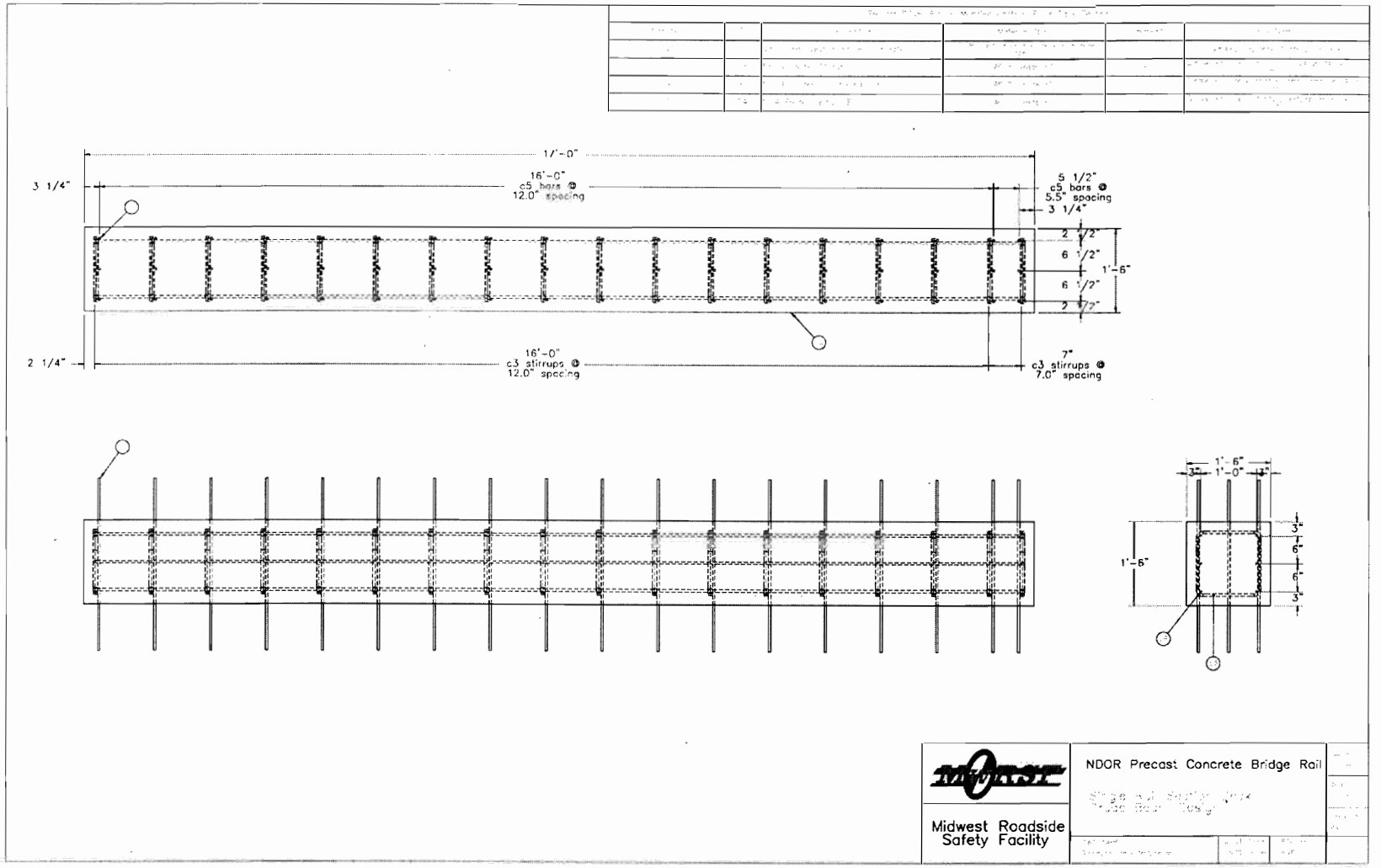

Figure 179. Schematic Details of Modified Bridge Deck Reinforcement

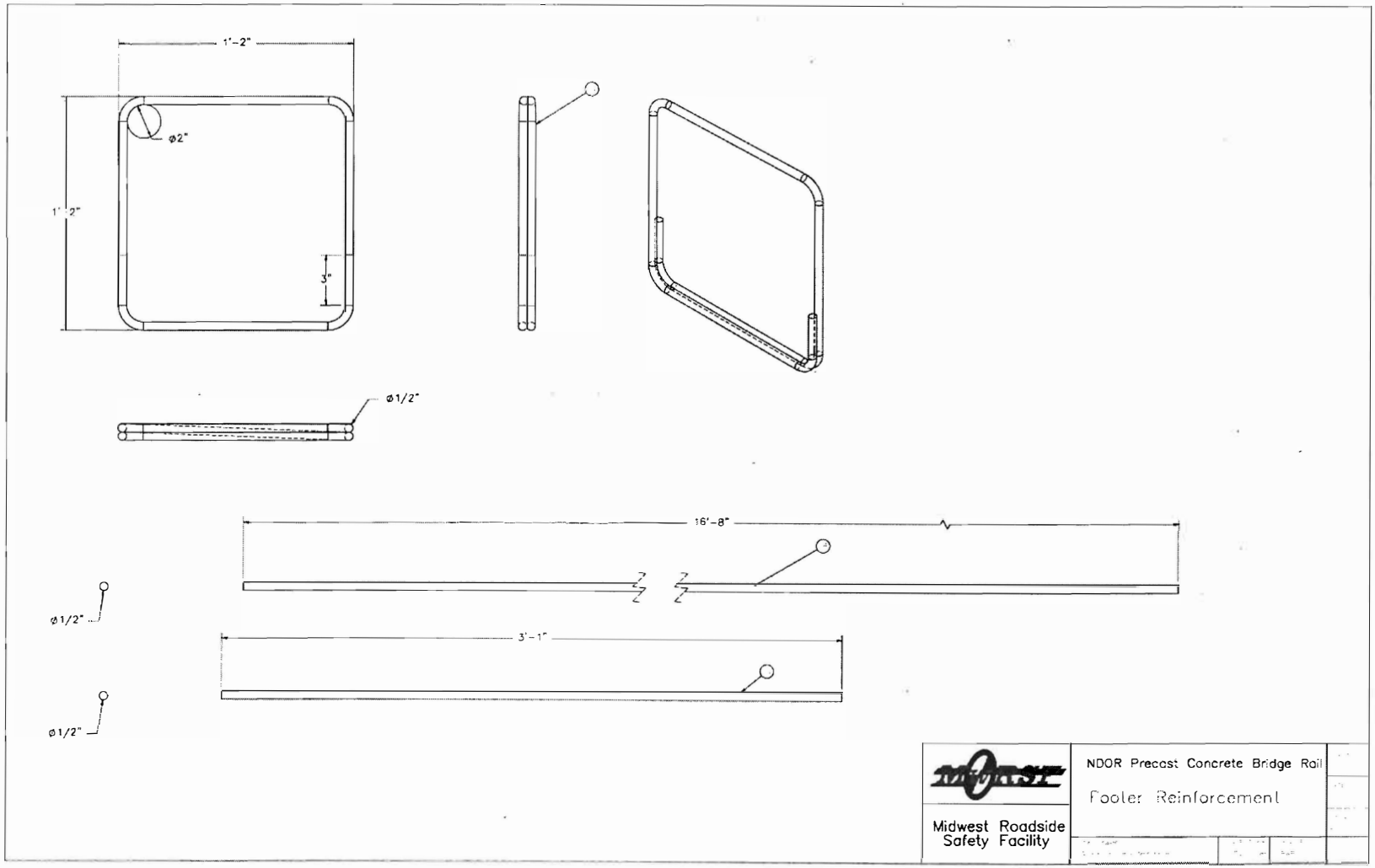

Figure 180. Schematic Details of Modified Bridge Deck Reinforcement

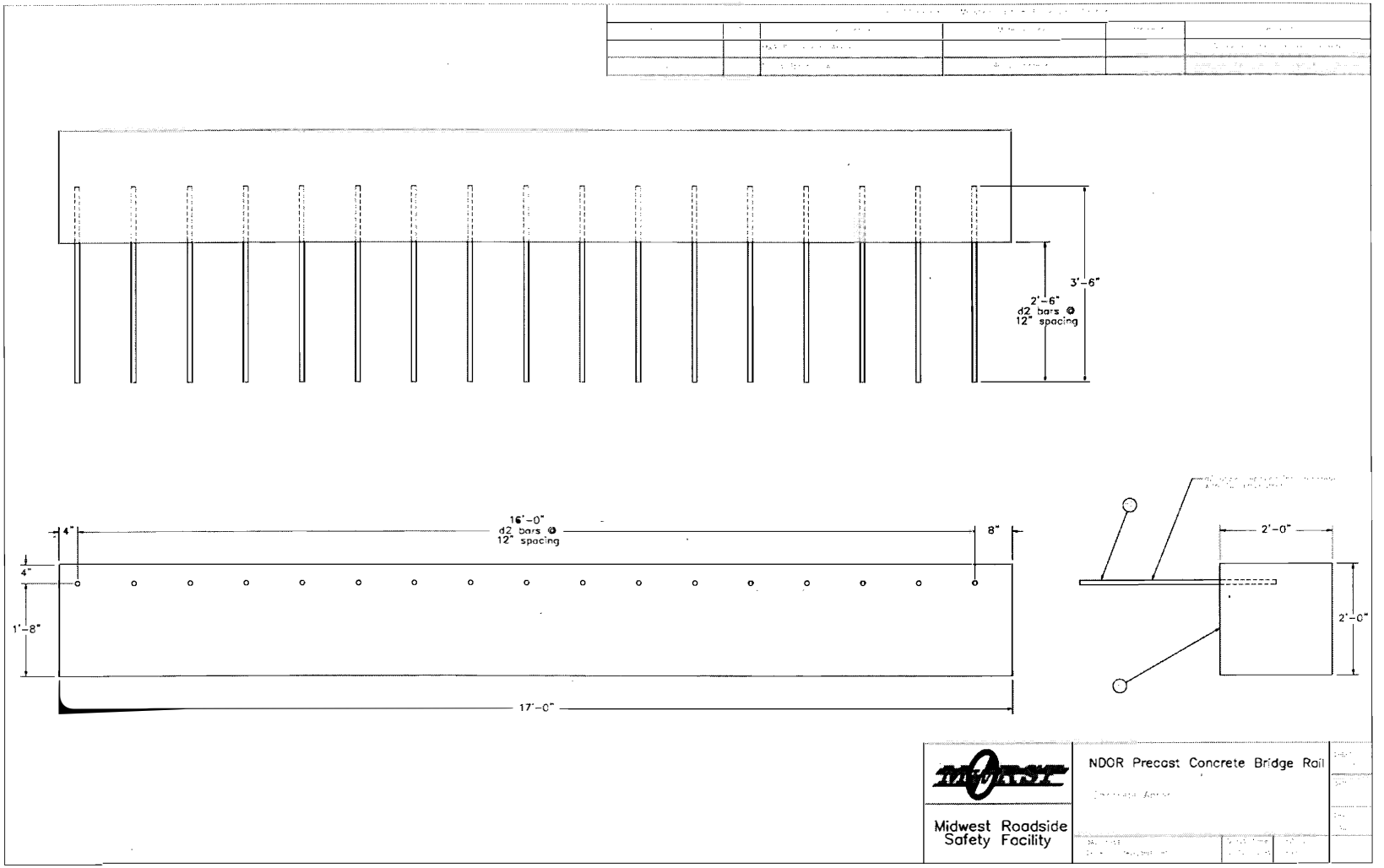

Figure 181. Schematic Details of Modified Bridge Deck Reinforcement

February 13, 2012
MwRSF Report No. TRP-03-239-12

10 FINAL PROTOTYPE DESIGN DETAILS

After completing the design of the basic rail geometry and structure, the rail segment connections, the post-to-deck attachment, and the revised bridge deck reinforcement, the researchers assembled design details and CAD for the complete bridge rail system required for full-scale crash testing of the precast concrete bridge rail prototype. The details for a single segment of the precast concrete bridge rail prototype are shown in Figure 182 through Figure 196. The details for the assembled bridge rail mounted on a simulated bridge deck at the MwRSF test facility, including the revised deck reinforcement, are shown in Figure 197 through Figure 209.

The precast bridge rail segment consisted of 191¾-in. (4.87-m) long rail segments with a ¼-in. nominal gap length between segments for a center to center distance of 16 ft. (4.88 m). The rail section was 36½ in. (927 mm) tall by 19 in. (483 mm) wide. The rail segment geometry was based on the Concept F (Fence) design selected in Chapter 4. This design consisted of two main rail segments separated by rail spacers or balusters. The upper rail segment incorporated geometry for mitigation of occupant head contact during passenger vehicle impacts. Reinforcement of both the upper and lower rail segments consisted of four no. 7 Grade 70 threaded rebar for the longitudinal steel and no. 4 Grade 60 epoxy coated stirrups at 8 in. (2093 mm) spacing on center for the shear reinforcement. The shear stirrup spacing was reduced to 4 in. (101 mm) for the final 13½ in. (343 mm) adjacent to the end connection pockets at each end of the rail. The balusters separating the top and bottom rail sections were 13 in. wide by 11 in. wide by 5¾ in. tall (330 mm wide by 279 mm wide by 146 mm tall). Each baluster was reinforced vertically with four no. 4 Grade 60 epoxy coated bars and used two no. 3 Grade 60 epoxy coated stirrups at 4 in. (102 mm) spacing on center for shear reinforcement.

Two posts were used to support the railing and attach the segments to the bridge deck. Each post was 25 in. wide by 11 in. deep by 12 in. tall (635 mm wide by 279 mm wide by 305 mm tall) and was spaced 71 in. (1,803 mm) from the adjacent post and 35 3/8 in. (899 mm) from the end of the rail segment. The vertical reinforcement of the post was comprised of the four 1¼-in. (32-mm) diameter, Grade 5 threaded rods used for anchoring the post to the bridge deck. The shear reinforcement for the post consisted of three no. 3 Grade 60 epoxy coated stirrups spaced at 4½ in. (114) mm on center. The base of the post was fitted with a 1/8-in. (3-mm) thick neoprene pad to form an evenly distributed connection bearing surface between the rough concrete that comprised the base of the post and the top of the bridge deck.

The connection between the post and the bridge deck was based on the Deck Attachment B, as detailed in Chapter 9. The connection consisted of the four 1¼-in. (32-mm) diameter Grade 5 threaded rods that were cast into the post and extended 12 in. (305 mm) from the base of the post. The threaded rods would pass through tubes cast into the bridge deck and then be affixed to the underside of the bridge deck with ½-in. (13-mm) thick plate washers and 1¼-in. (32-mm) diameter Grade 5 heavy hex nuts.

As detailed in Chapter 9, the bridge deck design used in conjunction with the precast concrete bridge rail prototype was based on Nebraska's standard, cast-in-place bridge deck reinforcement as supplied by NDOR. Steel tubes were inserted into the reinforcement to create mounting holes for the anchor rods. The steel tubes were connected by welded plates in order to help maintain the correct spacing during construction. Reinforcing steel was added around the steel tubes to tie the tubes into the existing deck reinforcement. The modifications required for the mounting of the precast concrete bridge rail required only the removal of on transverse no. 6

bar in the region of the steel tubes. No other modifications were necessary to the standard reinforcement.

The precast concrete bridge rail prototype segments were connected at both the top and bottom rail sections with the refined grouted joint design successfully tested in component test PCRB-3, as detailed in Chapter 8. This connection consisted of fabricated I-beam sections that dropped into open tube sections on each side of the joint. The open tube sections were then filled with grout to complete the connection. Full-details of the grouted connection design are located in the subsequent CAD details. This joint design had the developed very high loads and energy dissipation during component testing while retaining its integrity. In addition, the grouted connection required no shimming and was capable of handling joint tolerances and horizontal and vertical curves without additional hardware.

The system details shown for the precast concrete bridge rail prototype were developed for implementation and installation of the system at the MwRSF test facility. As such, the bridge deck and system length are configured for full-scale crash testing in the MwRSF simulated bridge pit on an existing girder system, as shown in Figure 210. Actual field installation details would vary from what is shown herein.

It should be noted that details for a closed rail system were also developed based on the open rail system shown here. The basic design of the closed rail system was unchanged from the open railing described above except for the addition of a reinforced concrete panel that ran flush with the front face of the posts on the closed rail system. This reinforcing steel for the panel was tied into the posts and the lower rail of the bridge rail. These details are available upon request but were not provided as part of this report.

Finally, it should be noted that the new, precast bridge rail system was developed with considerations for aesthetic treatments including the shape of the rail itself, additional surface treatments, dyes, and medallions. In order to evaluate the potential aesthetics of the new bridge rail design, a full-scale model of a single rail section was formed from Styrofoam and photographs with various vehicle types to provide a better feel for the actual aesthetics of the design, as shown in Figures 211 through 213. In addition to the full-scale model, renderings were prepared of potential aesthetic treatments for both the open and closed rail sections, shown in Figures 214 through 220. Many of these aesthetic treatments would not be possible without the use of precast concrete construction techniques. These efforts demonstrated the improved aesthetic qualities of the new design as compared to more conventional concrete bridge rails.

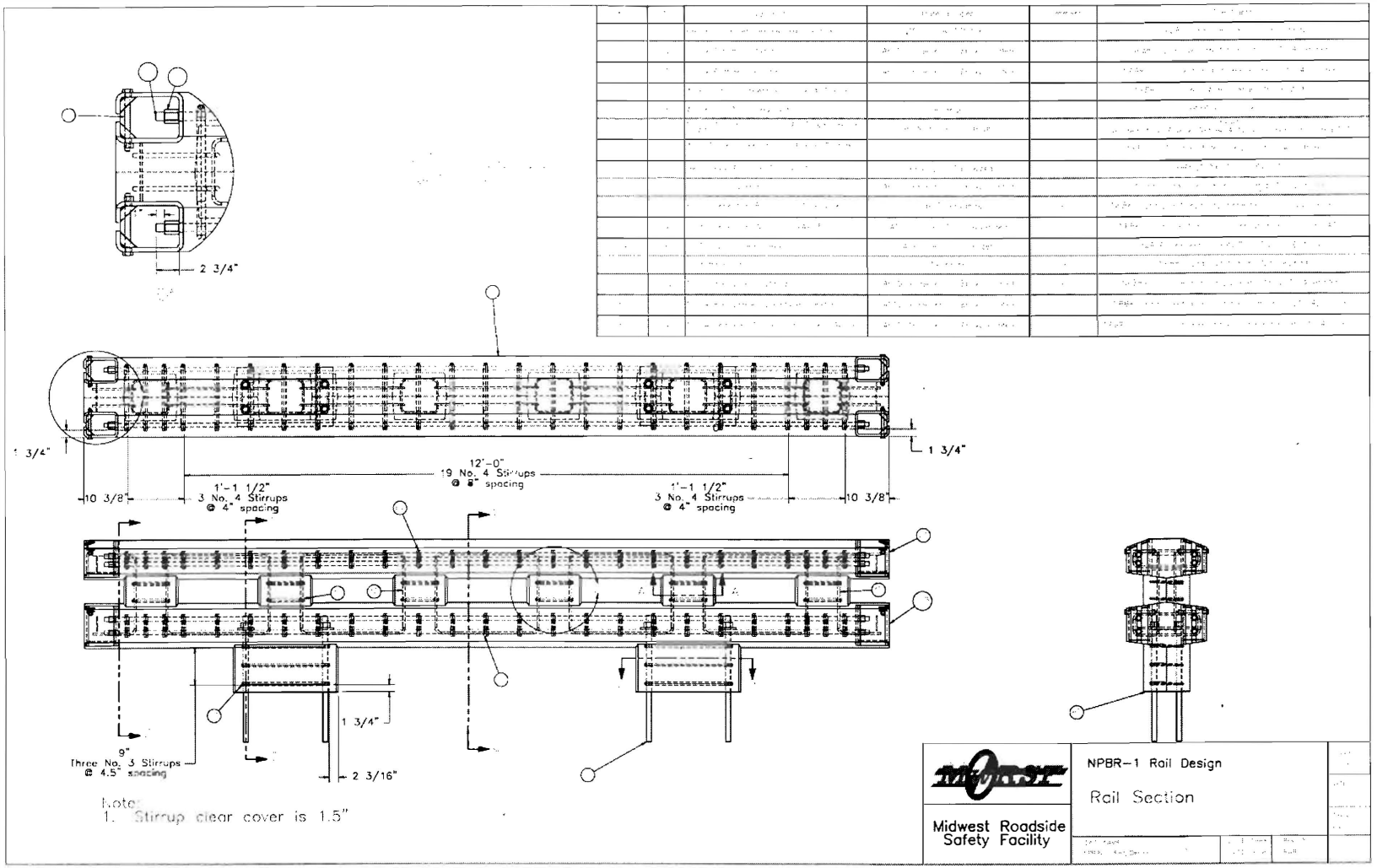

Figure 182. Precast Bridge Rail Segment CAD Details

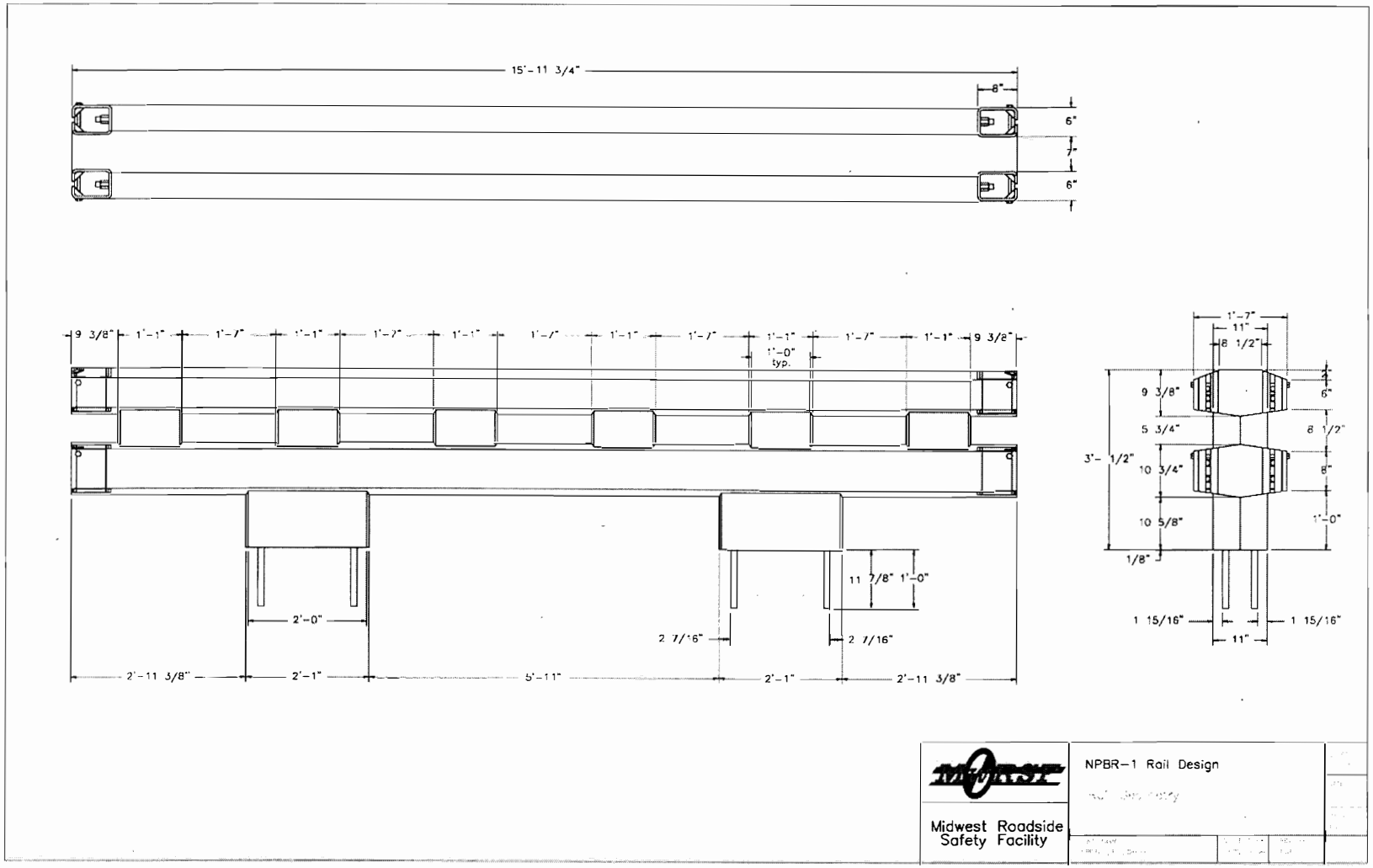

Figure 183. Precast Bridge Rail Segment CAD Details

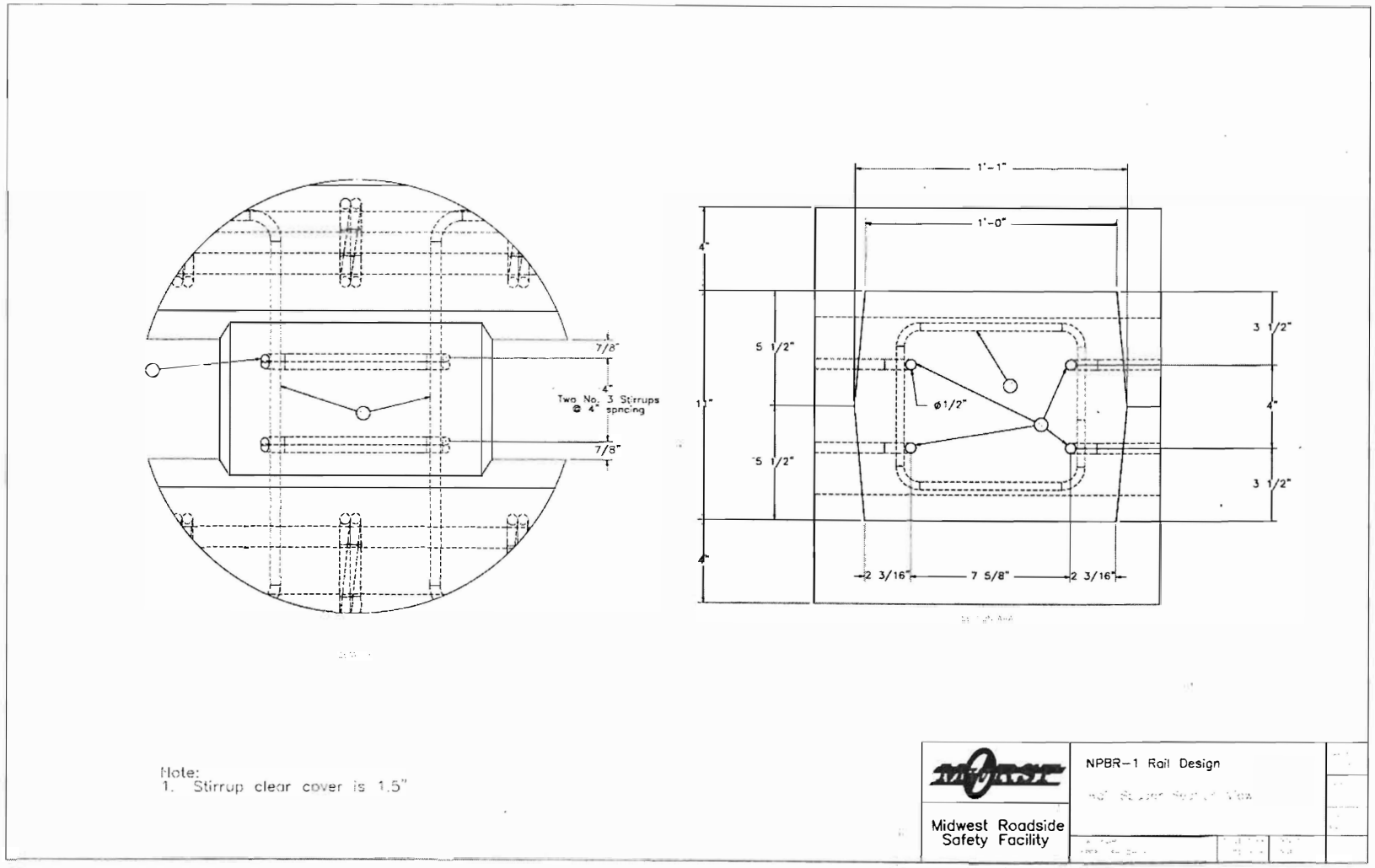

Figure 184. Precast Bridge Rail Segment CAD Details

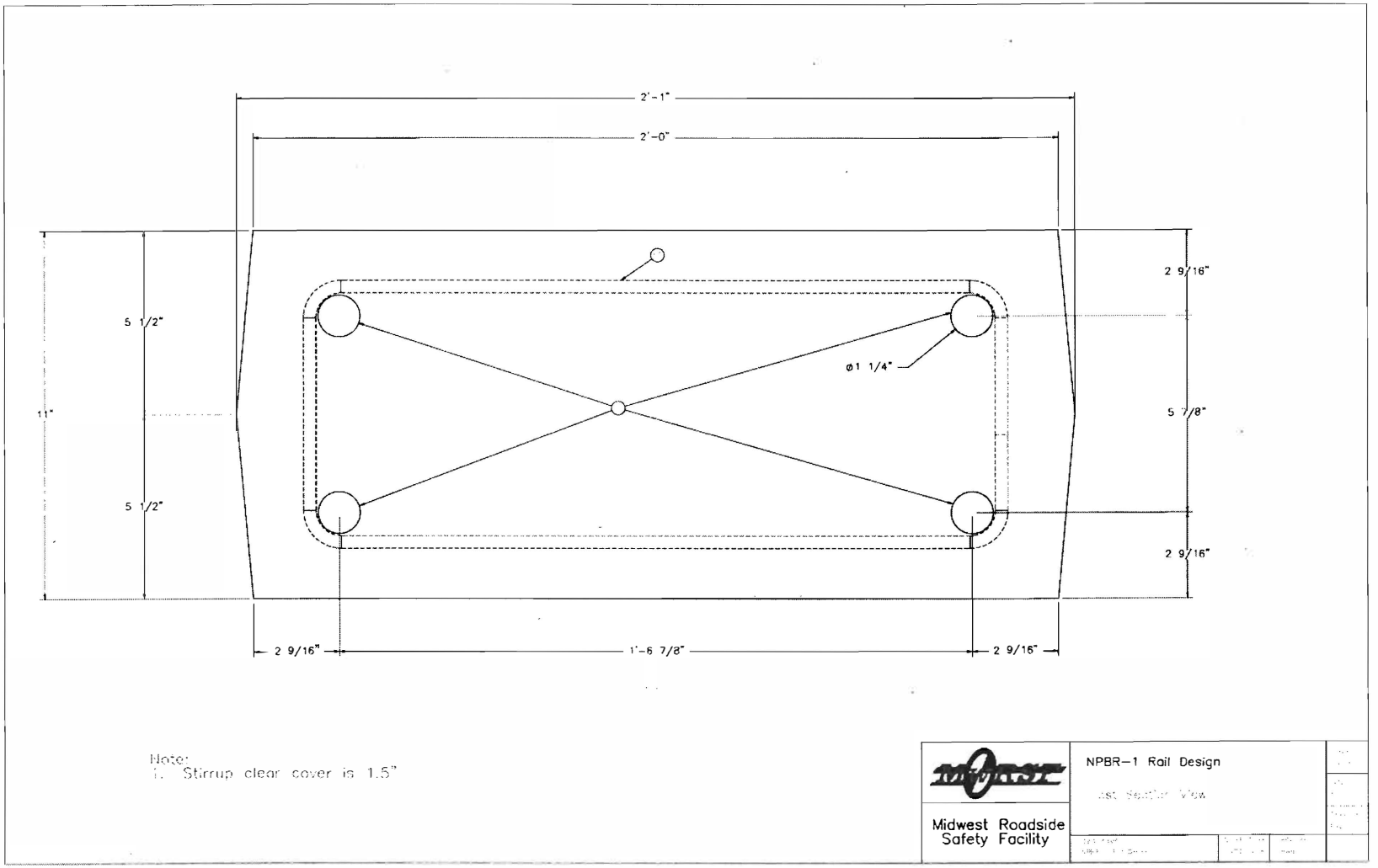

Figure 185. Precast Bridge Rail Segment CAD Details

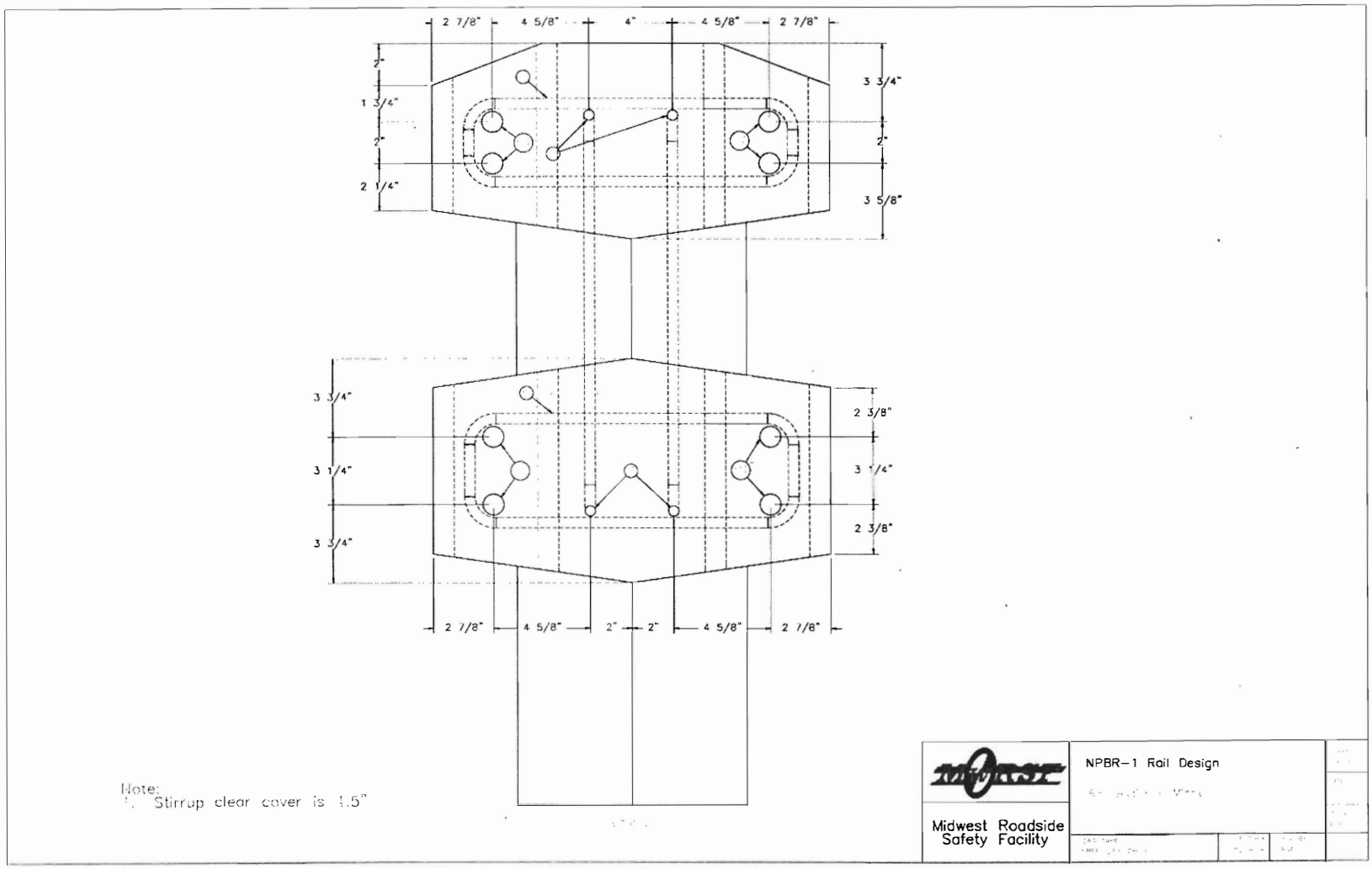

Figure 186. Precast Bridge Rail Segment CAD Details

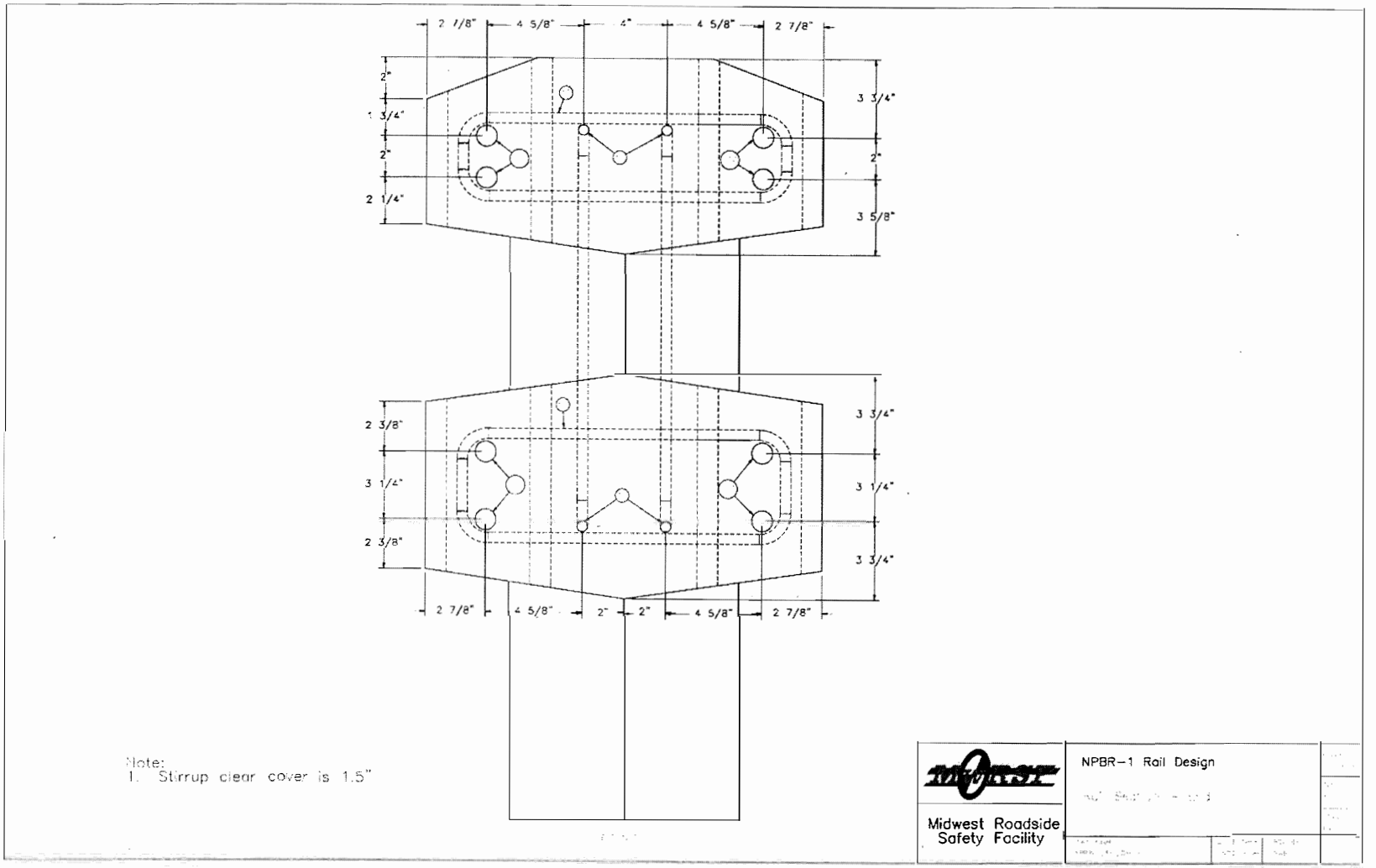

Figure 187. Precast Bridge Rail Segment CAD Details

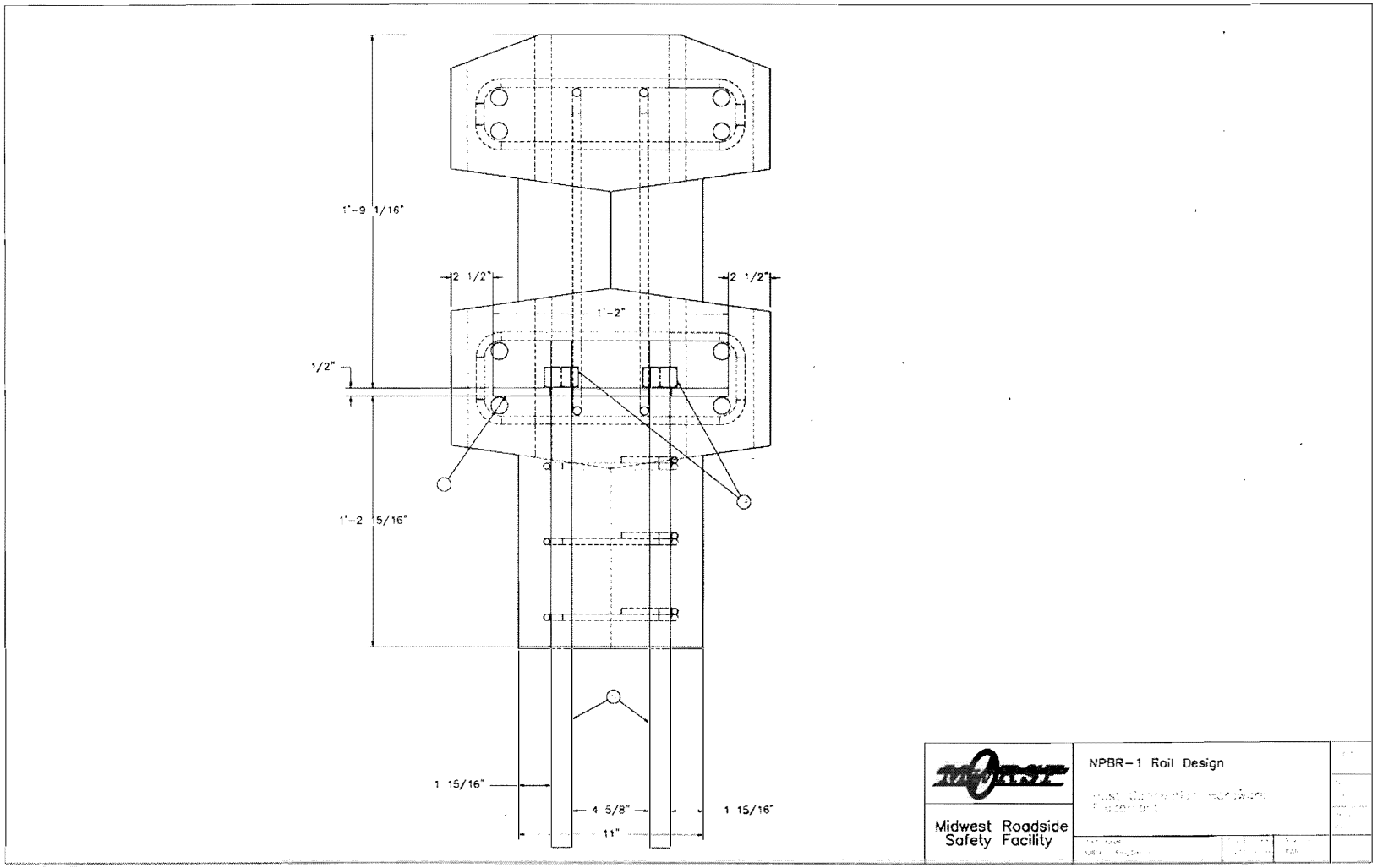

Figure 188. Precast Bridge Rail Segment CAD Details

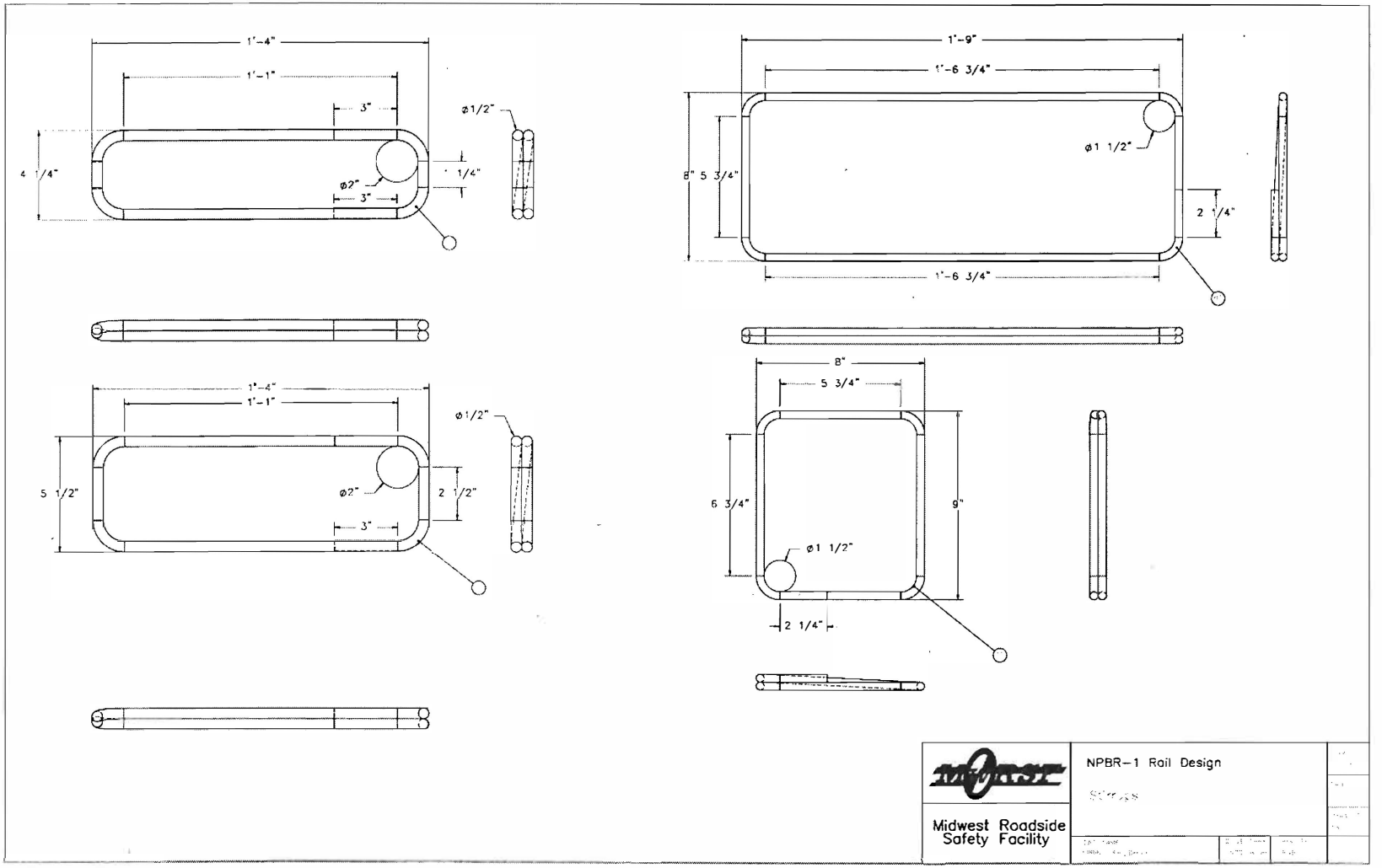

Figure 189. Precast Bridge Rail Segment CAD Details

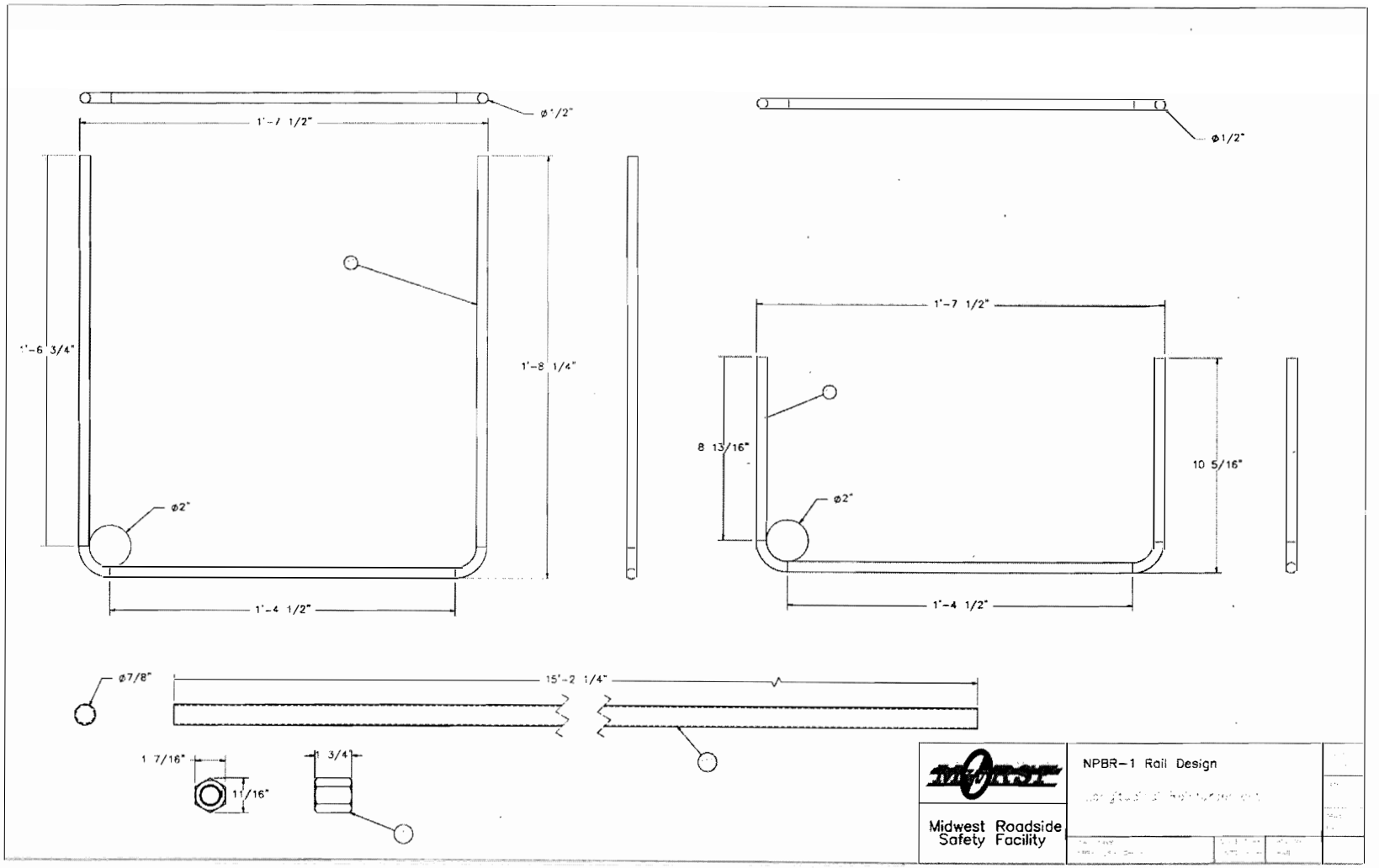

Figure 190. Precast Bridge Rail Segment CAD Details

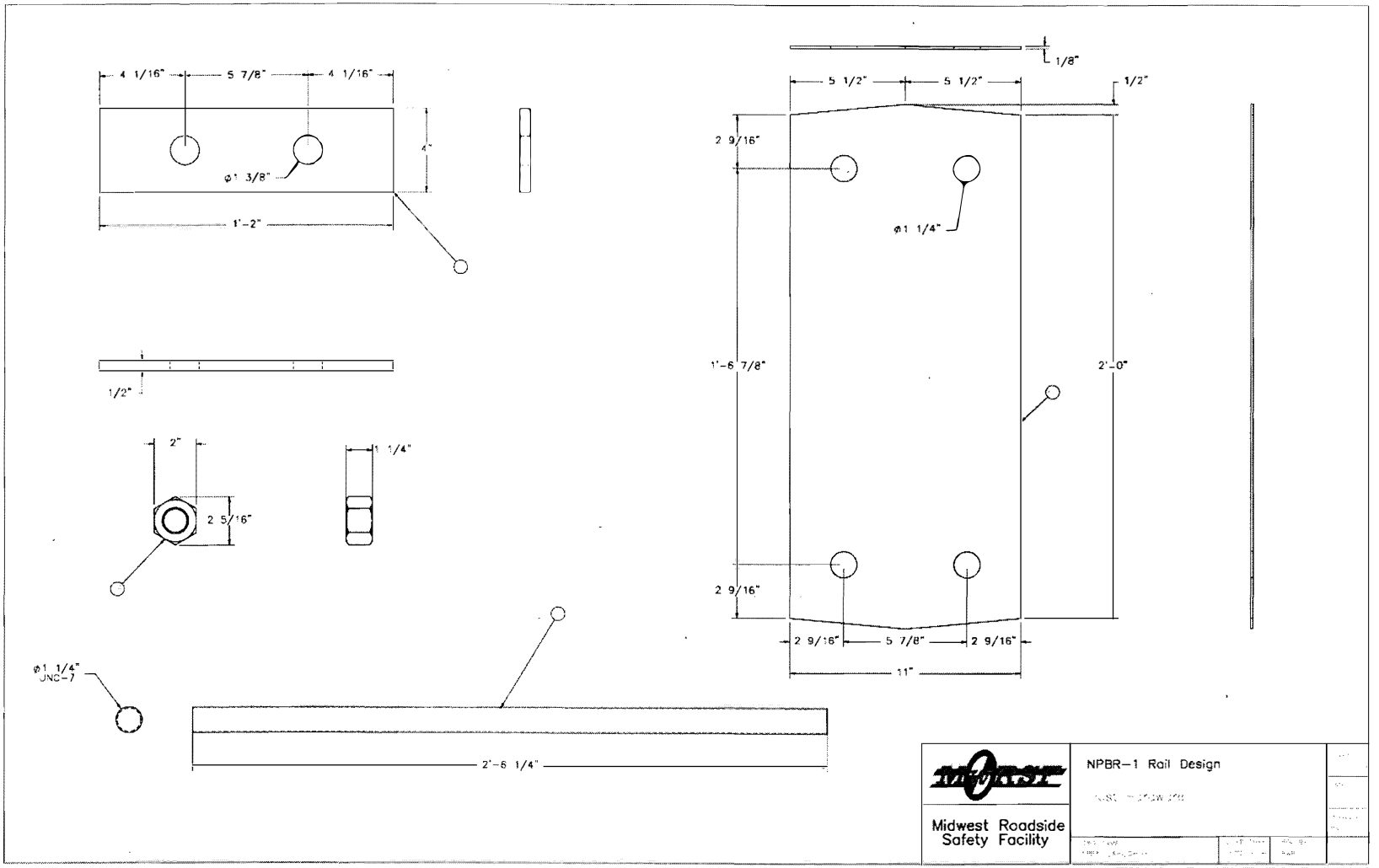

Figure 191. Precast Bridge Rail Segment CAD Details

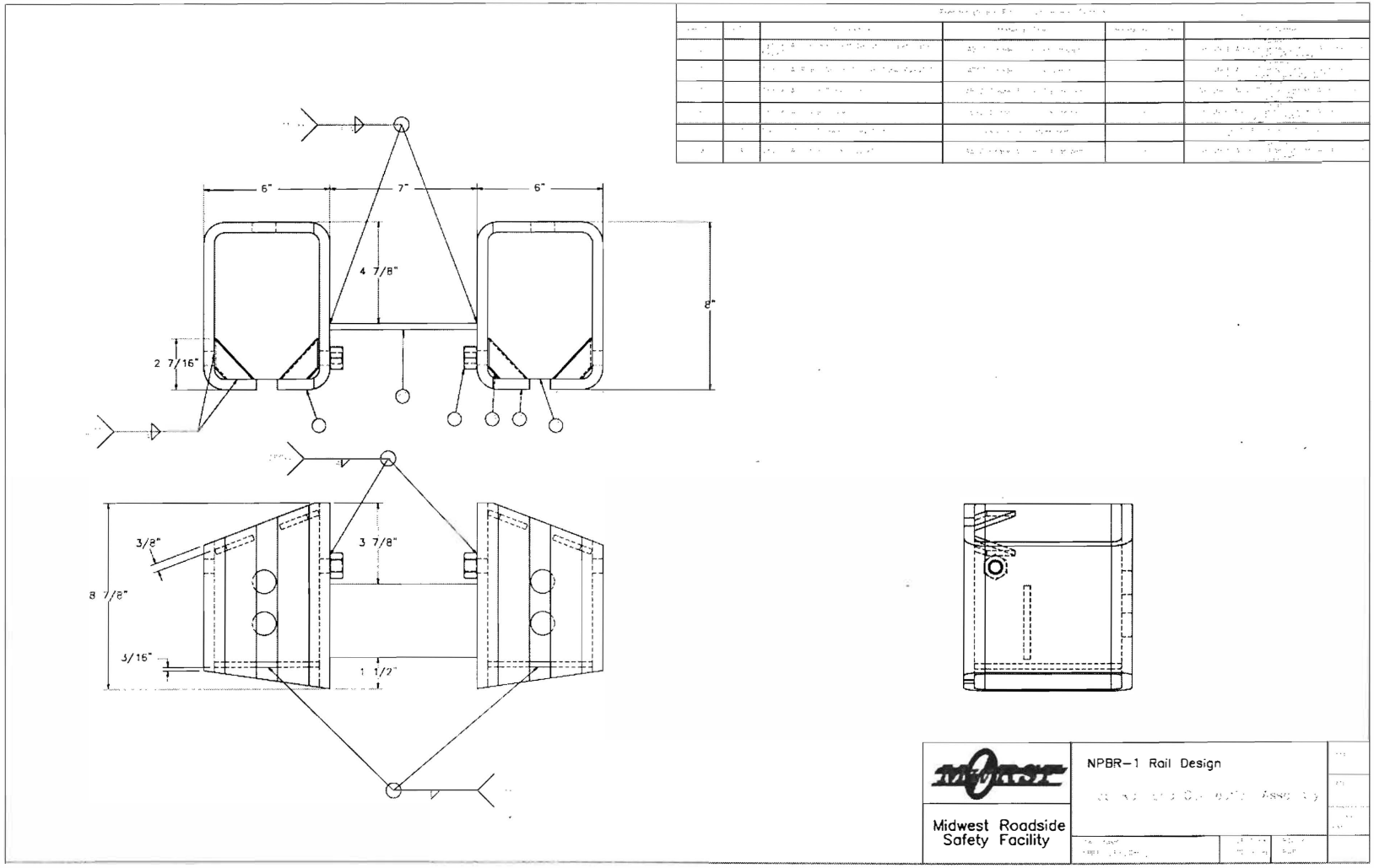

Figure 192. Precast Bridge Rail Segment CAD Details

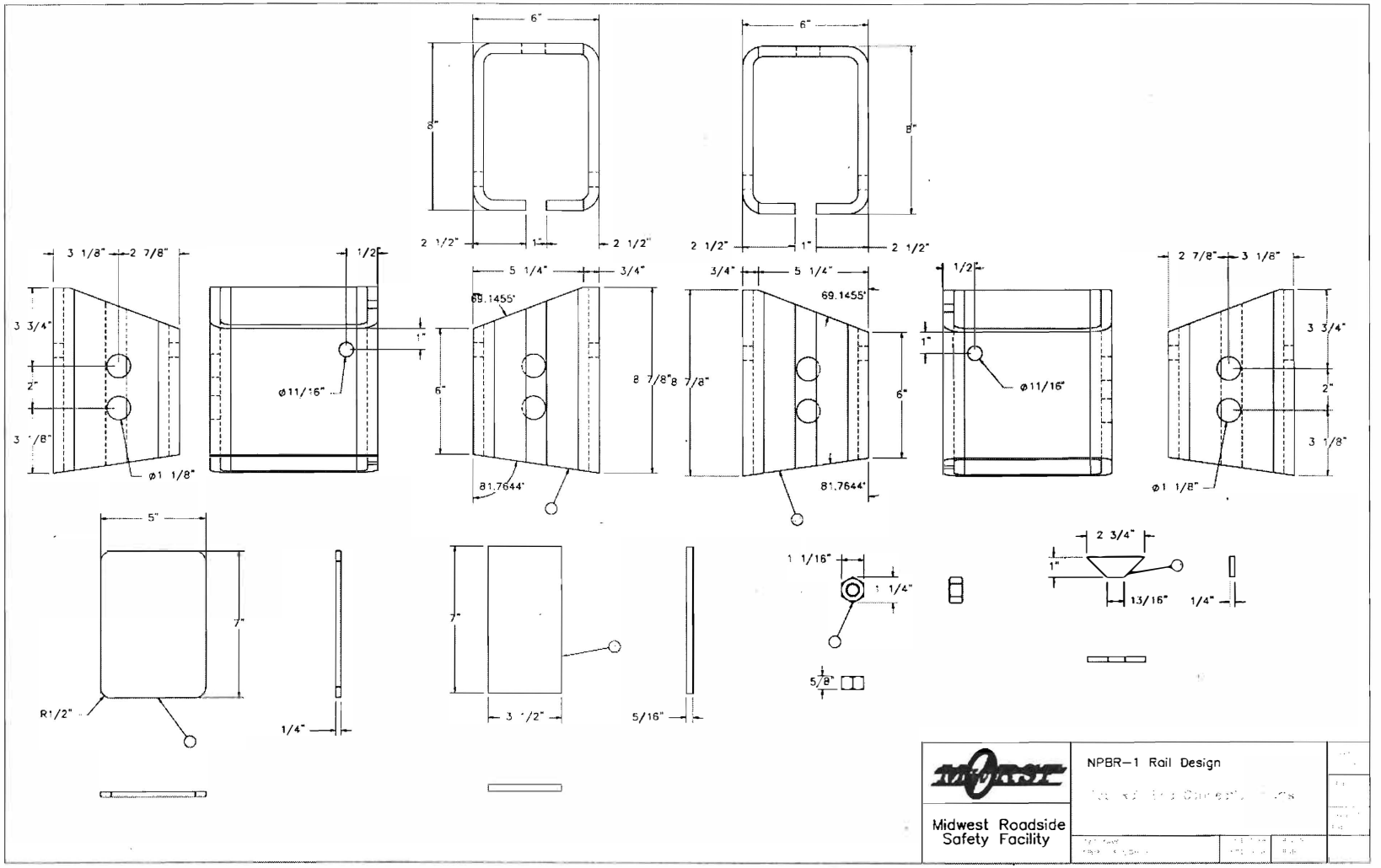

Figure 193. Precast Bridge Rail Segment CAD Details

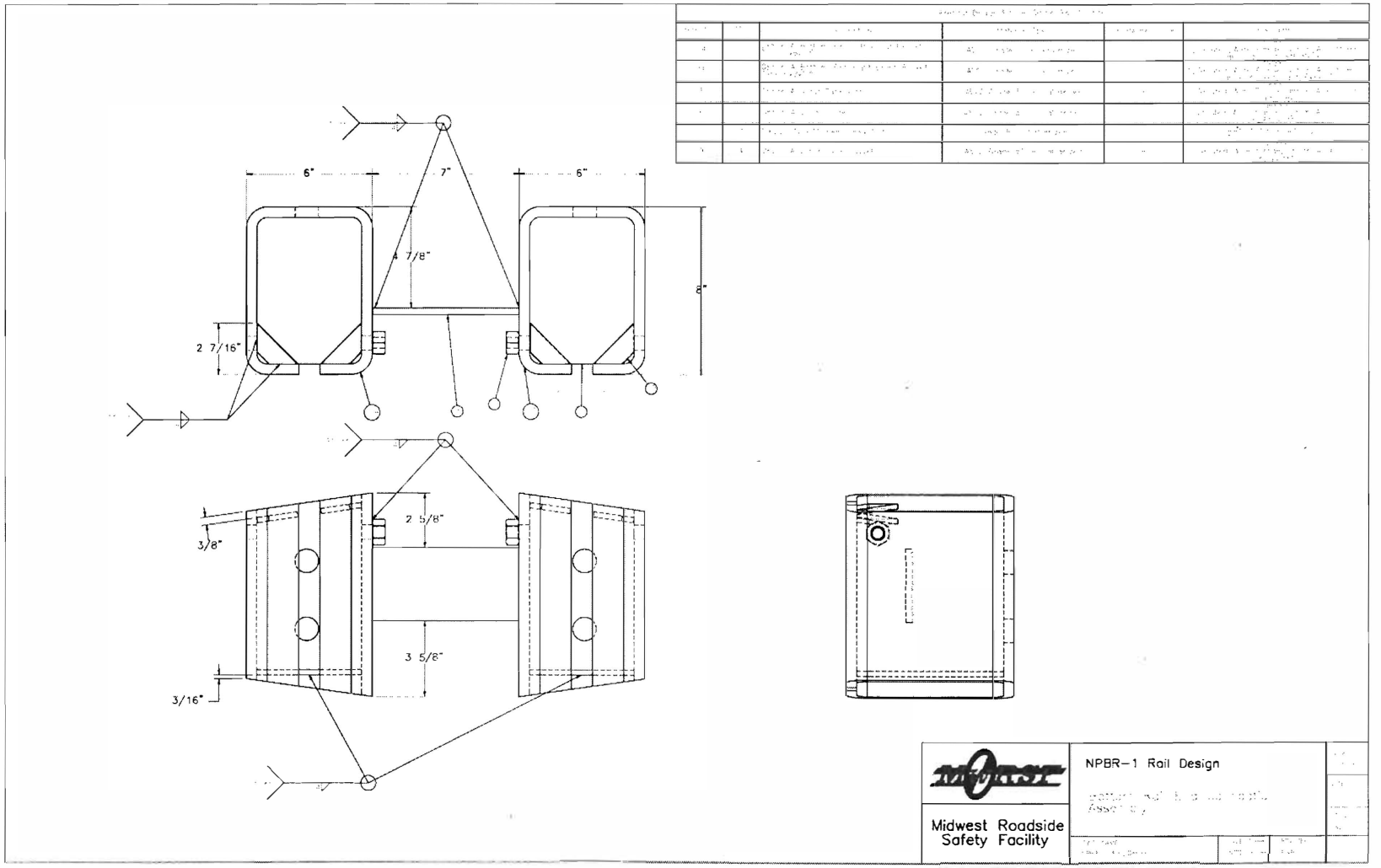

Figure 194. Precast Bridge Rail Segment CAD Details

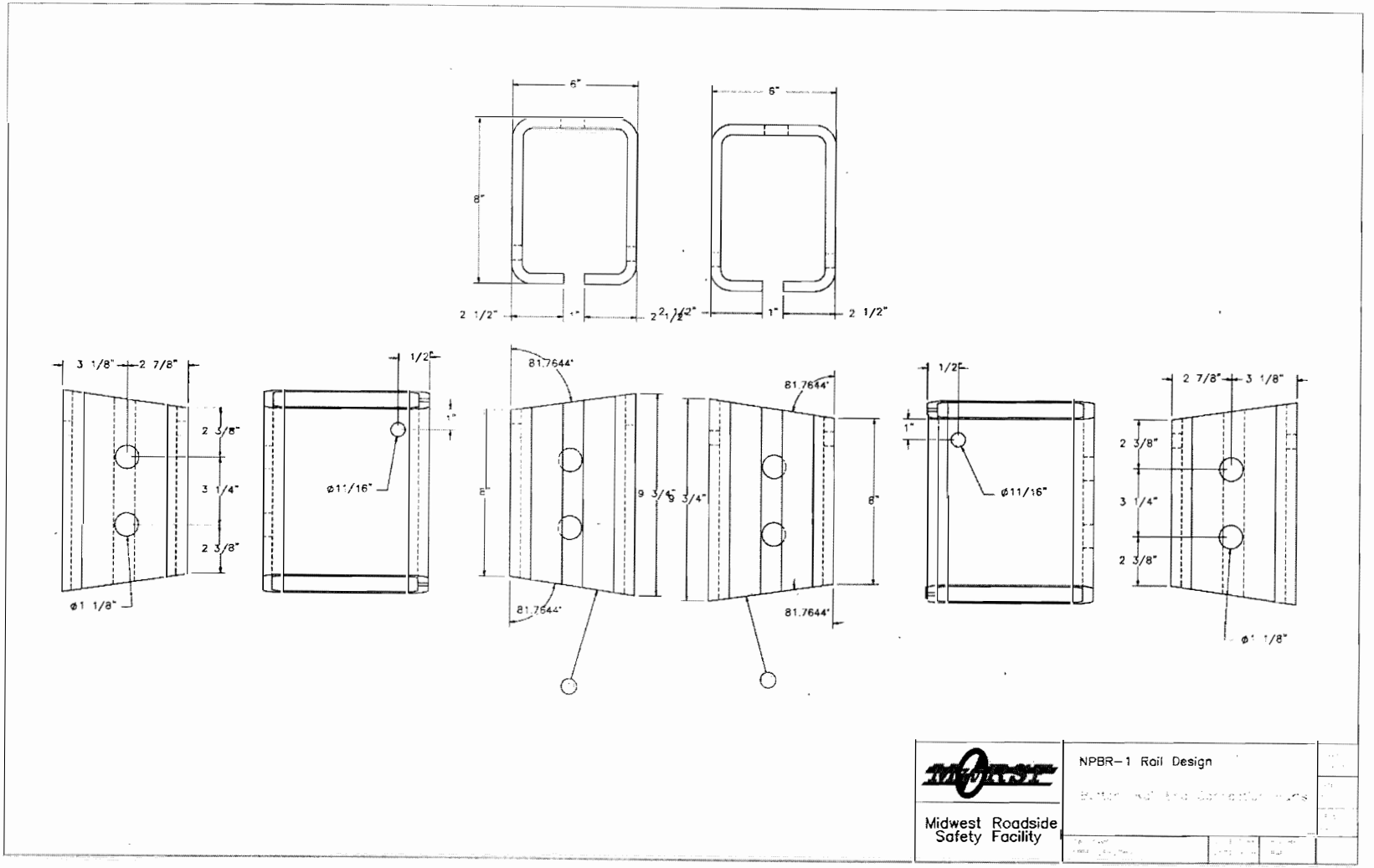

Figure 195. Precast Bridge Rail Segment CAD Details

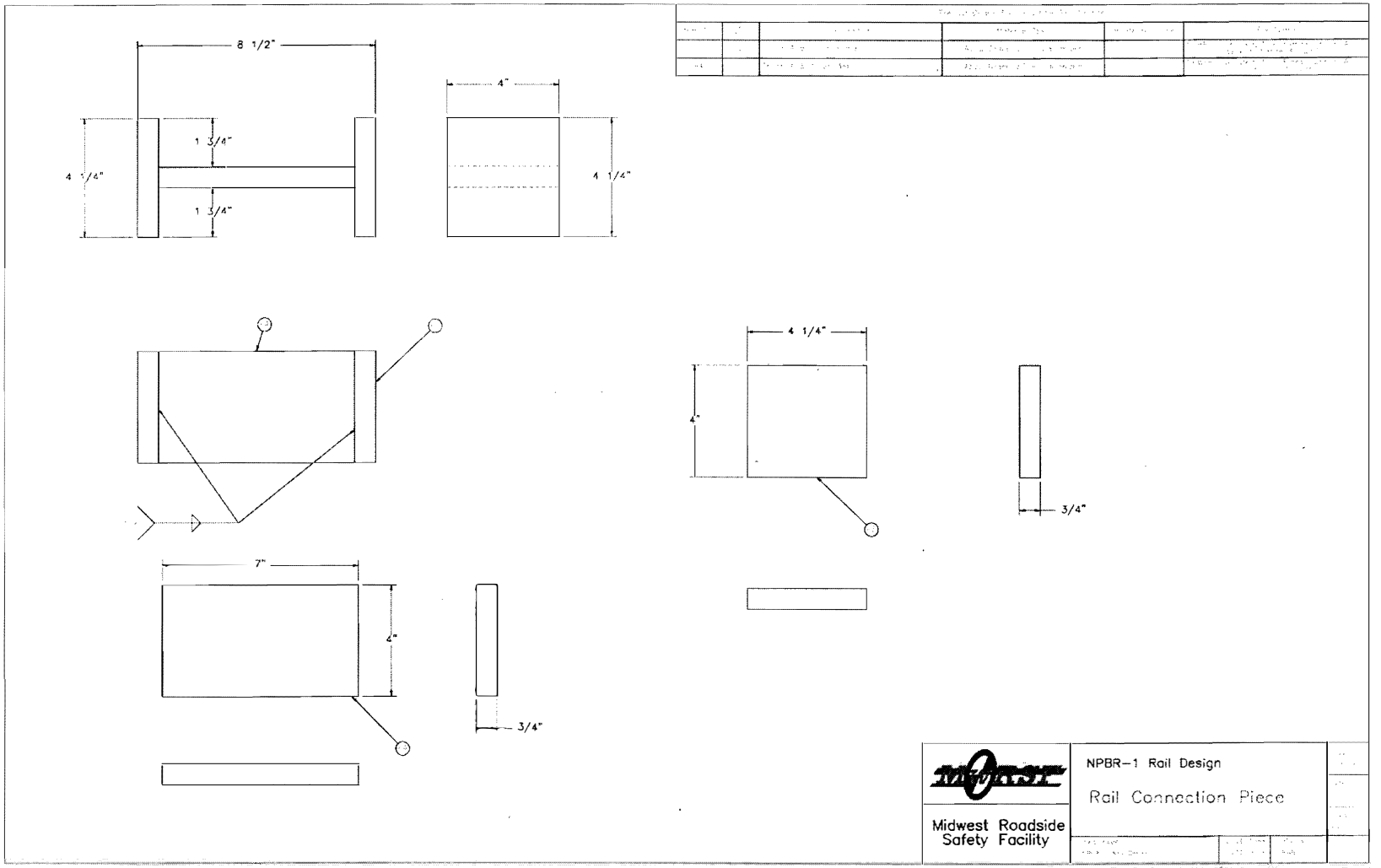

Figure 196. Precast Bridge Rail Segment CAD Details

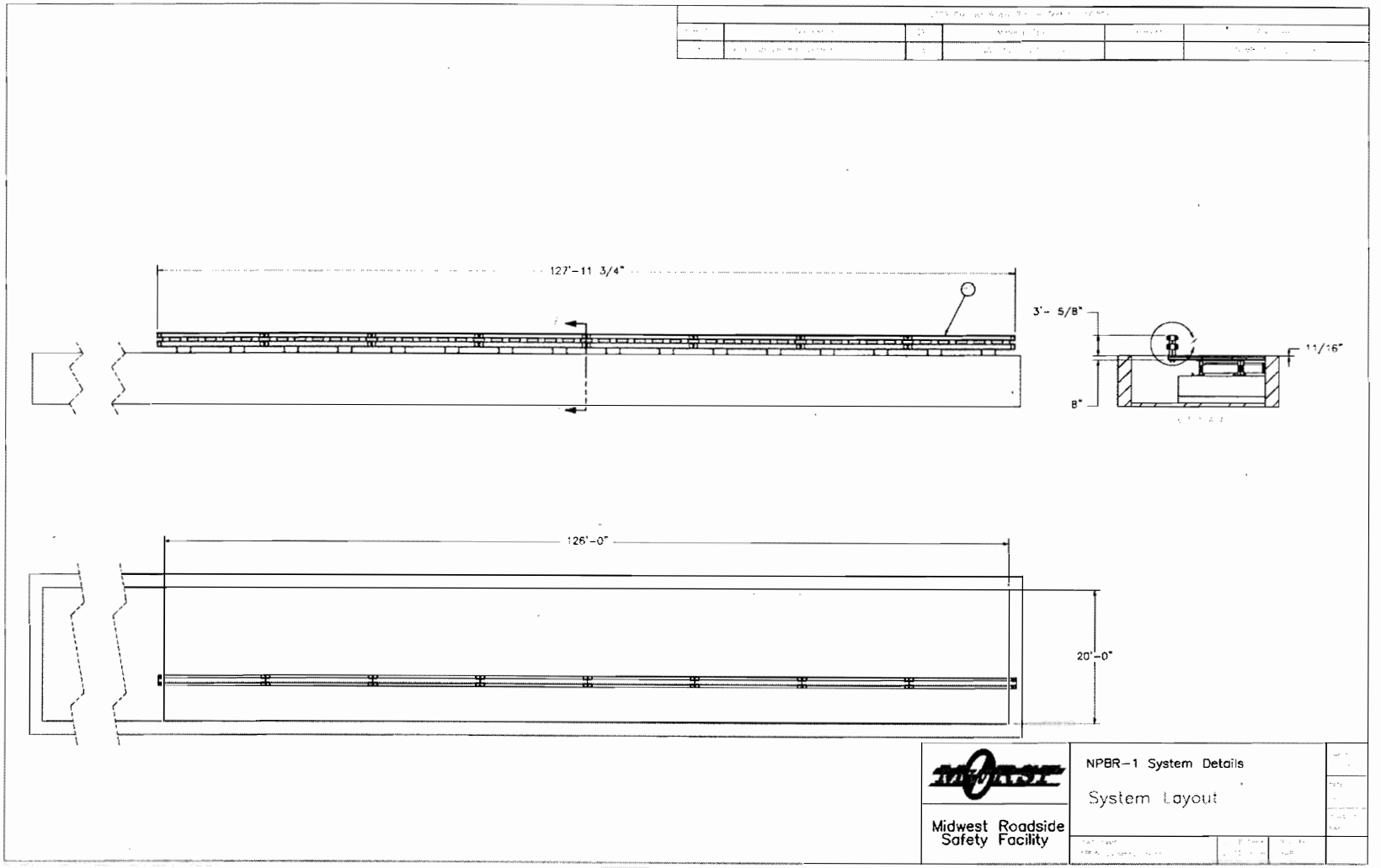

Figure 197. Precast Bridge Rail System Layout

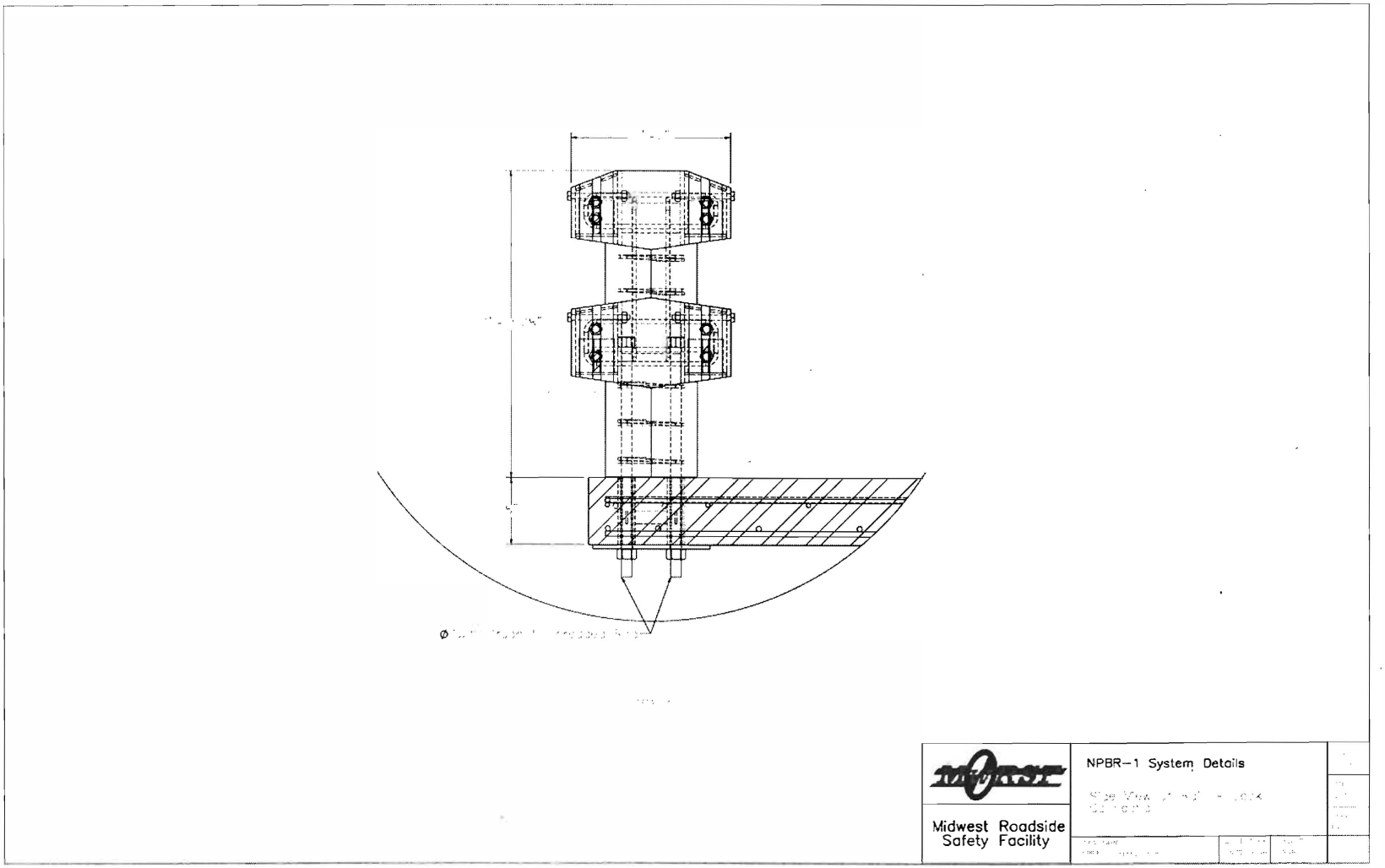

Figure 198. Precast Bridge Rail System Layout

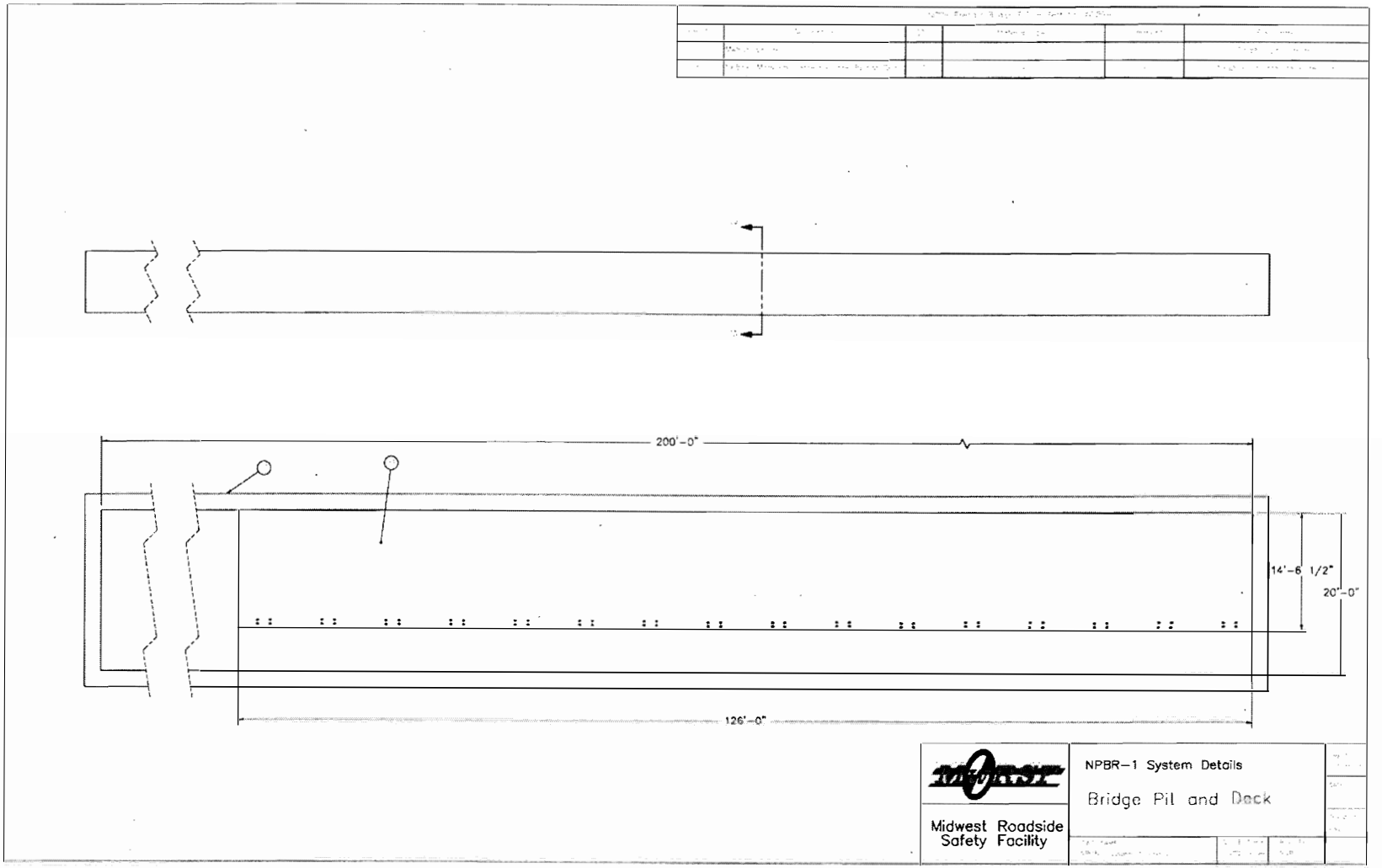

Figure 199. Precast Bridge Rail System Layout

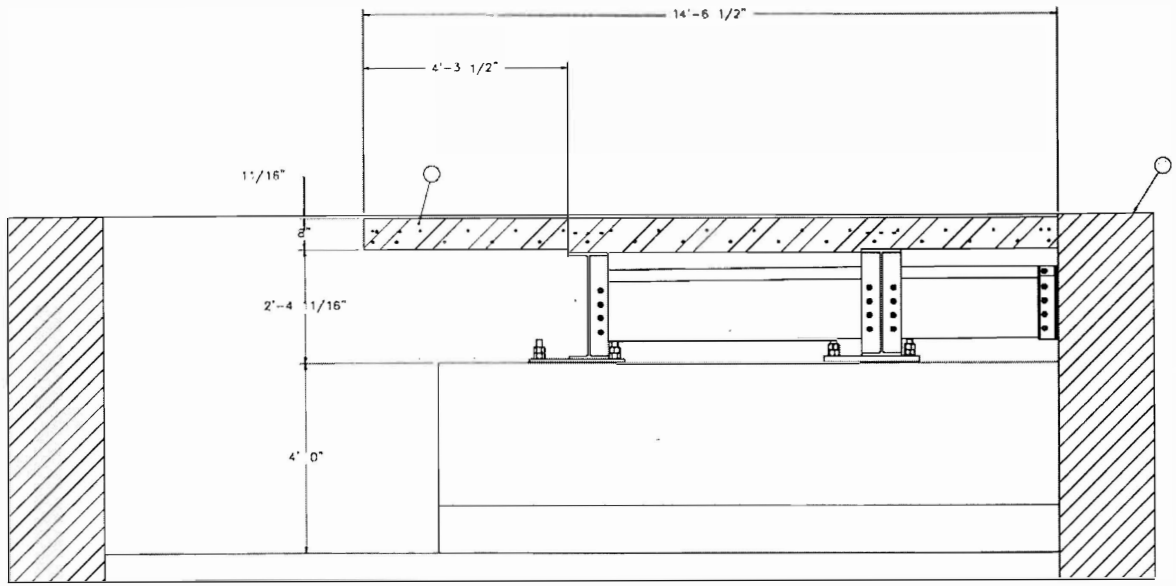

Midwest Roadside Safety Facility

NPBR-1 System Details

Bridge Pit and Deck Cross-Section

Figure 200. Precast Bridge Rail System Layout

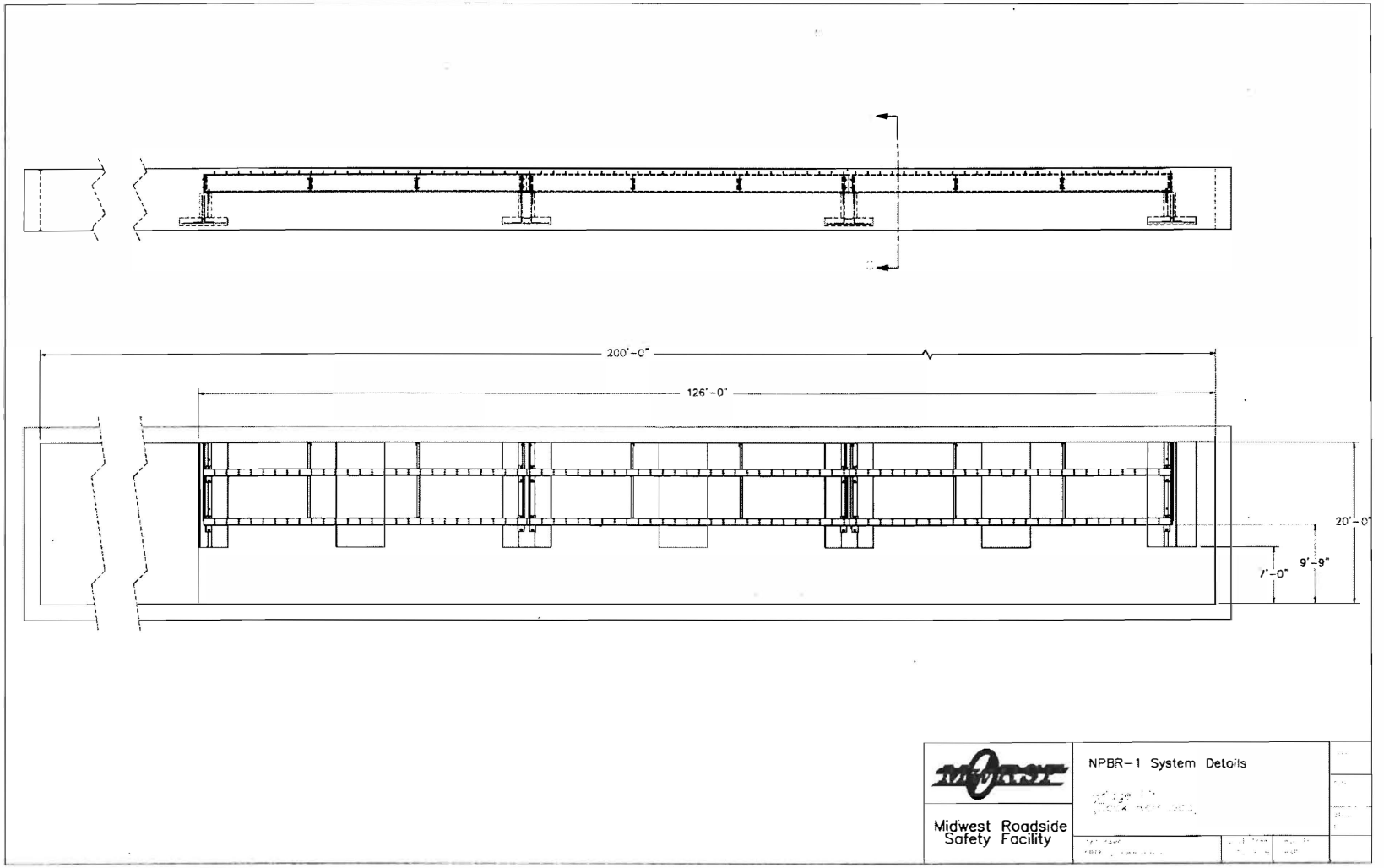

Figure 201. Precast Bridge Rail System Layout

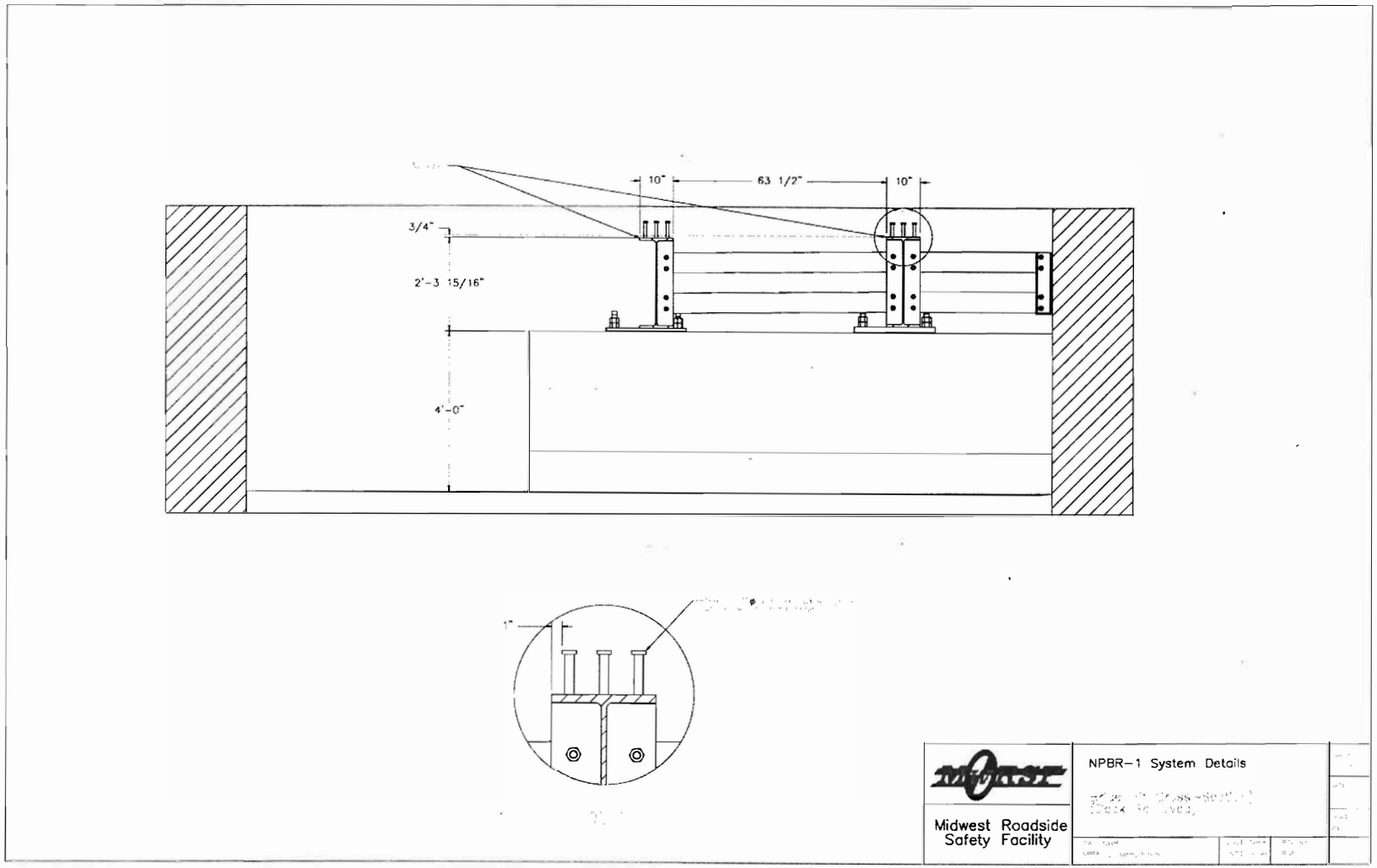

Figure 202. Precast Bridge Rail System Layout

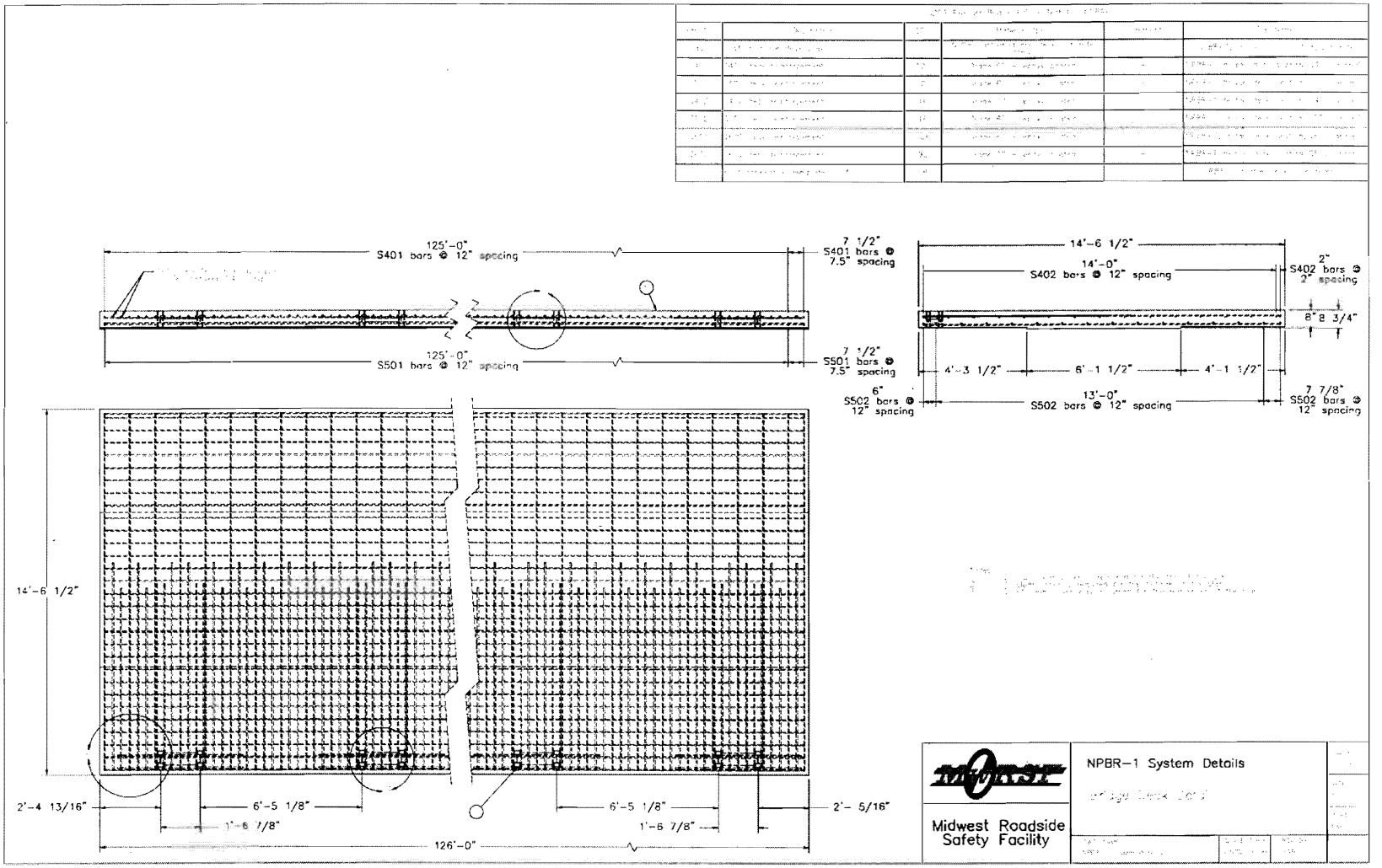

Figure 203. Precast Bridge Rail System Layout

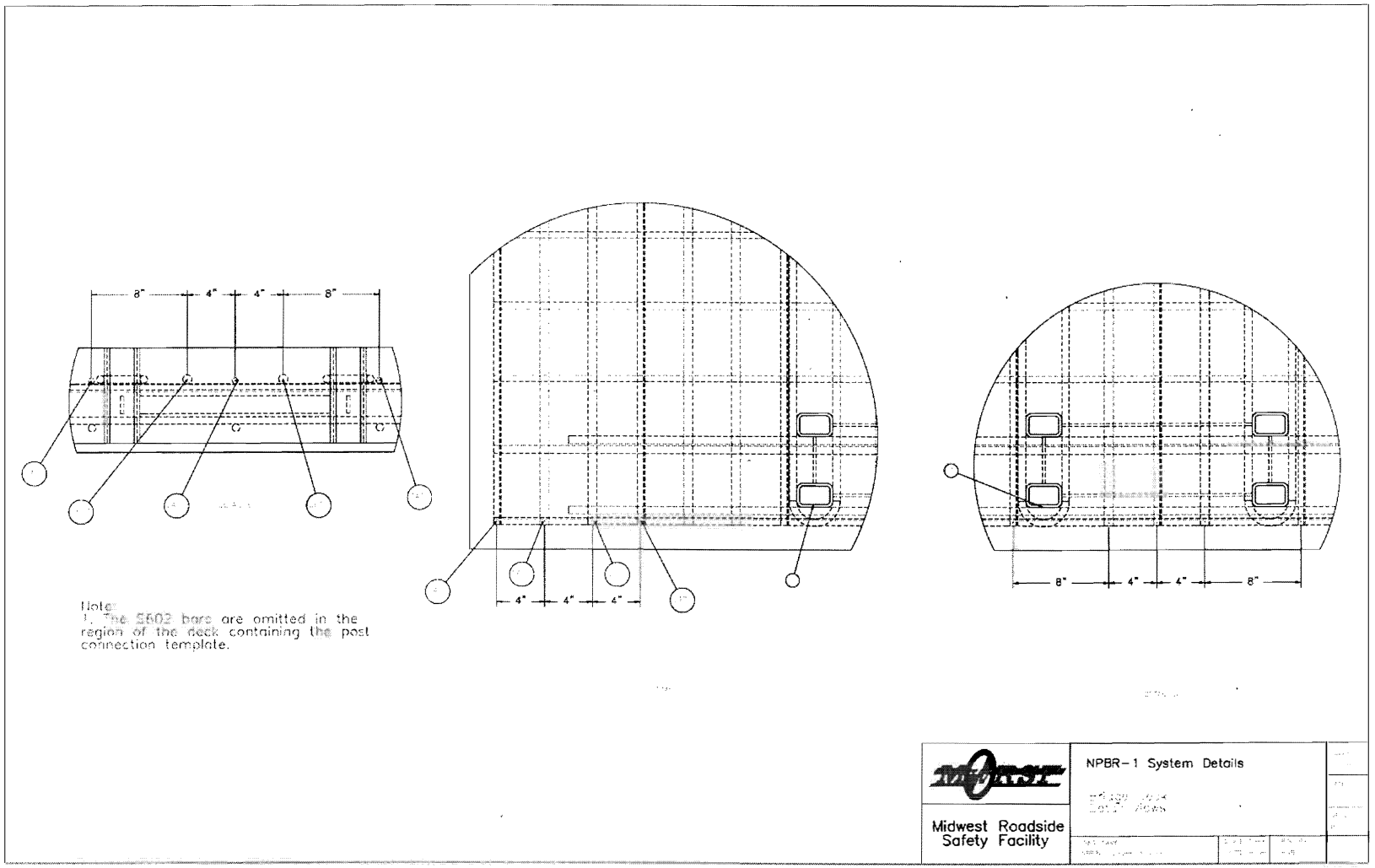

Figure 204. Precast Bridge Rail System Layout

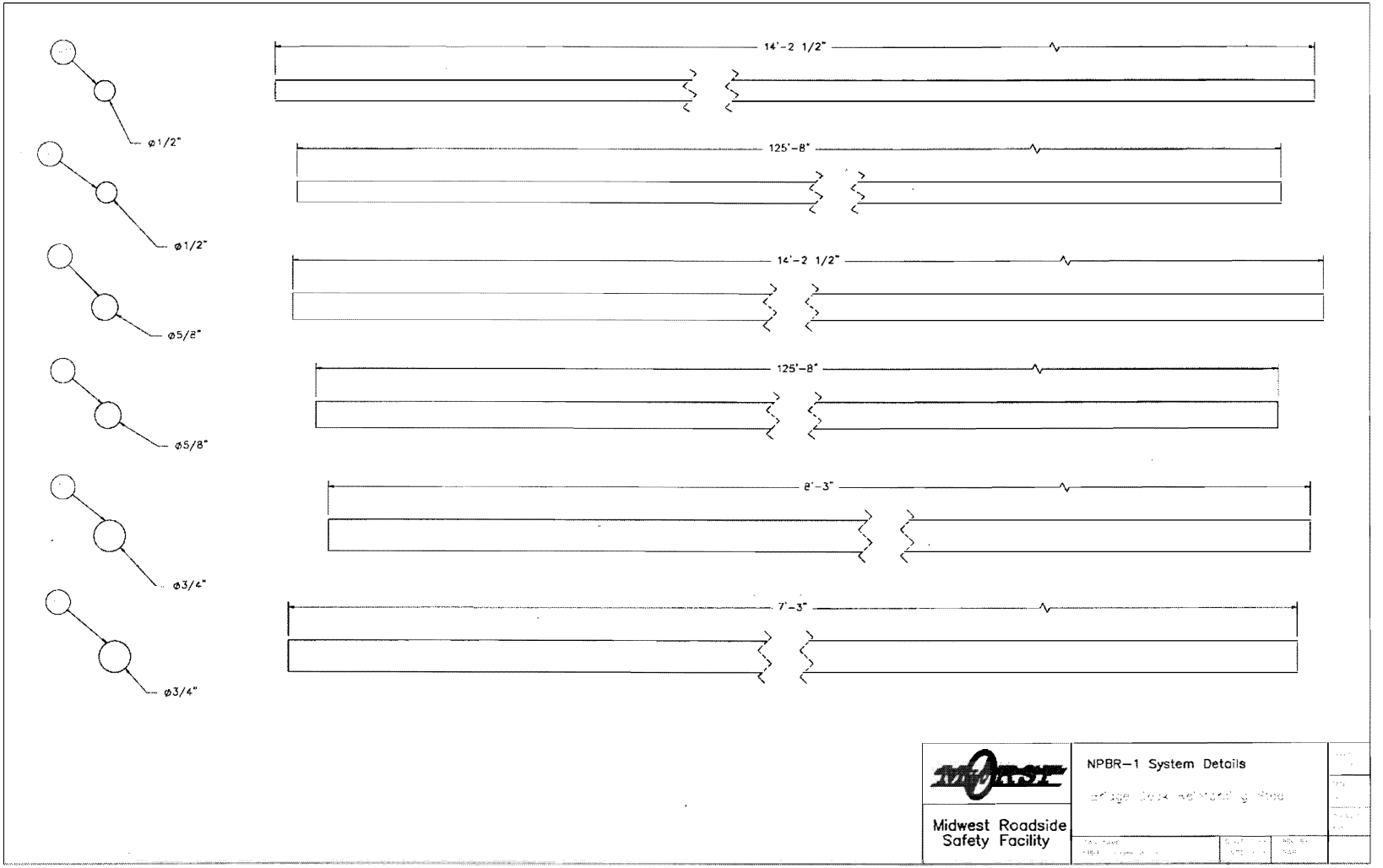

Figure 205. Precast Bridge Rail System Layout

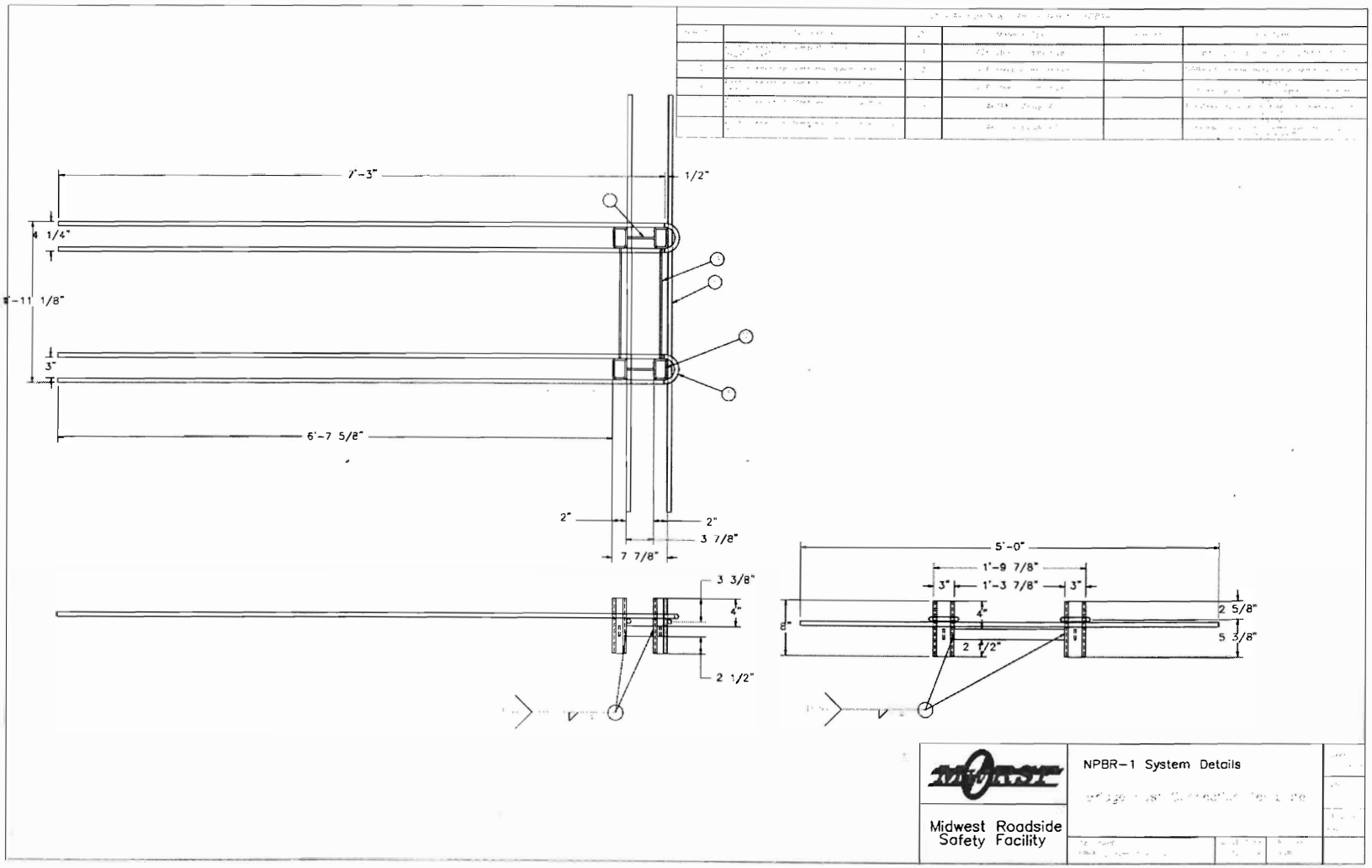

Figure 206. Precast Bridge Rail System Layout

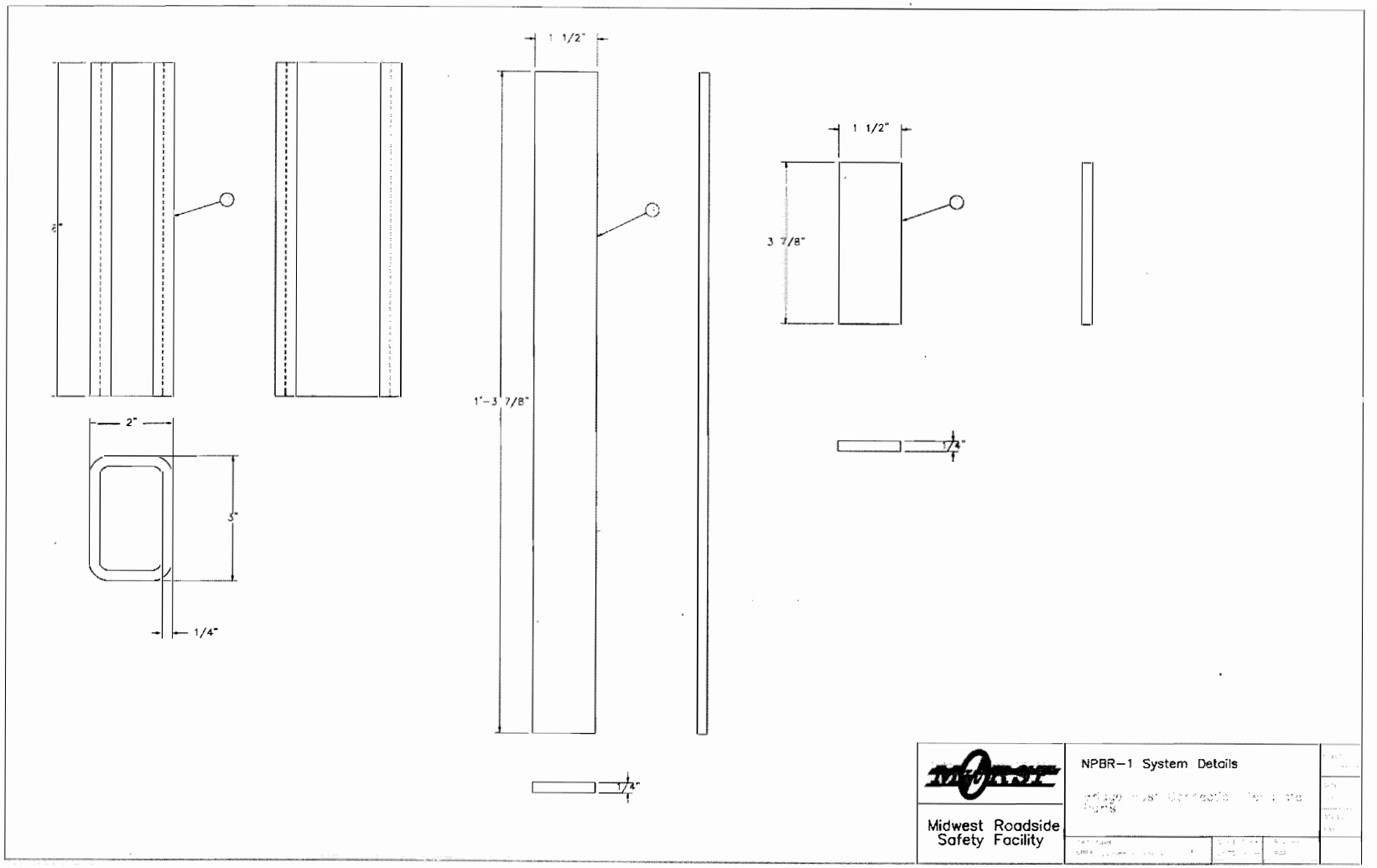

Figure 207. Precast Bridge Rail System Layout

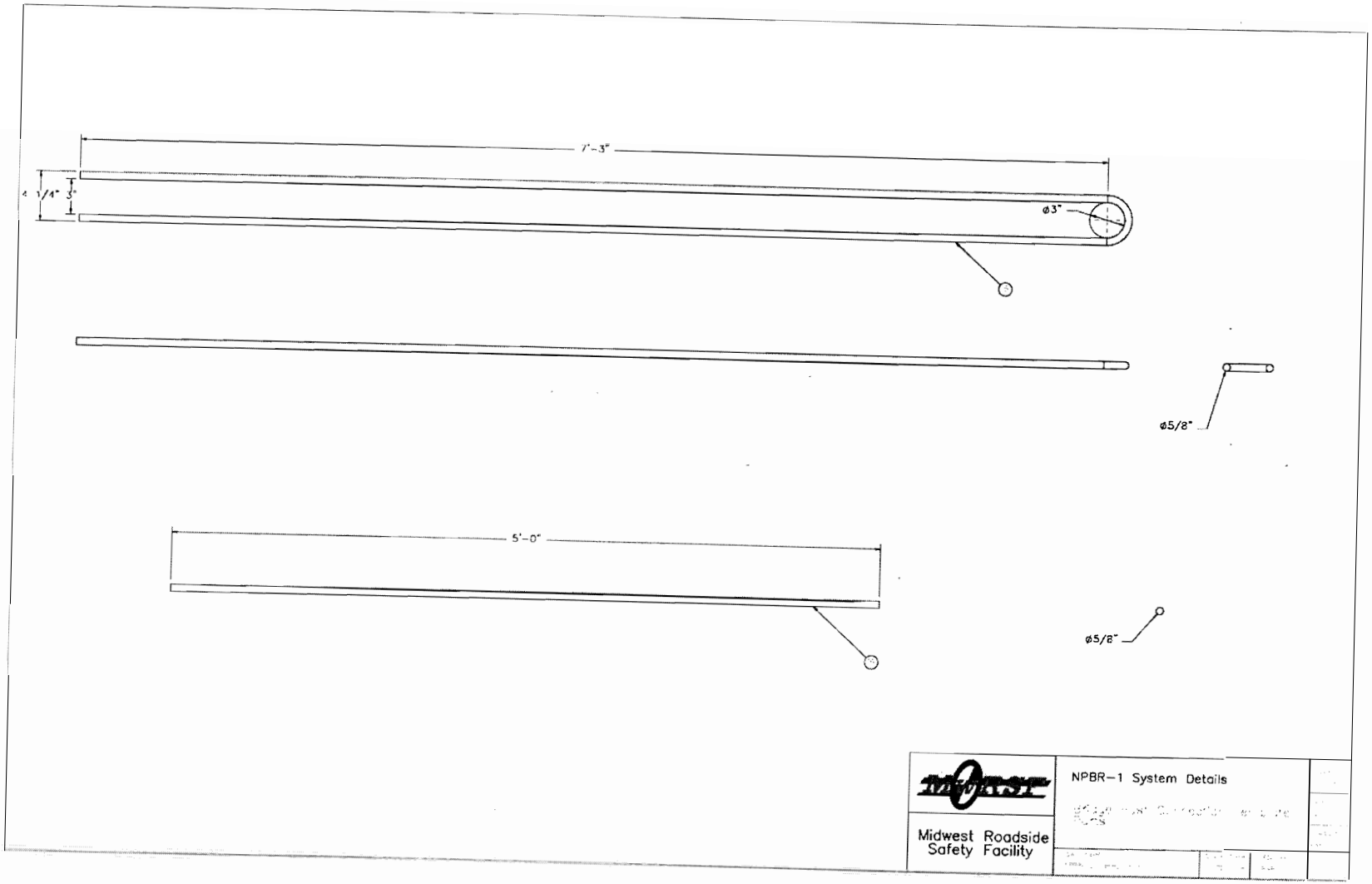

Figure 208. Precast Bridge Rail System Layout

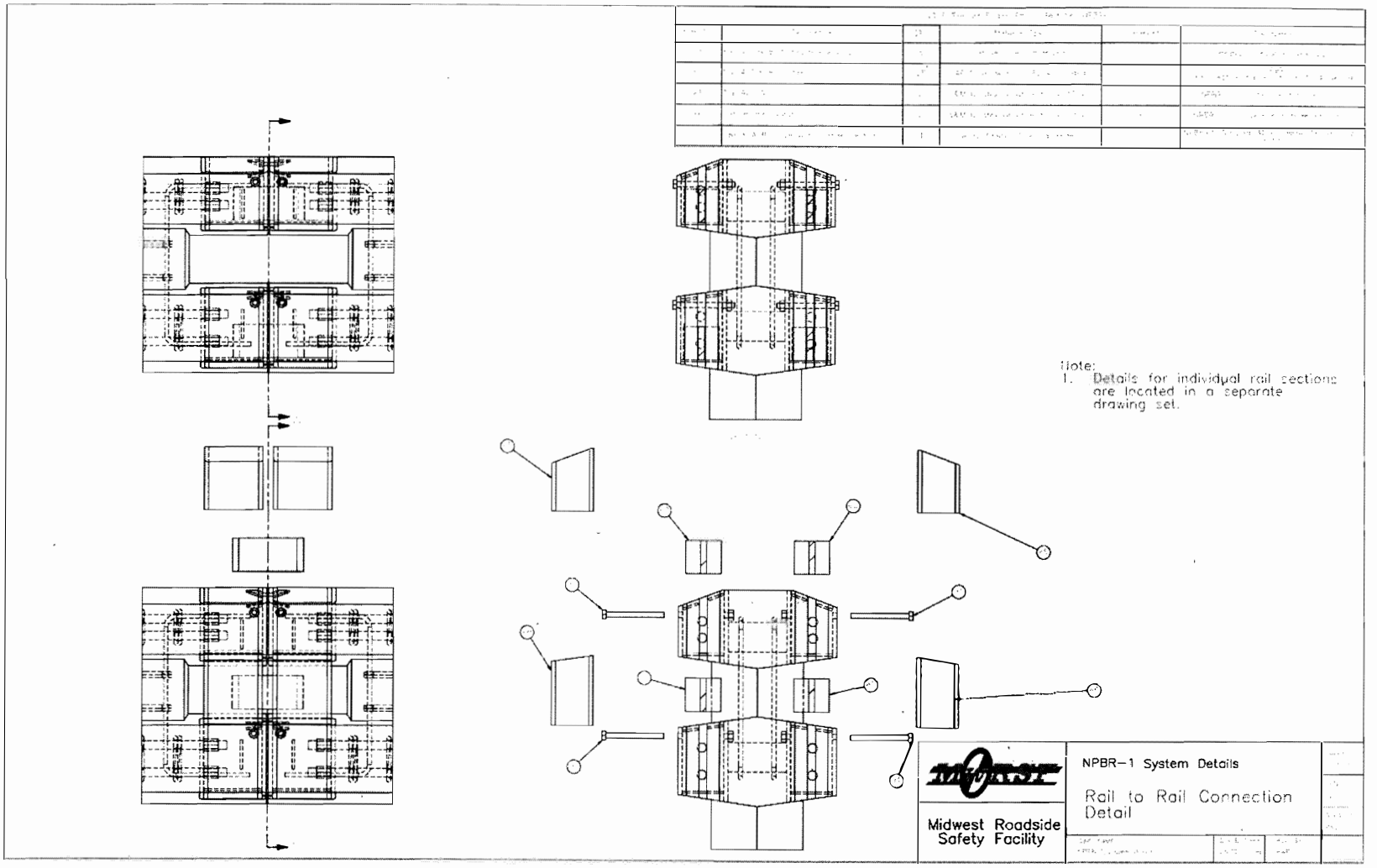

Figure 209. Precast Bridge Rail System Layout

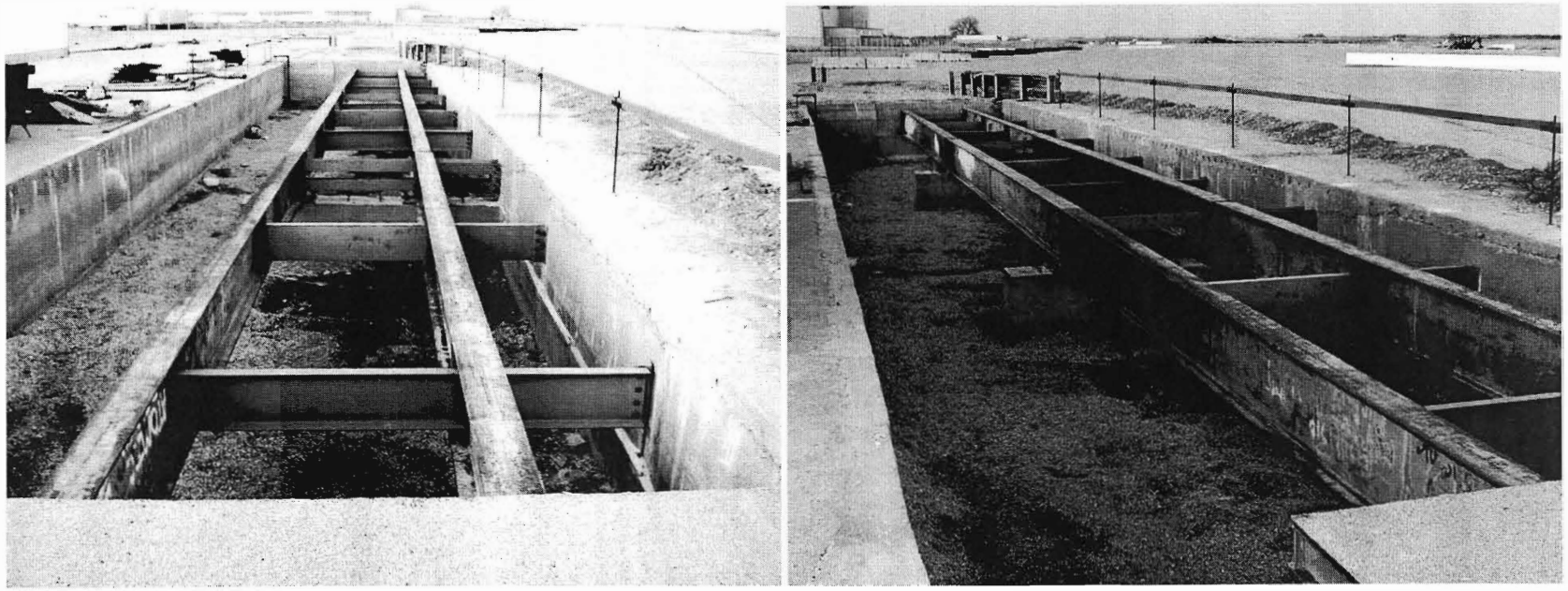

Figure 210. MwRSF Simulated Bridge Test Pit

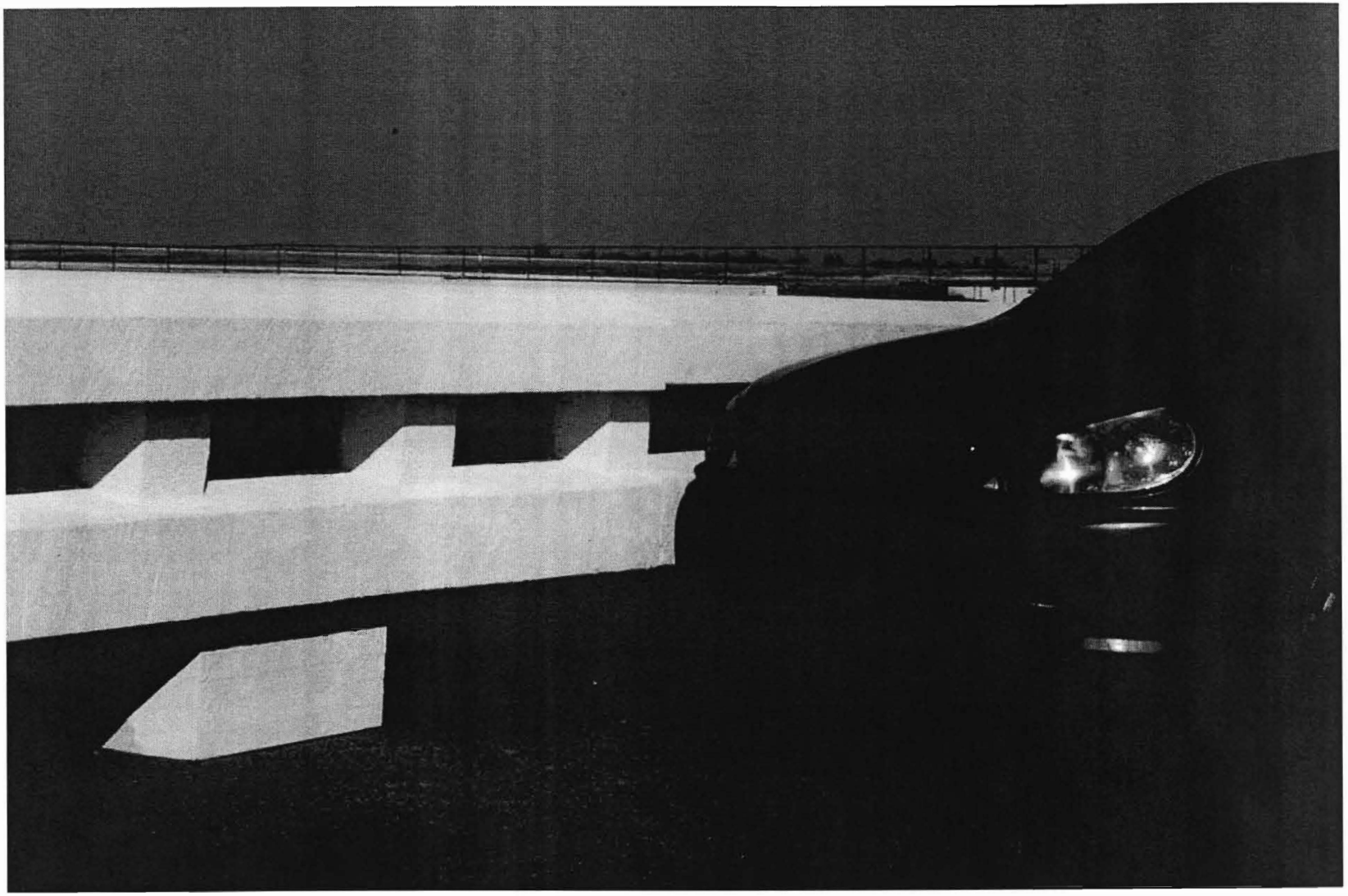

Figure 211. Precast Bridge Rail Foam Model with 1100C Vehicle

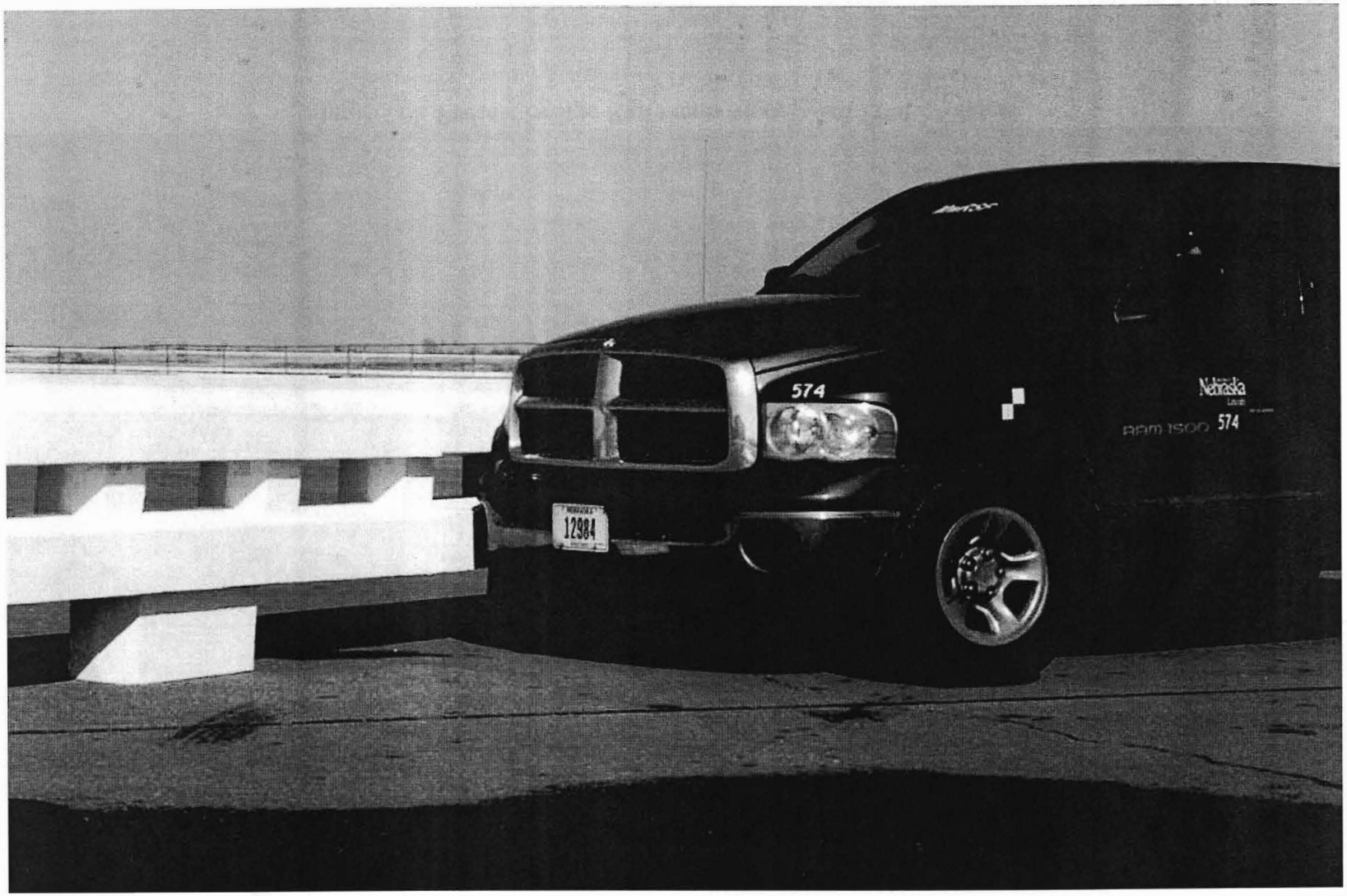

Figure 212. Precast Bridge Rail Foam Model with 2270P Vehicle

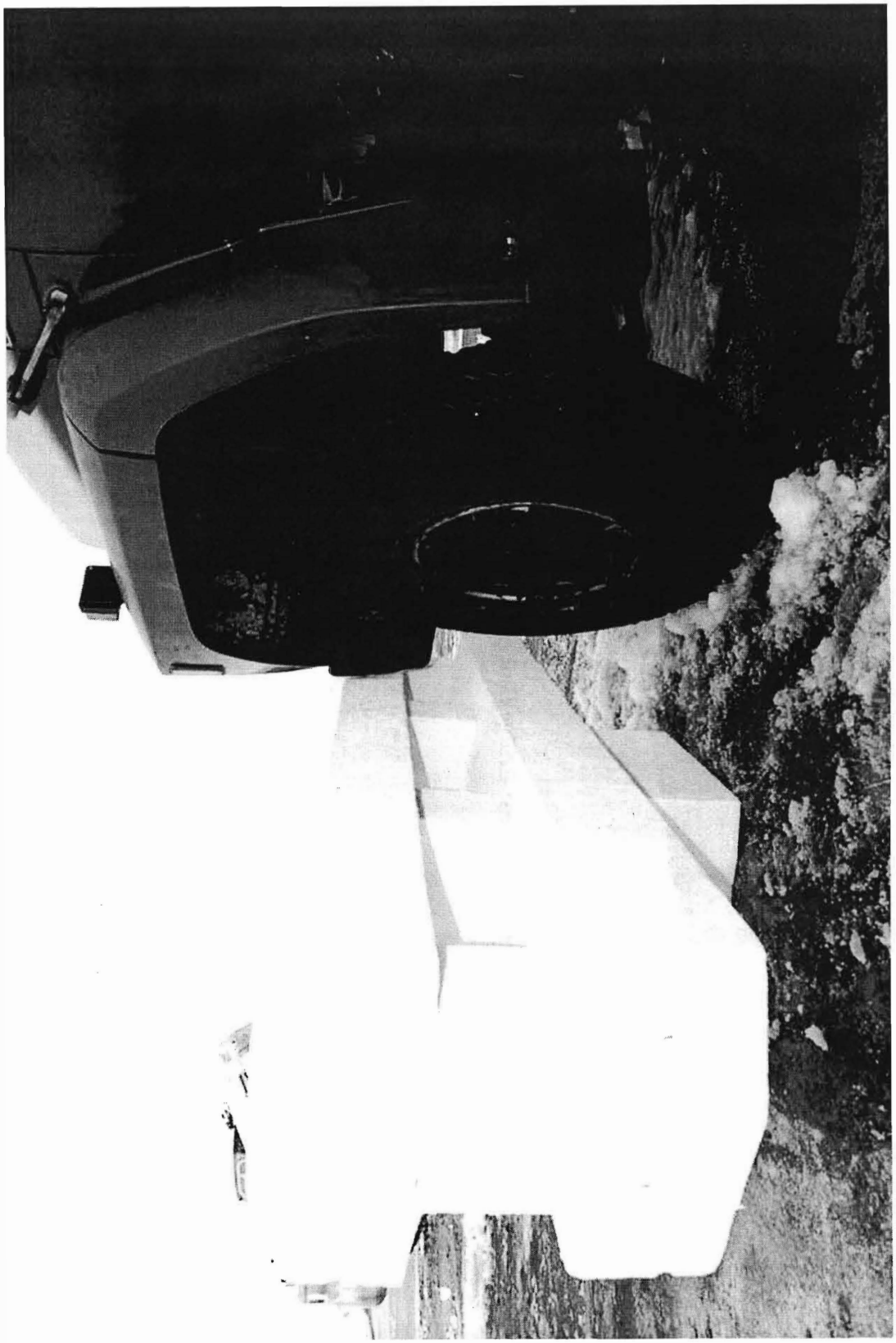

Figure 213. Precast Bridge Rail Foam Model with 10000S Vehicle

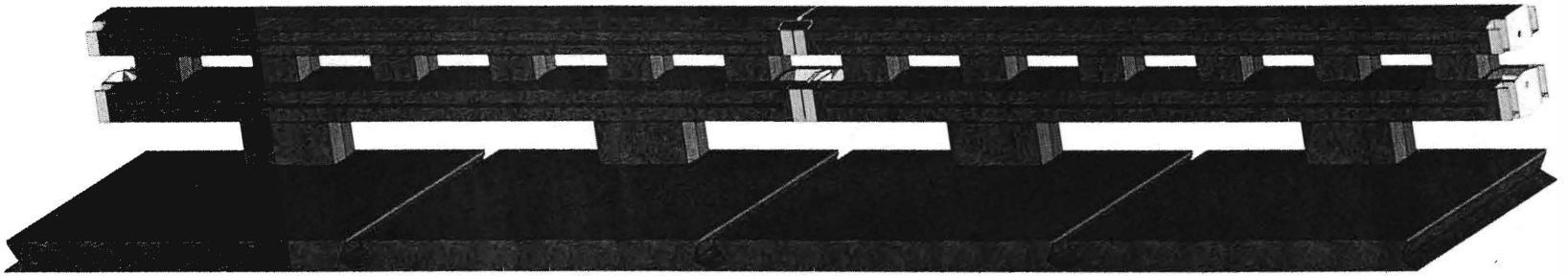

Figure 214. Precast Bridge Rail Aesthetic Treatment Concepts

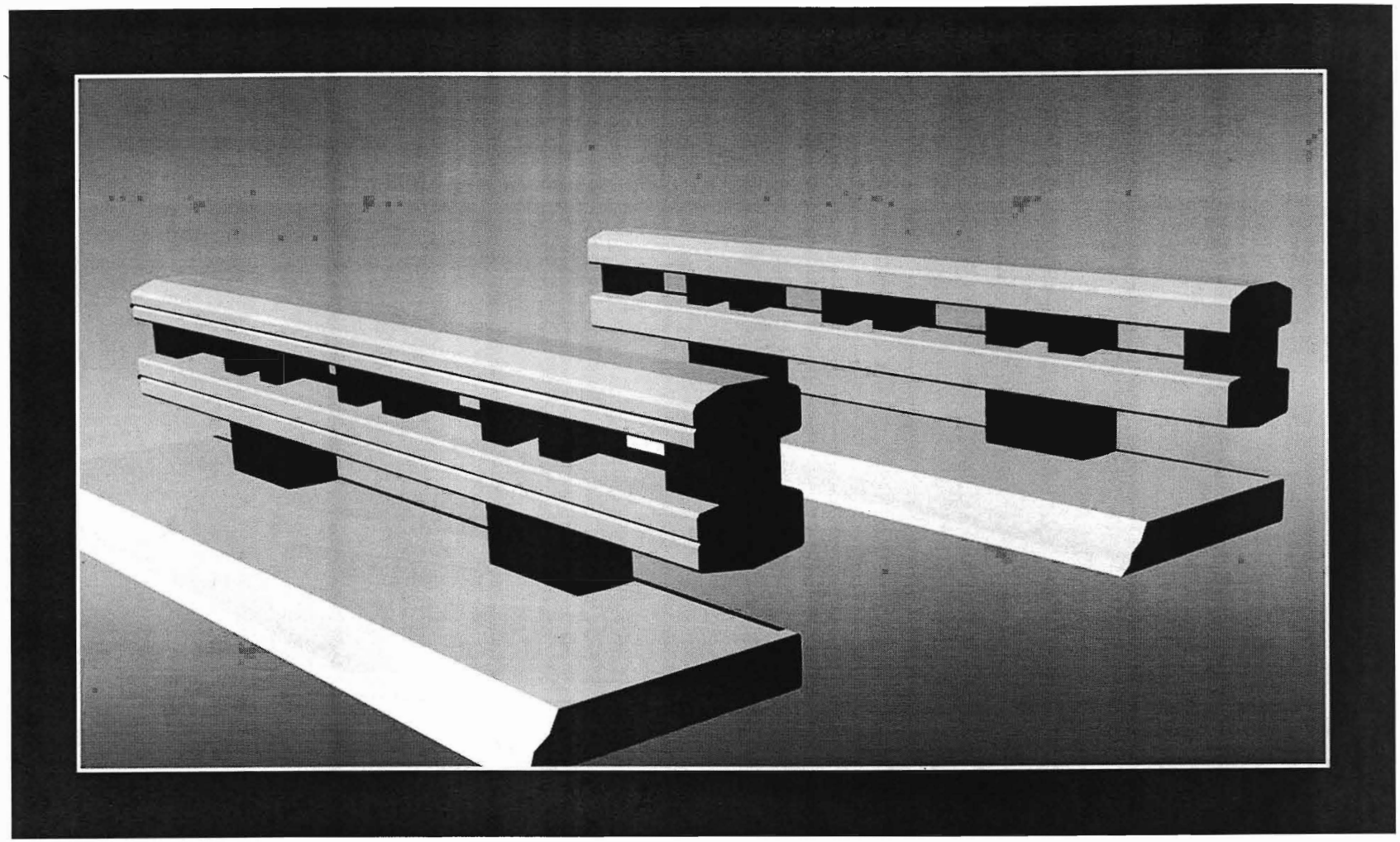

Figure 215. Precast Bridge Rail Aesthetic Treatment Concepts

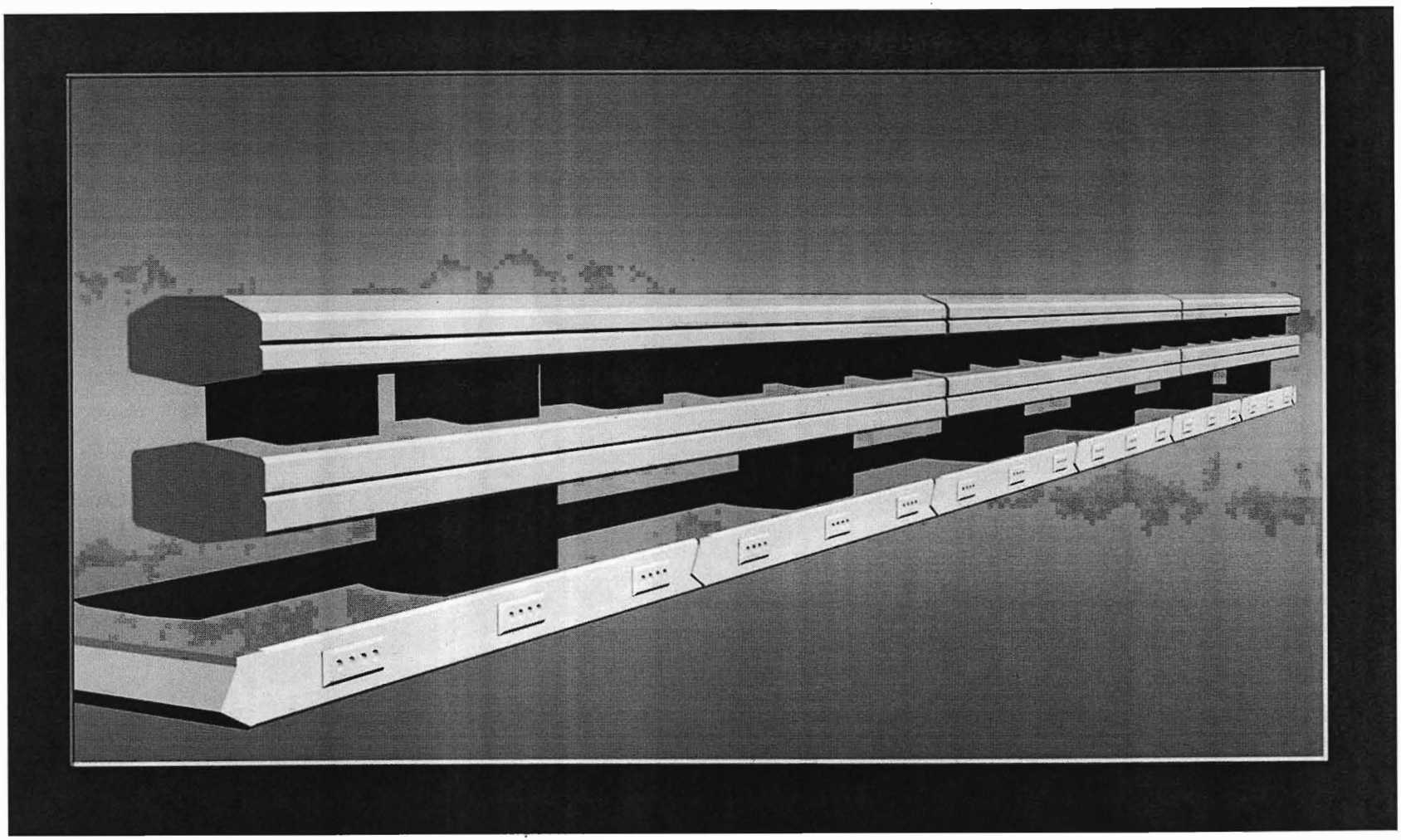

Figure 216. Precast Bridge Rail Aesthetic Treatment Concepts

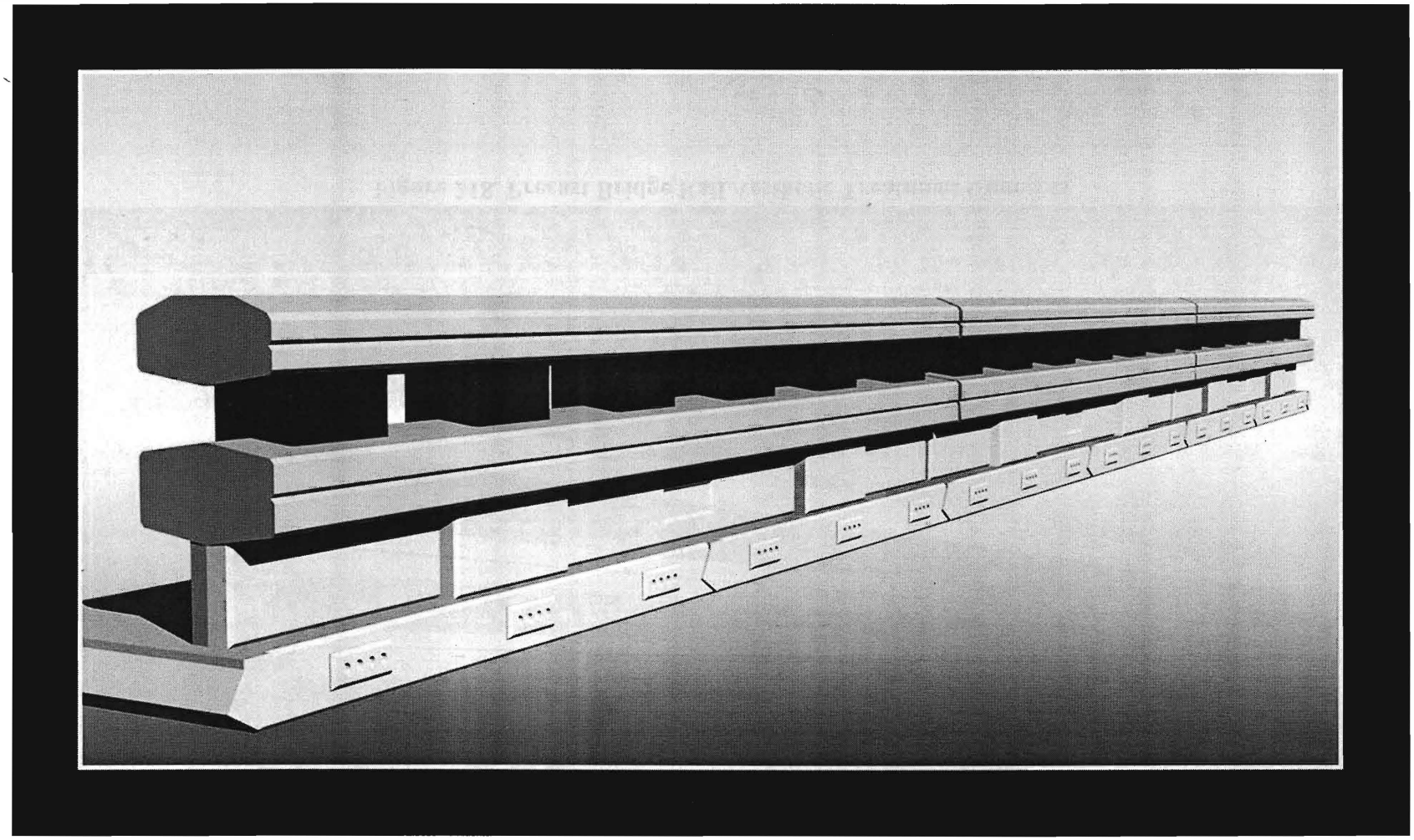

Figure 217. Precast Bridge Rail Aesthetic Treatment Concepts

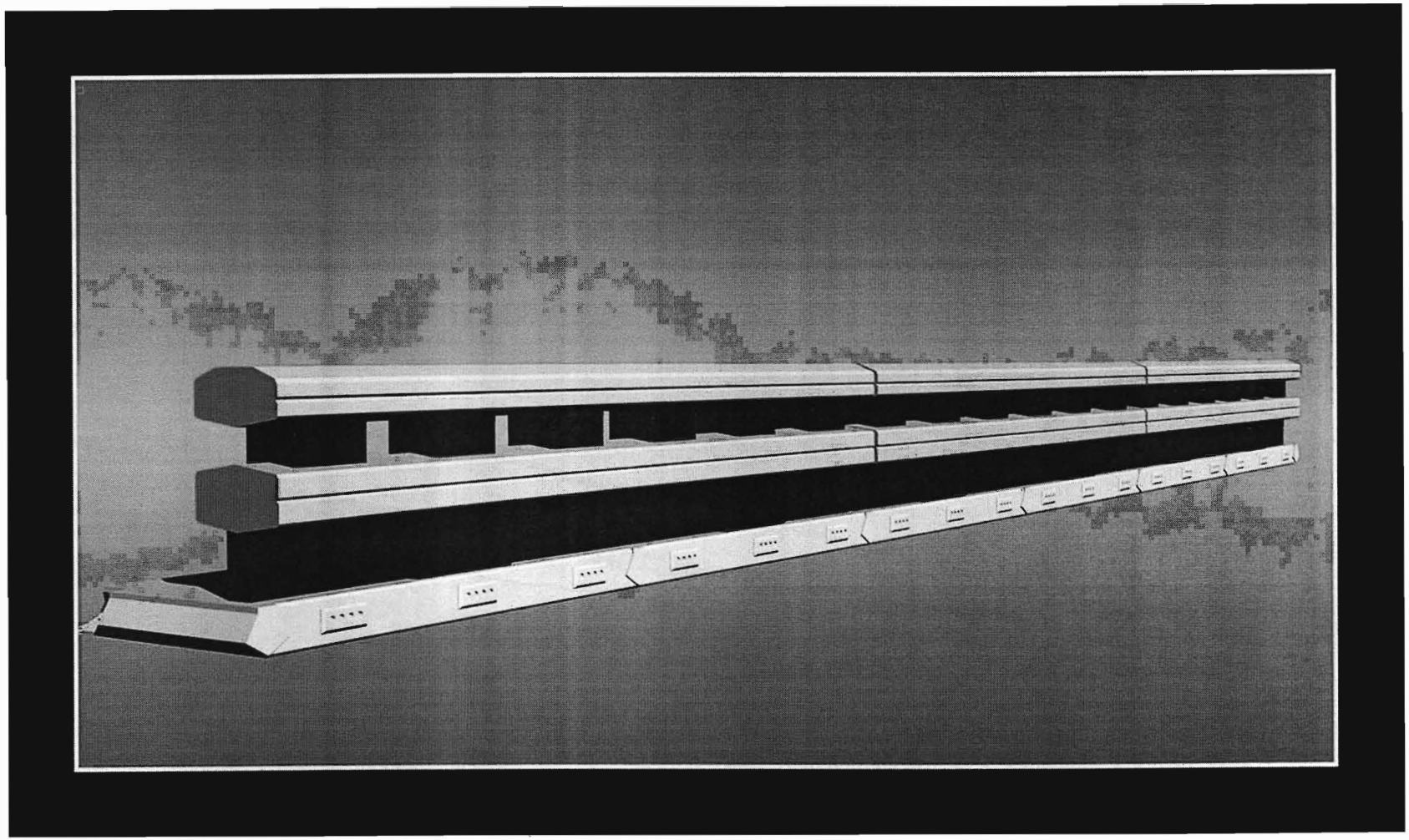

Figure 218. Precast Bridge Rail Aesthetic Treatment Concepts

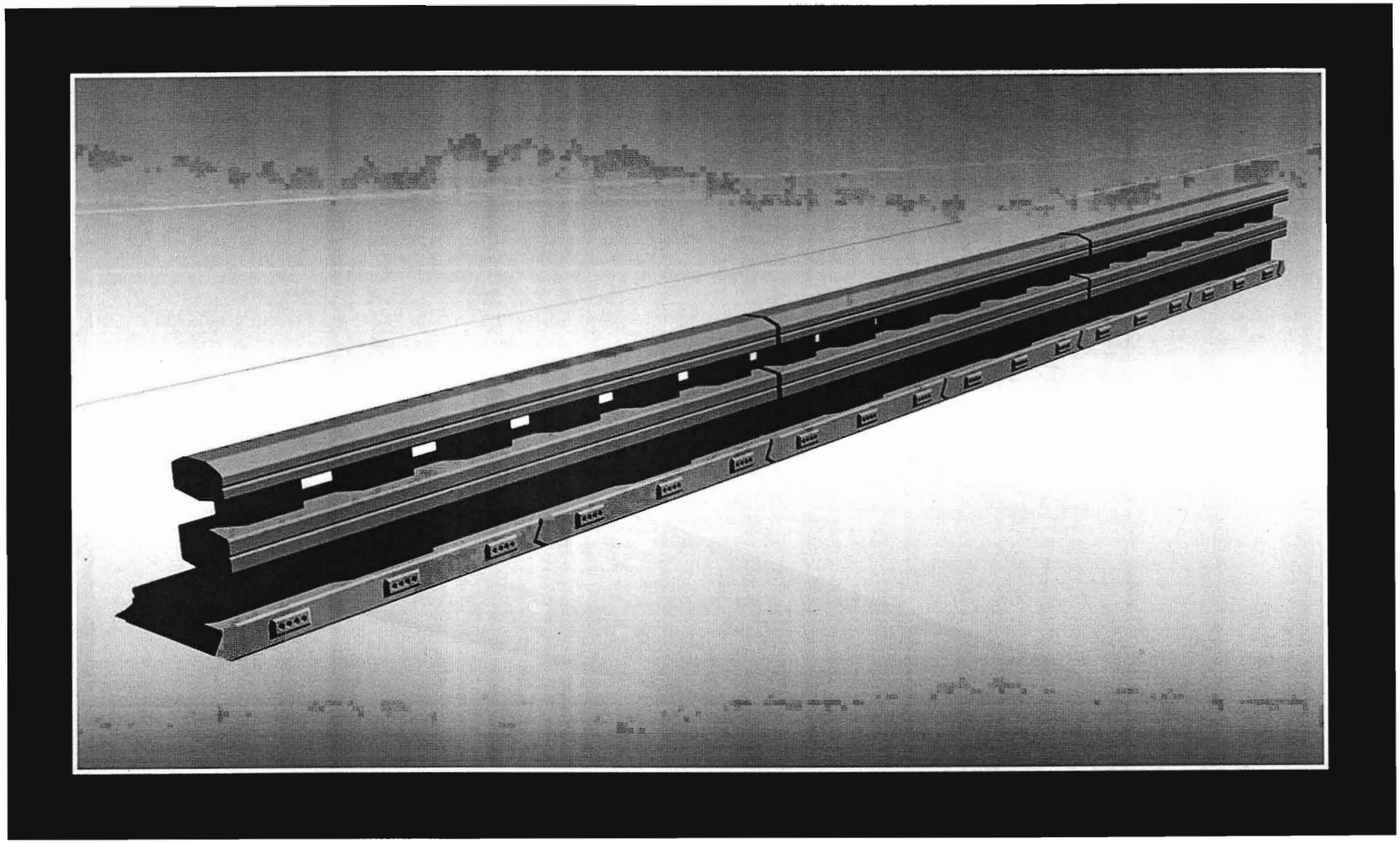

Figure 219. Precast Bridge Rail Aesthetic Treatment Concepts

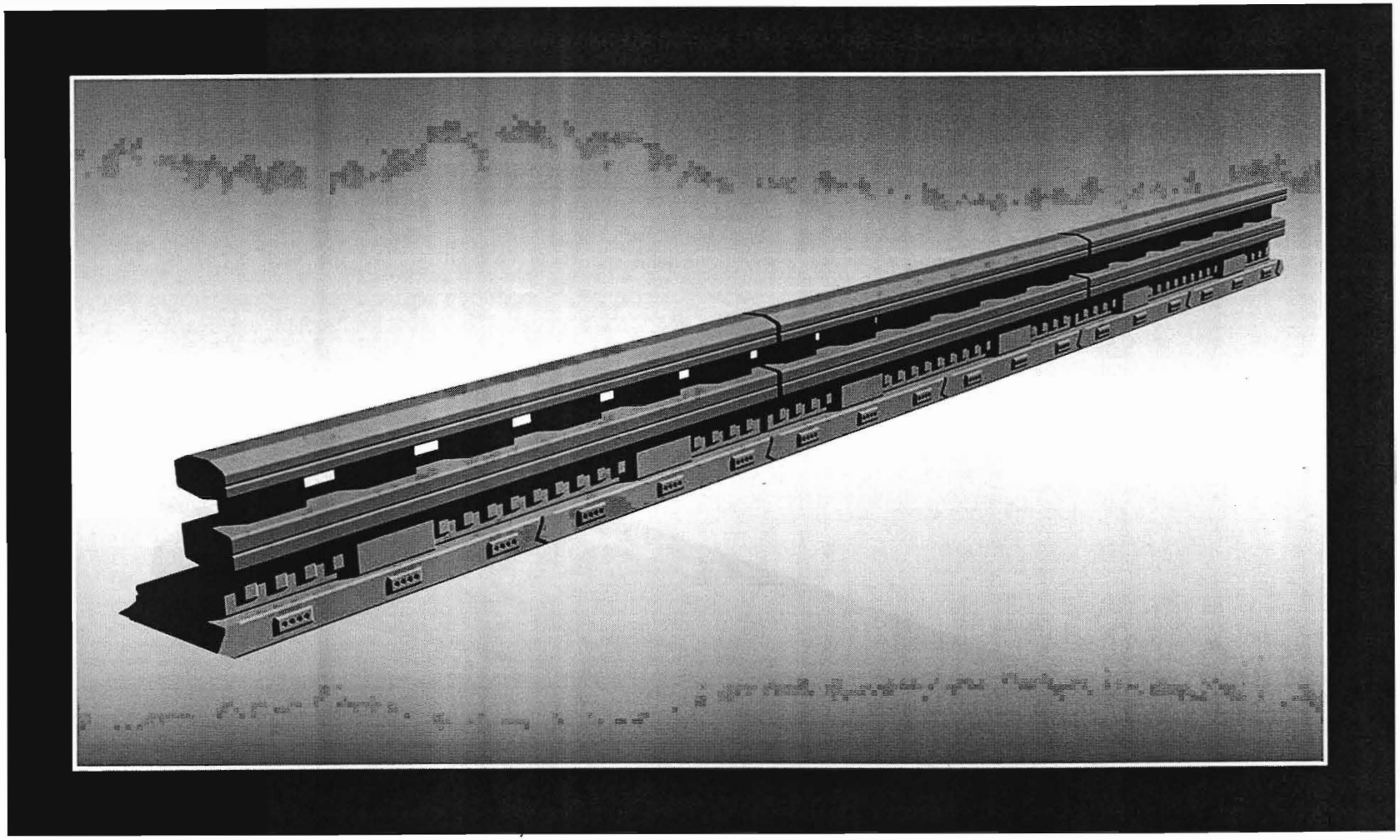

Figure 220. Precast Bridge Rail Aesthetic Treatment Concepts

11 SUMMARY, CONCLUSIONS, AND RECOMENDATIONS

11.1 Summary and Conclusions

The research effort described herein was focused on the development of a new, precast concrete bridge railing system. Precast concrete bridge rail systems offer several advantages over traditional cast-in-place rail designs, including reduced construction time and costs, installation in a wide range of environmental conditions, easier maintenance and repair, improved railing quality, and greater flexibility for aesthetic treatments. The objective of this project was to develop a precast concrete bridge rail system that met the TL-4 impact safety standards provided in MASH. The design criteria for the new bridge rail system included criteria for barrier geometry, provisions for open and closed rail options, constructability, weight limitations, segment length, design impact loads, connection of barrier segments, and connection to the bridge deck among other factors.

The research effort proceeded in several phases. First, the research focused on determining the overall concept for the new bridge rail system in terms of the rail configuration and geometry as well as the required barrier reinforcement. Next, design concepts for the joints connecting adjacent rail segments were designed and component tested in order to select a design capable of meeting design criteria for the precast bridge rail system. After selection of an appropriate rail joint, the researchers developed connection details for the attachment of the rail to the bridge deck. Once the design of the various precast bridge rail components was completed, a complete set of CAD details for the proto type precast concrete bridge rail system were completed.

Many design concepts for the precast concrete bridge rail system were developed in the first phase of the research. Review of previous TL-4 bridge rail research and finite element

computer simulation using LS-DYNA developed criteria for design impact loading, rail height, and barrier geometry guidelines to mitigation occupant head slap during passenger vehicle impacts. These criteria were combined with criteria for constructability, weight and segment length limitations, bridge rail width, load transfer to the bridge deck, and aesthetics to select the optimal precast bridge rail concept. Following detailed analysis and review of the various rail concepts, it was concluded that Concept F (Fence) was the optimal design. Concept F (Fence) was on open concrete railing that consisted of two stacked beams mounted at different heights and separated by balusters or spacers. This design provided advantages over the other design concepts in terms of aesthetics and constructability and met all of the other design criteria listed above.

Following selection of the basic bridge rail concept, the research was focused on development of a joint between adjacent rail segments. Analysis had shown that it was critical to develop continuity across the rail joints in order with potential TL-4 impact loads and limit the loads transferred to the bridge deck. The anticipated impacts loads required for the joint were calculated to be a shear loads of 35 kips (156 kN) and a moment of 700 k-in. (79 kN-m). A wide variety of joint designs were developed and considered based on load capacity, constructability, ease of repair, and aesthetics. Review of the initial design concept led to the selection of two potential joint designs for component testing. The designs selected for component testing were Joint Design H, a grouted, wide-flange beam joint connection and Joint Design D, a dry joint connection consisting of a shear tube and through bolts located in pockets at the outside edge of the rail beam.

The first round of component testing of the precast bridge rail joint designs was conducted to evaluate the feasibility of the two joint concepts and suggest potential

improvements to the designs. Test nos. PCRB-1 and PCRB-2 were conducted on Joint Design H and Joint Design D, respectively. The joints were tested by impacting short sections of the top rail beam of the bridge rail mounted on supports with the selected joint installed. The rail beam segments were then impacted by a bogie vehicle to produce the anticipated design loads. Both of the component test resulted in failure of the joint. Both joints displayed limited ductility and insufficient ability to sustain resistance to the design impact load during the impact. In addition, critical components of both joint designs failed during the testing. While the joint designs tested in test nos. PCRB-1 and PCRB-2 did not meet the design goals, they did demonstrate the potential to be used in the bridge rail design with the proper modifications.

Following the initial round of joint component testing, both the grouted and dry joint designs were revised to improve their capacity. A third joint design was also developed that considered an alternative grouted joint configuration. A second round of component testing was performed on these refined joint designs to determine if they met the design criteria. Test nos. PCRB-3, PCRB-4, and PCRB-5 were conducted on the refined grouted joint, the refined dry joint, and the alternative grouted joint design, respectively. The setup of the joint testing was similar to the previous testing. Results from the second round of bogie testing found that the revised grouted joint performed the best. This joint design met the design impact loads and retained its integrity. The revised dry joint proved to be capable of meeting similar impacts loads, but large pieces of concrete were disengaged from the joint during the component test. This behavior was undesirable, but it could be remedied through improved confinement of the concrete in the area of the joint pockets. The alternative grouted joint design fractured and failed very quickly and was deemed unacceptable for use in the bridge rail system. Following the results of the component testing, the revised grouted joint was chosen as the primary joint design

for the precast bridge rail system. It was believed that revised dry joint could be further revised to provide a second connection alternative if desired.

The final part of the design effort for the precast concrete bridge rail was to develop a connection between the bridge rail segments and the bridge deck. The design of the attachment focused on effectively transferring both shear and moment loads to the bridge deck without causing structural damage to the deck. Several attachment concepts were considered and evaluated based on capacity, constructability, and symmetry. Deck Attachment B was chosen as the most ideal design. This attachment employed four threaded rods of equivalent size to connect the rail posts to the bridge deck. This configuration allowed the rail segments to remain symmetric while utilizing a quick and simple method of fastening the segments to the bridge deck. Additional reinforcement details for the bridge deck were also designed to provide for the attachment of the post-to-deck anchorage. These reinforcement details provided additional capacity in the area of the post attachment to the deck while creating only minimal changes to the standard cast-in-place deck construction.

The individual design components of the new, precast bridge rail system were combined to create a prototype rail section design. Full CAD details of the prototype precast bridge rail design were prepared, including details for installation and mounting of the new design on a simulated concrete bridge deck at the MwRSF test facility.

The design of the new, precast concrete bridge railing system will significantly reduce construction time and should ultimately reduce overall costs as contractors and the precast industry gain experience with the new system. Construction of precast concrete railings will be much less weather sensitive as compared to the field installation cast-in-place, concrete railings. One additional benefit of the reduced construction time would result in a more-timely opening of

a bridge to the motoring public. The reduction in bridge construction time will improve work-zone safety for workers and motorists due to the reduced time period and exposure for the work zone near the bridge. Accident studies have found that accident and fatality rates increase in work zones. Thus, a reduced duration for the work zone should reduce accidents and improve safety. Further, a precast barrier system will greatly simplify barrier repair and maintenance should any damage occur during a moderate truck impact event. Standardized barrier components will allow maintenance personnel to easily remove and replace any damaged barrier components in a timely and efficient manner without requiring long periods of lane closure. Minimizing the bridge rail repair time also improves work-zone safety by reducing worker exposure to traffic. Finally, aesthetic features can be easily cast into the face of a precast barrier system without the high costs associated with field construction. Hence, the new barrier system allows designers much greater flexibility to develop bridge designs that contribute to the overall beauty of our nation's highways. In addition, it is believed that the rapid construction and innovative design allowed through the use of precast rail segments will provide the giant step in the advancement of bridge rail construction and safety.

11.2 Recommendations and Future Work

Only one design element of the precast bridge rail remained unfinished at the end of the research effort. The details for the bridge rail end sections were not finalized. MwRSF prepared preliminary concepts for the end section details, but the final details were left unfinished until the compliance testing of the new, precast bridge rail design was complete.

The original plan for the precast bridge rail project described herein included further component testing of a single rail section on a simulated concrete bridge deck to evaluate the connection between the bridge rail and the bridge deck. In addition, full-scale crash testing was

planned to evaluate the design and provide compliance for acquiring FHWA acceptance of the system. However, the intensive design and component testing efforts involved in the development of the precast bridge rail system did not leave sufficient funding for completion of these tasks. MwRSF researchers believe that the development of the precast bridge rail system could be completed through completion of the full-scale crash testing. Thus, it is recommended that the remaining full-scale crash testing be completed in order to finish the development of the new, precast bridge rail system.

Three crash tests are required according to the TL-4 impact conditions in MASH - a small car test, a pickup truck test, and a single-unit truck test. Since the railing geometry was designed to mitigate any propensity for small car wheel snag on the railing or post components, MwRSF believes that the small car test likely will be waived from the test matrix. However, MwRSF believes that both the pickup truck and single-unit truck crash tests will be required for certifying and garnering FHWA acceptance for the new bridge railing system. Thus, two full-scale crash tests will be required for evaluation and Federal acceptance under the requirements of MASH: (1) a 10,000-kg (22,000-lb) single-unit truck impacting at 56 mph (90 km/hr) and 15 degrees; and (2) a 2,268-kg (5,000-lb) pickup truck impacting at 62 mph (100 km/hr) and 25 degrees.

Full-scale crash testing and FHWA acceptance of the new bridge rail will aid implementation of the design as the benefits of the system become evident. New construction techniques will be developed to more rapidly install vehicular bridge railings, thus allowing for a more advanced bridge opening to the motoring public. The decreased construction time will result in improved safety of workers and motorists as well as decreased traffic congestion and the length of time that a work zone is operational. The completion of this effort will demonstrate to

other State DOTs that new, innovative bridge railings are feasible and available for use across the U.S.

12 REFERENCES

1. *Manual for Assessing Safety Hardware (MASH),* American Association of State and Highway Transportation Officials (AASHTO), Washington, D.C., 2009.

2. *FHWA Acceptance Letter No. B-5 – Precast Concrete Bolt-Down Barrier System*, Letter to E.F. Vines, L.B. Foster Company, Federal Highway Administration, March 14, 1989.

3. *Guide Specifications for Bridge Railings*, American Association of State Highway and Transportation Officials (AASHTO), Washington, D.C., 1989.

4. *Standard Type T503 – Precast Traffic Rail*, Bridge Division, Texas Department of Transportation, February 2003.

5. *Standard Type T504 – Precast Traffic Rail – Prestr Conc Box Beams, Slab Beams, or Dbl-T Beams (C-I-P Slab 5" Minimum)*, Bridge Division, Texas Department of Transportation, February 2003.

6. Ross, H.E., Sicking, D.L., Zimmer, R.A., and Michie, J.D., *Recommended Procedures for the Safety Performance Evaluation of Highway Features*, National Cooperative Highway Research Program (NCHRP) Report No. 350, Transportation Research Board, Washington, D.C., 1993.

7. Buth, C.E., Hirsch, T.J., and McDevitt, C.F., *Performance Level 2 Bridge Railings*, Transportation Research record No. 1258, Transportation Research Board, National Research Council, Washington, D.C., 1990.

8. Rosenbaugh, S.K., Sicking, D.L., and Faller, R.K., *Development of a TL-5 Vertical-Faced Concrete Median Barrier Incorporating Head Ejection Criteria*, Transportation Research Report No. TRP-03-194-07, Midwest Roadside Safety Facility, University of Nebraska-Lincoln, December 2007.

9. Mak, K.K. and Sicking, D.L., *Rollover Caused by Concrete Safety Shaped Barriers*, Transportation Research Record No. 1258, Transportation Research Board, National Research Council, National Research Council, Washington, D.C., 1990.

10. Rosenbaugh, S.K., Faller, R.K., Hascall, J.A.,Allison, E.M., Bielenberg, R.W., Rohde, J.R., Polivka, K.A., Sicking, D.L., and Reid, J.D., *Development of a Stand-Alone Concrete Bridge Pier Protection System*, Final Report to the Midwest State's Regional Pooled Regional Pooled Fund Program, Transportation Research Report No. TRP-03-190-08, Project No.: SPR-3(017), Project Code: RPFP-04-05 - Year 14, Midwest Roadside Safety Facility, University of Nebraska-Lincoln, April 18, 2008.

11. Schmidt, J.D., Faller, R.K., Lechtenberg, K.A., Sicking, D.L., and Reid, J.D., *Development and Testing of a New Vertical-Faced Temporary Concrete Barrier for Use*

on Composite Panel Bridge Decks, Final Report to the Kansas Department of Transportation, Transportation Research Report No. TRP-03-220-09, Sponsor Agency Code: SPR-3(017) Supplement No. 57, Midwest Roadside Safety Facility, University of Nebraska-Lincoln, October 13, 2009.

12. Bligh, R.P., Briaud, J.L., Kim, K.M., and Abu-Odeh, A., *Design of Roadside Barrier Systems Placed on MSE Retaining Walls*, National Cooperative Highway Research Program (NCHRP) Report No. 663, Transportation Research Board, Washington, D.C., 2010.

13. Buth, C.E., Hirsch, T.J., and Menges, W.L., *Testing of the New Bridge Rail and Transition Designs,* Technical Report, FHWA Contract No. DTFH61-86-C-00071, Report No. FHWA-RD-93-058, Federal Highway Administration, Washington D.C., September 1993.

14. Mak, K.K., Bligh, R.P., Menges, W.L., *Volume I: Technical Report Testing of State Roadside Safety Systems*, Report to Federal Highway Administration, Research Study No. RF 471470, Texas Transportation Institute, September 1996.

15. Holloway, J.C., Pfeifer, B.G., Faller, R.K., Post, E.R., *Full-Scale 18,000 lb. Vehicle Crash Test on the Kansas 32 Inch Corral Rail*, Report to Kansas Department of Transportation, Report No. TRP-03-26-91, Midwest Roadside Safety Facility, University of Nebraska-Lincoln, July 1991.

16. Polivka, K.A., Faller, R.K., Sicking, D.L., Rohde, J.R., Bielenberg R.W., Reid J.D., and Coon, B.A., *Performance Evaluation of the Permanent New Jersey Safety Shape Barrier - Update to NCHRP 350 Test No. 4-12 (2214NJ-2)*, Report No. TRP-03-178-06, Midwest Roadside Safety Facility, University of Nebraska-Lincoln, October 2006.

17. Bullard, D.L, Bligh, R.P., Menges, W.L., Haug, R.R., *Evaluation of Existing Roadside Safety Hardware Using Updated Criteria*, Report to National Cooperative Highway Research Program, Performed by Texas Transportation Institute, Texas A&M University, College Station, Texas, March 2010.

18. Halquist, L.O., *LS-DYNA Keyword User's Manual.* Version 970, Livermore California, Livermore software Technology Corporation, 2003.

19. Holloway, J.C., Faller, R.K., Pfeifer, B.G., and Post, E.R., *Performance Level 2 Tests on the Missouri 30-in. New Jersey Safety Shape Bridge Rail*, Final Report to the Missouri Highway and Transportation Department, Transportation Research Report No. TRP-03-27-91, Civil Engineering Department, University of Nebraska-Lincoln, November 1991.

20. Polivka, K.A., Hascall, J.A., Faller, R.K., Rohde, J.R., Holloway, J.C., Sicking, D.L., and Kurz, K., *Design and Evaluation of CYRO's Paraglas Soundstop TL-4 Noise Barrier System*, Final Report to CYRO Industries, Inc., Transportation Research Report No. TRP-

03-160-05, Midwest Roadside Safety Facility, University of Nebraska-Lincoln, April 22, 2005.

21. Holloway, J.C., Faller, R.K., Wolford, D.L., and Sicking, D.L., *Performance Level 2 Tests on a 29-in. Open Concrete Bridge Rail*, Final Report to the Nebraska Department of Roads, Project No. SPR-3(017), Transportation Research Report No. TRP-03-51-95, Midwest Roadside Safety Facility, University of Nebraska-Lincoln, June 1996.

22. *Tentative Service Requirements For Bridge Rail Systems*, National Cooperative Highway Research Report Program (NCHRP) Report No. 86, Washington, D.C., 1970.

23. Eller, C.M. and Reid, J.D., *Determination of Impact Forces From Vehicle-to-Barrier Crashes*, Report to University of Nebraska Honors Program, Midwest Roadside Safety Facility, University of Nebraska-Lincoln, April 2007.

24. Wiebelhaus, M.J., Polivka, K.A., Faller, R.K., Rohde, J.R., Sicking, D.L., Holloway, J.C., Reid, J.D., and Bielenberg, R.W., *Evaluation of Rigid Hazards Placed in the Zone of Intrusion*, Transportation Report No. TRP-03-151-08, Midwest Roadside Safety Facility, University of Nebraska-Lincoln, January 2008.

25. *AASHTO LRFD Bridge Design Specifications*, 2001 Interim Edition, Published by the American Association of State Highway and Transportation Officials, Washington D.C., 2001.

26. Hirsch, T.J., *Analytical Evaluation of Texas Bridge Rails to Contain Buses and Trucks*, Report No FHWA TX 78-230-2, Performed for the Texas State Department of Highways and Public Transportation, Performed by Texas Transportation Institute, Texas A&M University, College Station, Texas, August 1978.

27. Bligh, R.P., Sheikh, N.M., Menges, W.L., Haug, R.R., *Development of a Low-Deflection Precast Concrete Barrier*, Report No. FHWA/TX-05/0-4162-3, Texas Transportation Institute, Texas A&M University, College Station, Texas, January 2005.

13 APPENDICES

APPENDIX A. Additional Rail to Rail Joint Concepts

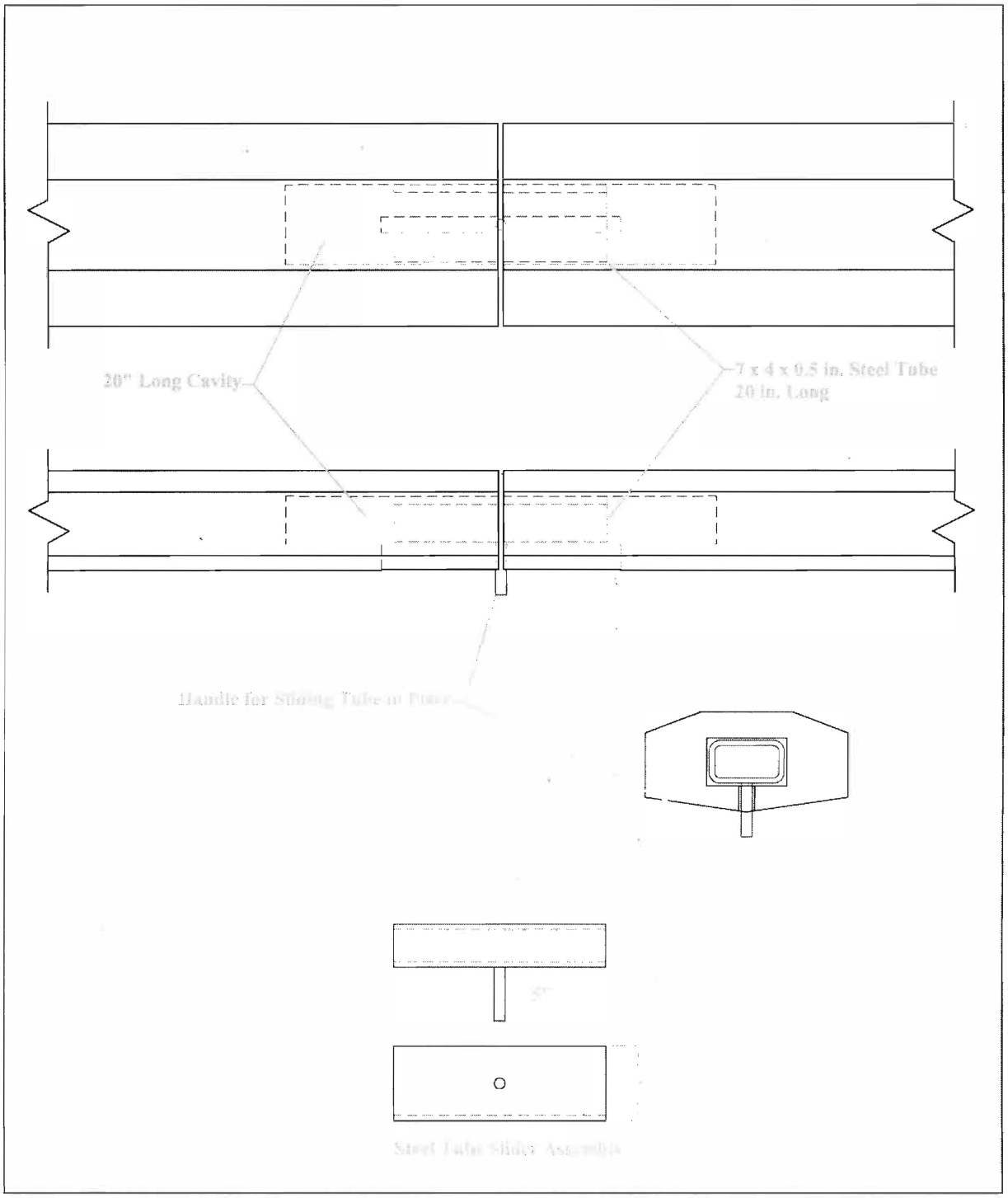

Figure A-1. Dry Rail Joint – Slider Tube

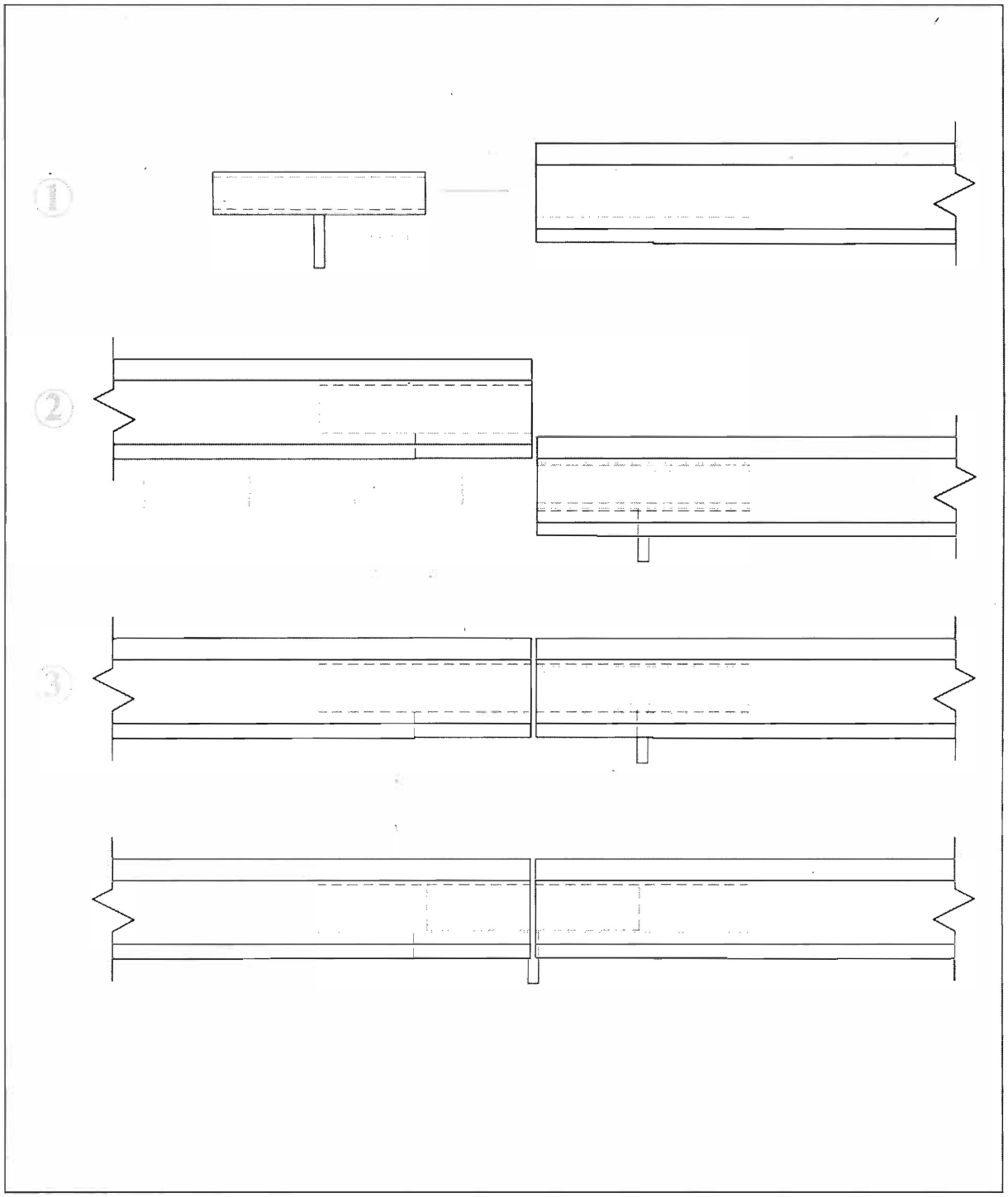

Figure A-2. Dry Rail Joint – Slider Tube Assembly

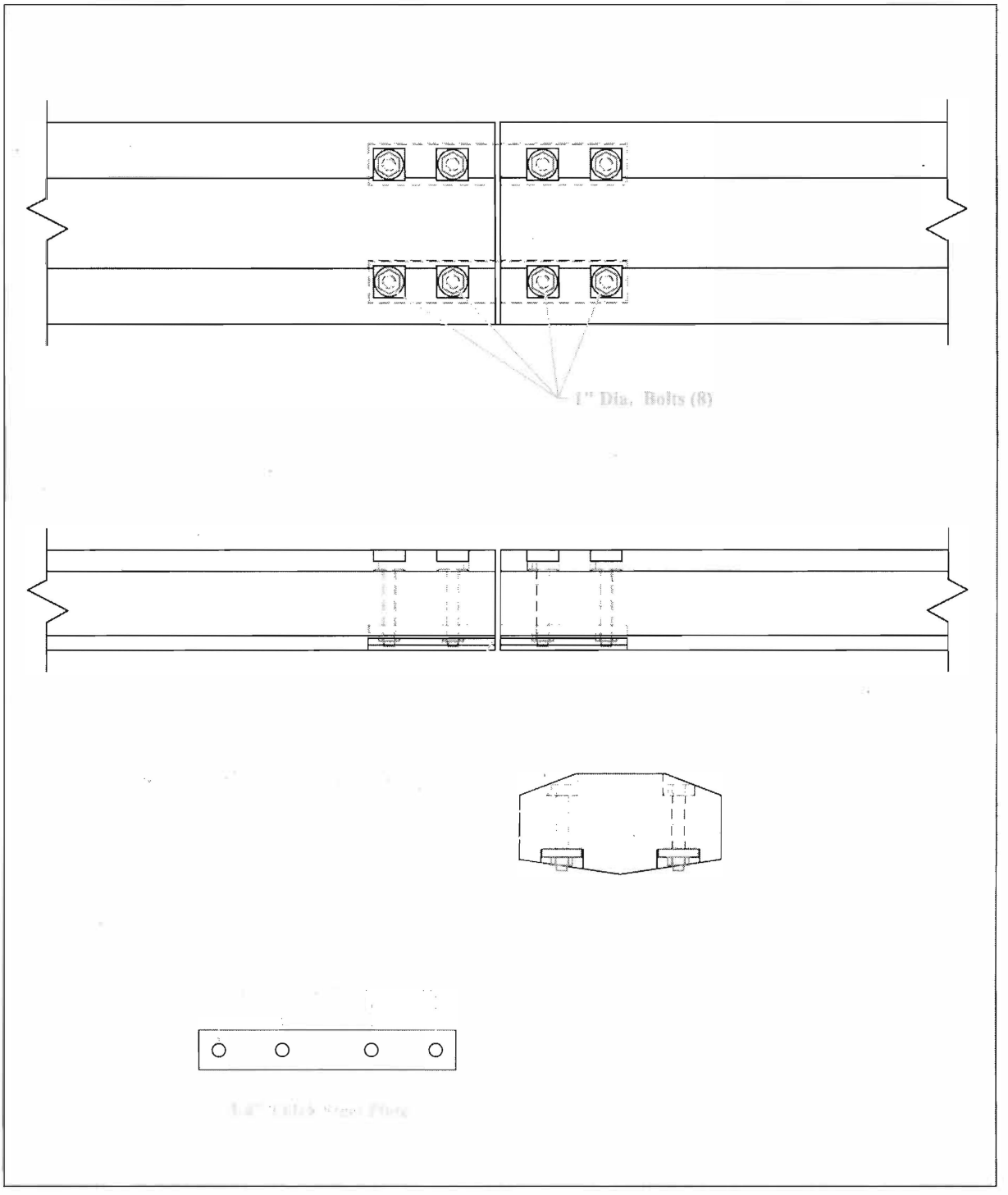

Figure A-3. Dry Rail Joint – Plates Underneath Rail

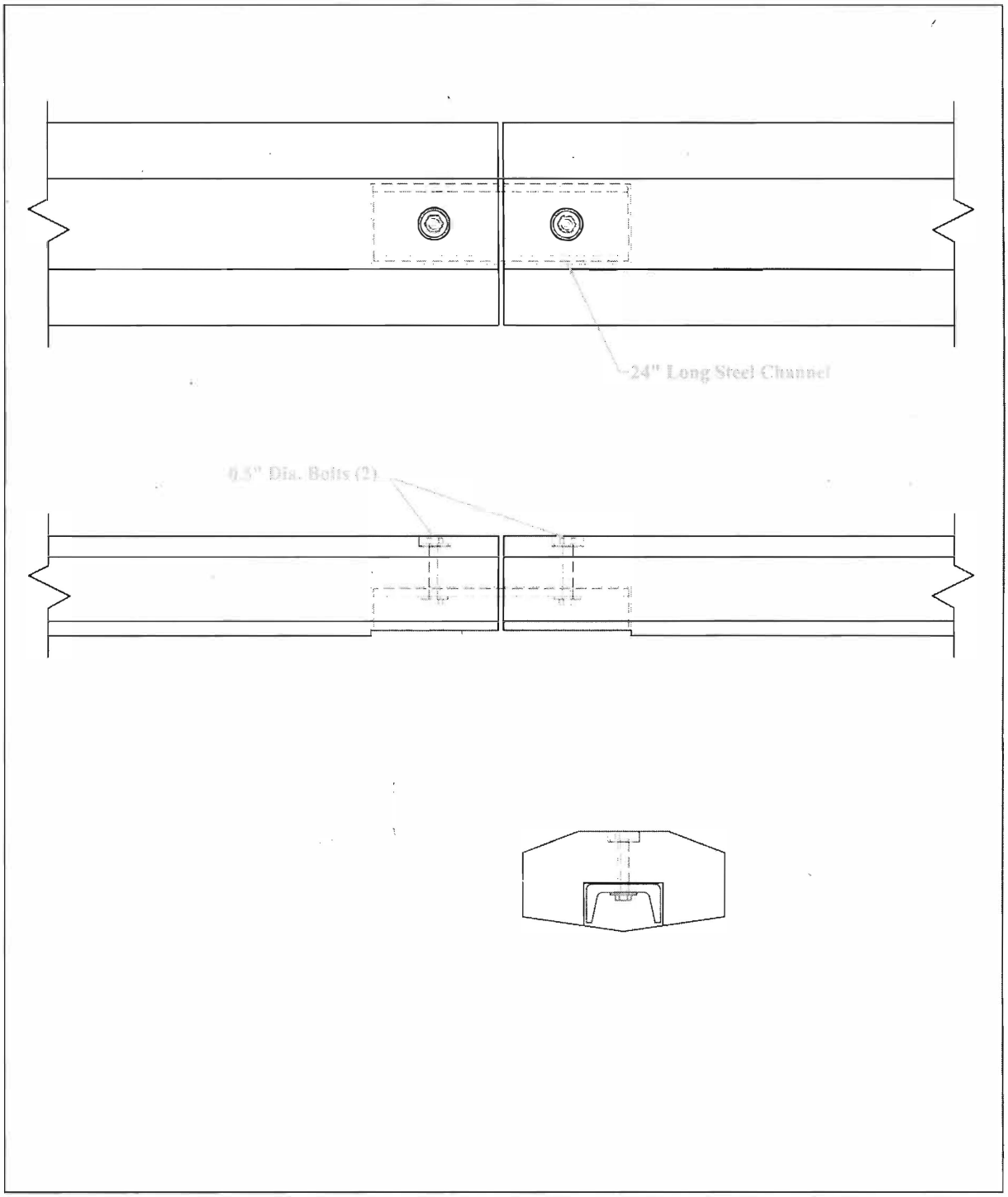

Figure A-4. Dry Rail Joint – Structural Steel Shape (C-Channel) Underneath Rail

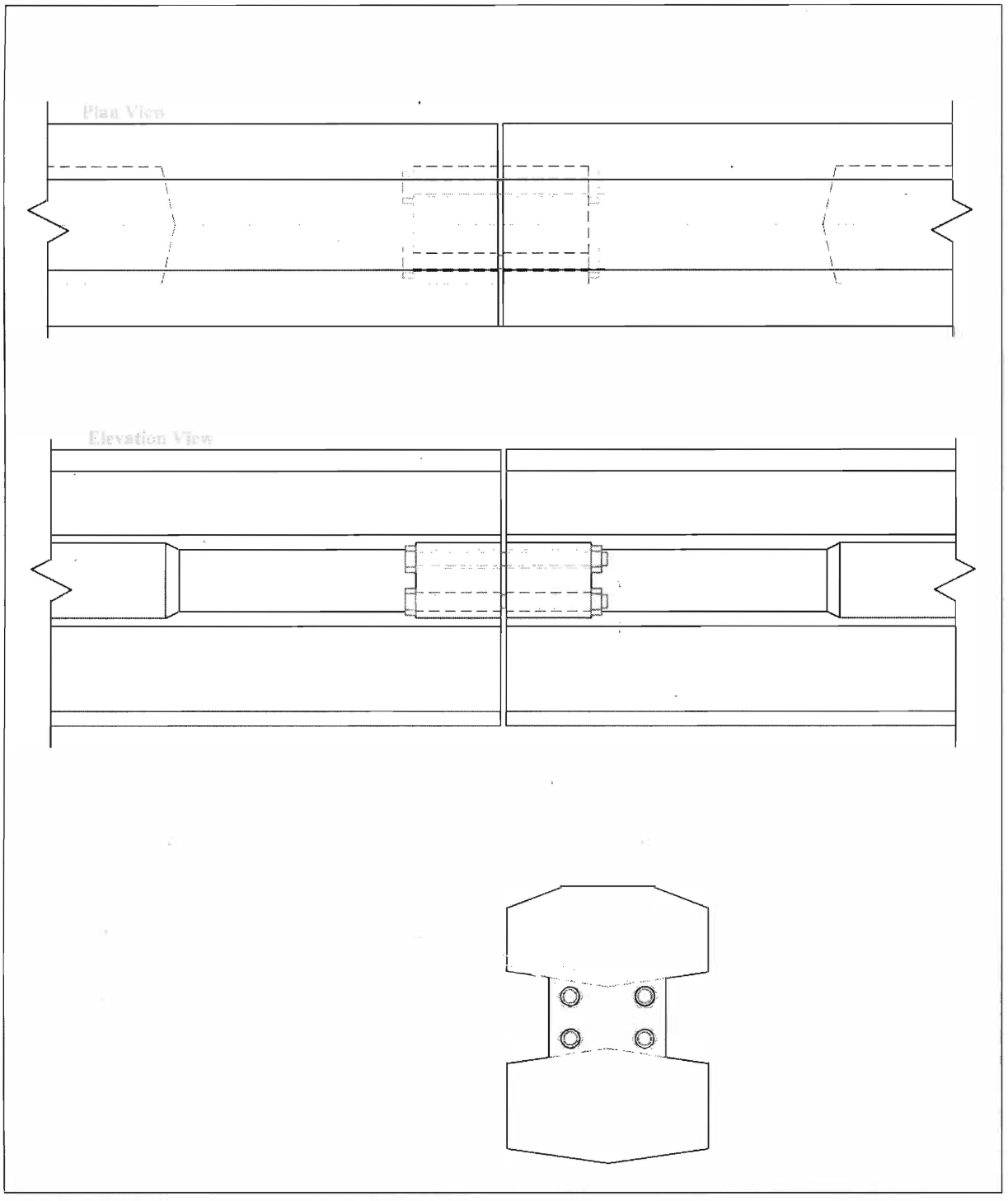

Figure A-5. Dry Rail Joint – Bolts Through End Balusters

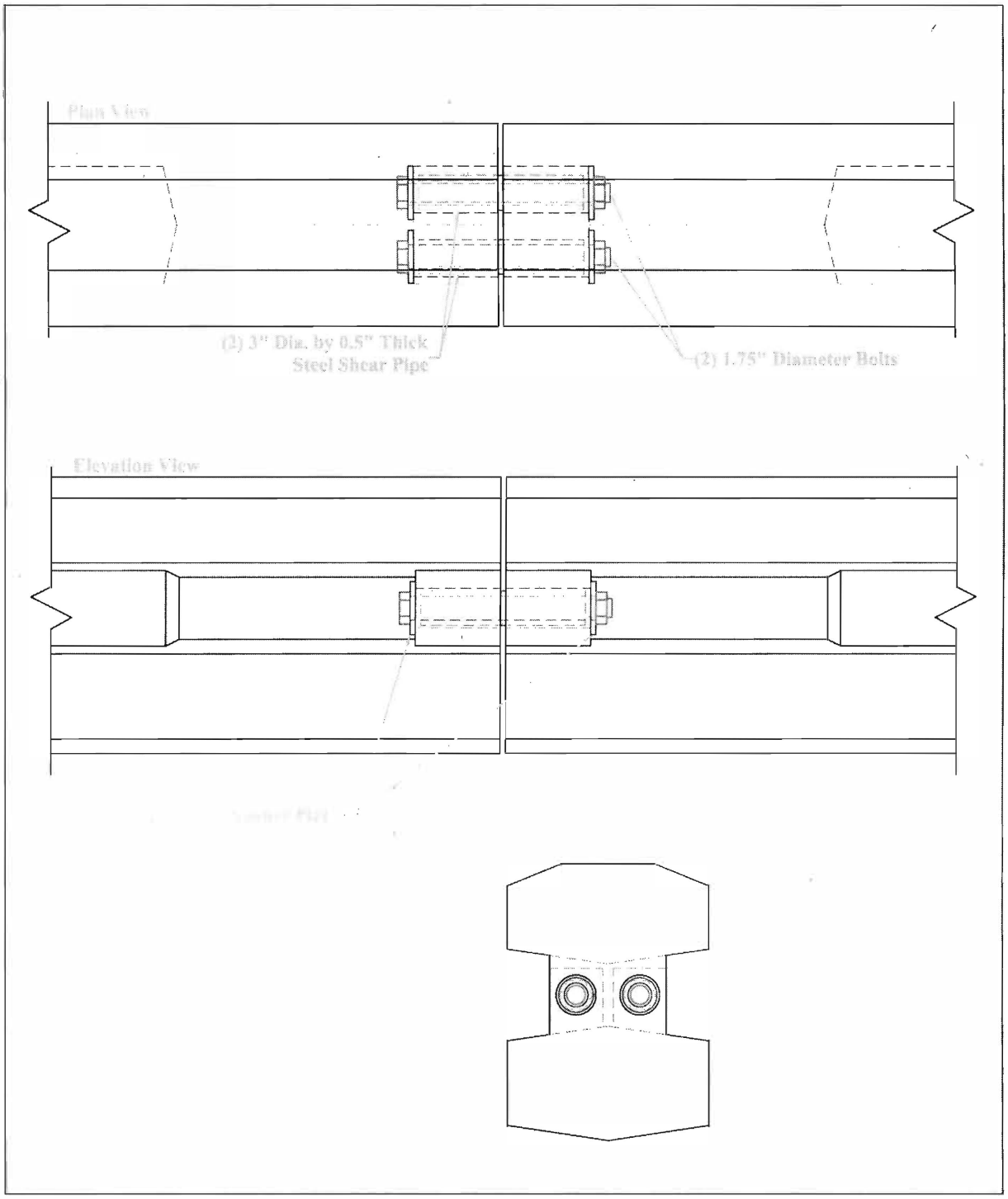

Figure A-6. Dry Rail Joint – Bolts and Shear Pipes Through End Balusters

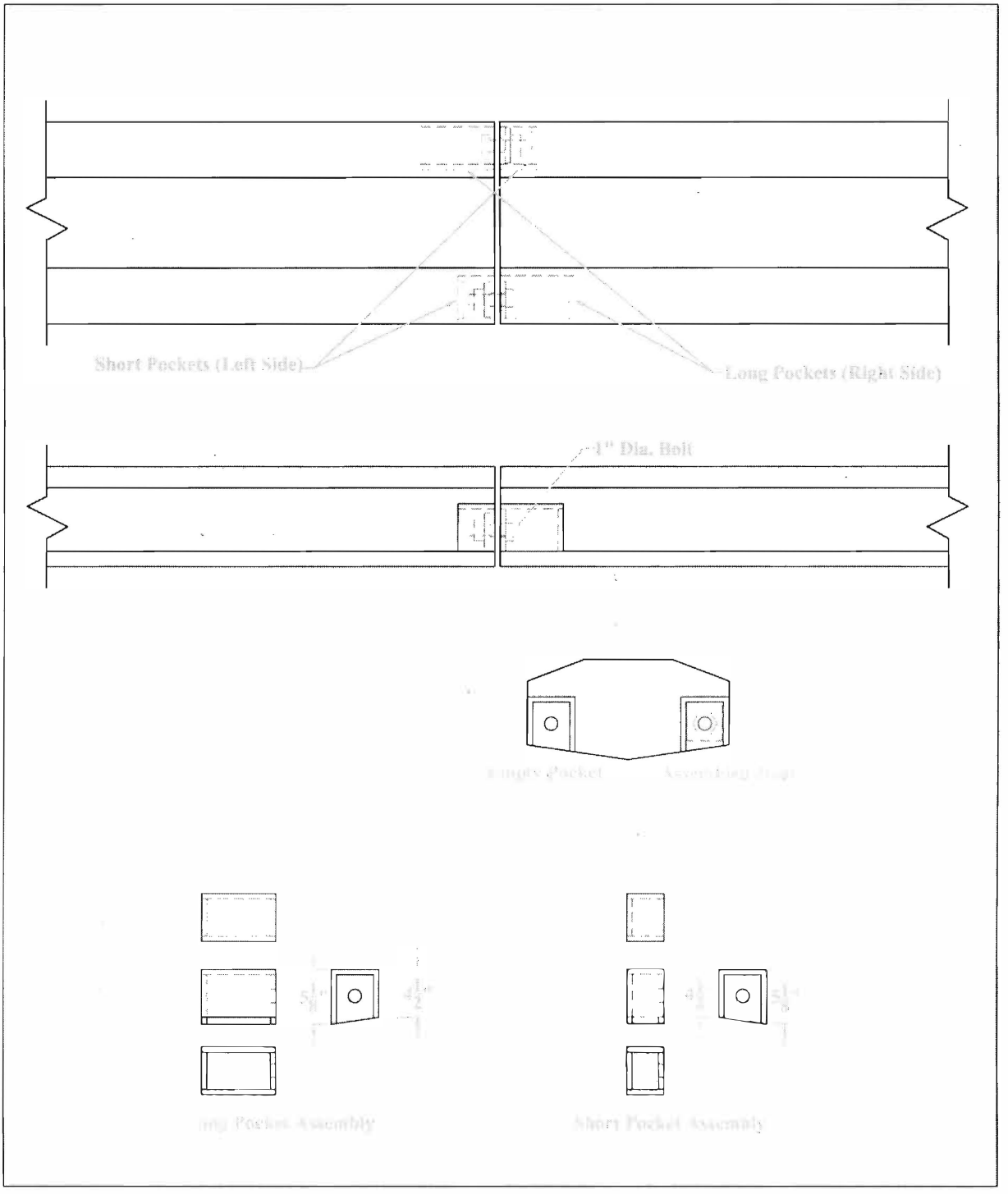

Figure A-7. Dry Rail Joint – Unsymmetrical, One-Way Bolt Assembly

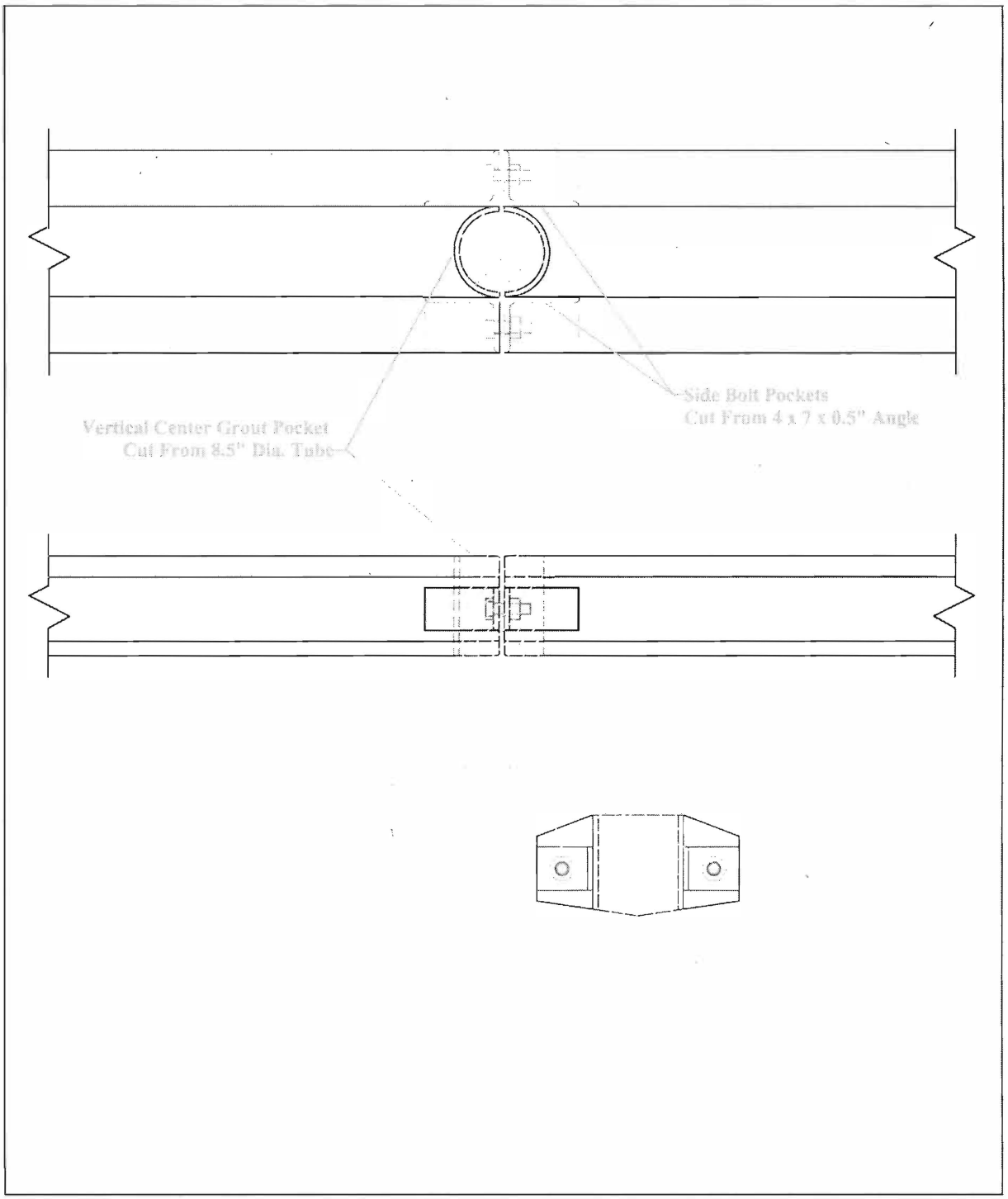

Figure A-8. Grouted Rail Joint – Side Bolts and Vertical, Center Grout Pocket

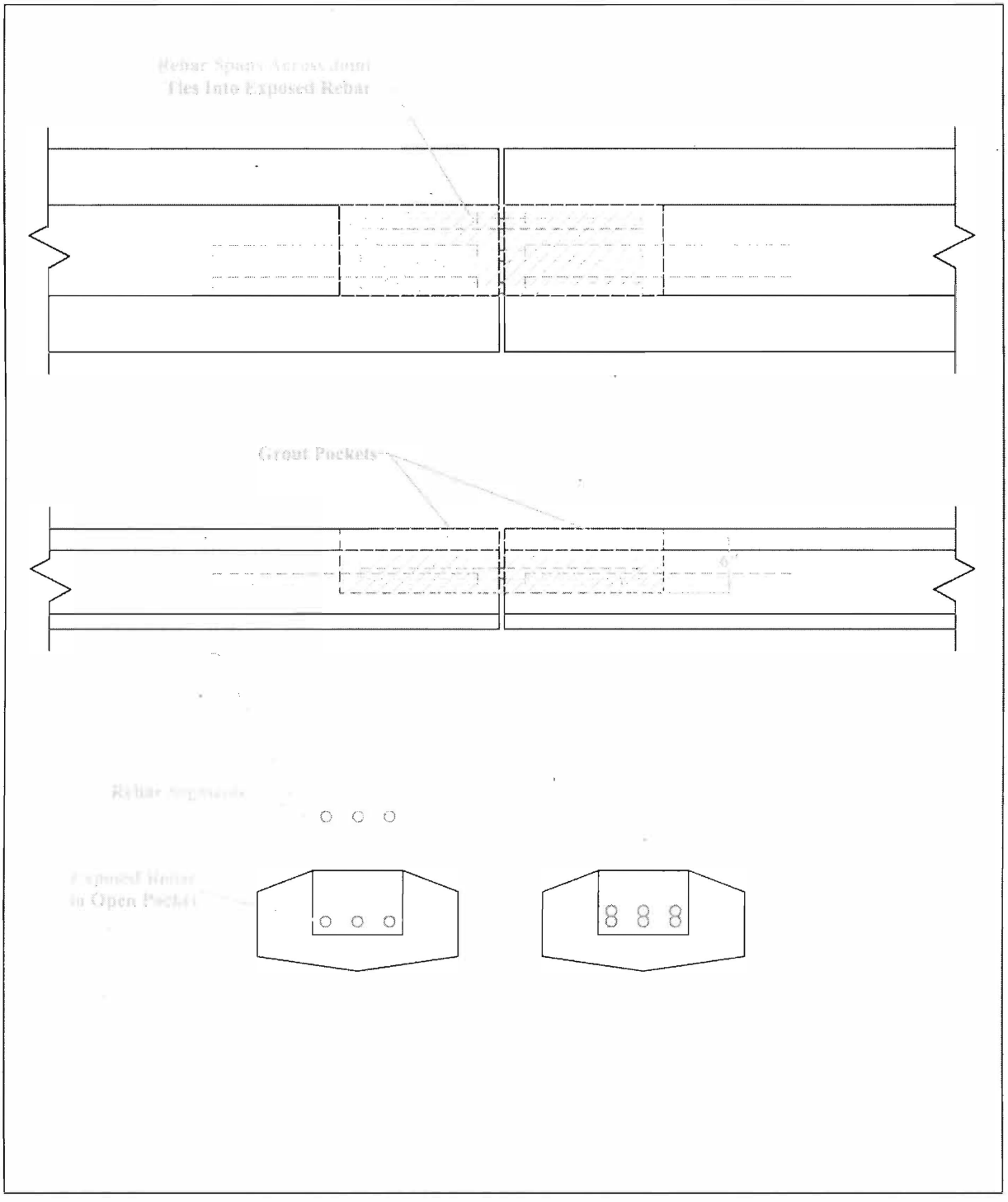

Figure A-9. Grouted Rail Joint – Large Grout Pocket with exposed Steel Reinforcement

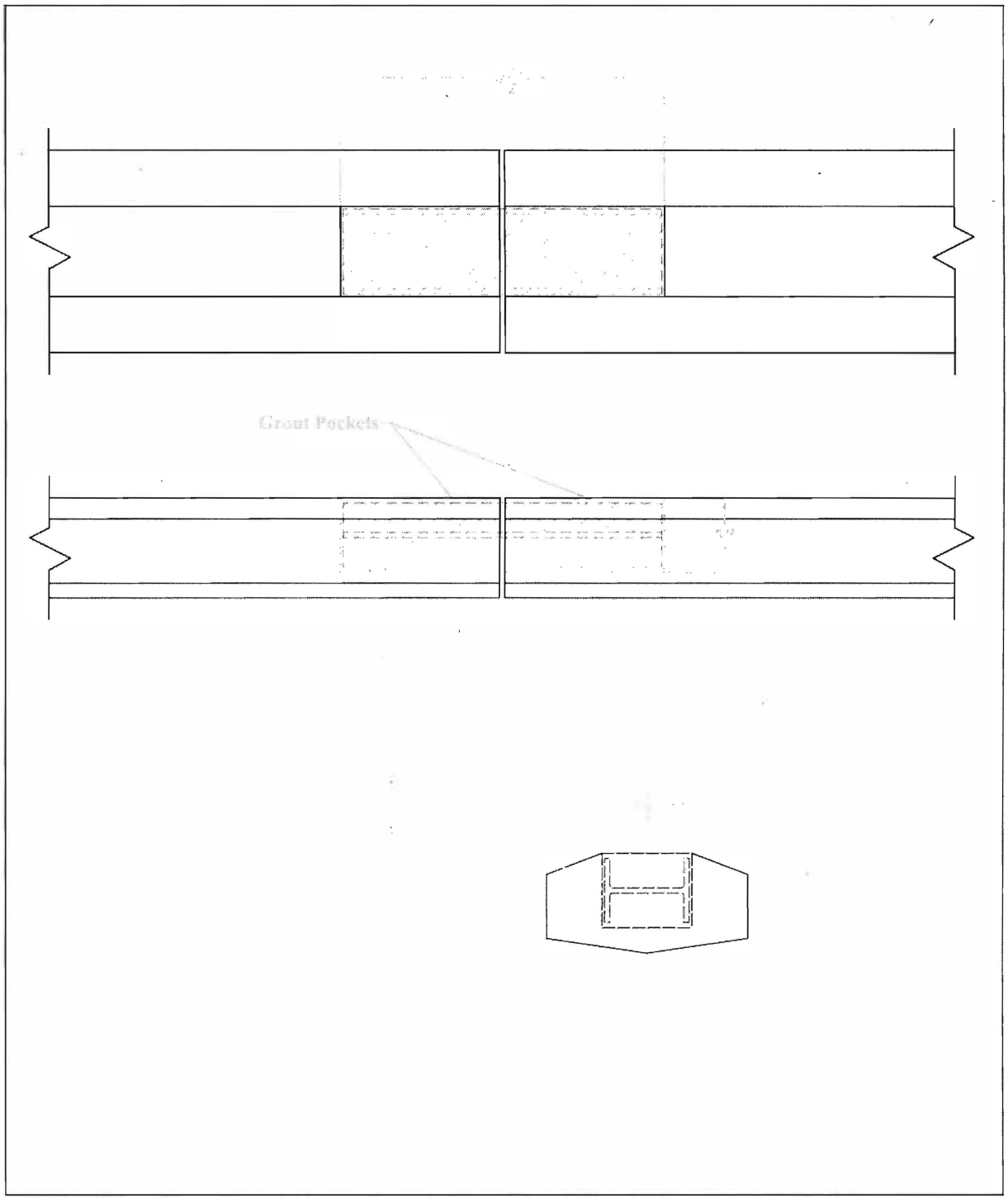

Figure A-10. Grouted Rail Joint – Structural Steel Shape in Center Grout Pocket

END OF DOCUMENT